

**HAGE and WT1 proteins as promising  
immunotherapeutic targets in chronic  
myeloid leukaemia**

**Rukaia Noori Sahdoon Almshayakhchi**

**A thesis submitted in partial fulfilment of the  
requirements of Nottingham Trent  
University for the degree of Doctor  
of Philosophy**

**Supervisors: Dr. Stephanie McArdle**

**Prof. Graham Pockley  
Prof. Sergio Rutella**

**May 2020**



# **Declaration of ownership**

This submission is the result of my work. All help and advice, other than that received from tutors, has been acknowledged and primary and secondary sources of information have been properly attributed. Should this statement prove to be untrue, I recognise the right and duty of the Board of Examiners to recommend what action should be taken in line with the University's regulations on assessment contained in the Handbook.

# Copyright statement

This work is the intellectual property of the author and may also be owned by the research sponsor(s) and/or Nottingham Trent University. You may copy up to 5% of this work for private study, or personal, non-commercial research. Any re-use of the information contained within this document should be fully referenced, quoting the author, title, university, degree level and pagination. Queries or requests for any other use, or if a more substantial copy is required, should be directed in the owner(s) of the Intellectual Property Rights.

# Ethical statement

1. All the pre-clinical work presented in this thesis was carried out under a Home Office approved PPL project licence (PB26CF602) which was approved on 28<sup>th</sup> November 2016.
2. Healthy blood samples used in this research were collected under an ethically approved study with approval given by the SST Human Invasive Ethics Committee (NTU) – application number 435 on 25th January 2016.

# Dedication

This Thesis is dedicated to my parents, my husband Firas, and my daughters; Fadak and Fatimah who have supported me all the way through my PhD journey. It is also dedicated to the soul of my grandma and to the souls of all the people who died due to *COVID-19*.

# Acknowledgements

First and foremost, I would like to express my deep gratitude to my supervisor, Dr Stéphanie McArdle. Stéphanie has indeed contributed to build-up my Knowledge and understanding in the area of cancer immunotherapy. Her scientific discussions, enthusiasm and devotion had provided a splendid environment for my project to move forward. I would also like to sincerely thank my supervisor Prof Graham Pockley for his excellent management and valuable feedback, his contribution in my research is highly appreciated. Many thanks to Prof Sergio for sharing with me his rich clinical expertise in leukaemia. I would also like to express gratitude to Prof Robert Rees who gave me the honour of being part of the immunology group. Next in line is Steve Reeder who offered me extraordinary help from the first day I started, assisting with all day-to-day issues, until now to this very moment. I would like to also say a big thank you to Prof Lindy Durrant, for providing me the ImmunoBody<sup>®</sup> vaccines- the secret to the novelty of my research.

I must acknowledge and thank The Higher Committee for Education Development in Iraq (HCED) for sponsoring my PhD study. Without their fund, I would not have had the opportunity to work here at John Van Gees Cancer Research Centre.

A special and deep thanks to Dr Jayakumar Vadakekolathu for his intellectuality and smart academic ideology that had guided me throughout my research, and particularly the molecular aspect. His significant knowledge, cheerful spirit and the eagerness to help others are just a flavour of his great personality, making him one of the kindest people who helped me to produce this project.

My sincere thanks to Dr Simon Hood and Dr Gemma Foulds for their continuous encouragement and support, particularly in experiments related to flow cytometry. A particularly grateful thanks to Dr Divya Nagarajan for her crucial support and guidance. Divya was always there for me during and after office hours; I will never forget her support, help and motivation.

I would like to heartily thank my dearest friend, Dr Shaymaa Al-Juboori, who recently graduated, and so all the best for her. Shaymaa is a real friend who was with me in happy and sad occasions, giving help and support, and of course sharing food!

Special appreciation should also go to Josh for his aid, I am really grateful for the kind response that I always receive whenever I ask for his help. Also, special thanks to Anna Di Biase for her endless support, encouragement and really friendly character.

My great thanks is also extended to Prof Graham Ball and Dr Sarah Wagner for help given in analysing bioinformatic data and complex statistics. Also, credit to Anne Schneider, Dr Tarik, Dr David, Dr Amanda, Catherine Johnson, and Dr Clare. Many

thanks should also go to the sweet group that has recently joined us at JVGCRG; Dr Cristina, Dr Maria and Dr Christopher, you are very welcome.

Deep thanks to Murrium for planning my experiments and managing the animal work. Special thanks to Andrew, Adam and Joe, for their help with immunisation and looking after my murine studies.

My heartfelt thanks to my fellow PhD colleagues; Abdullah, Pauline, Sarra Idri, Arif, Magdalena, Luisa, Marco, Jenny, Melissa and all friends who encouraged me, particularly Rebecca.

To far distance, a big thanks to my parents, parents in law, sister, brothers and all friends for the constant praying and encouragement to complete the second hardest academic experience in my life.

Finally, special heartily thanks to my husband, Firas, for being with me and on my side throughout this challenging part of my life. We have shared family duties, children care and pain, I would not be in good health today without his care.

All through this journey, my lovely daughter, Fadak, has provided me with all the love, hugs and support that I used to obtain from my Mum, thanks my sweetheart for your incredible moments. My sweet little daughter, Fatimah, thank you ever so much for your patience for the days that I did not spend enough time with you. Thank you very much my great family for understanding my situation and showing exceptional appreciation.

# Table of content

List of Figures .....	x
List of Tables.....	xv
Abbreviations .....	xvi
Abstract.....	xix
<b>1 Chapter I: Main introduction.....</b>	<b>1</b>
1.1 Chronic myeloid leukaemia (CML).....	1
1.1.1 Haematopoietic and leukaemic hierarchy.....	1
1.1.2 Definition, epidemiology and risk factors of CML.....	3
1.1.3 CML pathophysiology and molecular driving events.....	3
1.1.4 CML management: diagnosis and therapy.....	5
1.1.5 Immune dysregulation in the newly diagnosed CML .....	8
1.1.6 Imatinib immunological "On-target" and "Off-target" effects .....	13
1.2 Development of immunotherapy in CML .....	18
1.2.1 Resistance of CML stem cells to currently available therapy .....	18
1.2.2 Potential capability of immunotherapy to eradicate CML stem cells.....	19
1.2.3 Types of immunotherapy in CML.....	21
1.3 Helicase Antigen (HAGE) (DDX43) (CT-13) .....	33
1.4 Wilms tumour antigen (WT1) .....	35
1.5 Aims and hypothesis of the study .....	37
<b>2 Chapter-II: Material and methods .....</b>	<b>38</b>
2.1 Materials and Reagents.....	38
2.2 Methods.....	51
2.2.1 Cell lines, media and cultures .....	51
2.2.2 Genetic manipulation trials: Gene Knock-in and knockdown.....	53
2.2.3 Protein expression analysis .....	56
2.2.4 Gene expression analysis.....	59
2.2.5 Animals and immunisation .....	61
2.2.6 Preparation of T cell for the cytotoxicity assays.....	67
2.2.7 <i>in vivo</i> tumour challenge experiments: The prophylactic and the therapeutic settings.....	69
2.2.8 Gallios™ flow cytometer assays .....	72
2.2.9 Isolation of PBMCs from the blood of healthy volunteers .....	76
<b>3 Chapter III: Validation of HAGE and WT1 as potential targets for immunotherapy in leukaemia.....</b>	<b>77</b>
3.1 Introduction .....	77
3.1.1 Promising immunotherapeutic value of cancer testis antigens.....	77
3.1.2 The oncogenic function of cancer testis antigens.....	78
3.1.3 Pattern of cancer testis antigens expression in haematological malignancies .....	80
3.1.4 Current clinical applications of oncogenic C/T antigens.....	81
3.1.5 Epigenetic signature on C/T antigens expression in CML.....	82
3.1.6 HAGE (DDX43) antigen as a target for immunotherapy.....	84
3.1.7 WT1 antigen as a target for immunotherapy.....	85
3.2 Rationale of the chapter .....	86
3.3 Results .....	87
3.3.1 Expression of HAGE and WT1 in leukaemic cell lines.....	87

3.3.2	Expression of HAGE and WT1 transcripts in peripheral blood mononuclear cells from healthy volunteers.....	91
3.3.3	Expression of HAGE and WT1 transcripts in CML patients .....	92
3.3.4	Expression of HAGE and WT1 transcripts in AML patients .....	98
3.3.5	Expression of HAGE and WT1 transcripts in adult B-ALL .....	102
3.3.6	Patterns of Cancer Testis and WT1 gene expression in AML and CML, as determined by microarray analysis using the ArrayExpress database .....	106
3.4	Discussion .....	113
3.5	Conclusion and chapter impacts.....	121

## **4 Chapter IV: Immunogenicity of HAGE- and WT1-ImmunoBody<sup>®</sup> vaccines in HHDRII/DR1 mice ..... 122**

4.1	Introduction .....	122
4.1.1	Antigen Processing and Presentation .....	123
4.1.2	T cell development, differentiation and T cell mediated immunity .....	126
4.1.3	T cell exhaustion in the tumour milieu .....	129
4.1.4	Factors influencing vaccine success .....	130
4.1.5	DNA and ImmunoBody <sup>®</sup> based vaccines .....	131
4.2	Rationale of the chapter.....	135
4.3	Results .....	136
4.3.1	HAGE and WT1 peptides predication and synthesis.....	136
4.3.2	Peptide-HLA-A2 affinity and stability assays .....	138
4.3.3	Immunogenicity of HAGE- and WT1-ImmunoBody <sup>®</sup> vaccines administered individually .....	144
4.3.4	Immunogenicity of the combined HAGE- and WT1-ImmunoBody <sup>®</sup> vaccines .....	150
4.3.5	Proliferation, cytokine production and degranulation of CTLs derived from ImmunoBody <sup>®</sup> immunised mice .....	152
4.3.6	Influence of HAGE- and WT1-ImmunoBody <sup>®</sup> vaccines on naïve and memory T cell populations .....	156
4.3.7	Effect of immunisation on T cell activation and exhaustion .....	159
4.4	Discussion .....	161
4.5	Conclusion and chapter impacts:.....	166

## **5 Chapter V: Target cell preparation: ..... 167**

5.1	Introduction .....	167
5.1.1	Immortalized haematopoietic cell lines .....	167
5.1.2	Establishment of genetically modified cell lines .....	168
5.1.3	Role of IFN- $\gamma$ in cancer immunoediting :From immune-surveillance to immune evasion .....	169
5.2	Rationale of the chapter.....	177
5.3	Results .....	178
5.3.1	Evaluation of HAGE and WT1 expression by the respective targets... ..	178
5.3.2	Phenotypic analysis of the respective targets.....	179
5.3.3	Generation of K562/HHDII <sup>+</sup> /HAGE <sup>+</sup> cells to be a suitable target for cytotoxicity assay .....	181
5.3.4	Generation of KCL-22/HAGE <sup>+</sup> target cells for cytotoxicity assay.....	186
5.3.5	Generation of TCC-S/WT1.shRNA target cells for cytotoxicity assay..	187
5.3.6	Profile of hB16/HAGE <sup>+</sup> /Luc <sup>+</sup> cells:.....	188
5.3.7	Diverse biological functions of IFN- $\gamma$ on the respective CML cells:.....	190
5.4	Discussion .....	200
5.5	Conclusion and chapter impacts.....	204

<b>6 Chapter VI: <i>In vitro</i> cytotoxic activity of CTLs derived from mice immunised with the HAGE- and WT1-ImmunoBody® vaccines</b>	<b>205</b>
6.1 Introduction	205
6.1.1 T Cell-mediated cytotoxicity	205
6.1.2 Assays for monitoring cell-mediated cytotoxicity	207
6.2 Rationale of the chapter	208
6.3 Results:	210
6.3.1 Targets used in the cytotoxicity assay	210
6.3.2 Specific CTL activity against HAGE and WT1 peptide-pulsed T2 cells	211
6.3.3 Specific CTL activity against HHDII <sup>+</sup> /HAGE <sup>+</sup> and HHDII <sup>+</sup> /HAGE <sup>-</sup> K562 cells	216
6.3.4 Specific CTL activity against KCL-22 and TCC-S cells	221
6.3.5 Specific CTL activity against humanised B16 cells	226
6.3.6 Functional characterisation of CD8 <sup>+</sup> T cells from HAGE- and WT1-ImmunoBody® immunised animals	233
6.4 Discussion	238
6.5 Conclusion and chapter impacts	242
<b>7 Chapter-VII: The efficacy of HAGE/ WT1 ImmunoBody® combined regime as immunotherapeutic target in <i>in vivo</i> tumour models</b>	<b>243</b>
7.1 Introduction	243
7.1.1 Mouse cancer models in pre-clinical research	243
7.1.2 Generation of transgenic mice	245
7.1.3 Humanised mouse	247
7.2 Rationale of the chapter	250
7.3 Results	252
7.3.1 Profile of hB16/HAGE <sup>+</sup> /Luc <sup>+</sup> cells	252
7.3.2 Prophylactic and therapeutic efficacy of the combined HAGE/WT1 ImmunoBody® vaccines in HHDII/DR1 mice bearing the aggressive hB16/HAGE <sup>+</sup> /Luc <sup>+</sup> tumour	254
7.3.3 Capability of the combined HAGE/WT1 ImmunoBody® vaccines to provoke <i>in vivo</i> anti-tumour effector T cell function in HHDII/DR1 mice bearing hB16/HAGE <sup>+</sup> /Luc <sup>+</sup> tumour	260
7.3.4 Phenotypical characterisation of T cells and TILs from mice bearing hB16/HAGE <sup>+</sup> /Luc <sup>+</sup> tumour	265
7.4 Discussion	269
7.5 Conclusion and chapter impacts	273
<b>8 Chapter-VIII: Summary of discussion and recommendations</b>	<b>274</b>
8.1 Introduction	274
8.2 Validation of HAGE and WT1 as potential targets for immunotherapy	277
8.3 Immunogenicity of HAGE- and WT1 derived peptides	280
8.4 <i>in vitro</i> cytotoxic activity of HAGE- and WT1- specific CTLs	283
8.5 <i>in vivo</i> tumour challenge studies	285
8.6 Conclusion and future work	287
<b>9 Appendix</b>	<b>289</b>
<b>10 Bibliography</b>	<b>295</b>

# List of figures

<b>Figure 1.1: Schematic representation of haematopoiesis.</b> .....	2
<b>Figure 1.2: The translocation of t(9;22) (q34;q11) in CML creates various BCR-ABL1 variants.</b> .....	5
<b>Figure 1.3: Schematic representation depicts the diagnostic approaches of CML.</b> ...	6
<b>Figure 1.4: Balance between activating and inhibitory receptors expressed by the NK cells.</b> .....	9
<b>Figure 1.5: Effects of imatinib on various components of the anticancer immune-surveillance system.</b> .....	17
<b>Figure 1.6: Principle of CAR T cell therapy.</b> .....	23
<b>Figure 1.7: Schematic representation demonstrates the principle of immune checkpoint blockade therapy (anti-CTLA-4).</b> .....	26
<b>Figure 1.8: Schematic representation proposes that harness the synergistic interaction between targeted therapy and immunotherapy in CML leads to treatment-free remission</b> .....	33
<b>Figure 1.9: Schematic representation demonstrates DDX43 protein structure.</b> .....	34
<b>Figure 2.1: Schematic presentation of single ImmunoBody® immunisation regime</b> .....	65
<b>Figure 2.2: Schematic presentation of the combined HAGE- and WT1-ImmunoBody® vaccines regime</b> .....	65
<b>Figure 2.3: Scheme of the ELISpot procedure.</b> .....	66
<b>Figure 3.1: Oncogenic functions of some cancer testis antigens, which were described by Hanahan and Weinberg as the “Hallmarks of cancer”.</b> .....	80
<b>Figure 3.2: Targeting of C/T antigens in the current clinical settings.</b> .....	82
<b>Figure 3.3: HAGE expression in CML cell lines.</b> .....	87
<b>Figure 3.4: WT1 expression in CML cells lines.</b> .....	88
<b>Figure 3.5 HAGE expression in AML, AMoL and ALL cell lines.</b> .....	90
<b>Figure 3.6: WT1 expression in AML, AMoL and ALL cell lines.</b> .....	91
<b>Figure 3.7: HAGE expression in CML patients at mRNA level using RT-qPCR.</b> .....	94
<b>Figure 3.8: WT1 expression in CML patients at mRNA level using RT-qPCR.</b> .....	96
<b>Figure 3.9: A comparison of HAGE and WT1 expression in four pairs of CML patients at diagnosis and 12 months post-imatinib failure evaluated by RT-qPCR.</b> .....	97
<b>Figure 3.10: Validation of GUSB expression in seven AML at mRNA level using RT-qPCR technique.</b> .....	99
<b>Figure 3.11: HAGE expression in samples from patients with AML.</b> .....	100
<b>Figure 3.12: WT1 expression in samples from patients with AML.</b> .....	101
<b>Figure 3.13: β-actin expression in samples from patients with adult B-ALL.</b> .....	103
<b>Figure 3.14: HAGE expression in samples from patients with adult B-ALL.</b> .....	104
<b>Figure 3.15: Assessing WT1 expression in Adult B-ALL samples.</b> .....	105
<b>Figure 3.16: Expression patterns of C/T and WT1 genes in samples obtained from patients with AML and CML analysed from MILE study.</b> .....	112
<b>Figure 4.1: MHC class I and class II processing and presentation pathways.</b> .....	125
<b>Figure 4.2: Signal transduction required for the activation of naïve T cells.</b> .....	127
<b>Figure 4.3: Helios gene gun technique for delivering of ImmunoBody® DNA plasmid.</b> .....	132
<b>Figure 4.4: Dual mechanism of action of ImmunoBody® based vaccines.</b> .....	133

<b>Figure 4.5: Schematic vector maps demonstrate the design of WT1- and HAGE-ImmunoBody® DNA plasmids.</b> .....	135
<b>Figure 4.6: Position of the class I and class II HAGE peptides derived from the entire length of the HAGE protein.</b> .....	136
<b>Figure 4.7: Position of the long 15-mer and the short 9-mer WT1 peptides derived from the entire length of WT1 Isomer D.</b> .....	137
<b>Figure 4.8: Representative gating strategy used in T2 cell binding assay.</b> .....	139
<b>Figure 4.9: Affinity of class I WT1 and HAGE peptides to HLA-A2, as determined using the T2 binding assay</b> .....	141
<b>Figure 4.10 Time point analysis of class I HAGE and WT1 peptides binding stability to HLA-A2, as determined by brefeldin A decay assay using flow cytometer.</b> .....	143
<b>Figure 4.11: Frequency of HAGE-specific CTLs induced by the HAGE-ImmunoBody® vaccine, as determined using the IFN-<math>\gamma</math> ELISpot assay.</b> .....	145
<b>Figure 4.12: Frequency of WT1-specific CTLs induced by WT1 peptide/adjuvant immunisation, as determined using the IFN-<math>\gamma</math> ELISpot assay.</b> .....	146
<b>Figure 4.13: Frequency of WT1-specific CTLs induced by the ImmunoBody® vaccine, as determined using the IFN-<math>\gamma</math> ELISpot assay.</b> .....	147
<b>Figure 4.14: Frequency of immune response generated by WT1 peptide/adjuvant immunisation versus WT1-ImmunoBody® vaccine, as determined using the IFN-<math>\gamma</math> ELISpot assay.</b> .....	148
<b>Figure 4.15: Functional avidity of the immunogenic class I HAGE and WT1 peptides, as determined using peptide titration IFN-<math>\gamma</math> ELISpot assays.</b> .....	149
<b>Figure 4.16: Immune responses induced by different regimes of HAGE- and WT1-ImmunoBody® vaccines to evaluate HAGE immunogenicity, as assessed using the IFN-<math>\gamma</math> ELISpot assay.</b> .....	151
<b>Figure 4.17: Immune responses induced by different regimes of HAGE- and WT1-ImmunoBody® vaccines to evaluate WT1 immunogenicity, as assessed using the IFN-<math>\gamma</math> ELISpot assay.</b> .....	152
<b>Figure 4.18: Proliferation, cytokine production and degranulation of CTLs derived from mice immunised with ImmunoBody® vaccines, as determined using flow cytometry.</b> .....	154
<b>Figure 4.19: Representative gating strategy to determine upregulation in TNF-<math>\alpha</math>, IFN-<math>\gamma</math> and granzyme B expression by proliferating CTLs from mice immunised with the ImmunoBody® vaccines.</b> .....	155
<b>Figure 4.20: Fold change increase in TNF-<math>\alpha</math>, IFN-<math>\gamma</math> and granzyme B secretion from proliferating CTLs derived from mice immunised with ImmunoBody® vaccines, as determined using flow cytometry.</b> .....	155
<b>Figure 4.21: Representative gating strategy for characterising T cells induced by ImmunoBody® vaccines into naïve and memory T cells</b> .....	157
<b>Figure 4.22: Characterising T cells induced by ImmunoBody® vaccines into naïve and memory T cells using flow cytometry.</b> .....	158
<b>Figure 4.23: Representative gating strategy to assess the expression of markers of T cell activation and exhaustion.</b> .....	159
<b>Figure 4.24: Expression pattern of markers of T cell activation/exhaustion per CTLs derived from mice immunised with ImmunoBody® vaccines, as determined by flow cytometry.</b> .....	160
<b>Figure 5.1: Schematic representation depicts three phases of immunoediting process.</b> .....	170
<b>Figure 5.2: Immunomodulatory roles of IFN-<math>\gamma</math>.</b> .....	171
<b>Figure 5.3: Gene map of human HLA with especial emphasis of class I and class II molecules on chromosome 6.</b> .....	174
<b>Figure 5.4 The inhibitory role of IDO1 on the immune system.</b> .....	177

<b>Figure 5.5: Constitutive expression of HAGE and WT1 in target cells using RT-qPCR and Western blot.</b> .....	178
<b>Figure 5.6: Intracellular staining to detect WT1 expression in targets using flow cytometer.</b> .....	179
<b>Figure 5.7: Surface expression of HLA-A2 and HLA-DR1 on targets, as assessed by flow cytometer.</b> .....	180
<b>Figure 5.8: Transfection efficiency of HHDII<sup>+</sup> gene in K562 cells using lipofectamine reagent versus electroporation, as assessed by flow cytometry.</b> .....	181
<b>Figure 5.9: Gating strategy to determine HHDII expression by various HHDII<sup>+</sup> K562 clones.</b> .....	182
<b>Figure 5.10: Various levels of HHDII expression in randomly selected twelve HHDII<sup>+</sup>K562 clones, as assessed by flow cytometry.</b> .....	183
<b>Figure 5.11: Western blot analysis to assess HAGE transduction in K562/HHDII<sup>+</sup> cells.</b> .....	184
<b>Figure 5.12: Expressing of HAGE by different K562/HHDII<sup>+</sup>/HAGE<sup>+</sup> clones.</b> .....	185
<b>Figure 5.13 Immunofluorescence assay to determine the HAGE and WT1 proteins location in K562/HHDII<sup>+</sup>/HAGE<sup>+</sup> (Clone5).</b> .....	185
<b>Figure 5.14: HAGE transduction in KCL-22.</b> .....	186
<b>Figure 5.15: Knockdown of WT1 in TCC-S cells.</b> .....	187
<b>Figure 5.16: Stable genes expression by hB16/HAGE<sup>+</sup>/Luc<sup>+</sup> cells.</b> .....	188
<b>Figure 5.17: Constitutive WT1 expression by hB16/HAGE<sup>+</sup>/Luc<sup>+</sup> cells using IF and DAB immunochemical staining.</b> .....	189
<b>Figure 5.18: In vitro Optimisation of the hB16/HAGE<sup>+</sup>/Luc<sup>+</sup>cells bioluminescence.</b> .....	190
<b>Figure 5.19: CD119 constitutive expression on CML-derived target cells.</b> .....	191
<b>Figure 5.20: Upregulation of HLA-A, B, C and CD40 expression on CML-derived target cells after IFN-<math>\gamma</math> treatment.</b> .....	193
<b>Figure 5.21: Upregulation of HLA-E and HLA-G expression on CML-derived target cells after IFN-<math>\gamma</math> treatment.</b> .....	195
<b>Figure 5.22: Upregulation of PD-L1 expression on CML-derived target cells after IFN-<math>\gamma</math> treatment.</b> .....	196
<b>Figure 5.23: The effect of IFN-<math>\gamma</math> treatment on FasL expression by CML-derived target cells</b> .....	196
<b>Figure 5.24: The effect of IFN-<math>\gamma</math> on the expression of IDO1, WT1 and HAGE gene in TCC-S and K562 cells.</b> .....	198
<b>Figure 5.25: Kynurenine production upon induction of IDO by IFN-<math>\gamma</math>.</b> .....	199
<b>Figure 6.1: A workflow summarises cytotoxicity assays used in the present study.</b> .....	209
<b>Figure 6.2: Specific in vitro cytotoxicity induced by T cells derived from naïve mice against peptide pulsed/non-pulsed T2 cells, as assessed by the <sup>51</sup>Cr release assay.</b> .....	212
<b>Figure 6.3: Specific in vitro cytotoxicity induced by CTLs derived from ImmunoBody<sup>®</sup> immunised groups of mice against peptide pulsed/non-pulsed T2 cells, as assessed by the <sup>51</sup>Cr release assay.</b> .....	213
<b>Figure 6.4: IFN-<math>\gamma</math> response of CTLs produced by HAGE- and WT1-specific CTLs against peptides-pulsed T2 cells, as assessed using the IFN-<math>\gamma</math> ELISpot assay.</b> .....	215
<b>Figure 6.5: Specific in vitro cytotoxicity induced by CTLs derived from ImmunoBody<sup>®</sup> vaccinated groups of mice against K562 cells, as assessed using the <sup>51</sup>Cr release assay.</b> .....	217

<b>Figure 6.6: Specific in vitro cytotoxicity induced by the CTLs from ImmunoBody® immunised mice against the modified K562 “Clone5” cells, as assessed using the <sup>51</sup>Cr release assay.</b>	218
<b>Figure 6.7: IFN-γ secretion by HAGE- and WT1-specific CTLs in response to K562/HHDII<sup>+</sup> cells (with/without HAGE) cells, as assessed using the IFN-γ ELISpot assay.</b>	220
<b>Figure 6.8: Specific in vitro cytotoxicity induced by CTLs derived from ImmunoBody® immunised mice against KCL-22 cells (with/without HAGE), as assessed using the <sup>51</sup>Cr release assay.</b>	222
<b>Figure 6.9: Specific in vitro cytotoxicity of CTLs from ImmunoBody® immunised mice against KCL-22/HAGE<sup>+</sup> cells, as assessed using the <sup>51</sup>Cr release assay.</b>	223
<b>Figure 6.10: Specific in vitro cytotoxicity of CTLs from ImmunoBody® immunised mice against wild type and WT1-shRNA TCC-S cells, as assessed using the <sup>51</sup>Cr release assay.</b>	224
<b>Figure 6.11: Specific in vitro cytotoxicity of CTLs from ImmunoBody® immunised mice against the wild type TCC-S (HAGE<sup>+</sup>/WT1<sup>+</sup>) cells, as assessed using the <sup>51</sup>Cr release assay.</b>	225
<b>Figure 6.12: A comparative alignment between the murine and human WT1 protein sequences using “Align Sequences Protein BLAST” tool.</b>	227
<b>Figure 6.13: A comparison in the binding affinity scores between the murine and the human WT1 derived peptides toward HLA molecule, as determined using SYFPEITHI.</b>	228
<b>Figure 6.14: Specific in vitro cytotoxicity of CTLs derived from ImmunoBody® vaccinated mice against the hB16 cells, as assessed using the <sup>51</sup>Cr release assay.</b>	229
<b>Figure 6.15: Specific in vitro cytotoxicity of CTLs from ImmunoBody® immunised mice against the hB16/HAGE<sup>+</sup> cells, as assessed using the <sup>51</sup>Cr release assay.</b>	230
<b>Figure 6.16: Specific in vitro responses of CTLs from ImmunoBody® immunised mice against hB16/HAGE<sup>+</sup> cells (with/without HAGE), as assessed using the IFN-γ ELISpot assay.</b>	232
<b>Figure 6.17: Representative plate layout to assess responsiveness of CD8<sup>+</sup> T cells from ImmunoBody® immunised animals upon co-culture with targets.</b>	233
<b>Figure 6.18: Responsiveness of CD8<sup>+</sup> CTLs from immunised animals to peptide-pulsed/non-pulsed T2 cells.</b>	235
<b>Figure 6.19: Responsiveness of CD8<sup>+</sup> CTLs from immunised animals to HAGE<sup>+</sup>/WT1<sup>+</sup> (Clone5) and HAGE<sup>-</sup>/WT1<sup>+</sup> (Clone10) K562/HHDII<sup>+</sup> cells.</b>	237
<b>Figure 7.1: Various approaches for manufacturing transgenic mice.</b>	246
<b>Figure 7.2: Schematic representation of human (HLA) genes, mouse (H-2) MHC genes and the chimeric MHC (HHD) molecule.</b>	250
<b>Figure 7.3: Schematic representation of the in vivo experimental design.</b>	251
<b>Figure 7.4: In vivo kinetic optimisation of hB16/HAGE<sup>+</sup>/Luc<sup>+</sup> bioluminescence in naïve HHDII/DR1 mice.</b>	253
<b>Figure 7.5: Sequential real-time in vivo analysis of tumour burden in live animals, as assessed by Perkin Elmer IVIS Lumina III system.</b>	256
<b>Figure 7.6: Intra-tumoural luciferin bioluminescent signals in the vaccinated HHDII/DR1 mice bearing the aggressive hB16/HAGE<sup>+</sup>/Luc<sup>+</sup> tumour in comparison to the control.</b>	257
<b>Figure 7.7: Post-culled hB16/HAGE<sup>+</sup>/Luc<sup>+</sup> tumour weight and volume.</b>	258
<b>Figure 7.8: Survival analysis demonstrates the antitumor efficacy of the combined HAGE/WT1 ImmunoBody® vaccines in vaccinated tumour bearing mice.</b>	259
<b>Figure 7.9: Ex vivo IFN-γ ELISpot results of splenocytes derived from HHDII/DR1 tumour bearing mice vaccinated by the combined HAGE/WT1 ImmunoBody® vaccines.</b>	261

<b>Figure 7.10: Ex-vivo IFN-<math>\gamma</math> ELISpot assay of splenocytes processed from the last surviving tumour bearing mice assessed individually.....</b>	<b>262</b>
<b>Figure 7.11: IFN-<math>\gamma</math> secretion from splenocytes harvested from the last survivor tumour bearing mice, upon the recognition of the relevant targets, as assessed by ELISpot IFN-<math>\gamma</math> assay. ....</b>	<b>263</b>
<b>Figure 7.12: ICS of CTLs harvested from the last survivor tumour bearing mice in the prophylactic mice, induced by the HAGE/WT1 ImmunoBody<sup>®</sup> combined vaccines upon the recognition of the cognate peptides expressed by targets. ....</b>	<b>264</b>
<b>Figure 7.13: Gating strategy of splenocytes (A) and TILs (B) from immunised tumour bearing mice treated with HAGE/WT1-derived vaccine. ....</b>	<b>265</b>
<b>Figure 7.14: Overall T cells profile of spleens and TILs harvested from vaccinated and non-vaccinated tumour-bearing mice, as assessed by flow cytometry.....</b>	<b>266</b>
<b>Figure 7.15: T cell profile from fresh spleens <i>versus</i> TILs isolated from the last four survivor tumour bearing mice from the prophylactic group. ....</b>	<b>267</b>
<b>Figure 9.1: European LeukemiaNet recommendations for the management of CML: 2013.....</b>	<b>289</b>
<b>Figure 9.2: Representative density blot analysis to assess the purity of CD3<sup>+</sup> T cells before and after isolation using flow cytometer. ....</b>	<b>292</b>
<b>Figure 9.3: Spontaneous and maximum release of <sup>51</sup>Cr by targets. ....</b>	<b>292</b>
<b>Figure 9.4: Survival curve demonstrates prophylactic and therapeutic efficacy of the HAGE ImmunoBody<sup>®</sup> vaccines monotherapy in HHDII/DR1 mice bearing hB16/HAGE<sup>+</sup>/Luc<sup>+</sup> tumour. ....</b>	<b>293</b>
<b>Figure 9.5: Survival curve demonstrates the prophylactic and therapeutic efficacy of the WT1-ImmunoBody<sup>®</sup> vaccines monotherapy in HHDII/DR1 mice bearing hB16/HAGE<sup>+</sup>/Luc<sup>+</sup> tumour. ....</b>	<b>293</b>

# List of tables

<b>Table 2.1: Cell lines and media</b> .....	52
<b>Table 2.2: Doses of the selective markers to generate a stable transfection</b> .....	53
<b>Table 2.3: Cells and plasmids used in electroporation</b> .....	54
<b>Table 2.4: Cells transduced by PLenti.Puro plasmid</b> .....	55
<b>Table 2.5: Primary antibodies used in Western blot</b> .....	57
<b>Table 2.6: Secondary antibodies used in Western blot</b> .....	57
<b>Table 2.7: The primary antibodies used in Immunofluorescence assay</b> .....	58
<b>Table 2.8: The secondary antibodies used in Immunofluorescence assay</b> .....	58
<b>Table 2.9: Master mix preparation for cDNA synthesis</b> .....	60
<b>Table 2.10: Primers and annealing temperatures used for RT-qPCR</b> Error! Bookmark not defined.	
<b>Table 2.11: primary antibody used in the T2 binding/dissociation assay</b> .....	62
<b>Table 2.12: plasmids used and doses of the bacterial selective markers</b> .....	63
<b>Table 2.13A: A list of antibodies used in the single marker staining</b> .....	73
<b>Table 2.14: A panel of multicolour staining for murine cell surface staining</b> .....	74
<b>Table 2.15 : A panel of multicolour antibodies for the intracellular staining</b> .....	75
<b>Table 3.1: The pattern of C/T antigen expression in haematological malignancies</b>	81
<b>Table 3.2: CML samples studied</b> .....	93
<b>Table 3.3: AML and Adult B ALL samples studied</b> .....	98
<b>Table 3.4: Adult B-ALL samples studied</b> .....	102
<b>Table 4.1 The short HAGE peptides derived from the 30-mer sequence</b> .....	137
<b>Table 4.2: WT1 peptides derived from the 15-mer sequence</b> .....	138
<b>Table 4.3: Categorisation of the binding affinity of class I HAGE- and WT1-derived peptides toward HLA-A2 molecules, as assessed by T2 binding assay.</b> .....	140
<b>Table 5.5.1: Two shRNA sequences targeting WT1 gene.</b> .....	188
<b>Table 6.1: Summary information of targets used in the cytotoxicity assay</b> .....	210
<b>Table 9.1: Pattern of C/T and WT1 genes expression in CML samples analysed from MILE study</b> .....	290
<b>Table 9.2: Pattern of C/T and WT1 genes expression in AML samples analysed from MILE study</b> .....	291
<b>Table 9.3: Human WT1 protein isomers sequences</b> .....	294

# Abbreviations

<i>ABL1</i>	Abelson murine leukaemia
ACT	Adoptive cell transfer
AHR	Aryl Hydrocarbon Receptor
ALL	Acute lymphoblastic leukaemia
allo-HSCT	allogeneic hematopoietic stem cell
AML	Acute myeloid leukaemia
AMoL	Acute monocytic leukaemia
APCs	Antigen presenting cells
ATP	Adenosine triphosphate
ATRA	All-trans retinoic acid
AZA	AZAC 5'-aza-2'-deoxycytidine
BAGE	B Melanoma Antigen
<i>BCR</i>	Breakpoint cluster region
BFA	Brefeldin A
<i>BTK</i>	Bruton's tyrosine kinase
C/T	Cancer testis
CARs	Chimeric antigen receptors
CCyR	Complete cytogenetic response
CD	Cluster of differentiation
CDR	Complementarity determining region
CLL	Chronic lymphocytic leukaemia
CML	Chronic myeloid leukaemia
CPG	Cytosine triphosphate deoxynucleotide guanine
CRISPR	Clustered regularly interspaced short palindromic repeat system
CT45A	Cancer Testis 45A
CTAG1A	Cancer testis antigen 1B
CTLA-4	Cytotoxic T lymphocyte associated protein-4
DCs	Dendritic cells
DDX43	DEAD-Box Helicase 43
DLI	Donor lymphocyte infusion
DMR	Deep molecular response
DMSO	Dimethyl sulfoxide
DNA	Deoxyribonucleic acid
DNMTs	DNA methyltransferase enzymes
E:T ratio	Effector:Target ratio
ELISA	Enzyme-linked immunosorbent assay
ELISpot	Enzyme-linked immunospot
ELN	European LeukemiaNet recommendations
ER	Endoplasmic reticulum
FCR	FC receptor
FCS	Fetal calf serum
FDA	The Food and Drug Administration
FISH	Fluorescent in situ hybridisation
FITC	Fluorescein isothiocyanate
FoxP3	Forkhead box P3
FRI	Fluorescence intensity ratio
GAGE1	G Antigen 1
GDP	Guanidine diphosphate

GFP	Green-fluorescent protein 1
GIST	Gastrointestinal stromal tumours
GM-CSF	Granulocyte-macrophage colony-stimulating factor
GTP	Guanidine triphosphate
GvHD	Graft versus host disease
GvL	Graft versus leukemic effect
<sup>h</sup>	Humanised
HAGE	Helicase antigen
HKG	Housekeeping gene
HLA	Human leukocyte antigen
HSCs	Haematopoietic stem cells
hTERT	human telomerase reverse transcriptase
ICS	Intracellular cytokines staining
IDO	Indoleamine 2,3-dioxygenase 1
IFA	Incomplete Freund's adjuvant
IFN	Interferon
IFNGR1	Interferon gamma receptor 1
IL1RAP	IL1 receptor-associated protein
IS	International Scale
IVIS	In Vivo Imaging System
IVS	In vitro peptide re-stimulation
KIRs	Killer immunoglobulin-like receptors
LAAs	Leukaemic associated antigens
LAG3	Lymphocyte-activation gene 3
LILRB1	Leukocyte Immunoglobulin Like Receptor B1
LIR	Leukocyte Ig-like receptor
LPS	Lipopolysaccharides
LSCs	Leukaemic stem cells
Luc <sup>+</sup>	Luciferase reporter gene+
MAGE	Melanoma antigen gene
m-BCR	Minor cluster BCR
MDSCs	Myeloid-derived suppressor cells
MFI	Mean fluorescence intensity
MHC	Major histocompatibility complex
MICA	MHC class I chain-related genes A
MICB	MHC class I chain-related genes B
mm	Multiple myeloma
MMR	Major molecular response
MRD	Minimal residual disease
mRNA	Messenger ribonucleic acid
NK	Natural killer
NKG2D	NK cell activating receptor
NLS	Nuclear localization signal
NOD/SCID	Nonobese diabetic/severe combined immunodeficiency
NSG mice	NOD SCID Gamma mice
NY-ESO-1	New York Esophageal Squamous Cell Carcinoma 1
PCyR	Partial cytogenetic response
PD-1	Programmed death-1
PD-1L	programmed death ligand-1
PDGFR-β	Platelet-derived growth factor receptor-beta

PDX	Patient-derived xenograft
Ph	Philadelphia chromosome
PML-RARA	Promyelocytic leukaemia/retinoic acid receptor
PR3	proteinase-3
PRAME	Preferentially expressed antigen of melanoma
PTKs	Protein tyrosine kinases
RHAMM	Hyaluronan-mediated motility receptor
Rho-GEF	Rho guanidine nucleotide exchange factor
RMA	Robust multichip analysis
ROPN1	Rhopilin Associated Tail Protein 1
ROPN1	Rhopilin Associated Tail Protein 1 Like
RPM	Round per minute
RQ-MSP	Real-Time Quantitative Methylation-Specific PCR
RTCA	Real Time Cell Analysis
RTqPCR	Real time qPCR
SCID	Severe combined immunodeficiency
SEMG1	Semenogelin-1 antigen
sgRNA	Single guide RNA
shRNA	Small hairpin RNA
SPA17	Sperm Autoantigenic Protein 17
SSX	Synovial sarcoma X chromosome
STIM	Stop Imatinib
SYCP1	Synaptonemal complex protein-1
TAA	Tumour associated antigens
TAMs	Tumour-associated macrophages.
Tcm	Central memory T cell
TCR	T cell receptor
Tem	Effector memory T cell
TFR	Treatment free remission
TGF- $\beta$ 1	Transforming growth factor beta
Th-1	T helper 1
Th-2	T helper 2
TILs	Tumour-infiltrating lymphocytes
Tim-3	T cell immunoglobulin mucin-3
TKIs	Tyrosine kinase inhibitors
TMEFF2	Transmembrane Protein with EGF Like and Two Follistatin Like Domains 2
TNF	Tumour necrosis factor
Tregs	T regulatory cells
TSA	Tumour specific antigen
VEGF	Vascular endothelial growth factor
WT1	Wilm's tumour
WBCs	White blood cells
$\beta$ 2m	Beta 2 microglobulin
$\mu$ -BCR	micro cluster BCR
<i>Rag1<sup>null</sup>/Rag2<sup>null</sup></i>	Recombination activating genes 1 and 2
<sup>51</sup> Cr	<sup>51</sup> Chromium

# Abstract

Chronic myeloid leukaemia (CML) is a clonal myeloproliferative disorder resulting from a malignant transformation of the primitive HSCs. The disease is characterised by the breaking and re-assembling of chromosomes 9 and 22 t(9;22)(q34;q11) and the formation of a fusion gene called *BCR-ABL1* and its chimeric oncogenic protein (p210) which results in a permanent activation of tyrosine kinase (TK) enzyme. The clinical outcome of CML has significantly improved since the discovery of tyrosine kinase inhibitors (TKIs); however, they are not curative, and resistance against these therapies could develop at any phase of the disease. The molecular characteristic of CML pathology, the nature of cancerous-host immune cells interaction, in addition to the beneficial immunomodulatory role of the TKI therapy, would all offer "in theory" an excellent opportunity to combine TKIs with immunotherapeutic strategies. The cancer testis antigen DDX43 (HAGE) and the oncogene Wilms' tumour (WT1) antigens have previously been shown to be immunogenic and overexpressed in CML at mRNA level at 57-71% and 50-100%, respectively. With the aim to help patients who are on imatinib therapy to achieve a "definitive cure" by eliminating residual CML cells, patients who developed resistance to imatinib at any phase of the disease, and patients who are in blast crisis and not eligible to allo-HSCT, it was, therefore, hypothesised that a combination of HAGE and WT1 vaccines will be more effective against established CML tumours expressing both antigens than a vaccine incorporating peptides derived from either of these antigens alone.

This project investigated the use of HAGE- and WT1-derived ImmunBody® vaccines, alone and together in generating vaccine specific release of cytokines and in specifically killing target cells expressing the relevant antigens and HLA-A haplotype by the vaccine induced T cells. In order to achieve this, HHDII/DR1 mice were immunised with HAGE- and/or WT1-ImmunoBody® bullets of DNA vaccines in a prime-boost regime in two different flanks using gene gun technology. The immune responses generated against these two antigens were then assessed by measuring the number of IFN- $\gamma$  producing cells using ELISpot assay, cytokines released by flow cytometry and killing against specific targets using Chromium release assay. A number of CML-derived targets were genetically modified to either express or suppress the expression of HAGE/WT1 proteins, and the success of these modifications was confirmed by RT-qPCR and Western blot assays. Results showed that while both vaccines were independently capable of inducing the release of IFN- $\gamma$  in a high proportion of vaccine-induced cells and provoking substantial cell-mediated killing, the combined vaccines approach was able to induce a significantly higher number of CD8<sup>+</sup> T cells producing TNF- $\alpha$  and a significantly higher percentage of target cell death in comparison with the individual vaccines.

More importantly, in tumour challenges models, "humanised" B16 (HAGE<sup>+</sup>/WT1<sup>+</sup>) cells transplanted subcutaneously were employed as a "proof-of-concept" to demonstrate *in vivo* vaccine efficacy. The combination of HAGE/WT1 ImmunBody® vaccines was shown to significantly delay tumour growth and prolong mice survival in a prophylactic setting in comparison to mice that had not received the vaccines or even mice that had received only one of the vaccines. Overall, this work has demonstrated the significant value of combining both HAGE- and WT1-ImmunoBody® vaccines for treating patients harbouring HAGE<sup>+</sup>/WT<sup>+</sup> cancerous cells.



# 1 Chapter I: Main introduction

## 1.1 Chronic myeloid leukaemia (CML)

### 1.1.1 Haematopoietic and leukaemic hierarchy

Haematopoiesis is an essential multistep cellular process by which all blood cells are hierarchically produced from single pluripotent stem cells with self-renewal capacity called "haematopoietic stem cells" (HSCs) (Prosper, Verfaillie 2001). Self-renewal is defined as the ability of a cell to proliferate while completely preserving the differentiation potential of the parental cells, a unique feature shared by all kinds of stem cells. In the bone marrow milieu, HSCs differentiate into two main progenitor lineages in response to cytokines/growth factors and other microenvironmental stimuli: the common myeloid and the common lymphoid progenitors (Figure 1.1). The lymphoid progenitor proliferates and differentiates into T-lymphocyte, B-lymphocyte, and natural killer (NK) cells, whereas the myeloid progenitor differentiates into granulocyte, monocyte, erythrocyte, and megakaryocyte lineages (Kondo, Wagers *et al.* 2003, Weissman 2000). Another blood cell type, dendritic cells (DCs), is not clearly grouped under either myeloid or lymphoid lineage, since it can originally arise from either common lymphoid progenitors or common myeloid progenitors (Manz, Traver *et al.* 2001, Traver, Akashi *et al.* 2000).

Leukaemia is a cancer of the blood which affects white blood cells, and bone marrow. In leukaemia, leukaemic stem cells" (LSCs), are responsible for the initiation, maintenance and differentiation into more specific cell subtypes and can affect either of the lineages mentioned above (Riether, Schürch *et al.* 2015). Leukaemias are mainly classified into acute and chronic leukaemia. In the acute type, a rapid accumulation of the immature white blood cells (WBCs) occurs, whereas in the chronic type, an excessive build-up of relatively mature WBC happens. It is also classified into either myeloid or lymphoid, depending on the cell lineage that they developed from. Hence, the four main types of leukaemia are: acute lymphoblastic leukaemia (ALL), acute myeloid leukaemia (AML), chronic lymphocytic leukaemia (CLL) and chronic myeloid leukaemia (CML).

This project is particularly interested in the applicability of a T cell-based vaccine for the treatment of CML targeting specific tumour antigens, HAGE and WT1. Therefore, the first part of the introduction will explore mainly CML pathophysiology and onco-immunology drivers in CML aiming to obtain more comprehensive knowledge for how vaccines could interrupt the disease process. The second section will review the immunotherapeutic advancement in the treatment of haematological cancer with a special emphasis on CML.

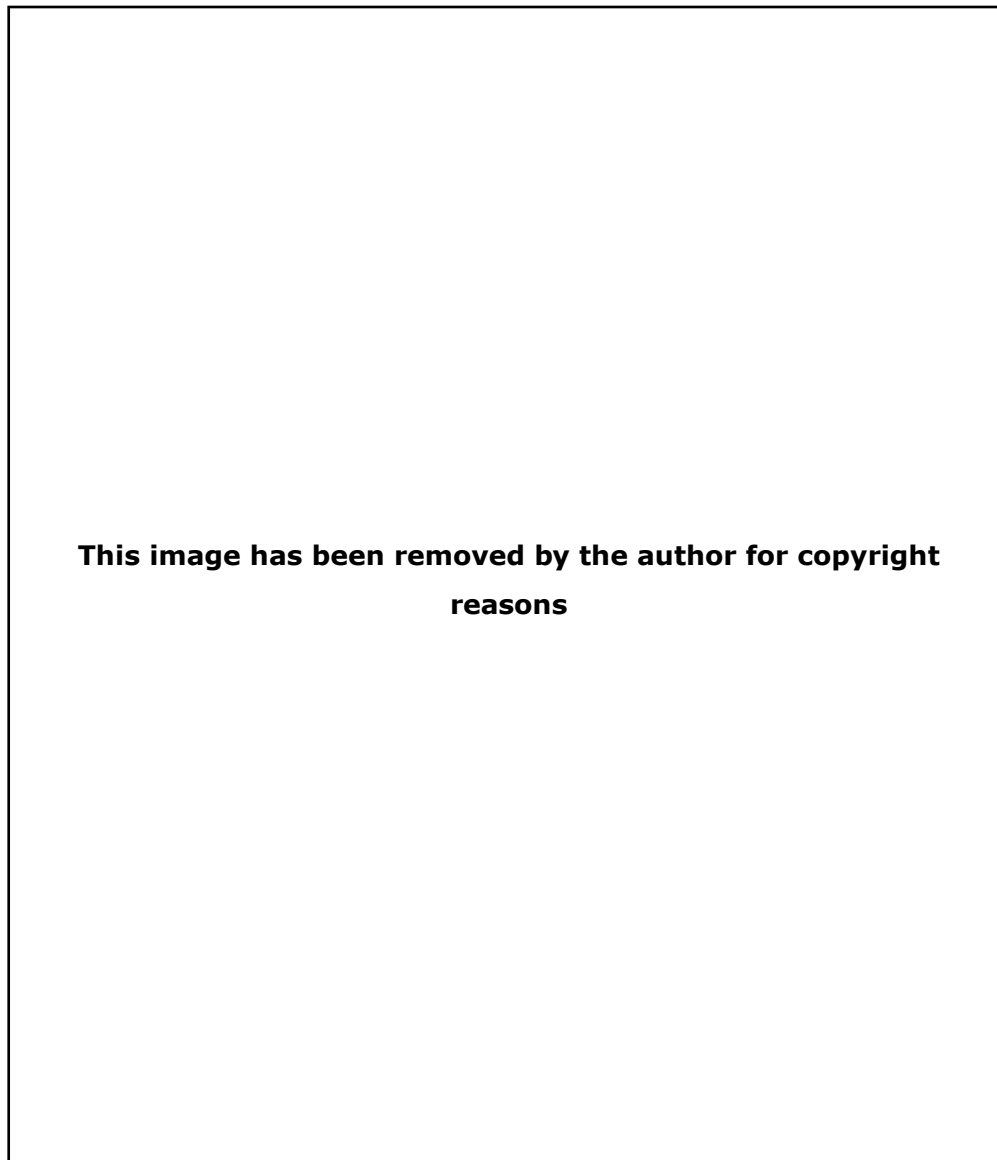


**Figure 1.1: Schematic representation of haematopoiesis.**

The figure demonstrates that all blood cells are hierarchically originated from pluripotent haemopoietic stem cells in the medulla of the bone marrow, which divided to give rise common myeloid and common lymphoid progenitors. The myeloid and lymphoid progenitors are then divided to produce various mature precursors that circulate in blood to produce various functions, however some of these cells take their way to residence tissues where they acquire different functional characterisation. Figure is reused from (Rodak and Carr 2015).

### 1.1.2 Definition, epidemiology and risk factors of CML

CML is a clonal myeloproliferative disorder resulting from a malignant transformation of the primitive HSCs into LSCs which then gives rise CML (Holyoake, Vetrie 2017). The disease is monoclonal in origin and affects myeloid lineage, in particular the granulocytes (neutrophils, basophils and eosinophils), wherein, a distinctive increase in the count of these cells can be identified in the bone marrow and peripheral blood of CML patients.

Annually, CML affects nearly 1 to 2 individuals per 100 000 population with a slight male to female predominance, which makes it account for 15% of all newly reported cases of leukaemias in the Western hemisphere (Apperley, Jane F. 2015).

CML is a disease of older people at age close to 60–65 years, with no obvious specific ethnic or geographical distribution (Baccarani, Pileri *et al.* 2012), however, exposure to a high level of ionising radiation seems to be a risk factor in CML development in accordance to what has been found post Hiroshima and Nagasaki nuclear bombing survivors health records (Hehlmann, Rüdiger, Hochhaus *et al.* 2007).

### 1.1.3 CML pathophysiology and molecular driving events

The primary pathological characterisation of the disease was discovered in 1960 by Peter Nowell and David Hungerford in Philadelphia/Pennsylvania, when an abnormally short chromosome, called later the “*BCR-ABL1* gene” or “Philadelphia chromosome” was found to be a constantly associated with CML samples (Nowell, Hungerford 1960). This was regarded as a breakthrough in cancer biology, since it was the first chromosomal aberration that demonstrated a consistent association with a particular type of leukaemia. Thirteen years later (when techniques of DNA study were developed), Philadelphia chromosome was found to be formed by a reciprocal translocation between chromosomes 9 and 22. In the 1980s, it was discovered that the fusion gene was formed as a result of reciprocal translocation of the Abelson murine leukaemia (*ABL1*) gene located on chromosome 9 with the breakpoint cluster region (*BCR*) gene located on chromosome 22, a mutation known as  $t(9;22)(q34;q11)$  (Heisterkamp, Groffen *et al.* 1982). About 10 years later, Daley and colleagues established CML disease at first time in a murine model (Daley, Van Etten *et al.* 1990). The  $t(9;22)(q34;q11)$  cytogenetic aberration is found virtually in all cases of CML at more than 95% and one third of adult ALL (Zitvogel, Laurence, Galluzzi *et al.* 2013, de Klein, van Kessel *et al.* 1982).

The protooncogenic *c-ABL* gene is the human homologue of the *v-abl* oncogene which is carried by the Abelson murine leukaemia virus (Abelson, Rabstein 1970), and it

encodes a non-receptor tyrosine kinase (Laneuville 1995). Structurally, the *ABL* gene encodes a protein containing several domains, three Src homology domains located toward the N-terminus; a tyrosine kinase activity domain (SH1) and two regulatory domains (SH2 and SH3), by which a protein-protein interaction is mediated. In the central part of the protein, numerous proline-rich regions are found which can combine the SH3 domains of other proteins. It also harbours nuclear localisation signals (NLS) which provide a shuttling function of ABL protein between nucleus and cytoplasm (Pane, Intrieri *et al.* 2002). The C-terminus contains DNA as well as actin binding motifs (Van Etten, Jackson *et al.* 1989, Kipreos, Wang 1992, McWhirter, John R., Wang 1993).

The fusion partner, the *BCR* protein, is characterised by the presence of numerous functional domains, including a serine–threonine kinase at the N-terminus, wherein, a coiled–coil domain allows dimer formation *in vivo* (McWhirter, J. R., Galasso *et al.* 1993). A region homologous to Rho guanine nucleotide exchange factors (Rho-GEF) that stimulate the exchange of guanine triphosphate (GTP) for guanine diphosphate (GDP) on Rho guanine exchange factors is found at the centre of the protein (Denhardt 1996). A site for calcium-dependent lipid binding (CaLB) and a domain with activating function for Rac-GTPase (Rac-GAP) are situated at the C-terminus (Diekmann, Brill *et al.* 1991).

In CML, each of the two genes are dislocated at a particular breakpoint and join to form the chimeric *BCR-ABL1* gene (Faderl, Talpaz *et al.* 1999). The most frequent rearrangements formed are the b2a2 or b3a2 transcripts, which in turn, are translated into a P210 kDa protein. However, breakpoints can occur in other region of the *BCR* gene; called minor cluster (m-*BCR*) or micro ( $\mu$ ) cluster ( $\mu$ -*BCR*) regions resulting in transcripts that encode either smaller (190 kDa) or larger (230 kDa) proteins, respectively, (Figure 1.2). In any of *BCR-ABL1* variants, the *ABL* tyrosine kinase domain is constitutively activated as a result of oligomerisation of the coiled coil region of p210 *BCR-ABL1* (McWhirter, J. R., Galasso *et al.* 1993), and removal of the inhibitory SH3 domain of *ABL* (Muller, Young *et al.* 1991). The deregulated *BCR-ABL1* tyrosine kinase activity is indeed responsible for the transformation of the HSC and conservation of the leukaemic phenotype. The mechanisms underpinning leukaemogenesis in CML are well-documented, and include a constitutive activation of mitogenic signalling, decreased apoptosis, changed cellular adhesion to stromal cells and extracellular matrix, and proteasome-mediated degradation of *ABL* inhibitory proteins. These processes happen via phosphorylation and activation of various downstream signalling pathways, such as *RAS* and *MAP* kinase pathway, *Jak-stat* pathway, *Myc* pathway, *RAF* and *JUN* kinase (Bennour, Saad *et al.* 2016).

The CML leukaemic clone is prone to acquire additional oncogenic mutations, which usually lead to disease progression into the terminal stages or resistance to tyrosine kinase inhibitors (TKIs). It has been estimated that mutations in the kinase domain

of *BCR-ABL1* accompany around 50% of imatinib resistance in the chronic phase, and 80% of the advanced phases (O'hare, Zabriskie *et al.* 2012).

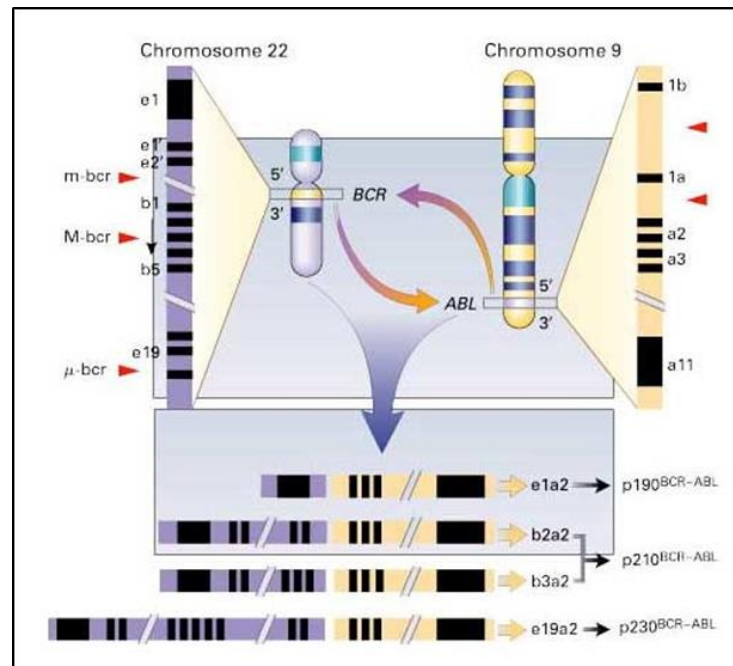


**Figure 1.2: The translocation of t(9;22) (q34;q11) in CML creates various *BCR-ABL1* variants.**

The Philadelphia chromosome corresponds to a shortened chromosome 22 form by a reciprocal translocation between 3' *ABL* segments (toward the telomere) on chromosome 9 and 5' *BCR* segments on chromosome 22. The breakpoints on *ABL* gene occur mainly at exon *a2*, whereas various breakpoint sites along the *BCR* gene on chromosome 22 were identified, thereby different-sized segments derived from *BCR* gene are joined with the *ABL* gene segment, producing different length RNA transcripts (*e1a2*, *b2a2*, *b3a2*, and *e19a2*). These products are then translated into chimeric proteins (*p190*, *p210*, and *p230*) with variable size and presumably variable activities. The abbreviation *m-bcr* refers to minor breakpoint cluster region, *M-bcr* refers to major breakpoint cluster region, and  $\mu$ -*bcr* to micro breakpoint. The image is reused with a reference from (Faderl, *et al.* 1999).

### 1.1.4 CML management: Diagnosis and therapy

The clinical course of CML disease is characterised by two or three phases. Firstly, a prolonged relatively stable phase called "chronic phase"; wherein most patients are in this phase when they are first diagnosed with CML. Patients in this phase are usually asymptomatic and they are either diagnosed by accident or due to simple complaints. However, without effective therapeutic interventions, the disease might progress through a period of a short but rapid instable phase known as "acceleration phase", in which patients fail to respond to therapies due to the increase in the percentage of the blast cells and/or associated mutations, to a critically terminal phase called "blast crisis", wherein the disease progressed rapidly to an acute leukaemia-like illness. Many definitions have been used to identify these stages, but according to the European LeukaemiaNet recommendations (ELN) for managing of CML disease updated in 2013 (the most reliable recommendations has been used in the clinical trials), accelerated phase is defined by the presence of one or more of the

following finding: <15-29% blasts in the peripheral blood or bone marrow,  $\geq 20\%$  basophils in the peripheral blood, and platelets  $< 100 \times 10^6/L$  unrelated to treatment, whereas the blast phase is identified by an increase in blast cells  $\geq 30\%$  in the peripheral blood or bone marrow, or the occurrence of extramedullary blast proliferation apart from spleen (Baccarani, Saglio *et al.* 2006, Baccarani, Cortes *et al.* 2009).

The presence of *BCR-ABL1* gene in almost all cases of CML, interestingly, leads to two clinically important consequences. Firstly, the *BCR-ABL1* gene provides a CML-specific biomarker for the CML diagnosis and follow-up, and secondly, the oncogenic protein tyrosine kinase being a sensitive target to the therapeutic interventions particularly TKIs.

The clinical suspicion of CML dictates several lab investigations, of which, complete blood count and morphological white blood cell differential are the most basic initial investigations. The blood cell picture should show a typical left sided- shift of the myeloid lineages with the detection of immature myelocytes and metamyelocytes, of eosinophilic and basophilic types. Secondly, bone marrow aspirate for cell count and differential can provide percentages of blasts, promyelocytes and myelocytes. Thirdly, traditional cytogenetics and karyotyping by G-banding with and without fluorescent in situ hybridisation (FISH) to identify chromosomal abnormalities and identify the t(9;22) translocation. Finally, RT-qPCR for *BCR-ABL1* mRNA transcripts detection which represents the most sensitive and prognostic test (Apperley, Jane F. 2015). Summary of these approaches is illustrated in Figure 1.3.

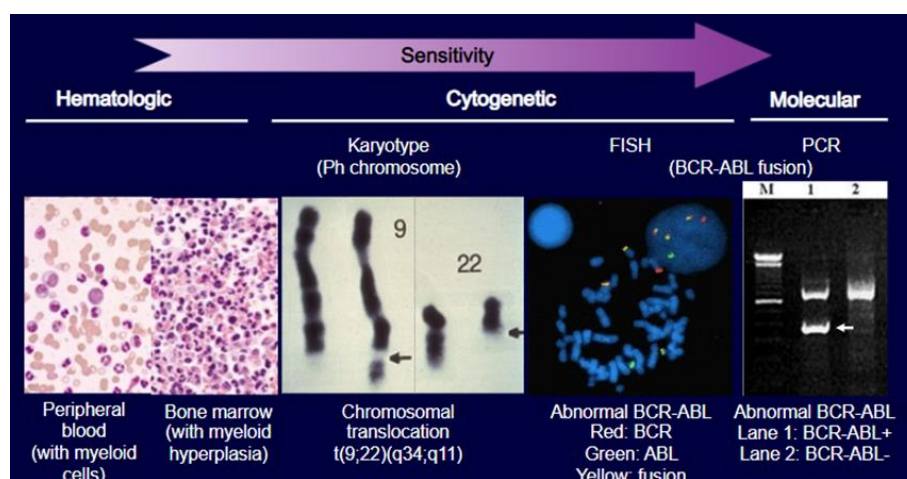


**Figure 1.3: Schematic representation depicts the diagnostic approaches of CML.**

Different approaches have been clinically implemented to diagnose patients with CML disease; Firstly, bone marrow aspirate shows a picture of hypercellularity and a significant myeloid hyperplasia. Secondly, traditional cytogenetics and karyotyping by G-banding to identify the t(9;22) translocation, supported by fluorescent in situ hybridisation (FISH) to detect *BCR* and *ABL1* genes fusion using specific markers. Finally, detection of *BCR-ABL1* transcripts using molecular techniques such as RT-qPCR. Permission to reuse this image was obtained with a reference to: Providing Optimal Care for Patients With Chronic Myeloid Leukemia. Clinical Care Options, LLC; Reston, Virginia, USA. Accessed 26 February, 2020, at: <https://www.clinicaloptions.com/oncology/programs/managing-cml/interactive-virtual-presentation>.

In terms of therapeutic intervention, until 2000, the therapeutic armamentarium for CML was limited to non-targeted chemotherapeutic agents, such as busulfan, hydroxyurea, and interferon-alpha (IFN- $\alpha$ ). While IFN- $\alpha$  led to regression of the disease and improvement in the survival rate, it was hindered by its modest efficacy and cytotoxicity. Allogeneic stem cell transplantation (allo-SCT) is the only curative strategy, but it carries the disadvantage of high rates of morbidity and mortality. In addition, allo-SCT is suitable only for patients who are generally well-health and have stable organ function (Jabbour, Elias, Kantarjian 2018).

After 2000, and upon the advent of "targeted therapy" with TKIs, the therapeutic landscape of CML has been substantially changed. These molecules competitively block the phosphorylation site of *BCR-ABL1* tyrosine kinase, thereby "switching-off" the downstream signalling pathways that promote leukaemogenesis. TKI therapy has indeed transformed the natural history of CML, improving the 10 year survival rate from nearly 20% up to 90% (Huang, X., Cortes *et al.* 2012, Deininger, Michael, O'Brien *et al.* 2009). During the course of the therapy, clinical response to the treatment is routinely evaluated by monitoring the count of white blood cells in the peripheral blood, and specifically by the quantification of *BCR-ABL1* transcripts against a reference gene (Cortes, J., Kantarjian 2012).

In 2013, the ELN expert panel updated recommendations that were made in 2009, wherein, imatinib, nilotinib, or dasatinib are recommended as initial first-line treatment. The response should be then assessed by RT-qPCR (molecular response) and/or cytogenetics analysis (cytogenetic response) at 3, 6, and 12 month post-treatment. The response is regarded as "optimal" if *BCR-ABL1* transcript levels assessed by PCR are  $\leq 10\%$  at 3 months,  $< 1\%$  at 6 months, and  $\leq 0.1\%$  from 12 months, whereas "failure" is defined if the transcripts are  $> 10\%$  at 6 months and  $> 1\%$  from 12 months, which would prompt a change in the treatment regime. In the same manner, "optimal response" can be determined by cytogenetic analysis where partial cytogenetic response (PCyR) at 3 months and complete cytogenetic response (CCyR) from 6 months are achieved, but "failure" defined when there is no CyR which means that Philadelphia stays positive  $> 95\%$  at 3 months, less than PCyR at 6 months, and less than CCyR from 12 months. The panel recommended that patient who achieved optimal response should remain on the therapy indefinitely. "Warning" is an intermediate degree of response between optimal and failure responses, where a strict monitoring is indicated. In this update, definitions are also provided to determine a response to second-line treatment, and particular recommendations for patients in the accelerated and blast phases are made, and also for allo-SCT. Details of the disease management, criteria for response (optimal, warning and failure), and time for cytogenetic and molecular ministering provided by the ELN-2013 are all attached in the appendix (Figure 9.1).

The molecular response is best weighed on the International Scale (IS) by finding the ratio between *BCR-ABL1* and *ABL1* transcripts. It is expressed as *BCR-ABL1*% on a log scale, wherein a 10%, 1%, 0.1%, 0.01%, 0.0032%, and 0.001% correspond to a reduction of 1, 2, 3, 4, 4.5, and 5 logs, respectively (Baccarani, Cortes *et al.* 2009, Cross, White *et al.* 2012).

Therefore, the major goal of the treatment in CML is to bring the molecular events into optimal response level, as this could improve patient survival. The optimal molecular response refers to an achievement of *BCR-ABL1* transcript levels at  $\leq 0.1\%$  at specific timepoints called "major molecular response" or shortly (MMR) (Baccarani, Deininger *et al.* 2013). However, the more recent aim in the treatment of CML is to obtain a state of a durable deep molecular response (DMR), wherein *BCR-ABL1* level at  $\leq 0.01\%$ , as this is a prelude to successful treatment free remission (TFR), which has been reported to occur in about 50% of all CML patients who stop TKI drug (Saussele, Richter *et al.* 2016). However, cessation of imatinib in chronic phase patients who achieve CCyR and MMR response for more than 2 years frequently leads to disease relapse but TFR seems to be more durable and frequent in patients who achieved deeper molecular responses (Mahon, Réa *et al.* 2010).

### **1.1.5 Immune dysregulation in the newly diagnosed CML**

The state of persistent immune dysfunction in CML patient at the time of diagnosis has been well-understood, precluding the development of efficient anti-leukaemic responses and enhancing disease progression unless efficacious TKIs are introduced. It has been found that most patients, at around 90%, are diagnosed with CML while they are at the chronic phase, which is characterized by abundant circulating functionally impaired myeloid cells, that are mainly produced and maintained by a small subset of LSCs (Nievergall, Ramshaw *et al.* 2014). Cells of both innate and adaptive immune responses (NK cells, CD8<sup>+</sup> and CD4<sup>+</sup> T cells), effector molecules, as well as intracellular signalling pathways exert indeed a sophisticated networking system to provide anti-cancerous response (Corthay 2014). However, cancer almost enables its self-protection and expansion by overwhelming the immune system through various means, such as; recruitment of immunosuppressive cells, release of immunosuppressive factors, and promoting of immune checkpoint pathways (Stevens, Netea *et al.* 2016, Shi, Chen *et al.* 2013). Understanding the immune imbalance in CML patients at the time of presentation is crucial for the development of new therapeutic strategies to enhance anti-tumour immune function and augment TFR success rates following TKI withdrawal. Therefore, aspect of immune dysfunction in CML will be covered in the following sections.

### 1.1.5.1 Effector cells dysfunction in pre-treated CML patients

The main cells of anti-tumour responses (NK cells, DCs and CTLs) are found to be severely impaired in CML.

NK cells are an important population of lymphocytes, characterised by the absence of antigen receptors like those found on T and B lymphocytes (Trinchieri 1989). These cells are able indeed to identify and kill stressed cells (tumour or virally infected cells) spontaneously without prior sensitisation, in a process termed "natural cytotoxicity" (Gismondi, Stabile *et al.* 2015, Herberman, Nunn *et al.* 1975). The activation of NK cells interestingly does not necessitate target cell expression of the major histocompatibility complex (MHC) class I molecules (Ljunggren, Karre 1990). In contrast, the MHC class I molecules expression defends targets from NK cells attack, suggesting that NK cells might be chronically inactivated and stimulated by the absence of 'self' epitopes, but T cells are, in contrast, triggered by the recognition of 'foreign' epitopes. This process gave rise to the "missing-self hypothesis" (Karre, Ljunggren *et al.* 1986), which postulates that NK cells constantly screen tissues for expressing normal level of MHC class I molecules, and accordingly they preferentially kill ones that displayed no/low/aberrant MHC class I.

The detection system of the NK cells includes an array of receptors that allow the identification of their targets while sparing normal cells, including activating, inhibitory, adhesion and cytokine receptors. The engagement of which determines indeed the intensity of the NK cell response (Vivier, Ugolini *et al.* 2012), balance between these signals is briefly described in Figure 1.4 below, where, MHC class I-specific inhibitory receptors, according to "missing-self hypothesis", provide means for NK cells to stay tolerant to the normal self-cells (healthy cells) while being lethal for stressed cells (virally infected or malignant cells) upon releasing of the stress signals detected by the NK cell activating receptors.

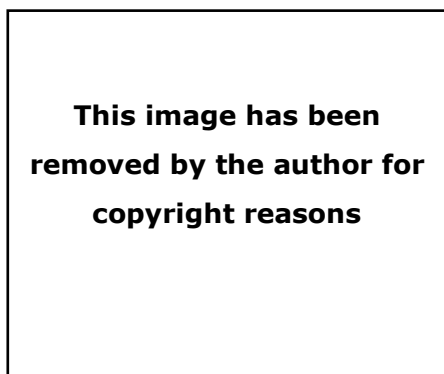


**Figure 1.4: Balance between activating and inhibitory receptors expressed by the NK cells.**

The inhibitory receptors (inhibitory killer immunoglobulin-like receptors (KIRs), leukocyte Ig-like receptor (LIR), and CD94/NKG2A) engaged with MHC class I molecules providing protection to autologous targets from NK killing whereas the activating receptors, natural cytotoxicity receptors (NKp30, NKp44, and NKp46), NKG2D, and DNAM-1 bind the ligands on target cells and trigger the NK cells toward cytotoxicity. Figure is reused from (Stagg and Galipeau 2007).

Technically, two distinct subsets of human NK cells have been identified depending on cell density of the surface marker CD56, wherein the majority (~90%) express

low level of CD56<sup>dim</sup> but express high levels of FcγRIII (CD16), and a minority (10%) express high levels of CD56<sup>bright</sup> but not or low levels of CD16<sup>dim/neg</sup> (Lanier, Le *et al.* 1986). NK cells are an essential element of the innate immunity, providing a front-line defence against tumour cells by exerting a powerful cellular cytotoxicity against cancerous cells (CD56<sup>dim</sup> NK cell subset) and produce immunoregulatory cytokines and chemokines, such as interferon gamma (IFN- $\gamma$ ) and tumour necrosis factor alpha (TNF- $\alpha$ ), supporting the development of the adaptive immunity (CD56<sup>bright</sup> NK cell subset).

In pre-treated CML patients, many reports have demonstrated various NK cell abnormalities and NK cell count reduction among other lymphocytes, which worsen during the blast crisis phase (Mellqvist, Hansson *et al.* 2000, Chen, C. I., Koschmieder *et al.* 2012, Pierson, Miller 1996). In addition, Boissel *et al.*, found a reduction in the expression of NKG2D-activating receptor in CML samples at diagnosis, promoting leukaemic cell immune escape (Boissel, Rea *et al.* 2006). Moreover, a recent study conducted by Hughes, *et al.*, 2017 revealed a reduction in three members of the NKG2 family of C-type lectin receptors expression, including CD94/NKG2A, CD94/NKG2C, and NKG2D (Hughes, Clarkson *et al.* 2017). In a similar pattern, the expression of natural cytotoxicity receptors NKp30 and NKp46 were previously reported for being impaired in CML pre-treatment cases in comparison to healthy donors (Sivori, Pende *et al.* 1999).

Another essential type of cells responsible for the activation of the anti-tumour immune response are the antigen presenting cell, especially dendritic cells (DCs). DCs trigger a potent activity of the naïve T cells and play a vital function in the initiation and regulation of the adaptive immune response (Ginhoux, Guilliams *et al.* 2016). DCs process antigens into short peptides and present them to CD4<sup>+</sup> and CD8<sup>+</sup> T cells in association with MHC class II and I molecules respectively, thereby initiating antigen-specific immune responses or immunological tolerance (Poltorak, Schraml 2015). Quantitative and functional impairments, such as non-efficient peptide presentation, have been described in a DC subset from CML patients (Mohty, Isnardon *et al.* 2002, Mohty, Jarrossay *et al.* 2001).

Interestingly, antigen-specific CTLs circulating in the peripheral blood of CML patient in chronic phase have been identified against *BCR-ABL1*, Wilms' tumour antigen 1 (WT1) and proteinase-3 (PR3), indicating the probable involvement of these CTLs in the immunological control of CML (Li, Y., Lin *et al.* 2012, Molldrem, Lee *et al.* 2000, Butt, Rojas *et al.* 2005). Studies, however have revealed functional impairment of T cells derived from pre-treated CML patients, these exhibit reduced TCR $\zeta$ -chain expression, lower cytotoxic activity, and limited immunoregulatory cytokines production, such as TNF- $\alpha$  or IFN- $\gamma$  (Chen, S., Yang *et al.* 2009, Li, Y., Geng *et al.* 2011, Zha, Yan *et al.* 2012). TCR $\zeta$ -chain expression is essential for proper T cell

function, such as T cell proliferation and IFN- $\gamma$  secretion (Baniyash 2004). Adding to that, the adhesion L-selectin molecule (CD62L) was found to be downregulated in CML patients at diagnosis (Sopper, Mustjoki *et al.* 2017), this could be another reason for effector CTL immune responses impairment, as CD62L is important in governing the traffic of T cells to the secondary lymphoid tissues and priming by APCs.

The antibody-secreting effector B cells, plasma cells, also protect the host by distinct B cell subsets mediating various kinds of antibody responses (Shapiro-Shelef, Calame 2005). While de Lavallade *et al.* previously found that CML patients at the time of diagnosis have a reduced number of memory B cell subsets (de Lavallade, *et al.* 2013), their clinical influence is not yet fully understood, since there have been no report of patients experiencing repeated infections despite the lack of B cells. In a line with de Lavallade's observation, Hughes and colleges (2017) performed an extensive characterisation of major B cell subsets in CML patients at the time of diagnosis, including transitional, naïve, non-switched memory, class-switched memory, plasmablasts, and plasma cells, and the authors detected that non-switched memory B cell expression was reduced in comparison to healthy people (Hughes, Clarson *et al.* 2017).

From what have been revealed, it seems that NK cells, DCs and CTLs, in addition to certain B cells subset are quantitatively and functionally impaired in patients with CML prior to the TKI therapy.

### **1.1.5.2 Suppressor cells activity in pre-treated CML patients**

As it is the case in other types of leukaemias, a significant immune dysregulation has been reported in CML due to the recruitment of immunosuppressive cells. The main immunosuppressive cells identified in CML are myeloid-derived suppressor cells (MDSCs) and Tregs cells. Recruitment of such cells in the bone marrow of patients with CML can facilitate the escape of cancerous cells from the natural immune control.

MDSCs are a heterogeneous population group of immature granulocytic and monocytic cells characterised by their powerful suppressive activity against the immune responses (Gantt, Gervassi *et al.* 2014). MDSCs expansion generally occurs in a disease associated with prolonged course, such as chronic infection, inflammation and cancer formation, wherein relatively low-strength signals induce modest but persistent increase in myelopoiesis. In patients with CML, monocytic and granulocytic MDSCs were found to be expressed at a high level at time of the diagnosis in comparison to healthy individuals (Hughes, Clarson *et al.* 2017), and also found that MDSCs induce significant suppressive function of the cytotoxic T cells, including leukaemia-specific CTLs, and NK cells (Gabilovich, Nagaraj 2009a). The expansion

of MDSCs in cancer is driven by multiple pro-inflammatory factors, mainly the vascular endothelial growth factor (VEGF) and the granulocyte-macrophage colony-stimulating factor (GM-CSF) produced within the immunosuppressive tumour milieu (Ostrand-Rosenberg, Sinha 2009, Dolcetti, Peranzoni *et al.* 2010). A number of mechanisms used by the MDSCs to mediate their suppressive activities have been reported, including high rate reactive oxygen and nitrogen species production and arginase-1 upregulation. The latter causing a local depletion of arginine which is an essential amino acid for T cell activity (Gabrilovich, Nagaraj 2009a, Ross, Branford *et al.* 2013, Rodriguez, Quiceno *et al.* 2004, Corzo, Cotter *et al.* 2009) and also depletion of cysteine which is necessary for antigen-presenting cells, mainly DCs (Srivastava, M. K., Sinha *et al.* 2010). Arginase-1 was found to be an inhibitory factor for NK cells proliferation and IFN- $\gamma$  production (Oberlies, Watzl *et al.* 2009), adding that MDSC itself induces NK cells anergy via the membrane-bound transforming growth factor beta TGF- $\beta$ 1 (Li, H., Han *et al.* 2009).

Moreover, while MDSCs negatively affect the immune responses by suppressing the function of CTLs and NK cells, it can facilitate the recruitment and the expansion of another type of immunosuppressive cells called "T regulatory cells" (Tregs), thereby adding more hostility against anti-tumour immune responses. Tregs are a specialised subpopulation of T cells (type of CD4<sup>+</sup> T cell), characteristically expressing forkhead box P3 (FoxP3), a transcription factor with anti-CD4<sup>+</sup>/CD8<sup>+</sup> T cells and antigen-presenting cell activity, this further enable the escape of tumour cells from the immune system (Gabrilovich, Nagaraj 2009a, Huang, B., Pan *et al.* 2006).

Many cancerous cells express indoleamine 2,3-dioxygenase 1 (IDO1) enzyme, which degrades the essential amino acid tryptophan into kynurenine, the latter has been shown to involve in immunosuppressive activity, such as promotion of Tregs and inhibition of the effector T cells (Takikawa, Yoshida *et al.* 1986, Munn, Sharma *et al.* 2005a). Interestingly, on-target effect of imatinib on oncogenic protein tyrosine kinases (PTKs) is found to be associated with reduced expression of IDO leading to decrease kynurenine production, increase apoptosis of Tregs and relative restoration of CTLs activity (Balachandran, Cavnar *et al.* 2011).

Zahran *et al.* (2014) reported that Tregs are significantly upregulated in newly diagnosed CML patients compared to normal individuals, which increased significantly more during the accelerated and blast phases than during the chronic phase (Zahran, Badrawy *et al.* 2014). In parallel, Bachy *et al.* states that high Tregs load is associated with CML patients who are scoring as intermediate or high-risk Sokal scores (Bachy, Bernaud *et al.* 2011). All these observations demonstrate the immunosuppressive state in patients with CML at the time of diagnosis induced by MDSCs and Tregs activities.

### **1.1.5.3 Immune checkpoints activity in pre-treated CML patients**

Another mechanism which compromises further the immune response of CML patient is the activation of immune checkpoints pathways, particularly, programmed death-1 (PD-1) and cytotoxic T lymphocyte associated protein-4 (CTLA-4). Programmed death ligand-1 (PD-L1) is a ligand for PD-1, and hence, the development of aberrant PD-1/PD-L1 signalling provides an inhibitory signal to activated T cells causing T cell anergy, exhaustion and apoptosis (Butte, Keir *et al.* 2007).

PD-1 expression occurs temporarily on the activated effector cells under normal circumstances; however, constitutive expression of PD-1 generates a state of immune-imbalance between effector and suppressive activities leading to the eventual deviation of the immune response from activation to suppression (skewed immune response) due to the attenuation of effector T cells function and the expansion of Tregs.

In CML, Mumprecht *et al.* previously showed PD-1 upregulation in CML-specific CTLs (Mumprecht, Schurch *et al.* 2009a), and Hughes *et al.* demonstrated increased PD-1 expression on both CD4<sup>+</sup> and CD8<sup>+</sup> T cells in CML patients at diagnosis (Hughes, Clarkson *et al.* 2017). Findings obtained from both studies adding the aforementioned observations suggesting the occurrence of a broadly immunocompromised status in CML patients at diagnosis. However, some of these events have been found altered after launching of TKIs by “on-target” and/or probably by “off-target” effects. The following section will demonstrate some aspects of these effects.

### **1.1.6 Imatinib immunological “On-target” and “Off-target” effects**

Imatinib represents a quintessential case of a successful precision medicine that has indeed altered the fate of not only patients with Philadelphia-positive CML but also gastrointestinal stromal tumours (GIST) by selectively targeting the oncogenic drivers of these diseases, *BCR-ABL1* and *KIT*, respectively. Imatinib treatment has also shown promising results in patients with myeloproliferative disorders with mutations in gene encoding platelet-derived growth factor receptor-beta (*PDGFR-β*) (Ottmann, Druker *et al.* 2002, Apperley, J. F., Gardembas *et al.* 2002). Interestingly, there has been an increasing line of evidence showing the critical contribution of the immune system in defining the imatinib therapeutic efficacy, as well as in controlling escape mutations (Zitvogel, L., Rusakiewicz *et al.* 2016).

It has been widely assumed that the therapeutic activity of cytotoxic anti-cancer drugs and targeted agents exert their effect on cancerous cells by two mechanisms; either via debulking capability thereby partial or complete responses could be

obtained followed by relapse, or by eradication of all tumour stem cells resulting in permanent cure (Zitvogel, L., Rusakiewicz *et al.* 2016). Imatinib, with high selectivity, kills Philadelphia positive myeloid lineage cells in both bone marrow and periphery because their survival relies on *BCR-ABL1* activity, but it does not affect the survival of Philadelphia positive HSCs (Corbin, Agarwal *et al.* 2011), indicating that relapse will be precipitated upon cessation of imatinib therapy. At odds with the above assumption, results from the French STIM trial which demonstrated that 41% of patient with CML were able to stop imatinib therapy intake without detectable relapse after reaching a complete molecular response lasting for 2 years duration (Mahon, Réa *et al.* 2010). These findings were further substantiated by several independent clinical trials as well as updates from the original STIM trial (Takahashi, N., Kyo *et al.* 2012, Ross, Branford *et al.* 2013, Shinohara, Takahashi *et al.* 2013, Thielen, van der Holt *et al.* 2013). These observations collectively introduce an important query about how this paradox could occur.

A plethora of reports indicates that some anti-cancer agents marshal the immune system against the cancer cells by different aspects which could explain the interrogation mentioned above; for example, i) via inducing immunogenic killing of the cancerous cells (Vacchelli, Aranda *et al.* 2014), ii) via sensitising cancerous cells to an immune attack (Zitvogel, Laurence, Galluzzi *et al.* 2013), iii) by inhibition of regulatory immune circuits, or by engaging activating immune receptors (Vanneman, Dranoff 2012), and finally iv) by induction or restoring immune-surveillance. Hence, the activity of conventional and targeted therapies might be prolonged beyond cessation of the treatment (Zitvogel, Laurence, Galluzzi *et al.* 2013). Imatinib, as an example of targeted anti-cancer therapies, also work by “off-target”, in addition to “on-target” mechanisms, a concept which has high practical consequences for firstly, defining novel immune-related biomarkers that could aid in prediction of the response or resistance to imatinib, and secondly, informing on probable novel combination regimens that include imatinib with immunotherapies.

At the haematopoietic level, *in vivo* murine studies show that imatinib modifies the process of haematopoiesis by *KIT*-dependent mechanism (Shin, Hu *et al.* 2014); causing an increase in the flux of both HSC and multipotent progenitor cell types; inducing the maturation of myeloid progenitors and increasing the migration of the mature myeloid cells to the periphery (Bodine, Seidel *et al.* 1993, Thoren, Liuba *et al.* 2008). Accumulation of these cells was noticed in the bone marrow of imatinib treated patients during various doses, whereas only low dose of imatinib can induce myeloid cells accumulation in peripheral blood and leads to an enhanced host anti-microbial immunity (Napier, Norris *et al.* 2015).

However, deleterious myeloid and lymphoid off-target effects of imatinib were also described involving the inhibition of DCs generation, with subsequent impairment in priming of CTLs, as it was demonstrated in several *in vitro* and *in vivo* murine studies,

the effects were found not to be mediated via on-target effect against *PDGFR* or *KIT* (Appel, Boehmler *et al.* 2004, Appel, Rupf *et al.* 2005, Taieb, Maruyama *et al.* 2004), but rather caused by reduction in phosphorylation of AKT/PKB and nuclear accumulation of NF- $\kappa$ B (off-target effect). In human, in imatinib-treated CML cases, incomplete recovery of circulating DC numbers was noticed, suggesting that imatinib can inhibit dendritopoiesis *in vivo* (Boissel, Rousselot *et al.* 2004).

Imatinib induces M2 reprogramming of TAM, tumour-associated macrophages. TAMs are a type of cells that belongs to the monocyte-macrophage lineage (Quatromoni, Eruslanov 2012). TAMs are known for their role in linking cancer with inflammation. It can promote proliferation, invasion, and migration of cancerous cells, induce tumour angiogenesis, and inhibit T cell response (Grivennikov, Greten *et al.* 2010). TAMs can be categorised into M1 and M2 phenotypes, wherein, M1 macrophages are identified as classically activated TAMs and show enhanced anti-tumoural (inflammatory) properties, whereas M2 polarised TAMs are the alternative activated version of macrophages and have pro-tumoural (anti-inflammatory) functions (Genard, Lucas *et al.* 2017). Immunohistochemistry analysis of immune cells infiltrates both primary and metastatic GIST revealed the presence of TAM with an M1-like phenotype that restrict tumour growth; however, this phenotype then shifted towards an M2 pattern upon imatinib therapy demonstrated in the murine models and in imatinib-treated GIST (Cavnar, Zeng *et al.* 2013, van Dongen, Savage *et al.* 2010). This reprogramming probably results from tumour cell apoptosis induced by the on-target imatinib activity.

Furthermore, imatinib targets *ABL1*, *ABL2*, and *LCK* which have a role in T cell development, causing *in vitro* decrease of T cell receptor (TCR)-mediated T cell proliferation and activation and diminished *in vivo* delayed-type hypersensitivity (Dietz, Souan *et al.* 2004, Seggewiss, Lore *et al.* 2005).

Moreover, CD4<sup>+</sup> T cells derived from imatinib-treated CML patients were found secreting less effector cytokines upon TCR-mediated stimulation than cells derived from healthy controls (Gao, Lee *et al.* 2005). The off-target inhibition of the Bruton's tyrosine kinase (*BTK*) by imatinib might also explain the clinical observation that imatinib causes a reduction in the numbers of IgM-producing memory B cells, a general hypogammaglobulinemia, and an alteration of the phenotype of bone marrow plasma cells (Carulli, Cannizzo *et al.* 2010, Steegmann, Moreno *et al.* 2003). In spite of these inhibitory effects of imatinib on a defined population of immune cells, patients with CML do not experience repeated infections during their long term imatinib treatment (Druker, Talpaz *et al.* 2001).

Imatinib also demonstrated a direct inhibitory effect on NKG2D ligand expressed by cancerous cells, thereby preventing their recognition by NKG2D-expressed by the NK cells (Cebo, Da Rocha *et al.* 2006).

In addition, imatinib inhibits transcription of the vascular endothelial growth factor (VEGF)(Legros, Bourcier *et al.* 2004), a factor that has found frequently overexpressed in many malignancies. VEGF, in addition to its well know function in angiogenesis, has an essential role in leukaemic cells expansion and survival, and drives various immunosuppressive activities (Voron, Colussi *et al.* 2015, Terme, Tartour *et al.* 2013, Motz, Santoro *et al.* 2014). Following diagnosis, the high count of MDSCs in CML patients is found to be normalised after imatinib treatment, which could be due to the direct effect of imatinib or as a result of reduced VEGF level.

Imatinib can also promote expansion of a specific bone marrow subset of CD20<sup>+</sup> CD5<sup>+</sup> IgM<sup>+</sup> B lymphocytes, inducing higher plasma levels of IgM specific for O-linked sugars expressed by leukaemic cells (Catellani, Pierri *et al.* 2011).

Imatinib can rescue immune polarisation caused by *c-kit/SCF* axis activity in the DCs (which skewed towards a type 2 T-helper ( Th-2) profile), by re-direction of the immune response toward the more favourable T helper1 ( Th-1) type profile to induce tumour eradication (Oriss, Krishnamoorthy *et al.* 2014). Imatinib also restores the count of Th-1 which are found at a low number in patient with CML at the time of diagnosis (Aswald, Lipton *et al.* 2002). Moreover, specific *BCR-ABL1* effector memory CD4<sup>+</sup> and CD8<sup>+</sup> T cells have been found in patients who are on long-term imatinib therapy, and after imatinib withdrawal (Riva, Luppi *et al.* 2010, Riva, Luppi *et al.* 2014).

In human and mice models, imatinib has been shown to be a potent stimulator of NK cells, this activity was found in mice to be exerted indirectly by the stimulation of bone marrow derived DCs which in turns could activate resting NK cells which then release IFN- $\alpha$  (Borg, Terme *et al.* 2004). In GIST, around half of the patients who were treated with imatinib demonstrated an enhanced NK cell derived IFN- $\alpha$ , and therefore, NK cells response has been regarded as an immunological predictor of GIST prognosis (Borg, Terme *et al.* 2004, Menard, Blay *et al.* 2009).

Accumulating evidence also implicates NK cells in the cure of CML by achieving sustained complete molecular remission as it was initially indicated in preclinical models, in addition to several clinical trials of imatinib cessation have proved that higher NK cell numbers or NK cell function at the time of discontinuation was associated with prolonged maintenance of the sustaining complete molecular remission (Menard, Blay *et al.* 2009, Ilander, Olsson-Strömberg *et al.* 2014, Dulphy, Henry *et al.* 2013). Moreover, a study conducted by Binotto and colleagues, revealed that CML patients receiving imatinib exhibited preferential expression of activating NK receptors (Binotto, Frison *et al.* 2014).

Collectively, the aforementioned observations have revealed that imatinib has a long-term effect able to trigger anti-cancer responses in patients with CML or GIST mediated principally by T cells and NK cells, although there has been some deleterious imatinib effects stated to compromise the immune response; however,

no ample evidence has demonstrated that patients receiving imatinib have experience an opportunistic infection due to depressed immunity. It is, therefore, proposed that a novel therapeutic strategy would be to combine imatinib with immunotherapies and that this will allow long term relapse-free survival to be achieved in a bigger number of CML patients and will avert the emergence of imatinib resistant issues (Zitvogel, *et al.* 2016).

These effects of imatinib on various components of the anti-tumour immune-surveillance system are summarised in Figure 1.5.

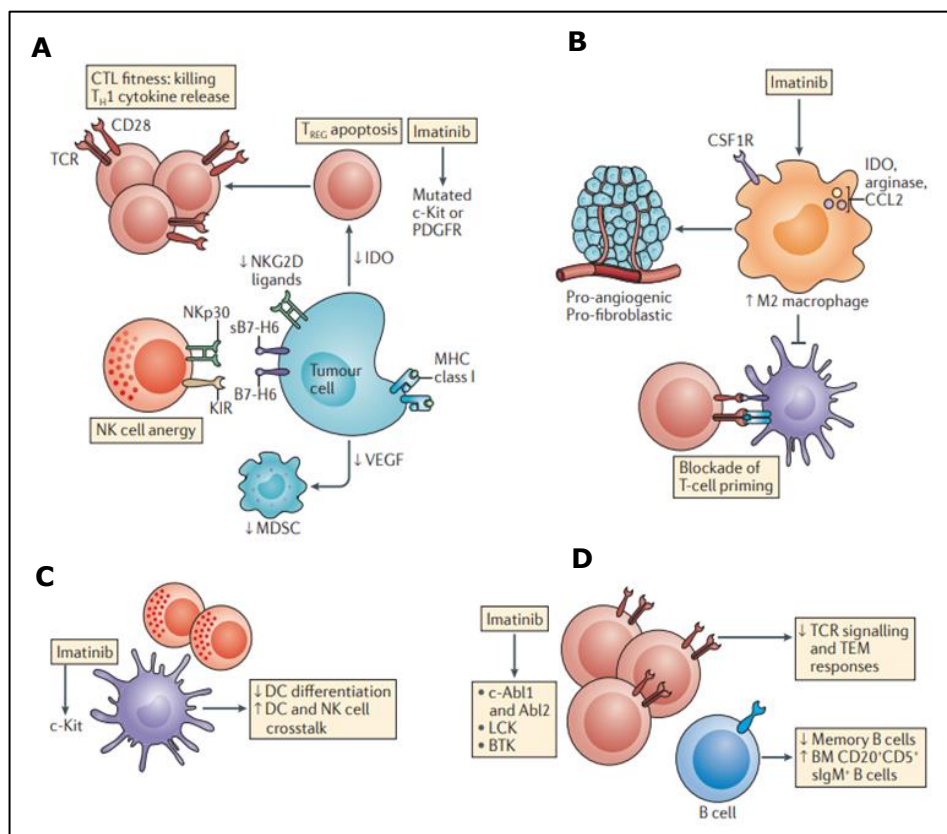


**Figure 1.5: Effects of imatinib on various components of the anticancer immune-surveillance system.**

**(A)** Imatinib targets the oncogenic protein tyrosine kinases (PTKs) causing apoptosis of Tregs and expansion of CTLs, by reducing the expression of IDO, and also by targeting the VEGF secretion. This direct effect of imatinib also reduces the expression of NKG2D ligand on neoplasm, thereby negatively hinder their recognition by NKG2D-expressing NK cells. MDSCs are normalised following imatinib therapy or as a result of reduced VEGF serum level. **(B)** Imatinib induces the polarisation of TAMs to M2 phenotype, which can induce tumour angiogenesis, and inhibit T cell response **(C)** through targeting *kit* on DCs, it has been found that while imatinib therapy reduces spontaneous and FLT3L induced DCs differentiation, it permits DC–NK cell crosstalk in the spleen and the lymph nodes. **(D)** Imatinib targets *ABL1*, *ABL2* and *LCK*, which involve in T cell development, leading to a reduced TCR-mediated T cell proliferation and activation *in vitro* and decreasing in the delayed type hypersensitivity reaction *in vivo*. Imatinib off-target inhibition of Bruton tyrosine kinase (*BTK*) induces a decline in both IgM-expressing memory-B-cell count and hypogammaglobulinemia. However, imatinib can promote the expansion of a specific bone marrow subset of CD20<sup>+</sup>CD5<sup>+</sup>sIgM<sup>+</sup> B lymphocytes, inducing higher plasma levels of IgM specific for O-linked sugars expressed by leukaemia cells. Permission from the Springer Nature is obtained to reuse this image with a reference from (Zitvogel, *et al.* 2016).

## 1.2 The development of immunotherapies in CML

### 1.2.1 Resistance of CML stem cells to the currently available therapies

In spite of the significant success that has been achieved in the management of CML disease, only a minority of patients have reached an ultimate “cure” via the currently available TKIs therapy. Indeed, even though CML patients who have reached complete remission, their primitive leukaemic progenitors continue to be readily detectable (Gerber, Qin *et al.* 2011).

It has been clearly shown that bone marrow microenvironment in CML patients produced aberrant signals and cellular genetic and epigenetic alterations contribute to the persistence of a quiescent LSCs, cells which are responsible for TKIs resistance and subsequent progression of the disease into the blast crisis phase (Perrotti, Silvestri *et al.* 2017). It has been found that while imatinib exerts strong toxicity against the differentiated CML progenitors, LSCs demonstrate a relative or even complete resistant to imatinib (Bhatia, Holtz *et al.* 2003).

Currently, imatinib, nilotinib, and dasatinib are the standard first-line treatment for treating newly diagnosed CML patients at chronic phase (Jabbour, E., Kantarjian 2014, Apperley, Jane F. 2015). The majority of imatinib-treated CML patients in that phase are reported to achieve a significance and persistent response, however, approximately 20-40% of them develop *BCR-ABL1* mutation-induced drug resistance (Goldman 2009, Jabbour, E., Kantarjian 2014, Ross, Hughes 2014), and similarly, around 35-50% of patients become resistant to the second generation TKIs (Jabbour, E., Kantarjian 2014, Ross, Hughes 2014, Wei, Rafiyath *et al.* 2010). For patients who fail the frontline regime, other second or third generation TKIs are being used where their utility principally depends on the type of *BCR-ABL1* mutations identified, ponatinib, for example, is used for managing patients with the *BCR-ABL1 T315I* mutation; however, only 50% of TKI-resistant CML patients at the chronic phase and only 35% patients in the blast crisis show a significant response to ponatinib (Jabbour, E., Kantarjian 2014, Ross, Hughes 2014, Apperley, Jane F. 2015), although the latter group of patients (patients in the crisis phase ) do not show long-term response to ponatinib drug (Hehlmann, R. 2012). Adding to that, ponatinib could be associated with considerable organs failure, as it was reported in some cases, such as cardiac failure and hepatotoxicity (Cortes, J. E., Kim *et al.* 2013). Depending on these observations and on the evidence showing selective LSCs outgrowth and disease relapse even years after cessation of TKIs, it is now becoming clear that TKIs do not cure CML disease (Ross, Hughes 2014).

In addition, whilst allogeneic haematopoietic stem cell transplantation (allo-SCT) remains the only available curative therapy, it is only feasible for 30% of patients (Kessler, JH, Bres-Vloemans *et al.* 2006) and is associated with high mortality and morbidity rates, and other non-TKIs therapies, such as interferon- $\alpha$ , are also found not to be effective in elimination of LSCs (Graham, Jorgensen *et al.* 2002, Jorgensen, Allan *et al.* 2007). Considering these observations, it seems that, in general, there is no definitive curative drug for CML patients regardless of the disease stage, and no feasible drug to treat patients who developed multiple TKIs resistance in particularly the blast phase, and hence, this issue sparks an important and urgent necessity in the field of clinical haematology to find an alternative or assistive therapeutic strategy to the existing approaches capable to eradicate the minimal residual disease (MRD) and generating long lasting protection. The considerable progress in understanding the molecular and the immunological aspects related to CML, together with the evidence provided in the following section have raised expectations that CML patients could achieve a definite cure by combining the current targeted therapies with immunotherapeutic approaches.

### **1.2.2 Potential capability of immunotherapies to eradicate CML stem cells**

It has been considered that T cell immune response might play a significant role in the success of allo-SCT. This has been shown in an exceptional clinical situation where more than 90% of CML relapsed cases post transplantation found to achieve complete molecular remission after receiving a donor lymphocyte infusions (DLI), and also, the rate of relapse found to be higher among those who had T cell depleted grafts (Pinilla-Lbarz, Shah *et al.* 2009). These observations point out the significance of CTLs in eradication of leukaemic cells and the feasibility of applying T cell-based immunotherapy in CML. This hypothesis is particularly reasonable in CML disease because the cancerous cells are circulating in the blood and lymphatic system, thus, it makes them an easier target than solid tumours. Additionally, several factors have made CML theoretically an ideal target for immunotherapeutic approaches; i) its well-known disease pathology; understanding the onco-molecular pathways driving the development of CML disease and the subsequent immune response have contributed to the development of various vaccines targeting these pathways, ii) relative long chronic phase, this give an opportunity to monitor the immune response over a period of time, iii) CML is not a disease treated by the chemotherapeutic agents that are known to compromise the immune system and interfere with immune response intended, and iv) CML overexpresses numerous leukaemia-associated antigens (LAAs) especially at the advance phases (Rosenfeld, Cheever *et al.* 2003).

The concept of therapeutic immunotherapy is based on the stimulation of the patient's own immune responses to kill cancerous cells. In theory, distinctive features assume immunotherapy superior to other traditional anti-cancer therapies is the high degree of specificity thereby minimizing normal tissue cytotoxicity, and ability to generate long term memory response to prevent subsequent reoccurrence (Emens 2008). Therefore, a key technical element for the development of successful immunotherapies is to find antigens that are specifically expressed by tumour, called "tumour-specific antigens", thereby the immune system would be able to attack tumour while sparing normal cells (Adam, Odhav *et al.* 2003).

The first one to ever be considered in CML is the *BCR-ABL1* derived peptides, especially those encompassing the breakpoint region (*BCR-ABL1* Junctional peptides), as these are exclusively present in CML cells and should therefore be recognised as novel antigens by the immune system. These were, therefore, thought to be able to induce high avidity T cells associated with an excellent recognition efficacy. However, it has been found that the numbers of junctional breakpoint peptides potentially being presented by HLA class I molecules are very limited and restricted to certain HLA haplotypes (Clark, Dodi *et al.* 2001, Bocchia, Wentworth *et al.* 1995), and that the circulating specific T cells against junctional peptides in CML patients were low, and no high-avidity T cells could be demonstrated (Posthuma, van Bergen *et al.* 2004, Bocchia, Gentili *et al.* 2005). It has been therefore hypothesised that not *BCR-ABL1* gene, *per se*, but rather other genes that are induced by the *BCR-ABL1* kinase activity might represent the critical antigens for CTLs activation against Philadelphia positive CML cells (Deininger, M. W., Vieira *et al.* 2000, Grunebach, Mirakaj *et al.* 2006). Furthermore, Scheich, *et al.* 2007 addressed the question of whether a T cell response derived from CML patients is also directed against *BCR-ABL1*-regulated antigens or against *BCR-ABL1* itself by stimulating CD8<sup>+</sup> cells with DCs transfected with RNA coding for *BCR-ABL1* wild-type and a kinase-deficient mutant. The authors suggested that immunotherapy targeting multiple immunogenic *BCR-ABL1*-associated antigens could be superior to immunisation targeting *BCR-ABL1* breakpoint peptides alone, and the authors therefore point out the importance of inducing synergistic effect by including to imatinib therapy other CML-associated antigens, such as proteinase-3 (PR3) or helicase antigen (HAGE), while imatinib directly targeted the *BCR-ABL1* kinase to induce major molecular remission, the tumour antigens might exert their potentiality to overcome resistance for imatinib by eradication of Philadelphia positive LSCs (Scheich, Duyster *et al.* 2007).

In this respect, numerous LAAs have been described as overexpressed in CML, and therefore, they have been subjected to active investigations to determine the rationale for being suitable targets for immunotherapy. Various peptides derived from these antigens have been extensively studied and the majority of them were found to be able to activate CML-specific T cell responses in HLA-restricted manner. Some

of these TAAs are: Wilm's tumour protein (WT1) (Bellantuono, Gao *et al.* 2002), proteinase-3 (Knights, Weinzierl *et al.* 2006), helicase antigen (HAGE) (Knights, Weinzierl *et al.* 2006, Martelange, De Smet *et al.* 2000), Preferentially expressed antigen of melanoma (PRAME) (Kessler, J. H., Beekman *et al.* 2001), hyaluronan-mediated motility receptor (RHAMM)/CD168 (Schmitt, Li *et al.* 2006), human telomerase reverse transcriptase (hTERT) (Gannage, Abel *et al.* 2005), survivin (Hernandez-Boluda, Bellosillo *et al.* 2005), CML28 (Han, Zhao *et al.* 2006) and CML66 (Suemori, Fujiwara *et al.* 2008), but are also expressed by normal cells, albeit to a lesser extent (Greiner, Dohner *et al.* 2006). Among these TAAs, this project focuses on HAGE and WT1 as suitable targets for immunotherapy against CML due to several merits as it will be demonstrated in the following sections.

### **1.2.3 Types of immunotherapy in CML**

Therapeutic immunotherapy can be categorised into active and passive types. Active immunotherapy promotes the activation of the patients own immune system to generate a specific anti-tumour cytotoxic and humoral immune responses with long-lasting immunological memory pool, whereas the passive immunotherapy involves the modulation of pre-existing immune responses by infusion of preformed antibodies or cells directly to eliminate the transformed cells.

#### **1.2.3.1 Passive immunotherapy**

##### **1.2.3.1.1 Donor leukocyte infusion (DLI)**

DLI is a process by which leukocytes from stem cell donors are infused into patients who have relapsed haematologic malignancies, mainly used after allo-SCT to boost an anti-tumour immune response and/or to ensure that the donor stem cells remain engrafted (Porter, David, Levine 2006). It has been found that DLI post marrow transplantation induces long-lasting remission in the majority of CML relapsed patients (Li, Y., Lin *et al.* 2012). The principle of DLI is based on induction of remission by a process called graft *versus* leukaemic effect (GvL), where the donor T cells attack and inhibit the growth of residual cancer cells. It is thought that GvL effect is maintained by host APCs that stimulate the donor T cells by presenting target antigens expressed on the specific haematopoietic cells (Dolstra, Fredrix *et al.* 1999). Importantly, donor T cells can also inhibit leukaemic cells by targeting aberrantly expressed antigens on leukaemic cells, but not normal colony formation (Molldrem, Clave *et al.* 1997). The main compelling evidence supported GvL effect principally mediated by donor T cells is that firstly, patients who received syngeneic-SCT relapsed more often than patients received allo-SCT, and secondly, higher number

of relapses were noticed in those who received T cell depleted grafts (Horowitz, Gale *et al.* 1990, Marmont, Horowitz *et al.* 1991).

Although the application of DLI has been dramatically decreased due to the advent of the TKIs and to avoid the possible risk of severe graft *versus* host disease (GvHD), DLI is still a viable option for treating relapsed cases after allo-SCT.

### **1.2.3.1.2 Adoptive T cell therapy**

Although relapsed CML patients after allo-SCT have benefited from DLI, efforts to enhance GvL have been limited by the potential to induce lethal GvHD. Adoptive T cell therapy has been developed for augmenting GvL and relies on the infusion of *ex vivo*-generated T cells with particular specificities.

Single and multiple TAA-specific T cells have found to be applicable for a wide-range of haematological malignancies. For example, Chapuis and colleagues (Chapuis, Ragnarsson *et al.* 2013) created WT1-specific donor-derived CD8<sup>+</sup> T cell clones, and infused 11 patients with advanced MDS, AML, CML or ALL post-HSCT with and without IL-21, as means to prolong survival of CTL *in vivo*, in an attempt to harness the GvL effect while reducing the possible risk of GvHD. Results demonstrated that; i) there was direct evidence of anti-leukaemic effect in two patients; one of them was with advanced progressive disease developed a transient response, and the second patient with MRD had a prolonged remission, ii) three patients who were expected at high risk for relapse post-HSCT survived without any leukaemic relapse or GvHD, and without additional anti-leukaemic therapies, iii) Interestingly, CTLs produced with IL-21 (transferred into three patients and the patient with MRD) persisted over long-term and acquired phenotypic and functional characterisation of memory CD8<sup>+</sup> T cells. This trial although may not be adequate to achieve a clinical benefit to all treated patients, it supports the growing efforts to target WT1 as a target for immunotherapy and provides the elements needed to establish effective persistent T cell responses in leukaemic patients.

Other groups have developed polyclonal polyfunctional T cells that are able to target multiple TAAs in a single product of cell therapy to increase the applicability of TAA-specific CTLs in a wide range of cancer. In this respect, Gerdemann *et al.*, have generated T cells that target multiple cancer testis antigens; PRAME, SSX2, NY-ESO-1, MAGEA4 and Survivin from healthy people and from patients with lymphoma. It has been found that these activated CTLs demonstrated *in vitro* cytotoxic activity toward autologous lymphoma cells, but they have not been established in a human trial yet (Gerdemann, Katari *et al.* 2011). Several Phase I clinical trials are testing this concept using mainly cancer testis antigens and WT1 available at: <https://clinicaltrials.gov/> with accession number (NCT01333046) and (NCT02203903).

### 1.2.3.1.3 Chimeric Antigen Receptors (CARs) therapy

This approach represents a recent advancement in the transfer immunotherapy. It is based on *in vitro* manipulation of TCR gene to express chimeric antigen receptors (CARs) on the surface of T cells, engineered to target defined TAAs. CAR T cells are expanded and then reinfused into patients' blood circulation where they should kill tumour cells expressing these particular antigens (Figure 1.6).

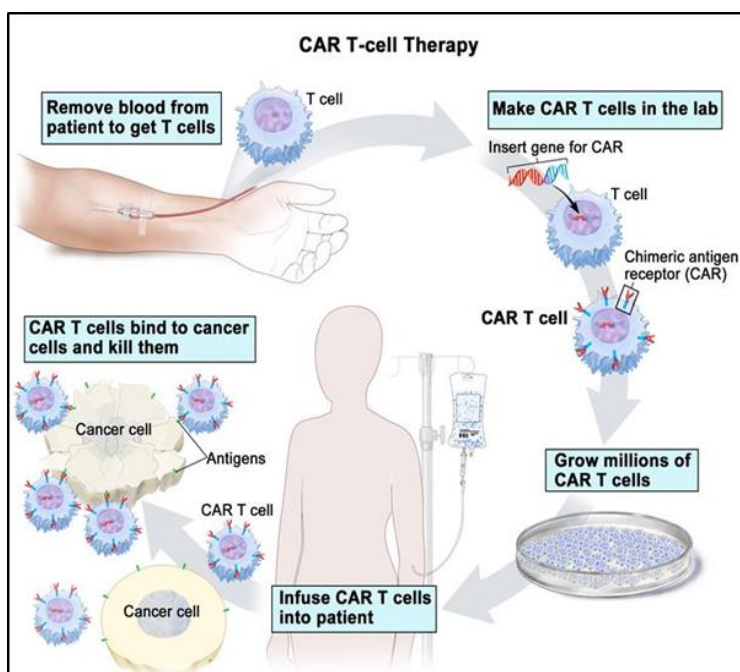


**Figure 1.6: Principle of CAR T cell therapy.**

Permission to reuse this image is obtained from the National Cancer Institute® (2017) Terese Winslow LLC, U.S. Govt. has certain rights. Image is available at: <https://www.cancer.gov/images/cdr/live/CDR774647-750.jpg>.

Structurally, these receptors consist of an extracellular recognition domain that is derived from an antibody variable region attached to intracellular signalling domains of both TCR complex and costimulatory molecule signalling (Maher, Brentjens *et al.* 2002). This type of therapy have shown unprecedented success in the field of the immunotherapy, not only in haematological malignancies such as refractory/relapse ALL and CLL (Maude, Frey *et al.* 2014, Porter, D. L., Levine *et al.* 2011), but also in solid type of tumours (Brown, Alizadeh *et al.* 2016). In addition, other many promising preclinical studies have been established, mainly AML (CD33 or CD123), multiple myeloma (CD38 or CD44v6), lymphomas (CD30) and T cell malignancies (CD5) (Maus, Grupp *et al.* 2014). The "first-generation" CARs were limited by poor clinical responses and general lack of persistence, wherein TCR  $\zeta$  chain was used as the only signalling domain (Jensen, Popplewell *et al.* 2010). Later, and upon addition of costimulatory molecules in the construct of the "second-generation" CARs, such as CD28 costimulatory domain, their persistent antitumor activity was improved *in*

*vivo* (Kowolik, Topp *et al.* 2006, Savoldo, Ramos *et al.* 2011). Since then, this approach has been frequently modified to improve the overall efficacy. A group at the National Cancer Institute, for example, applied a lymphodepletion regimen consisting of cyclophosphamide and fludarabine before T cell infusion to improve CAR T cells persistence (Kochenderfer, Wilson *et al.* 2010), the result demonstrated clinical responses in 6 out of 8 patients suffering from progressive B-cell malignancies (CLL and follicular lymphoma) (Kochenderfer, Dudley *et al.* 2012a). Later, the University of Pennsylvania used customised chemotherapy regimens followed by a lentivirus vector expressing 4-1BB as a costimulatory signalling domain instead of CD28, where results initially showed impressive responses in 2/3 of patients with CLL, as each CAR T cell was able to kill more than 1000 CLL cells (Kalos, Levine *et al.* 2011), but these findings in CLL have not been sustained.

The more impressive success achieved upon using the second-generation CD19-CAR T cells is for the treatment of adult and paediatric patients with ALL demonstrated by the University of Pennsylvania/Children's Hospital of Philadelphia Seattle and BCM, wherein, response rates between 70% and 90% have been achieved in some patients with the poorest prognosis ALL (Brentjens, Davila *et al.* 2013, Cruz, Micklethwaite *et al.* 2013, Grupp, Kalos *et al.* 2013, Kochenderfer, Dudley *et al.* 2012).

Warda and colleagues, 2019 have recently demonstrated in a "proof-of-concept" of a CAR T cell immunotherapy approach in the context of CML. They have developed CAR T cells targeting IL1 receptor-associated protein (IL1RAP) in an attempt to induce permanent cure by targeting quiescent CML stem cells based on the fact that IL1RAP is expressed by the leukaemic but not the normal HSC compartment. Results demonstrated that IL1RAP CAR T cells were triggered by IL1RAP<sup>+</sup> cell lines and primary CML cells, leading to proinflammatory cytokines secretion and specific *in vitro* killing. In a xenograft murine model, NSG mice were transplanted (intraperitoneally or intravenously) with Luc<sup>+</sup>/IL1RAP<sup>+</sup>/GFP<sup>+</sup> tumour, and CML cell lines with or without administration of the effector CAR T cells, results demonstrated that only the group that received the CAR therapy led to decrease tumour size until complete elimination (Warda, Larosa *et al.* 2019). Based on the same concept, the *ClinicalTrials.gov* is currently recruiting 40 participants for a trial entitled "Targeting Leukaemic Stem Cell Expressing the IL-1RAP Protein in Chronic Myelogenous Leukaemia (CML) (CAR-LMC)" (NCT02842320), the study is due to be finished by the end of April, 2020.

From what has been seen it seems that CAR therapy is very promising in haematological malignancies, and therefore, the FDA has recently approved two CAR-based therapies in treatment of haematological malignancies; i) tisagenlecleucel for B cell ALL and tocilizumab for cytokine release syndrome, available at:

<https://www.fda.gov/drugs/resources-information-approved-drugs/fda-approves-tisagenlecleucel-b-cell-all-and-tocilizumab-cytokine-release-syndrome> and ii) tisagenlecleucel for adults with relapsed or refractory large B-cell lymphoma, available at: <https://www.fda.gov/drugs/resources-information-approved-drugs/fda-approves-tisagenlecleucel-adults-relapsed-or-refractory-large-b-cell-lymphoma>.

In spite of these very promising results, it is difficult to determine an ideal CAR-based approach due to many factors, such as variability of CAR design, T cell generation, tumour burden and prior chemotherapy (Brentjens, Curran 2012).

#### **1.2.3.1.4 Immune checkpoint blockade therapy**

The principle of this strategy is based on the administration of preformed antibodies with the aim of harnessing the tumour immune environment in favour of the host, as demonstrated in Figure 1.7. The most clinically established checkpoint blockade strategies are those targeting PD-1/PD-L1 and CTLA-4 pathways, with impressive responses seen in a wide variety of tumour types in particular in melanoma, renal cell carcinoma, lung cancer, and other solid tumours due to boosting of immune-surveillance (Lesokhin, Callahan *et al.* 2015).

Normally, humans have been evolved to keep immune homeostasis via multiple complex mechanisms designed in the thymus to prevent autoimmunity, wherein a constant balance between recognition of non-self-epitopes and avoidance of recognition of self is maintained through a process of positive and negative selection of developing T cells in the thymus. Naïve T cell activation in the lymphatic tissue relies on TCR recognition of antigen in the context of MHC molecules and effective co-stimulation of CD28 by CD80/86 on APCs, which in turn lead to upregulation of CTLA-4 on the surface of T cells, and through competition with CD28 to bind CD80/CD86, inhibits activated T cells (Walunas, Lenschow *et al.* 1994).

Tregs, unlike T cells, constitutively express CTLA-4 and therefore represent a major player in peripheral tolerance (Topalian, Drake *et al.* 2015), hence, blockade of the CTLA-4 can stop Tregs negative signals that could inhibit T cells activity, causing a persistent activation of T cells, but this can precipitate the development of an autoimmune disease (Maker, Attia *et al.* 2005).

Similarly, engagement of the programmed cell death 1 receptor (PD-1) on the activated T cells with its ligands PD-L1 and PD-L2 in tissues keeps immunologic tolerance by suppression of autoreactive T cells. APCs and tumour cells expressing PD-L1 are able to engage PD-1 on T cells causing T cell exhaustion and dysfunction, thereby protects PD-L1-expressing cells from T cells attack (Chen, L., Han 2015), and in haematological malignancy, PD-L1 expression by cancerous cells seems to be an inherent feature in the disease biology (Roemer, Advani *et al.* 2016). CTLA-4 is

found expressed on the surface and in the cytoplasm of various type of leukaemias, including AML, CML and CLL (Perez-Garcia, Brunet *et al.* 2009, Ciszak, Frydecka *et al.* 2016). It has been reported that immune escape of leukaemic cells in CML is mediated by PD-1 pathway (Christiansson, Soderlund *et al.* 2013). Currently, there are two CTLA-4 inhibitors, ipilimumab (FDA approval) and tremelimumab, both of them in various stages of clinical development in solid and haematological malignancies (Wolchok, Weber *et al.* 2013, Wolchok, Neyns *et al.* 2010). Nivolumab and pembrolizumab are the two anti-PD1 agents that have been used in the most advanced stages of clinical development in haematological malignancies. Pianko and colleagues have provided a recent review where they showed many clinical trials adopted checkpoints inhibitors with/without combination with other strategies in haematological malignancies (Pianko, Liu *et al.* 2017). Thus far, the majority of clinical data targeting checkpoint blockade in haematological malignancies has been collected from lymphoid cancers, however considerable preclinical findings support the value of using immune checkpoint inhibition in myeloid cancer as well (Pianko, Liu *et al.* 2017).

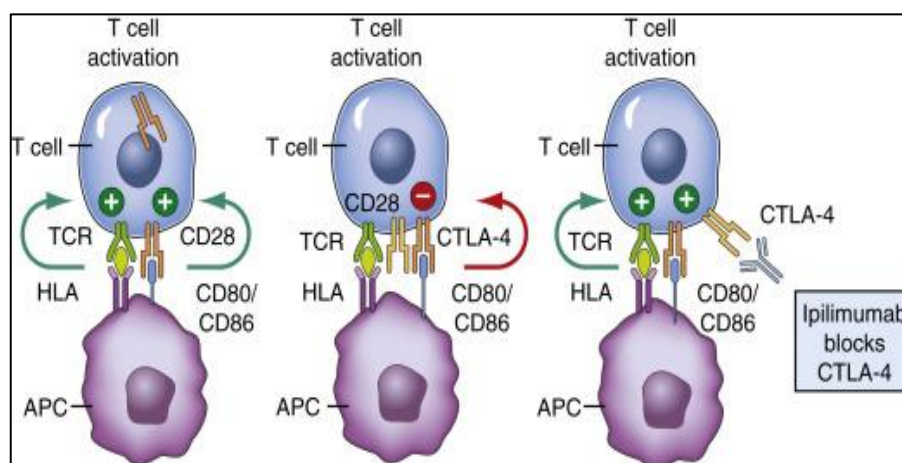


**Figure 1.7: Schematic representation demonstrates the principle of immune checkpoint blockade therapy (anti-CTLA-4).**

CTLA-4 is a CD28 homologue expressed transiently on the surface of activated CD8 T cells. The inhibition of CD8 T cells by CTLA-4 occurs by binding of CTLA-4 on CD8 T cells to the costimulatory molecules CD80/CD86 on the APCs, causing dephosphorylation of TCR signalling proteins and subsequently T cell inhibition. Ipilimumab is an antibody that targets CTLA-4 on the surface of CD8 T cells and inhibits this pathway, thereby retaining the effector function of the CD8<sup>+</sup> cells. Permission from Elsevier is obtained to reuse this image with a reference from (Bell, *et al.* 2018).

### 1.2.3.2 Active immunotherapy /cancer vaccines

In general, cancer vaccines developed in relation to the treatment of leukaemia include DNA, dendritic cell (DC) and peptide-based vaccines. However, clinical trials using vaccines for the treatment of CML are still in early development. The following sections will discuss the available vaccine types in treatment of cancer with especial emphasis on CML.

### 1.2.3.2.1 DNA-based vaccines

DNA vaccines are an attractive delivery system for inducing immune response against TAAs in cancer patients. DNA vaccine is a bacterial plasmid designed to express a specific antigen (protein) after *in vivo* administration and subsequent cell transfection. Many advantages are associated with DNA vaccines, such as cost effective, safe, easily manufactured and administered (Anderson, Schneider 2007, Dermime, Armstrong *et al.* 2002). It has been found that DNA vaccines can mount both arms of adaptive immune responses, humoral and cell-mediated responses (Vatakis, Koh *et al.* 2005, Yan, Cheung *et al.* 2007), and might also help avoid pre-existing immunity and immunodominance (Yu, Z., Restifo 2002). However, these types of vaccines have limited capacity to break *in vivo* tolerance and provide long term effect (Tsang, Zaremba *et al.* 1995).

DNA vaccines provide opportunity to design vaccine of interest depending on the theoretical and conceptual requirement of the researchers. In general, DNA plasmid constructs contain basic components involving an optimal eukaryotic promoter and polyadenylation site to encode the elements of the interest (Ghanem, Healey *et al.* 2013). Inside the construct, different inserts can be introduced to be co-expressed with the antigen of interest, such inserts are; immune costimulatory molecules, cytokines, chemokines, inhibitors of immuno-suppression (CTLA4, PD-1/PD-L1) and many other co-signalling molecules (Li, L., Petrovsky 2017). DNA vaccines are often introduced to the muscle cells under the skin (myocytes) and DCs of the skin (Langerhans cells) by either intra-muscular injection or electroporation, during which, both CD8<sup>+</sup> T cells and CD4<sup>+</sup> T cells can be triggered upon presentation of the processed peptides by MHC class I and II molecules, respectively by employing both direct and cross presentations pathways (Rice, Ottensmeier *et al.* 2008). ImmunoBody<sup>®</sup>, developed by Scancell Ltd, represents an ideal DNA vaccine, encoding an antibody containing the peptide sequence of the gene of the interest in its CDR region and has been shown to generate high frequency and high avidity T cells (Pudney, Metheringham *et al.* 2010). This type of vaccine has been used in this project and will be explained in more details in Chapter-4.

Numerous studies have demonstrated the applicability of DNA vaccines in pre-clinical models and human clinical trials (Phase I / II), which are available at [clinicaltrials.gov](http://clinicaltrials.gov), with accession numbers: NCT00807781, NCT01493154, NCT00849121, and NCT01138410, these target mainly HPV-related cancers, breast cancer, prostate, and melanoma.

In leukaemias, the majority of the DNA vaccines are in the pre-clinical stage (Liu 2011). For example, a DNA-based vaccine was developed in an animal model of acute promyelocytic leukaemia by fusing the human promyelocytic leukaemia-retinoic acid receptor-alpha (*PML-RARA*) oncogene to tetanus fragment C (FrC) sequences. It was

found that this DNA vaccine specifically targeted an oncoprotein producing a significant outcome on the mice survival rate, both alone and when incorporated with all-trans retinoic acid (ATRA) (Padua, Larghero *et al.* 2003).

WT1-based vaccine was also evaluated in preclinical studies. A plasmid DNA encoding the full-length murine WT1 gene was inoculated into C57BL/6 mice intramuscularly. Specific WT1-CTLs against the WT1 protein were detected, and these were shown to specifically kill WT1-expressing cancer cells in a MHC class I-restricted manner (Tsuboi, Oka *et al.* 2000).

### **1.2.3.2.2 Dendritic cell-based vaccine**

DCs are professional antigen-presenting cells (APCs) characterised by their powerful capacity to capture, process and present antigenic peptides to launch both cellular and humoral immune responses (Banchereau, J., Steinman 1998, Sloma, Jiang *et al.* 2010). Proper DCs functionality is of a particular importance in anti-tumour immunity to elicit fully functional T cell responses. CML patients have been found to have a significant lower DCs count in comparison to healthy individuals, of which, the immature cells exert abnormally deficient pinocytosis which then negatively impacted the process of processing and presentation of the antigens (Sloma, Jiang *et al.* 2010, Andrea Erika Held, Heine *et al.* 2013). Mature DCs, in CML patients, are also defective in their antigen presentation capacity, due to the downregulation of MHC and the costimulatory molecules; CD80, CD83, CD86 (Eisendle, Lang *et al.* 2003). Therefore, loading leukaemia-derived antigens into CML-DCs could enable them to trigger strong CML-specific CTL cytotoxicity, and this is the concept of "Dendritic cell-based vaccine".

In human, DCs develop from two independent pathways; CD34<sup>+</sup> haemopoietic progenitors and CD14<sup>+</sup> monocytes (Romani, Gruner *et al.* 1994, Sallusto, F., Lanzavecchia 1994). Advance technologies nowadays have indeed permitted the generation of autologous DCs from these cells in large quantities, wherein they are *ex vitro* co-cultured with cytokines to become fully matured and then re-infused back to the patient. This process involves an initial induction of autologous DCs maturation *in vitro* in the presence of granulocyte-macrophage colony stimulating factor and interleukin 4 (GM-CSF/IL-4) to produce immature DCs (Yu, L., Hu *et al.* 2016), cells are then loaded with particular tumour antigens which could be in the form of a peptide, protein, lysate, RNA or DNA derived from tumour extracts derived from a TAA (Bergant, Meden *et al.* 2006, Berzofsky, Ahlers *et al.* 2001). After being loaded, additional inflammatory signals to induce final DCs maturation are used, such as TNF- $\alpha$ , toll-like receptors (LPS) and CD40-ligand receptors, this is important in order to avoid tolerance before they are re-infused back into the patient (Mocellin, Semenzato *et al.* 2004). The immature DCs are characterised by a powerful capacity

to capture and process antigenic elements but are weak T cell activator. In contrast, the mature DCs are identified by their lost capability of antigenic capture and acquisition of increased capacity to stimulate T cells through increased antigen presentation and expression of co-stimulatory molecules (Cella, Sallusto *et al.* 1997), such as by upregulation of MHC molecules.

Several clinical trials are currently assessing the efficacy of DC-based vaccines in various cancer, such as AdHER2/neu DC Vaccine (NCT01730118), Autologous dendritic cell-adenovirus (NCT00049218), dendritic cell fusion vaccine for myeloma (NCT01067287), renal cell carcinoma (NCT01441765), prostate cancer (NCT01420965), acute myeloid leukaemia (NCT01096602) and many other, of which the DCs vaccination has shown to be safe and feasible in many clinical trials, and that DC-based vaccine called (Sipuleucel-T)/phase III trials induced a survival benefit (Bol, Schreiber *et al.* 2016). However, in general, DC-based immunotherapy and particularly the monotherapy have their own limitations principally due to immunosuppressive mechanism in the tumour milieu and therefore combination therapy could play an important role in improving the subsequent treatment outcomes (Bol, Schreiber *et al.* 2016).

In CML, it is assumed that DC-based vaccines are an attractive therapy due to the fact that progenitor cells express many TAAs, and also tumour specific antigen (TSA) (*BCR-ABL1*), which they can be used to generate APC (Orsini, Calabrese *et al.* 2006). In clinical trials, there was a pilot study performed on three CML patients to assess the capability of autologous DCs loaded *ex vivo* with leukaemia-specific peptide (b3a2 type) to stimulate anti-tumour immunity, wherein mature and immature pulsed DCs administered in different occasions; intravenously and intradermally. Results demonstrated that the vaccine was well tolerated, with no major adverse reaction observed. In addition, a peptide-specific cellular immune response was generated in all three patients, however, there was a weak clinical response (assessed by detection of *BCR-ABL1* FISH and Ph<sup>+</sup> chromosome in patients bone marrow). Since it generated immunological response, it is therefore assumed that this type of vaccine needs further development to obtain the clinical benefits intended (Takahashi, T., Tanaka *et al.* 2003).

Another study has recently described the efficacy of autologous DCs pulsed with WT1 peptide from a phase I/II study for the treatment of advanced breast, ovarian, and gastric cancers (Zhang, W., Lu *et al.* 2019), wherein, the study provides evidence that patients can be effectively vaccinated with autologous DCs pulsed with WT1 peptide with two doses of vaccine administration per week. The result showed that the vaccine was well tolerated with no serious toxicity noticed and that the clinical response included stable disease in seven out of ten patients, Karnofsky Performance Scale scores were increased, and radiology scan image demonstrated shrinkage in tumour size in three of seven patients. Importantly, the immunological responses to

this vaccine were significantly correlated with lower MDSCs in comparison to the pre-treated peripheral blood.

### 1.2.3.2.3 Peptides/protein-based vaccine

The development of antigen/protein-based vaccines has been an attractive area in the field of cancer research since the identification of various TAAs expressed by many cancerous cells (Parmiani, De Filippo *et al.* 2007). The principle of which, generally relies on *in vivo* pulsing of synthetic (exogenous) peptides onto MHC molecules to stimulate T cells (Bertram 2000), but they can also be used *in vitro* to pulse DCs before being re-infused back into the patient's circulation. The main benefit of these vaccines are the relative low cost and the ease to monitor the immune response upon administration of such kind of vaccines (Dermime, Gilham *et al.* 2004). However, the main two disadvantages of this type of vaccine are HLA-restriction and the development of tolerance.

Several factors have been found to influence peptide/protein-based vaccine efficacy, and these include: Firstly, peptide length; under this category, short sequences peptides are found to be directly presented by MHC class I (as they do not need processing) and generate CD8<sup>+</sup> T cell response which has been found to be transient and functionally impaired. This impairment could be attributed to peptide uptake and presentation by non-professional APCs that lack the appropriate co-stimulation signal leading to dysfunctional T cell immune response (Bijker, van den Eeden *et al.* 2007). Whereas longer peptide needs to be processed to smaller peptides before being presented and therefore long peptides offer the benefit of delivering different MHC class II and MHC class I epitopes, consequently the latter strategy has been found to trigger stronger and more durable immune response than the short sequence regime (Rosalia, Quakkelaar *et al.* 2013, Bijker, van den Eeden *et al.* 2007). This concept is of crucial importance in vaccine development because efficient immune responses against a given antigen require an integrated responses of both T helper CD4<sup>+</sup> and cytotoxic CD8<sup>+</sup> cells, wherein, the former produces cytokines such as TNF- $\alpha$ , IL-2, IFN- $\gamma$  to promote the proliferation of the latter cells and support subsequent cytolytic function (Gattinoni, Klebanoff *et al.* 2005, Kim, H. P., Imbert *et al.* 2006). Whole protein vaccination strategy, on the other hand, thought to offer larger number of presented epitopes; however, Melief's group reveals that long peptide sequence vaccines rather than the entire protein produce stronger immune response against HPV (Rosalia, Quakkelaar *et al.* 2013). Secondly, number of epitopes encompassing peptide vaccine: With identification of large number of immunogenic epitopes derived from TAAs, it is now possible to incorporate series of overlapping epitopes in a single vaccine called multi-epitope vaccine, which is found to be an ideal approach in vaccination settings against tumours and viruses (Buonaguro, HEPAVAC Consortium

2016). Interestingly, multi-epitope vaccines have many advantages over single epitope vaccines or classical vaccines (Lu, Meng *et al.* 2017, Saadi, Karkhah *et al.* 2017) indeed: i) they can stimulate multiple clones from various T cell subsets because they express multiple MHC-restricted epitopes that can be recognised by different TCRs, ii) they can induce strong humoral and cellular immune responses simultaneously due to co-expression of B-cell, CTLs, T helper cells epitopes, iii) they can expand the spectra of targeting tumours or viruses because they could express multiple epitopes from different tumour or virus antigens, and iv) they can decrease undesirable components of immune responses that could activate pathological immune responses and/or adverse activities. Therefore, a well-designed multi-epitope vaccine should carry considerable prophylactic and therapeutic agents against cancer and viral infection (Zhang, L. 2018). The third factor that is found to improve peptide-based vaccine is amino acid sequence within the peptide itself; in this aspect, modifying one or more amino acid sequence in some peptides can significantly improve peptide binding affinity toward the MHC molecule or to the TCR (Yu, Z., Restifo 2002).

Many other factors have been found to affect peptide-based vaccine, such as the route of the vaccine administration, frequency of vaccination, prime-boost immunisation, and usage of appropriate adjuvants (Sultan, Fesenkova *et al.* 2017).

There is a growing body of evidence showing that WT1 peptide-based vaccines may become a reliable, safe and cure-oriented therapy for treating patients with CML who have residual disease, particularly those who are resistant to TKIs. As is the case with a CML patient who was treated with WT1-based vaccine, the patient developed WT1-specific CTLs in the peripheral blood (Oji, Yusuke, Oka *et al.* 2010). The vaccine was administered 22 times over 18 months, and lead to remarkable decrease in the *BCR-ABL1* transcripts to major molecular response level, indicating its beneficial effects on minimal residual disease (Saitoh, Narita *et al.* 2011).

### **1.2.3.3 Harness the synergistic interaction between targeted therapy and immunotherapy in CML**

Although imatinib therapy has significantly transformed the outlook of CML disease, in fact, it is not able to eradicate Philadelphia positive HSC, and drug withdrawal rapidly precipitates relapse in a high proportion of patients with CML, in addition resistance to imatinib which is estimated to happen in approximately 20% of patients, often occurs during the first 5 years of treatment. Hence, there is a growing need to combine imatinib with immunotherapy as this may exert a synergistic effect which will be able to harness anti-tumour immune responses to induce definitive cure in a high percentage of patients and overcome disease resistance by eradication of the quiescent HSCs population.

Harnessing the adaptive immune arm in CML seems to be quite rationale since the impressive results of cure obtained upon introducing of DLI post-allo-SCTs. In addition to the evidence suggested by imatinib withdrawal in some patients who achieved a durable deep molecular response in spite of the presence of very low levels of leukaemic cells (Lemoli, Salvestrini *et al.* 2009), this implies that immunological governor has played a critical role in minimizing cancerous cells load and aid maintaining a complete molecular response (Ross, Branford *et al.* 2010), and hence this immune response could be boosted by immunotherapy.

In those patients who have achieved durable deep molecular response, it is important to assess CML specific T cell responses directed to specific CML antigens as it would help determine the role of imatinib-induced T cells in the ultimate cure of CML. Several clinical trials have been conducted most of which employed vaccines encompassing epitopes spanning the *BCR-ABL1* fusion region (Li, Y., Lin *et al.* 2012, Greiner, Schmitt 2008), wherein, phase I and phase II trials on patients who were treated concomitantly with imatinib and vaccines demonstrated development of cellular response against *BCR-ABL1* epitopes led in clinical responses (Bocchia, Gentili *et al.* 2005, Cathcart, Pinilla-Ibarz *et al.* 2004). However, unlike *BCR-ABL1* peptides, which are presented by a limited number of HLA molecules, other antigens, either selectively expressed or overexpressed in CML cells, are of particular promising candidates for therapeutic approaches. Among them, the WT1 antigen, is an attractive target for immunotherapeutic interventions in CML (Thielen, van der Holt *et al.* 2013, Shinohara, Takahashi *et al.* 2013, Mahon, Réa *et al.* 2010) because of its overexpression in the majority of leukaemias and solid tumours and its selective expression in bone marrow HSCs but not in somatic tissue (Sato, Onai *et al.* 2009). In addition to WT1, several other antigens have also been reported in CML, including proteinase 3 and members of the cancer testis antigen family, such as PRAME (Quintarelli, Dotti *et al.* 2011) and HAGE (Adams, Sahota *et al.* 2002).

Considering the observations reported above, CML has been described as one of the cancer most susceptible to immunological manipulation (Vonka, Petrackova 2015). Combined and integrated immunological interventions of imatinib, vaccines targeting overexpressed TAAs, TNF- $\alpha$ , immune checkpoint inhibitors, and CAR-T cells have raised the hope for treatment-free remission (TFR) in CML patients in the near future (Chiba, Mizuguchi *et al.* 2014), as it is illustrated in Figure 1.8.

It is assumed that if many CML patients can be cured and safely discontinuing imatinib, a dramatic reduction in the medical expense will be provided for both patients and governments.

Among these antigens, HAGE and WT1 antigens have been selected for this project as suitable target for immunotherapy in CML. We hypothesise that the use of such vaccines together with imatinib would help cure patient with CML in term of eradication of MRD and overcome TKI resistance by eradication of the LSCs.

**This image has been removed by the author for copyright reasons**

**Figure 1.8: Schematic representation proposes that harness the synergistic interaction between targeted therapy and immunotherapy in CML leads to treatment-free remission.**

Combined and integrated immunological interventions of imatinib, vaccines targeting overexpressed TAAs, TFN- $\alpha$ , immune checkpoint inhibitors, and CAR-T cells has been raising the hope for treatment free remission in CML patients. Image is reused with a reference from (Chiba, *et al.* 2014).

## **1.3 Helicase Antigen (HAGE)/ (DDX43)/ (CT-13)**

Helicases have been regarded as molecular motors moving along the nucleic acid backbone separating (unwind) the two nucleic acid strands into single oligonucleotide strand utilising energy generated by ATP hydrolysis. The functions of helicases involve many cellular processes of nucleic acid metabolism, such as replication, repair, transcription, recombination and chromosome segregation (Jarmoskaite, Russell 2014, Linder, Jankowsky 2011, Lohman, Bjornson 1996). In general, different strategies have been used to categorise helicases; firstly, according to the direction of the nucleic acid that they bind to and move along, helicases are classified as (5' to 3') or (3' to 5') direction. Based on substrates that they catalysed, helicases are grouped as DNA and or RNA helicases (Pyle 2008). Depending on their conserved motifs, they are classified into 6 super-families, of which, SF2 is the major superfamily that embraces DEAD-box helicases (Singleton, Dillingham *et al.* 2007). Structurally, DEAD-box helicases possess nine conserved motifs; Q-motif (unique for D-E-A-D helicases), motif-I, motif-Ia, motif-Ib, motif-II, motif-III, motif-IV, motif-V,

and motif-VI, wherein motif-II contains four amino acids (asp-glu-ala-asp) and from which the D-E-A-D name is derived. Q-motif, motif-I, motif-II and motif-VI are involved in ATP binding and hydrolysis whereas motif-Ia, motif-Ib, motif-III, motif-IV, and motif-V could involve in RNA interaction and intramolecular rearrangements essential for remodelling activity (Tanner, N. K., Cordin *et al.* 2003).

Helicase Antigen (HAGE), also called D-E-A-D-box polypeptide 43 (DDX43), a 73kDa protein and 648 amino acids length, is encoded by the DDX43 gene on chromosome 6 (6q12-q13 gene). HAGE is a Cancer-Testis antigen (CT-13) and a member of the DEAD box family of ATP-dependent RNA helicases, it was first identified in human sarcoma cell line in 2002 wherein authors found that HAGE was associated with tumour-specific expression (Martelange, De Smet *et al.* 2000).

As it is shown in Figure 1.9, HAGE holds signature motifs of SF2 RNA helicases which include, including motif-Q, motif-I, motif-Ia, motif-Ib, motif-II, motif-III, motif-IV, motif-V, and motif-VI, as well as conserved motifs Ic, Va, and Vb that also exist in other particular proteins of DEAD-box family. In addition to the helicase core domain that is situated in its C terminus, HAGE also has (KH) domains at its N terminus with its distinguished sequence, GXXG, (Valverde, Edwards *et al.* 2008), a domain that has been recently found to be required for full nucleic acid unwinding function (Talwar, Vidhyasagar *et al.* 2017).

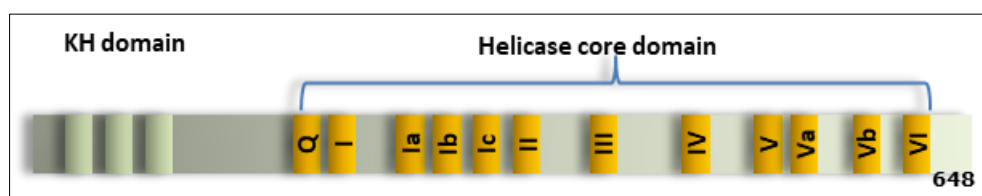


**Figure 1.9: Schematic representation demonstrates DDX43 protein structure.**

The figure demonstrates conserved helicase motifs located at C terminus are coloured yellow, one potential KH domain located at N-terminus and coloured pink, and two GXXG motifs coloured olive green.

Since it is a relatively new antigen, very little is known about its actual function, however, RNA metabolism, regulation of cell cycle, spermatogenesis and embryogenesis are among possible functions that HAGE might exert. HAGE overexpression has been frequently related with tumorigenesis. Recently, Lin and colleagues, 2018 demonstrated that DDX43 overexpression in CML cell lines (K562) promoted cells survival and colony formation, inhibited apoptosis, enhanced tumorigenesis, as well as CML progression, whereas silencing of HAGE resulted in inhibition of cell survival and tumorigenesis (Lin, J., Ma *et al.* 2018), thereby implicating HAGE as being required for CML cells survival.

HAGE overexpression has been reported in various solid and haematological malignancies but low/absent expression in normal tissues, except testis (Mathieu,

Linley *et al.* 2010, Martelange, De Smet *et al.* 2000), indicative of its high tissue specificity and therefore making it a good target for immunotherapy (Lin, J., Ma *et al.* 2018). Details on HAGE over expression in cancer in general, and in CML in particular, will be further discussed in Chapter-3.

Regarding HAGE immunogenicity, limited work has been performed to determine the presence of HAGE specific T cells in CML patients. In our group, previous students, however, were able to identify several immunogenic HAGE-derived HLA-A2 and HLA-DR1 peptides which were found to be naturally processed. Tumorigenicity of HAGE as a novel DNA vaccine was previously also assessed in our group, wherein a tumour model was developed in double transgenic HHDII/DR1 mice using B16 cells that artificially overexpressed HAGE, and as a "proof-of-concept", authors found that B16 tumour growth significantly slowed down by HAGE DNA vaccine <http://irep.ntu.ac.uk/id/eprint/33>, <http://irep.ntu.ac.uk/id/eprint/34884/>.

## 1.4 Wilms tumour antigen (WT1)

The oncogenic WT1 antigen, ~50 kb in length, is a zinc finger transcription factor, encoded by WT1 gene which is located on the short arm of chromosome 11p13. In mammals, WT1 gene encodes proteins from as many as ten exons and hence, 36 isoforms have been found. A combination of events, such as alternative transcription start sites, translation start sites, splicing and RNA editing, have all contributed to this wide-range diversity. These isomers seem to have various shared but also distinctive roles in the development of organs during embryonic development (Hastie 2017).

WT1 is, indeed, involved in the regulation of important cell activities, such cell growth and differentiation, apoptosis, and organ development (Sugiyama 2001, Oka *et al.* 2006).

In tumours, a plethora of studies have reported the potent contribution of WT1 in essential processes of tumorigenesis, such as cells proliferation, progression, invasion, metastasis and angiogenesis in different types of cancer, and it has also been demonstrated that silencing WT1 causes inhibition of cell proliferation and subsequent cancer cells death (Barbolina, Adley *et al.* 2008, Brett, Pandey *et al.* 2013, Toska, Roberts 2014, McCarty, G., Awad *et al.* 2011). Suggesting that WT1 is required for cancer cell survival.

WT1 upregulation has been well-documented in a variety of haematogenous and solid malignancies, including acute and chronic myelogenous leukaemia, myelodysplastic syndrome and acute lymphocytic leukaemia, glioblastoma, breast cancer, lung cancer, thyroid cancer, colorectal cancer, bone/soft tissue sarcoma, renal cancer, and head/neck squamous cell carcinoma (Oka *et al.* 2006), among these cancer WT1 was

found to be particularly upregulated in CML, more details on WT1 expression in CML can be found in Chapter-3.

Moreover, in patient bearing cancer, WT1-specific CTLs, helper T cells and anti-WT1 antibodies both IgG and IgM-types have been detected (Oji, Y., Kitamura *et al.* 2009, Oka, Tsuboi *et al.* 2004, Qi, Zhang *et al.* 2015).

More importantly, WT1 vaccine have already been used in clinical trials for treating patients with haematological malignancies, such as acute myeloid leukaemia (AML), myeloma and myelodysplastic syndrome (MDS), and solid tumours, such as brain tumour, breast cancer, thyroid cancer, colorectal cancer, leiomyosarcoma (Oka, Tsuboi *et al.* 2008). Clinical and immunological responses generated from many WT1-based vaccine clinical trials were reviewed and assessed by Van Driessche and colleagues, 2012, wherein, the authors concluded that vaccine-induced immunological responses were detected virtually in all clinical trials studied where objective clinical responses in the vaccinated patients with solid tumours and haematological malignancies were observed in 46% and 64% respectively, and most importantly, immunogenicity of WT1-based cancer vaccines was found in 35% and 68% of solid tumours and haematological malignancies cases, respectively. These findings demonstrate the feasibility of WT1-based vaccines as an immunotherapeutic strategy in both haematological and solid cancers and dominant responses are found to be higher in the haematological malignancies (Van Driessche, Berneman *et al.* 2012).

The concept of combination of imatinib with WT1 to treat imatinib-resistant cases is quite feasible, since a study conducted by Narita and colleagues, 2010 described how a CML patient who was in chronic phase and developed resistance to imatinib after 2.5 years post therapy (Narita, Masuko *et al.* 2010) was able to achieved complete molecular remission after 11 months of every 4 week administration of modified type 9mer WT1 peptides (CYTWNQMNL/HLA-A2 restricted) in combination with imatinib. WT1/MHC tetramer<sup>+</sup>CD8<sup>+</sup> CTLs developed as early as after the second dose of the WT1 peptides and continued circulating in patient blood on 14<sup>th</sup> month post-vaccine withdrawal. Moreover, *in vitro* cytotoxicity study of the candidate lymphocytes demonstrated the capability of WT1-specific cells to kill WT1 expressing leukaemic cells in a MHC class I restricted manner. This study reveals the rationale to implement WT1-based vaccine in combination with TKI in treating patients suffer from imatinib-resistant.

## 1.5 Aims and hypothesis of the study

The overall aim and overarching theme of my PhD project was the development of a combined HAGE and WT1 based vaccine for the treatment of CML. We hypothesised that a combination of HAGE and WT1 vaccines will be more effective against established CML tumours expressing both antigens than a vaccine incorporating peptides derived from either of these antigens alone. Finding such vaccine could help patients who are on imatinib therapy to achieve a “definitive cure” by eliminate residual CML cells, patients who developed multi-TKIs drugs resistance at any phase of the disease, and patients who are in crisis phase and not eligible to SCT.

### **The specific objectives were:**

1. To validate HAGE and WT1 antigens as potential immunotherapeutic targets by measuring their expression pattern in samples from patients with CML and in human cancer cell lines at the mRNA and protein level experimentally and from publicly available clinical datasets. The results of these studies will be shown and critically discussed in Chapter-3.
2. To assess the immunogenicity of HAGE and WT1 derived peptides individually and in combination using the double transgenic HHDII/DR1” humanised” mice. The results of these studies will be shown and critically discussed in Chapter-4.
3. To generate genetically engineered CML derived targets that have been either induced or inhibited the expression of HAGE and/or WT1 proteins. These modified cells were utilised as suitable targets for assessing in *in vitro* cytolytic effects of the HAGE and WT1 derived CTLs. The results of these studies are detailed in Chapter-5.
4. To assess the ability of CD8<sup>+</sup> CTLs derived from spleens of vaccinated mice using either HAGE-ImmunBody® or WT1-ImmunBody® vaccines or both to recognise and kill relevant targets. The results of these studies are detailed in Chapter-6.
5. To provide a “proof-of-concept” for the anti-tumour efficacy of the vaccine in a prophylactic and therapeutic tumour model using dual HAGE<sup>+</sup> and WT1<sup>+</sup> expressing “humanised” B16 cells, in which murine MHC was knocked-out and replaced by the HHDII/HLA-DR1 construct. These experiments will be covered in Chapter-7.

## 2 Chapter II: Material and methods

### 2.1 Materials and Reagents

All reagents were stored as per manufacturer instructions and used before the end of the shelf life and the expiry date.

<b>2.1.1. Cell culture media</b>	<b>Supplier</b>
IMDM, RPMI 1640, DMEM	SLS (Lonza)
McCoy's 5A	SLS (Lonza)
Opti-MEM® I Reduced Serum Medium	Thermo Fisher

<b>2.1.2. Supplements to media</b>	<b>Supplier</b>
Foetal calf serum (FCS)	Fisher (GE Healthcare)
L-Glutamine	SLS (Lonza)
D-glucose	Sigma
HEPES	SLS (Lonza)
2-mercaptoethanol	Sigma
Sodium Pyruvate	SLS (Lonza)
GM-CSF	PeptoTech
Insulin	Sigma
transferrin	Sigma
β2-Microglobulin from human urine	Sigma
Recombinant human IFN-γ protein	R&D system

<b>2.1.3. Cell culture related reagents</b>	<b>Supplier</b>
Dimethyl sulfoxide (DMSO)	Insight Biotechnology
Dulbecco's phosphate buffered saline (DPBS)	SLS (Lonza)
Trypan Blue solution 0.4%	Sigma
Trypsin/Versene	SLS (Lonza)
Trypsin from porcine pancreas	Sigma
EDTA 0.5M	Ambion
Dextran sulphate	Sigma

<b>2.1.4. Antibiotics and antifungal</b>	<b>Supplier</b>
Geneticin	Sigma
Hygromycin	Sigma
Zeocin	Invitrogen
Puromycin	Sigma
Geneticin (G418)	Promega
Penicillin/Streptomycin	SLS (Lonza)
Ampicillin	Sigma
Pen/strep antibiotic solution	SLS (Lonza)
Fungizone (amphotericin B)	Promega

<b>2.1.5. Adjuvants, peptides, ILs and Supplier toxins</b>	<b>Supplier</b>
Incomplete Freund's adjuvant (IFA)	Sigma
CPG	Eurofins Genomics
Peptides	GeneScript
Lipopolysaccharide (LPS)	Sigma
Staphylococcal Enterotoxin B (SEB)	Sigma
Mitomycin C	Sigma
Collagenase type1 from Clostridium histolyticum	Sigma
$\beta$ 2-Microglobulin from human urine	Sigma
Recombinant Human IFN- $\gamma$ Protein	R&D system

<b>2.1.6. Chemical reagents</b>	<b>Supplier</b>
Acetic acid	Fisher Scientific
Anhydrous ethanol	Sigma
Agar	Bioline
Ammonium Persulphate (APS)	Geneflow
Agarose	Bioline
Avidin D solution	Vector Laboratories
Biotin solution	Vector Laboratories
Bovine serum albumin (BSA)	Merck
Bromophenol blue	Arcos Organics

Butane	Fisher Scientific
Brefeldin A	BioLegend
CRYO-EM-BED Embedding compound	Bright
Calcium chloride (CaCl <sub>2</sub> )	Sigma
Chromium-51	Biosciences
Clarity Western ECL Substrate	Bio Rad
dNTP	Promega
M-MLV Reverse transcriptase	Promega
RNasin ribonuclease inhibitor	Promega
DNA ladder (1kp Plus)	Promega
DAPI VECTASHIELD Mounting media	Vector Laboratories
Double distilled water (ddH <sub>2</sub> O)	Barnstead, Nanopure
Ethanol	Fisher Scientific
Ethyl alcohol absolute	VWR chemicals
Ethyldiamine tetraacetic acid (EDTA)	Sigma
Ficoll Paque	GE Healthcare Life Sciences
Glycerol	Sigma
Glycine	Sigma
Gold micrpcarrier (1.0mm)	BioRad
Goat serum	Sigma
Glacial acetic acid	Sigma
Hydrochloric acid (HCl)	Fisher Scientific
heparin	Sigma
Horse serum	Vector Laboratories
Isopropanol	Sigma
LB broth with agar	Sigma
LB broth	Sigma
Liquid nitrogen	BOC
Marvel skimmed milk	Co-operative
Murine IL-2	Sigma
Monensin	BioLegend
Methanol	Fisher Scientific

Orange-G	Sigma
Paraformaldehyde	Arcos
Phosphate Buffer Saline (PBS) Tablets	Oxoid
Polyvinyl pyrrolidone (PVP)	Sigma
Protein Assay Dye Reagent Concentrate	Bio-Rad
Propidium iodide	Sigma
Protease Inhibitor Cocktail	Sigma
Protogel (30% Acrylamide mix)	Geneflow
Ponceau S	Sigma
Polybrene	Sigma
p-dimethylaminobenzaldehyde	Sigma
Sodium chloride (NaCl)	Calbiochem
Sodium dodecyl sulphate (SDS)	Sigma
Sodium Hydrogen Carbonate (NaHCO <sub>3</sub> )	Fisher Scientific
Sodium hydroxide (NaOH)	Fisher Scientific
Solution 18	ChemoMetec
SYBR green supermix	BioRad
SYBR® Safe DNA Gel Stain	Invitrogen
Spermidine	Sigma
2-methylbutane (isopentane)	Acro Organics
Tetraethylammonium bromide (TEAB) 25mM	Sigma
TEMED	Sigma
10x Transfer buffer	Gene Flow
10x Running buffer	Gene Flow
Trichloro-acetic acid (TCA)	Sigma
Triton-X-100	Sigma
Tris	Fischer Scientific
Trizma base	Sigma
1M Tris-HCl	Invitrogen
Trizma (Tris) base	Sigma
TES	Sigma
Tryptone	Sigma
Tween-20	Sigma

<b>2.1.7. Immunochemical Reagents</b>	<b>Supplier</b>
Rabbit anti-human WT1	Abcam
Rabbit anti-human DDX43	Sigma
Mouse anti-human $\beta$ -actin	Sigma
Anti-Rabbit IgG HRP-linked Ab	Cell Signalling
Anti-Mouse IgG HRP-linked Ab	Cell Signalling
D-Luciferin	PerkinElmer
Precision protein TM strep Tactin –HRP conjugate	Bio Rad
Alexa - FluroR 488 goat anti rabbit IgG	Invitrogen
Alexa FluroR 568 goat anti rabbit IgG	Invitrogen
Alexa Fluor 488 donkey anti-rabbit IgG	Abcam
pan-specific biotinylated secondary anti-mouse/rabbit IgG antibody	Vector Laboratories
ABC kit streptavidin complex	Vector Laboratories
Mayer's Hematoxylin.	Sigma Aldrich
DPX mounting media	Sigma Aldrich

<b>2.1.8. Flow cytometer related reagents and kits</b>	<b>Supplier</b>
APC anti-human HLA-A2 Antibody	BioLegend
PE anti-human HLA-DR Antibody	BioLegend
Monoclonal Anti- $\beta$ 2m-FITC, antibody produced in mouse	Sigma
Brilliant Violet 421™ anti-mouse CD3	BioLegend
APC/CY7 anti-mouse CD8a	BioLegend
Alexa-fluor700 anti-mouse CD4	BioLegend
APC anti-mouse/human CD44	BioLegend
FITC anti-mouse CD62L	BioLegend
FITC anti-mouse CD357 (GITR)	BioLegend
OX-40 (CD134) PE	BioLegend
CTLA-4 (CD152) PE/Dazzle™ 594	BioLegend
LAG-3 (CD223) PerCp-Cy5.5	BioLegend
Tim-3 (CD366) PE-Cy7	BioLegend
APC anti-mouse CD279 PD-1	BioLegend

CD28	BD Biosciences
CD49d (Integrin $\alpha$ 4 chain)	BD Biosciences
FITC anti-mouse CD107a (LAMP-1) Antibody	BioLegend
PE anti-mouse TNF- $\gamma$	BioLegend
PE-eFluor <sup>®</sup> 610 anti- Ki-67	BD Biosciences
PerCP/Cy5.5 anti-mouse IL-2	BioLegend
PE/Cy7 anti-mouse IFN- $\gamma$	BioLegend
APC anti-human/mouse Granzyme B Recombinant	BioLegend
PE anti-human CD119 IFN- $\gamma$ R $\alpha$ Chain	BioLegend
Alexa Fluor <sup>®</sup> 488 anti-human MICA/MICB	BioLegend
PE anti-human CD178 (Fas-L)	BioLegend
PE/Dazzle <sup>™</sup> 594 anti-human CD80	BioLegend
PerCP/Cy5.5 anti-human HLA-E	BioLegend
PE/Cy7 anti-human HLA-G)	BioLegend
APC anti-human CD274 (B7-H1, PD-L1)	BioLegend
Alexa Fluor <sup>®</sup> 700 anti-human CD40	BioLegend
APC/Cy7 anti-human HLA-A, B, C	BioLegend
Pacific Blue <sup>™</sup> anti-human CD86	BioLegend
PerFix-nc Kit 150 tests	Beckman Coulter
Foxp3 / Transcription Factor Staining Buffer Set	Thermo Fisher
FcR Blocking Reagent	Miltenyi Biotec
LIVE/DEAD Fixable Violet Dead Cell Reagent	Thermo Fisher
OneComp eBeads Compensation Beads	Thermo Fisher
Flow check	Beckman Coulter
Flow set	Beckman Coulter
Isoton sheath fluid	Beckman Coulter

<b>2.1.9. Reagent kits</b>	<b>Supplier</b>
Dynabeads Untouched mouse CD3+ T cell isolation	BioLegend
Murine IFN- $\gamma$ cytokine ELISpot kit	Mabtech
Cell Line Nucleofector <sup>®</sup> Kit V	Amax / Lona
Lipofectamine 3000 Transfection Reagent	Invitrogen
Lipofectamine <sup>®</sup> LTX & PLUS <sup>™</sup> Reagent	Invitrogen
RNeasy Mini Kit (250)	QIAGEN
QIAGEN QIA-filter Plasmid Midi	QIAGEN
Protein assay kit	BioRad

<b>2.1.10. Cell lines</b>	<b>Suppliers</b>
K562	ATCC
LAMA-84	Tubingen
KCL-22	Anthony Nolan
K812	Anthony Nolan
TCC-S	Dr Barbara Guinn
PCI 13	Pittsburgh
HEK293	Thermo Scientific
KYO-1	Anthony Nolan
KASUMI	ATCC
KG-1	ATCC
MV4-11	DSMZ
THP-1	ATCC
AML-139	ATCC
SIG-M5	DSMZ
SUPB-15	DSMZ
Humanised B16 (Knocked out murine MHC, knock in of human MHC HHDII/DR1)	Scancell Ltd.

<b>2.1.11. Plasmids and mice</b>	<b>Suppliers</b>
PLenti-puro	Addgene
pLKO.1 puro	Addgene
Enveloped plasmid pMD2.G	Addgene
packaging plasmid psPAX2	Addgene
Pc DNA-3.1	Addgene
shRNA.WT1	Mission/sigma
HAGE ImmunoBody® (PDCORIG HIB HAGE 243-272/h2 huigG1+wt kappa)	Scancell Ltd.
W1 ImmunoBody® (P VITRO2-hygro-mcd)	Scancell Ltd.
HHDI/DR1 mice	Charles River laboratories

<b>2.1.12. Laboratory plastics and glassware</b>	<b>Suppliers</b>
Cell culture flasks (T25, T75, T175)	Sarstedt, UK
Coverslips	SLS
Conical flasks (50 mL, 100 mL)	Pyrex
Eppendorf tubes (0.5 mL, 1.5 mL, 2 mL)	Sarstedt, UK
FACS tubes	Tyco healthcare group
Falcon tubes (50 mL, 15 mL)	Sarstedt, UK
Filter tips (0.5-10 µL, 2-20 µL, 20-200 µL, 200-1000 µL)	Greiner bio-one/Sarstedt
Flat-bottom culture dishes (6, 24, 96-well)	Sarstedt, UK
Glass coverslips	SLS
Glass slides	SLS
Micro tips (0.5-10 µL, 20-200 µL, 200-1000 µL)	Sarstedt, UK
Magnetic cell separators Mini MACS	Miltenyi Biotech
Pasteur pipettes	Sarstedt, UK
Petri dishes	Sarstedt, UK
Rotor-Gene® Style 4-Strip Tubes and Caps, 0.1 mL 4-strip tubes and caps	Star lab
Pipettes (5mL, 10mL, 25mL)	Sarstedt, UK

PVDF blotting membrane	GE Healthcare, Life science
Scalpels	SLS (Swann Morton)
Serological pipettes	Sarstedt
Superfrost™ Microscope Slides	Thermo Scientific Fisher
Syringes (10mL,20mL)	Becton Dickenson
Multichannel pipette	Sartorius
Superfrost™ Microscope Slides	Thermo Scientific Fisher
Tefzel tubing	BioRad
Universal tubes (20mL)	Greiner
Western blot filter paper	Schleicher-Schuell
0.45 µm syringe filter	Sartorius
0.22 µm syringe filter	Sartorius
40 µm nylon strainer	Greiner
70 µm nylon strainer	Greiner
Plate L-shape spreader	Sigma
96 well Black microplate	PerkinElmer
96 well scintillator LumaPlate™	PerkinElmer
Nucleocuvette™ Vessels	Lonza

<b>2.1.13. Laboratory equipment</b>	<b>Suppliers</b>
4°C refrigerators	Lec
-20°C freezers	Lec
-80°C freezers	Revco/ Sanyo
96-well plate reader	Tecan
Autoclave	Rodwell
Bacterial cell orbital incubator	Stuart
Bacterial cell culture plate incubator	Genlab
Balance	Fisher
Cell culture incubator	Sanyo
Centrifuges	Sanyo, Eppendorf
Class II safety cabinets	Walker

4D-Nucleofector System (electroporator)	Lonza
Fluorescence microscope	ZEISS
Gallios™ flow cytometer	Beckman Coulter
G: BOX XT4: Chemiluminescence and Fluorescence Imaging System	Syngene
Haemocytometers	SLS
Heatblocks	Lab-Line
ImmEdge pen	Vector Laboratories
Light microscope	Nikon/Olympus
Microcentrifuge	MSE
Mo Flo™ cell sorter	Beckman Coulter
Nanodrop 8000 Spectrophotometer	Thermo scientific
Nucleocounter cell counting machine	Chemometec
pH meters	Metler Toledo
Pipettes and multichannel pipettes	Gilson, Star Labs, Eppendorf
Plate rocker	VWR, Stuart
Sonicator	VWR
Rotor-Gene Q real-time PCR cycler	Qiagene
Spectrophotometer for 96-well plate	Tecan ULTRA
Transfer tank	BioRad
Tubing prep station	BioRad
Ultrapure water dispenser	Barnstead
Vortex	Scientific industries
Water baths	Grant Bio
Laser Capture Microdissector	ZEISS

### 2.1.14. Buffers and gels

#### 2.1.14.1. LB agar plate

**For 1L**

LB broth with agar powder (sigma, L3147)	40g
ddH <sub>2</sub> O	Up to 1L
Autoclaved, cooled down to 50°C	
Ampicillin	50mg to the melted LB agar

Poured on Petri dishes, left to solidify and stored at 4°C for up to a week.

<b>2.1.14.2. LB broth</b>	<b>For 1L</b>
---------------------------	---------------

LB broth powder (Sigma, L3522)	40g
--------------------------------	-----

ddH <sub>2</sub> O	Up to 1L
--------------------	----------

Autoclaved, cooled down to 50°C before antibiotic addition

Stored at 4°C for up to a week

<b>2.1.14.3. TRIS-EDTA (TE) buffer</b>	<b>For 500mL</b>
--	------------------

1 M Tris pH 8	5mL
---------------	-----

0.5 M EDTA pH 8	1mL
-----------------	-----

ddH <sub>2</sub> O	Up to 500mL
--------------------	-------------

<b>2.1.14.4. TRIS-Acetate EDTA (TAE) buffer</b>	<b>For 50x</b>
---	----------------

1 M Tris base	242g
---------------	------

Disodium EDTA	18.61g
---------------	--------

Glacial acetic acid	57.1mL
---------------------	--------

<b>ddH<sub>2</sub>O</b>	Up to 1L
-------------------------	----------

Dilute to 1x using distilled water before use, store at 4°C

<b>2.1.14.5. 4X SDS-PAGE loading buffer</b>	<b>For 10mL</b>
---	-----------------

1M Tris-HCl pH 6.8	2.4mL
--------------------	-------

Sodium dodecyl sulfate (SDS)	0.8g
------------------------------	------

Glycerol	4mL
----------	-----

DTT	0.5mL
-----	-------

Bromophenol blue	4mg
------------------	-----

ddH <sub>2</sub> O	3.1mL
--------------------	-------

Aliquots were stored at -80°C.

<b>2.1.14.6. 5% Stacking gel</b>	<b>For 4mL</b>
----------------------------------	----------------

ddH <sub>2</sub> O	2.7mL
--------------------	-------

30% Acrylamide mix	0.67mL
--------------------	--------

1.5M Tris-HCL (pH 6.8)	0.5mL
------------------------	-------

10% SDS	0.04mL
---------	--------

10% Ammonium persulfate	0.04mL
-------------------------	--------

TEMED	0.004mL
<b>2.1.14.7. 10% Resolving gel For 10mL</b>	
H <sub>2</sub> O	4.0mL
30% Acrylamide mix	3.3mL
1.5 M Tris-HCL (pH 8.8)	2.5mL
10% SDS	0.1mL
10% Ammonium persulfate	0.1mL
TEMED	0.004ml
<b>2.1.14.8. 10 X TRIS-buffered saline (10 X TBS) For 1L</b>	
Trizma base	24.2g
NaCl	80g
ddH <sub>2</sub> O	Up to 1L
Adjust pH to 7.6 with concentrated HCl.	
<b>2.1.14.9. TRIS-buffered saline (TBST) For 1L</b>	
10 X TBS	100mL
ddH <sub>2</sub> O	900mL
<b>2.1.14.10. Laemilli buffer Volume</b>	
10% SDS (w/v) (4% final)	4mL
Glycerol (20%)	2mL
1M Tris-HCL (125mM)	1.2mL
10% 2-mercaptoethanol	1mL
Distilled water	0.8mL
<b>2.1.14.11. Ehrlich's reagent</b>	
p-dimethylaminobenzaldehyde	100mg
Glacial acetic acid	5mL

### **2.1.15. Preparation of glycerol stock**

30% sterile glycerol stock	250μL
Bacterial culture	250μL

Mix both in a 1.5mL Eppendorf sterile tube, and then dip it in a liquid nitrogen until completely frozen. Then transfer the tube into -80°C.

## 2.1.16. Primary culture media

### 2.1.16.1. Complete T cell media

### Concentrations

RPMI 1640	-
FCS	10%
L-Glutamine	1%
Pen-Strep	2%
HEPES	1%
Fungizone	0.00%
2-mercaptoethanol (to be freshly added)	50mM

### 2.1.16.2. Mojosort buffer

### Concentrations

Phosphate buffered saline (PBS), pH 7.2	1X
Bovine Serum Albumin (BSA)	0.5 % (w/v)
Ethylene Diamine Tetra-acetic acid (EDTA)	2mM

This solution then needs sterile filtering through a 0.2  $\mu$ M membrane.

## 2.1.17. Software

Rotor gene 6000 real-time PCR 1.7 software	Qiagene
Tecan microplate reader	Tecan
Live image (IVIS Spectrum Series)	PerkinElmer
ELISpot CTL software	CTL
GraphPad Prism 7	Graph Pad software
Kaluza 1.3 version	Beckman Coulter
NanoDrop™ 8000 Spectrophotometer	Thermo Fisher Scientific

## 2.2 Methods

### 2.2.1 Cell lines, media and cultures

Thawing of cryopreserved cells was the initial step in the cell culture process. It involved quick thawing of the required vials taken from either liquid nitrogen or  $-80^{\circ}\text{C}$  in the hood under sterile conditions. After that, the thawed cells were transferred dropwise into a centrifuge tube containing the desired amount of pre-warmed complete growth medium appropriate for the thawed cell line. Cells were then pelleted by centrifugation. The centrifugation speed and duration varies depending on the cell type. After centrifugation, the supernatant was aseptically decanted without disturbing the cell pellet and the cells were gently resuspended in an appropriate growth medium. The suspension was then transferred into an appropriate culture vessel and incubated into the recommended culture environment typically, at 5%  $\text{CO}_2$  in a humidified incubator at  $37^{\circ}\text{C}$ . For sub-culturing of suspension cells, culture flasks were incubated in an upright position. Once cells reached  $\sim 80\text{-}90\%$  confluency, the entire contents were then transferred into a collection tube and centrifuged for 5 minutes. Cell pellet was then re-suspended in cell-specific medium. According to the type of experiments, a specific amount from that suspension was then re-cultured into a fresh culture flask. Adherent cell lines were also employed in this project, such as HEK 293T cells for transfection experiments, PCI-13, as a positive control for HAGE expression, "humanised" B16 cell line ( $_{\text{h}}\text{B16}$ ) that were knocked-out for murine MHC and replaced by human MHC for *in vitro* and *in vivo* experiments. These cells were routinely passaged when cell density reached  $\sim 80\%$  confluency. Medium from the flask was discarded and cells were washed twice with Dulbecco's phosphate buffered saline (DPBS). Cells were then detached by incubating with 0.05 % trypsin mixed with 0.02 % versene for (v/v) 5-15 minutes at  $37^{\circ}\text{C}$ . Following trypsinisation, an equal amount of FCS-containing medium was immediately added to the cell culture flask, the cells were then transferred into a centrifuge tube and centrifuged at 400g for 5 minutes. The resulting cell pellets were re-suspended in fresh medium. Depending upon the required experimental purposes, a particular amount from that suspension was re-cultured into proper cell culture flasks and kept in a flat position. All cell lines (together with supplements and antibiotics) utilised in this study are summarised in Table 2.1. On daily basis, cultures were visually and microscopically examined for the assessment of growth density and exclusion of any microbial contamination.

With respect to cell counting and viability, either manual haemocytometry or automated nucleocounter cell counting was performed by staining the cells with trypan blue and solution 18 dye, respectively.

For a cryopreservation of stocks, cell pellets were re-suspended in freezing medium consisting of 90% FCS and 10% dimethyl sulfoxide (DMSO) with a final concentration of  $1 \times 10^6$  cells/mL/cryo-vial. Cells were then immediately frozen at  $-80^\circ\text{C}$  until further use. All culture procedures were performed under completely aseptic conditions.

**Table 2.1: Cell lines and media**

Name	Description	Media
K562	CML/expressing b3a2 (Goss, Lee et al. 2006)	IMDM+10% (v/v) FCS.
KCL-22	CML/expressing b2a2 positive (Goss, Lee et al. 2006)	RPMI+10% (v/v) FCS+2mM L-Glutamine
TCC-S	CML/expressing P210 and P190 BCR/ABL transcripts (Van Thanh, Xinh et al. 2005)	RPMI+10% (v/v) FCS+2mM L-Glutamine
CMLT-1	CML/expressing e13a2 (Volpe, Cignetti et al. 2007)	RPMI+10% (v/v) FCS+2mM L-Glutamine
LAMA-84	CML/expressing b3a2 (Haass, Kleiner et al. 2015)	RPMI+10% (v/v) FCS+2mM L-Glutamine
K812	CML/expressing b3a2 (Goss, Lee et al. 2006)	RPMI+10% (v/v) FCS+2mM L-Glutamine
KYO-1	CML/expressing b2a2 (Patel, H., Marley et al. 2008)	RPMI+10% (v/v) FCS+2mM L-Glutamine
KASUMI-1	AML, subtype M2	RPMI-1640+20% (v/v) FCS+ 2mM L-Glutamine.
KG-1	AML	RPMI+10% (v/v) FCS+2mM L-Glutamine
MV4-11	Biphenotypic; B myelomonocytic leukaemia	IMDM+10% (v/v) FCS
THP-1	AMoL	RPMI 1640 +10% FCS+1% L-Glutamine + 1% HEPES (5mL) +0.44% glucose (2.2mL)
AML-139	AMoL	IMDM with 0.005 mg/ml insulin, 0.005 mg/ml transferrin and 5 ng/ml GM-CSF, 95%; fetal bovine serum, 5%
SIG-M5	AMoL	IMDM +10% (v/v) FCS
SUPB-15	ALL	McCoy's 5A +20% (v/v) FCS
T2	lymphoblastoid cell line	RPMI+10%(v/v) FCS+2mM L-Glutamine.
PCI 13	Squamous cell carcinoma of the head and neck cell	RPMI+10%(v/v) FCS+2mM L-Glutamine
HEK293	Human embryonic kidney 293 cells	DMEM+10%(v/v) FCS+2mM L-Glutamine
<sup>h</sup> B16(HHDII <sup>+</sup> /DR1 <sup>+</sup> )	Murine melanoma (humanised)	RPMI 1640+10%(v/v) FCS+2mM L-Glutamine + 300µg/mL Hygromycin+500µg/mL Geneticin
<sup>h</sup> B16(HHDII <sup>+</sup> /DR1 <sup>+</sup> /HAGE <sup>+</sup> /Luc <sup>+</sup> )	Murine melanoma (humanised)	RPMI 1640 +10% FCS+1% L-Glutamine + 300µg/mL hygromycin+500µg/mL geneticin+ 550µg/mL zeocin+ 1µg/mL puromycin

## 2.2.2 Genetic manipulation: Gene Knock-in and knockdown

### 2.2.2.1 Dose-response curve for antibiotic selection (kill curve)

The generation of stable transfectants requires the uses of an antibiotic to select only cells that have acquired the antibiotic resistant gene as a part of a plasmid construct introduced during transfection. In order to achieve this, it is necessary to determine the minimum concentration of antibiotic needed to kill all non-transfected cells. An appropriate antibiotic was used according to the gene of resistance carried by the plasmid of interest. Cells were seeded in duplicates, in 6-well plates at a density of  $0.5 \times 10^6$  cells/mL and treated with serial antibiotic concentrations. Antibiotic containing selection medium was replenished every 2-3 days, and cells were checked for detection of significant cell death. The number of viable cells was determined by trypan blue exclusion assay and counted using a haemocytometer for each check. The minimum dose required to kill the non-transfected cell line was determined for each of the cell lines of interest and these doses are detailed in Table 2.2. It was found that 14-20 days were necessary for the antibiotic G418 to achieve maximum effect whereas 3 days with puromycin were sufficient.

**Table 2.2: Doses of the selective markers to generate a stable transfection**

Cells used	plasmid	Selection marker	Dose
K562	Pc DNA-3.1/HHDII	G418	2000 $\mu$ g/mL
K562/HHDII <sup>+</sup>	PLenti-Puro/HAGE	Puromycin (In addition to G418)	1 $\mu$ g/mL
TCC-S	shRNA/WT1	puromycin	1 $\mu$ g/mL
KCL-22	PLenti-Puro/HAGE	Puromycin	1 $\mu$ g/mL

### 2.2.2.2 Lipofectamine transfection

#### 2.2.2.2.1 LTX Lipofectamine transfection

This technique was carried out according to the manufacturer's instructions for the 24-well format of Lipofectamine transfection for suspension cells (Lipofectamine<sup>®</sup> LTX and PLUS<sup>™</sup> Reagent/ Invitrogen/ catalogue number:15338-030). For each well,  $0.1 \times 10^6$  cells in 0.5mL of complete growth medium were plated. On the day of the transfection, cell density was checked, and cells were used only if a confluency of  $\geq 80\%$  was reached. For each well, 0.5 $\mu$ g of DNA was diluted in 100 $\mu$ L of Opti-MEM<sup>®</sup> I Reduced Serum Medium. PLUS<sup>™</sup> Reagent was used to increase the efficacy of the transfection in a volume of 1:1 ratio to the DNA. Therefore, for each well, 0.5 $\mu$ L was

added directly to the diluted DNA and then incubated for 15 minutes at room temperature. After that, 2 $\mu$ L of Lipofectamine<sup>®</sup> LTX was added into the diluted DNA solution, mixed gently and incubated for 30 minutes at room temperature. This results in the formation of DNA-Lipofectamine<sup>®</sup> LTX complex. After that, 100 $\mu$ L from that mixture was directly added to each well and gently mixed by rocking the plate before being incubated in a CO<sub>2</sub> incubator at 37°C. An appropriate antibiotic was then added one day-post transfection.

### 2.2.2.2.2 Lipofectamine 3000 transfection

All Lipofectamine 3000 transfection was carried out in a similar manner to HEK-239T transfection, this will be elaborated in section:2.2.4.1, below.

### 2.2.2.3 Electroporation

The procedure was applied according to manufacturer's instructions for the electroporation technique using SF cell line 4D nucleofection™ Xkit/ Amaxa. 0.3X10<sup>6</sup> cells/mL were sub-cultured two days before the transfection. At the day of transfection, a pellet of 1X10<sup>6</sup> cells was obtained in a 1.5mL Eppendorf tube and the supernatant was then completely removed. Once the entire supplement was added to the Nucleofector™ Solution, the pellet was then carefully re-suspended. 5 $\mu$ g of plasmid DNA was then added and the mastermix of cells-DNA was carefully transferred to the bottom of Nucleocuvette™ Vessels avoiding air bubble formation. At that point, the cuvette was inserted into the electroporation machine and cells were immediately electroporated by selecting an appropriate Nucleofector™ Programme. Pre-loaded electroporation programmes suited for each cell line were determined by the supplier. In this experiment, Programme T-016 displayed on the electroporator screen was selected to electroporate K562 cells. After that, 500 $\mu$ L of pre-warmed appropriate medium was added to the suspension and the mixture transferred carefully to 1.2mL of pre-warmed medium plated in a 12 well-plate. At the same time, a positive control of 2 $\mu$ g of pmaxGFP™ Vector was run. At the end of the experiment, the plate was incubated in a humidified 37°C/5% CO<sub>2</sub> incubator for 24 hours. After 24 hours, an appropriate antibiotic was added.

**Table 2.3: Cells and plasmids used in electroporation**

Cells	Plasmid	Antibiotic
K562	5 $\mu$ g of Pc DNA-3.1/HHDII	2000 $\mu$ g/mL of G418
K562	2 $\mu$ g of pmaxGFP™ Vector (positive control)	N. A

## 2.2.2.4 PLentiviral transduction

### 2.2.2.4.1 HEK-293T transfection

1X10<sup>6</sup> of HEK-293T cells were grown in 4mL of cell dedicated medium in T25 flask. On the day of the transfection, cell confluency was confirmed to be no more than 70-80%. For each transfection, 20µL Lipofectamine 3000 (Invitrogen) and 500 µL Opti-MEM®I Reduced Serum Medium (Gibco) was mixed and incubated at room temperature for 30 minutes. A second mixture consisting of 8µg target plasmid (PLenti.Puro/HAGE), 6µg packaging plasmid psPAX2 (Addgene, catalogue number: 12260), 2µg envelope expressing plasmid pMD2.G (Addgene, catalogue number: 12259) and 12µL P3000 reagent was prepared, then both mixtures were carefully mixed, After that, the 4mL of medium from T25 flask containing HEK-293T cells was removed and replaced with 4mL fresh medium, and a 1mL of the transfection mixture. Cells were then incubated at 37°C/5%CO<sub>2</sub> for ~16 hours. On the next day, medium was replaced with fresh one (5mL/T25 flask) and incubated for 24 hours. On the next day, a supernatant (fraction 1) from the transfected HEK-293T cells was collected into a tube and filtered through a sterile 0.45µm syringe filter. Fraction 1 was aliquoted into 1mL cryovials and stored at -20°C. The procedure was repeated one day after to collect and store fraction 2.

### 2.2.2.4.2 Cells transduction

The aim of this experiment was to transfect K562/HHDII<sup>+</sup> cells (already containing Pc DNA-3.1/HHDII gene) and KCL-22 cells with the PLenti.Puro/HAGE plasmid. On the day of transfection, 0.5X10<sup>6</sup> cells were collected into a 15mL tube. The cells were pelleted and re-suspended in 500µL of cell-specific medium and 500µL of fraction 1 prepared from the previous section. This mixture also contained 8µL/mL of polybrene (Hexadimethrine bromide 1mg/mL in 0.9%NaCl) to increase the efficacy of the transduction. An empty plasmid control was also used, PLenti.Puro/empty vector, which contains the antibiotic resistant gene, puromycine, but does not contain the HAGE gene. Tubes then underwent hourly shaking in the first 6 hours, and then they were incubated overnight inside the viral incubator at 37°C/5%CO<sub>2</sub>.

**Table 2.4: Cells transduced by PLenti.Puro plasmid**

Cells	Plasmids	Puromycine dose	G418 dose
HHDII <sup>+</sup> K562	PLenti.Puro/HAGE	1µg/mL	2000µg/mL
HHDII <sup>+</sup> K562	PLenti.Puro/empty vector	1µg/mL	2000µg/mL
KCL-22	PLenti.Puro/HAGE	1µg/mL	-

On next day, cells were centrifuged, resuspended in medium containing 1µg/mL puromycin and 2000 µg/mL G418, transferred into a 24-well plate and incubated at 37°C/5%CO<sub>2</sub>. The transfection was then confirmed by Western blotting.

In a similar manner, two shRNA sequences targeting the human WT1 gene were ordered from MISSION/Sigma in a form of bacterial glycerol stock and used to knockdown WT1 from TCC-S cells, wherein supernatants (Fractions-1) from the respectively transfected HEK-293T cells was collected to transduce the TCC-S cells. After being transduced, cells were selected with 1µg/mL puromycin and assessed for WT1 expression.

## **2.2.3 Protein expression analysis**

### **2.2.3.1 Western blotting**

#### **2.2.3.1.1 Lysate preparation and protein assay for SDS-PAGE**

Briefly, cell pellets were washed twice with cold DPBS, lysed in bromophenol blue free-Laemmli lysis buffer and boiled for 15 minutes at 95°C to denature proteins, lysates were then immediately kept on ice. To determine the quantity of protein in the lysates obtained, a BioRad DC protein assay was performed following the manufacturer's protocol. Standards were prepared by serial dilutions of BSA diluted in bromophenol blue free-Laemmli lysis buffer. In brief, 25µL of Reagent S and Reagent A (1:40 dilution) was added to 5µL of standards and samples loaded in a 96-well plate in triplicates. 200µL per well of Reagent B was then added. The reaction was left to develop in the dark for 15 minutes at room temperature. Absorbance of the developed colorimetric reactions was read at 750nm on a Tecan 96-well plate reader. Cell lysates were then mixed with 10% of 2-mercaptoethanol and 10% of protease inhibitor cocktail, and 1% of bromophenol blue.

#### **2.2.3.1.2 SDS-PAGE and protein transfer**

A pre-calculated volume of sample giving 30µg of protein was loaded into each well of SDS-PAGE gel alongside 5µL of the ladder. Electrophoresis was run at 70V through the 4% stacking gel for 30 minutes, and then 90V through the 10% resolving gel (~two hours). Protein bands were then transferred onto PVDF membrane for 60 minutes at 100V in a cold room.

#### **2.2.3.1.3 Immunoprobings**

To make sure that proteins were successfully transferred, the membranes were stained with Ponceau S. Following this staining, the membrane was washed 5 times for 5 minutes with agitation using a washing buffer of 1XTBS and 0.1% Tween-20.

The membrane was then blocked with TBS-Tween containing 5% Marvel milk powder under constant agitation for 60 minutes at room temperature. Next, primary antibodies to detect the protein of interest and housekeeping protein (as a loading control) were added at a concentration recommended by the manufacturer's instructions outlined in Table 2.5. These primary antibodies were diluted in 5% Marvel milk powder in TBST. Blots were then kept rocking overnight at 4°C. The next day, membrane was washed 5 times for 5 minutes, and secondary antibodies were added according to the recommended dilutions by the suppliers (Table 2.6) and incubated under agitation for 2 hours at room temperature. After five washes, the membrane was developed using Clarity™ Western ECL Substrate (Bio-Rad, catalogues number:170-5061) and luminescence was detected by G:BOX XT4: Chemiluminescence and Fluorescence Imaging System.

**Table 2.5: Primary antibodies used in Western blot**

Antibody	Supplier	Product Code	Dilution
Rabbit anti-WT1	Abcam	Ab89901	1:1000
Rabbit anti-DDX43	Sigma	HPA031381	1:250
Mouse anti-β actin	Sigma	A5441	1:5000

**Table 2.6: Secondary antibodies used in Western blot**

Antibody	Supplier	Product Code	Dilution
Anti-rabbit IgG- HRP- linked antibody	Cell signalling	70745	1:1000
Anti-mouse IgG- HRP- linked antibody	Cell signalling	70765	1:1000
Precision protein™ strep Tactin –HRP conjugate	Bio Rad	161-0380	1:5000

### 2.2.3.2 Immunofluorescence assay (IF)

In a microcentrifuge tube,  $1 \times 10^5$  cells were collected, washed twice with cold DPBS and fixed with 1mL of chilled 100% methanol for 5 minutes at -20°C. After drawing a hydrophobic barrier, cells were smeared on a slide surface using the side of pipette tips. Once all the liquid had evaporated at room temperature, the slides were washed once with cold PBST for 5 minutes. For the blocking step, cells were incubated with a mixture of 1% BSA, 0.1% Tween-20, 10% normal goat serum, and 0.3M glycine in PBS for 30 minutes at room temperature. After giving three washes with PBST, slides were incubated with the primary antibody (Table 2.7) diluted in 1% BSA and 0.1% Tween-20 in PBS overnight at 4°C. After three washes, cells were incubated

with fluorescently labelled secondary antibody for one hour at room temperature (Table 2.8). Slides were then washed, and nuclei stained with mounting medium containing DAPI and finally visualised with a ZEISS laser microscope.

For staining adherent cells, hB16 cells were grown on glass cover slips, fixed by paraformaldehyde and permeabilised with Triton. After that, cells were blocked with BSA and incubated in the rabbit anti-WT1 antibody in BSA overnight at 4°C. On the next day, cells were incubated in donkey anti-rabbit IgG Alexa Fluor 488 for 1 hour in the dark. Cells on the coverslips were then mounted to slides using VECTASHIELD HardSet mounting medium with DAPI before they were imaged.

**Table 2.7: The primary antibodies used in Immunofluorescence assay**

Antibody	Supplier	Product Code	Dilution
Rabbit Anti-WT1	Abcam	Ab89901	1:50
Rabbit DDX43	Sigma	HPA031381	1:100

**Table 2.8: The secondary antibodies used in Immunofluorescence assay**

Antibody	Supplier	Product Code	Dilution
Alexa Fluor 488 goat anti-rabbit IgG	Invitrogen	A11008	1:1000
Alexa Fluor 568 goat anti-rabbit IgG	Invitrogen	A-11011	1:1000
Alexa Fluor 488 donkey anti-rabbit IgG	Abcam	ab150073	1:500

### 2.2.3.3 DAB immunochemical staining

In brief, the hB16 cells were grown on glass cover slips, fixed in 4% paraformaldehyde in PBS and permeabilised with 0.1% Triton in PBS. After that, cells were blocked with 2.5% horse serum and incubated with avidin D solution. Biotin solution was then added to cells and then they were incubated with the rabbit anti-WT1 antibody (1:200 dilution) in 2.5% horse serum overnight at 4°C. On the next day, cells were incubated in pan-specific biotinylated secondary anti-mouse/rabbit IgG antibody, washed, incubated in ABC kit streptavidin complex and then incubated in DAB solution. After that, cells were counterstained with Mayer's Hematoxylin. Cells on the coverslips were finally mounted to slides using DPX mounting medium before they were imaged.

### 2.2.3.4 Kynurenine assay

In this type of assay, IFN- $\gamma$  was used at 100ng/mL to induce the expression of IDO in various leukaemic cell lines at different time points. At each time point, pellets

were assessed for IDO expression in addition to WT1, HAGE, costimulatory and inhibitory molecules using RT-qPCR and flow cytometry, whereas the supernatants were collected to determine the Kynurenine concentration. Briefly, Kynurenine standards were prepared starting with 10 $\mu$ M L-Kynurenine and up to 200 $\mu$ M. For optimal measurements, standards were made in same medium used for culturing the cells and processed along with the samples. In 1.5mL Eppendorf tubes, 200 $\mu$ L of supernatants/standards were mixed thoroughly with 100 $\mu$ L of 30% Trichloro-acetic acid. After being centrifuged at 8,000g for 5 minutes at 4°C, 75 $\mu$ L of supernatants were transferred into 96-well flat-bottom plates and an equal volume of Ehrlich's reagent was then added. Finally, the plate was incubated for 20-30 minutes at room temperature and read at 495nm absorbance on a Tecan 96-well plate reader. All readings were blanked using corresponding cell culture medium.

## **2.2.4 Gene expression analysis**

### **2.2.4.1 RNA extraction**

Total RNA was isolated from cell lines following the manufacturer's instructions for the RNeasy Mini Kit (Qiagen, catalogue number: 04053228006121). Briefly, cell pellets were lysed by RLT buffer in a volume of 350 $\mu$ L for 5x10<sup>6</sup> cells. After ensuring that the lysates were properly homogenised, one volume (350 $\mu$ L) of 70% ethanol was then added to precipitate the RNA. This 700 $\mu$ L mixture was then transferred to a RNeasy spin column placed in a 2mL collection tube, followed by centrifugation for 15 seconds at 10,000 RPM. To wash the RNeasy spin column membrane, 700 $\mu$ L of RW1 washing buffer was added to the column and then centrifuged for 15 seconds at 10,000 RPM. A further two washes were performed with 500 $\mu$ L of RPE buffer. An additional spin using a clean 1.5mL collection tube was performed to remove any residual buffer. Finally, the column was placed in a new 1.5 mL collection tube and the RNA was eluted with 30–50 $\mu$ L RNase-free water. The quantity and purity of the produced RNA was evaluated using a NanoDrop 8000 Spectrophotometer.

### **2.2.4.2 cDNA synthesis**

2 $\mu$ g of RNA was reverse transcribed into cDNA along with 0.5 $\mu$ g of Oligo-dT (15) primers in a small 500 $\mu$ L Eppendorf tube. The tube was then heated to 70°C for 5 minutes and placed immediately on ice for at least 3 minutes. 15 $\mu$ L from a master mix consisting of 5 $\mu$ L of 5X Reaction Buffer, 1 $\mu$ L of dNTP (12.5mM), 25 units of RNasin ribonuclease inhibitor and 200 units of M-MLV reverse transcriptase (see Table 2.9), was then added to the tube. Nuclease free water was then added to make the final volume to 25 $\mu$ L. The mixture was then gently mixed and heated to 40°C for 60

minutes followed by stopping the reaction at 95°C for 5 minutes before storing at -20°C.

**Table 2.9: Master mix preparation for cDNA synthesis**

Contents	Volume for a single reaction
5x Reaction Buffer	5µL
M-MLV Reverse transcriptase	1µL
RNasin ribonuclease inhibitor	0.7µL
dNTP	1µL
Nuclease free	7.3µL
Total	15µL

### 2.2.4.3 Real time quantitative PCR (RT-qPCR)

RT-qPCR was used to assess the expression pattern of the genes of interest at mRNA level, (Table 2.10). For each reaction, 1µL of cDNA was mixed with 6.75µL of SYBR Green supermix, 0.5µL (5pmol) of the forward and 0.5µL (5pmol) of the reverse primer and 3.25µL of molecular grade water. Each sample was run in triplicate on a Rotor-Gene Q real-time PCR cycler. qRT-PCR setting started by a melting phase, followed by 40 cycles of a denaturation phase, annealing at the corresponding annealing temperatures and extension phases, and stopped at 4°C. The run was set to end upon completing 40 cycles, and a threshold of 0.06 was defined as the cut off for the definition of positive and negative signals in our analysis. For each sample, CT (cycle threshold) values were reported, where CT represents the cycle number at which the fluorescent signal intensity of a particular gene in the reaction crosses the setting threshold (i.e. exceeds background level), and hence the difference in CT values between samples and controls is termed as delta CT ( $\Delta CT$ ). The Relative gene expression was calculated using the formula:  $2^{-\Delta CT}$ . The reaction efficiency of WT1 primers was determined according to the qPCR results of five-fold serial template cDNA dilutions produced from K562 cells (at >97%). Whereas the reaction efficiency for HAGE primers were optimised by a previous researcher (Divya Nagarajan, previous PhD student).

**Table 2.10: Primers and annealing temperatures used for RT-qPCR**

Primers	Sequence	Annealing Temp
WT1 forward	GACTCATAACAGGTGAAAAGC	58°C
WT1 reverse	GAGTTTGGTCATGTTTCTCTG	
DDX43 forward	CAACACCTATTCAGTCACAG	58°C
DDX43 reverse	GACCAGATGAATAAATCCAGG	

GUSB forward	ACTGAACAGTCACCGAC	58°C
GUSB reverse	AAACATTGTGACTTGGCTAC	
β actin forward	CTCTTCCAGCCTTCCTTCT	61°C
β actin reverse	AGCACTGTGTTGGCGTACAG	
HAGE forward (codon optimised)	CCACATGCACTTTTCGACGAT	58°C
HAGE forward (codon optimised)	ATTCCTGGTCGGTTCCTCTG	
IDO forward	TTGTTCTCATTTCTGTGATGG	58°C
IDO reverse	TACCTTGATTGCAGAAGCAG	

#### 2.2.4.4 Agarose gel electrophoresis

For visualisation of DNA of interest by size, RT-qPCR products amplified from cDNA synthesised were run on 2% (w/v) agarose gel by electrophoresis. Briefly, 150mL of 1xTAE buffer was added to 3g agarose and mixed thoroughly. The mixture was then microwaved for 1-2 minutes until a well-homogenised melted agar was obtained. A SYBR safe dye (Invitrogen) was then added to the warm mixture at 4μL to each 50mL buffer (v/v). After that, the melted agarose was poured into a centre of a comb containing casting tray and left to solidify for an hour. During incubation time, a loading dye, Orange-G (sigma), was added at 3μL into each RT-PCR product together with DNA ladder. After careful removal of the comb from the gel assembly, samples and ladder were then loaded at 10μL per well and run at 60V for 2 hours. Bands were then visualised under UV light using a Syngene G-box.

### 2.2.5 Animals and immunisation

#### 2.2.5.1 Animals

The “humanised” double transgenic HHDII/DR1 mice (originally C57BL/6 mice), purchased from Charles River laboratories, were used as a host for testing the immunogenicity of the putative peptides. Animals were maintained inbred by ensuring they have a common F0 ancestor. Upcoming generations were bred at Nottingham Trent University animal house in accordance with the Home Office Codes of Practice for the housing and care of animals. The genotype of mice from different generations was periodically assessed.

#### 2.2.5.2 HAGE and WT1 Peptides

Using a web-based algorithm ([www.syfpeithi.de](http://www.syfpeithi.de)), the WT1 protein sequence was screened for peptides binding to HLA-A2. Peptides were then chosen according to their binding score. Hence, a 15 amino acid long peptide (VRDLNALLPAVPSLG) derived from the WT1 protein containing two known and previously published HLA-

A2 9-mer have been used to evaluate their capacity to induce immune response in the humanised HHDII/DR1 mice. Whereas for HAGE, a 30-mer long peptide (QTGTGKTLCYLMPGFIHLVLQPSLKGQRNR) derived from the HAGE (DDX43) protein has previously been identified by a previous student and shown to be immunogenic when used as an ImmunoBody® or combined with CpG/IFA adjuvants. Various class I and class II derived from this length was assessed. Details of these peptides are provided in Chapter-4 ([Section:4.3.1](#)). All peptides were synthesised by GenScript Ltd with a minimum purity of 80%. After being received, they were reconstituted in DMSO to a stock concentration of 10mg/mL and stored at -80°C until use.

### 2.2.5.3 Peptides-HLA-A2 affinity assay/T2 binding assay

A T2 peptide-binding assay was performed to evaluate the binding affinity of the HAGE and WT1 class I peptide sequences predicted by SYFPEITHI to the HLA-A2 molecule. Briefly, in a sterile 96-well rounded-bottom plate, T2 cells were plated and at  $0.05 \times 10^6$  cells/100µL in serum free RPMI medium supplemented with 3µg/mL human β2m in the presence of HAGE and WT1 class I peptides at a concentration of 10, 30, 50, 60 and 100µg/mL and incubated at 26°C overnight. The next day, T2 cells were washed and stained with APC anti-human HLA-A2 Antibody (Table 2.11) for 30 minutes at 4°C. Cells were then washed and stained with propidium iodide to exclude dead cells, and run immediately to assess HLA-A2 expression using Beckman Coulter Gallios™ flow cytometer.

**Table 2.11: primary antibody used in the T2 binding/dissociation assay**

Antibody	clone	Company	Catalogue #	Volume µL
APC anti-human HLA-A2 Antibody	BB7.2	BioLegend	343308	5µL/100µL

### 2.2.5.4 Peptides-HLA-A2 dissociation assay/Brefeldin A (BFA) decay assay

To evaluate the stability of the class I peptide-HLA-A2 complex on the cell surface, a BFA decay assay was performed as following: in a sterile 96-well plate, T2 cells were seeded overnight at a concentration of  $1 \times 10^6$  cells/mL in serum free RPMI medium containing 3µg/mL human β2m. Cells were cultured with either the candidate peptides at a final concentration of 50µg (as determined by T2 binding assay) or with DMSO as a negative control and incubated at 26°C overnight. On the next day, one batch of cells was washed and incubated with 10µg/mL BFA for 1 hour at 37°C (this batch was indicated as time 0). After incubation, cells were gently transferred into a

FACS tube, washed and stained with APC anti-HLA-A2 (BB7.2) fluorescent monoclonal antibody for 30 minutes at 4°C and analysed using flow cytometer. Dead cells were excluded by staining with suitable fluoresces. For the following batches, cells were harvested and stained in the same manner but at different time points, these were 2, 4, 6 and 8 hours.

### 2.2.5.5 Plasmid bulk up and Transformation into XL1-Blue E. coli

XL1-Blue, a strain of *Escherischia coli*, is often used for nucleotide transformation. Briefly, a previously prepared aliquot of XL1-B bacteria was initially kept on ice for slow defrosting, and then 10µL of the DNA was mixed with the bacteria and incubated for 30 minutes on ice. After that, cells were heat-shocked for 3 minutes at 42°C and then immediately cooled on ice. Luria-Bertani (LB) broth was then added at a volume of 250µL and mixed with cells in a shaker at 37°C for 1 hour. 150µL of the transformed cells were then plated onto LB agar plates containing an appropriate selection antibiotic depending on the resistance gene expressed by the plasmid used for transformation (See Table 2.12). Plates were then shifted in a 37°C/5%CO<sub>2</sub> incubator where they were kept in inverted position overnight. On the next day, single colonies from the agar plates were picked up using a pipette tip and placed in a 37°C shaker to grow overnight in a culture flask containing LB broth with the corresponding antibiotic.

**Table 2.12: plasmids used and doses of the bacterial selective markers**

Plasmid	Antibiotic express by the plasmid	Antibiotic dose	Media
HAGE ImmunoBody®	Zeocin	35µg/mL	LB broth with a low salt agar
WT1 ImmunoBody®	Zeocin	35µg/mL	LB broth with a low salt agar
PC DNA-3.1 HHDI	Ampicillin	100µg/mL	LB broth

### 2.2.5.6 DNA plasmid isolation and purification

DNA isolation was performed using a QIAfilter plasmid midi kit following the manufacturer's instructions (QIAfilter plasmid Midi Kit, catalogue number: Q12143). Briefly, overnight bacterial culture containing the plasmid of interest was pelleted by centrifugation at 6000 RPM for 30 minutes at 4°C. Bacterial pellet was then re-suspended in 4mL pre-chilled Buffer P1. Thereafter, 4mL of pre-warm Buffer P2 was added and mixed thoroughly by vigorously inverting the tube few times and incubated at room temperature for 5 minutes. After that, 4mL of pre-chilled Buffer P3 was added and mixed thoroughly by vigorously inverting the tube and then the mixture was incubated on ice for 5 minutes. The formed lysate was then poured into

a barrel and incubated at room temperature for 10 minutes and then filtered into a previously equilibrated QIAFilter cartridge. Following the filtering of the lysate the QIAGEN-tip was washed twice with 10mL Buffer QC. Next, DNA was eluted with 5mL of pre-warmed Buffer QF at 65°C to increase DNA yield. For the precipitation of the DNA, 3.5mL isopropanol was added to the eluted DNA. This was followed by centrifugation at 6000 RPM for one hour at 4°C. Finally, the DNA pellet was then washed twice with 1mL 70% ethanol and centrifuged at 13,000g for 10 minutes. Once the resultant DNA pellet was air-dried, DNA was re-dissolved in an appropriate volume of TE buffer. The obtained DNA was quantified using NanoDrop 8000 Spectrophotometer.

### **2.2.5.7 DNA vaccine-bullets preparation**

Expression vectors encoding HAGE- and WT1-ImmunoBody® were coated onto 1.0µm gold microcarriers as per manufacturer's instructions. Briefly, 200µL of 0.05M spermidine containing 16.6mg of gold was mixed with 36µg of DNA. After giving a short sonication, 200µL of 1M CaCl<sub>2</sub> was added dropwise to the mixture whilst still vortexing, and then the DNA-gold mixture was kept for 10 minutes at room temperature. The pellet was then re-suspended in 2mL of 0.025mg/mL Polyvinylpyrrolidone after being washed twice with anhydrous ethanol. After that, whilst the tube was sonicating, the sample was syringed into dried Tefzel tubing and kept stand for five minutes in a Tubing Prep Station. Without disturbing the gold, the ethanol was then gradually expelled using a syringe. Nitrogen gas was turned on while the tube was kept spinning for 7-10 minutes inside the station. When completely dried out, the tubing was detached from the station and cut by a guillotine. The bullets were then kept at 4°C until used.

### **2.2.5.8 Immunisation programmes**

#### **2.2.5.8.1 Single vaccine immunisation regime**

##### **2.2.5.8.1.1 Simple single peptide/adjuvant immunisation regime**

At the beginning of the study, the efficacy of simple WT1 peptide immunisation with Incomplete Freund's adjuvant (IFA) and cytosine triphosphate deoxynucleotide guanine (CPG) adjuvants was assessed in HHDII/DR1 double transgenic mice using *ex vivo* IFN-γ ELISpot assays. In this set of study, three mice were immunised with 100µL of emulsion containing 50µg CpG and 50µg WT1 long 15-mer peptide in 50% IFA injected subcutaneously at the base of the tail. Two boosts of immunisation with the peptides cocktail were undertaken at 7-day intervals.

The immunogenicity of HAGE peptides with different adjuvant was assessed by previous students.

### 2.2.5.8.1.2 Single ImmunoBody® immunisation regime

In this set of experiments, each HHDDII/DR1 mouse received a total of three injections with one bullet containing approximately 1µg of DNA coding for either HAGE or WT1-ImmunoBody® vaccines coated onto gold particles using gene gun technology. Mice were immunised with either HAGE or WT1 bullet for three rounds of immunisation with the same ImmunoBody® DNA at 7-day intervals.

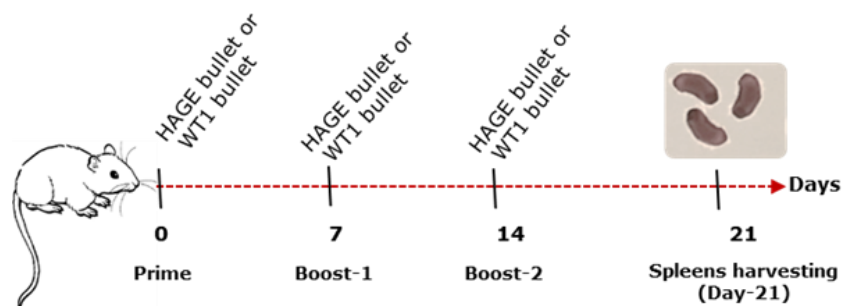


**Figure 2.1: Schematic presentation of single ImmunoBody® immunisation regime**

Prime-boost strategy was applied to assess the immunogenicity of single DNA immunisation of HAGE- and WT1-ImmunoBodies® administered in separate sets of mice, wherein, each mouse received a total of 3 injections at 7-day intervals. Spleens were then harvested on day-21 for IFN- $\gamma$  ELISpot assay.

### 2.2.5.8.2 Combined HAGE- and WT1-ImmunoBody® vaccination regime

After having determined the immunogenicity of a single vaccine DNA regime, a combination therapy was then tried by incorporating both HAGE- and WT1-ImmunoBody® vaccines. Mice were immunised for both vaccines at the same time where the round was repeated for three rounds at 7-day intervals.

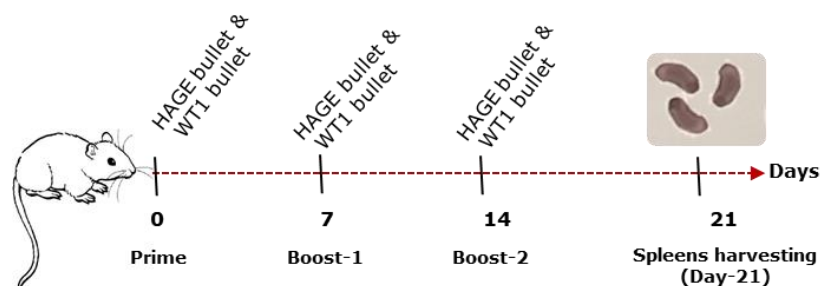


**Figure 2.2: Schematic presentation of the combined HAGE- and WT1-ImmunoBody® vaccines regime**

Prime-boost strategy was applied to assess the immunogenicity of the combined HAGE- and WT1-ImmunoBody® vaccines, wherein, each mouse received a total of 6 injections at three sessions at 7-day intervals, two bullets per session in two different flanks. Spleens were then harvested on day-21 for IFN- $\gamma$  ELISpot assay.

### 2.2.5.9 IFN- $\gamma$ enzyme-linked immunospot (ELISpot) Assay

The immunogenicity of either HAGE or WT1 peptides was determined in splenocytes harvested from the immunised mice using *ex vivo* IFN- $\gamma$  ELISpot assay (ELISpot kit for mouse IFN- $\gamma$ / MABTECH). One day before spleens were harvested, 96-well ELISpot plates (milipore) for IFN- $\gamma$  ELISpot assay were firstly activated with 70% ethanol in a volume of 100 $\mu$ L/well for two minutes, followed by 4 washes with ddH<sub>2</sub>O. Plates were then coated with 50 $\mu$ L of mouse anti-human IFN- $\gamma$  antibody diluted in DPBS and incubated overnight at 4°C. The day after, the plates were then washed with DPBS to remove unbound antibodies and then were blocked with T cell medium for a minimum of one hour at room temperature. After being flushed out, washed and counted using nucleocounter, splenocytes from immunised animals were plated at a density of 0.5X10<sup>6</sup> cell per well in triplicate with 1 $\mu$ g/mL of class I and 10 $\mu$ g/mL of class II relevant peptides, and incubated at 37°C/5%CO<sub>2</sub> for 48 hours. Thereafter, 5 times washing of plates with DPBS containing 0.05%Tween was performed, and 50 $\mu$ L/well (1/1000 dilution) of biotinylated detection antibody against mouse IFN- $\gamma$  was then added and incubated for 2 hours at room temperature. Plates were then washed 5 times with 200 $\mu$ L/well PBS/Tween, followed by the addition of 50 $\mu$ L/well streptavidin alkaline phosphatase (1/1000 dilution)/well, this was then incubated for 1-2hours at room temperature. After incubation, plates were washed again 6 times with PBS/Tween and then 50 $\mu$ L/well development solution (BCIP/NBT, BioRad) was added, and left in dark at room temperature for 20-45 minutes or until spots could be seen. Once spots developed, the reaction was then stopped by rinsing the plates under tap water and left to dry. Spots were then quantified using an ELISpot plate reader (Cellular Technology Limited). Cells of all groups were stimulated with SEB, the staphylococcal enterotoxin-B, at (2.5 $\mu$ g/mL) as a positive control, and unstimulated cells (cells alone) were used as a negative control for every ELISpot assay.

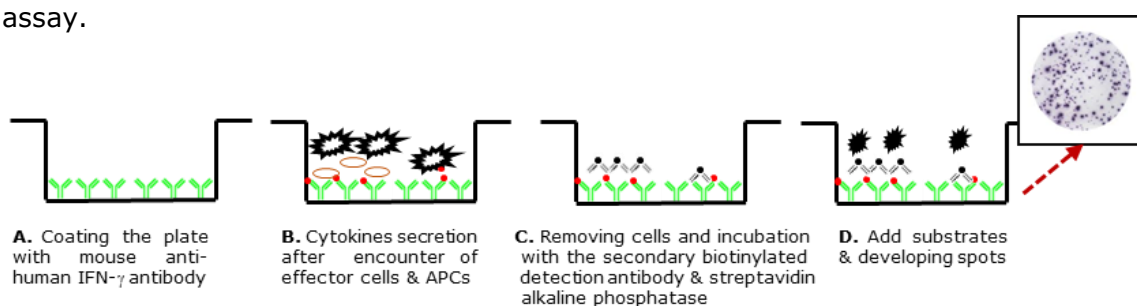


**Figure 2.3: Scheme of the ELISpot procedure.**

The primary monoclonal antibody coated on an ethanol-treated membrane **(A)** binds to the secreted cytokine upon cells stimulation **(B)**. After cell removal, a secondary, biotinylated detection antibody specifically binding the respective cytokine was added, followed by a streptavidin-biotin-horse radish peroxidase conjugate complex **(C)**. The developing insoluble enzyme complex then precipitated when a colorimetric substrate was added **(D)**.

Animals were scored as having a positive reaction when the number of spots in cell-alone wells did not reach more than 20 spots and when the response in the peptide containing wells were at least was twice that of standard deviation of the mean of the control wells. General principle of this assay is shown in Figure 2.3.

## **2.2.6 Preparation of T cell for the cytotoxicity assays**

### **2.2.6.1 Preparation of LPS blasts**

Two days before harvesting spleens (day-21), LPS blasts were prepared, wherein spleens from naïve mice were flushed out with T cell medium, and then  $60 \times 10^6$  splenocytes were seeded in 40mL T cell medium supplemented with 25µg/mL of LPS and 7µg/mL of dextran sulphate in a T75 flask. LPS blasts were then incubated at 5% CO<sub>2</sub> humidified atmosphere incubator at 37°C. After 48 hours, cells from LPS blasts were harvested and treated with mitomycin-C, which can stop the proliferation of cells, at a dilution of 1µg/mL per  $1 \times 10^6$  splenocytes for 20 minutes at 37°C. Following incubation, cells were washed 4 times using 10mL complete T cell medium to remove mitomycin. After that, cells were counted and the required number of splenocytes incubated with the immunogenic class-I peptides that were determined to be immunogenic by *ex vivo* IFN-γ ELISpot assay (mentioned-above) for 90 minutes at 37°C. Peptide-pulsed LPS cells were then washed thoroughly with 10mL T cell medium and co-cultured with freshly isolated splenocytes from immunised mice at a ratio of (1) LPS:(5) splenocytes in the presence of β-mercaptoethanol at 50mM and mIL-2 at 50U/mL and incubated at 37°C for 6 days. After incubation, LPS blast/T cells were then harvested, washed and counted ready for co-culture with target cells for the chromium release assay.

### **2.2.6.2 Chromium (<sup>51</sup>Cr) release assay**

All institutional radiation safety procedures were followed during working with <sup>51</sup>Cr to avoid the radioactivity biohazard. The <sup>51</sup>Cr release assay measures the release of <sup>51</sup>Cr from labelled target cells as they are lysed by specific effector T cells. Different target cells have been employed for this assay; these include T2 cells pulsed/non-pulsed with 50µg/mL of the relevant peptide a day prior to the cytotoxicity assay. Besides these, target tumour cells prepared in Chapter-5 (modified by either knock-in or knock down of the genes of the interest) were all labelled with <sup>51</sup>Cr and incubated with LPS-blast/T cells. Briefly,  $1.5 \times 10^6$  of target cells were re-suspended in 500µL of respective medium containing 20% heat shocked FCS (65°C for 30 minutes). Afterwards, cells were incubated with 1.85Mbq of <sup>51</sup>Cr isotope in a water bath at 37°C for one hour. Cells were then rested for another hour at 37°C after giving them a

single wash. Meanwhile, LPS blast/T cells (prepared 6 days prior to the cytotoxicity assay) were harvested and plated in a 96-well rounded bottom plate at a volume of 100µL and then incubated with an equal volume of target cells at different effector: target ratios of 100:1, 50:1, 25:1 and 12.5:1. In parallel, controls of spontaneous release and maximum load were set up in 4 replicates using plain medium and 1% SDS, respectively. After 4-24 hours of incubation at 37°C/5% CO<sub>2</sub>, 50µL supernatants were then transferred into 96-well Luma plates. <sup>51</sup>Cr release was measured using a Top Count Microplate Scintillation Counter, and then percentages of specific cytotoxicity was determined by calculating the values of the spontaneous and maximum release.

The spontaneous release refers to the quantity of <sup>51</sup>Cr released from the labelled target cells spontaneously without the influences of the effector cells. In fact, it represents the level of background death and it should be therefore subtracted from the actual target killing produced by the effector CTLs. Maximum release, on the other side, refers to the maximum amount of <sup>51</sup>Cr release from the labelled targets when they are being fully lysed by detergents (1% SDS) and it also should be normalised by subtracting the value coming from the background (spontaneous release). All <sup>51</sup>Cr release assay were performed in triplicate, and data were considered only if spontaneous release was less than 30% of maximum release.

The percentage of normalised experimental release to the normalised maximum release represents the percentage of cytotoxicity, a lysis which is produced by the net effect of CTLs on targets, calculated as the following:

$$\text{Percentage of cytotoxicity} = \frac{(\text{Experimental release} - \text{Spontaneous release})}{(\text{Maximum release} - \text{Spontaneous release})}$$

In addition, naïve splenocytes derived from non-immunised mice were also pulsed with LPS, treated with mitomycin-C and stimulated by the immunogenic class I peptides (in a similar manner to the splenocytes derived from the immunised mice). These were used for comparison with vaccine-induced killing upon incubation with different targets.

### **2.2.6.3 *In vitro* peptide re-stimulation (IVS) of the murine splenocytes**

Fresh splenocytes isolated from each vaccinated group of mice at a density of 2x10<sup>6</sup>/mL were re-stimulated *in vitro* by either the HAGE 30-mer long peptides, the WT1 15-mer long peptides or both, at a concentration of 1µg/mL in the presence of β-mercaptoethanol and 50U/mL murine IL-2 for 7 days in a 37°C/5% CO<sub>2</sub> incubator. Cells were then washed and counted using the nucleocounter machine.

To ensure that other cells do not take over the desirable effector cell function, non-CD3<sup>+</sup> cell removal by negative selection was performed using MACS technology. After non-CD3<sup>+</sup> cells depletion, the obtained cells (CD3<sup>+</sup>) were either re-stimulated with short cocktail peptides for *ex vivo* IFN- $\gamma$  ELISpot, or plated with target cells at pre-defined ratio (1:10) to assess their ability to produce IFN- $\gamma$  upon target recognition.

#### **2.2.6.4 Murine non CD3<sup>+</sup> cell depletion**

Non-CD3<sup>+</sup> T cells were depleted using "MojoSort™ Mouse CD3 T Cell Isolation Kit", (BioLegend, catalogue number:480031). The principle relies on that an incubation of splenocytes with a biotinylated antibody cocktail against many non-CD3 markers, using magnetic streptavidin nanobeads, results in the magnetically labelled fraction being retained by a magnetic separator and the untouched CD3<sup>+</sup> T cells stay in the tube, these can then be collected for assessment.

In this study, according to the manufacturer's instructions, splenocytes that harvested from after one-week IVS were initially filtered with a 70 $\mu$ m cell strainer, centrifuged at 300xg for 5 minutes, and re-suspended in an appropriate volume of MojoSort™ Buffer at a density of 100X10<sup>6</sup> cells/mL. For that concentration of cell, 100 $\mu$ L of the Biotin-Antibody Cocktail was then added, and incubated on ice for 15 minutes. After being vortexed thoroughly, 100 $\mu$ L of streptavidin nanobeads were then added and incubated on ice for another 15 minutes. 2.5mL of MojoSort™ Buffer was then added and the tube was placed in a magnetic separator for 5 minutes. The obtained liquid (containing CD3<sup>+</sup> cells) was collected in a clean fresh tube for further study. In order to increase the yield, the magnetic separation was repeated twice. The purity and yield of process were monitored before and after depletion using flow cytometry.

### **2.2.7 *In vivo* tumour challenge experiments: The prophylactic and therapeutic settings**

#### **2.2.7.1 Culture and maintenance of hB16 cells**

The hB16 cells previously knockout for the murine  $\beta$ 2-microglobulin and transfected with HHDII (chimeric HLA-A2) and HLA-DR1 were a kind gift from Prof. Lindy Durrant. These humanised cells were additionally transfected by a previous student with luciferase and HAGE constructs. In this project, these cells have been shortly named as (hB16/HAGE<sup>+</sup>/Luc<sup>+</sup>). These cells were maintained in RPMI-1640 medium supplemented with 10% FCS, 1% L-Glutamine, 300 $\mu$ g/mL hygromycin (to maintain HLA-DR1 gene), 500 $\mu$ g/mL G418 (to maintain HHDII gene), 550 $\mu$ g/mL zeocin (to maintain luciferase gene) and 1 $\mu$ g/mL puromycin (to maintain HAGE gene). hB16/HAGE<sup>+</sup>/Luc<sup>+</sup> cells were used to establish the relevant tumour model as a "proof-

of-concept" to test the efficacy of the candidate vaccines in the tumour challenge experiments in both the prophylactic and therapeutic settings in the "humanised" HHDII/DR1 double transgenic mice.

### **2.2.7.2 *In vitro* optimisation of luciferin bioluminescence activity in $_{h}B16/HAGE^{+}/Luc^{+}$ cells**

Prior to every tumour implantation,  $_{h}B16/HAGE^{+}/Luc^{+}$  cells were assessed *in vitro* for optimisation of luciferin bioluminescence activity, wherein cells were trypsinised, washed and counted using nucleocounter cell counting machine. Cells were then titrated and plated in a black 96-well microplate for at least 6 serial concentrations. After that, 0.15µg of D-Luciferin/well was added, and the plate was wrapped in foil and immediately sent for measuring the total flux of luciferin using IVIS machine.

### **2.2.7.3 *In vivo* optimisation of $_{h}B16/HAGE^{+}/Luc^{+}$ cells: Tumorigenicity and luciferase bioluminescence activity**

Prior to tumour challenge experiments, the tumorigenicity of the B16 cells was optimised in the naïve HHDII/DR1 double transgenic mice at three different doses to determine which dose can induce steady tumor growth and at the same time to determine the *in vivo* luciferase bioluminescence activity. On the day of implantation, cells were washed twice in DPBS, re-suspended in serum-free medium and counted using nucleocounter machine. Three different concentrations of B16 cells were prepared in three different studies, these were  $0.25 \times 10^6$ ,  $0.5 \times 10^6$  and  $0.75 \times 10^6$  cells suspended in 100µL of serum free medium. Three different groups of naïve mice were then challenged by implanting these doses subcutaneously and mice were then regularly monitored for tumour growth. In each session, mice were injected with luciferin, anaesthetised immediately after injection and imaged in a real time analysis to monitor tumour growth upon detection of luciferin bioluminescence signal.

### **2.2.7.4 Tumour challenge programmes**

In the prophylactic setting, prior to the tumour challenge, mice were subcutaneously vaccinated with 1µg of HAGE-ImmunoBody® in one flank and 1µg of WT1-ImmunoBody® into the contralateral flank simultaneously for three rounds of vaccination occurring every seven days. In the therapeutic setting, mice were firstly challenged by tumour cells and vaccines were administered on the next day which was then followed by two boosts at 7-day intervals. The control group of mice received the same dose of tumour cell implant but not the vaccines.

Tumours were monitored twice weekly by callipers until a palpable tumour was detected. Thereafter, mice were monitored twice weekly until termination by callipers and by *in vivo* imaging weekly. For each imaging session, luciferin was administered intraperitoneally at 150mg/kg, and anaesthesia induction began 10 minutes afterwards. All mice were anaesthetised with an appropriate concentration of isoflurane and imaged using the Perkin Elmer IVIS Lumina III system. Mice were sacrificed when tumour volume reached predefined threshold endpoints, including tumour diameter of more than 1.2cm<sup>2</sup> in the prophylactic group and more than 1.5cm<sup>2</sup> for the therapeutic group. In addition to tumour caliper measurement and tumoural luciferin bioluminescent signals (>10<sup>9</sup>), other additional clinical factors, such as body weight, hydration status and skin integrity over the tumour implant, were all collectively considered when determining the endpoint of a given tumour bearing mouse.

## **2.2.7.5 Processing of B16 tumours tissue**

### **2.2.7.5.1 Tumour volume and weight**

After the threshold endpoints were reached, tumours were taken, weighted, scaled and snap-frozen in liquid nitrogen until use. Approximate tumour volume was measured applying the formula:  $\pi/6 \times (\text{length} \times \text{width}^2)$ .

For the purpose of studying tumour-infiltrating lymphocytes (TILs), prior to freezing, small portions weighing ~1g were resected.

### **2.2.7.5.2 Snap-freezing of tumours**

Slow freezing can cause distortion of tissue architecture due to ice crystal formation. Therefore, snap freezing in this study was performed as a means of rapid cooling for preservation of fresh tumour tissue. Briefly, a specimen of tumour tissue was fixed on a pre-labelled cork piece and covered with cryo-embedding medium. The assembly was then immersed into a glass beaker of isopentane (2-methylbutane) which was chilled in a drawer of liquid nitrogen for 10 minutes. Sample was immersed in the beaker for 2-3 minutes or until the cryo-embedding medium turned solid-white. To make sure that the whole tissue was thoroughly frozen, the assembly was submerged completely in the isopentane for a further 10 to 20 seconds using long forceps and then the frozen tumours were quickly transferred onto dry ice and stored at -80°C.

### **2.2.7.5.3 Isolation of tumour infiltrating lymphocytes (TILs)**

Briefly, ~1g was resected from B16 tumours, chopped into small pieces using scissor and incubated with 5mL of RPMI containing 1mg/mL collagenase-I (Sigma, catalogue number:C0130) at 37°C for 30 minutes under gentle shaking. After that, the suspensions were filtered through a 70-µm filter, washed with PBS to get rid the dissociation medium and re-suspended in 5mL of T cell medium. TILs were analysed by flow cytometry for the expression of CD8, CD4, CD3 and PD-1.

## **2.2.8 Gallios™ flow cytometer assays**

Flow cytometry has been performed for many purposes throughout the chapters in this thesis to confirm either the presence or the absence of a particular antigen expressed on the surface of cells or expressed intracellularly. The following sections therefore describe different applications of these assays where they were used.

### **2.2.8.1 Surface staining of cell lines**

On the day of the experiment,  $0.5 \times 10^6$  cells were harvested per tube from different cell lines together with an appropriate control. Cells were washed with 2mL of DPBS and incubated with fluorochrome-conjugated antibodies at concentrations recommended by the manufacturer for 30 minutes at 4°C. When the incubation time was over, cells were washed with 2mL of DPBS to remove any excess unbound antibodies by centrifuging at 400g for 5 minutes. Cells were also stained with an appropriate fluorescein to exclude dead cells from the analysis, such as propidium iodide (PI) or LIVE/DEAD™ Yellow stain. At the end of the assay, cells were re-suspended with 320µL isoton and run immediately on the flow cytometer.

Surface staining was performed for studying markers expressed by different cell lines throughout this thesis, either as a single marker staining or as a multicolour staining. For example, single marker staining was applied to characterise cells phenotypically, such as anti-HLA-A2 and anti-DR1 antibodies and was also used in T2 binding assay and BFA decay assay which employed anti-HLA-A2 antibody as a marker for peptide-HLA-A2 affinity and surface stability. It was also used to assess the success of HHDII gene transfection and cloning experiment of K562 cells upon staining with anti-β2m antibody. CD119 (IFN-γRα Chain receptors) were also assessed in particular targets of cells.

**Table 2.13A: A list of antibodies used in the single marker staining**

Antibody	Supplier	clone	Product Code	Species	Dilution per 100µL
Monoclonal Anti-β2m-FITC	Sigma	β2m-01	SAB4700012	Mouse	1µL
APC anti-human HLA-A2 Antibody	BioLegend	BB7.2	343308	Mouse	5µL
PE anti-human HLA-DR Antibody	BioLegend	L243	307606	Mouse	5µL
PE anti-human CD119 IFN-γRα Chain	BioLegend	GIR-94	308704	Mouse	5µL

Upregulation of some inhibitory and costimulatory molecules on CML cell lines upon IFN-γ treatment were assessed as a panel of multicolour staining (listed in Table 2.13B), wherein, 10µL of human Fc receptor blocking antibody (BioLegend) per tube were added and incubated with the cells at 4°C for 15 minutes prior to the staining.

**Table 2.13B: A panel of multicolour staining to study the effect of IFN-γ on CML cells**

Antibody	Clone	Product Code	Dilution per 100µL
Alexa Fluor® 488 anti-human MICA/MICB	6D4	320912	2.5µL
PE anti-human CD178 (Fas-L)	NOK-1	306406	2.5µL
PE/Dazzle™ 594 anti-human CD80	2D10	305229	2.5µL
PerCP/Cy5.5 anti-human HLA-E	3D12	342609	2.5µL
PE/Cy7 anti-human HLA-G)	87G	335911	2.5µL
APC anti-human CD274 (B7-H1, PD-L1)	29E.2A3	329707	2.5µL
Alexa Fluor® 700 anti-human CD40	5C3	334327	2.5µL
APC/Cy7 anti-human HLA-A, B, C	W6/32	311425	2.5µL
Pacific Blue™ anti-human CD86	IT2.2	305417	2.5µL
Zombie Yellow™ Fixable Viability Kit	N. A	423103	2.5µL

### 2.2.8.2 Surface staining of murine T cells

In this project, splenocytes isolated from the vaccinated mice were assessed using an activation marker panel and a memory panel. Therefore, fresh  $1 \times 10^6$  splenocytes were washed and stained for CD3, CD4 and CD8 markers together with either an

activation marker panel or memory panel (listed in Table 2.14), but prior to each staining, cells were incubated with anti-mouse FCR block (BioLegend) which was added at 1µg/tube for 15 minutes at 4°C. After incubation, cells were washed once and resuspended in 320µL isoton before being run on the flow cytometer.

In a similar manner, splenocytes isolated from tumour bearing mice in tumour challenge experiments and TILs were stained with CD8, CD4, CD3, PD-1, and LIVE/DEAD™ Yellow.

**Table 2.14: A panel of multicolour staining for murine cell surface staining**

Antibody	Clone	Product Code	Quantity (µg) Volume (µL)
Brilliant Violet 421™ anti-mouse CD3	17A2	100228	0.2µg/1µL
APC/CY7 anti-mouse CD8a	53-6.7	100714	0.5µg/2.5µL
Alexa-fluor700 anti-mouse CD4	GK1.5	100430	0.25µg/0.5µL
Live/Dead Yellow	N. A	L34968	2.5µL
APC anti-mouse/human CD44	IM7	103012	0.25µg/1.25µL
FITC anti-mouse CD62L	MEL-14	104405	0.25µg/0.5µL
FITC anti-mouse CD357 (GITR)	DTA-1	126308	1µg/2µL
OX-40 (CD134) PE	OX-86	119410	0.25µg/1.25µL
CTLA-4 (CD152) PE/Dazzle™ 594	UC10-4B9	106318	0.5µg/2.5µL
LAG-3 (CD223) PerCp-Cy5.5	C9B7W	125212	0.5µg/2.5µL
Tim-3 (CD366) PE-Cy7	RMT3-23	119716	0.5µg/2.5µL
APC anti-mouse CD279 PD-1	29F.1 A12	135210	0.5µg /2.5µL

### 2.2.8.3 Intracellular staining of WT1 protein expressed by cell lines

For intracellular WT1 staining,  $0.2 \times 10^6$  cells from K562, TCC-S and KCL-22 were washed twice with DPBS and fixed with 200µL of fixative solution prepared from Foxp3 staining buffer set at a ratio of one-part concentrate to three parts diluents, cells were then incubated in the dark for 20 minutes at 4°C. After that, cells were washed with 2mL of DPBS and incubated with 200µL permeabilisation buffer for 10 minutes at room temperature. The primary rabbit anti-WT1 antibody, was diluted in permeabilisation buffer at a 2:50 dilution and incubated for 30 minutes at 4°C. Cells were then washed once with 2mL of permeabilisation buffer and incubated for 30 minutes at 4°C with the secondary antibody; Alexa Flour 488 goat anti rabbit IgG (Invitrogen, catalogue number: A11008) at 1:200. Cells were then washed once with 2mL permeabilisation buffer, and thereafter 300µL of isoton was added, samples were then run on the flow cytometer.

### 2.2.8.4 Intracellular cytokine staining of splenocytes

In this aspect, immunophenotyping of murine splenocytes following 6 hours of peptide stimulation was performed as following: In a 96-well rounded bottom plate,  $1 \times 10^6$  of freshly isolated splenocytes from immunised mice were seeded at a volume of  $50 \mu\text{L}$ /well. Cells were then stimulated by addition of  $1 \mu\text{g}/\text{mL}$  final concentration of either class-I relevant peptides (4xconcentration) at a volume of  $50 \mu\text{L}$ /well. Costimulatory molecules, soluble anti-CD28 (BD Bioscience, catalogues number:553294), and anti-CD49d (BD Bioscience, catalogues number:553314) were prepared at 4xconcentration to be added to the microplate at a final concentration of  $1 \mu\text{g}/\text{mL}$  and incubated at  $37^\circ\text{C}$  for 60 minutes. After that, brefeldin A (BioLegend, catalogue number:420601) and monensin (BioLegend, catalogue number:420701) were diluted 1/1000 and added at  $50 \mu\text{L}$ /well as protein secretion inhibitors. At this point,  $3 \mu\text{L}$ /well of CD107a antibody was added, mixed well and incubated for 5 hours at  $37^\circ\text{C}$ , and then stored overnight at  $4^\circ\text{C}$ .

On the next morning, splenocytes were transferred into FACS tubes, washed, and re-suspended in  $50 \mu\text{L}$  FCS. FCR blocking agent anti-CD16/CD32 was added at  $0.5 \mu\text{g}/\text{tube}$  and incubated for 15 minutes at  $4^\circ\text{C}$ . After that, anti-CD3, -CD4 and -CD8 surface antibodies and fixable LIVE/DEAD™ Yellow were added and incubated for 30 minutes at  $4^\circ\text{C}$ .

After having completed staining of the surface antigens, intracellular cytokine staining was then performed. Cells were fixed and permeabilised as per the manufacturer's instructions provided for the PerFix-nc kit (Beckman Coulter, catalogue number: B31168), wherein,  $25 \mu\text{L}$  of the fixative reagent (Reagent R1) per tube were added to the cells and incubated in the dark at  $4^\circ\text{C}$  for 15 minutes, then  $300 \mu\text{L}$  of the permeabilisation reagent (Reagent R2) was added to each tube together with an appropriate volume of intracellular antibodies (as listed in the Table 2.15, except anti-CD107a antibody which was added on the day before) at  $4^\circ\text{C}$  for 30 minutes.

**Table 2.15 : A panel of multicolour antibodies for the intracellular staining**

Antibody	Clone	Product Code	Quantity( $\mu\text{g}$ ) Volume( $\mu\text{L}$ )
FITC anti-mouse CD107a (LAMP-1) Antibody	1D4B	104405	$1.5 \mu\text{g}/3 \mu\text{L}$
PE anti-mouse TNF- $\alpha$	MP6-XT22	506306	$0.25 \mu\text{g}/1.25 \mu\text{L}$
PE-eFluor® 610 anti- Ki-67	SolA15	61-5698-82	$0.125 \mu\text{g}/0.6 \mu\text{L}$
PerCP/Cy5.5 anti-mouse IL-2	JES6-5H4	503822	$0.6 \mu\text{g}/3 \mu\text{L}$
PE/Cy7 anti-mouse IFN- $\gamma$	XMG1.2	505826	$0.6 \mu\text{g}/3 \mu\text{L}$
APC anti-human/mouse Granzyme B Recombinant	QA16A02	QA16A02	$3 \mu\text{L}$

Finally, cells were washed with 1X of the washing solution (Reagent R3), and re-suspended in 320 $\mu$ L isoton and run on the flow cytometer.

## 2.2.9 Isolation of PBMCs from blood of healthy volunteers

After having taken their formal consent, 30mL blood was collected from healthy volunteers in sterile 50mL polypropylene Falcon™ tubes containing 300 $\mu$ L of heparin (10 IU/mL, Sigma). After that, blood was diluted at a ratio of 1:1 with DPBS. In a 50mL LeucoSep R tube, 15mL of Ficoll Paque (GE Healthcare Life Sciences) was added and spun for 30 seconds at 1100g to push the Ficoll Paque below the disc. After that, diluted blood was carefully layered over the Ficoll Paque in the LeucoSep R tubes, which should sit on the upper compartment of the disc. After that, samples were centrifuged at 800g for 30 minutes at room temperature on a swing out rotor with the breaks off. The most upper, serum layer was aspirated carefully and discarded, and the PBMCs layer was then collected and washed twice with 10mL DPBS at 400g for 10 minutes while brakes on. Cells were then resuspended in RPMI media, counted and prepared for further analysis.

## 2.3 Statistical analysis

All experiments in this work dealt with a quantitative type of data which was statistically analysed using GraphPad Prism version-7. In order to identify statistically significant differences between two or more sets of data, two kinds of analysis were applied: parametric and non-parametric tests. Parametric tests applied herein include the mean, the SD/SEM, t-test and for the analysis of multiple independent groups, the analysis of variance (ANOVA) test was used. Whereas for non-parametric analysis, the median and Mann-Whitney test were mainly performed. Overall, the type of test used was chosen on the bases of sample size and whether the data were normally distributed or not. For tumour challenge studies, the survival proportion was evaluated by both the Gehan-Breslow-Wilcoxon test and the log-rank test.

For each test, *P-value* (probability value) was calculated, and was found to be significant if \**p-value*=<0.05, very significant if \*\**p-value*=<0.01 and highly significant in case \*\*\**p-value*=<0.001 or \*\*\*\**p-value* =<0.0001.

## **3 Chapter III: Validation of HAGE and WT1 as potential targets for immunotherapy in leukaemia**

### **3.1 Introduction**

It is evident that the majority of tumours are immunogenic, and the immune system can limit cancerous growth in response to tumour immunogenicity under certain circumstances. However, it is also obvious that the immune response *per se* is not sufficient to control the progression of malignant cells, especially when growth is well-established. Therefore, significant efforts have been undertaken to enhance the efficacy of anti-tumour immune responses by applying various immuno-modulatory interventions. Cytotoxic T cells (CTLs) are the main contributors in the process of immune-surveillance by virtue of their capability to identify quantitative and qualitative alterations in the presented antigens on the surface of transformed cells. Since progression of carcinogenesis produces an altered protein repertoire (Gjerstorff, M. F., Andersen *et al.* 2015), targeting the correct repertoire of tumour antigens is of critical importance for the delivery of more effective immunotherapy. Hence, the ideal tumour antigen should typically have a combination of four essential criteria; i) be expressed specifically by cancerous cells and no/minimal expression in normal cells, ii) be expressed stably and homogeneously by the majority of tumour cells, iii) have a vital role in tumorigenesis, and iv) induce a strong immune response which makes it an explicit target for T tumour antigen-specific CTLs (Simpson, Caballero *et al.* 2005). Identification of such tumour antigens would indeed strengthen the cancer vaccine development. Among various categories of tumour antigens, cancer testis (C/T) antigens have emerged as promising targets in the field of cancer immunotherapy.

#### **3.1.1 Promising immunotherapeutic value of cancer testis antigens**

The main hallmarks of cancer were essentially described by Hanahan and Weinberg in 2000 as the following; i) capacity for unlimited cells growth due to induction of abnormal cell cycle regulatory mechanisms, ii) developing strategies to resist apoptosis and death, iii) tendency for migration and distal implantation, and iv) ability to enhance angiogenesis. It would therefore be very feasible to target proteins or protein patterns responsible for, or associated with, these features of cancer for the development of therapeutic interventions (Hanahan, Weinberg 2000). Examples of

such tumour antigens are telomerase, Survivin Cyp1B1 (targeted cell division), Bcl-2, Bcl-X(L) (targeted resistance to apoptosis), RhoC (targeted metastatic potential), and VEGFR (targeted angiogenesis), however, none of these have a cancer-specific expression like C/T antigens (Gjerstorff, M. F., Andersen *et al.* 2015).

The cancer testis antigen family constitutes one of the most promising therapeutic targets identified to date due to their unique and specific set of characteristics. Firstly, they are mostly expressed in cancerous cells with diminished expression in healthy cells. In normal adults, C/T antigen expression is restricted to testis and trophoblast of the placenta, however ectopic expression has been detected in many human cancers (Hofmann, Caballero *et al.* 2008, Zendman, de Wit *et al.* 2001, Gjerstorff, MF, Johansen *et al.* 2006). In fact, male germ cells are 'immune-privileged' in that they lack HLA class I molecule expression and therefore cannot present antigens to T cells (Janitz, Fiszler *et al.* 1994). This reduces the induction of peripheral immune tolerance to these antigens and renders C/T antigens promising targets for immunotherapeutic programmes (Fijak, Meinhardt 2006). Secondly, the majority of C/T antigens have been shown to be immunogenic (Mahmoud 2018). In this aspect, it has been reported that humoral and cellular immune responses against C/T are often detected in many types of cancers (Tsuji, Altorki *et al.* 2009, Andersen, R. S., Thruue *et al.* 2012, Wang, Yu, Wu *et al.* 2004, Akcakanat, Kanda *et al.* 2004, Ayyoub, Rimoldi *et al.* 2003a, Gnjatic, Atanackovic *et al.* 2003, Qian, Gnjatic *et al.* 2004, Milne, Barnes *et al.* 2008). In addition, studies have also reported a correlation between the upregulation of these genes and the cytotoxic effects of immune infiltrates into tumours (Rooney, Shukla *et al.* 2015). Thirdly, C/T antigens exerts an oncogenic function (a feature that will be covered in the next section below). Collectively, these unique features render C/T antigens as one of the most promising antigen group for the development of novel and effective immunotherapeutic strategies.

### **3.1.2 The oncogenic function of cancer testis antigens**

In general, C/T antigens are allocated into two groups relying on the chromosomal localisation of their encoding genes; A) the chromosome X-encoded C/T antigens which are generally highly germ cell-specific and immunogenic, such as MAGE, GAGE, SSX, CT45 etc. C/T antigens of this group have undergone extensive diversification selection during primate development resulting in the production of various subfamilies with multiple members (Stevenson, Iseli *et al.* 2007). The MAGE antigens, for example, developed in three different groups on chromosome X forming three subfamilies; MAGE-A, -B and -C with 12, 6 and 2 members, respectively (Sang, Wang *et al.* 2011). B) the non-X chromosome C/T antigens which are composed

principally of proteins encoded by solitary copy genes placed on the autosome, such as BAGE, HAGE, SP17 etc.

Interestingly, it has been proposed that the germ line cells and some trophoblasts share several vital traits with malignant cells. For instance, the ability of primitive germ cells that originated in the wall of the yolk sac to rapidly move and penetrate tissues as they migrate to the gonadal primordium (Mamsen, Brochner *et al.* 2012), a process which in many aspects resembles the expansion of cancer cells from primary tumour to metastatic sites. Moreover, the continuous differentiation of immature spermatogonia to spermatocytes throughout life, which go through meiosis, is comparable to the genetic alterations observed in most cancers. Furthermore, trophoblasts express characteristics similar to tumour cells as they can invade and burrow into the endometrium to implant the fertilised ovum and can vigorously proliferate to form the non-maternal part of the placenta (Gjerstorff, M. F., Andersen *et al.* 2015). Placenta accreta, increta and percreta represent an excellent example of the seriously invasive feature of placenta, wherein placental cells which adhere and invade rapidly into different uterine layers causing a critical postpartum haemorrhage (Fitzpatrick, Sellers *et al.* 2012).

These observations led to the assumptions that activation of gametogenic and or embryonic programmes are among the strongest predisposing factors of tumorigenesis, a concluding concept stems from the fact that numerous placental and germ cell proteins, including C/T antigens, are abnormally expressed in tumour tissues. These observations collectively suggest C/T antigens as being targets for extensive investigations to determine their functions in normal *versus* malignant tissues. Although their functions are not yet fully understood, studies utilising transgenic mice have revealed that several C/T members play a significant role in male fertility (Greve, Pøhl *et al.* 2014). At the molecular level, C/T antigens have been implicated in cell metabolism, cytoskeleton dynamics, maintenance of genomic integrity, and control the expression of mRNA during spermatogenesis.

In cancer, re-expression of C/T antigens points out their role in the regulation of tumour cell survival and epithelial mesenchymal transition (Rooney, Shukla *et al.* 2015). Some aspect of the oncogenic functions of C/T antigens are summarised in Figure 3.1. As provided by Gjerstorff, *et al.* 2015; SSX and CAGE have been shown to control sustained growth, CAGE also has a role in angiogenesis, whereas resistance to apoptosis is shown to be influenced by MAGE-A, -B, and -C, PAGE, GAGE and CAGE which have also anti-apoptotic features. Local and systemic invasion seems to be organised by MAGE-C2, GAGE, XAGE1, CT45A1 and also by CAGE. The effect of C/T antigens on genomic instability appears to be induced by FMR1NB, NXF2 and SSX2 (Gjerstorff, M. F., Andersen *et al.* 2015).

These oncogenic features have drawn the attention of the onco-immunologists to the importance of targeting C/T antigens in cancer vaccine development. Although the majority of C/T antigen studies have essentially focused on the solid cancer in particularly melanoma, recent studies have been directed to employ these antigens as immunological targets for the treatment of haematological malignancies as well.

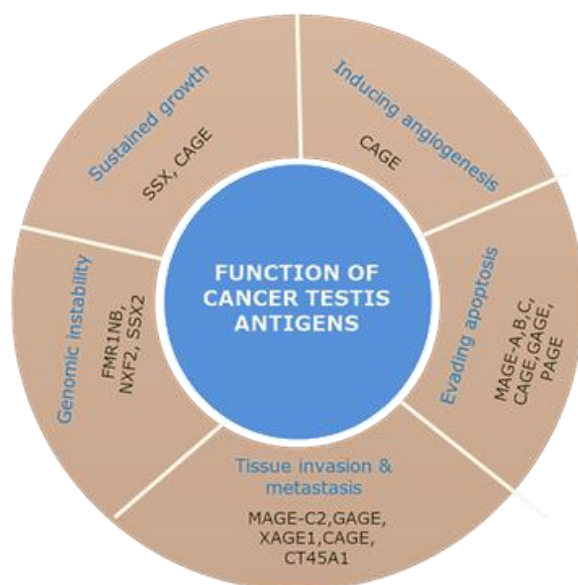


**Figure 3.1: Oncogenic functions of some cancer testis antigens, which were described by Hanahan and Weinberg as the “Hallmarks of cancer”.**

This set of specific features, including unlimited cell growth, resistance to apoptosis, the capability for invasion and metastasis, induction of angiogenesis, etc are originally caused by genomic instability, wherein several genetic variations are generated, and the acquisition of these hallmarks are then accelerated. Involvement of C/T antigens in these processes indicates that C/T antigens are directly implicated in the process of tumorigenesis. Figure is adapted from (Gjerstorff, M. F., Andersen, and Ditzel 2015).

### 3.1.3 Pattern of cancer testis antigens expression in haematological malignancies

Over the last few years, there have been several reports demonstrating C/T antigen expression in haematological malignancies. Table 3.1 summarises the pattern of cancer testis antigen expression in haematological malignancies and has been taken from a review provided by Meklat, Li *et al.* (Meklat, Li *et al.* 2007). The majority of these antigens were studied in multiple myeloma (MM). HAGE, SPANX, SCP1, PASD1 and SEMG have been studied in CML and SPAN-Xb, SLLP, PRAME and PASD1 in AML.

**Table 3.1: The pattern of C/T antigen expression in haematological malignancies**

C/T antigens	Disease and frequency of expression (%)	References
NY-ESO-1	MM: 60%	(van Rhee, Szmania <i>et al.</i> 2005)
MAGE C1	MM: Stage III: 82%	(Jungbluth, Ely <i>et al.</i> 2005)
SP17	MM: 26%	(Lim, S. H., Wang <i>et al.</i> 2001)
SLLP1	AML: 22%, CLL: 27% CML: 29%, MM: 35%	(Wang, Z., Zhang <i>et al.</i> 2004)
MAGE-A	MM: Stage III: 100 % MM: Stage I/II: 33 % MGUS: 83%	(Jungbluth, Ely <i>et al.</i> 2005)
GAGE1	MM: Stage II: 41%	(van Baren, Brasseur <i>et al.</i> 1999)
BAGE	MM: Stage: 14%	(van Baren, Brasseur <i>et al.</i> 1999)
SSX	Lymphoma: 36%	(Türeci, Chen <i>et al.</i> 1998)
HAGE	CML: 55%, AML: 23%	(Adams, Sahota <i>et al.</i> 2002)
SPANX	MM: 20%, CML: 60% CLL: 33%, AML: 50%	(Wang, Z., Zhang <i>et al.</i> 2003)
SCP1	MM: 10%, CML: 23% AML: 5-7%	(Lim, SH, Austin <i>et al.</i> 1999)
PASD1	AML: 33%, CML: 17%	(Guinn, Bland <i>et al.</i> 2005)
SEMG	CML: 62%, CLL: 42% MM: 7%	(Zhang, Y., Wang <i>et al.</i> 2003)

### 3.1.4 Current clinical applications of oncogenic C/T antigens

In general, the principal goal of therapeutic immunotherapies is to stop immune escape by overriding tolerance and expanding tumour-reactive T cells, an objective that can be achieved by enhancing the existing immune responses against tumour-associated antigens (TAAs). In fact, the therapeutic efficacy of the oncogenic C/T antigens has been studied in many clinical settings and been reviewed elsewhere (Gjerstorff, Morten Frier, Burns *et al.* 2010). Clinical trials indicate that targeting MAGE-A3 in melanoma and NY-ESO-1 in ovarian cancer are generally well-tolerated and promising.

In general, two types of C/T immunotherapeutic regimens are used; vaccination and adoptive transfer (illustrated in Figure 3.2). The concept of combining C/T antigens with other TAAs is currently being tested in several clinical trials in solid and haematological malignancies with or without adoptive T cell therapy. For example, presently, a phase I clinical trial for the treatment of AML and MDS ("Administration of Donor Multi TAA-Specific T Cells for AML or MDS (ADSPAM)"), was established in February 2016 (<https://www.clinicaltrials.gov/ct2/show/NCT02494167>).

The principle of this study involves *in vitro* education of a patients' stem T cells to recognise multiple TAAs that are known to be overexpressed by the majority of AML and MDS cancerous cells; two C/T antigens (NY-ESO-1 and PRAME), WT1, and Survivin, followed by expansion and re-infusion of cells at least one month after allo-HSCT. The study is expected to conclude in February 2024.

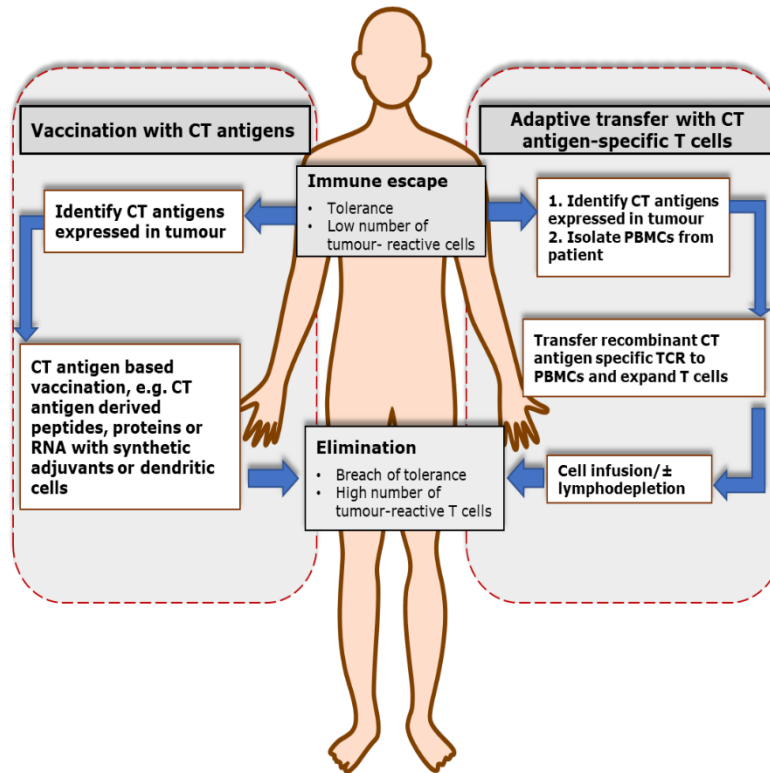


**Figure 3.2: Targeting of C/T antigens in the current clinical settings.**

Two regimens of C/T antigen-specific immunotherapy are currently applied: vaccination and adoptive transfer. Vaccination aims to activate the patient's own immunity toward C/T antigens expressed on the surface of cancer cells, by administration of immunogenic proteins or peptides loaded on dendritic cells or administered together with synthetic adjuvants. C/T antigens are also common targets for adoptive transfer in which recombinant C/T antigen epitope-specific T cell receptors (TCRs) are inserted into patient T cells, wherein and after being expanded, they are transferred back to the patients. These two strategies might greatly lower the risk of outgrowth of cancer variants. Figure is adapted from (Gjerstorff, Andersen and Ditzel 2015) with modification.

### 3.1.5 Epigenetic signature on C/T antigens expression in CML

Understanding the molecular mechanisms that regulate C/T gene expression is vitally important in order to increase the applicability and efficacy of potential tumour vaccines (Meklat, Li *et al.* 2007). In general, gene expression is primarily controlled by complex interactions which mainly involves DNA methylation and histones deacetylation. The interaction of these two processes results in structural alterations

in the chromatin configuration from a structure in which DNA transcription happens to a structure in which transcription is inhibited (Jones, Baylin 2002). It has been revealed that aberrant methylation of cancer suppressor gene promoters plays an important role in the pathogenesis and progression of various types of cancer, wherein global DNA hypomethylation and gene-specific hypomethylation are the more frequent epigenetic alterations that predispose to cancer development (Pogribny, Beland 2009). DNA hypomethylation predisposes to cancer development via the production of chromosomal instability and re-stimulation of transposable elements. Hypermethylation is generally achieved by the transfer of a methyl group to the gene's promotor site by DNA methyltransferase enzymes (DNMTs) (Herman, Lu *et al.* 2003), where over-crowding by methyl groups interferes with gene transcription. DNMTs inhibitors (also called demethylating agent), such as azacytidine and 5'-aza-2'-deoxycytidine, are able to incorporate into the DNA of dividing cells, causing irreversible inhibition of DNMTs and subsequent stopping of CpG island hypermethylation.

In this context, it has been demonstrated that there is a correlation between C/T antigen expression and hypomethylated CpG dinucleotides in gene promoters described in tumour cell lines and in tissue samples (Cho, Lee *et al.* 2003, Grunau, Sanchez *et al.* 2005, Lim, Jun Hee, Kim *et al.* 2005, Wang, Zhiqing, Zhang *et al.* 2006). Interestingly, Sigalotti and colleagues found that all C/T antigens that they studied can be upregulated in all C/T antigen negative melanoma clones upon treatment with demethylating agents (Sigalotti, Fratta *et al.* 2004). In CML, Chen, *et al.* studied the methylation status of the HAGE promoter in 87 Chinese CML patients employing Real-Time Quantitative Methylation-Specific PCR (RQ-MSP), and they investigated the HAGE transcripts in 35 patients using RT-qPCR. Overall, findings demonstrated that the promoter of HAGE was hypomethylation in 22 (25.3%). The frequency of HAGE hypomethylation was found to be increased as the disease progressed; at 23.4% (15/64) in patients who were diagnosed during the chronic phase, and at 25.0% (2/8) and 33.3% (5/15) in the accelerated phase and blast crisis, respectively (Chen, Qin, Lin *et al.* 2013). Thus, the authors suggest that hypomethylation of the HAGE promoter could be an early and frequent molecular events in the development of this type of leukaemia in Chinese people.

In AML, as in CML, the level of HAGE expression is also significantly correlated with hypomethylation of the HAGE promoter. However, in contrast to CML, HAGE hypomethylation is a favourable prognostic factor in AML and MDS (Lin, Jiang, Chen *et al.* 2014, Chen, Qin, Lin *et al.* 2012). The discrepancy in the findings linking HAGE expression to disease outcome may be due to that HAGE enrolls different functions in different diseases.

An aberrant methylation of WT1 promotor regions has been also reported in CML/chronic phase patients (Maupetit - Mehoulas, Court *et al.* 2018), wherein authors studied DNA methylation pattern in a big number of genes including WT1 in CML/chronic phase in comparison to healthy controls, and it was found an aberrant methylation occurred which affected the transcriptional profile of cancerous cell, and thus suggested a combination of epigenetic modulators with TKIs to treat CML/chronic phase. In addition, a solid correlation between methylation of the Intron 1 CpG island and WT1 silencing has been reported in AML patients and myeloid cell lines (McCarty, Gregory, Loeb 2015), no methylation issues were detected in one study of ALL patients (Alimohammadi, Alizadeh *et al.* 2018).

As the main aim of this chapter was to validate HAGE and WT1 as suitable targets for immunotherapy, a brief introduction about the expression pattern of these antigens in cancer will be provided in the sections below.

### **3.1.6 HAGE (DDX43) antigen as a target for immunotherapy**

Helicase Antigen (HAGE), a 73kDa protein, is encoded by the DDX43 gene on chromosome 6 (6q12-q13gene). HAGE is a cancer testis antigen (CT13) and a member of the D-E-A-D box family of ATP-dependent RNA helicases. HAGE expression at the mRNA and protein levels has been confirmed in many solid and haematological malignancies by many research groups (Mathieu, Linley *et al.* 2010, Adams, Sahota *et al.* 2002, Abdel-Fatah, McArdle *et al.* 2016, Chen, Yao - Tseng, Hsu *et al.* 2009, Martelange, De Smet *et al.* 2000). Interestingly, our group has previously reported that HAGE is expressed in multiple malignant tissues at mRNA and protein levels, but not their normal counterparts. Indeed, Mathieu and colleagues in 2010 were able to study HAGE expression in multiple human normal and malignant tissues using RT-qPCR and immunohistochemistry assays. Interestingly, they demonstrated the lack of HAGE expression at the protein level in normal microarrays tissues, whereas HAGE was overexpressed in cancerous tissues. HAGE expression in tissue microarrays (TMAs) from normal human bladder, brain, larynx, liver, lung, kidney, skin, thymus, uterus, oesophagus and ovary was compared to the expression in normal testicular tissue (high level) using immunohistochemistry (Mathieu, Linley *et al.* 2010). High levels of HAGE expression was present in oesophagus small cell carcinoma, hepatocellular carcinoma, kidney clear cell carcinoma, stomach adenocarcinoma and small intestine papillary adenocarcinoma, an intermediate expression of HAGE in astrocytoma, colon adenocarcinoma and lung squamous cell carcinoma, and a low level of HAGE expression in breast invasive ductal carcinoma

and bladder transitional cell carcinoma; but not in their respective matched normal tissues. These results suggest that HAGE can be employed as a basis of an immunotherapy for specifically targeting cancerous cells.

In CML, Adams and colleagues used RT-PCR analysis to demonstrate HAGE overexpression at the mRNA level in 55% and 71% of patients in chronic and blast crisis phases, respectively (Adams, Sahota *et al.* 2002). In addition, Chen, *et al.* in 2011 studied the expression status of HAGE in bone marrow mononuclear cells at the mRNA level using RT-qPCR. Results indicated that HAGE transcript overexpression was detected in 9 CML cases (34.6%) and more frequently observed at accelerated phase and blast crisis (4/4, 100%) than that at chronic phase (5/22, 22.7%)(Chen, Q., Lin *et al.* 2011).

### **3.1.7 WT1 antigen as a target for immunotherapy**

The second putative protein is WT1, a zinc finger transcription factor. It is encoded by the WT1 gene on the short arm of chromosome 11. WT1 was identified as a gene responsible for a paediatric nephroblastoma and called "Wilms' tumour" (Call, Glaser *et al.* 1990, Gessler, Poustka *et al.* 1990). WT1 is, indeed, involved in the regulation of important cell activities, such cell growth and differentiation, apoptosis, and organ development (Sugiyama 2001, Oka *et al.* 2006a). Recently, interest in WT1 as promising target for cancer immunotherapy has significantly increased due to factors such as its overexpression in various haematological and solid tumours, its low level of expression in normal tissues and its involvement in carcinogenesis (Pinilla-Ibarz, May *et al.* 2006a). In a prioritisation of cancer antigens study organised by National Cancer Institute (NCI), WT1 was, interestingly, categorised as the most promising TAA out of 75 selected antigens, depending on particular predefined and pre-weighted criteria (Cheever, Allison *et al.* 2009). In this article, experts listed 9 standard criteria that the ideal cancer antigen should have, as the following: i) the therapeutic function of the ideal antigen in the clinical trial should be excellent, ii) the immunogenicity should be demonstrated by T cell and/or antibody responses elicited in clinical trials, iii) the ideal antigen should be oncogenic, i.e. it is essential for cancer cell survival, iv) it should be absolutely specific; specificity of the antigens is determined by how much the antigen is specific to a given tumour, absolute specificity for example offers 100% of the value for that criterion, whereas overexpressed antigens received only 35% of that value, v) the expression level and % positive cells of the antigen should be high on all tumour cells in patients selected for therapy, vi) stem cell expression of the antigen should exist, vii) Number of patients with antigen-positive cancers should be high, viii) Number of epitopes should be multiple and they should have potential to bind with most MHC molecules,

and finally ix) the cellular location of antigen expression should be normally on the cell surface with no or few circulating antigens. Cumulative scores for each antigen were then calculated by mathematic equation. The outcome of this pilot demonstrated that there was no antigen exhibiting all of the above-mentioned criteria; however, WT1 was ranked the top in the list of 75 promising targets as a consequence of its oncogenic potential, presumptive immunogenicity and its widespread expression across various malignancies. WT1-reactive T cells are found in patients with leukaemia after allo-HSCT or donor lymphocyte infusions (DLI) (Rezvani, Yong *et al.* 2007, Tyler, Jungbluth *et al.* 2013).

The WT1 mutation has been reported in a wide-range of haematologic malignancies. Kreuzer and colleagues found that WT1 expression is an important tool for monitoring MRD (Minimal Residual Disease) (Kreuzer, Saborowski *et al.* 2001) and for predicting a patient's resistance to imatinib therapy when expressed in peripheral blood cells (Otahalova, Ullmannova-Benson *et al.* 2009) and in bone marrow (Cilloni, Messa *et al.* 2004). Moreover, WT1 is regarded as a predictive biomarker of the treatment and prognosis of leukaemic patients after allo-HSCT (Shahrabi, Yazdanpanah *et al.* 2017). In CML, the detection of WT1 level depends on the disease phase and the method of analysis used. It appears that it is significantly overexpressed during the blast phase in 50-100% (4/4 cases) of cases using Northern blot, but not during the chronic or accelerated phase. However, other researchers have detected WT1 expression in all cases they studied at different levels using quantitative RT-qPCR (Inoue, Sugiyama *et al.* 1994, Karakas, Miething *et al.* 2002). In fact, WT1 has been a very attractive antigen in clinical trials, and many of which have already demonstrated the usefulness of WT1 in immunotherapy, these are reviewed by Van Driessche, Berneman *et al.* 2012 (Van Driessche, Berneman *et al.* 2012).

## 3.2 Rationale of the chapter

1. To validate HAGE and WT1 as targets for immunotherapy in CML by assessing their expression in human CML cell lines at mRNA and protein levels. Validation also involves assessing their expression in CML patients at the mRNA level.
2. To assess the expression of HAGE and WT1 at the mRNA level in other types of leukaemias, such as AML and Adult B-ALL, using cell lines and patient samples.
3. To assesses the expression of cancer testis family genes and WT1 genes in CML and AML human samples obtained from clinical microarray data published in ArrayExpress website.

## 3.3 Results

### 3.3.1 Expression of HAGE and WT1 in leukaemic cell lines

#### 3.3.1.1 Screening a panel of CML cell lines for HAGE and WT expression

A panel of CML cell lines were evaluated for their expression of HAGE and WT1 at transcriptional and protein levels using RT-qPCR and Western blot assays, respectively. These cells (shown in Figure 3.3 and Figure 3.4) are KCL-22, K562, TCC-S, CML-T1, LAMA-84, KYO-1 and K812 cell lines. The LAMA-84 cell line showed extremely poor amplification with GUSB primers (i.e. came in a very late cycle) and it was therefore excluded from PCR analysis. However, it was included in Western blot analysis to assess expression at the protein level.

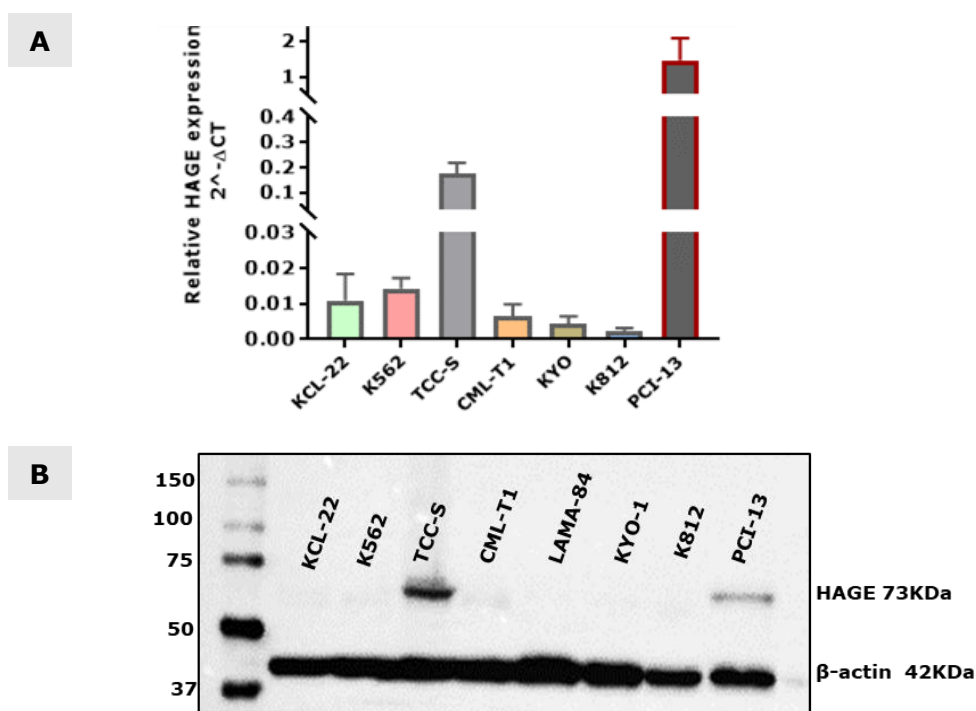


**Figure 3.3: HAGE expression in CML cell lines.**

**(A)** Bar graph illustrates HAGE expression at the mRNA level. 2000ng of mRNA per sample were utilised for cDNA synthesis using oligo (dT) primers, which were then amplified using RT-qPCR. Data were plotted as  $2^{-\Delta CT}$  values where all CT values were normalised to an internal control gene (GUSB). Each bar represents mean  $\pm$ SD of three replicates of three independent experiments. **(B)** Western blot analysis demonstrates HAGE expression at the protein level. Lysates of cells were obtained using Laemmli buffer for Western blot analysis. 30 $\mu$ g of lysates were loaded onto 10% w/v SDS gel and then blotted onto PVDF membrane. The membranes were blocked in TBS-Tween-5% w/v Marvel milk under a constant agitation for 1 hour at room temperature. The above blot shows result of membrane probed with rabbit anti-HAGE antibody in 1:200 dilution.  $\beta$ -actin (42KDa) was used as a loading control. Results demonstrate different level of constitutive HAGE transcripts expressed by different cell lines, and that only TCC-S cells translate HAGE at protein level.

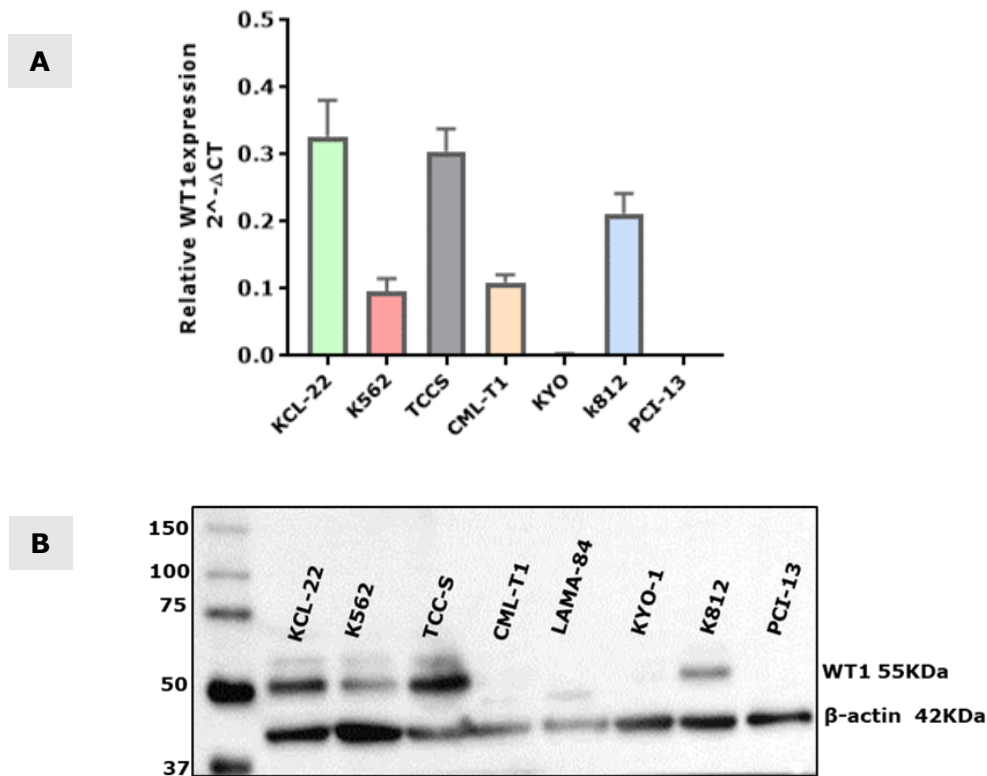


**Figure 3.4: WT1 expression in CML cells lines.**

**(A) Bar graph illustrates WT1 expression in CML cell lines at mRNA level.** 2000ng of mRNA per sample were utilised for cDNA synthesis using oligo (dT) primers, which were then amplified using RT-qPCR. Data were plotted as  $2^{-\Delta CT}$  values wherein all CT values were normalised to an internal control gene (GUSB). Each bar represents mean  $\pm$ SD of three replicates of three independent experiments. **(B) Western blot analysis demonstrates WT1 expression in CML cell lines at protein level.** Lysates of cells were obtained using Laemilli buffer for Western blot analysis. 30 $\mu$ g of lysates were loaded onto 10%SDS gel and then blotted onto PVDF membrane. The membranes were blocked in TBS-Tween-5% Marvel milk under a constant agitation for 1 hour at room temperature. The above blot shows result of membrane probed with rabbit anti-WT1 antibody in 1:1000 dilution.  $\beta$ -actin (42KDa) was used as a loading control. Results demonstrate different level of constitutive WT1 transcripts expressed by different cell lines, and that KCL-22, K562, TCC-S and K812 cells express WT1 at protein level.

In each run, 2000ng of RNA were reverse transcribed into cDNA using oligo (dT) primers, which were then amplified using RT-qPCR. Data are expressed as  $2^{-\Delta CT}$  value of relative gene expression normalised by GUSB as a housekeeping gene. Results in Figure 3.3A show that these cell lines are expressing HAGE mRNA to varying degrees. The predominant expression was in TCC-S cells, followed by KCL-22 and K562 cells which express a low level of HAGE. HAGE mRNA expression in CML-T1 and KYO were similar and slightly lower than that in KCL-22 and K562 cells, whereas HAGE transcripts were present at the lowest level in K812 cells. In addition, HAGE expression was assessed at protein level using Western blot analysis (Figure 3.3B). Lysates from PCI-13 cells, a squamous cell carcinoma of the head and neck cell line known to express HAGE, were used as a positive control for HAGE expression. For

the Western blot, 30µg of protein were loaded onto 10% w/v SDS gels and a rabbit anti-DDx43 antibody at 1:200 dilution was used to stain the PVDF membrane. Only TCC-S cells expressed detectable levels of HAGE at the protein level (Figure 3.3B). Regarding WT1 expression, the majority of cells express WT1 mRNA, with the highest expression being found with KCL-22 and TCC-S cells, followed by K812, k562 and CML-T1 cells (Figure 3.4A). KCL-22, K562, TCC-S and K812 cells express WT1 at the protein level (Figure 3.4B), as indicated by an intense band at the expected molecular weight (55KDa). Blots for the CML-T1 and LAMA-84 cells revealed very faint bands of protein at slightly lower molecular weight, probably indicating the expression of one of the WT1 isomers. KYO-1 cells did not express detectable levels of WT1 protein. In summary, HAGE and WT1 were expressed at the mRNA level by the majority of CML cell lines studied, as was WT1 at the protein level. Only TCC-S cells expressed detectable levels of HAGE protein.

### **3.3.1.2 Screening a panel of acute myelogenous (AML), acute monocytic leukaemia (AMoL) and acute lymphoblast leukaemia (ALL) cell lines for HAGE and WT expression**

HAGE and WT1 expression at transcriptional and protein levels (using RT-qPCR and Western blot assay, respectively) were determined in three cell lines from acute myelogenous (AMoL) disease; KASUMI, KG-1 and MV4-11 (Biphenotypic; B myelomonocytic leukaemia), three cell lines of monocytic leukaemia; THP-1, AML-139 and SIG-M5 and one cell line from acute lymphoblastic leukaemia, SUPB-15 cells line. As shown in Figure 3.5 (A and B), all AMoL and AML cell lines do not express HAGE, except MV4-11 cells which express HAGE transcripts at a low level. HAGE mRNA transcripts; however, were the highest in the SUPB-15 ALL cells which also seems to translate HAGE protein at a low quantity.

In both assays, TCC-S cells were used as a positive control.

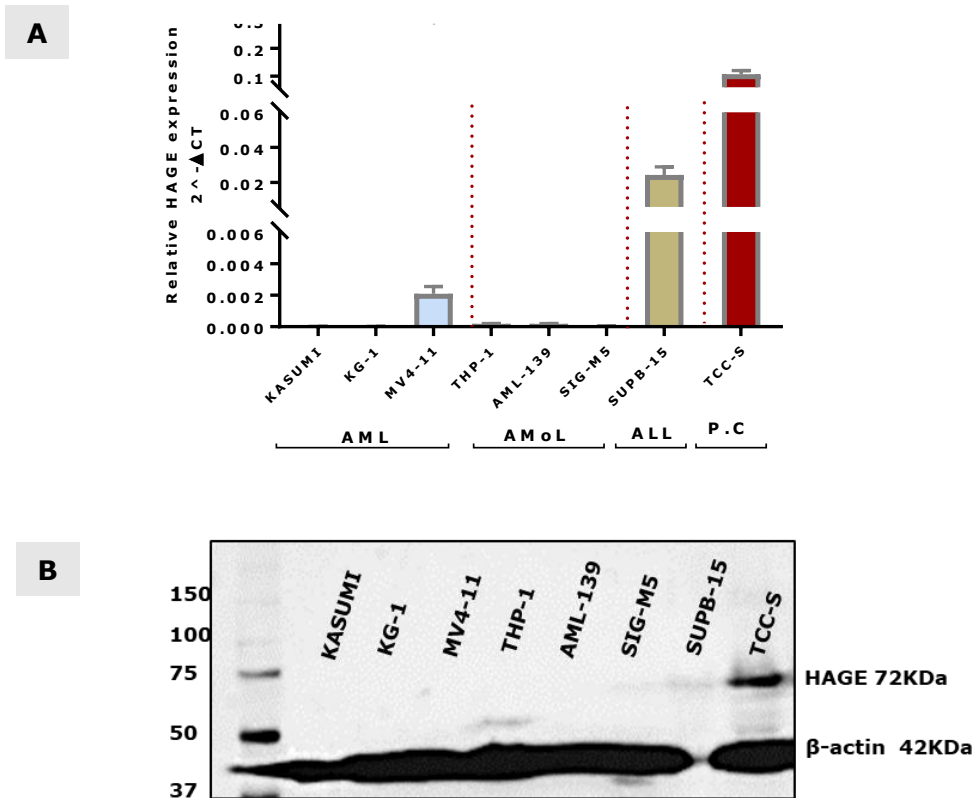


**Figure 3.5 HAGE expression in AML, AMoL and ALL cell lines.**

**(A) HAGE expression at the mRNA level.** 2000ng of mRNA per sample were utilised for cDNA synthesis using oligo(dT) primers, which were then amplified using RT-qPCR. Data were plotted as  $2^{-\Delta CT}$  values where all CT values were normalised to an internal control gene (GUSB). Each bar represents mean $\pm$ SD of three replicates of three independent experiments. **(B) Western blot analysis demonstrates HAGE expression at protein level.** Lysates of cells were obtained using Laemilli buffer for Western blot analysis. 30 $\mu$ g of lysates were loaded onto 10% w/v SDS gel and then blotted onto PVDF membrane. The membranes were blocked in TBS-Tween-5% w/v Marvel milk under a constant agitation for 1 hour at room temperature. The above blot shows result of membrane probed with rabbit anti-HAGE antibody in 1:200 dilution.  $\beta$ -actin (42KDa) was used as a loading control. Overall, results demonstrate low/nill constitutive expression of HAGE at mRNA level, with no expression could be detected at protein level except SUPB-15 cells.

Regarding WT1 expression, the majority of leukaemic cell lines express WT1 at the mRNA level, the highest of which was detected in SUPB-15 cells and the lowest in SIG-M5 cells (Figure 3.6A). All of the cell lines express WT1 at the protein level (Figure 3.6B).

In summary, none of the acute myelogenous leukaemia, acute monocytic leukaemia and acute lymphoblastic leukaemic cell lines examined in this study expressed HAGE at the protein level, whereas all of the cell lines expressed WT1 at the protein level.

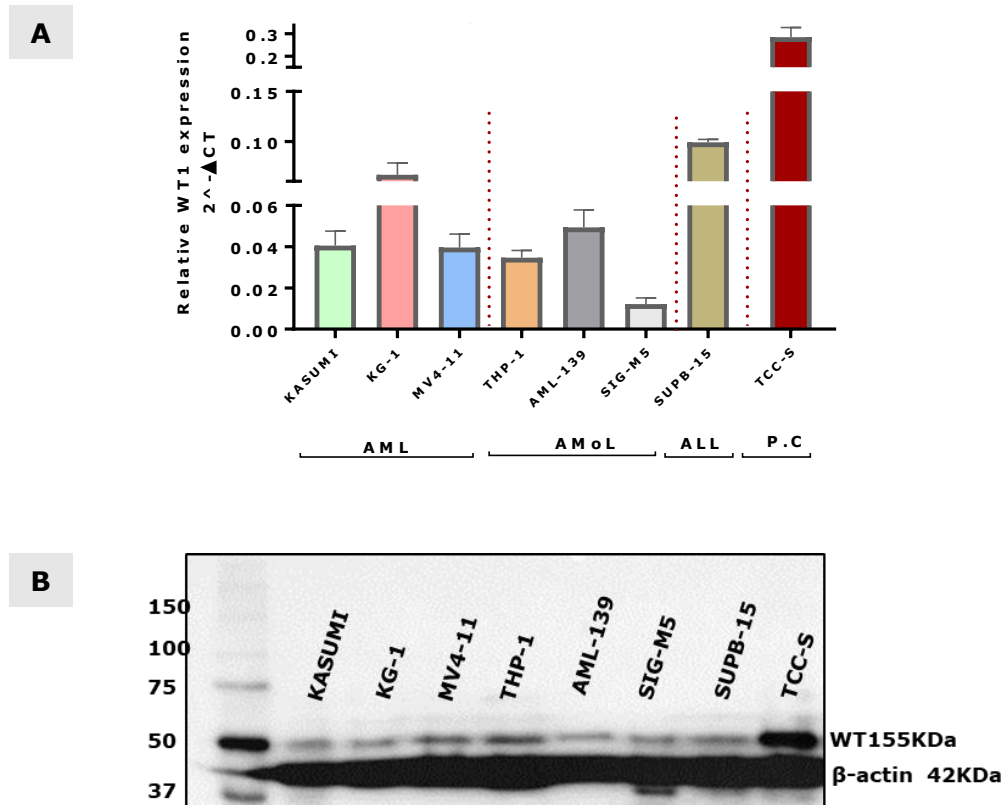


**Figure 3.6: WT1 expression in AML, AMoL and ALL cell lines.**

**(A) WT1 expression at mRNA level.** 2000ng of mRNA per sample were utilised for cDNA synthesis using oligo (dT) primers, which were then amplified using RT-qPCR. Data were plotted as  $2^{-\Delta CT}$  values where all CT values were normalised to an internal control gene (GUSB). Each bar represents mean  $\pm$ SD of three replicates. **(B) Western blot analysis demonstrates WT1 expression at protein level.** Lysates of cells were obtained using Laemilli buffer for Western blot analysis. 30 $\mu$ g of lysates were loaded onto 10% w/v SDS gel and then blotted onto PVDF membrane. The membranes were blocked in TBS-Tween-5% w/v Marvel milk under a constant agitation for 1 hour at room temperature. The above blot shows result of membrane probed with rabbit anti-WT1 antibody in 1:1000 dilution.  $\beta$ -actin (42KDa) was used as a loading control. Interestingly, results demonstrate constitutive WT1 overexpression in the all cell lines studies at mRNA and protein levels.

### 3.3.2 Expression of HAGE and WT1 transcripts in peripheral blood mononuclear cells from healthy volunteers

In the context of cancer vaccine specificity, it is necessary to demonstrate no/low expression of the candidate protein in normal tissues while confirming its overexpression in the cancerous tissue. As mentioned earlier, our group demonstrated no/low HAGE expression in multiple normal tissue sections in comparison to testicular and malignant tissues. However, unfortunately, in this project few samples were obtained from healthy volunteers. Herein, we collected whole blood from 4 volunteers, from which were isolated peripheral blood

mononuclear cells (PBMCs). Thereafter, mRNA was extracted from the PBMCs and used to reverse transcribe cDNA using oligo (dT) primers, HAGE and WT1 expression was then assessed by RT-qPCR. Data from these samples will be presented alongside those from leukaemic samples in the following sections, where appropriate, for comparative purposes.

### **3.3.3 Expression of HAGE and WT1 transcripts in CML patients**

Previous studies confirmed HAGE and WT1 overexpression in human leukaemias including CML. Herein, in an attempt to support these observations and for the purpose of validating HAGE and WT1 as suitable targets for immunotherapy in CML, the expression of both genes was assessed in 13 CML samples at the time of diagnosis using RT-qPCR. Among these samples, there were four pairs of non-responder patients at 12 months post-imatinib failure. These samples were received in a form of cDNA from a collaborative work at the University of Liverpool. The method of cDNA preparation and their final concentrations were not stated, although it would be ideal to check the original quality and quantity of mRNA used for cDNA synthesis, 1 $\mu$ L of cDNA was then utilised for PCR HAGE and WT1 gene amplification.

Data in Figure 3.7 illustrate HAGE expression in these samples in comparison with TCC-S cells (as a positive control) and PBMCs from the four healthy volunteers, for which all data were normalised using GUSB. Results show that there is different degree of HAGE expression in different samples studied, but in general most samples expressed HAGE transcripts to varying degrees. For ease of presentation and interpretation, findings are presented according to the relative gene expression into: Group-1: includes samples that exhibit HAGE expression at a level below 0.1 (shown as beige-coloured bars), Group-2: refers to samples that reveal HAGE expression in a range between 0.1 to 0.4 (shown as light grey-coloured bars), and Group-3: involves samples that express HAGE at a level higher than 0.4 (shown as dark grey-coloured bars).

In previous experiments, samples with HAGE mRNA levels less than 0.2 did not express HAGE protein. In the samples assessed here, 4 CML samples out of 13 expressed HAGE at levels comparable or higher than those obtained with TCC-S cells (0.2). HAGE mRNA expression in PBMCs of healthy volunteers was less than 0.1, and it is important to assess whether such low levels of HAGE mRNA in PBMCs of healthy volunteers generates detectable levels of protein.

**Table 3.2: CML samples studied**

<b>#</b>	<b>Patient ID</b>	<b>Samples at diagnosis</b>	<b>12 months post imatinib therapy</b>
<b>1.</b>	6	2735	3795
<b>2.</b>	14	2990	
<b>3.</b>	21	3171	4427
<b>4.</b>	123	4964	
<b>5.</b>	199	5604	
<b>6.</b>	206	5777	
<b>7.</b>	219	6052	
<b>8.</b>	220	6107	
<b>9.</b>	290	6529	
<b>10</b>	296	6776	7846
<b>11.</b>	385	8463	9716
<b>12.</b>	395	8564	
<b>13.</b>	467	9409	

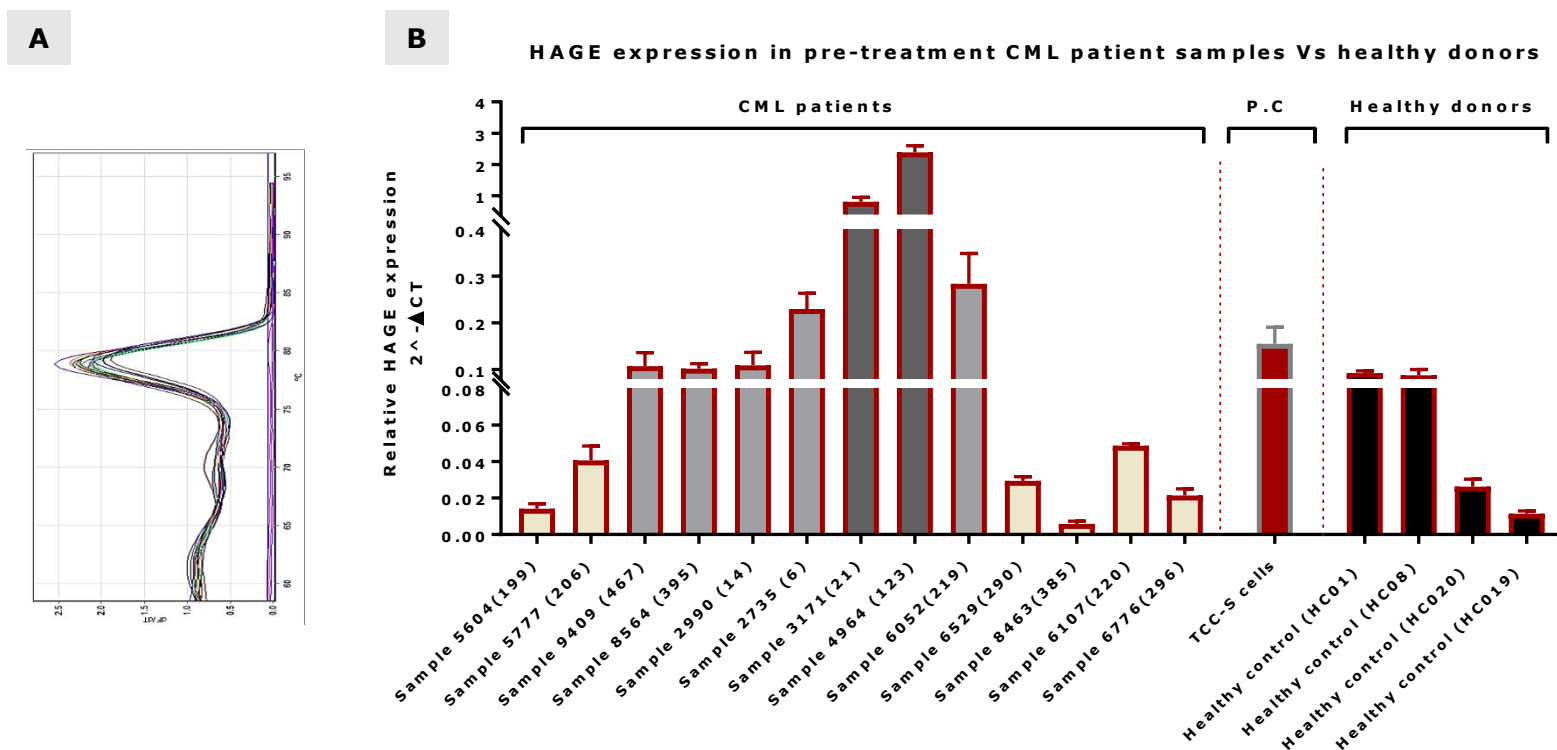


**Figure 3.7: HAGE expression in CML patients at mRNA level using RT-qPCR.**

1 $\mu$ L of already synthesized cDNA was utilised for RT-PCR amplification. **(A) Melt curve analysis to assess the dissociation characteristics of HAGE double stranded DNA during heating.** Results show a single pure amplicon synthesised by HAGE-specific primers indicating the specificity of the amplified fragments. **(B) HAGE expression using RT-qPCR in comparison to healthy donors.** Data were plotted as 2<sup>- $\Delta$ CT</sup> values where all CT values were normalised to an internal control gene (GUSB). Each bar represents mean $\pm$ SD of two replicates of two repetitions. TCC-S cells were used as a positive control (P.C). Overall, HAGE was overexpressed in more than half of CML samples.

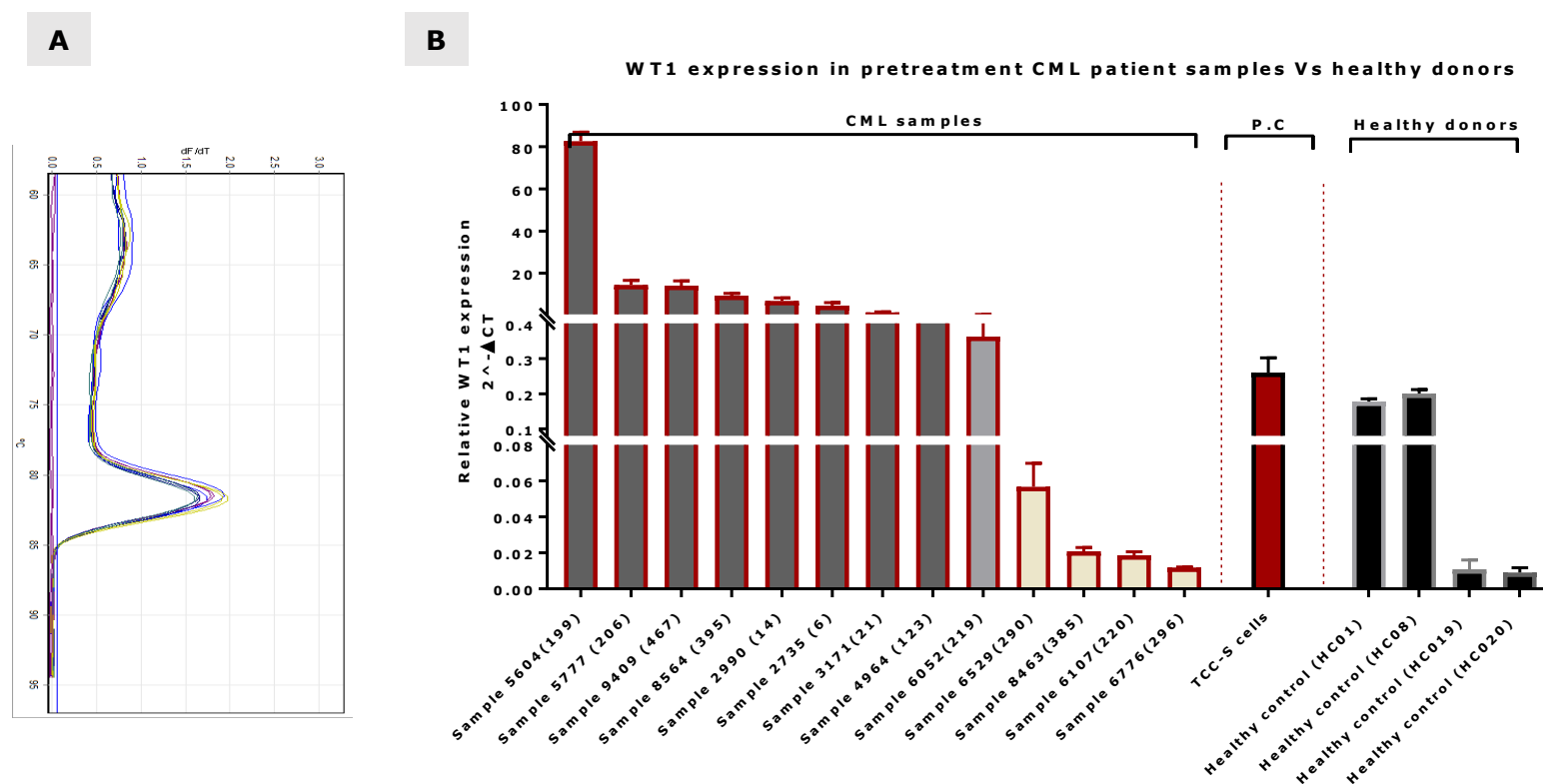
Regarding WT1 expression, mRNA levels above 0.1 were detected in almost all the CML samples, as well as in two of the PBMCs taken from healthy donors (Figure 3.8). Previous experiments indicated that samples with mRNA levels of 0.1 and above produced a detectable level of WT1 protein. The fact that a similar level was detected in two healthy donors (possible indication of protein expression as well as mRNA) is not entirely surprising since some researchers have found that healthy individuals have a detectable level of WT1-specific CD8<sup>+</sup> T cells in their circulation (Schmied, Gostick *et al.* 2015), as WT1 has an essential function in the normal development of the urogenital tract and has been reported to be expressed in some normal tissue (Klattig, Sierig *et al.* 2007).

Interestingly, Ichinohasama *et al.* (2010), reported a discrepancy between WT1 expression at the mRNA level and protein levels, wherein the authors found that although the WT1 mRNA transcript expression in PC-14 cells was very weak, the protein expression level was almost the same as in the other cell lines they tested (Ichinohasama, Oji *et al.* 2010). Moreover, this difference between WT1 mRNA and protein expression has also been reported by Kerst G *et al.* (2008) in childhood leukaemia (Kerst, Bergold *et al.* 2008), which means that there is no direct correlation between WT1 mRNA expression and its protein expression.

Interestingly, cross-matching to find out a possible simultaneous correlation between HAGE and WT1 transcripts expression in these samples demonstrates that all samples that overexpressed WT1 also express HAGE, except the first two samples in Figure 3.7 and Figure 3.8, sample 5604 (199) and sample 5777 (206). In addition, all the 4 samples that showed down-regulated WT1 expression expressed very low levels of HAGE, indicating a possible concurrent HAGE and WT1 expression in CML disease.

In summary, although the number of samples is small, data demonstrate upregulation of both HAGE and WT1 at the mRNA level in this set of CML patients in comparison to the healthy individuals, and that there is a high possibility of concomitant expression of both genes.

In addition, among these 13 samples obtained at the time of diagnosis, follow-up samples at 12 months post-imatinib failure were available from four patients, and HAGE and WT1 expression was assessed in paired samples from these. Interestingly, disease progression at 12 months post-imatinib failure is associated with a significant simultaneous increase of both HAGE and WT1 transcripts (Figure 3.9 A and B), this trend is shown in 2 pairs out of 4 which might indicate that HAGE and WT1 could be regarded as markers for disease progression and poor response to imatinib, and it would be interesting to assess that in a larger number of pairs.

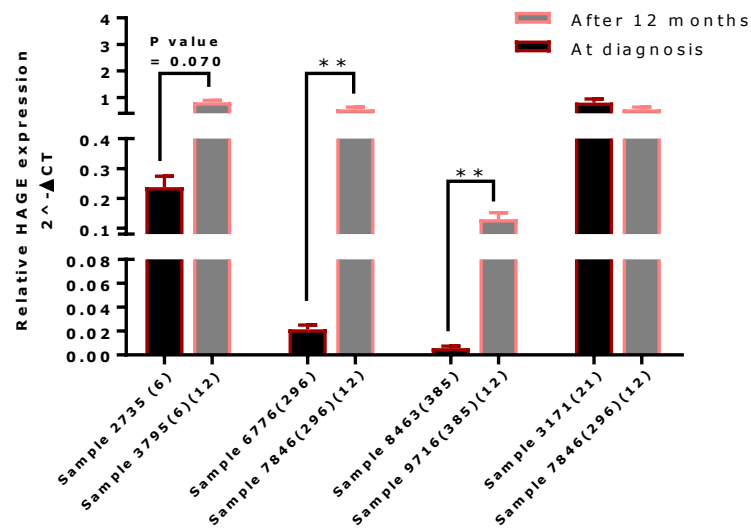


**Figure 3.8: WT1 expression in CML patients at mRNA level using RT-qPCR.**

1 $\mu$ L of already synthesized cDNA was utilised for RT-PCR amplification. (A) Melt curve analysis to assess the dissociation characteristics of WT1 double stranded DNA during heating. Results show a single pure amplicon synthesised by WT1-specific primers indicating the specificity of the amplified fragments. (B) WT1 expression using RT-qPCR. Data were plotted as  $2^{-\Delta CT}$  values where all CT values were normalised to an internal control gene (GUSB). Each bar represents mean  $\pm$  SD of three replicates of three repetitions. TCC-S cells were used as a positive control (P.C). Overall, results demonstrate that WT1 was expressed in an impressive number of samples.

**A**

**A comparison of HAGE expression at diagnosis Vs 12 months post-imatinib therapy in four pairs of non-responder CML samples**

**B**

**A comparison of WT1 expression at diagnosis Vs 12 months post-imatinib therapy in four pairs of non-responder CML samples**

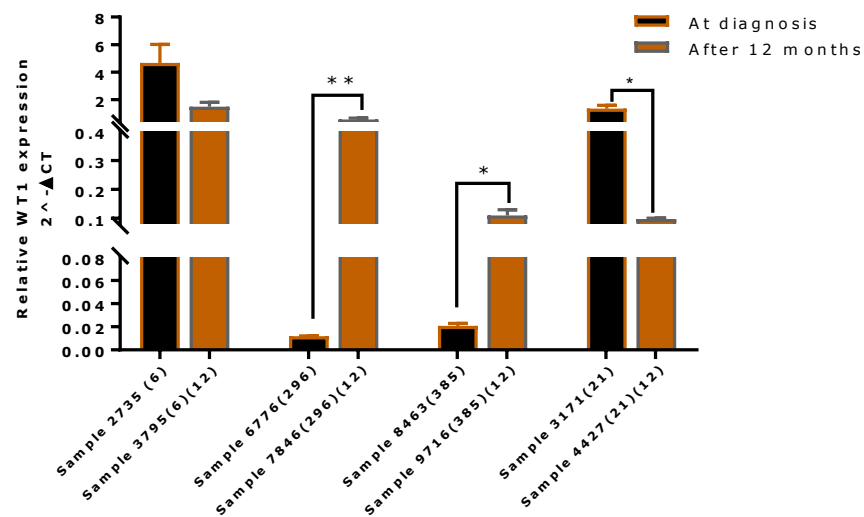


**Figure 3.9: A comparison of HAGE and WT1 expression in four pairs of CML patients at diagnosis and 12 months post-imatinib failure evaluated by RT-qPCR.**

A comparison of HAGE expression in the four pairs is demonstrated at **(A)** whereas WT1 expression is demonstrated in **(B)**. Data were plotted as  $2^{-\Delta CT}$  values where all CT values were normalised to an internal control gene (GUSB). Each bar represents mean $\pm$ SD of two replicates of two repetitions. Statistically, the level of the significance was assessed using paired t test. Overall, results demonstrate that both HAGE and WT1 are upregulated with the disease progression in two out of four pairs of non-responders CML patients.

### 3.3.4 Expression of HAGE and WT1 transcripts in AML patients

In this frame of study, cDNA from 7 AML samples at a concentration of 300ng/ $\mu$ L, (listed in Table 3.3) was assessed for HAGE and WT1 expression in collaborative work at the University of Hull. For this, 1 $\mu$ L of cDNA was utilised for RT-qPCR assay using GUSB for normalisation. Given the fact that non-specific and primer-dimer products could be formed during PCR reaction, all products were run on 2% w/v agarose gel including the HKG. Melting curves analysis was also shown to demonstrate the specificity of the amplified fragments.

**Table 3.3: AML and Adult B ALL samples studied**

#	Reference number	Diagnosis/disease stage
1.	3206838	AML – M4
2.	138072291	AML
3.	3950386	AML/MDS
4.	3720369	AML
5.	3956624	AML
6.	0175263	AML
7.	3990310	AML
<b>P.C</b>	Positive control	TCC-S cells
<b>N.C</b>	Negative control	ddH2O

Figure 3.10 below demonstrate GUSB amplification of the studied samples, wherein a specific peak in the melt curve (shown in A) illustrates the dissociation characteristics of GUSB double-stranded DNA during heating in real time PCR analysis. Results confirm the specificity of the amplified fragments, as reflected by single pure amplicon synthesised by GUSB-specific primers. Furthermore, PCR products were run on 2% w/v agarose gel stained with SYBR safe dye and visualised under UV light (shown in B). All samples display an intact reference gene, as reflected by a single band signal intensity in the corresponding GUSB molecular size (155bp). Therefore, it was used to normalise the gene of the interest in this batch of samples.

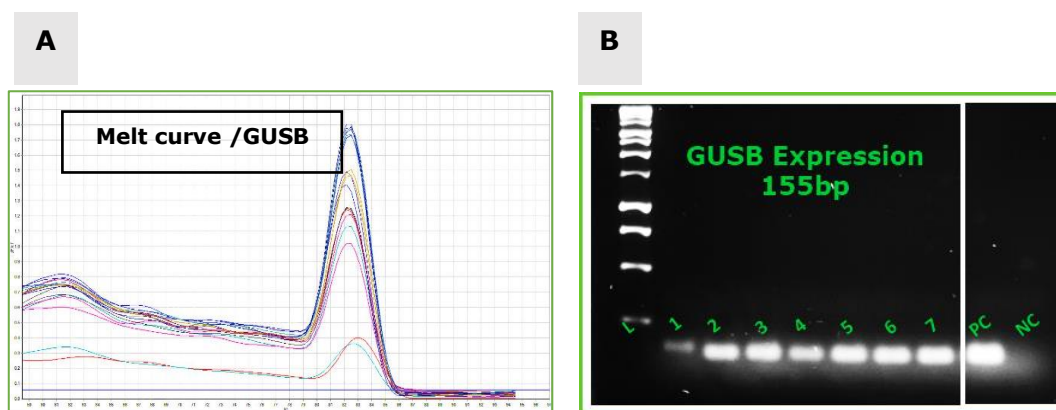


**Figure 3.10: Validation of GUSB expression in seven AML at mRNA level using RT-qPCR technique.**

cDNA samples were initially amplified using RT-qPCR and the products were then run on 2% w/v agarose gels. **(A) Melt curve analysis to assess the dissociation characteristics of GUSB double stranded DNA during heating.** Results show a single pure product synthesised by GUSB-specific primers indicating the specificity of the amplified fragments. **(B) Image of agarose gel electrophoresis of the studied samples.** PCR products was run on 2% w/v agarose gel stained with SYBR safe and then visualised under UV light for assessing GUSB expression in the samples studied. cDNA from TCC-S cells was utilised as a positive control whereas a master mixed containing H<sub>2</sub>O instead of cDNA was used as a negative control. Overall, finding shows that all samples have the intact reference gene as reflected by single band signal intensity in the corresponding GUSB molecular size.

Similarly, HAGE expression relative to that in healthy volunteers was also assessed (Figure 3.11). Interestingly, all AML samples demonstrated HAGE overexpression in comparison with healthy controls. A melt curve and agarose electrophoresis (Figure 3.11B, C) confirmed the specificity of HAGE primers. WT1 expression in all samples studied was higher than that in healthy volunteers and TCC-S cells (Figure 3.12A). Primer specificity was confirmed which demonstrate a single codon of amplification in the melt curve and single band densities on the gel, respectively (Figure 3.12B, C).

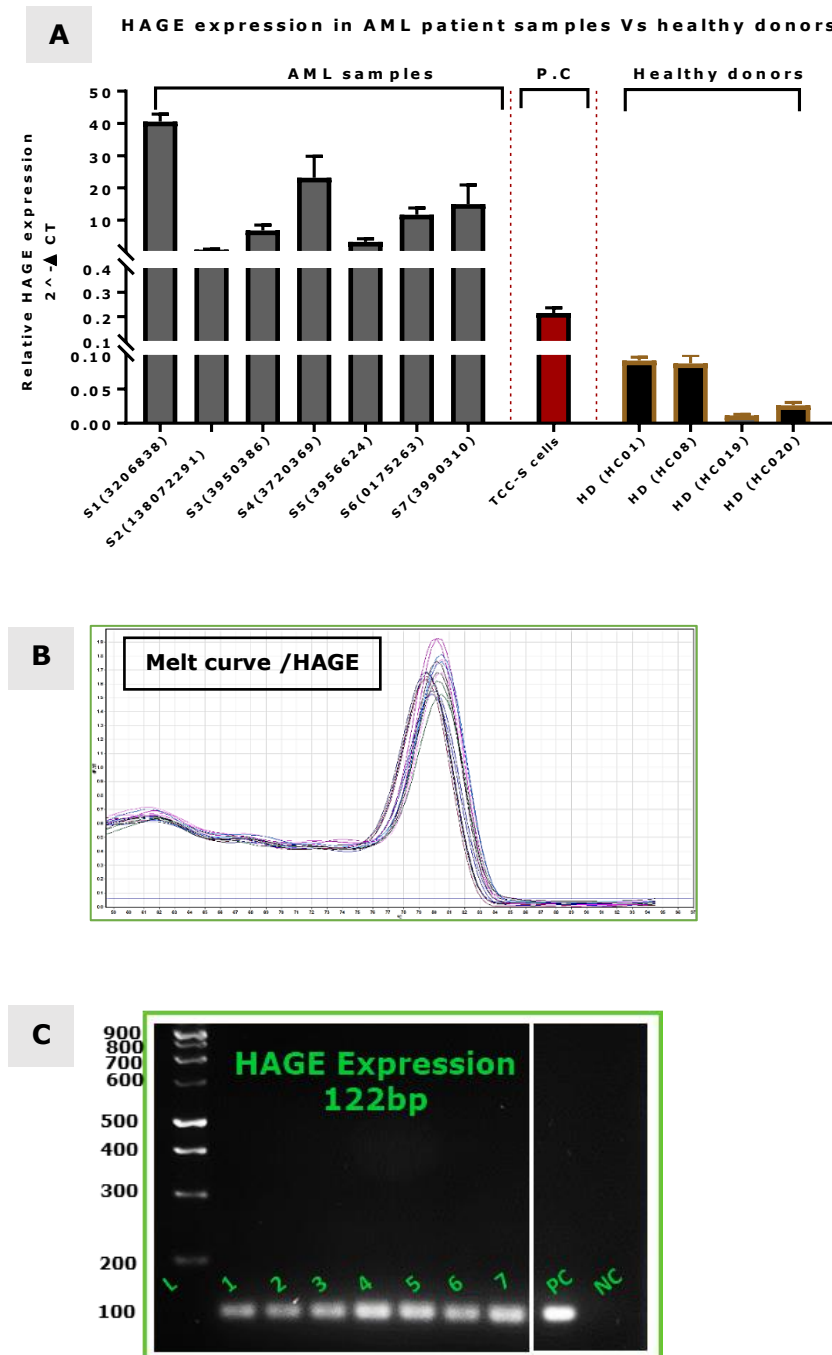


**Figure 3.11: HAGE expression in samples from patients with AML.**

cDNA samples were amplified using RT-qPCR and the products were then run on 2% w/v agarose DNA gel. **(A) Bar graph demonstrates HAGE expression using RT-qPCR.** Data are plotted as  $2^{-\Delta CT}$  values. All the CT values were normalised to an internal control gene (GUSB). Each bar represents mean  $\pm$  SD of two replicates of two repetitions. **(B) Melt curve analysis to assess the dissociation characteristics of HAGE double stranded DNA during heating.** Results show a single pure amplicon/product synthesised by HAGE-specific primers indicating the specificity of the amplified fragments. **(C) Image of agarose gel electrophoresis of the studied samples.** PCR products were run on 2% w/v agarose gel and then visualised under UV light for assessing HAGE expression in the samples studied. cDNA from TCC-S cells was utilised as a positive control whereas a master mixed containing H<sub>2</sub>O instead of cDNA was used as a negative control. Overall, finding shows impressive HAGE expression in all samples studied in comparison to the healthy donors (HD).

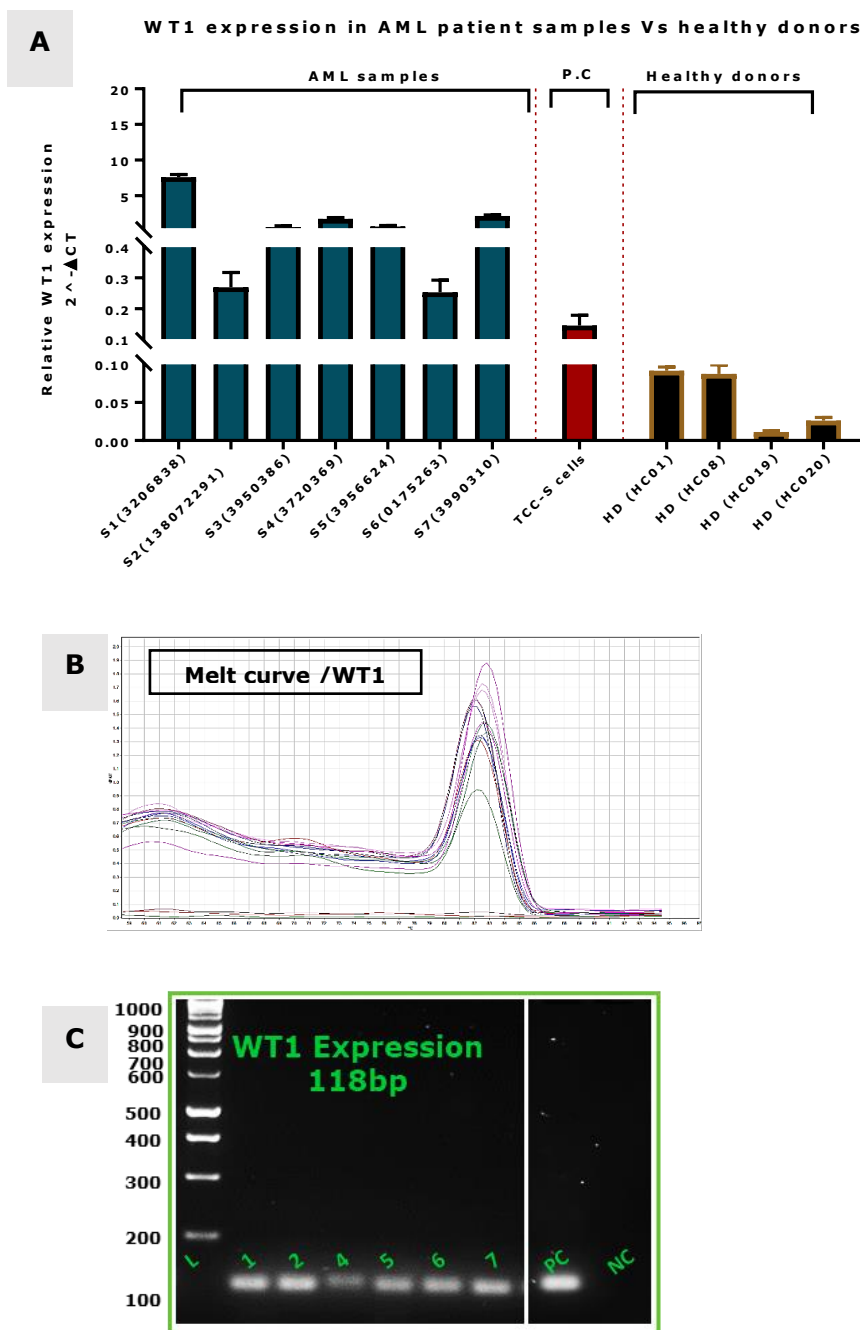


**Figure 3.12: WT1 expression in samples from patients with AML.**

cDNA samples were amplified using RT-qPCR and the products were then run on 2% w/v agarose DNA gel. **(A) Bar graph demonstrates WT1 expression using RT-qPCR.** Data are plotted as  $2^{-\Delta CT}$  values. All the CT values were normalised to an internal control gene (GUSB). Each bar represents mean  $\pm$  SD of two replicates of two repetition. **(B) Melt curve analysis to assess the dissociation characteristics of WT1 double stranded DNA during heating.** Results show a single pure amplicon/product synthesised by WT1-specific primers indicating the specificity of the amplified fragments. **(C) Image of agarose gel electrophoresis of the studied samples.** PCR products was run on 2% w/v agarose gel stained with SYBR safe and then visualised under UV light for assessing WT1 expression in the samples studied. cDNA from TCC-S cells was utilised as a positive control whereas a master mixed containing H<sub>2</sub>O instead of cDNA was used as a negative control. Overall, finding shows notable WT1 expression in all studied samples in comparison to the healthy donors (HD).

### 3.3.5 Expression of HAGE and WT1 transcripts in adult B-ALL

Additional cDNA generated from leukaemia samples from a collaboration at the University of Hull were analysed. These included 9 cDNA samples from adult acute lymphoblastic leukaemia (Adult B-ALL) pre-treatment, at a concentration of 1ng/ $\mu$ L, listed in Table 3.4. It was decided to assess the pattern of HAGE and WT1 expression in these samples as a part of general screening of the candidate genes in leukaemia, as far as the samples were available. Like previous samples, HAGE and WT1 expression were initially assessed using RT-qPCR technique and their products were then run on 2% w/v agarose gel to make sure that neither non-specific amplification nor primer-dimer products were produced. GUSB was initially used as an HKG for normalisation, but there was no amplification even until the end of cycle-40 neither by the RT-qPCR, nor on the gel electrophoresis. Unfortunately, similar results were obtained upon using the HKG GAPDH. However,  $\beta$ -actin revealed a peak of amplification on the RT-qPCR melt curve and a single band on the agarose gel at the desired molecular size. Data in Figure 3.13 confirm the specific amplification of  $\beta$ -actin expression, as a consequence of which  $\beta$ -actin was used as an internal reference normaliser for the genes of interest.

**Table 3.4: Adult B-ALL samples studied**

#	Reference number	Samples used
1.	Q115931	Adult B-ALL / Pre-treatment
2.	1380722	Adult B-ALL / Pre-treatment
3.	7310036	Adult B-ALL / Pre-treatment
4.	1394825	Adult B-ALL / Pre-treatment
5.	5014584	Adult B-ALL / Pre-treatment
6.	7310337	Adult B-ALL / Pre-treatment
7.	7257763	Adult B-ALL / Pre-treatment
8.	3849843	Adult B-ALL / Pre-treatment
9.	1411274	Adult B-ALL / Pre-treatment
PC	Positive control	TCC-S cells
NC	Negative control	ddH2O

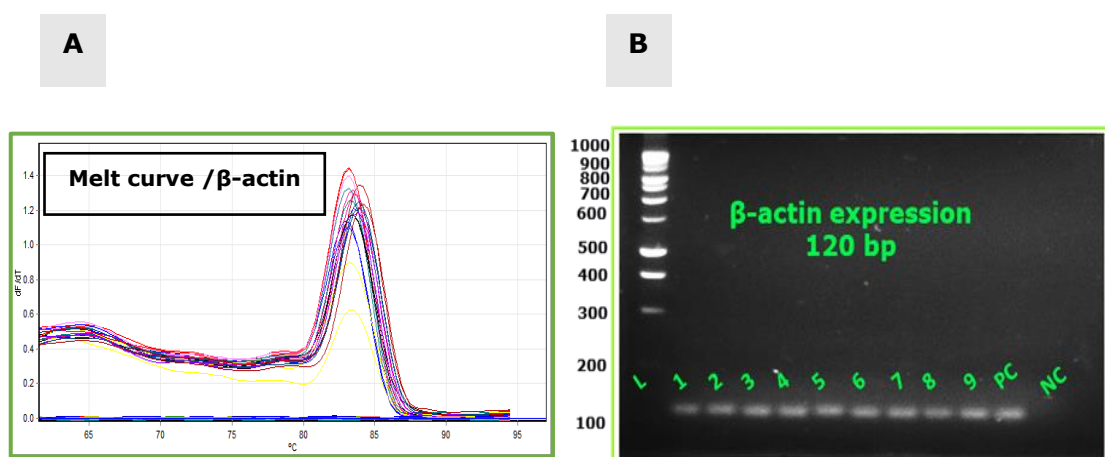


**Figure 3.13: β-actin expression in samples from patients with adult B-ALL.**

cDNA samples were initially amplified using RT-qPCR assay and the products were then run on 2% w/v agarose gels. **(A) Melt curve analysis to assess the dissociation characteristics of β-actin double stranded DNA during heating.** Results show a single pure product synthesised by β-actin-specific primers indicating the specificity of the amplified fragments. **(B) Image of agarose gel electrophoresis of the studied samples.** PCR products was run on 2% w/v agarose gel stained with SYBR safe and then visualised under UV light for assessing β-actin expression in the samples studied. cDNA from TCC-S cells was utilised as a positive control whereas a master mixed containing H<sub>2</sub>O instead of cDNA was used as a negative control. Overall, all samples contain the intact reference gene as reflected by single band signal intensity in the corresponding β-actin molecular size. therefore, they are suitable normalising the genes of interest.

The pattern of HAGE expression in the studied samples is illustrated in Figure 3.14 A, RT-qPCR data clearly demonstrated that 3 out of 9 (33%) patients had detectable level of HAGE mRNA transcripts, while the others had no or very low level of expression in comparison with TCC-S cells and healthy volunteers (that were normalised by β-actin) as reflected by absence/very low values of  $2^{-\Delta CT}$ .

WT1 mRNA transcripts, on the other hand, were detected in 7 out of 9 (77.7%) as the PCR product bands appeared clearly on the agarose gel (Figure 3.15). The low level of genes expression might be attributed to the low concentration of cDNA that were initially used for PCR amplification as the samples provided were very diluted and/or might be due to the incorrect HKG as a normaliser because β-actin came in very early cycle, therefore the calculated  $2^{-\Delta CT}$  were found to be low.

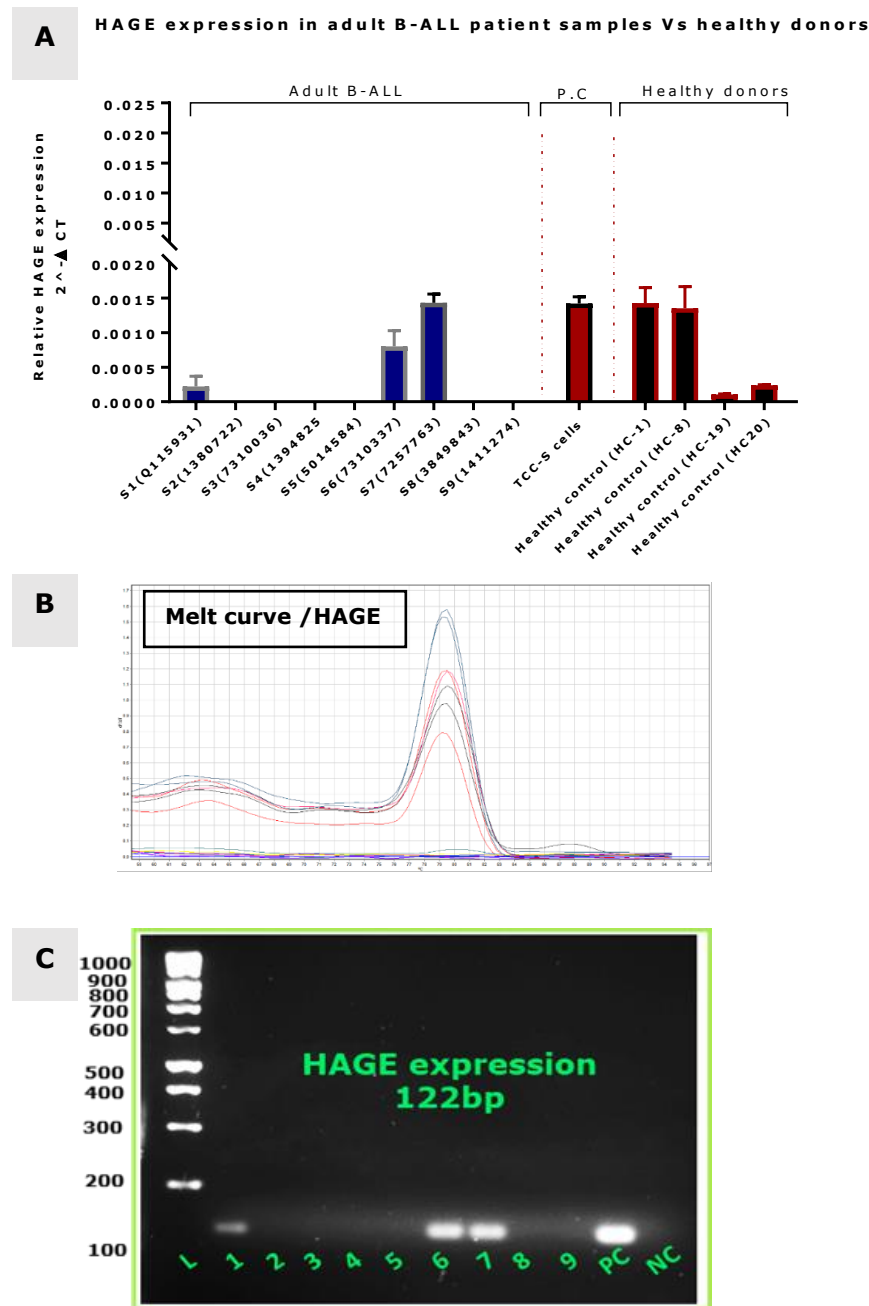


**Figure 3.14: HAGE expression in samples from patients with adult B-ALL.**

cDNA samples were amplified using RT-qPCR and the products were then run on 2% w/v agarose DNA gel. **(A) Bar graph demonstrates HAGE expression using RT-qPCR.** Data are plotted as  $2^{-\Delta CT}$  values. All the CT values were normalised to an internal control gene ( $\beta$ -actin). Each bar represents mean  $\pm$  SD of two replicates of two repetitions. **(B) Melt curve analysis to assess the dissociation characteristics of HAGE double stranded DNA during heating.** Results show a single pure amplicon synthesised by HAGE-specific primers indicating the specificity of the amplified fragments. **(C) Image of agarose gel electrophoresis of the studied samples.** PCR products was run on 2% w/v agarose gel stained with SYBR safe and then visualised under UV light for assessing HAGE expression in the samples studied. cDNA from TCC-S cells was utilised as a positive control whereas a master mixed containing H<sub>2</sub>O instead of cDNA was used as a negative control. Overall, findings show HAGE expression in 3/9 studied samples.

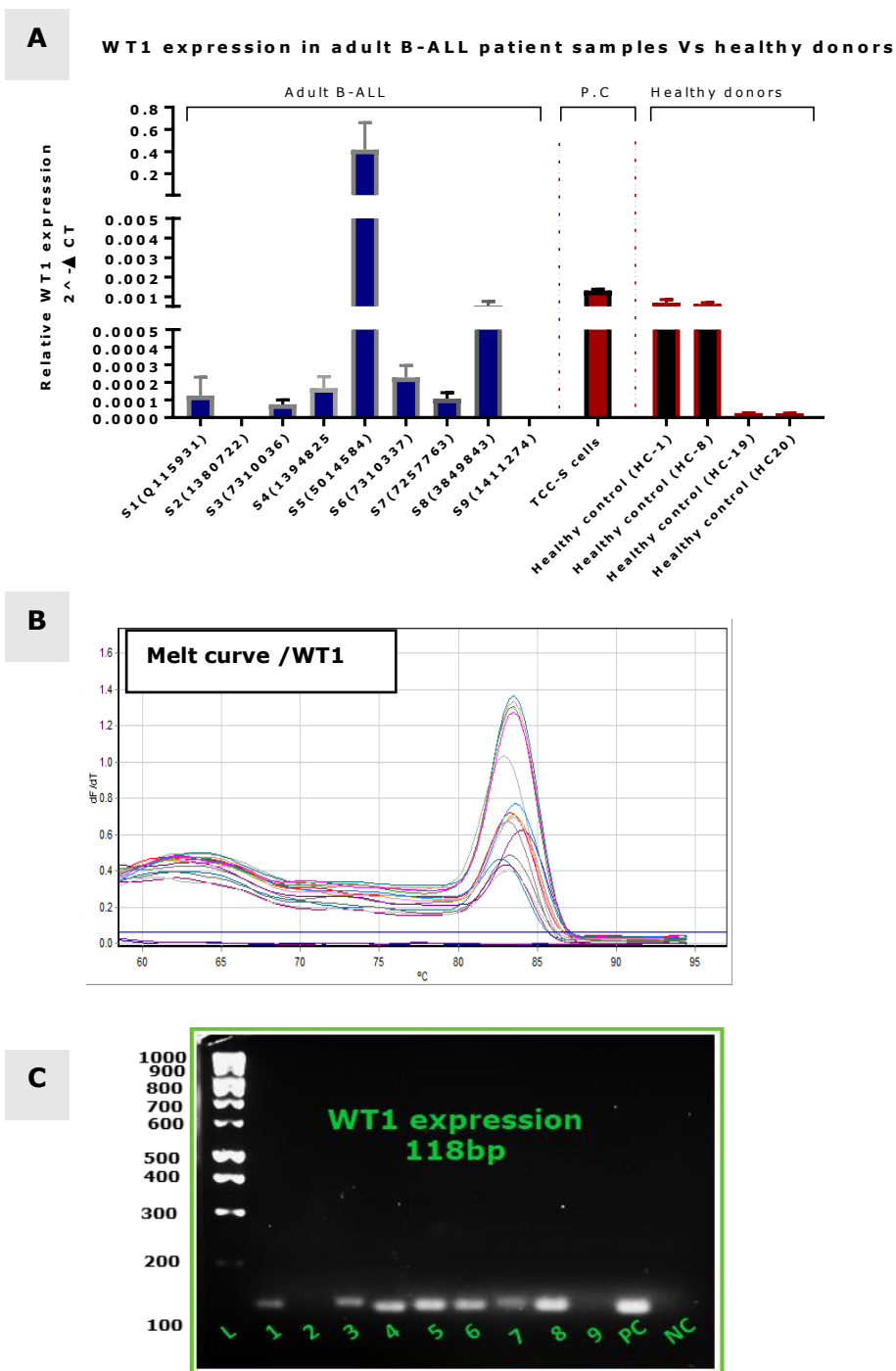


**Figure 3.15: Assessing WT1 expression in Adult B-ALL samples.**

cDNA samples were amplified using RT-qPCR and the products were then run on 2% agarose DNA gel. **(A) Bar graph demonstrates WT1 expression using RT-qPCR.** Data are plotted as  $2^{-\Delta CT}$  values. All the CT values were normalised to an internal control gene ( $\beta$ -actin). Each bar represents mean and SD of three replicates. **(B) Melt curve analysis to assess the dissociation characteristics of WT1 double stranded DNA during heating.** Results show a single pure amplicon synthesised by WT1-specific primers indicating the specificity of the amplified fragments. **(C) Image of agarose gel electrophoresis of the studied samples.** PCR products was run on 2% agarose gel stained with SYBR safe and then visualised under UV light for assessing WT1 expression in the samples studied. cDNA from TCC-S cells was utilised as a positive control whereas a master mixed containing H<sub>2</sub>O instead of cDNA was used as a negative control. Overall, findings point out WT1 expression in 7/9 studied samples.

### **3.3.6 Patterns of Cancer Testis and WT1 gene expression in AML and CML, as determined by microarray analysis using the ArrayExpress database**

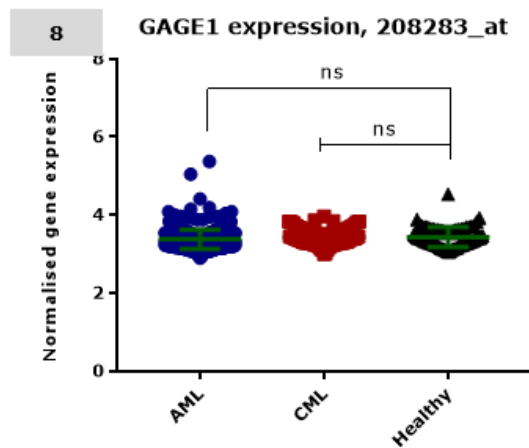
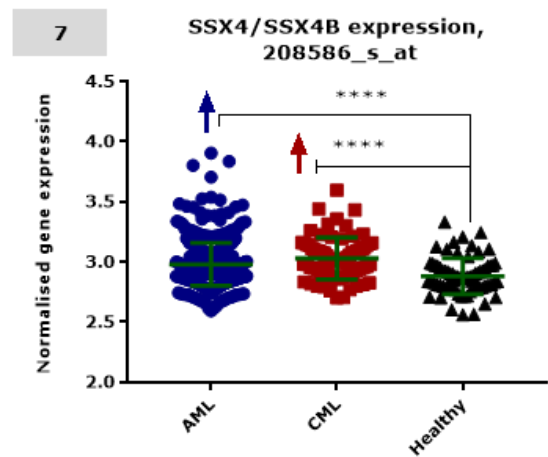
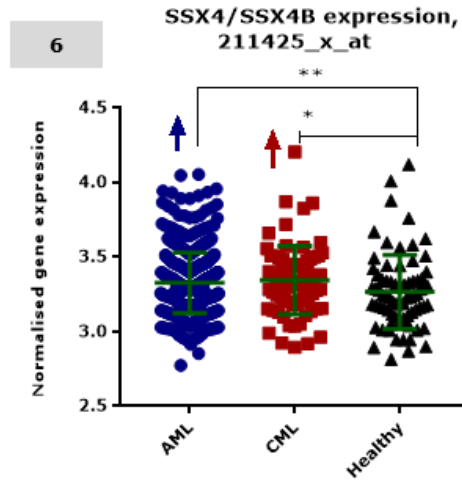
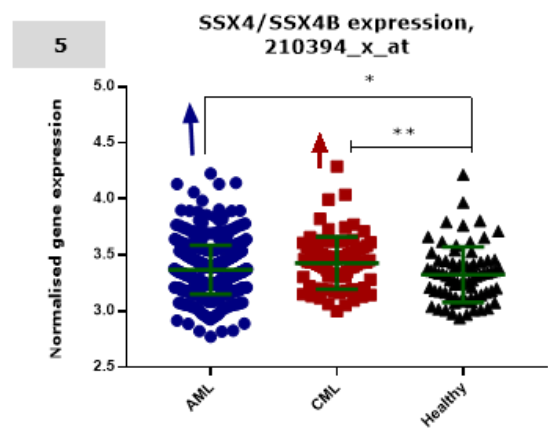
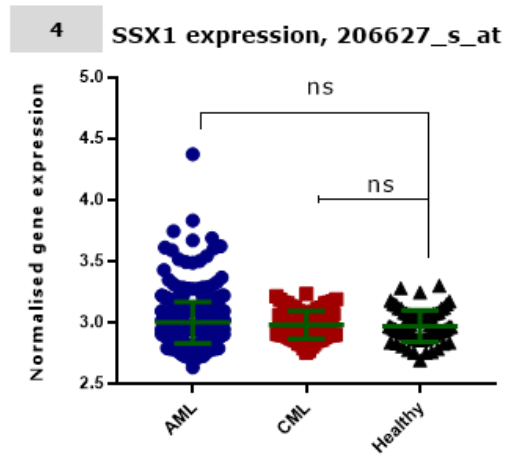
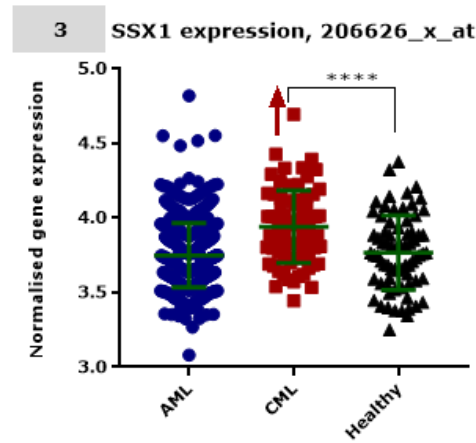
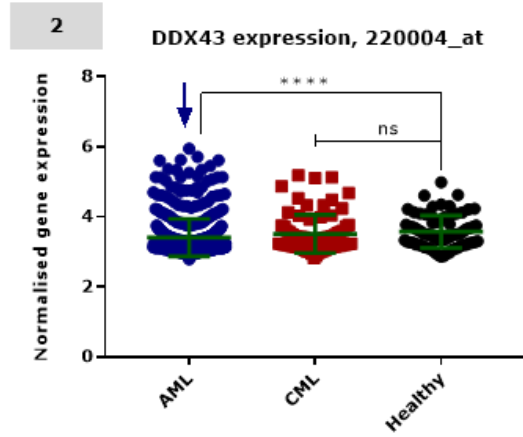
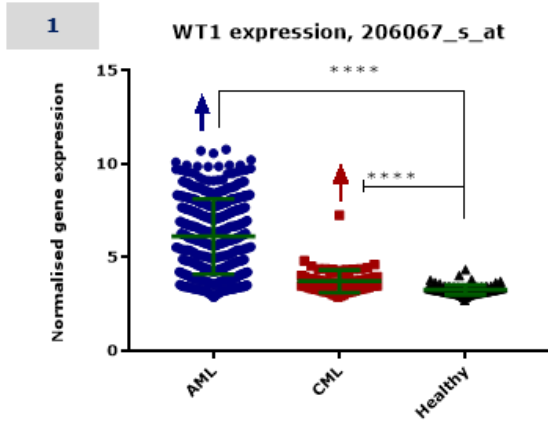
In this section, in addition to the data above that demonstrated HAGE and WT1 expression in CML and AML patient samples using RT-qPCR, cancer testis antigens and WT1 expression in CML and AML was investigated using a clinical database published in ArrayExpress website. ArrayExpress is the biggest repository of data collected from microarray and RNA sequencing platforms with experimental details, clinical annotation, and other relevant biological experimental details. Such a database can provide a guide and or preliminary information to generate reproducible research and a platform for testing multiple hypothesis in patient gene expression data.

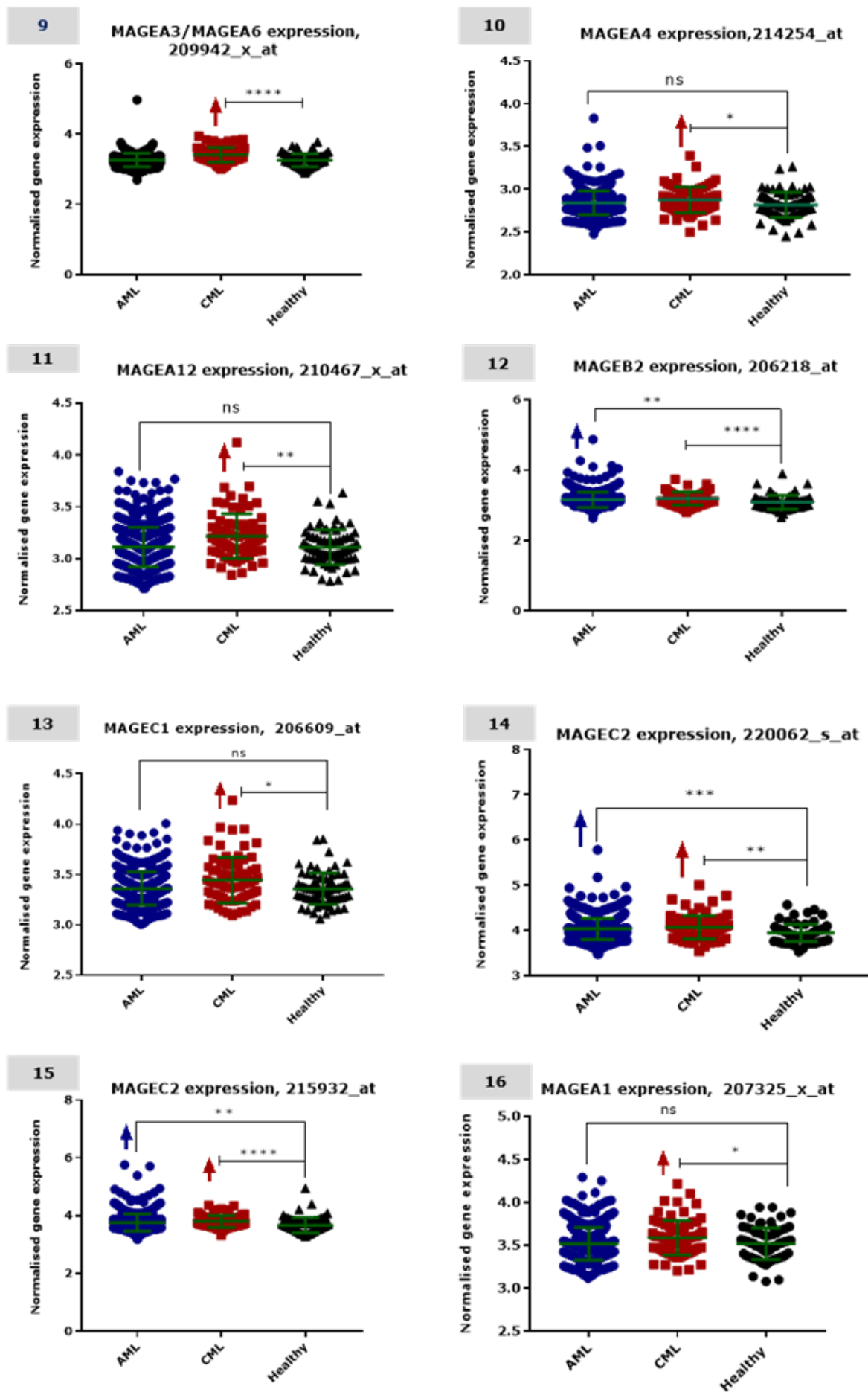
In this project, raw data were collected from a leukaemia study (ArrayExpress accession number E-GEOD-13159) named as "Microarray Innovations in LEukemia (MILE) study: Stage 1 data", (stander reference=2096), which is a part of the MILE Study "Microarray Innovations in LEukemia", available at: <https://www.ebi.ac.uk/arrayexpress/experiments/E-GEOD-13159/>.

The MILE study is an international multi-centre study, established in 2005, to define the clinical value of microarray-based gene expression profiling in the diagnosis and sub-classification of leukaemia. It was released on 30<sup>th</sup> of September 2009 and finally updated on 27<sup>th</sup> March 2012. The MILE study involved 11 participating centres distributed in three continents, wherein, in the first stage of the study, blood or bone marrow samples of acute, chronic leukaemia and myelodysplastic syndromes patients were hybridised to Affymetrix HG-U133 Plus 2.0 GeneChips for the discovery of biomarkers and generated whole-genome expression profiles from 2,143 patients. In the second stage, further validation of the gene expression profiling-based diagnostic accuracy was done of an independent cohort of 1,191 patients. The method of this study, as described by the authors, involved the following steps; initially, PBMCs were obtained from *de novo* untreated patients using Ficoll density centrifugation (Haferlach, Kohlmann *et al.* 2010). Total RNA from each sample was then converted into double-stranded cDNA by reverse transcription using an oligo(dT)24 – T7 primer and Poly-A control transcripts. The generated cRNA was then purified and quantified using the GeneChip Sample Cleanup Module (Affymetrix) and the NanoDrop ND-1000 spectrophotometer, respectively. The incubation steps during the cDNA transcription and target fragmentation were achieved using the Hybex Microarray Incubation and Eppendorf ThermoStat plus systems.

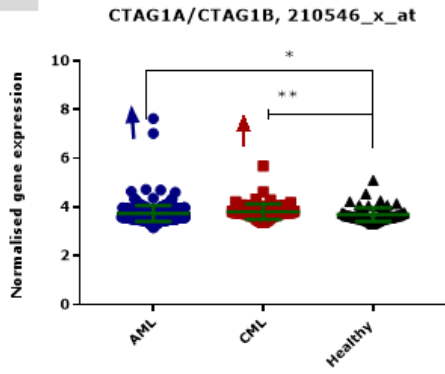
Our contribution in the present study was to collect the raw data generated from MILE study and normalised them using Robust Multichip Analysis (RMA). RMA is a normalisation procedure for microarrays that corrects background, normalises and summarises the probe level information as log<sub>2</sub> values. All possible probes of each genes of interest were searched in Affymetrix annotation and it is found that some genes have more than one possible probe; however, all the possible probes were herein analysed. Each probe was then essentially used to collect the relevant values from the processed (normalised) excel sheet of 542 AML, 76 CML and 73 healthy samples.

Values in each set (AML, CML, healthy volunteers) were firstly assessed for being normally distributed using at least two normality tests D'Agostino and Pearson normality test, and Shapiro-Wilk normality test using GraphPad Prism-7, followed by plotting of the frequency distribution histograms. Data that failed normality distribution tests and showed abnormal frequency distributed histograms was examined in comparison to the healthy control group using non-parametric test followed by Mann Whitney test. Data from control and disease samples that passed the tests for normality distribution was compared using the unpaired t-test. Summary results of the pattern of the gene expression in CML and AML is provided in Table 9.1 and Table 9.2 respectively, (see Appendix), in addition to the multigraphs chart in Figure 3.16.

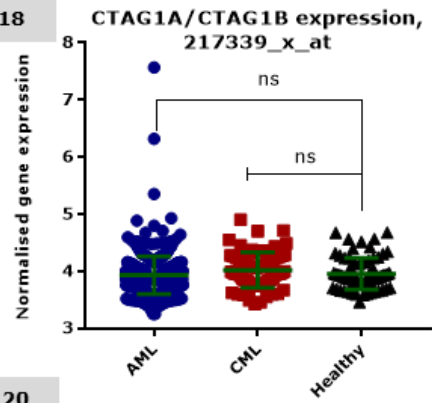




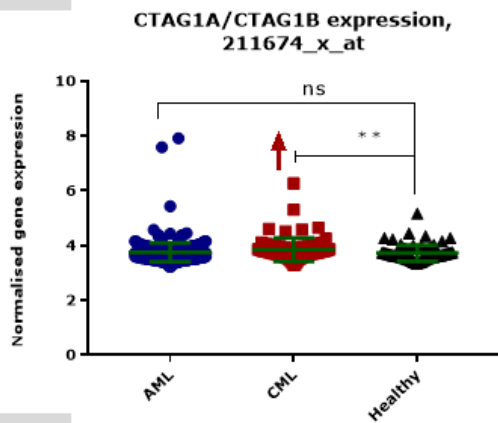
17



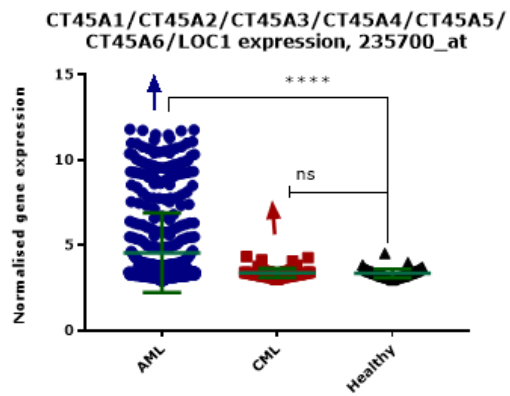
18



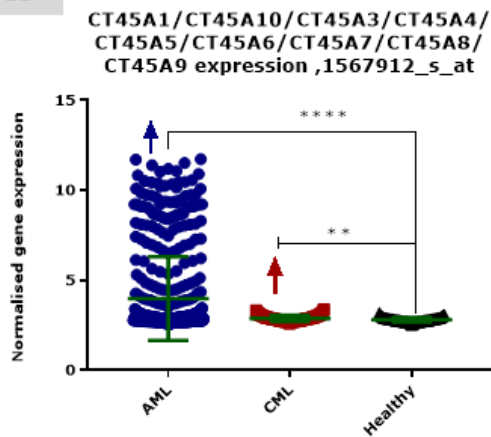
19



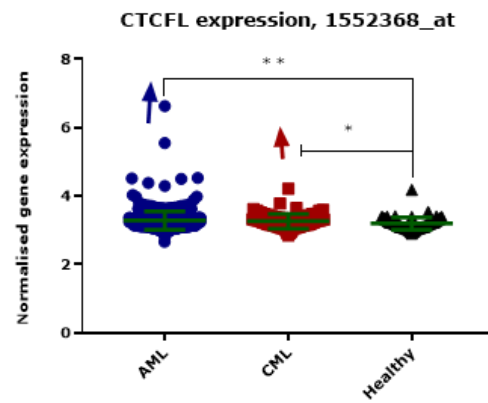
20



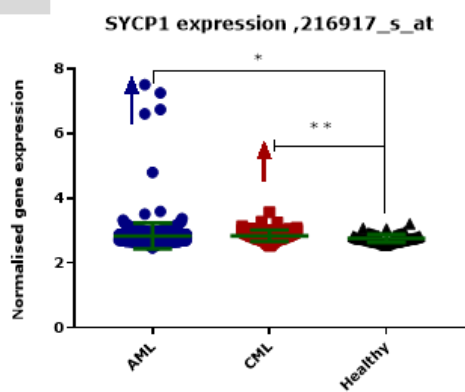
21



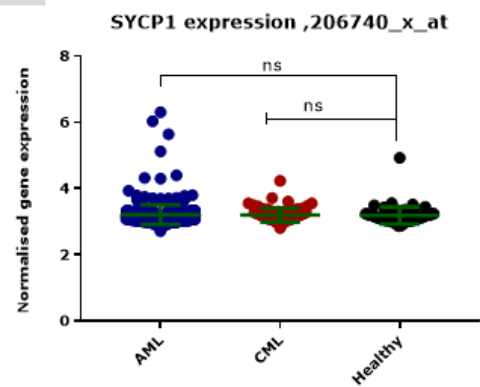
22

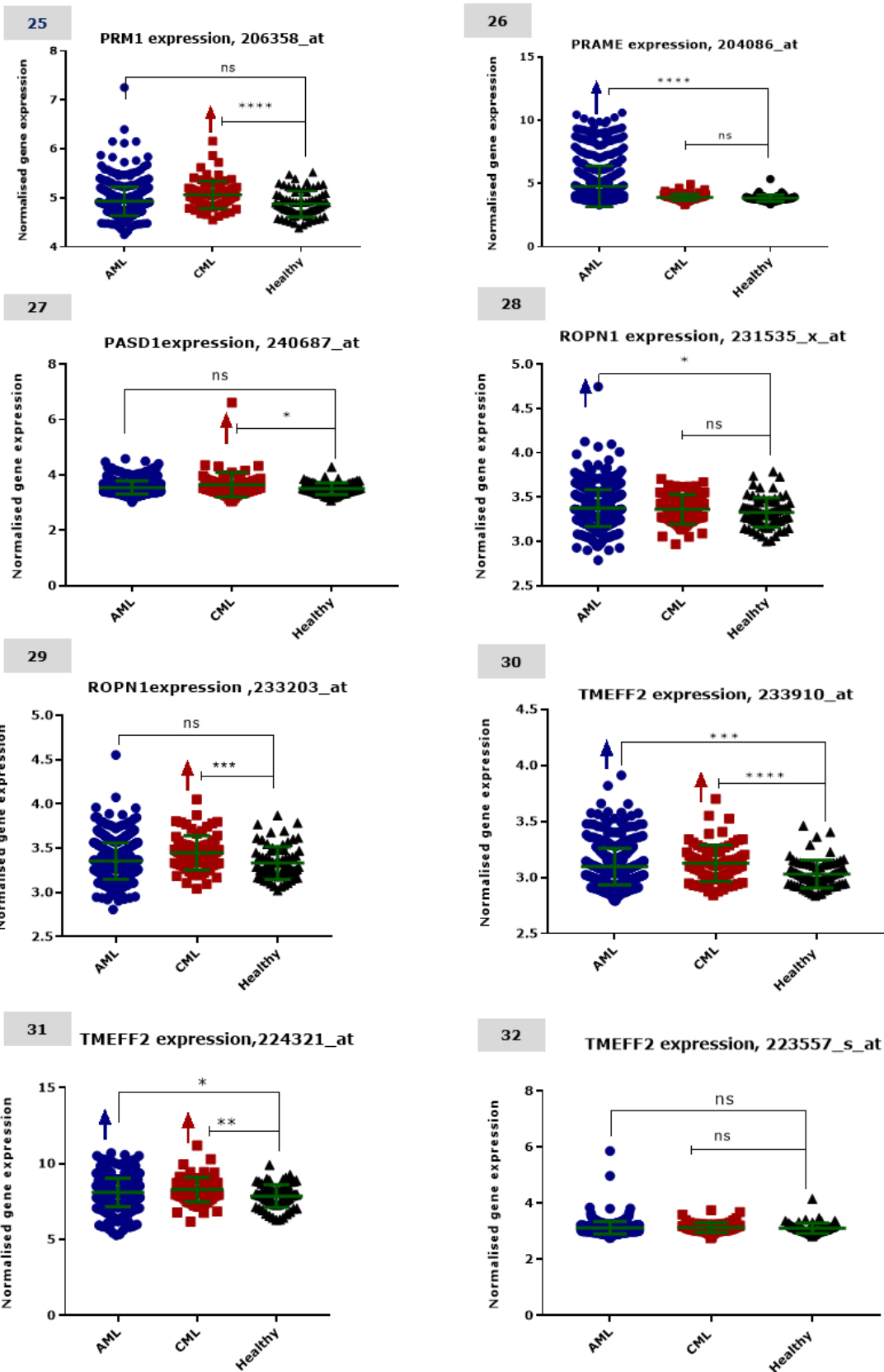


23



24





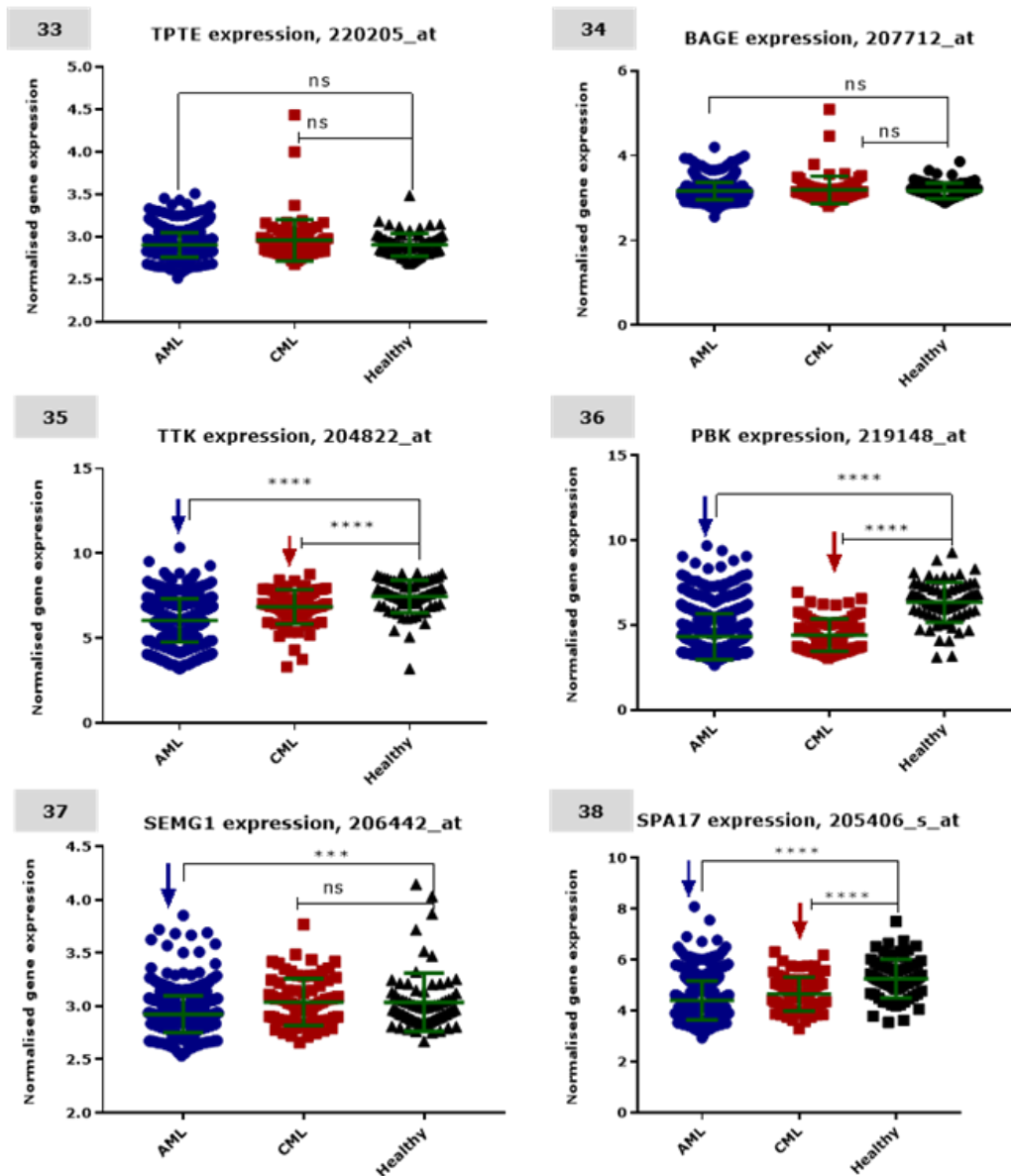


**Figure 3.16: Expression patterns of C/T and WT1 genes in samples obtained from patients with AML and CML analysed from MILE study.**

Data were collected from a study called "E-GEOD-13159-Microarray Innovations in LEukemia (MILE) study: Stage 1 data" published on ArrayExpress website, normalised using Robust Multichip Analysis (RMA), and processed using GraphPad Prism (version 7.04). Each graph is titled by the name of the gene of interest and the prob used. Blue, red and black colour symbols represent AML, CML and healthy volunteers respectively. Statistically, each group was firstly tested for the normality distribution using at least two test D'Agostino & Pearson normality test and Shapiro-Wilk normality test. Group that passed the normality distribution tests and showed normal shape frequency distribution histogram (bell-shape histogram) was analysed using unpaired t-test Whereas group that failed normality distribution test and showed abnormal shape frequency distribution histogram (skewed) was processed by non-parametric test followed by Mann Whitney test. In each graph, *P-value* was used to point out the significance in the difference between the diseased group and the healthy. Overall, results in graphs show different patterns of C/T and WT1 genes expression in AML and CML samples; wherein the majority of samples were showed different degrees of upregulation, few of them showed no upregulation, and very few genes showed downregulation. Number of AML samples=542, CML=76 and healthy volunteers=73.

## 3.4 Discussion

Immunotherapy is an attractive therapeutic option in the field of haematological malignancies. However, to date, progress in the development of cancer vaccines for such aggressive diseases has not been very impressive, principally due to the lack of suitable targets. Importantly, the delivery of effective antigen-based immunotherapy essentially depends on the recognition of the cancer antigen displayed on the cancer cell surface by antigen-specific T cells.

In general, C/T antigens are shown to be epigenetically upregulated on cancer cells following demethylating chemotherapeutic agents, a strategy that could be applied before giving a C/T based vaccine to circumvent the problem of heterogeneity in antigens expression and to make tumour cells more vulnerable to antigen-specific T cell recognition and killing. Employing a similar concept, McCarty, Loeb (2015) found a solid correlation between the Intron 1 CpG island methylation and WT1 silencing in AML patient samples as well as cell lines (McCarty, Gregory, Loeb 2015).

In the first section of this chapter, attempts to validate HAGE and WT1 as potential targets for cancer immunotherapy were described. Although previous studies proved this observation, our purpose was mainly to substantiate consistency with the previously published data. To achieve this, a panel of leukaemic cell lines from CML, AML, AMoL and ALL available in our laboratory were initially scanned for HAGE and WT1 expression at transcriptional and protein levels. Expression of these genes in samples from patients with CML, AML, adult B-ALL was also assessed.

Regarding HAGE expression in CML cell lines, HAGE transcript was expressed by 3 out of 7 cell lines but none, except TCC-S cells, expressed it at protein level. These data were not surprising since it has previously been shown that HAGE promoter is hypermethylated in CML cell lines which influence its expression. For example, a previous PhD student in our group, Morgan, 2007 confirmed this observation by treating K562 and KYO-1 cells with a demethylating agent (5'-aza-2'-deoxycytidine), with and without a deacetylase inhibitor, (trichostatin A) and showed HAGE re-expression at mRNA level. The author found that this treatment significantly enhanced the expression of HAGE transcript in the studied CML cell lines (Morgan Mathieu, a PhD thesis, 2007). Similarly, Lin and *et al.* found that HAGE expression could be restored after treating K562 cells with a demethylating agent (Lin, Jiang, Chen *et al.* 2014). Together, these observations imply that hypermethylation is an essential mechanism via which HAGE transcription is silenced in CML cell lines.

The expression of HAGE was also assessed in three acute myelogenous cell lines, three acute monocytic leukaemia cell lines and one acute lymphoblast leukaemia cell line. Interestingly, none of these cell lines express HAGE at protein level, and few of them express barely detectable quantities of HAGE transcripts, except SUPB-15 cells which expressed HAGE transcript at similar levels to KCL-22 and K562 cells and few

quantity of protein, suggesting a possible epigenetic derived mechanism, i.e. hypermethylation that could constrain HAGE transcription in the selected cell lines. This assumption needs to be proved in the future work since there is no available report studying HAGE DNA hypermethylation in these specific cell lines. Similarly, many other C/T antigens were not expressed in AML cell lines unless they were treated with demethylating agents due to hypermethylation (Atanackovic, Luetkens *et al.* 2011). Taken together, these results indicate that C/T antigens are often not expressed in leukaemic cell lines due to hypermethylation of their promoters, but that they can be re-expressed after treatment with demethylation agents. This could make HAGE a good target for immunotherapy for the treatment of leukaemia regardless of its expression at the time of diagnosis since these patients could first receive a demethylation agent prior to receiving a HAGE-derived vaccine.

Regarding WT1 expression, interestingly, WT1 is expressed by all the CML, AML, AMoL and ALL, except KYO-1 cells. These findings are consistent with many studies that have shown WT1 to be among the most predominant antigens expressed by myeloid cancerous cells.

In addition to the cell lines, HAGE and WT1 transcripts expression in cDNA samples obtained from CML, AML and adult B-ALL human patients were assessed.

Pre-treatment CML cDNA samples was kindly provided from collaborative work at the University of Liverpool where the samples were already processed, and cDNA synthesised. We detected HAGE expression in 54% of the samples, a result which is comparable to that found by Adam, *et al.* at 55% of CML bone marrow and peripheral blood samples using RT-qPCR (Adams, Sahota *et al.* 2002). WT1 expression was detected in all CML samples studied, with expression being higher than that found in TCC-S cells in 9/13 (70%). This high percentage of WT1 expression is consistent with other studies that have reported WT1 overexpression in CML (Inoue, Sugiyama *et al.* 1994, Karakas, Miething *et al.* 2002).

Furthermore, HAGE expression in these samples was correlated to WT1 expression to identify possible associations, and it was found that the majority of samples that over-expressed WT1 also expressed HAGE, indicative of synchronised expression of both genes in CML. In all cases (4/4), samples that showed low levels of WT1 expression also expressed lower levels of HAGE. These findings of co-expression are of particular importance since we hypothesised a promising outcome upon incorporation of HAGE and WT1.

For 4 patients, additional samples were available after failure of imatinib treatment. A significant increase of both HAGE and WT1 transcripts were found in 2 concomitant pairs (i.e. simultaneous upregulation of both HAGE and WT1) out of 4 pairs. Although, it is difficult to know whether this increase is due to a larger number of cancer cells present in the samples or whether the level of mRNA has increased *per se*. Moreover, it is not possible to know whether they are the results or the cause of imatinib failure.

It would be therefore very interesting if one could follow HAGE expression over time in a large cohort of patients as is done for *BCR-ABL1* transcript monitoring. Collectively, both HAGE and WT1 can be considered feasible targets for immunotherapy and as biomarkers of disease progression although the latter observation needs to be investigated in a larger cohort of paired samples.

HAGE and WT1 expression were also assessed in cDNA of AML patients using RT-qPCR. These samples were assessed according to collaborative work at the University of Hull, where samples were initially assessed using RT-qPCR and normalised using GUSB as an internal reference control. Since some samples show no amplification of GUSB using the RT-qPCR (a case might be attributed to the disease heterogeneity among the studied samples), all PCR products were run on 2% w/v agarose gel to make sure that GUSB is valid gene for normalising the genes of the interest. Few samples that were found not to express GUSB were accordingly excluded from the analysis. Overall, all AML samples (100%) showed HAGE overexpression in comparison with healthy controls. This percentage seems to be high in comparison with what Adam, *et al.* found in 2002 at 23% of AML bone marrow and peripheral blood samples using RT-qPCR (Adams, Sahota *et al.* 2002). These variations might be attributed to the specificity of pair primers and or sensitivity of PCR applied, number of samples, or disease stages.

Similarly, WT1 transcripts were detected in all AML patient samples studied, a result that is consistent with other study that demonstrated WT1 overexpression in 37-100% of AML (Inoue, Sugiyama *et al.* 1994, Karakas, Miething *et al.* 2002). It is also in agreement with study conducted by Aydin (2013) in which WT1 is revealed to be expressed by 100% AML blasts in the bone marrow at diagnosis (Aydin, Riera *et al.* 2013).

In addition, there was an opportunity to study 9 cDNA samples from patients with adult B-ALL - it was interesting to study the pattern of HAGE and WT1 expression in this disease alongside with other types of leukaemias. Therefore, these samples were investigated for HAGE and WT1 expression at the mRNA level using RT-qPCR together with the internal reference gene, GUSB. Surprisingly, some samples showed amplification of HAGE and WT1, but not GUSB by RT-qPCR and on the agarose gel. Similar to GUSB, there was no amplification detected upon using another HKG (GAPDH). Therefore,  $\beta$ -actin was tried, which returned a successful specific amplification, as demonstrated by PCR and agarose gel electrophoresis. HAGE is expressed by 33.3% (3/9) and WT1 by 77.7% (7/9) of the samples, but at a low level in comparison to the TCC-S cells and healthy individuals. These results are aligned with results from Menssen, Renkl *et al.* which showed that WT1 is expressed in 12 of 14 (86%) of samples from patients with pre-B-ALL (Menssen, Renkl *et al.* 1995). However, it is not in agreement with study conducted by Chiusa, *et al.* which

indicated that WT1 gene expression is present in 100% cases of samples from patients with adult ALL that they studied (Chiusa, Francia di Celle *et al.* 2006). Variations in detection of a gene expression in general could be due to the variability in handling of samples, quality and quantity of RNA/cDNA utilised for PCR amplification (since adult ALL- cDNA samples that we used in the present study were so diluted), and also might be due to the type of the internal control chosen for normalisation, as  $\beta$ -actin is amplified in very early cycles of PCR run; therefore, the values of relative gene expression ( $2^{-\Delta CT}$ ) could be subsequently low. Overall, data obtained in this batch of samples is not very conclusive and a larger cohort of samples would be required.

Recently, there has been a renewed interest in studying the role of C/T antigens in cancer and their possible usage as target therapeutic vaccines against cancer. Therefore, in the second section of this chapter, our search was extended to validate the expression of a comprehensive range of cancer testis family members including HAGE, as well as WT1 as targets for immunotherapy in AML and CML from a large cohort study titled as "E-GEOD-13159-Microarray Innovations in LEukemia (MILE) study: Stage 1 data", from which, raw clinical data were collected, normalised and plotted. Microarray chips assay represent a potent technology for measuring the expression of thousands of genes concomitantly. Providing such profiling has led to substantial advances in the understanding of cellular events at the molecular level, which could lead to the development of molecular diagnostics and personalised medicine (Jain 2004).

Overall, the majority of the genes studied were found to be highly expressed in AML and CML in comparison to the healthy individuals. However, some of these genes did not show any significant difference in their expression, and very few of them had a significant downregulation.

In the discussion below, the patterns of C/T and WT1 expression in CML and AML will be discussed, and the consistency with other published studies will be cross matched whenever they are available since the expression of many members of the C/T family in leukaemia have not been quite covered yet. Delivering such analysis could provide basic preliminary information that could assist in the development of C/T based immunotherapy in leukaemia.

WT1 was found to be significantly more expressed in both diseases in comparison to the controls with \*\*\*\* $p$ -value<0.0001 each, indicating the validity of WT1 as immunotherapeutic target for these diseases. These observations are in line with studies and results demonstrating WT1 overexpression in cDNA of CML and AML patient samples as well as cell lines mentioned above.

However, the expression of HAGE (DDX43), despite being expressed by both leukaemias, was found to be significantly downregulated in samples from patients with AML (\*\*\*\* $p$ -value<0.0001), and no significant difference in its expression was

found between CML samples and healthy individuals. These results are in direct contradiction with what has been found in the above-mentioned collaborative studies performed on AML and CML samples. However, the number of samples studied is small and the primers used are different to the probes used and it is therefore possible that the probes are affected by the methylation status of HAGE. The possibility of epigenetic control of HAGE expression in leukaemia was referred in a study conducted by Lin, Chen *et al.* in 2014, wherein the authors found that HAGE DNA was methylated in 85% (182/214) of patients with AML, whereas it was hypomethylated in 15% (32/214), and they confirmed that the level of HAGE expression was significantly correlated with HAGE hypomethylation using Real-Time Quantitative Methylation-Specific PCR (RQ-MSP) and bisulfite sequencing to evaluate the methylation density of CpG in DDX43 promoter (Lin, Jiang, Chen *et al.* 2014). Adding these observations to results arguing the methylation status of HAGE in the CML cell lines described-above; it seems that the application of HAGE vaccine in leukaemias as an immunotherapy might need a prior treatment with demethylated agents to restore the silenced promoter.

The expression of the synovial sarcoma X chromosome breakpoint (SSX) family was also studied in CML and AML in comparison to healthy controls. SSX family were reported to be associated with advanced cancer stages and poor prognosis (Smith, H. A., McNeel 2010). Herein, data from CML samples show a significant upregulation of SSX1 when the 206626\_x\_at probe is used, whereas no significant difference could be found with the 206627\_s\_at probe. SSX4/SSX4B were also assessed in both AML and CML *versus* healthy controls using three different probes: (210394\_x\_at), (211425\_x\_at) and (208586\_s\_at). Results demonstrate a significant difference between leukaemic and healthy control samples in all three probes; however, the maximum upregulation is noticed when the 208586\_s\_at probe is used. Within the available published data related to our study, Niemeyer, *et al.* studied the expression of five C/T genes in AML and ALL using RT-PCR, including SSX-1 and SSX-2, where the authors found that there were no detectable expression of any genes in AML, whereas four out of five C/T genes showed frequent expression in ALL (Niemeyer, Türeci *et al.* 2003). Unfortunately, there is no available data for SSX family expression in CML.

The expression of some members of the melanoma antigen gene (MAGE) were also assessed. In fact, MAGE family that constitutes a subset of more than 40 human proteins has been extensively studied in various cancers, in which their expression has been found to be associated with a poorer clinical outcome (Weon, Potts 2015). In addition, it has been revealed that DNA hypomethylation plays a key element in the regulation of MAGE expression in solid tumours (De Smet, Lurquin *et al.* 1999). Herein, six members of MAGE family were studied in AML and CML using different probes, and as the following; MAGEA3/MAGEA6 (209942\_x\_at), MAGEA4

(214254\_at), MAGEA12 (210467\_x\_at), MAGEB2 (206218\_at), MAGEC1 (206609\_at), MAGEC2 (220062\_s\_at) MAGEC2 (215932\_at) and MAGEA1 (207325\_x\_at) . Data demonstrate that there is upregulation of all the candidate genes in CML group with maximum upregulation detected in MAGEA3 and MAGEA6 (209942\_x\_at), MAGEB2 (206218\_at) and MAGEC2 (215932\_at) at \*\*\*\**p-value*<0.0001, and less upregulation is noticed when MAGEA4 (214254\_at) , MAGEC1 (206609\_at) probes are used with \**P-value* only. These results are partially consistence with Mendoza-Salas *et al.*, 2016 study which was conducted on 65 *de novo* CML patients, wherein, authors demonstrated that the most prevalent MAGE genes were MAGEA4 and MAGEA3 at 63% and 32.4%, respectively whereas the expression of MAGEB2 and MAGEC1 genes was less prevalent at 3.07% and 1.50%, respectively (Mendoza-Salas, Olarte-Carrillo *et al.* 2016). On the other hand, the AML group shows lower upregulation of MAGE gene expression. For example, MAGEA4 (214254\_at), MAGEA12 (210467\_x\_at) and MAGEC1(206609\_at) demonstrate no significant statistical upregulation in the studied probes whereas a considerable overexpression in MAGEB2 (206218\_at) and MAGEC2 (220062\_s\_at) is significantly present. It has been reported that some members of the MAGE family in AML is associated with a dense methylation of the promotor which silences their expression. For example, MAGEA3/6 was found to be expressed at low levels in 100% at the time of diagnosis, yet there was a statistically significant increase in its expression after treatment with demethylating agents (Srivastava, P., Paluch *et al.* 2016). Therefore, we assume that a possible epigenetic regulation prevents the expression of the most MAGE members studied herein in AML.

In addition, genes responsible for the expression of the cancer testis antigen 1A (CTAG1A) and cancer testis antigen 1B (CTAG1B) were also studied. Data were generated using three different probes targeting both genes concurrently. Findings indicate that both genes are upregulated more in CML than AML in comparison to the same control group in two probes applied (211674\_x\_at) and (210546\_x\_at). Nevertheless, no statistical upregulation could be detected when the 217339\_x\_at probe was used.

Moreover, members of C/T 45A gene family (CT45A) were investigated for their expression in CML and AML *versus* the healthy. This family is known to be expressed in many types of cancer (Chen, Yao -Tseng, Hsu *et al.* 2009). The CT45A1/CT45A10/CT45A2/CT45A3/CT45A4/CT45A5/CT45A6/CT45A7/CT45A8/CT45A9 genes were simultaneously studied using a single probe (235700\_at). Interestingly, it has been found that AML is associated with strong overexpression at \*\*\*\**p-value*<0.0001 whereas no statistically significant difference was found in CML. Similarly, the expression of CT45A1/CT45A10/CT45A3/CT45A4/CT45A5/CT45A6/CT45A7/CT45A8/CT45A9 was assessed using a single probe (1567912\_s\_at),

wherein a significant upregulation of these set of genes was detected at \*\*\*\**p-value*, and \*\**p-value* in AML and CML samples, respectively.

The synaptonemal complex protein-1 (SYCP1) gene expression was also herein assessed. A significant upregulation in both leukaemias was found when one probe was used (216917\_s\_at), whereas no upregulation could be detected using another probe sequence (206740\_x\_at). Again, there is no available published data for cross matching with our data.

The cancer testis gene responsible for the expression of the Preferentially Expressed Antigen in Melanoma (PRAME) was herein also assessed, and it was found to be associated with a very impressive upregulation in AML (\*\*\*\**p-value*<0.0001), whereas no significant upregulation of PRAME in CML could be seen. This result is consistent with a study conducted by Baren, which tested the PRAME expression on more than 250 bone marrow and blood samples collected from patients with various haematological cancer using RT-PCR, where a remarkable overexpression of PRAME in all acute myeloblastic leukaemias was detected (Baren 1998). Results are also in agreement with a study conducted by Atanackovic, Luetkens *et al.* on C/T gene expression in AML cell lines and AML bone marrow samples, wherein the author found that there was upregulation of PRAME gene in 53.1% of the studied samples using RT-qPCR, and that the level of PRAME can be induced upon a treatment with 5-azacytidine (Atanackovic, Luetkens *et al.* 2011). Such results support the preferential targeting of PRAME in the development of AML immunotherapy.

In contrast to PRAME, the Protamine1 (PRM1), which was recently found to be associated with poor outcome of colonic cancer (Chen, Zhi, Shi *et al.* 2018), herein is shown to be highly overexpressed in CML in comparison with healthy donors at \*\*\*\**p-value*, whereas no significant difference in its expression in AML could be detected. In myeloid leukaemias, there are few reports describing the pattern of PRM1 expression. Meklat, Zhang *et al.* 2009, for example, detected transcripts of PRM1 in 26.8% of CLL patients and therefore it could potentially be an appropriate target for the development of cancer immunotherapy in the early stage of CLL (Meklat, Zhang *et al.* 2009).

The expression of the TMEFF2 (Transmembrane Protein with EGF Like and Two Follistatin Like Domains 2) gene is also assessed in this study. TMEFF2 expression has been recently shown to be downregulated in colorectal, gastric and gallbladder cancers, suggesting a tumour suppressive function. In contrast, TMEFF2 is found to be significantly increased in prostate cancer implying its role in promoting cancer progression. In the present study, the expression of this gene is shown to be significantly upregulated in both leukaemias in two different probes. This might highlight the significance of targeting this antigen in the future work, as there is no available study has demonstrated such association.

Furthermore, a group of C/T genes (GAGE1, ROPN1, TPET and BAGE) shows no significant difference in their expression in AML and or CML in comparison to the control group. It is assumed that these genes might be also under the influence of the epigenetic control, and therefore an induction by demethylating agents might be suggested in the future work. However, ROPN1 expression is significant ( $*P\text{-value}=0.0482$ ) when the 231535\_x\_at probe was used. These results are inconsistent with data from Atanackovic, Luetkens *et al.* 2011 which showed that the ROPN1 expressed in a minority of AML patients (Atanackovic, Luetkens *et al.* 2011). Interestingly, a third group of C/T genes shows generally a remarkable downregulation in either AML, CML or both. For example, the TTK gene, a dual-specificity protein kinase that was considered to be implicated in the mitotic spindle assembly and controlling cell cycle system (Miao, Wu *et al.* 2016), herein was shown to be significantly downregulated in both leukaemias with  $****p\text{-value}<0.0001$  each. In a similar pattern to TTK expression, the PDZ binding kinase, PBK (another cell cycle controller protein) demonstrates a strong downregulation in AML and, to a lesser extent in CML. This protein was described by its upregulation in a variety of haematologic malignancies and possible role in leukaemic cell growth (Nandi, Tidwell *et al.* 2004).

In addition to the above-mentioned two downregulated genes, herein the gene responsible for the expression of the Semenogelin-1 antigen (SEMG1), an important protein of human semen coagulum, was found to be strongly downregulated in AML and not significantly upregulated in CML in comparison to the healthy donor group, suggesting an aberrant gene silencing of SMG1 in these leukaemias. These results disagree with a study by Zhang, Wang *et al.* 2003, in which SEMG1 expression was found to be frequently expressed in CML (62.5%, 5 of 8) and CLL (41.7%, 5 of 12) using PCR (Zhang, Y., Wang *et al.* 2003). However, the difference in the sample size and method of analysis between our study and Zhang's study should be considered. Finally, the SPA17 (sperm Autoantigenic Protein 17) gene interestingly found to be among the genes that were strongly downregulated in CML and AML. Again, there is not much literature or experimental work focussed on this gene in such leukemias. However, Figueroa, Chen *et al.* 2013 provided a list of genes that are commonly involved in methylation signature in ALL where the authors described the regulation of SPA17 expression by methylation process (Figueroa, Chen *et al.* 2013).

However, the microarray findings are all limited to detect the candidate genes only at mRNA level, and inconsistencies between mRNA and protein levels are frequently observed due to i) differing in mRNA molecules stability, ii) translation regulatory process, iii) post-translational modifications and iv) proteasomal degradation (Chen, G., Gharib *et al.* 2002, Rogel, Popliker *et al.* 1985). Therefore, in order to correctly validate the expression of the C/T antigens, assessment at protein level is needed.

### 3.5 Conclusion and chapter impacts

Overall, the pattern of C/T antigens expression in AML and CML was shown to be heterogenous, with most family members being significantly upregulated, some others being non-significantly upregulated or even downregulated. Collectively, according to the data obtained in the present study and from previous reports, it seems that an epigenetic-driven mechanism could be the most feasible explanation behind this inconsistency. However, this reason should be explored more in-depth, especially those C/T antigen members that have not been studied yet using methylation-specific assays. It, therefore, seems logical to combine C/T antigen-based immunotherapy with epigenetic modulators such as demethylating agents in particular AML patients who are not eligible for standard remission induction chemotherapy. The potential role of the demethylating agent (5-aza-2'-deoxycytidine) in the treatment of AML have been already explored in several clinical trials (Du, Lu *et al.* 2014).

HAGE, a member of the C/T antigen family, was found to be overexpressed in cDNA derived from PBMCs of CML and AML patients assessed by RT-qPCR, and also by TCC-S cell line. However, employing a large-scale study using a publicly available clinical dataset assessed by microarray demonstrated that there is no significance HAGE expression in both diseases in comparison to healthy controls, therein, we assume methylation issues might be the cause of this discrepancy or the difference in the methods of assessment.

On the other hand, the expression of WT1 was found to be considerably upregulated in both diseases regardless of whether the methylation mechanism is involved or not. Therefore, it is proposed that a combination of HAGE and WT1 vaccines in CML preceded by demethylating agents would benefit patients whose genes might be particularly hypermethylated, especially during the blast crisis. Another advantage of using demethylating agents in CML blast phase is to restore the expression of several tumour suppressor genes that were reported frequently methylated in CML patients and cell lines during the blast crisis (Janssen, Denkers *et al.* 2010).

## **4 Chapter IV: Immunogenicity of HAGE- and WT1-ImmunoBody<sup>®</sup> vaccines in HHDRII/DR1 mice**

Having demonstrated the pattern of HAGE and WT1 expression in different leukaemias in the previous chapter, the immunogenicity of the respective vaccines was then assessed as a basic requirement for cancer vaccine development. Therefore, this chapter will explore immune responses generated upon the administration of novel DNA vaccines, HAGE- and WT1-ImmunoBody<sup>®</sup>, both individually and in combination in HHDRII/DR1 double transgenic mice. The immunogenicity was mainly assessed by ELISpot assays, as well as by intra-cellular cytokine staining (ICS) assay. Some aspects of effector and memory profile characterisation upon ImmunoBody<sup>®</sup> vaccines administration was also investigated.

### **4.1 Introduction**

The principal objective of T cell-mediated cancer immunotherapy is to induce cancerous cell death by stimulating tumour-specific CTLs (Ribas, Butterfield *et al.* 2003, Rosenberg 2004), against tumour antigens expressed in association with MHC class I molecule on the tumour cell surface. Upon engagement, CTLs rapidly differentiate, clonally expand and develop into effector cells, releasing powerful cytotoxins, including perforin and granzymes which result in target cell lysis (Banchereau, Jacques, Steinman 1998, Gridelli, Rossi *et al.* 2009, Kelly, Gulley *et al.* 2010). Under this scenario, IFN- $\gamma$  carries a central role in promoting various immunoregulatory effects (Babiak, Steinhauser *et al.* 2014) and therefore its release is frequently assessed to monitor the ability of specific CTLs to recognise and respond to vaccine-containing peptides or to target cells expressing the relevant antigen using an IFN- $\gamma$  ELISpot assay. By finding the number of spots in a working ELISpot plate, responder T cell frequencies can be quantified, which in turn reflects the potency of the vaccine used. Hence, the immunogenicity of HAGE- and WT1-ImmunoBody<sup>®</sup> were herein assessed primarily using the IFN- $\gamma$  ELISpot assay.

Pathways involved in the processing and presentation of a given antigen/vaccine in the context of MHC restriction and subsequent stimulation of T cell immune responses are discussed in the following sections.

## 4.1.1 Antigen Processing and Presentation

In general, antigens need to be processed and presented to immune cells in order to be capable of engaging the main elements of the adaptive immunity, such as specificity, diversity, memory and self/non-self-discrimination. Antigen presentation is driven by the MHC class I molecules and class II molecules expressed on the surface of APCs and other cells. In fact, both molecules are similar in their definitive functions which involve degradation and delivering of shorter peptides to the cell surface through a cascade of reactions allowing the cytotoxic CD8<sup>+</sup> and the helper CD4<sup>+</sup> T cells respectively, to specifically recognise and engage with these complexes. The key factor that determines which pathway peptides should follow is the origin of the protein. Endogenous (intracellular) peptides predominantly follow MHC class I pathway, whereas the exogenous (extracellular) peptides mainly follow MHC class II pathway. However, cross-presentation wherein extracellular antigens are presented by MHC class I molecules and endogenous antigens are presented by MHC class II can also occur (Nierkens, Tel *et al.* 2013). Cross-presentation is of vital importance in tumour immunotherapy since dead and inflamed tumour tissues are engulfed by scavenging dendritic cells (DCs) and antigens processed and presented to the class I and class II pathway to trigger both CD8<sup>+</sup> and CD4<sup>+</sup> T cells, hence providing excellent tumour immune-surveillance (Brusic, Hainz *et al.* 2012).

### 4.1.1.1 MHC class I presentation

MHC class I molecules are principally expressed by all nucleated cells, where they are fully assembled in the lumen of the endoplasmic reticulum (ER). The mature MHC class I molecules consist of two categories of chains; a polymorphic transmembrane heavy chain (3 $\alpha$  polypeptides) and soluble  $\beta$ 2-microglobulin chain. Originally, MHC class I protein is produced in the ribosome and transported into the ER, wherein prior to binding the  $\beta$ 2-microglobulin, the heavy chain is typically stabilised by the chaperone molecule called calnexin, and later, the complex is stabilised by other chaperones; calreticulin and ERp57 (Neefjes, Momburg 1993, Williams, D. B., Watts 1995). Tapasin is another chaperone which has a binding affinity towards a specialised transporter protein that allows the passage of peptide from the cytosol into the ER called TAP (transporter associated with antigen processing). The role of tapasin is to control peptide translocation to the MHC class I binding groove and prevent MHC class I- $\beta$ 2-microglobulin complex degradation (Reits, Vos *et al.* 2000).

Outside of the ER, proteolysis of intracellular protein occurs in the cytoplasm wherein a multi-catalytic complex, called the proteasome, mediates the process of protein cleavage and degradation into small antigenic determinants (Kloetzel, Ossendorp 2004). Peptides are then actively driven into the lumen of the ER in an ATP-dependent

manner by TAP molecules ( TAP1 and TAP2) which translocate peptides of 8–11 amino acids length (Germain 1995), some of which might require an additional trimming in the ER prior to their binding to MHC class I molecules. Once the correct peptides bind to the appropriate MHC class I molecules, all chaperones are then dissociated and peptide–MHC class I complexes leave the ER for the Golgi apparatus for further maturation and finally reach the cell membrane using a Golgi vesicle. Peptides are then displayed to the T cell receptors (TCRs) expressed on CD8<sup>+</sup> T cells (Figure 4.1, 4.2).

#### **4.1.1.2 The MHC class II presentation pathway**

MHC class II molecules are mainly expressed by cells of immune system that are involved in antigen presentation, such as DCs, macrophages and B cells. In fact, MHC class II molecules often bind peptides produced from degraded proteins in the endocytic pathway (extracellular proteins). Structurally, MHC class II complexes comprise two  $\alpha$ - and two  $\beta$ -chains produced in the ribosome and assembled in the ER. At the early stage of assembly, the MHC class II molecule is stabilised by a third chain called the invariant chain (Ii), a chaperone that prevents the engagement of other peptides present in the ER lumen to the MHC groove. The invariant chain (Ii) also has a potentially important role in trafficking the class II molecules to the endosomal compartments (Bikoff, Huang *et al.* 1993). After being transported through Golgi into a new compartment, the invariant chain (Ii) is digested due to the activation of proteases cathepsin S and cathepsin L leaving a new molecule called “class II-associated Ii peptide” (CLIP) in the MHC peptide-binding groove (Bennett, Levine *et al.* 1992). Eventually, the CLIP is exchanged for an antigenic peptide produced from a protein degraded in the endosomal pathway after fusion of vesicles harbouring the MHC class II molecules with the ones encountering the antigenic peptides. It has been reported that the peptide fragment length that could be comfortably loaded onto MHC class II molecules is within a range of 13-18 amino acid length (Germain 1995). Peptide-MHC class II complexes are then transported to the cytoplasmic membrane to display the processed peptide to CD4<sup>+</sup> T cells via their engagement with a particular TCR (Figure 4.1, 4.2).

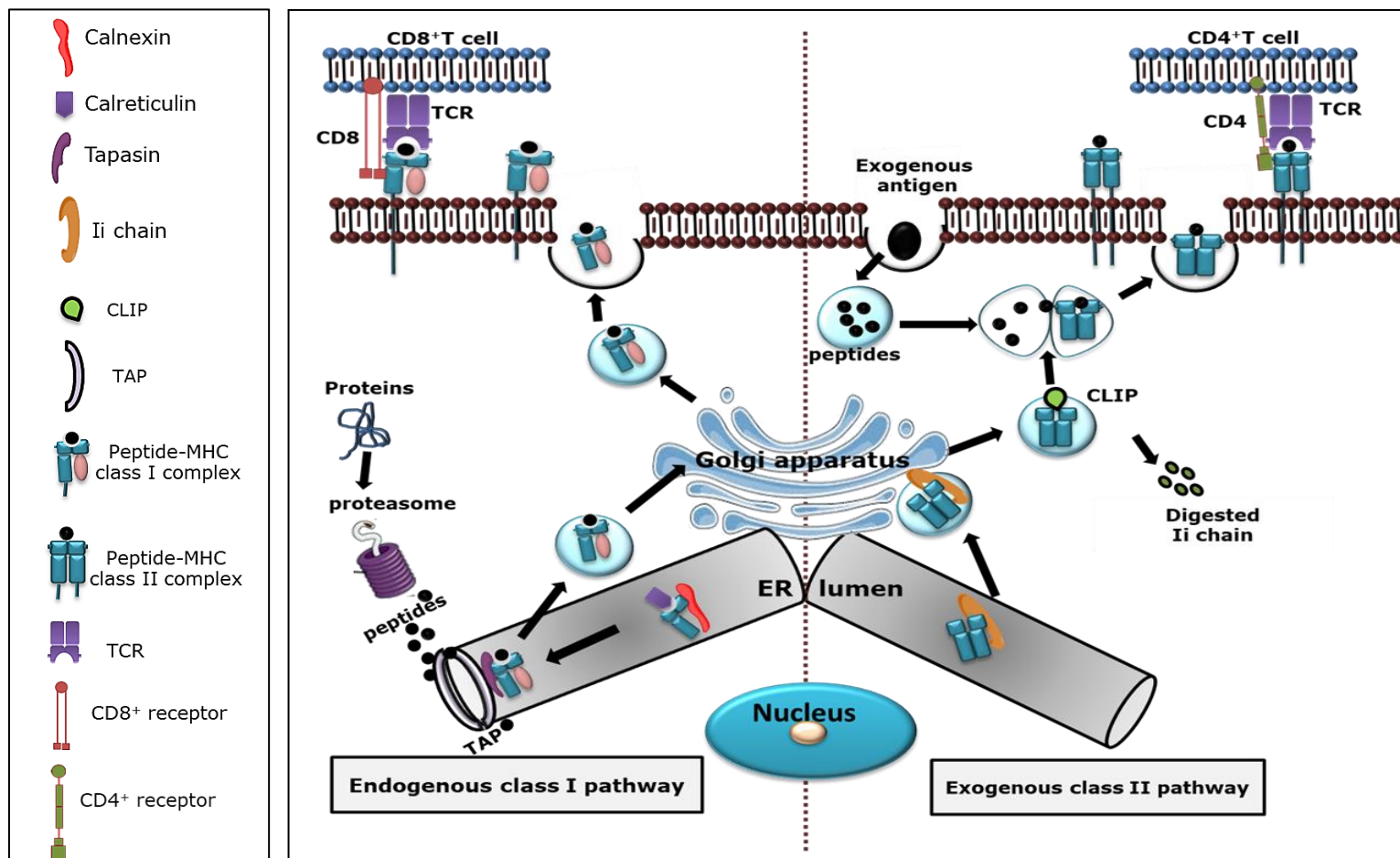


**Figure 4.1: MHC class I and class II processing and presentation pathways.**

The left panel represents the endogenous MHC class I pathway, wherein antigenic protein is degraded by proteasome, transposed into the ER by TAP and bind MHC class I molecules that were assembled inside the ER lumen by the help of various chaperones, the peptide-MHC class I complexes are then transported to the cell surface to present peptides to the CD8<sup>+</sup> T-lymphocytes. The right panel summarises exogenous MHC class II pathway, wherein the exogenous antigens are processed and bind the MHC class II in endocytic compartments rather than the ER, the peptide-MHC class II complexes are then transported to the cell surface to present peptide to B- and CD4<sup>+</sup> T cells.

## 4.1.2 T cell development, differentiation and T cell mediated immunity

T cells are originally produced in the bone marrow and developed in the thymus where each cell undergoes DNA rearrangement to create a unique TCR and are 'scanned' against autoreactivity issues and for an affinity restriction for self/nonself-MHC antigens. T cells that are released from the thymus, naïve T cells, are constantly circulating in the periphery between the blood and lymph system searching for a specific peptide presented by appropriate APCs (Kindt *et al.*, 2007).

Naïve T cells pass from blood to lymph nodes through regions known as high endothelial venules, wherein each individual cell scans DC networks in the T cell zone of the lymph node called the paracortex. The fate of an individual naïve cell after being aggregated in this zone is principally determined by the availability of specific peptide-MHC complex loaded by the DCs. In the absence of such a complex the naïve cell will exit via the efferent lymphatics, which eventually is drained into the thoracic duct and then back into the blood circulation. However, if a naïve T cell encounters an APC that expresses the desirable peptide-MHC, an activation program will be rapidly initiated (Punt 2013).

Three signals are required for the full activation of a naïve T cell; the first signal is delivered through the interaction between the TCR/CD3 complex and the specific peptide-MHC complex. The second signal is delivered via the binding of the costimulatory receptor CD28, a homodimer expressed by the majority of naïve CD4<sup>+</sup> and CD8<sup>+</sup> T cells, and B7-1 (CD80) and B7-2 (CD86). Cytokines provide important third signals for T cell activation. When cytokines bind their receptors, an intracellular signal is produced which enhances T cell proliferation, prolongs their survival and stimulates effector function that a T cell acquires. IL-2 contributes an important role for naïve T cell activation. IL-2, produced by T cell itself, binds IL-2 receptor on the surfaces of activated T cells, keeping cells in a continuous cycle of activation. In addition, a network of other cytokines produced by DCs, T cells, and other cells of the immune system also defines the functional fate of T lymphocytes (Punt 2013), these events are described in Figure 4.2.

Three subsets of T cells are critically engaged presentation of an antigen by the APCs; i) Cytotoxic CD8<sup>+</sup> T cells, which recognise and kill infected or malignantly transformed cells by releasing effector granules. ii) T helper CD4<sup>+</sup> cells (Th1) exchange information with APCs and have a critical role in the activation of CTLs. iii) T helper CD4<sup>+</sup> cells (Th2), mediate the humoral arm of immune response by influencing the activity of B cells. Categorisation of helper CD4<sup>+</sup> T cells into Th1 or Th2 principally depends on the functional cytokine profile they produced, (Mosmann, Kobie *et al.* 2009). While Th1 set largely secretes pro-inflammatory cytokines, such as IL-2, IFN- $\gamma$  and TNF- $\alpha$ , Th2

cells predominantly produce anti-inflammatory mediated cytokines, such as IL-4, IL-5, IL-6, IL-10, and IL-13 (Yamane, Paul 2013).

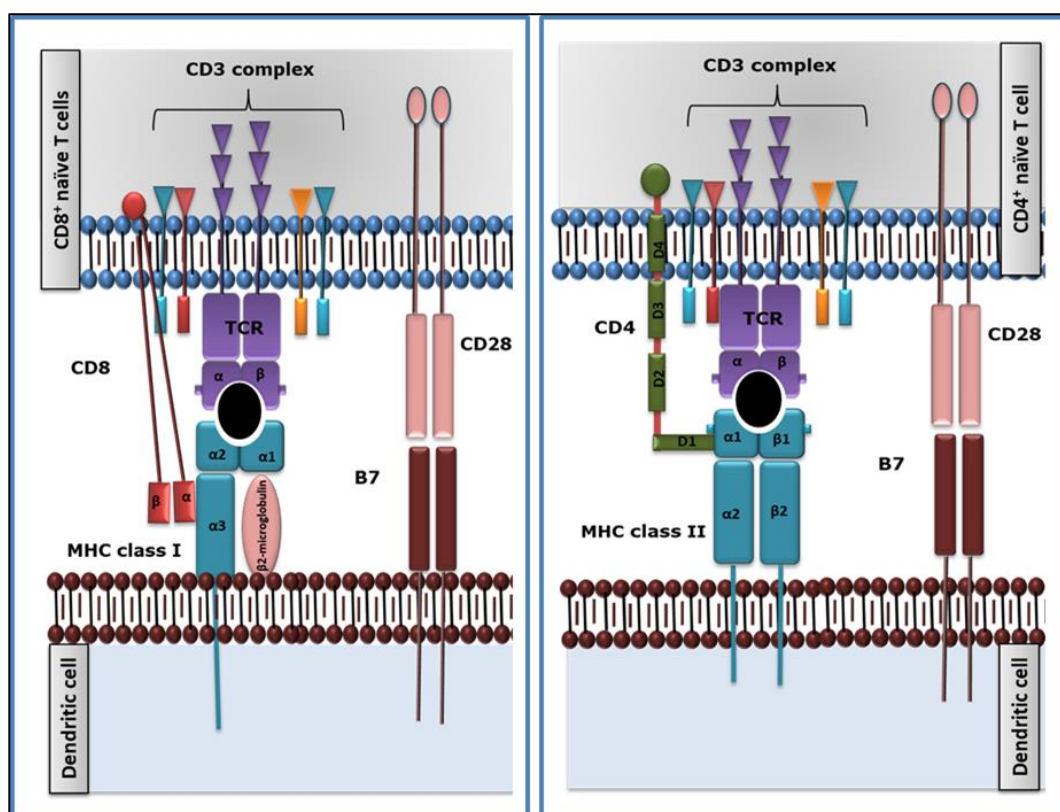


**Figure 4.2: Signals transduction required for the activation of naïve T cells.**

The figure demonstrates the structure and complex engagement of naïve T cell receptors (TCRs) with receptors expressed by APC upon peptide presentation. In the first signal transduction event, the CD8 co-receptors expressed by the naïve CD8<sup>+</sup> T cells (composed from  $\alpha$  and  $\beta$  chain) firstly check the MHC molecule for being MHC class I through binding of its  $\alpha$  chain with  $\alpha3$  chain of the MHC class I, then immediately TCR scans the particular peptide carried by the candidate MHC molecule for being match the binding groove in the TCR (shown in the left panel). Similarly, the CD4 co-receptors expressed by the naïve CD4<sup>+</sup> T cells (composed of 4 segments called D1, D2, D3 and D4) check the MHC molecule for being MHC class II through their binding to  $\alpha$  portion of MHC class II molecule and then TCR scans the particular peptide carried by the candidate MHC molecule for being match the binding groove in the TCR (shown in the right panel). The second signal event involves a cascade generated through the binding of the costimulatory receptor CD28 expressed by the majority of naïve CD4<sup>+</sup> and CD8<sup>+</sup> T cells with one of two members of the B7 family proteins: B7-1 (CD80) and B7-2 (CD86). The multimeric CD3 complex is composed of the  $\gamma$ ,  $\delta$ ,  $\epsilon$  and  $\xi$  subunits. The third signal (not shown on the figure) is provided by cytokines.

Collectively, DCs are attracted to the tumour site by the mediators of the innate response, where they phagocytise tumour cell debris and other apoptotic cell fragments. APCs then migrate to the lymph nodes and present the antigen-MHC complex to cells of the immune system, CD8<sup>+</sup> and CD4<sup>+</sup> Th1 T cells. These three subsets of cells create a trivalent complex which results in the maturation of DCs mediated by cytokine secretion and cell surface receptor interactions between the DCs and CD4<sup>+</sup> T cells. This, in turn, facilitates communications between DCs and CD8<sup>+</sup> T cells leading to the differentiation of the latter into CTLs. After being activated,

CTL cells migrate back to the tumour where they exert their specific cytotoxicity on any tumour cells harbouring the specific antigen against which they have been stimulated in the lymph node during peptide presentation process, through the secretion of perforin and granzyme B.

Interestingly, Kaech and colleagues in 2002 described three phases that a naïve cell passes through in order to be developed (Kaech, Wherry *et al.* 2002). The first stage is known as the "expansion phase" in which naïve T cells are clonally expanded and differentiated into effector T cells to form CD4<sup>+</sup>T helper cells or CD8<sup>+</sup>cytotoxic T lymphocytes. This occurs upon the engagement of specific peptide-MHC loaded on the DCs with their respective TCR in the secondary lymphoid organs. After that, more than 90% of effector T cells die (Gourley, Wherry *et al.* 2004), and this is the period of the second stage known as the "contraction phase". However, less than 5% T cells survive and are maintained for long periods of time (memory T cells) (Ahmed, Gray 1996, Sprent, Tough 2001, Wong, Pamer 2003) - the "memory phase".

Memory T cells have a unique ability to remember a previously encountered antigen by leaving a long-lasting pool of phenotypically and functionally distinctive population of T cell (Kaech, Wherry *et al.* 2002, Dutton, Bradley *et al.* 1998). This population has the merit of rapid and efficient responses for detecting and killing any potentially new cells that could harbour this particular antigen, keeping an individual protected during the rest of their life. Depending on the expression of specific surface markers (shown below), cytokine production and some other effector particles, memory cells are further categorised into two subsets; central memory (T<sub>cm</sub>) and effector memory (T<sub>em</sub>) T cells (Champagne, Ogg *et al.* 2001, Appay, Dunbar *et al.* 2002, Zanetti, Castiglioni *et al.* 2010), with the former homing primarily the lymphoid tissues and the latter circulating in the peripheral tissues (Gourley, Wherry *et al.* 2004). Factors such as altered gene expression patterns, epigenetic regulation and transcription factors influence the development of the naïve and effector cells into memory cells and their long-term maintenance (Weng, Araki *et al.* 2012).

Phenotypically, T cells in various stages of differentiation have been characterised depending on the expression of specific surface markers which are thought to mediate various migratory patterns. One of these markers is the adhesion molecule L-selectin (CD62L), also called homing receptor; upon binding with their ligands expressed on the endothelial cells, T cells are kept rolling through the blood stream toward the secondary lymphoid tissue (Kansas, Ley *et al.* 1993). This is typically the case of a naïve T cell that has not yet encountered a specific antigen, and thus needs to enter the secondary lymph nodes to find a particular antigen expressed by APCs (Nolz, Starbeck-Miller *et al.* 2011). Secondly, the adhesion mediated by CD44 (H-CAM), has been found to be continuously up-regulated on memory cells (Puré, Cuff 2001) and, in addition to its well-established function to control T cell extravasation from lymphoid tissue to the blood, CD44 has also a vital

role in inducing cell migration (Ponta, Sherman *et al.* 2003). As a result, a raised expression level of CD44 is commonly used to identify antigen-experienced T cells. Hence, murine naïve T cells are widely characterised by surface expression of CD62L and low expression of CD44, shortly abbreviated as CD62L<sup>high</sup>CD44<sup>low</sup>. In addition, it has been reported in two separate studies that memory CD8<sup>+</sup> T cells segregate into two distinct populations during lymphocytic choriomeningitis virus and Sendai virus infection of mice (Oehen, Brduscha-Riem 1998, Usherwood, Hogan *et al.* 1999). These populations are a CD44<sup>high</sup>CD62L<sup>low</sup> population mainly located in the spleen and exerts an immediate effector function (effector memory), and a CD44<sup>high</sup>CD62L<sup>high</sup> population that is shown homing mainly to the spleen and the lymph nodes with no rapid effector function (central memory). However, several surface markers have been found to be expressed on effector T cells as well as memory T cells, a situation that has made the differentiation between both types is relatively complicated (Oehen, Brduscha-Riem 1998).

In humans, the phenotypic and functional characterisation of memory CD4<sup>+</sup> and CD8<sup>+</sup> cells is mainly based on the expression of CD62L and CCR7 markers (Sallusto, Federica, Lenig *et al.* 1999, Kaech, Wherry *et al.* 2002) wherein the CD62L<sup>low</sup>CCR7<sup>-</sup> tissue homing effector memory T population which exerts an immediate effector function is distinguished from the CD62L<sup>high</sup>CCR7<sup>+</sup> lymph node homing central memory T cells which lack the effector function.

However, recently, it has been found that the hostile cancer microenvironment would result in what is called "T cell exhaustion", wherein proliferation and cytokine secreting capacity of T cells is reduced, a subject that will be discussed in the following section.

### **4.1.3 T cell exhaustion in the tumour milieu**

As mentioned above, naïve T cells differentiate upon encountering an antigen into effector cells, wherein cytokines/proteins which are required for correct and effective immune function are produced and released. However, due to exhaustion by extended/chronic stimulation, T cells fail to proliferate and deliver effector functions. Until recently, many studies have identified a sustained expression of the inhibitory molecule PD-1 by exhausted T cells and that blockade of PD-1/PD-L1 interactions can restore T cell effector function and improve clinical outcome in several cancers settings (Blank, Kuball *et al.* 2006, Yamamoto, Nishikori *et al.* 2008, Mumprecht, Schurch *et al.* 2009b, Zhang, L., Gajewski *et al.* 2009). However, it has also been reported that such pathway blockade does not constantly reverse T cell exhaustion (Blackburn, Shin *et al.* 2008, Gehring, Ho *et al.* 2009) and that PD-1 expression is not always associated with an exhausted T cell phenotype (Petrovas, Casazza *et al.* 2006, Fourcade, Kudela *et al.* 2009), thereby suggesting the involvement of other

molecules in T cell exhaustion. Tim-3 has also been extensively studied as a marker of T cell exhaustion or dysfunction (Wherry 2011, Pauken, Wherry 2015). Antibodies targeting Tim-3 have been found to boost T cell function in some settings, but could work better in synergy with PD1/PDL1 pathway blockade (Jin, Anderson *et al.* 2010, Fourcade, Sun *et al.* 2010, Sakuishi, Apetoh *et al.* 2010). In addition, other checkpoint receptors, such as LAG-3, CTLA-4, and TIGIT, have been found to be highly expressed on exhausted T cells. Given these observations, it seems that targeting multiple pathways will deliver the most effective strategy for restoring exhausted T cells.

#### 4.1.4 Factors influencing vaccine success

Over the era of cancer vaccine development, various key factors have been identified as strong influencers on vaccine efficacy, including i) the selection of the appropriate tumour antigens, ii) the addition of molecular adjuvants and immunostimulatory signals, iii) the choice of delivery systems, and iv) ensuring prime-boost strategies have been optimised (Tiptiri-Kourpeti, Spyridopoulou *et al.* 2016).

Importantly, the proper selection of tumour antigens is a basic necessity for vaccine development. One should therefore be careful when choosing the antigen and this process should consider the high level of immunogenicity and low-level risk of inducing autoimmunity to avoid toxicity against normal cells.

Adjuvants, (originally Latin word *adjuvare*, which means “to help”) were firstly defined by Ramon in 1924 as compounds that can induce higher immune response when they are used in combination with a particular antigen than using the antigen alone (Ramon, 1924). Since then, diverse classes of compounds have been assessed for their ability to boost the immunogenicity of a given vaccine, such as mineral salts, microbial products, saponins, polymers, cytokines, emulsions, liposomes, and microparticles (Guy 2007). Interestingly, although the precise mechanism of action for every single adjuvant has not yet been fully understood, recent advance reports suggests that they can work via one or more of the following ways to provoke the desired immune responses: i) sustained slow antigen release at the site of inoculation (depot effect), ii) induction of cytokines and other chemokines, iii) increased antigen uptake and presentation to APCs, iv) activation and maturation of APC by improving the expression of MHC class II and costimulatory molecules and inducing migration to the draining lymph nodes, v) cells recruitment at administration site, and (vi) activation of inflammasomes (Cox, Coulter 1997, Hoebe, Janssen *et al.* 2004, Fraser, Diener *et al.* 2007).

In contrast, a more immunogenic antigen might benefit from a particular delivery system which could enable the targeting and/or release of the antigen to DCs.

According to Bolhassani, *et al.*, approaches for delivering a DNA plasmid aiming to mount immunity against TAAs could be classified into two major classes; I) Physical approaches which include; tattooing, gene gun, ultrasound, electroporation and laser methods, and II) Non-physical delivery methods which include biological gene delivery systems (viral vectors) and non-biological gene delivery systems (non-viral vectors), such as cationic lipids/liposomes, polysaccharides and cationic polymers, micro-/Nano-particles, cationic peptides/cell-penetrating peptides (Bolhassani, Safaiyan *et al.* 2011).

Additionally, the route of administration of various immunotherapeutic modalities has been shown to have a significant influence on immune response outcomes. For example, in 2011, Lesterhuis, de Vries *et al.* found that an intradermal injection of DCs induces a significant anti-cancerous immunity when compared with intranodally injection of DCs (Lesterhuis, de Vries *et al.* 2011).

In this regard, various types of vaccines aimed at harnessing immune responses to eradicate cancerous cells with high efficacy and minimum toxicity have been developed. Among different type of vaccines, this chapter mainly focuses on cell-mediated immunity produced upon the administration of a particular type of DNA vaccine called "ImmunoBody<sup>®</sup>" developed by Scancell Ltd and kindly provided by Prof. Lindy Durrant. Some relevant aspects of DNA vaccines will be briefly discussed in the following sections.

#### **4.1.5 DNA and ImmunoBody<sup>®</sup> based vaccines**

DNA vaccination has recently gained a special interest in the field of cancer immunotherapy because it offers a safe, simple and promising strategy for harnessing immune responses. DNA vaccines are generally designed to deliver one or more genes encoding tumour antigens thereby provoking and/or augmenting immune responses against tumour cells harbouring particular tumour antigens that have a central role in tumorigenesis (Chlichlia, Schirrmacher *et al.* 2005, Herrada, Rojas-Colonelli *et al.* 2012, Coulie, Van den Eynde, Benoît J *et al.* 2014).

Structurally, DNA vaccines consist of a bacterial plasmid encoding the tumour protein of interest, a strong modified and/or chimeric viral CMV promoters to improve expression efficiency (Fioretti, Iurescia *et al.* 2010), a selection marker and polyadenylation signal to stabilise the transcripts.

The ImmunoBody<sup>®</sup> vaccine is a circular DNA plasmid which encodes a human antibody/fusion protein designed to express both cytotoxic and helper T cell epitopes derived from tumour antigens that are known to be overexpressed by tumour cells. An antibody-based approach was chosen based on the fact that they have long half-

lives and are capable of efficiently delivering their cargo to DCs via their Fc receptors, thereby helper and cytotoxic T cell stimulations can be generated, more details can be found in Figure 4.4.

ImmunoBody® can be delivered via intradermal, intravenous, intramuscular, subcutaneous and intraperitoneal routes (Doria-Rose, Haigwood 2003). However, the standard method of DNA ImmunoBody® delivery is via the intradermal route using a gene gun device. This has the merit of delivering the DNA directly into skin and Langerhans cells at highly efficient rates, followed by rapid migration of APCs into the regional lymph nodes (Porgador, Irvine *et al.* 1998).

The Helios gene gun is a handheld device used to transfect a wide range of targets *in vivo* using adjustable low-pressure helium pushes the biomaterial gold coated particles from inside the Tefzel tube directly into target cells (Raska, Turanek 2015). The efficacy of DNA transduction using this technology is substantially higher than the other approaches because the particles are directly delivered to the cytosol and cell nucleus (Trimble, Lin *et al.* 2003) – very small doses of DNA plasmid are sufficient. Interestingly, Pudney, Metheringham, *et al.* reported that a prime-boost immunisation regime using gene gun technology enhances the efficacy of the DNA vaccine by generating higher avidity epitope-specific responses (Pudney, Metheringham *et al.* 2010).

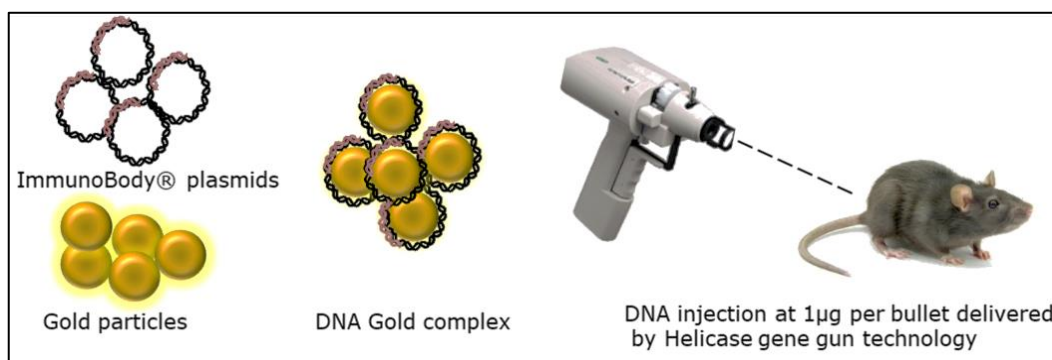


**Figure 4.3: Helios gene gun technique for delivering of ImmunoBody® DNA plasmid.**

Prior to the immunisation, the DNA ImmunoBody® of the interest was coated onto gold microcarrier particles, the mixture was then loaded into a Tefzel tube and immediately dried over a slow flow of N<sub>2</sub> gas. The tube was then chopped into small bullets and the mice were eventually injected intradermally.

This project uses two, HAGE- and WT1-ImmunoBody® vaccines at a 1µg plasmid DNA, which were separately coated onto 1.0 µm gold particles prior to the immunisation. DNA bullets were then injected intradermally into different flanks of the mice using the BioRad Helios® gene gun technology, in a prime-boost immunisation regime involving three rounds of vaccination seven days apart, Figure 4.3.

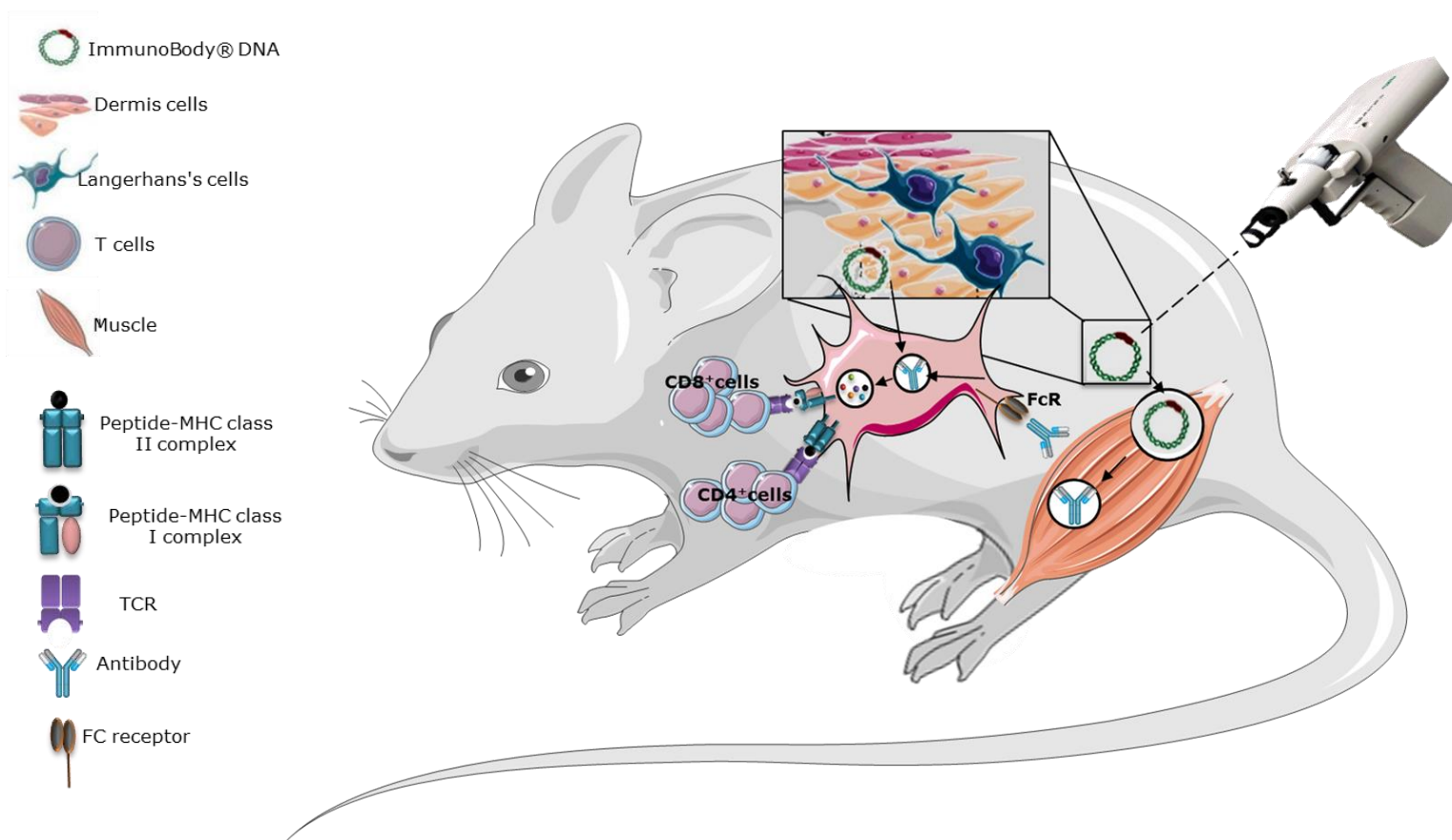


**Figure 4.4: Dual mechanism of action of ImmunoBody® based vaccines.**

Overall, the figure demonstrates the ability of the ImmunoBody® to initiate both direct and cross-presentation of epitopes to T-cells. DCs can employ various pathways by which can process antigens, wherein the highest avidity T cell response are produced if more than one pathway is used to present the same epitope. The ImmunoBody® DNA is designed to be taken up and processed directly by DCs that are present in the dermal layers (Langerhans's cells). It is also taken indirectly, the protein generated by smooth muscle taking up the DNA at the site of the injection is secreted, binds the Fc receptors on DCs and is cross-presented. As a result of both the direct and cross-presentation, both CD8<sup>+</sup> cytotoxic and CD4<sup>+</sup> T helper cell responses are generated with high avidity and at a high frequency. The figure was produced using drawing facilities provided by Servier Medical Art, available at: <https://smart.servier.com/>.

ImmunoBody<sup>®</sup> DNA vaccines maximise T cell activation by producing both high frequency and high avidity T cells. Functional avidity is defined by the lowest amount of peptide required for effector T cell activation and function (Kroger, Alexander - Miller 2007). It therefore measures the overall strength of CTL interactions with a target cell (Sandberg, Franksson *et al.* 2000). In the new era of vaccine development, it is widely accepted that the production of high frequency T cell responses does not necessarily reflect a competent immune response as the existence of antigen-specific T cells seldom correlates with positive clinical outcome, whereas the presence of high avidity T cells could be a better indicator of clinical response (Zeh, Perry-Lalley *et al.* 1999, Ayyoub, Rimoldi *et al.* 2003b). In fact, viral infection and tumour growth in pre-clinical models have only been found to be eliminated by high avidity, not low-avidity specific CTLs (Dutoit, Rubio-Godoy *et al.* 2001, Sedlik, Dadaglio *et al.* 2000).

Although the exact mechanisms by which high avidity CTLs are generated have not yet been fully understood, several factors have been implicated in the modulation of functional avidity, these include the production of IL-12 and IL-15 (Oh, Hodge *et al.* 2003, Xu, Koski *et al.* 2003), the expression of CD8 $\alpha\beta$  (Cawthon, Lu *et al.* 2001, Kroger, Alexander - Miller 2007), specific TCR affinity (Oh, Hodge *et al.* 2003, Hodge, Chakraborty *et al.* 2005) and also the level of DCs maturation.

SCIB1 DNA was the first ImmunoBody<sup>®</sup> based vaccine developed, it encodes a human IgG1, engineered to express two cytotoxic T cell epitopes and two helper T cell epitopes derived from the melanoma antigens Tyrosinase-Related Protein 2 (TRP2) and gp100 within the CDR regions. This antibody, produced by the transfected cells, is able to target DCs *in vivo* via their high affinity Fc fragment leading to a significant enhancement of both frequency and avidity of T cells (Patel, P. M., Ottensmeier *et al.* 2018). The high avidity T cells induced towards TRP2 were able to destroy both primary and metastatic tumours and lead to significantly prolonged survival rates in a Phase I/II clinical trial (accession number: NCT01138410) of patients with advanced metastatic melanoma (Patel, P. M., Ottensmeier *et al.* 2018). The majority of tumour vaccines are unable to specifically target DCs *in vivo*, and hence require an *ex vivo* antigen pulsing of DCs followed by the re-infusion of these cells into individual patients, a process which is expensive and time-consuming (Turnis, Rooney 2010). ImmunoBody<sup>®</sup> has been designed specifically to circumvent such limitations.

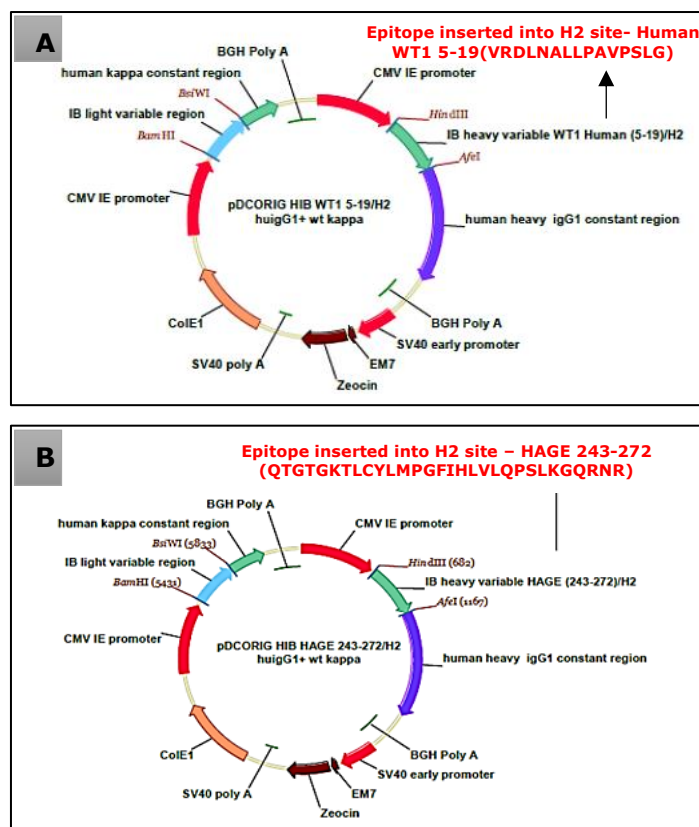


**Figure 4.5: Schematic vector maps demonstrate the design of WT1- and HAGE-ImmunoBody® DNA plasmids.**

ImmunoBody® platform comprises the double expression vector (pDCorig) designed with two reading frames; the ImmunoBody (IB) heavy variable ( $V_H$ ) and human heavy IgG1 constant regions are inserted in one frame, and human kappa constant and IB light variable ( $V_L$ ) regions are inserted into another frame. Both frames are controlled by two separated CMV promoters (as immediate early promoter) and end with Bovine Growth Hormone (BGH) polyadenylation signals (to ensure an effective termination). The WT1-ImmunoBody® construct designed to carry gene encodes for the WT1 15-mer [VRDLNALLPAVPSLG] peptide which is inserted in the heavy variable region (shown in A), whereas the HAGE-ImmunoBody® encodes the HAGE 30-mer [QTGTGKTLCYLMPGFIHLVLPQSLKGQRNR] peptide is also inserted in the heavy variable region (shown in B). Both images/maps are reused with a reference to the vaccine supplier (Scancell Ltd. Nottingham, UK).

## 4.2 Rationale of the chapter

1. To determine the affinity of the HAGE- and WT1-derived peptides for HLA-A2 molecules, followed by studying the peptide-MHC complex stability on the surface of T2 cells.
2. To ascertain the immunogenicity of HAGE- and WT1-ImmunoBody® derived peptides individually and in combination, by studying T cell frequency and avidity induced by the candidate vaccines using IFN- $\gamma$  ELISpot assay.
3. To provide a phenotypical characterisation of the vaccine-induced T cells in term of memory cells formation provoked.

## 4.3 Results

### 4.3.1 HAGE and WT1 peptides prediction and synthesis

The immunogenic region of the HAGE antigen was previously identified in our group using a combination of approaches; matrix-screening method of overlapping peptides and reverse immunology.

A 30-mer peptide sequence [QTGTGKTLCYLMPGFIHLVLQPSLKGQRNR]/[position; 286-316] derived from the HAGE protein was found to be associated with high immunogenicity, as detected by *ex-vivo* IFN- $\gamma$  ELISpot assay (Divya Nagarajan, previous PhD student). From that sequence, various short peptides were predicted to bind to MHC class I (HLA-A2) and class II (HLA-DR1) by the freely available software SYFPEITHI, as shown in Table 4.1 and Figure 4.6. Only HLA-A2 and HLA-DR1 restricted peptides were selected to be used in our HLA-A2/DR1 double transgenic mice (HHDII/DR1).

SYFPEITHI, an internet-based access algorithm, was used to predict the peptide-binding affinities for specific HLA molecules depending on the position of anchor residues. The software allows an entire protein to be screened and predicts peptides that are likely to bind to given HLA haplotypes. This saves time, effort and cost by avoiding the need to purchase and assess a panel of overlapped peptides. This software is available at:

<http://www.syfpeithi.de/bin/MHCServer.dll/EpitopePrediction.html>.

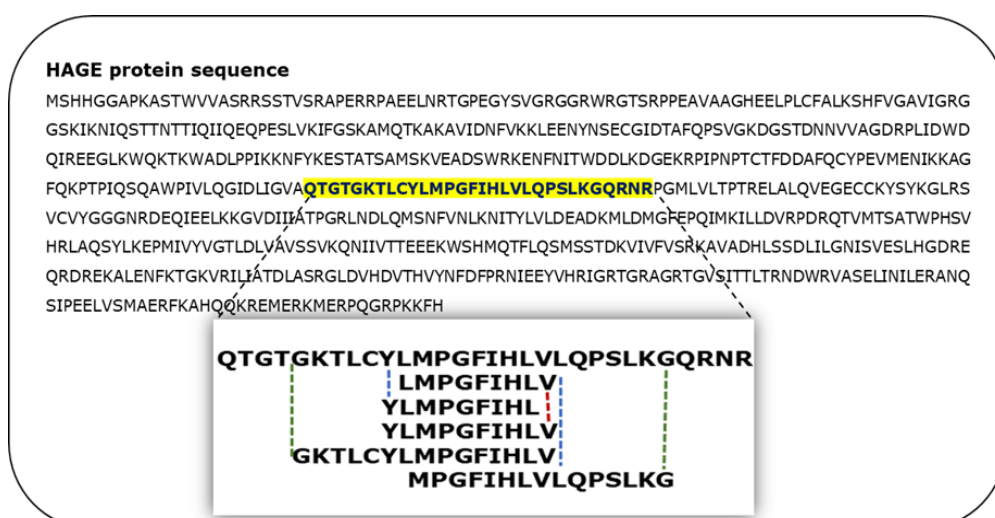


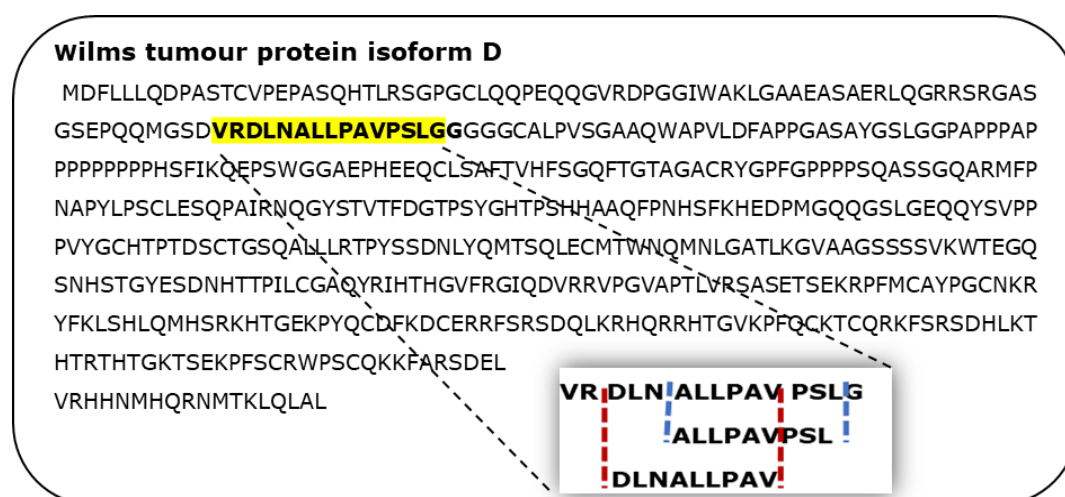
**Figure 4.6: Position of the class I and class II HAGE peptides derived from the entire length of the HAGE protein.**

The figure demonstrates the entire HAGE protein sequence of 648 amino acid length, from which the long 30-mer (yellow highlighted) and other short 9- 15-mer peptides derived from the long 30-mer (shown in the big window) are illustrated. This length was fully copied from NCBI website/FASTA available at: <https://www.ncbi.nlm.nih.gov/protein/Q9NXZ2.2?report=fasta>.

**Table 4.1 The short HAGE peptides derived from the 30-mer sequence**

Peptides	Peptide sequence	Length	Position	SYFPEITHI Score	Haplotype binding
<b>HAGE/P4</b>	LMPGFIHLV	9	296-305	28	HLA-A2
<b>HAGE/P5</b>	YLMPGFIHL	9	295-304	27	HLA-A2
<b>HAGE/P6</b>	YLMPGFIHLV	10	295-305	30	HLA-A2
<b>HAGE/P7</b>	GKTLCYLMPGFIHLV	15	290-305	30	HLA-DR1
<b>HAGE/P8</b>	MPGFIHLVLQPSLKG	15	297-312	26	HLA-DR1

Similarly, a 15 amino acid long HLA-DR1 binding peptide [VRDLNALLPAVPSLG] derived from the WT1 protein containing two known and previously published HLA-A2 9-mer (Pinilla-Ibarz, May et al. 2006b) was initially assessed for its binding affinity using the SYFPEITHI database (Figure 4.7, Table 4.2). It should be noted that human WT1 protein presents as several isomers (see Appendix/[Table 9.3](#)), and Figure 4.7 below represents "WT1 protein Isoform D", the longest isomer of 522 amino acid length.

**Figure 4.7: Position of the long 15-mer and the short 9-mer WT1 peptides derived from the entire length of WT1 Isoform D.**

The figure demonstrates the entire WT1 isoform D protein sequence of 522 amino acid length, wherein the long 15-mer (yellow highlighted) and the two others short peptide derivatives (shown in the big window) are illustrated. This length was fully copied from NCBI website/FASTA available at: [https://www.ncbi.nlm.nih.gov/protein/NP\\_077744.4?report=fasta](https://www.ncbi.nlm.nih.gov/protein/NP_077744.4?report=fasta).

HAGE and WT1 peptides were then synthesised and purchased from GenScript (Piscataway, USA), which provided us the requested peptides with a purity of more than 80%.

**Table 4.2: WT1 peptides derived from the 15-mer sequence**

Peptides	Peptide sequence	Length	Position	SYFPEITHI Score	Haplotype binding
WT1 P1	VRDLNALLPAVPSLG	15	78-93	31	HLA-DR1
WT1 P3	ALLPAVPSL	9	83-92	33	HLA-A2
WT1 P5	DLNALLPAV	9	80-89	27	HLA-A2

The HAGE and WT1 short peptides were then further validated for the binding/dissociation affinity toward MHC using T2 binding and dissociation assays, respectively, as detailed in the following sections.

### 4.3.2 Peptide-HLA-A2 affinity and stability assays

Of all the factors affecting the capability of peptide-MHC complexes to stimulate T cells, the two main ones are the affinity of the peptide for the MHC molecule and the cell surface stability of the peptide-MHC complex (Baker, Gagnon *et al.* 2000, Holler, Kranz 2003). It is true that computer algorithm predictions are very useful for scoring peptide binding, however its accuracy is not more than 70–80% (Dao, Korontsvit *et al.* 2017). Therefore, in this study, the strength of the interaction between the respective HAGE and WT1 class I peptides and the HLA-A2 molecules was assessed *in vitro* using a peptide-HLA-A2 T2 binding and stability assay.

T2 cells are an HLA-A2 human lymphoblast suspension cell line that have been genetically modified to produce mutated non-functional transporter-associated proteins (TAPs) that are necessary to transport MHC class I restricted peptides into the ER. This defect results in a failure to present internal TAP-dependant peptide and instead MHC molecules leave the ER and Golgi compartments empty, leading to a 70–80% reduction of HLA-A2 expression on T2 cell surface. These empty molecules are not stable and are quickly recycled. However, it is thought that a small proportion of peptides still reach MHC molecules in a TAP independent manner and are eventually presented on the cell surface. The empty HLA-A2 molecules on the surface of the cells can, however, be stabilised by the exogenous addition of peptides for which they have an affinity (van der Burg, Visseren *et al.* 1996). In contrast to the TAP deficient cells, the endogenously processed peptides upon proteasomal degradation in the TAP competent cells (shown in Figure 4.1) are transported into the ER where they are loaded onto MHC class I molecules before they are presented on the cell surface.

Taking advantage of this defect, T2 cells are frequently used to validate the binding of exogenously administered peptides.

### 4.3.2.1 Peptide-MHC affinity assay (T2 binding assay)

HAGE and WT1 HLA-A2 derived epitopes predicted to bind by SYFPEITHI software were experimentally evaluated for their MHC binding affinity *in vitro* upon loading them onto T2 cells. These exogenous synthetic peptides can directly engage with the MHC class I complex and display on the surface of T2 cells in a TAP-independent mechanism.

As per the method described in Chapter-2 ([Section:2.2.5.3](#)), T2 cells suspended in a serum-free medium containing human  $\beta$ 2m at 3 $\mu$ g/mL and serial concentrations of the short class I HAGE and WT1 peptides (at 10, 30, 50 and 100 $\mu$ g/mL) were plated in a rounded-bottom 96-well plate overnight at 26°C, alongside cells incubated with similar concentrations of DMSO instead of peptides as a negative control. On the next day, cells were stained using an APC-conjugated anti-human HLA-A2 antibody and propidium iodide to exclude dead cells, samples were then immediately run using a Beckman Coulter Gallios™ flow cytometer. Gating strategies are shown in Figure 4.8.

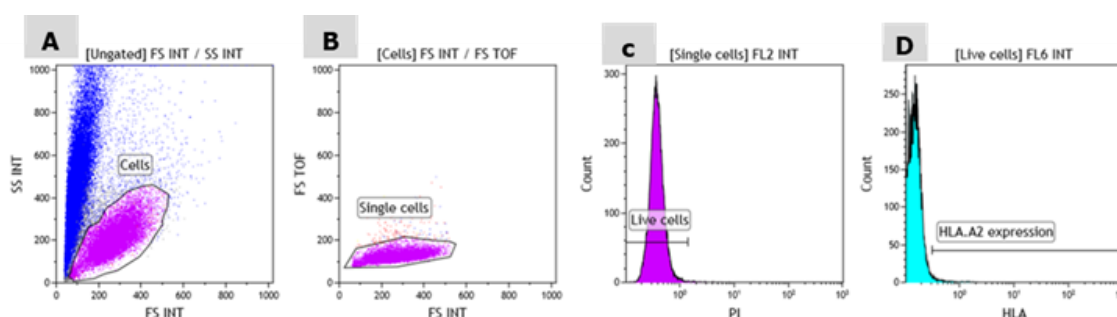


**Figure 4.8: Representative gating strategy used in T2 cell binding assay.**

Using density plots of Forward Scatter Linear (FS-INT) *versus* Side Scatter Linear (SS-INT) axis, the cells were firstly gated as “Cells” populations (shown in A). “Single cells” were then gated out of “Cells” populations in order to eliminate doublets using Forward Scatter Linear (FS-INT) *versus* FS TOF (time of flight) axis (shown in B). To exclude the dead cells from the analysis, “Live cells” were gated out of “Single cells” (shown in histogram plot C), wherein cells were stained with propidium iodide (PI) detected at FL2. Finally, the level of surface HLA-A2 expression/FL6 was determined on basis of fluorescence intensity depicted by a shift to the right of the histogram in comparison to unstained samples.

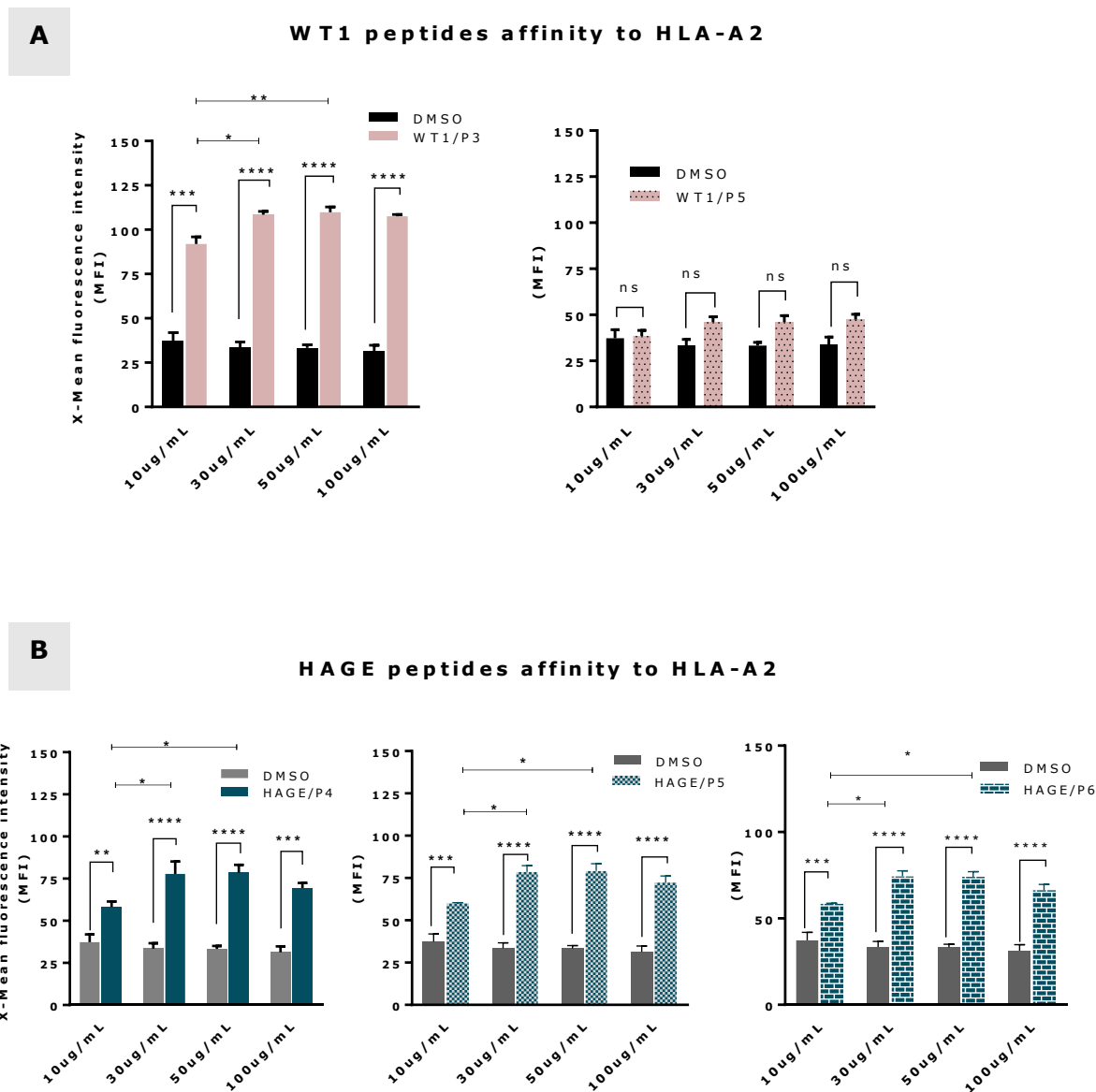
Overall, results in the Figure 4.9 demonstrate that the intensity of fluorescein produced due to HLA-A2 expression measured by the Mean Fluorescence Intensity (MFI) progressively increases in a dose-dependent manner in comparison with the control (MFI produced by cells that were treated with match doses of DMSO instead of peptides), indicating a successful peptide-MHC engagement, apart from WT1/P5 which did not increase the MFI, thereby reflecting a poor binding affinity towards MHC class I molecule.

In addition, the Fluorescence Intensity Ratio (FIR) was calculated for each indicated concentration using the MFI of HLA-A2 expressed by T2 cells incubated with a peptide and the MFI of HLA-A2 expressed by T2 cells that were incubated in the absence of that peptide, but with the same concentrations of DMSO. It is widely accepted that peptides with  $FIR=1$  are categorised as being non-binders,  $1 < FIR \leq 1.5$  as weak binders,  $1.5 < FIR < 2$  as moderate binders and  $2 \leq FIR < 3$  as strong binders. Interestingly, all HAGE peptides demonstrated a strong affinity towards HLA-A2 molecules, although the FIR slightly dropped to a moderate binding score at low concentrations (10 µg/mL). Regarding the WT1 peptides, data prove that WT1/P3 is a strong binder even in the lower concentrations, this anticipates a potent ability to stimulate CTL activation *in vitro* and *in vivo*. WT1/P5 exhibited the least binding ability with a score of 1 (non-binder) at 10 µg/mL, although the score slightly increased to between 1.4 to 1.5 at the higher concentrations but was still categorised as a weak binder peptide.

**Table 4.3: Categorisation of the binding affinity of class I HAGE- and WT1-derived peptides toward HLA-A2 molecules, as assessed by T2 binding assay.**

Peptides	FIR obtained from various HAGE and WT1 peptides doses			
	10µg/mL	30µg/mL	50µg/mL	100µg/mL
HAGE/P4	1.8 (moderate)	2.3 (strong)	2.4 (strong)	2.3 (strong)
HAGE/P5	1.9 (moderate)	2.4 (strong)	2.4 (strong)	2.3 (strong)
HAGE/P6	1.8 (moderate)	2.3 (strong)	2.3 (strong)	2.2 (strong)
WT1/P3	2.6 (strong)	3.3 (very strong)	3.4 (very strong)	3.5 (very strong)
WT1/P5	1.0 (non)	1.4 (weak)	1.4 (weak)	1.5 (weak)

Serial doses were used to assess peptides binding affinity toward HLA-A using flow cytometry, peptides were then categorised for being a strong, moderate and weak HLA-A2 binder according to Fluorescence Intensity Ratio (FIR).



### 4.3.2.2 Peptide-MHC dissociation assay (brefeldin A decay assay)

The stability of peptide-MHC complexes on the surface of the target cells is an important component for effective CTL activity. Therefore, the goal of this assay was to monitor the persistence of the peptide-MHC class I complex on the cell surface and resistance to the endocytosis and or dissociation in time course analysis using a brefeldin A decay assay. Brefeldin A obstructs the anterograde transport of vesicles from the ER to the Golgi apparatus (trap effect), thereby preventing peptide-MHC proteins from being transported to the cell surface. T2 cells were used for this assay.

The assay is based on the incubation of 50µg/mL each HAGE and WT1 class I short peptide with T2 cells suspended in a serum-free medium containing human β2m at 3µg/mL overnight at 26°C. According to FIR values showed in Table 4.3, the minimum concentration that seemed to work best for the majority of peptides studied was 30 and 50µg/mL, hence, in this study 50µg/mL was selected to test peptide-MHC dissociation pattern, as it was also used by other researchers for studying the stability assay (Chen, Fei, Zhai *et al.* 2012). On the next day, cells were washed and incubated with 10µg/mL brefeldin A at different time points in 37°C. After each incubation, cells were washed and stained with anti-HLA-A2 antibody for 30 minutes at 4°C, after which dead cells were excluded using PI and samples run immediately on flow cytometer. Regarding gating strategy, the approach used was similar to the T2 cells binding assay shown in Figure 4.8.

The stability of each peptide-HLA-A2 complex was assessed by calculating of DC<sub>50</sub> value, which is defined as the time required for a 50% reduction in the level of MFI recorded at time 0 (Chen, Fei, Zhai *et al.* 2012), the longer the time for reduction, the more stable the complex is. The DC<sub>50</sub> was calculated according to the formula: (MFI at different time points/MFI at time 0) X100%. T2 cells incubated in the absence of peptide, but in the presence of the same concentration of DMSO were used as negative controls.

Results show that there is a steady reduction in the level of MFI in a time dependent manner in all the complexes in the first hours of the study, but then the reduction stopped after 6 hours (Figure 4.10). With regards of the DC<sub>50</sub> value, all HAGE and WT1/P3 -HLA-A2 complexes on the T2 cell surface were stable as their DC<sub>50</sub> values were all more than 8 hours. However, WT1/P5 HLA-A2 complex exhibited poor stability, as DC<sub>50</sub> value fell earlier than 6 hours.

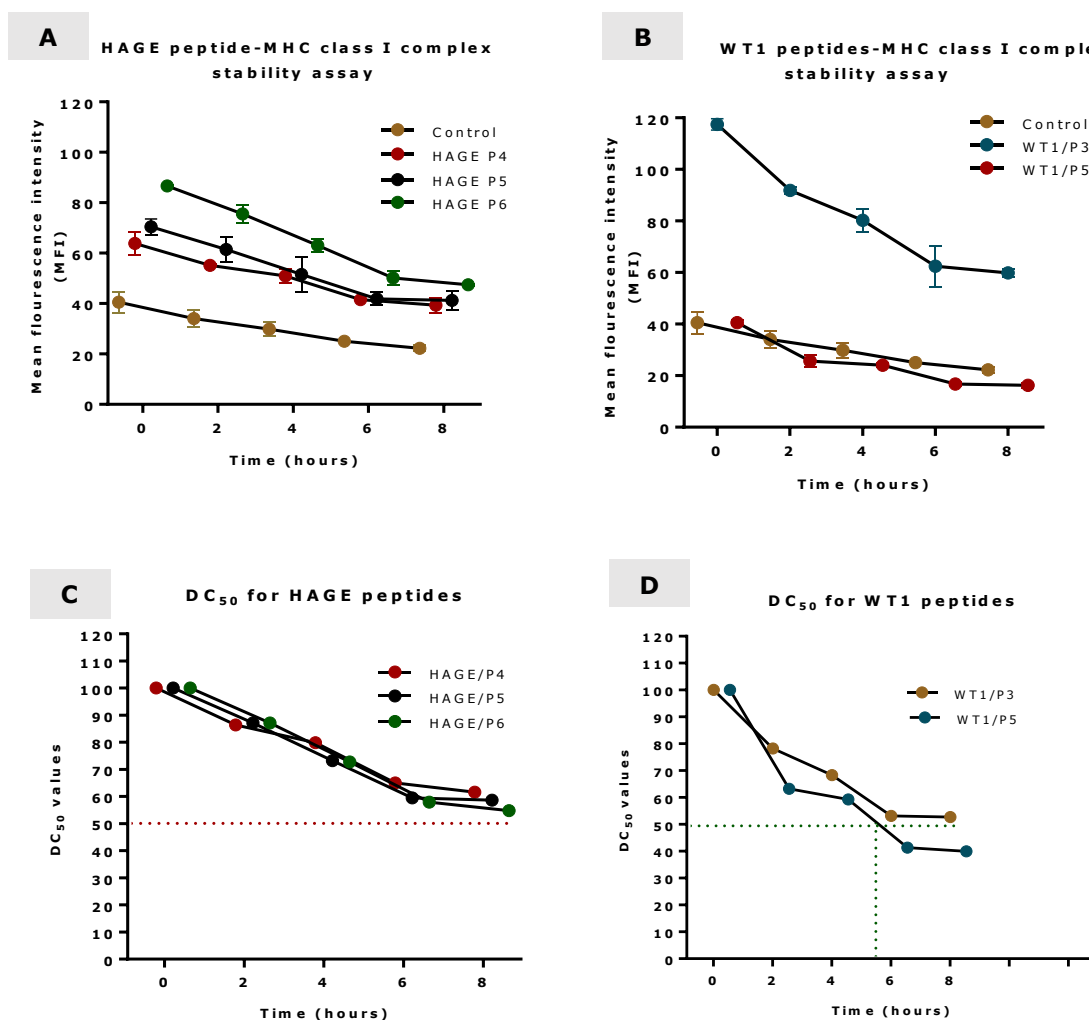


**Figure 4.10 Time point analysis of class I HAGE and WT1 peptides binding stability to HLA-A2, as determined by brefeldin A decay assay using flow cytometer.**

The binding stability (measured by MFI) of class I HAGE peptides (HAGE/P4, HAGE/P5 and HAGE/P6) is shown in (A) and WT1 peptides (WT1/P3 and WT1/P5 shown in (B) in comparison to cells that were incubated with the same concentrations of DMSO. Whereas DC<sub>50</sub> for HAGE peptides and WT1 are shown in (C) and (D), respectively. T2 cells in serum-free medium containing human  $\beta$ 2m at 3 $\mu$ g/mL were incubated with respective peptides overnight at 50 $\mu$ g/mL and assessed in time course analysis for HLA-A2 using flow cytometer. Values are expressed as the mean $\pm$ SEM of two independent experiments. All peptide-HLA complexes studied are stable on the T2 cells surface as their DC<sub>50</sub> values were > 8 hours, apart from the WT1/P5- HLA-A2 complex which shows poor stability as there was a drop in DC<sub>50</sub> value earlier between 5-6 hours. n=2.

In conclusion, from what the results obtained with the T2 binding/dissociation assays, it seems that the candidate class I HAGE and WT1 peptides are associated with strong affinity toward the HLA-A2 molecules and are relatively stable on T2 surface except for WT1/P5. In the following sections, these peptides were assessed for their immunogenicity in HHDII/DR1 mice, using a novel delivery system based on intradermal administration of ImmunoBody® DNA vaccines which encode the HAGE 30-mer and WT1 15-mer peptides sequence by means of gene gun technology (separately and in combination) in order to explore their potential competition in generating T cell response in HHDII/DR1 mice.

### 4.3.3 Immunogenicity of HAGE- and WT1-ImmunoBody<sup>®</sup> vaccines administered individually

Having determined the binding ability and peptide stability of the candidate peptides, the immunogenicity of the chosen peptides was then assessed in HHDII/DR1 mice using IFN- $\gamma$  ELISpot.

#### 4.3.3.1 HAGE-specific CTL immune responses induced by the HAGE-ImmunoBody<sup>®</sup> vaccine

In the context of peptide vaccine development, peptide dose, route of administration, single *versus* combined adjuvants, delivery system and other factors have been found to affect vaccine success, depending on the type of the vaccine and the experimental design. The previous PhD student, Divya Nagarajan, compared the efficacy of the long 30-mer HAGE delivered either as ImmunoBody<sup>®</sup> DNA vaccine or as a peptide with adjuvants. Her results demonstrated that the intradermal injection of the HAGE-ImmunoBody<sup>®</sup> vaccine using a gene gun once a week for three consecutive weeks was associated with more potent immunogenicity than the peptide/adjuvant vaccination regime.

Hence, in the present study only ImmunoBody<sup>®</sup> vaccine regime using gene gun technology was used. The programme of this strategy, as indicated by the supplier, includes; immunisation of group of mice by single DNA bullet containing 1 $\mu$ g of HAGE DNA ImmunoBody<sup>®</sup> which as mentioned previously encodes the HAGE 30-mer sequence [QTGTGKTLCYLMPGFIHLVLQPSLKGQRNR]/(vector map in Figure 4.5B) coated onto gold particles and administered by gene gun device in two boosts at 7 days interval apart. On day 21, mice were culled and splenocytes were immediately harvested and re-stimulated *in vitro* using 1 $\mu$ g/mL class I, LMPGFIHLV (HAGE/P4), YLMPGFIHL (HAGE/P5) and YLMPGFIHLV (HAGE/P6) and 10 $\mu$ g/mL of class II, GKTLCYLMPGFIHLV (HAGE/p7) and MPGFIHLVLQPSLKG (HAGE/P8) peptides, followed by measuring IFN- $\gamma$  production using the ELISpot. These two concentrations were used as they were found to work best in previous experiments conducted by our group. The direct *in vitro* re-stimulation with the short peptides enabled the assessment of the immunogenicity of each individual peptide separately. Results in Figure 4.11 verify the immunogenicity of two class I peptides (HAGE/P5 and HAGE/P6) and one class II (HAGE/P7) in comparison to cell alone (cells that did not receive any peptide) as it is reflected by the high number of IFN- $\gamma$  producing cells, at \*\*\*\**P-value*<0.0001 for each peptide. HAGE/P4 and HAGE/P8 peptides did not, however, produce any release of IFN- $\gamma$  indicating that these peptides were not endogenously produced and presented to T cells *in vivo*.

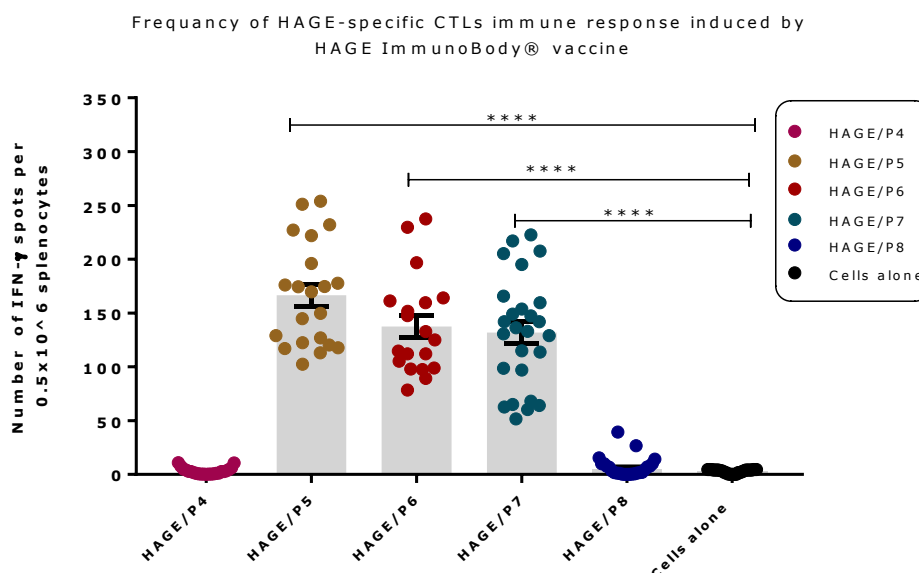


**Figure 4.11: Frequency of HAGE-specific CTLs induced by the HAGE-ImmunoBody® vaccine, as determined using the IFN- $\gamma$  ELISpot assay.**

The level of IFN- $\gamma$  produced by fresh  $0.5 \times 10^6$  splenocytes harvested from a group of mice immunised and boosted with HAGE-ImmunoBody® were assessed using the ELISpot assay. Values are expressed as the mean  $\pm$  SEM of 8 independent experiments (3 mice/group), and the level of significance was assessed using One Way ANOVA followed by Dunnett's multiple comparisons test. Results demonstrate the immunogenicity of the two class I peptides; HAGE/P5 and HAGE/P6 and one class II; HAGE/P7 in comparison to cells alone, whereas the class I HAGE/P4 and class II HAGE/P8 are shown to be poorly immunogenic.  $n=8$  (3 mice/group).

### 4.3.3.2 WT1-specific CTL immune responses induced by WT1 vaccines

Using a similar approach mentioned-above (that was followed in HAGE vaccine experiments), a comparison between responses to WT1 simple peptide/adjuvant immunisation *versus* WT1 ImmunoBody® vaccine was assessed.

In the first instance, the experiment was set up as the following; a set of three mice per group were immunised with the long WT1-15mer [VRDLNALLPAVPSLG] peptide (WT1/P1) emulsified in IFA and CPG, after which they were boosted by an equal ratio of a cocktail of MHC class I restricted short peptides; ALLPAVPSL (WT1/P3) and DLNALLPAV (WT1/P5), emulsified in the same adjuvants mixture, in two rounds at seven day interval. Seven days from the last immunisation (day-21), splenocytes were harvested and re-stimulated with the same short peptides (separately) and assessed for IFN- $\gamma$  production using the ELISpot assay. Results in Figure 4.12 point out the strong immunogenicity of WT1/P3 at\*\*\* $P$ -value in comparison to the cells alone, and poor immunogenicity of WT/p5.

**Frequency of WT1-specific CTLs immune response induced by simple WT1 peptides/adjuvant vaccination**

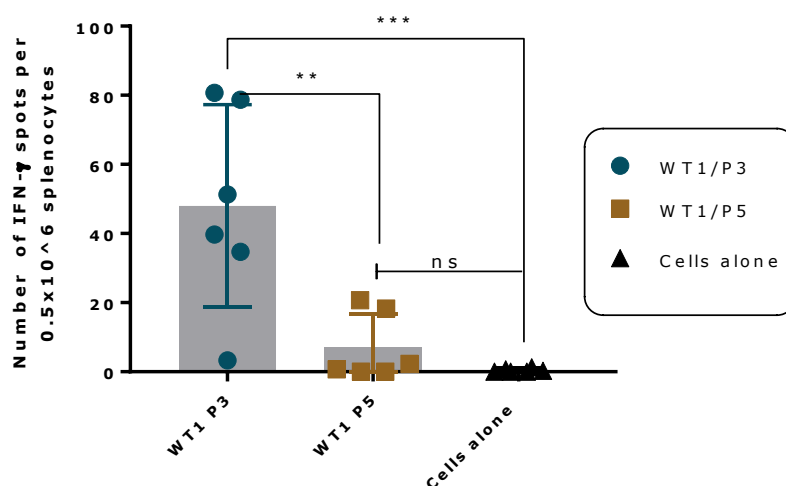


**Figure 4.12: Frequency of WT1-specific CTLs induced by WT1 peptide/adjuvant immunisation, as determined using the IFN- $\gamma$  ELISpot assay.**

The level of IFN- $\gamma$  produced by fresh  $0.5 \times 10^6$  splenocytes harvested from a group of mice that were immunised by the long WT1 15-mer peptide VRDLNALLPAVPSLG (WT1/P1) emulsified in IFA and CPG and boosted by equal ratio of a cocktail of MHC class I restricted short peptides; ALLPAVPSL (WT1/P3) and DLNALLPAV (WT1/P5) emulsified in the same adjuvants mixture were assessed using the ELISpot assay. Values are expressed as the mean  $\pm$  SEM of two independent experiments (3 mice per group) and the level of significance was assessed using One Way ANOVA followed by Dunnett's multiple comparisons test. Results point out the immunogenicity of WT1/P3 in comparison to cells alone (not received peptide re-stimulation), and poor immunogenicity of WT/p5. n=2, (3 mice/group).

In the second set of the experiments, WT1-specific CTL responses induced by a novel WT1 DNA ImmunoBody<sup>®</sup> vaccine (kindly provided by Prof. Lindy Durrant) was assessed, and this is the first time that the efficacy of WT1 vaccine in the form of DNA ImmunoBody<sup>®</sup> vaccine is studied. The same programme as that used for the HAGE-ImmunoBody<sup>®</sup> immunisation was followed, wherein, a set of three mice per group immunised by single DNA bullet containing 1  $\mu$ g of WT1 DNA which was designed to encode the long WT1 15-mer sequence [VRDLNALLPAVPSLG]/(vector map in Figure 4.5A) coated onto gold particles and administered by gene gun device in two boosts at seven days interval apart. On day-21, splenocytes were immediately harvested and re-stimulated *in vitro* using 1  $\mu$ g/mL class I, (WT1/P3) and (WT1/P5), and 10  $\mu$ g/mL of the class II long 15-mer itself (WT1/P1). Then the level of IFN- $\gamma$  production was assessed using ELISpot assay. Results in Figure 4.13 verify the immunogenicity of WT1/P1 and WT1/P3, and also show (once again) the poor immunogenicity of WT1/P5.

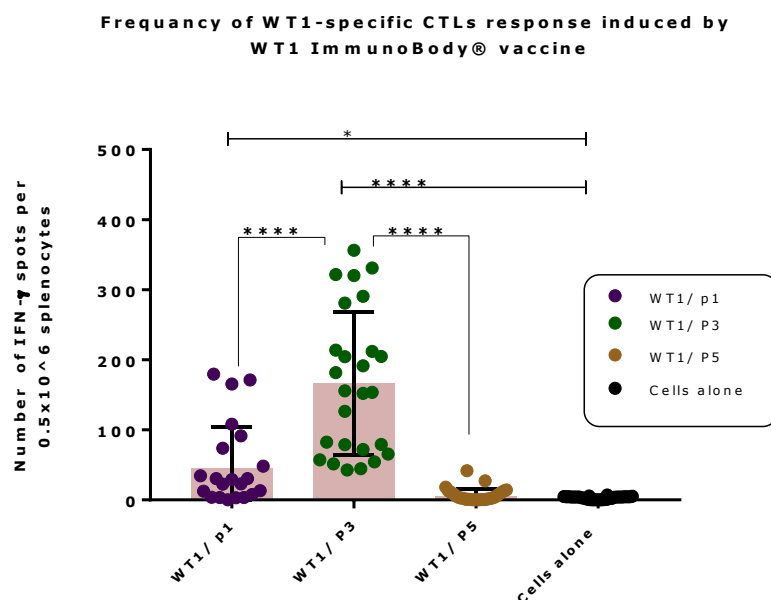


**Figure 4.13: Frequency of WT1-specific CTLs induced by the ImmunoBody® vaccine, as determined using the IFN- $\gamma$  ELISpot assay.**

The level of IFN- $\gamma$  produce by fresh  $0.5 \times 10^6$  splenocytes harvested from a group of mice immunised and boosted with the HAGE-ImmunoBody® were assessed using ELISpot assay. Values are expressed as the mean  $\pm$  SEM of 8 independent experiments and the level of the significance was assessed using One Way ANOVA followed by Dunnett's multiple comparisons test. Results point out the immunogenicity of WT1/P1 and WT1/P3, and poor immunogenicity of WT1/P5 in comparison with cell alone. n=8 (3 mice/group)

After having demonstrated the immunogenicity of WT1 vaccine using the two above mentioned strategies, a comparison of the WT1 simple peptide/adjuvant and WT1-ImmunoBody® immune response was plotted in Figure 4.14 to compare and summarise the responses elicited by these approaches. Results show that there is a significant enhancement in the immune response toward WT1/P3 when the ImmunoBody® was used with \*\*\**P-value*= 0.0004. These data highlight once again the superiority of the ImmunoBody® vaccine at inducing a high frequency of T cells over the simple peptide/adjuvant regime. WT1/P5, however, did not show any improvement within the range of the experiment condition and design. Hence, the data collected for WT1/P5 in the form of T2 binding/dissociation assays and IFN- $\gamma$  ELISpot assay strongly indicate that this peptide is of low affinity to HLA-A2 molecules, and even if one assumes that some peptide-HLA complex was formed, it was of low stability and was easily dissociated from the cell surface, and most likely was not endogenously processed which resulted in weak/lack of T cell immune response.

**A comparison of the immune response generated by WT1 simple peptide/adjuvant immunisation versus WT1 ImmunoBody®**

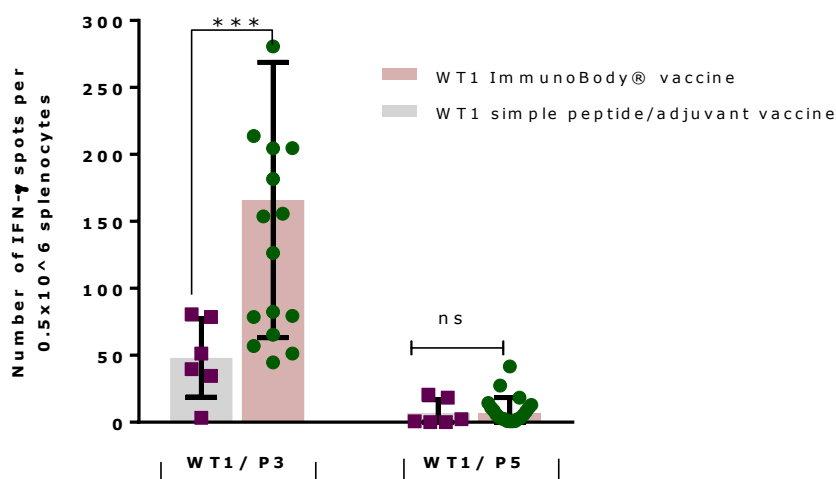


**Figure 4.14: Frequency of immune response generated by WT1 peptide/adjuvant immunisation versus WT1-ImmunoBody® vaccine, as determined using the IFN- $\gamma$  ELISpot assay.**

The level of IFN- $\gamma$  produced by fresh  $0.5 \times 10^6$  splenocytes harvested from a group of mice immunised and boosted with the HAGE-ImmunoBody® were compared with a group of mice that were immunised with the WT1 long 15-mer and boosted with a cocktail of short 9-mer WT1 peptides assessed using ELISpot assay. Values are expressed as the mean  $\pm$  SEM and the level of significance was assessed using two-way ANOVA followed by Tukey's multiple comparisons test. Results show that there is a significant enhancement in the frequency of the immune response toward WT1/P3 when ImmunoBody® was used. Nevertheless, no improvement in WT1/P5 could be detected in comparison with cell alone.

### 4.3.3.3 Functional avidity of the immunogenic HAGE and WT1 peptides, as assessed by peptide titration IFN- $\gamma$ ELISpot assays

Having demonstrated the binding affinity, stability and immunogenicity of the HAGE and WT1 peptides, the functional avidity of the immunogenic class I short peptides; HAGE/P5, HAGE/P6 and WT1/P3, were assessed.

Fresh splenocytes isolated from a group of mice immunised with HAGE-ImmunoBody® and another group immunised with WT1-ImmunoBody® were re-stimulated with serial dilutions of the immunogenic class I peptides; HAGE/P5, HAGE/P6 and WT1/P3 at  $1 \mu\text{g}$  to  $10^{-7} \mu\text{g/mL}$  (corresponding to the  $10^{-6}$  to  $10^{-12}$  LogM), and responses were assessed using IFN- $\gamma$  ELISpot. The effector function is often measured by half maximal activation ( $EC_{50}$ ) which refers to the concentration needed to produce 50% maximum effector function of T cells, and this can be calculated by plotting dose response sigmoid curves against the logarithms of molarity (LogM) of the cognate peptide. Figure 4.15 (B and C) demonstrates that the three peptides can induce IFN- $\gamma$  release even with very low concentrations of peptide, as it is reflected by their

corresponding low  $EC_{50}$  values, indicating that high avidity T cells were produced by the candidate peptides. The figure also demonstrates that each  $EC_{50}$  value calculated for HAGE/P6 and WT1/P3 are very similar and both are higher than the one obtained for HAGE/P5.

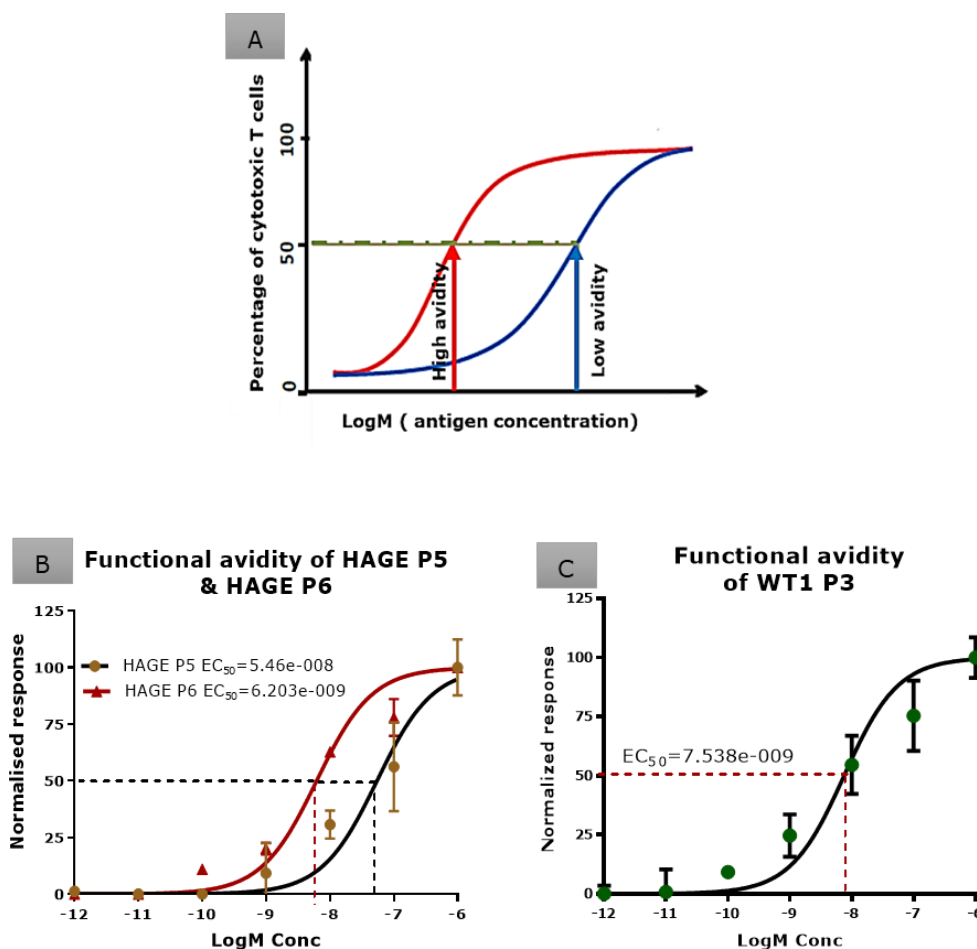


**Figure 4.15: Functional avidity of the immunogenic class I HAGE and WT1 peptides, as determined using peptide titration IFN- $\gamma$  ELISpot assays.**

Fresh splenocytes from group of mice immunised with the HAGE-ImmunoBody<sup>®</sup> vaccine and another group vaccinated with WT1-ImmunoBody<sup>®</sup> vaccine were isolated and re-stimulated by serial dilutions of the immunogenic short class I peptides (HAGE/P5, HAGE/P6 and WT1/P3) and then assessed for their functional avidity profile using IFN- $\gamma$  peptide titration ELISpot assays. (A) Representation of high and low avidity T cell responses adapted from Jayakumar Vadakekolathu thesis (Vadakekolathu 2013), wherein the red sigmoid curve refers to high avidity T cell response as it appeared to be triggered by a very low antigen dose, whereas low avidity T cells response shown in the blue sigmoid curve requires a higher concentration of antigenic peptides for its optimal activation. (B&C) dose response curves point out the minimum concentration of HAGE/P5, HAGE/P6 and WT1/P3 required to induce 50% maximum function ( $EC_{50}$ ). Logarithms of molarity (LogM) for each peptide were calculated and plotted against the normalised response,  $EC_{50}$  was then calculated using non-regression analysis. Data expressed as the mean of the three replicated of two independent experiments. Overall, results demonstrate that all peptides studied can induce T cell responses (IFN- $\gamma$  release) even at low concentrations, reflecting high avidity of T cells induced by the candidate peptides, and that  $EC_{50}$  values of each HAGE/P6 and WT1/P3 are almost close and both are higher than HAGE/P5. n=2 (3 mice/group).

### 4.3.4 Immunogenicity of the combined HAGE- and WT1-ImmunoBody<sup>®</sup> vaccines

Having demonstrated the immunogenicity of HAGE- and WT1-ImmunoBody<sup>®</sup> vaccines individually, this section studied the applicability of using both vaccines in combination without peptide/antigen competition on the APC surface which could interfere with optimal function of T cells.

Two programmes were designed in an attempt to optimise the interval between HAGE and WT1 vaccines and identify the one that generates the highest T cell activity for implementation in future experiments. In the first programme, both ImmunoBody<sup>®</sup> vaccines were administered concurrently (same day immunisation programme), wherein each mouse received a single HAGE-ImmunoBody<sup>®</sup> bullet inoculated intradermally into one flank and a single WT1 bullet into the contralateral flank at the same time using a BioRad Helios<sup>®</sup> gene gun technology, three times with 7 days in between. The second protocol (HAGE then WT1 vaccination programme) was similar but started with administering the HAGE-ImmunoBody<sup>®</sup> vaccine at one flank, then after 2 days, administration of the WT1-vaccine into the contralateral flank.

To potentially reduce variations in the optimisation assay that could occur due to reasons, such as bullet preparation, bullet firing, material used to assess IFN- $\gamma$  and other variables, all optimisation experiments were carried out using freshly made bullets that were prepared with the same reagents and conditions, and they were tested for adequate firing and the absence of remnants in the tube. As much as possible, the same ELISpot kit and other reagents for spot development were used.

Figure 4.15 shows the results of this comparison. No statistically significant difference was found between the number of HAGE peptide specific IFN $\gamma$  released when both vaccines were administered concurrently (same day immunisation) in comparison to vaccine given alone. However, a significant lower number of spots against HAGE peptide was obtained when WT1 vaccination was applied two days after HAGE vaccination, with *\*\*p-value* for HAGE/P6 re-stimulation and *\*P-value* for each HAGE/P5 and HAGE/P7 re-stimulation, highlighting the deterioration of HAGE-immunogenicity by WT1 peptide when this programme is applied.

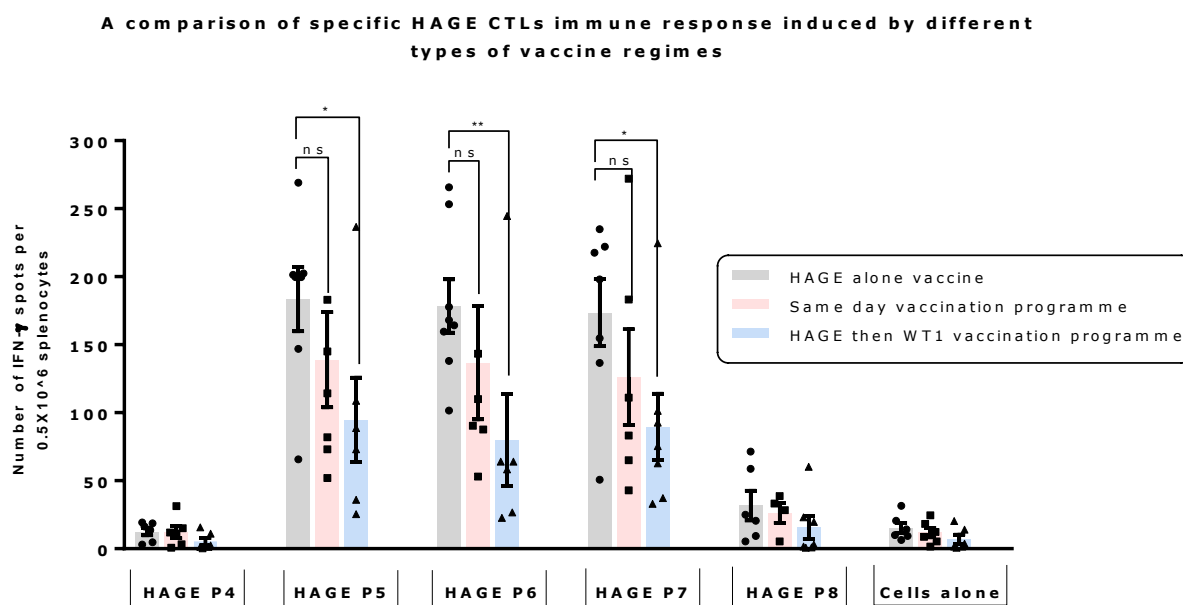


**Figure 4.16: Immune responses induced by different regimes of HAGE- and WT1-ImmunoBody<sup>®</sup> vaccines to evaluate HAGE immunogenicity, as assessed using the IFN- $\gamma$  ELISpot assay.**

The level of IFN- $\gamma$  produced by fresh  $0.5 \times 10^6$  splenocytes harvested from groups of mice immunised and boosted with a combination of HAGE- and WT1- ImmunoBody<sup>®</sup> vaccines, but in different intervals between the doses was assessed using the ELISpot assay, alongside with a group of mice that were immunised and boosted with HAGE-ImmunoBody<sup>®</sup> alone. In the same day immunisation programme, each mouse received HAGE and WT1 bullets simultaneously, but into different flanks. whereas in the HAGE then WT1 programme, mice first received the HAGE bullet, and two days later the WT1 bullet. On day-21, splenocytes were harvested and re-stimulated by the short HAGE peptides (HAGE/p4), (HAGE/p5), (HAGE/P6), (HAGE/P7) and (HAGE/P8). Values are expressed as the mean  $\pm$  SEM and the level of the significance was assessed using two Way ANOVA followed by Tukey's multiple comparisons test. Results show that same day immunisation is better than when HAGE administered then WT1. n=2 (3 mice/group).

At the same time, IFN- $\gamma$  produced by WT1-specific CTLs was assessed upon re-stimulation of splenocytes harvested from different programmes by the short WT1/P3 and WT/P5 peptides. Interestingly, as is shown in Figure 4.16, there was no statistical difference in the immune response obtained when both vaccines were administered at the same day, nor when the HAGE vaccine preceded the WT1 vaccine, highlighting the predominance of WT1 peptide over HAGE.

From what was found, it seems that WT1 could competitively inhibit the immunogenicity HAGE when the HAGE vaccine was administered before WT1, but that the same day administration could work best in term of improvement of HAGE immunogenicity. For that reason, this programme was selected for all forthcoming *in vitro* and *in vivo* studies and from now and on, the word "combined vaccines" indicates that both HAGE- and WT1-ImmunoBody<sup>®</sup> vaccines were given on the same day but into different flanks.

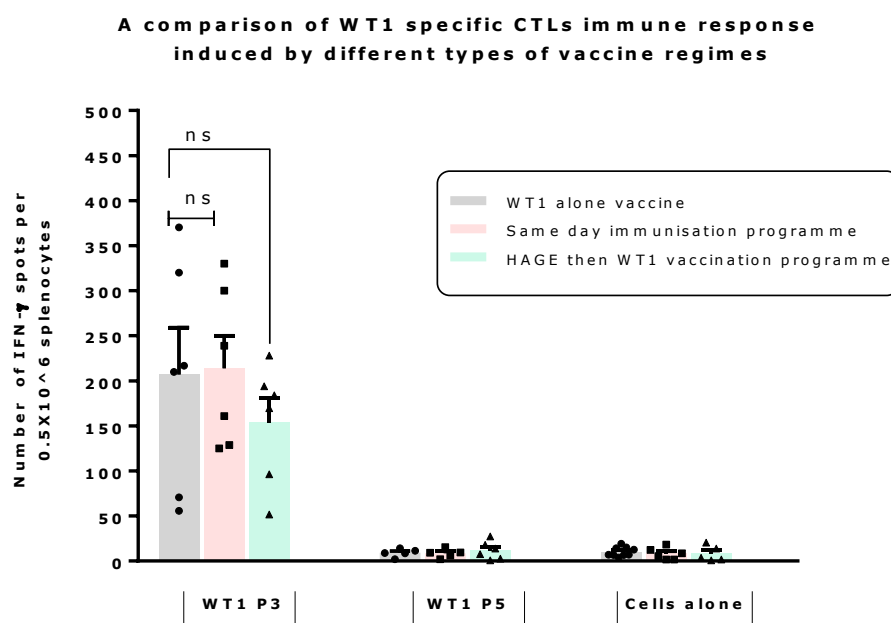


**Figure 4.17: Immune responses induced by different regimes of HAGE- and WT1-ImmunoBody® vaccines to evaluate WT1 immunogenicity, as assessed using the IFN- $\gamma$  ELISpot assay.**

The level of IFN- $\gamma$  produce by fresh  $0.5 \times 10^6$  splenocytes harvested from groups of mice immunised and boosted with a combination of HAGE- and WT1-ImmunoBody® vaccines, but in different intervals was assessed using ELISpot assay, alongside with a group of mice that were immunised and boosted with WT1-ImmunoBody® alone. In the same day immunisation programme, mice received HAGE and WT1 simultaneously, but into different flanks, whereas in the HAGE then WT1 programme, mice first received the HAGE bullet, and two days later the WT1 bullet. On day-21, splenocytes were harvested and re-stimulated by the short WT1 peptides (WT1/p3) and (WT1/P5). Values are expressed as the mean  $\pm$  SEM and the level of the significance was assessed using two Way ANOVA followed by Tukey's multiple comparisons test. Results show that there was not statistically significance difference in responses induced by the different regimes. n=2 (3 mice/group).

### 4.3.5 Proliferation, cytokine production and degranulation of CTLs derived from ImmunoBody® immunised mice

Multi-colour flow cytometry gives a distinctive advantage over other available techniques used to detect cytokine/protein production, such as ELISpot and ELISA assays in that it can identify secreting cell populations. Indeed, combining intracellular staining (ICS) and cell surface staining enables one to simultaneously identify and characterise multiple phenotypic, differentiation and functional parameters of responder T cells (Smith, S. G., Smits, Joosten, van Meijgaarden, Satti, Fletcher, Caccamo, Dieli, Mascart, and McShane 2015).

In ICS, it is important to inhibit protein transport prior to staining in order to retain cytokines inside the cells, this was achieved by using brefeldin A and monensin. Brefeldin (derived from fungi; *Penicillium brefeldianum*) interrupts protein secretion

early in a pre-Golgi compartment whereas monensin (isolated from *Streptomyces cinnamonensis*) acts at the final stages of secretory vesicle maturation in Golgi compartment (Mollenhauer, Morr   *et al.* 1990).

In this study, to characterise the response induced by the HAGE, WT1 and combined ImmunoBody<sup>®</sup> vaccines, ICS to measure and compare the expression of IFN- $\gamma$ , TNF- $\alpha$ , IL-2, Granzyme B (serine protease) and Ki-67 (marker of proliferation) and CD107a (marker of degranulation) derived from CD8<sup>+</sup> T population was performed on freshly isolated splenocytes from mice immunised with the candidate vaccines. For each mouse (vaccinated/na  ve), T cells were assessed for these markers in two settings; firstly, when cells stimulated with a cocktail of class I peptides, and in the absence of peptide (cells alone). All samples were treated exactly by the same reagents, such as protein inhibitor (brefeldin A and monensin) and the costimulatory molecules (soluble anti-CD28 and anti-CD49d). Cells were then incubated for 5 hours at 37  C and then stored overnight at 4  C for ICS the next day. Staining for cells alone is important in order to be able to subtract background noise from values that are generated with the test samples. The levels of expression for the markers was gated on single live CD8<sup>+</sup> T cells, and the level of the cytokine production for each mouse was determined by comparing the fluorescence intensity of the peptide-stimulated with that of no stimulation (cells alone).

Fold change increase in the cytokines/proteins was calculated as a ratio between the percentage of CD8<sup>+</sup> T cells expressing the indicated proteins in the immunised groups relative to the na  ve group, and thus, bars in Figure 4.17 below indicate these ratios after noise background being subtraction. TNF- $\alpha$  and Ki-67 (a marker of proliferation) were the most upregulated markers seen in all vaccine regimes at almost equal folds, ~9-fold for TNF- $\alpha$  and ~6.5-fold for Ki-67. The cell degranulation marker CD107a was also upregulated by both HAGE and WT1 vaccines at ~2 and ~3 fold than of the na  ve splenocytes, respectively, and the combination of the two vaccines further increased the level of degranulation (~6 fold), indicating the advantageous effect of the combined vaccines over the single regimes for inducing T cell degranulation. In a similar manner, IFN- $\gamma$  production triggered by the WT1 and HAGE vaccines was shown to be 4 and 5 times that of the na  ve respectively, while the combined vaccines enhanced IFN- $\gamma$  level further at ~6 fold. However, no notable upregulation of granzyme B was found.

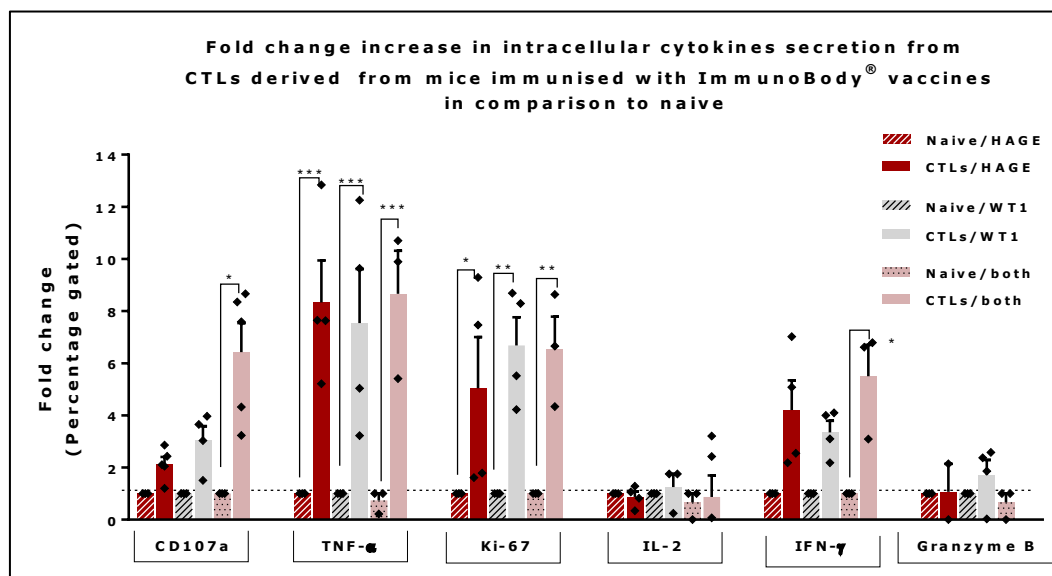


**Figure 4.18: Proliferation, cytokine production and degranulation of CTLs derived from mice immunised with ImmunoBody<sup>®</sup> vaccines, as determined using flow cytometry.**

$1 \times 10^6$  of splenocytes freshly harvested from mice immunised with the HAGE- and WT1-ImmunoBody<sup>®</sup> vaccines (individually and in combination), and from naïve mice were all re-stimulated *in vitro* with short cocktail of class I peptides at  $1 \mu\text{g}/\text{mL}$  together with protein transport inhibitors for 5 hours, cells were then analysed for the expression of the indicated proteins by flow cytometry. According to gating strategy mentioned-above, the level of the cytokines secretion per single live  $\text{CD8}^+$  T cells were determined and compared with the naïve T cells. Statistical analysis was performed using two-way ANOVA test. Results show that there is an upregulation of the candidate antigens in almost all groups studied, except IL-2 and granzyme B.  $n=2$  (2 mice/group).

TNF- $\alpha$ , IFN- $\gamma$  and granzyme B production per single  $\text{CD8}^+/\text{Ki67}^+$  cells from the immunised mice and cells from naïve mice was compared. Hence, according to the gating strategy of this population shown in Figure 4.18, a notable upregulation was observed to be 30-55% for TNF- $\alpha$ , 45-55% for IFN- $\gamma$  and around 10% for granzyme B, as shown in Figure 4.19. The combined vaccines was shown to induce a greater increase in the production of TNF- $\alpha$  than when HAGE and WT1 were given individually, this again highlights the benefit of combining the vaccines.

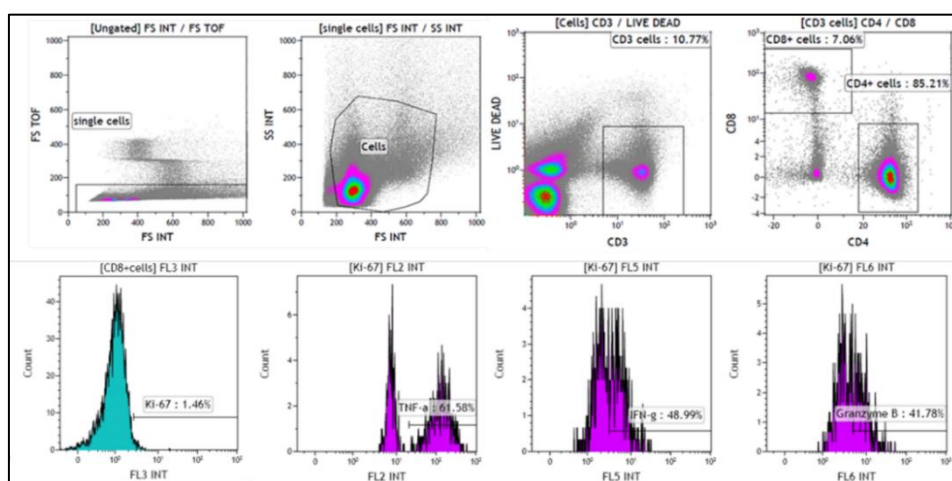


**Figure 4.19: Representative gating strategy to determine upregulation in TNF- $\alpha$ , IFN- $\gamma$  and granzyme B expression by proliferating CTLs from mice immunised with the ImmunoBody® vaccines.**

In the upper row, “Single cells” were first gated according to their Forward Scatter Linear (FS-INT) *versus* FS TOF (time of flight) axis to remove doublets. “Cells” were then gated by Side Scatter and Forward Scatter profile, and then single cells were selected, leaving out the doublets, Cells were then gated on “Cells” as “CD3” populations *versus* LIVE/DEAD™ Yellow stain to exclude the dead cells from the analysis. Categorisation into CD8<sup>+</sup> and CD4<sup>+</sup> T cells obtained by a density plot gated on CD3<sup>+</sup> cells. The level of Ki-67 expression gated on CD8<sup>+</sup> cells (demonstrated in the lower row) determined on basis of fluorescence intensity depicted by a shift to the right of histograms in comparison to sample obtained from non-stimulating sample (cells alone). TNF- $\alpha$ , IFN- $\gamma$  and granzyme B are all then gated on population of cells shown to be a positively stained for Ki-67.

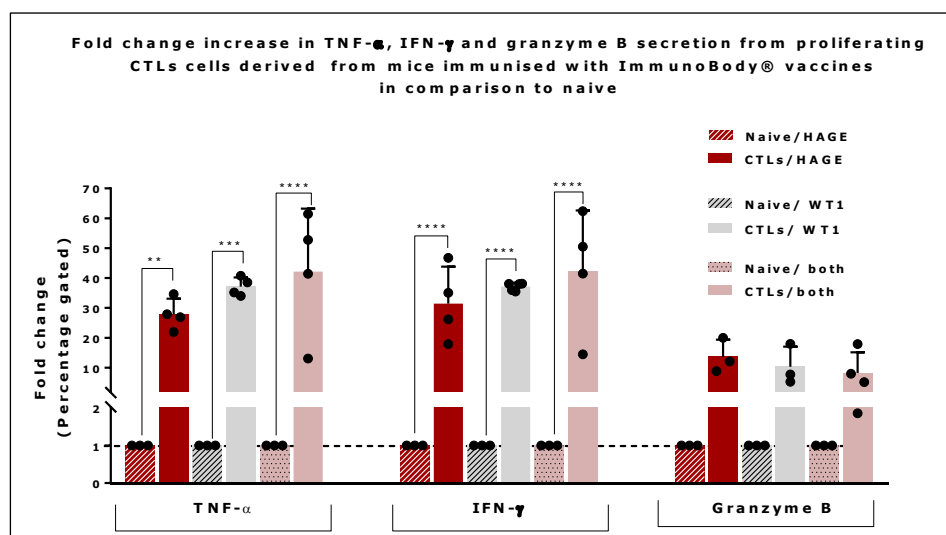


**Figure 4.20: Fold change increase in TNF- $\alpha$ , IFN- $\gamma$  and granzyme B secretion from proliferating CTLs derived from mice immunised with ImmunoBody® vaccines, as determined using flow cytometry.**

$1 \times 10^6$  of fresh splenocytes from mice immunised with HAGE- and WT1-ImmunoBody® vaccines (individually and in combination) and from naïve mice were all re-stimulated *in vitro* with a cocktail of short class I peptides at 1ug/mL together with protein transport inhibitors for 5 hours, cells were then stained with surface markers and intracellular cytokines and run on flow cytometer. According to gating strategy mentioned above, the level of TNF- $\alpha$ , IFN- $\gamma$  and granzyme B secretion from single live proliferating CD8<sup>+</sup> T cells (Ki-67 positive) were estimated and compared with naïve T cells that were treated exactly as the immunised mice. Statistical analysis was performed using two-way ANOVA test. Results show that there is a significant upregulation of TNF- $\alpha$  and IFN- $\gamma$  in all groups studied. n=2 (2 mice/group).

From this study, it can be concluded that HAGE and WT1 vaccines or a combination upregulate the majority of cytokines/proteins studied in comparison to the naïve cells, and that the combined regime is associated with more degranulation and IFN- $\gamma$  secretion. In addition, a high proportion of proliferating cells generate TNF- $\alpha$  and IFN- $\gamma$  when both vaccines were used.

### 4.3.6 Influence of HAGE- and WT1-ImmunoBody<sup>®</sup> vaccines on naïve and memory T cell populations

In response to a specific antigen, naïve T cells undergo complex transformational changes leading to cell proliferation and differentiation into effector function. These events are associated with alteration of different surface markers that are responsible for a specific cell function, such as homing (Oehen, Brduscha-Riem 1998).

In mice, T cells are frequently characterised into naïve and memory cells depending on the expression of the adhesion molecules CD62L and CD44, where naïve T cells are identified as being CD62L<sup>high</sup>CD44<sup>low</sup> and memory cells as CD62L<sup>low</sup>CD44<sup>high</sup>.

In an attempt to phenotypically characterise the T cells generated upon the administration of HAGE- and WT1-ImmunoBody<sup>®</sup> vaccines either individually or in combination, splenocyte harvested from immunised and naïve mice were stained using a panel of monoclonal antibodies: anti-CD3-BV421<sup>™</sup>, CD4-Alexa-Fluor<sup>™</sup>700, CD8-APC-Cy7<sup>™</sup>, CD62L-FITC, CD44-APC and viability determined by including the LIVE/DEAD<sup>™</sup> Yellow stain. Gating strategy of this analysis is shown in Figure 4.20.

Data in Figure 4.21 show significant upregulation of CD62L<sup>low</sup>/CD44<sup>high</sup> population and significant down-regulation of CD62L<sup>high</sup>/CD44<sup>low</sup> population in the vaccinated mice in comparison to the naïve. The percentage of CD62L<sup>high</sup>/CD44<sup>low</sup> population was significantly lower after the administration HAGE and WT1 vaccines at *\*p-value* and *\*\*p-value*, respectively in comparison to the naïve group, however, the frequency of this population declined further when the vaccines were combined at *\*\*\*P-value*. In reverse, the proportion of CD62L<sup>low</sup>/CD44<sup>high</sup> cells was significantly increased in comparison to the naïve group at *\*\*P-value* in the HAGE alone group and at *\*\*\*\*P-value* in the WT1-ImmunoBody<sup>®</sup> group, as well as in the group of mice immunised with both HAGE- and WT1-ImmunoBody<sup>®</sup> (*\*\*\*\*P-value*) vaccines. These observations indicate that both HAGE- and WT1-ImmunoBody<sup>®</sup> independently or together can induce the differentiation of naïve T cells into memory repertoires, and that combining vaccines improves the memory pool in terms of down regulating the CD62L<sup>high</sup>/CD44<sup>low</sup> population.

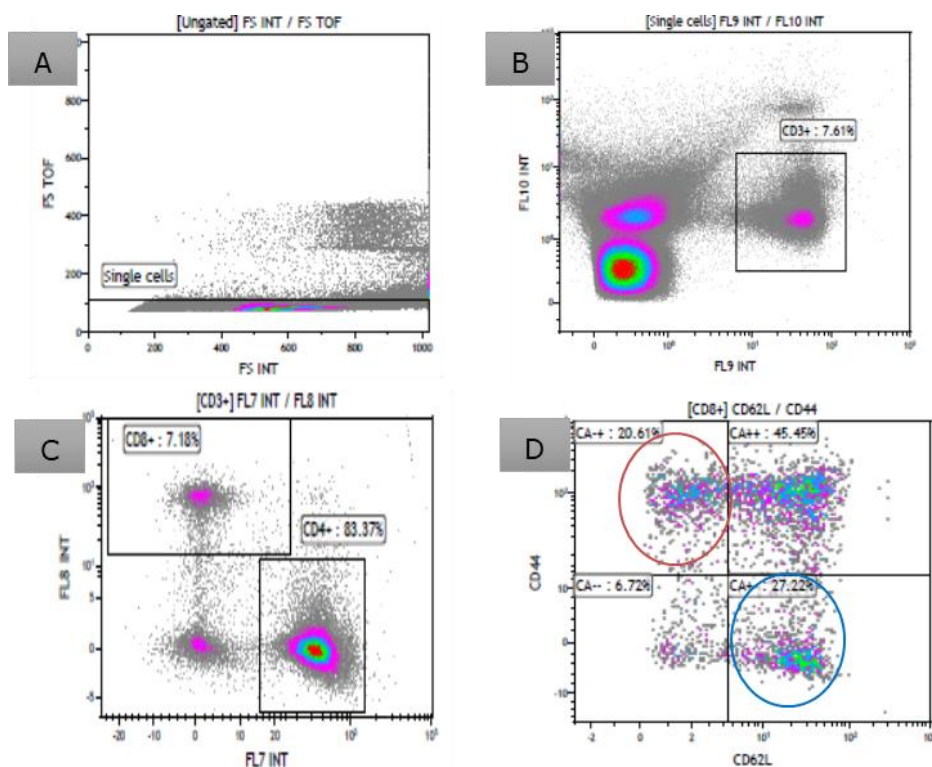


**Figure 4.21: Representative gating strategy for characterising T cells induced by ImmunoBody® vaccines into naïve and memory T cells.**

To eliminate doublets "Single cells" population, Forward Scatter Linear (FS-INT) versus FS TOF (time of flight) axis was firstly plotted (shown in A). Cells were then gated on single cells as "CD3" populations (shown in B) which detected at FL9 versus LIVE/DEAD™ Yellow stain (detected at FL10) to exclude the dead cells from the analysis. Categorisation into CD8<sup>+</sup> and CD4<sup>+</sup> T cells obtained by plotting a density plot gated on CD3<sup>+</sup>, wherein CD8<sup>+</sup> T cell detected at FL8 at the upper left quadrant in C and the CD4<sup>+</sup> T cells detected at FL7 at the right lower quadrant. Finally, the CD62L<sup>high</sup>CD44<sup>low</sup> population which represents naïve T cells gated on CD8<sup>+</sup> T cells is identified at the lower right quadrant in D (blue-outline circle). The CD62L<sup>low</sup>CD44<sup>high</sup> population representing memory T cells is in the upper left quadrant (red-outline circle).

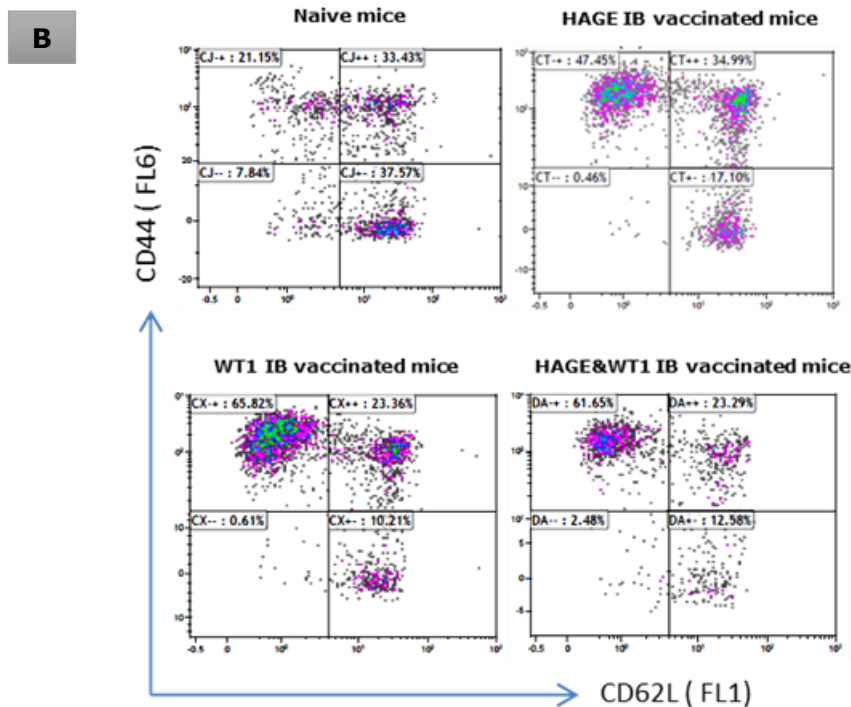
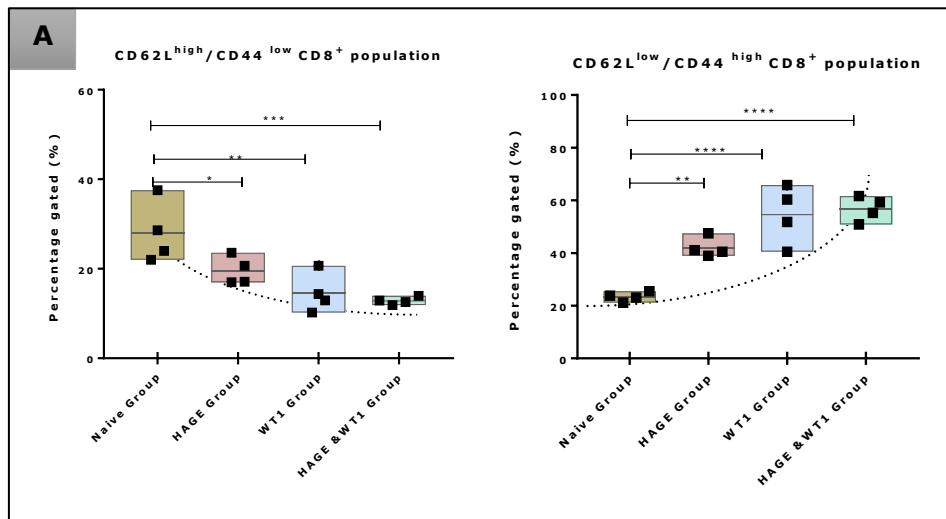


**Figure 4.22: Characterising T cells induced by ImmunoBody<sup>®</sup> vaccines into naïve and memory T cells using flow cytometry.**

(A) Floating bar graphs demonstrate two patterns of CD8<sup>+</sup> populations expressed by ImmunoBody<sup>®</sup> vaccine derived T cells: CD62L<sup>low</sup>/CD44<sup>high</sup> (memory) and CD62L<sup>high</sup>/CD44<sup>low</sup> (naïve) populations.  $1 \times 10^6$  of fresh splenocytes from each indicated group were stained with anti-CD3, -CD4, -CD8, -CD44, -CD62L and LIVE/DEAD<sup>™</sup> Yellow stain and run on flow cytometer. Values are expressed as the mean  $\pm$  standard deviation of 4 mice. The level of the significance was assessed using Two Way ANOVA. (B) Representative density plots for CD62L and CD44 expression by cells from immunised and naïve animals. The CD62L<sup>low</sup>/CD44<sup>high</sup> (memory) population is gated in the upper left quadrant of each plot, whereas the CD62L<sup>high</sup>/CD44<sup>low</sup> (naïve) population is indicated in the lower right quadrant. Results show that there is significant upregulation of CD62L<sup>low</sup>/CD44<sup>high</sup> population and significant down-regulation of CD62L<sup>high</sup>/CD44<sup>low</sup> population in immunised mice in comparison to the naïve mice. n=1 (4 mice).

### 4.3.7 Effect of immunisation on T cell activation and exhaustion

Recent studies have confirmed that T cell dysfunction/exhaustion is one of the main mechanisms that can hinder productive properties of the anti-cancerous immunity. In this respect, the effect of different ImmunoBody<sup>®</sup> vaccines on the expression of some inhibitory and stimulatory markers of T cell was determined.

Splenocytes from mice immunised with HAGE- and WT1-ImmunoBody<sup>®</sup>, individually or in combination, and naïve non-immunised mice were stained with the following panel of antibodies of; anti-CD3-BV421<sup>™</sup>, CD4-Alexa-Fluor<sup>™</sup>700, CD8-APC-Cy7, PD-1-APC, CTLA-4(CD152)-PE/Dazzle<sup>™</sup>594, Tim-3 (CD366)-PE-Cy7<sup>™</sup>, LAG-3 (CD223)-PerCp-Cy5.5<sup>™</sup>, OX-40 (CD134)-PE, GITR (CD357)-FITC and viability determined by including the LIVE/DEAD<sup>™</sup> Yellow stain, Samples were analysed using flow cytometry.

Details of gating strategy are illustrated in Figure 4.22, where, the levels of the respective markers produced per single live CD8<sup>+</sup> T cells were determined.

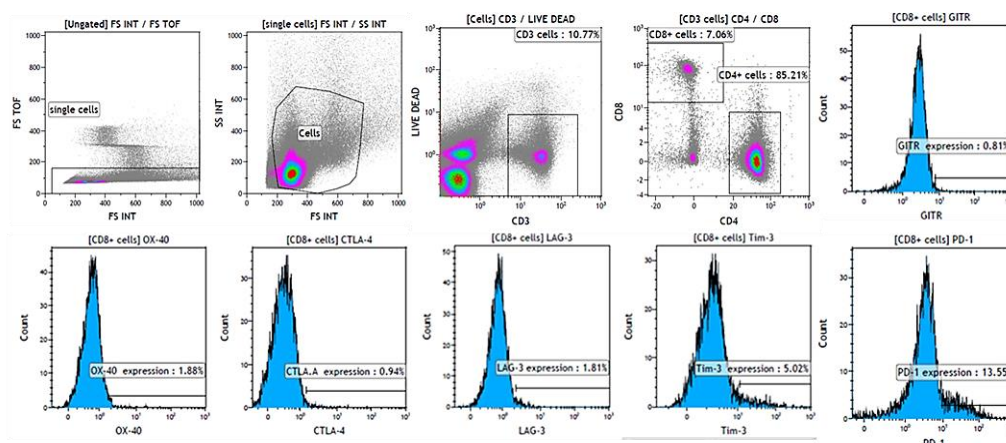


**Figure 4.23: Representative gating strategy to assess the expression of markers of T cell activation and exhaustion.**

In the upper row, “Single cells” were first gated according to their Forward Scatter Linear (FS-INT) *versus* FS TOF (time of flight) axis to remove doublets. “Cells” were then gated by Side Scatter and Forward Scatter profile, and then single cells were selected, leaving out the doublets, Cells were then gated on “Cells” as “CD3” populations which detected at FL9 *versus* LIVE/DEAD<sup>™</sup> Yellow stain (detected at FL10) to exclude the dead cells from the analysis. Categorisation into CD8<sup>+</sup> and CD4<sup>+</sup> T cells obtained by plotting a density plot gated on CD3 cells, wherein CD8<sup>+</sup> T cell detected at FL8 and the CD4<sup>+</sup> T cells detected at FL7. The levels of surface markers expression (demonstrated in the lower row) were determined based on fluorescence intensity depicted by a shift to the right of histograms in comparison to a sample obtained from a naïve mouse.

Data in Figure 4.23 show the expression of the costimulatory molecules (GITR and OX-40) and the inhibitory molecules (CTLA-4, LAG-3, Tim-3 and PD-1) by CTLs derived from mice vaccinated with the respective ImmunoBody<sup>®</sup> vaccines. Interestingly, the findings demonstrate significance upregulation in the level of the PD-1 which is shown to be highly upregulated in comparison to naïve non-vaccinated mice at \*\*\*\**P-value* in all ImmunoBody<sup>™</sup> vaccine groups. Nevertheless, no significant upregulation in other markers could be detected.

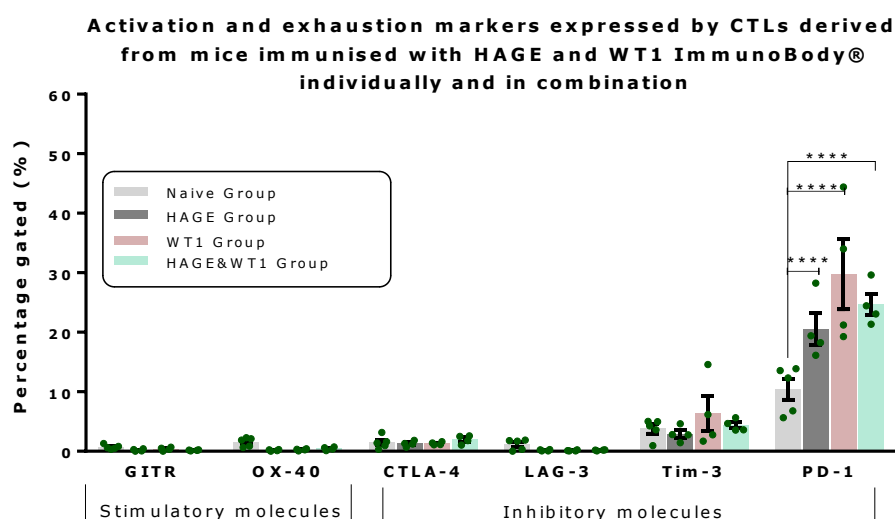


**Figure 4.24: Expression pattern of markers of T cell activation/exhaustion per CTLs derived from mice immunised with ImmunoBody<sup>®</sup> vaccines, as determined by flow cytometry.**

$1 \times 10^6$  of fresh splenocytes from each indicated group were stained with anti-CD3, -CD4, -CD8, -GITR, -Ox-40, -CTLA-4, -LAG-3, -Tim-3, -PD-1 and LIVE/DEAD<sup>™</sup> Yellow stain. Values are expressed as the mean  $\pm$  SEM of 4 mice and the level of the significance was assessed using Two Way ANOVA followed by Tukey's multiple comparisons test. Results show that there is significant upregulation of the inhibitory molecules PD-1 in all three vaccinated groups in comparison to the naïve, suggesting an exhaustion indicator of the T cells. n=1 (4 mice/group).

## 4.4 Discussion

The ever-increasing number of TAAs has induced a major incentive for the development of various therapeutic peptide-based vaccines. However, peptide immunogenicity and specificity are crucial basic elements for the success of peptide-based vaccine. Initially, peptide vaccines exclusively targeted CTL responses, which is why initial vaccine trials employed vaccines based on short peptides. However, Melief and colleagues later proved that long peptide vaccines harbour multiple CD8<sup>+</sup> and CD4<sup>+</sup> T cell epitopes and are therefore more efficient at generating durable anti-tumour responses (Melief, Van Der Burg, Sjoerd H 2008).

The cancer testis antigen, HAGE, and the zinc finger transcription factor, WT1, have previously been shown to be immunogenic. More specifically, the HAGE long 30-mer peptide sequence [QTGTGKTLCYLMPGFIHLVLQPSLKGQRNR] was found to be immunogenic and encompass several immunogenic short class I and class II epitopes restricted to HLA-A2 and HLA-DR1 haplotypes. The efficacy of this 30-mer sequence in the form of HAGE-ImmunoBody<sup>®</sup> was also compared with that of the HAGE 30-mer peptide/adjuvant vaccination programme. Previous student in our group (Divya Nagarajan found that the intradermal administration of the HAGE-ImmunoBody<sup>®</sup> vaccine using gene gun technology is more potent at enhancing the vaccine immunogenicity than the peptide/adjuvant vaccination regime, as was assessed by IFN- $\gamma$  ELISpot assay. Hence, the present study focused on HAGE-ImmunoBody<sup>®</sup> vaccines regime only. In a similar manner, a 15 amino acid peptide [VRDLNALLPAVPSLG] derived from the WT1 protein containing two known and previously published HLA-A2 9-mer was selected for studying the efficacy of WT1 vaccine. The efficacy of WT1 15-mer peptide/adjuvant vaccination was compared with the WT1 15-mer ImmunoBody<sup>®</sup> based vaccination programme.

First, both HAGE and WT1 HLA-A2 restricted epitopes predicted by SYFPEITHI software were evaluated for their MHC binding affinity *in vitro* upon loading them onto T2 cells. Interestingly, all HAGE HLA-A2 restricted peptides; HAGE/P4, HAGE/P5, and HAGE/P6 stabilised HLA-A2 on the surface of T2 cells, as was reflected by high FIRs and, therefore, they were classified as strong HLA-A2 binders, which correlated with SYFPEITHI predication. Likewise, WT1 peptides binding affinity for HLA-A2 was experimentally studied. WT1/P3 was found to be a very strong HLA-A2 binder, which has therefore the potential to lead to potent T cells activation *in vitro* and *in vivo* studies. On the other hand, although WT1/P5 was scored 27 by the SYFPEITHI, it exhibited low binding capability to HLA-A2 which could not be improved using even at higher peptide concentrations. It was therefore categorised as being a weak HLA-A2 binder. However, although it is true that high peptide binding affinity to MHC is associated with high frequency peptide-MHC complex production, it does not

necessarily mean that these complexes will induce potent T cell activation, as in some instances these peptide-MHC complexes are relatively unstable and subject to recycling and endocytosis, thereby hindering T cell recognition and subsequent killing. In addition, it has been reported that the peptide-MHC stability more than the peptide-MHC binding affinity is linked with T cell activation (Rudolph, Speir *et al.* 2001). It was therefore decided to study the stability of the respective peptide-MHC complex on T2 cells using DC<sub>50</sub> as an indicator (the time required for a 50% reduction in the MFI), for which the higher the DC<sub>50</sub> the more stable is the interaction between peptide-MHC. This was estimated by loading the respective peptides on the T2 cells and monitored for the persistence of the peptide-MHC class I complex on the cell surface and resistance to the dissociation in a time course analysis using brefeldin A decay assay. This study interestingly reveals that all HAGE-MHC and WT1-MHC complexes were associated with rapid dissociation within the first 6 hours of the experiment as reflected by the drop in the MFI values, however this decline seems to stop after that time. As far as the DC<sub>50</sub> value is concerned, results indicated that all complexes are technically stable as there was no 50% reduction in MFI in comparison to time zero during this range of time (>8 hours), except for WT1/P5-HLA-A2 complex which showed poor stability as its DC<sub>50</sub> value was between 5-6 hours. Collectively, the feasibility of using the candidate peptides for future experiments was validated as they are associated with strong binding attitudes toward MHC molecules as well as potential resistance to the dissociation except WT1/P5 which demonstrated low binding and early dissociation from HLA-A2 molecules.

Next, the immunogenicity of these peptides, when incorporated into an ImmunBody<sup>®</sup> vaccine, was assessed using direct *ex vivo* IFN- $\gamma$  ELISpot to determine the frequency of T cell response to re-stimulation with short peptides. Class I HAGE/P5, HAGE/P6 and the class II HAGE/P7 epitopes were all associated with potent triggering of T cell responses, indicating that these peptides are endogenously processed and presented in association with class I and class II MHC molecules, respectively, thereby inducing the activation of T cells. However, no immunogenicity was detected for the class I peptides HAGE/P4, indicating that this peptide was not endogenously processed, despite being a strong stable HLA-A2 binder. However, it should be noted that these assays were used to confirm the SYFPEITHI predictions and cannot determine whether the peptides are endogenously processed since the exogenous peptides were loaded directly onto T2 cells. Interestingly, while the biochemical structure of the 9-mer HAGE/P4 [LMPGFIHLV] is quite close to the 10-mer HAGE/P6 [**Y**LMPGFIHLV] with only one amino acid difference (presence of Tyrosine (Y) at position 1 in HAGE/P6, bold), it seems this amino acid is of an important in term of TCR binding and subsequent recognition. This could potentially justify the question of why HAGE/P6,

but not HAGE/P4 is a potent immunogenic peptide. It was also noticed that HAGE peptide ending with Valine (V) residue was associated with higher MHC binding score as it is the case in (HAGE/P6) at score 30 compared with (HAGE/P5) at score 2, respectively, suggesting that the presence of Valine could be also important to improve HAGE binding score to the MHC molecule.

In a similar manner to what has been applied for HAGE-ImmunoBody<sup>®</sup>, WT1 ImmunoBody<sup>®</sup> was herein validated for its superior capability to induce WT1-specific immune responses in HHDII/DR1 mice compared to WT1 15-mer peptide/adjuvant. The novel WT1-ImmunoBody<sup>®</sup> DNA vaccine encoding the 15-mer sequence was kindly provided by Prof. Lindy Durrant (Scancell), and herein is the first study that assesses the efficacy of this ImmunoBody<sup>®</sup> vaccine in HHDII/DR1 mice using gene gun technology and applying prime-boost programme. The WT1/P3 epitope was found to elicit stronger T cells immune response upon ImmunoBody<sup>®</sup> vaccination than a peptide/adjuvant vaccination regime, demonstrating the importance of the mode of delivery in enhancing the immune response as this could be a reflection of dual stimulation of CD4<sup>+</sup> and CD8<sup>+</sup> T cells due to cross presentation induced by the ImmunoBody<sup>®</sup> vaccine. On the other hand, peptide WT1/P5 was not recognised by vaccine-induced splenocytes which did not produce any significant level of IFN $\gamma$ .

Having demonstrated the high frequency T cell response induced by the class I peptides HAGE/P5, HAGE/P6 and WT1/P3, the functional avidity of these peptides was then assessed. High T cell frequency was found not to correlate with clinical outcomes and functional avidity might be a more reliable way to assess the quality of the immune response (Lee, Wang *et al.* 1999, Anichini, Molla *et al.* 1999, Jonuleit, Giesecke - Tuettenberg *et al.* 2001). In general, functional avidity refers to the overall strength of interactions that T cell could receive upon encountering of an antigen at particular densities (Appay, Douek *et al.* 2008). In fact, T cells with high avidity could perform fast and readily effector function at lower antigenic dose thresholds (Almeida, Sauce *et al.* 2009, Appay, Douek *et al.* 2008) as it exerts rapid proliferation and expansion *in vivo*, shaping their immuno-dominance to eradicate tumour cells (Almeida, Price *et al.* 2007, Almeida, Sauce *et al.* 2009, Appay, Iglesias 2011, Mothe, Llano *et al.* 2012). In this regard, various techniques has been described to measure T cell functional avidity; firstly, cytokine release-based assays, such as the intracellular cytokine staining and peptide titration using ELISpot assay, and secondly, cytolytic-based assays, which depend on measuring a cytolytic activity produce by T cells against TAP deficient cells that were pulsed with titrated concentrations of cognate peptides, measured by <sup>51</sup>chromium release, for example (Pudney, Metheringham *et al.* 2010, McKee, Roszkowski *et al.* 2005). Therefore, the immunogenic class I peptides; HAGE/P5, HAGE/P6 and WT1/P3 which were identified for their high frequency IFN- $\gamma$  induction, were herein selected to study their functional

avidity profile using IFN- $\gamma$  peptide titration ELISpot assays. DNA ImmunoBody<sup>®</sup> vaccines were shown to induce T cells of high avidity, as indicated by low EC<sub>50</sub> values derived from these immunogenic short peptides.

Nowadays, the concept of incorporation of two or more therapies to accumulate or synergise a clinical benefit has become widely accepted. This helps to overcome the issue of antigenic heterogeneity and phenotypic alteration that often accompany cancerous growth. Taking melanomas as an example, as they expand they frequently lose one or more melanocytic differentiation antigens expression (Slingluff Jr, Colella *et al.* 2000), and C/T antigens are expressed in only a subset of patients. It therefore appears that no single antigen will be suitable for all melanomas, rather a broad immune response against multiple antigens would immunologically control such expansion. In addition, it has been hypothesised that the generation of efficient immune responses against an individual antigen could induce epitope spreading and subsequent activation of immune responses against other antigens (Slingluff 2011). This concept is currently implemented in various clinical trials. For example, one clinical study involves *in vitro* education of patients' stem T cells to recognise two C/T antigens (NY-ESO-1 and PRAME), WT1 and Survivin for treatment of patients with AML and MDS disease, followed by expansion and re-infusion of cells at least one-month post-allo-SCT (<https://www.clinicaltrials.gov/ct2/show/NCT02494167>).

Hence, having explored many advantageous features of HAGE and WT1 mono-vaccines, we were encouraged to try the combination strategies. However, one should consider an important issue which could negatively impact the development of multi-vaccines strategy, in that co-administration of peptides engaging the same MHC molecule could induce competitive inhibition of lower-MHC affinity peptides by higher-affinity peptides (Slingluff 2011). To overcome this, vaccines are often inoculated at different body sites (Powell, Rosenberg 2004) and/or the interval between vaccines administrations are optimised. Therefore, in this study, the interval between administering both ImmunoBody<sup>®</sup> vaccines into two different flanks was optimised by testing at least two instances: in the first setting both HAGE and WT1 vaccines were administered at the same day, whereas in the second setting mice were initially immunised using the HAGE vaccine then the WT1 vaccine two days later. Findings generated from the latter setting demonstrate a significant drop in HAGE immunogenicity whereas no significant decline in WT/P3 was noticed in this programme, indicating the probability of competitive inhibition of the HAGE peptides by the WT1. However, immunising on the same day appears to be the best combination with both vaccines working independently without significant competition. Therefore, this approach was applied for the future experiments.

Moreover, in cancer vaccine-based developmental studies, evaluating the effector function of T cells induced by vaccines, such as cytokine production, is important.

Consequently, several assays have been established to detect cytokine secretion from either bulk populations or at a single cell level. Taking advantage of the multi-parametric flow cytometry in simultaneous assessments of numerous cytokines or effector molecule expression per an individual cytokine/protein-secreting cell, we studied and compared the expression pattern of IFN- $\gamma$ , TNF- $\alpha$ , IL-2, granzyme B and Ki-67 (marker of proliferation) and CD107a (marker of cytolytic degranulation) from CD8<sup>+</sup> T populations derived from different ImmunoBody<sup>®</sup> vaccination programmes by flow cytometry using intracellular and cell surface staining. Keeping in mind that several factors could affect this type of assay, such as cell type, method and time of stimulation, type of protein transport inhibitors and finally the ways of cell fixation and permeabilisation.

Interestingly, levels of TNF- $\alpha$  and Ki-67 produced from CD8<sup>+</sup> cells in the immunised group were notably higher than those generated in the naïve group, but all ImmunoBody<sup>®</sup> vaccines delivered almost equal responses. However, CD107a and IFN- $\gamma$  are shown to be higher in the incorporated type of vaccines. These data indicate that all three vaccines were able to induce proliferation of CD8<sup>+</sup> T cells and secretion of TNF- $\alpha$ , IFN- $\gamma$ . However, the combined regime was able to induce a higher degree of degranulation and IFN- $\gamma$  secretion than the individual vaccines.

To further characterise the responses induced by ImmunoBody<sup>®</sup> vaccination regimes, the production of TNF- $\alpha$ , IFN- $\gamma$  and granzyme B per single live proliferating CD8<sup>+</sup> cells was assessed, in which, the respective markers were all gated on Ki-67<sup>+</sup> cells (proliferating CD8<sup>+</sup> cells). Interestingly, the staining illustrates an overall induction of CD8<sup>+</sup>TNF- $\alpha$ <sup>+</sup>, CD8<sup>+</sup>IFN- $\gamma$ <sup>+</sup> and CD8<sup>+</sup> granzyme B<sup>+</sup> T cells upon ImmunoBody<sup>®</sup> vaccination, among these cytokines, TNF- $\alpha$  and IFN- $\gamma$ <sup>+</sup> show an obvious enhancement upon vaccines incorporation.

The aim of cancer immunotherapy is to induce long-lasting specific memory responses of the adaptive arm of immune response for durable tumour regression and subsequent possible cure (Disis 2014). Therefore, antibodies against CD62L and CD44 molecules, known to be able to distinguish between naïve, effector and memory cells were also used. Naïve T cells are known to express the CD62L homing receptor, and that its level reduces upon encountering antigen, while at the same time cells acquire CD44 expression. This phenomenon was confirmed in mice which have been immunised, in which the predominant phenotype of CD8<sup>+</sup> cells was CD62L<sup>low</sup>CD44<sup>high</sup>, a typical effector/memory phenotype. The CD62L<sup>low</sup>CD44<sup>high</sup> population was found in abundance following immunisation with all three ImmunoBody<sup>®</sup> vaccines in comparison to the naïve, and the lowest expression was induced by the HAGE-vaccine which was further increased when combined with the WT1-vaccine, suggesting that the combined vaccines induce a higher number of memory cells during the course of

immunisation, which might provide long-lasting immune response. However, one would need to re-assess these markers after a longer period of time to be able to firmly establish this.

In addition, markers associated with dysfunctional T cells were studied. This is because it has been reported that T cells could undergo a state of exhaustion/dysfunction in the context of chronic antigen exposure, such as in chronic viral infections and cancer, wherein the T cells exhibit notable defective proliferative capacities and decline in the cytokine producibility, however, these cells are not entirely inert and could exert lytic functions (Zarour 2016). Importantly, the exhausted T cells undergo typical phenotypical changes in the form of upregulation of various inhibitory receptors, such as CTLA-4 and PD1 receptors, which can inhibit/suppress the immune responses upon binding with their ligands expressed on tumour cells and APCs. Targeting such molecules is nowadays a hotspot topic since it has been found that immune checkpoint inhibitors successfully reinvigorate tumour-infiltrating T lymphocytes and can induce durable clinical benefits to a significant number of patients suffering from advanced cancer (Zarour 2016) which were until then incurable. This big success of the cancer immunotherapy fostered the development of combinatorial strategies to target numerous mechanisms by which cancer induced T cell dysfunction. Therefore, the influence of our ImmunoBody® vaccines on the expression of a comprehensive number of cell surface costimulatory and inhibitory markers by CTLs were assessed. GITR and OX-40 as a representative of the activation markers and the inhibitory molecules CTLA-4, LAG-3, Tim-3 and PD-1. PD-1 is significantly overexpressed by T cells that are derived from HAGE- and WT1-ImmunoBody® vaccines, indicating a state of T cell exhaustion, although additional markers would be required to confirm this since PD1 on its own is not sufficient to make such a statement. Taken together, these findings have shed some light on the necessity to incorporate immune checkpoint blockades to the ImmunoBody® vaccines to reinvigorate the exhausted T cells in our future *in vivo* tumour model experiments.

## 4.5 Conclusion and chapter impacts

The HAGE 30-mer and the WT1 15-mer long peptides were found to have several predicted MHC class I and class II peptides binders. The binding affinity and the off-rate were assessed for all HLA-A2 predicted peptides. HAGE/P5, HAGE/P6 and the WT1/P3 were confirmed as strong binders. They were found associated with high frequency and avidity T cell immune responses, and strong effector and memory function. We have also found that our vaccines induced PD-1 expression on T cells surface, a marker of both stimulation and T cell exhaustion.

## 5 Chapter V: Target cell preparation

The previous chapter demonstrated that both HAGE- and WT1-ImmunBody® vaccines generated T cells capable to producing high level of IFN- $\gamma$  and that they could be injected together without inducing immunodominance. In order to assess whether the vaccine-induced T cells can recognise cancer cells in an antigen and HLA-A-restricted manner an appropriate cell need to be produced. This chapter will explain how this has been achieved.

### 5.1 Introduction

#### 5.1.1 Immortalised haematopoietic cell lines

It is very important to provide an appropriate *in vitro* model system in order to demonstrate the efficacy of the vaccines before going into *in vivo* model and later to the clinic. In general, primary cell cultures have a finite number of cell cycles which limits their lifespan, indeed after a certain number of proliferation cycles, they undergo senescence and death, whereas the immortalised cell lines, continuous cell lines, are able to establish an indefinite proliferation and division in cell cultures (Kaur, Dufour 2012). In CML-related research, the Philadelphia positive haematopoietic cell lines offer a basic platform to assess the molecular events of CML and assess drug efficacy, adding to delivering indefinite source of cellular material for many *in vitro* assays. They are also cost effective and easy to manipulate. More interestingly, these cells provide consistent and reproducible results because they are originally generated from pure genetically identical population of cells. However, data obtained from these cells should be utilised with caution for the reasons that they typically derived from patients in blast crisis and mutations are often there. Nonetheless, immortalised haematopoietic cell lines are commonly utilised in early-stage research prior to the preclinical trials and their utility should not be undervalued (Clarke, Holyoake 2017). It has been reported that the vast majority of haematologic cell lines including CML retain their main pathways even after frequent passaging. For instance, Andersson, Eden *et al.* in 2005 reported that the majority of the 40 haematologic cell lines they studied kept their molecular and clinical subtypes of origin regardless of their diverse origin and frequent passages *in vitro*. This finding indicates their validity and therefore justifies their usage (Andersson, Edén *et al.* 2005).

Before any cancer vaccine can be used in a phase 0/I trial, it is vital to demonstrate that vaccine-induced T cells can recognise and kill targets in an antigen and HLA-restricted manner. It has been reported that killing of antigen-bearing cells by specific

T effector cells could be highly influenced by the density of antigen expressed by that targets (Velders, *et al.* 1998), and accordingly transfection would artificially induce high expression of the gene transfected which would not be physiologically relevant. However, it is not always possible to find cells expressing both the relevant antigen and the relevant HLA haplotype. In addition, genetic manipulations allow researchers to create all the necessary controls to ensure that T cell recognition is both antigen- and HLA-specific.

### **5.1.2 Establishment of genetically modified cell lines**

Transfection is defined as a process by which genetic materials (DNAs/RNAs) are introduced into target cells for either long term (stable transfection) or short term (transient transfection) depending on the experiment requirements (Recillas-Targa 2006). Transfection is mainly used to study a particular gene function and or gene products, by boosting or constraining specific gene expression in target cells (Wurm 2004). In the stable transfection, the nucleic acid integrates into the host genome and remains there even after host cell divisions (Glover, Lipps *et al.* 2005), whereas in the transient transfection, the genetic materials neither integrated into the host genome nor sustained the expression of the gene for a long period of time (Recillas-Targa 2006). With the recent technology, various approaches have been adopted, and the selection of the appropriate method depends principally on cell type and the purpose of transfection. Technically, the ideal method should be associated with minimal cell toxicity, high transfection efficiency, low effects on cell physiology, and easy to perform (Kim, T. K., Eberwine 2010). In general, methods are broadly categorised into biological, chemical, and physical approaches. The biological approach (using a virus as a genomic vehicle) is the most popular technique because of its high efficiency rate and its simplicity to produce sustainable transgene expression. The virus DNA integrates into the host genome, resulting in transmission of this DNA into daughter cells, which could permit sustainable transgene expression (Kim, T. K., Eberwine 2010). In the chemical transfection, however, chemicals are used to introduce the gene of interest into mammalian cells, such as cationic polymer, calcium phosphate, cationic lipid and cationic amino acid (Schenborn, Goiffon 2000, Washbourne, McAllister 2002, Holmen, Vanbrocklin *et al.* 1995). The general principle involves the formation of complexes between the positively charged chemicals and the negatively charged nucleic acids. These complexes then pass the cell membrane and deliver the plasmid construct to the nucleus. The most recent method is the physical transfection whereby diverse physical tools are used to directly deliver nucleic acids into the cytoplasm or nucleus, such as direct micro-injection, electroporation, and laser-based transfection (Mehier-Humbert, Guy 2005).

In this project, the main purpose of the transfection was to generate various cell lines expressing the correct antigens and the correct HLA haplotype and the controls necessary to prove that specificity of the vaccine-induced T cells. This was achieved by enhancing or constraining the expression of the cognate genes in leukaemic cell suspension targets (known for their resistance to transfection) by knock-in and knockdown assays, respectively. The modified cells were then used (in the next chapter) to assess the cytotoxicity of T cells derived from the candidate vaccines. IFN- $\gamma$  production is one of the commonest indicators of immune response. Therefore, it is important to provide some understanding related to its contribution on the immune system, as it will be shown in the following section.

### **5.1.3 IFN- $\gamma$ role in cancer immunoediting: From immune-surveillance to immune evasion**

Cancer immune-surveillance has been often described as an important defence process by which carcinogenesis can be inhibited and cellular homeostasis could be maintained (Kim, R., Emi *et al.* 2007). The concept was first proposed by Ehrlich in 1909, however, experimental evidence for the potential involvement of the immune system in tumour regression came from tumour transplantation models by Burnet and Thomas in the mid-20<sup>th</sup> century (Burnet 1957). In the late 1990s, the idea became widely accepted, when experimental animal models were developed, such as knockout mice model. Castello, Gastaut *et al.* in 1999, for example, point out several lines of evidence demonstrating the role of immune system in tumour elimination at the clinical level, then many other reports concluded that immune-surveillance does certainly exist (Kim, R., Emi *et al.* 2007). In this framework, three phases (designated as three **E**'s) of host- tumour cells interactions have been proposed in a process called "cancer immunoediting ". The initial phase involves efficient eradication of the nascently transformed cells by the immune effector cells derived from the innate and the adaptive immune responses, known as "**E**limination phase". However, cancerous cells might enter the "**E**quilibrium phase" where immune sculpting is induced by immune selection due to the effect of immuno-editors resulting in the development of foci of tumour variants that have acquired dangerous mutations reducing their immunogenicity, such as down regulation of MHC molecules and resistance to effector cell killing. When such tumour variants grow and become clinically detectable, a hostile immunosuppressive network in the tumour microenvironment has been established. The fast-accumulated events of immunosuppressive influences make it difficult indeed to provoke an efficient immune response to either stop or eliminate cancer progression. This detrimental phase of invasion is called "**E**scape/**E**vasion phase", during which malignant growths usually evolve mechanisms thereby deceive T cells and sooner or later escape immune destruction (Stewart, Abrams 2008a).

Examples of immune evasion strategies adopted by tumour cells include; i) capability of malignant cells to downregulate the expression of MHC molecules which are necessary to display the tumour antigens to T cells, ii) secretion of inhibitory molecules by tumour tissues, such as IDO and immuno-suppressive/immuno-regulating cytokines, such as IL-4, IL-5, IL-6, IL-10, IL-13 and transforming growth factor-beta, iii) regional recruitment of immunosuppressor cells, such as Tregs and MDSCs. iv) dysregulation of T cell checkpoint pathways, including sending inhibitory signals to the activated T cells by upregulation of PD-L1 expression causing T cell death (Davies 2014). This inversed correlation is depicted in the triangular *versus* inverted triangular in Figure 5.1 shown below.

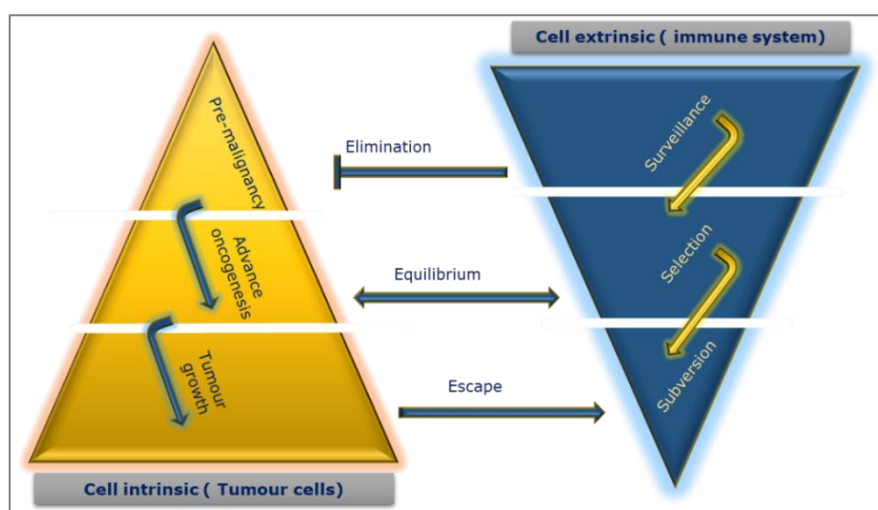


**Figure 5.1: Schematic representation depicts three phases of immunoeediting process.**

Elimination, equilibrium, and escape are three phases involved in crosstalk between tumour growth and immune system defence. Overall, carcinogenesis is a multistep process resulting from crosstalk of malignant cell and host immune system. In the elimination phase, the immune system in its maximum activity and hence can effectively recognise and eradicate malignantly transformed cells. In the equilibrium phase, the cancerous cells develop genetic alterations whereby immune cells cannot restrict tumour growth. At this stage, the tumour cells select and maintain the less immunogenic variants. With expansion of these clones, the oncogenesis process will be strongly intensified while the immune-surveillance quickly dropped down, a state where the immune system become unable to recognise or effectively kill tumour cell due to the development of various escape mechanisms that tumour can adapt to circumvent the immune-surveillance. This stage is called the 'escape' phase. The yellow pyramid indicates tumour expansion, whereas the blue inverted pyramid indicates immune system deterioration. Permission from Springer Nature is obtained to adapt this image with a reference from (Zitvogel *et al*, 2006).

IFN- $\gamma$  is a cytokine molecule, known for its cytotoxic effect and anti-tumour activity during both the innate and cell-mediated immune responses (Farrar, Schreiber 1993). In spite of ample evidence that substantiates the role of IFN- $\gamma$  in tumour immune-surveillance and recent successful achievements in the field of cancer immuno-therapies, such as re-invigoration of anti-tumour immunity with immune-checkpoint inhibitors or autologous tumour-infiltrating lymphocytes (TILs)/ adoptive transfer of chimeric antigen receptor (CAR) T cells (Mojic, Takeda *et al*. 2017), there

has been a steady flow of observations showing its possible pro-tumorigenic role under special circumstances (Zaidi, M. R., Merlino 2011) due to a large percentage of resistance to immunotherapy and cases of relapse. Arguments have blamed the prolonged presence of IFN- $\gamma$  in the tumour microenvironment during the equilibrium phase for the failure of eradication of tumour cells, and instead, it generates tumour variants with more carcinogenic potentials that could negatively impact the process of immune-surveillance. Therefore, some studies have proposed that IFN- $\gamma$  blockade could inhibit the establishment of an immunosuppressive milieu or suppress IFN- $\gamma$ -induced genetic changes in tumour cells. However, premature inhibition of IFN- $\gamma$  might hinder the generation of an effective anti-tumour response. That is why an extensive future work is required to understand such complex paradoxical pro- and anti-tumour roles of IFN- $\gamma$ . By boosting its advantageous anti-tumour activity alongside with reducing pro-tumour effects, IFN- $\gamma$  could participate in establishing promising immunotherapy against cancer. Therefore, it is worth studying the immunomodulatory aspects of IFN- $\gamma$  on CML cell lines chosen herein to be used as targets for cytotoxicity assays, because successful vaccine-induced T cells will produce high level of IFN- $\gamma$  in response to the TCR/peptide-MHC engagement.

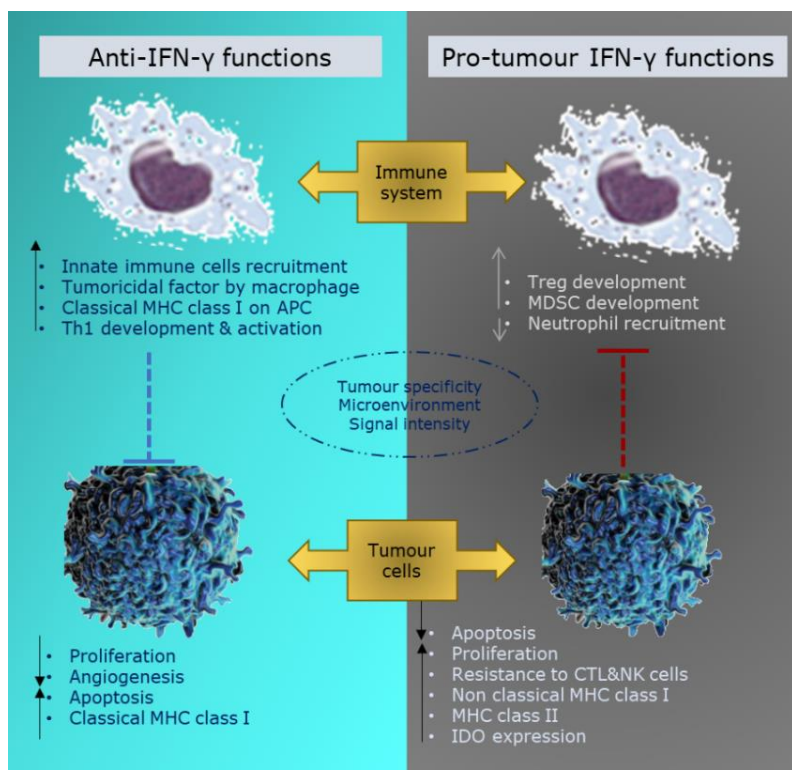


**Figure 5.2: Immunomodulatory roles of IFN- $\gamma$ .**

IFN- $\gamma$  shows evidence of dual contradictory functions, pro- and anti-tumour. Under both scenarios, IFN- $\gamma$  affects the cancerous cells directly as well as indirectly by manipulating the cells of the immune system. The anti-tumour effects result in direct inhibition of tumour cell growth, and recognition and elimination of the tumour cells. The pro-tumorigenic effects, on the other hand, include promoting proliferative and anti-apoptotic signals, and tumour escape from CTLs and NK cells. Idea adapted from American Association of Cancer Research, 2011.

### 5.1.3.1 Effect of IFN- $\gamma$ on the expression of HLA molecules on tumour cells

As it is well-known, there are two main MHC molecules that have a fundamental role in modulation of immune responses: the MHC class I and the MHC class II molecules. The MHC class II molecules play a vital role in the regulation of immune process by presenting peptides that have primarily originated from processed extracellular antigens to CD4<sup>+</sup> T cells (Mach, Steimle *et al.* 1996, van den Elsen, Peter J, Gobin *et al.* 1998). Classically, there are three types of MHC class II molecules; HLA-DP, HLA-DQ, and HLA-DR, each of which is a form of 2 $\alpha$  and 2 $\beta$  chains (Ting, Trowsdale 2002). Interestingly, it has been found that even though they are constitutively displayed on the professional APCs, such as DCs, monocytes/macrophages and B cells, their expression can be triggered by IFN- $\gamma$  in the majority of cells (Mach, Steimle *et al.* 1996, Boss 1997, Reith, Mach 2001).

MHC class I, on the other hand, is allocated into two main groups of molecules; MHC class Ia (classical) and MHC class Ib (non-classical), both of which are expressed at the cell surface in combination with  $\beta$ 2m. In humans, MHC class Ia molecules are subdivided into HLA-A, HLA-B, and HLA-C (Bjorkman, Parham 1990, Rodgers, Cook 2005). HLA-class Ia molecules represent the main players in adaptive immunity against viruses and transformed cells through their direct interaction with TCR and with the CD8 co-receptor on CTLs surface (Braciale 1992). HLA-class Ia molecules can also interact with NK cells through killer Inhibitory Receptors (KIRs), thereby controlling NK cell functions (Moretta, Bottino *et al.* 2001). It has been confirmed that one of the well-established functions of IFN- $\gamma$  in the context of cell mediate immunity is upregulation of MHC class I molecules to aid antigen priming and presentation to the APCs (Zaidi, M. R., Merlino 2011).

Although the best characterised HLA class Ib family members are non-classical HLA-E and HLA-G molecules, it also includes less characterised members, such as HLA-F and HLA-H. In contrast to HLA class Ia, HLA class Ib are characterised by low genetic diversity due to a limited polymorphism and few alleles control the production of a small number of proteins (<http://hla.alleles.org/nomenclature/stats.html>). There are seven different isoforms of HLA-G produced by alternative splicing of the same primary mRNA. Namely; HLA-G1, -G2, -G3, and -G4 isomers are membrane-bound molecules and HLA-G5, -G6, and -G7 isoforms are released as soluble molecules (Pistoia, Morandi *et al.* 2007). Similarly, HLA-E can be expressed as membrane bound and/or soluble isoforms. Observations proved that both HLA-G and HLA-E have immunomodulatory function on the immune system by engagement with specific inhibitory receptors expressed on various immune effector cells (Le Bouteiller,

Lenfant 1996). It has been reported that these molecules are overexpressed by a variety of malignant cells and they are potential biomarkers of poor prognosis (Kochan, Escors *et al.* 2013). Interestingly, upregulation of HLA-G and HLA-E following IFN- $\gamma$  treatment indicates that they might carry potentially pro-inflammatory responses. Despite the fact that the inflammatory responses are necessary to eradicate tumour cells, they also prompt strong immunoregulatory mechanisms that could impair the immune system and hence favour tumour development, such as the recruitment of the immunosuppressive Tregs and MDSCs. Additionally, non-classical MHC class I molecules could adopt other strategies which enable tumour cells to bypass immune-surveillance. These molecules can arrest the immune response by ligating to inhibitory receptors expressed by effector cells (Contini, Ghio *et al.* 2003, Contini, Ghio *et al.* 2000). For instance, Paul and collaborators reported that HLA-G plays a notable role in defending malignant cells from the cytotoxic effect of NK cells and cytotoxic T lymphocytes by its ligation to Leukocyte Immunoglobulin-Like Receptor (LILRB1, best known as ILT-2) (Contini, Ghio *et al.* 2003, Rouas-Freiss, Moreau *et al.* 2005). HLA-G can also exert immunosuppression by inducing a Th2 cytokine profile, by stimulating the release of IL-3, IL-4, and IL-10, and down-regulating IFN secretion by T cells (Rouas-Freiss, Moreau *et al.* 2005). Moreover, HLA-G has been shown to stimulate the inhibitory HLA-E molecule, thereby favouring tumour cell escape from immune-surveillance through ligation to the inhibitory CD94/NKG2A receptor expressed by NK cells and CTLs (Braud, Allan *et al.* 1998).

Other MHC related molecules that have gained a particular area of interest by researchers are the costimulatory MHC class I chain-related genes A (MICA) and B (MICB). They are located on chromosome 6 close to HLA-B as shown in Figure 5.3. They have been described as a stress marker of the cells because their expression is induced by viral infection, inflammation, heat and DNA damage (Özlü, Akçalı *et al.* 2017). Although they are structurally similar to HLA class I, they neither bind peptides nor engage with TCR, they instead engage with NKG2D activating receptor expressed by NK cells and certain T cells. As a consequence, upregulation of MICA/MICB expression induces tumour cell killing by these cells (Santoni, Zingoni *et al.* 2007). However, a part of immune evasion mechanism, studies have found that some tumour cells have autoregulatory mechanisms by which they can simultaneously upregulate the expression of MICA/MICB and their ligand NKG2D on the tumour surface resulting in a strong proliferative response of the malignant cells upon such binding (Weiss-Steider, Soto-Cruz *et al.* 2011).

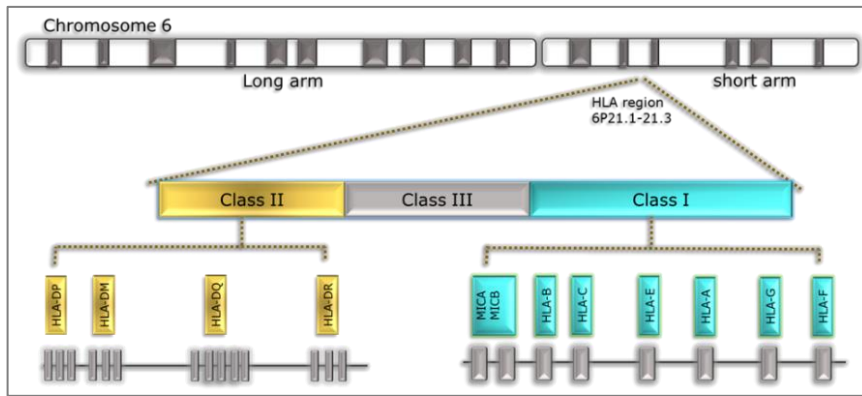


**Figure 5.3: Gene map of human HLA with especial emphasis of class I and class II molecules on chromosome 6.**

The figure illustrates three main classes of HLA molecules which are located on the short arm of chromosome 6. MICA/MICB are located close to HLA-B and HLA-C locus whereas HLA-A allele located in between HLA-E and HLA-G loci.

### 5.1.3.2 Effect of IFN- $\gamma$ on the expression of the costimulatory molecules CD80, CD86 and CD40 on tumour cells

The generation of functionally activated T cells requires not only the binding of TCR with specific peptides-MHC complex on APCs, but also synchronising with proper ligation of cell surface accessory molecules. Among the best-established co-stimulation molecule system are binding of B7 family members (CD80 and CD86) with CD28/CTLA-4 and CD40 with CD40 ligand (CD40L) (Yin, Zhang *et al.* 1999).

CD80 (B7-1) and CD86 (B7-2) molecules are members of the immunoglobulin superfamily expressed on APCs (Freeman, Gribben *et al.* 1993). They deliver critical co-stimulatory signals for T cells via interactions with the T cell receptors CD28 and CTLA-4 (Lenschow, Walunas *et al.* 1996). Studies reported that these ligands shared receptors that have contradictory functions, i.e. engagement of either CD80 or CD86 to the CD28 receptor produced a costimulatory signal thereby triggering T cell proliferation and IL-2 production (Lenschow, Walunas *et al.* 1996), whereas binding to CTLA-4 exerts an inhibitory signal causing T cell anergy (Krummel, Allison 1995). It has been speculated that a paucity of B7 costimulatory molecules create a state of T cell anergy resulting from the absence of the particular signal, thereby enabling cancer cells to escape immune-surveillance (Chang, Chang *et al.* 2007).

Similarly, the activation of the costimulatory CD40, a member of the tumour necrosis factor (TNF) receptor superfamily, was shown to be vital for T cell activation and also for B cell proliferation and differentiation (Lane 1995). It has been noticed that engagement of CD40 on APCs with CD40L expressed by T cells boosts the expression of MHC and costimulatory molecules on APCs, triggers the synthesis of pro-inflammatory cytokines, and leads to the activation of T cells (Grewal, Flavell 1998).

In addition, an *in vivo* study has demonstrated that engagement of CD40 on tumour cells inhibits the growth of solid tumours and advance B-cell lymphoma lines, causing regression of tumours (Funakoshi, Longo *et al.* 1994). Hence, the lack of CD40 expression by cancerous cells might favour tumour escape from activated T cells expressing CD40 ligand. Moreover, Van Mierlo and colleagues in 2002 demonstrated that systemic administration of anti-CD40 agonistic antibodies into tumour-bearing mice leads to eradication of tumour upon the activation of specific CD8<sup>+</sup> T cells (van Mierlo, den Boer *et al.* 2002). Recently, there has been a plethora of pre-clinical observations that provide a basis of distinct strategies to use CD40 agonists in the area of cancer immunotherapy, details are provided in a review by Beatty (Beatty, Li *et al.* 2017).

### **5.1.3.3 Effect of IFN- $\gamma$ on the expression of the inhibitory molecules FasL, PD-L1 and IDO1 on tumour cells**

FasL CD178 (CD95L) is type II glycoprotein belonging to the TNF superfamily and is widely expressed on activated T lymphocytes, NK cells and B cells. Ligation of FasL expressed by immune cells to Fas (CD95) expressed by tumour cells inducing their death by apoptosis. This is one mechanism employed by cancer cells to elude immune attack. Thereby, TILs infiltrating into the tumour bed would undergo programmed cell death when they come into contact with tumour cells expressing FasL (Chappell, Restifo 1998). In addition, it has been found that activation of T cells through TCR after encountering tumour cells induces an upregulation of FasL resulting in self T cell killing (T cell suicide) in a classical negative feedback loop (Daniel, Kroidl *et al.* 1997). Studies have confirmed that IFN- $\gamma$  can induce tumour cell apoptosis in general, by triggering the expression of Fas receptor (Akiyama, Ino *et al.* 2003) and it can also induce apoptosis in K562 cells, in particular by simultaneously elevating Fas and FasL protein expression (Xia, Li *et al.* 2017).

Programmed cell death ligand 1 (PD-L1), also called (B7-H1 or CD274), is a transmembrane protein member of the B7 family. Recently, it has gained a particular interest because of evidence demonstrating its over expression in various types of tumours, in addition to the strong correlation of its overexpression to cancer grades and stages (Wilmotte, Burkhardt *et al.* 2005). PD-L1 upregulation, which can be induced by exposure to IFN- $\gamma$ , conveys inhibitory signals via the PD-1 receptor on T cells, this could facilitate tumour escape from immune-surveillance (Dong, Strome *et al.* 2002). Targeting this signalling pathway, therefore, is of critical importance for the clinical development of immune checkpoint blockade therapies (Garcia-Diaz, Shin *et al.* 2017).

Another inhibitory molecule that can be induced by IFN- $\gamma$  is IDO. It is an intracellular enzyme, and can present into two types, IDO1 and IDO2. The latter is expressed by a small subset of tissue and has a lower enzymatic activity than the former and it has less clear function in malignancy (Ball, Sanchez-Perez *et al.* 2007, Prendergast, Metz *et al.* 2014, Metz, Duhadaway *et al.* 2007). Another important difference is that while IDO1 is strongly upregulated upon treatment with IFN- $\gamma$ , IDO2 shows a weak response to IFN- $\gamma$  (Munn, Mellor 2016). In recent years, IDO1 has gained considerable attention because of its immunosuppressive activity that contribute essentially to tumor escape and progression (Lob, Konigsrainer *et al.* 2008). The general concept proposes that malignant cells or myeloid cells express high levels of IDO1 in the tumor microenvironment (Platten, von Knebel Doeberitz *et al.* 2015), which in turn cleaves the amino acid "L-tryptophan" into N-Formyl kynurenine and serotonin, hence, resulting in a local depletion of L-tryptophan and the accumulation of L-tryptophan degradation products called "kynurenines" in the tumor milieu (Mbongue, Nicholas *et al.* 2015). Under these starving conditions, T cells, for which L-tryptophan is an essential amino-acid, are stressed, and then a stress response signal is induced via uncharged tRNAs which in turn activates the kinase general control non-depressible 2 (GCN2) resulting in cell cycle arrest and death (Munn, Sharma *et al.* 2005b). Besides that, activation of GCN2 favours *de novo* Tregs differentiation and activation, leading to highly immunosuppressive microenvironment. In addition, kynurenines activate the transcription of the Aryl Hydrocarbon Receptor (AHR). Through the AHR, kynurenine metabolites promote the differentiation of Tregs and suppression of anti-tumour immune responses (Thaker, Rao *et al.* 2013). Figure 5.4 shows a simple diagram representing the inhibitory contribution of IDO1 on the immune system.

IDO upregulation has been detected in many solid malignancies and in AML (Curti, Pandolfi *et al.* 2007, Uyttenhove, Pilotte *et al.* 2003). In these cancer, IFN- $\gamma$  has been considered to be the primary cytokine stimulus driving IDO expression (Folgiero, Goffredo *et al.* 2014, Iachininoto, Nuzzolo *et al.* 2013, Takikawa, Kuroiwa *et al.* 1988). Hence, and from a clinical standpoint, IDO1 expression is associated with a significant poor prognosis, and therefore, it has been already targeted in clinical trials, with the aim to overcome cancer-induced immunosuppression.

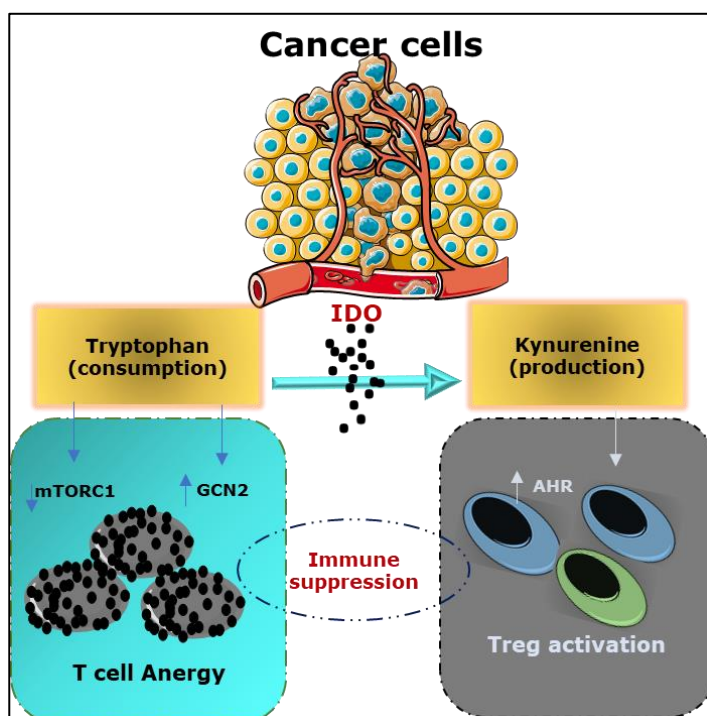


**Figure 5.4 The inhibitory role of IDO1 on the immune system.**

By cleaving the aromatic indole ring of L-tryptophan by the enzyme IDO1, a variety of kynurenines are produced. Consequently, IDO1 causes L-tryptophan deficiency, which results in inhibition of mTORC1 and activation of GCN2, in turn leading to T cells anergy. On the other arm of equation, Tryptophan's consumption leads to production of kynurenine compounds, and consequent AHR stimulation, a transcription factor that promotes Tregs differentiation. Overall, the effects of IDO1 enzyme on both sides of equation favours immunosuppressive environment and provides a basis for tumour escape from immune-surveillance.

## 5.2 Rationale of the chapter

1. To induce or inhibit the expression of HAGE and WT1 proteins in the CML cell lines by either knock-in or knock-down, respectively, so that they can be used as targets for vaccine-induced T cells in *in vitro* cytotoxicity assays (Chapter-6).
2. To confirm the expression of HAGE, WT1, HHDII (chimeric HLA-A2) and HLA-DR1 proteins in the humanised B16 ( $hB16/HAGE^+/Luc^+$  cells) prior to *in vivo* tumour model (Chapter-7).
3. To investigate the capacity of IFN- $\gamma$  to influence the sensitivity of the CML cell lines to T cell-mediated cytotoxicity.

## 5.3 Results

### 5.3.1 Evaluation of HAGE and WT1 expression by the respective targets

As part of screening of CML cell lines for the candidate genes (Chapter-3), the constitutive expression of HAGE and WT1 at the mRNA and protein level were determined in the respective targets using RT-qPCR and Western blotting. As a reminder, these findings are summarised in Figure 5.5. Bar graph in Figure 5.5A illustrates the level of HAGE natural expression by the three targets at mRNA level. It is clear that TCC-S cells express HAGE at a much higher level than KCL-22 and K562 cells. These findings were further confirmed by Western blot analysis, which confirms that TCC-S cells are expressing HAGE at protein level (as reflected by dense band signal), whereas no HAGE expression could be detected in KCL-22 or K562 cells. WT1, on the other hand, is shown to be constitutively expressed by all these targets at mRNA and protein levels (Figure 5.5B).

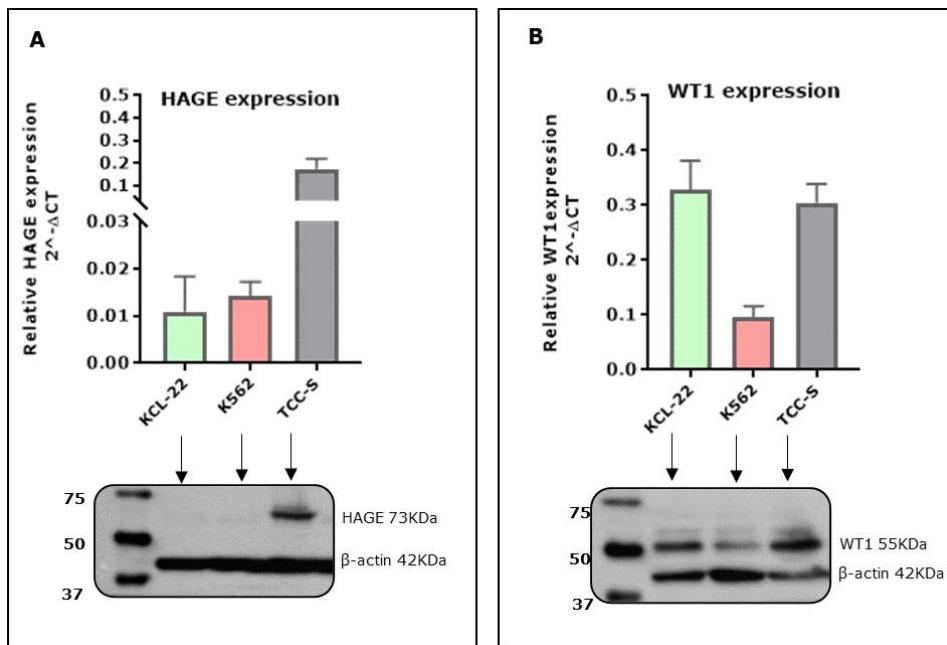


**Figure 5.5: Constitutive expression of HAGE and WT1 in target cells using RT-qPCR and Western blot.**

**(A)** HAGE expression at the mRNA and protein levels using RT-qPCR and Western blot. HAGE is expressed at low levels at the mRNA level by KCL-22 and K562, but not at protein level. In contrast, TCC-S cells constitutively express high levels of HAGE at the mRNA and protein levels. **(B)** WT1 is expressed by all cells studied at both mRNA and protein levels. Values of PCR are expressed as the mean  $\pm$  SD of three independent experiments. The doublet on WT1 in the Western blot might represent WT1 isoforms resulting from an alternative splicing event.

Taking advantage of the availability of a WT1 antibody used for Western blot but is also valid for flow cytometry, target cells were fixed, permeabilised and stained with rabbit anti-WT1 primary antibody followed by goat anti-rabbit IgG for another 30 minutes, and samples were then run on the Beckman Coulter Gallios™ flow cytometer. As shown in Figure 5.6, WT1 is expressed at 96.67% by KCL-22 cells, 97.87% by TCC-S cells and 90.04% by K562 cells in comparison to un-stained samples. These are consistent with relative gene expression obtained from the RT-qPCR and Western blot.

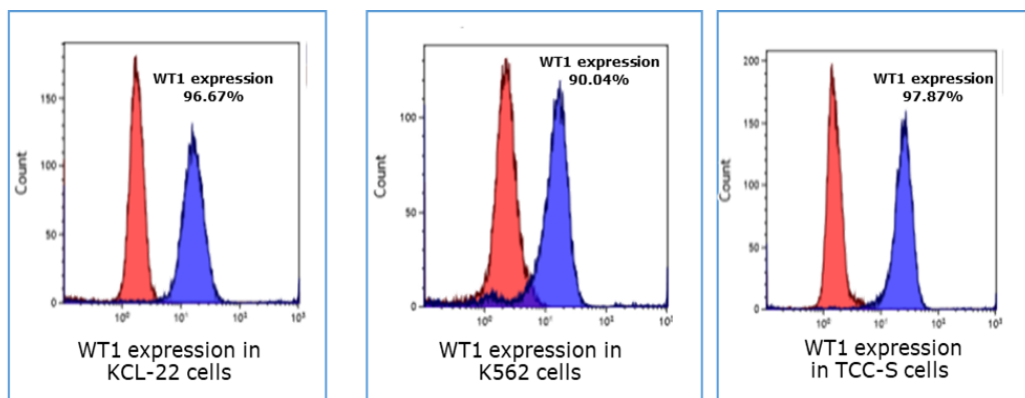


**Figure 5.6: Intracellular staining to detect WT1 expression in targets using flow cytometer.**

Overlay histograms show the percentage of WT1 expression in the considered CML targets. Cells were fixed with fixative solution prepared from [Foxp3 staining buffer set] in dilution of 1 part of concentrate /3 parts diluent, permeabilised by permeabilisation buffer for 10 minutes and stained with rabbit anti-WT antibody for 30 minutes. Secondary antibody [Alex Fluor™ 488-conjugated goat anti-rabbit IgG] were then added at 1:200 dilution and cells were incubated for 30 minutes. Red histograms refer to the control/unstained cells as negative controls whereas blue histograms represent the stained cells. Results thus confirm the natural expression of WT1 by targets chosen. n=2.

In summary, TCC-S cells express both HAGE and WT1, whereas KCL-22 and K562 cells express only WT1. Accordingly, these cells were chosen for further gene modifications in order to be targets for future proposed *in vitro* cytotoxicity studies.

### 5.3.2 Phenotypic analysis of the respective targets

K562, KCL-22 and TCC-S cells were stained for phenotypical characterisation using flow cytometry, as it was mentioned in the methodology ([Section:2.2.8.1](#)). Histograms in Figure 5.7B illustrate the percentage of HLA-A2 surface expression in these cells in comparison to non-stained samples taken from the candidate cell lines as negative controls, wherein, results demonstrates that only a small percentage of K562 cells expressed HLA-A2, whereas high percentages of KCL-22 and TCC-S cells were positive. Furthermore, these cells were assessed for the surface expression of

HLA-DR, Figure 5.7C indicates that there was no HLA-DR1 expression in comparison with non-stained sample could be detected.

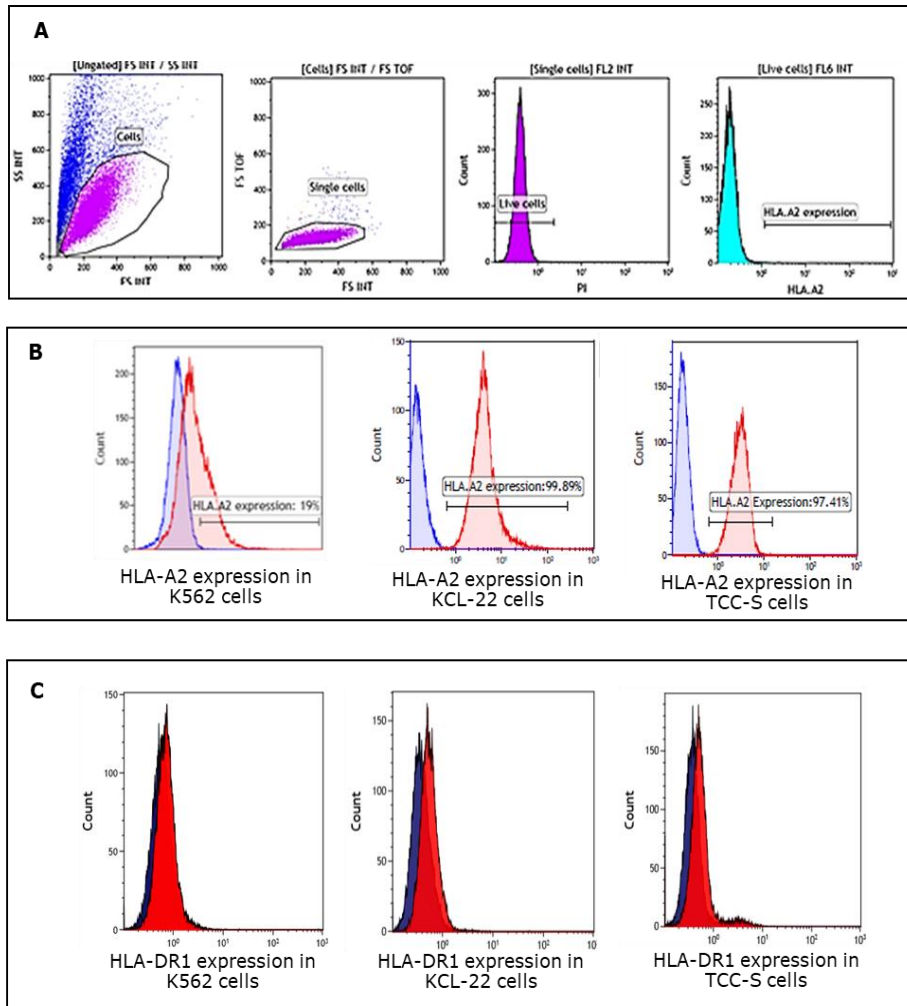


**Figure 5.7: Surface expression of HLA-A2 and HLA-DR1 on targets, as assessed by flow cytometer.**

**(A)** Representative gating strategy used in this type of analysis. Live cells were first gated according to their Side Scatter and Forward Scatter profile, and then single cells were selected, leaving out the doublets, the level of surface HLA-A2 and HLA-DR1 expression were determined on basis of fluorescence intensity depicted by a shift to the right of the histogram in comparison to unstained samples. **(B)** Overlay histograms illustrate HLA-A2 surface expression in comparison to negative controls (non-stained samples). **(C)** Overlay histograms illustrate HLA-DR1 surface expression in the candidate cells in comparison to negative controls (non-stained sample), n=2.

In summary, KCL-22 and TCC-S were confirmed to be HLA-DR1 negative and HLA-A2 positive, whereas K562 cells are negative for both HLA-DR1 and HLA-A2. Since K562 cells do not express HLA-A2, it was transfected with the chimeric HLA-A2 plasmid (HHDII) gene to be a suitable target for T cells derived from HHDII/DR1 mice (details in the following section).

### 5.3.3 Generation of K562/HHDII<sup>+</sup>/HAGE<sup>+</sup> cells

#### 5.3.3.1 Transfection of K562 cells with the HHDII gene, and clone selection

Since K562 cells were shown to be negative for the expression of HLA-A2, they were transfected with the chimeric HLA-A2 gene (HHDII) in order to be a suitable target for vaccine-induced T cells from immunised HHDII/DR1 mice. The PcDNA-3.1/HHDII construct was designed to carry the antibiotic G418 as a marker of selection to maintain HHDII gene. As transfection of cells in suspension is known to be difficult, and hence several methods were used. Lipofectamine-based transfection (Lipofectamine® LTX and PLUS™ Reagent / Invitrogen) was first tried and the results showed low level of transfection efficiency. Thereafter, the electroporation technique was tried using the SF cell line 4D nucleofection TM X kit / Amaxa, Programme T-016. Post transfection, cells were selected using G418 at 2mg/mL, a concentration that was found to kill all parental, non-transfected cells, within 3 weeks, as mentioned in the methodology ([Section:2.2.2.1](#)), Cells that survived the antibiotic selection were assessed for HHDII expression using an antibody against  $\beta$ 2m (a key component of MHC class I molecule stability) and assessed by flow cytometer. Overlay graphs in Figure 5.8 demonstrate a comparison in the percentages of the outcome between the two transfection methods. It clearly shows that electroporation is much more efficient than lipofectamine with 71% compare to 14%, respectively.

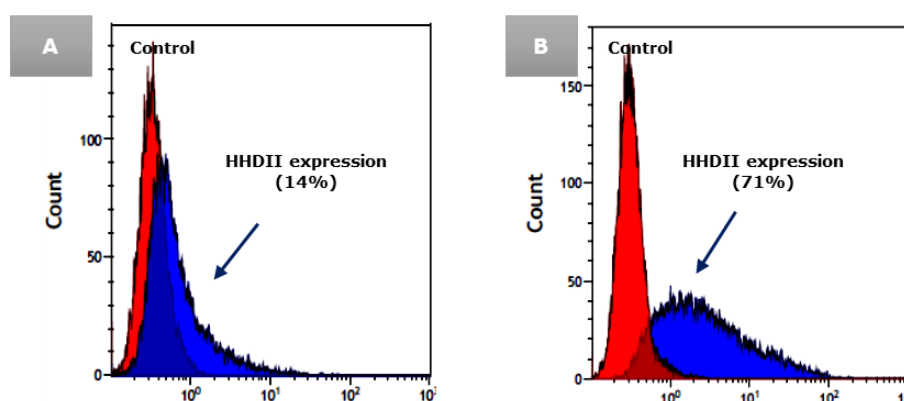


**Figure 5.8: Transfection efficiency of HHDII<sup>+</sup> gene in K562 cells using lipofectamine reagent versus electroporation, as assessed by flow cytometry.**

Red histograms represent parental non-transfected K562 cells, whereas blue histograms represents transfected cells. Results demonstrate high percentage of K562/HHDII<sup>+</sup> cells produced by electroporation in comparison with lipofectamine, at 71% versus 14%, respectively. It also demonstrates the need to clone the cells since some of them express very little FI of 10<sup>0</sup> and very few cells express a lot FI almost 10<sup>2</sup>.

However, in order to obtain consistent results from cytotoxicity experiments involving T cells from immunised HHDII/DR1 mice, it is important to generate a homogenous cell population, all of which express the same levels of HHDII. Cells were therefore cloned by limited dilution in a 96-well rounded-bottom plate and then expanded to larger culture flasks. Each clone was then stained for HHDII expression.

Density plots in Figure 5.10 demonstrate HHDII expression by randomly selected clones derived from single HHDII<sup>+</sup> K562 cells. Non-transfected K562 cells were also stained for comparison. Gating strategy is shown in Figure 5.9.

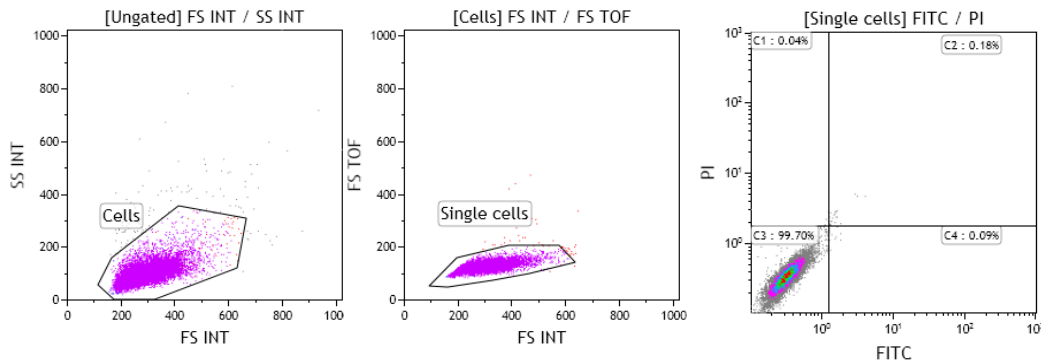


**Figure 5.9: Gating strategy to determine HHDII expression by various HHDII<sup>+</sup> K562 clones.**

Cells were first gated at the single cell level and then on the basis of viability and HHDII positivity. C3 quadrant indicates the percentage of cells that do not express HHDII (HHDII<sup>-</sup>), whereas C4 indicates the percent of cells that are expressing HHDII.

Data in Figure 5.10 show that these clones expressed different levels of HHDII, ranging from 0.75% to 91%. Clone12 comprised two populations, one with HHDII low expression at 38.09% and the other of moderate expression at 59.43%. Nevertheless, Clone10 and Clone11 were associated with the highest percentages of HHDII expression at 91.80% and 91.96% respectively and therefore, they were expanded and reserved for further studies.

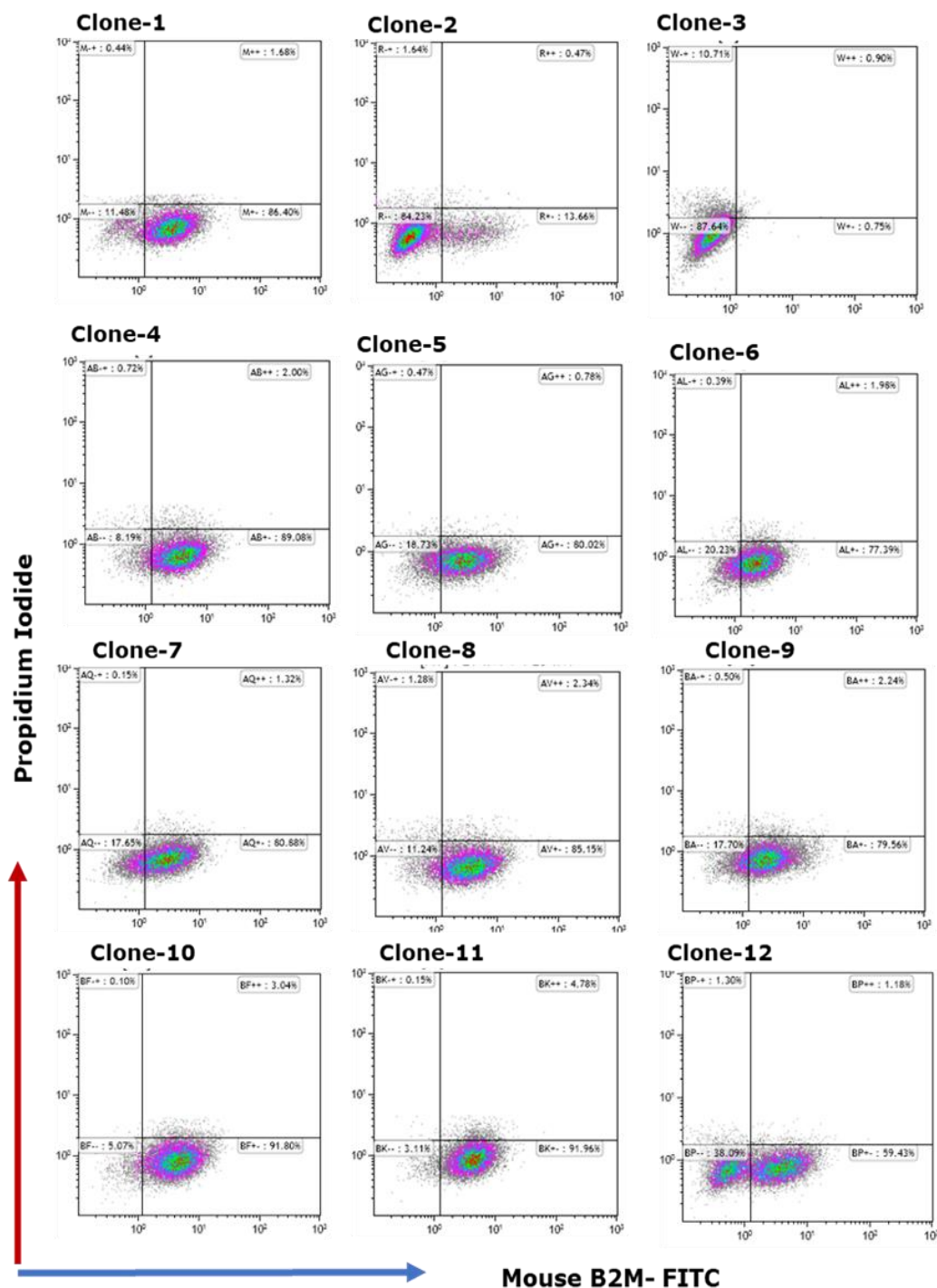


**Figure 5.10: Various levels of HHDII expression in randomly selected twelve HHDII<sup>+</sup>K562 clones, as assessed by flow cytometry.**

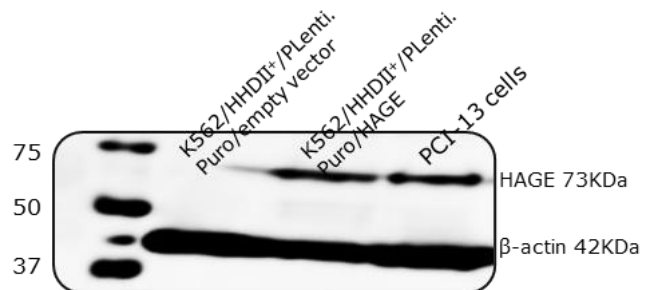
Data represent an example of 12 selected clones of HHDII expression analysed by Gallios flow cytometer. Cells were stained with anti- $\beta$ 2m antibody and then run by flow cytometry. Results point out that both Clone10 and Clone11 are associated with the highest level of expression.

### 5.3.3.2 Transfection of K562/ HHDII<sup>+</sup> cells with HAGE, and clonal selection

Since K562 cells naturally express WT1, there was no need to transfect them with the WT1 gene. However, the previous data also showed that K562 cells are deficient in HAGE protein expression. Thus, K562/HHDII<sup>+</sup> cells (Clone10) was virally transduced with PLenti-Puro/HAGE plasmid construct prepared by a previous researcher (for more details about this construct, please see Divya Nagarajan PhD thesis, 2018 available at: <http://irep.ntu.ac.uk/id/eprint/34884/>). HEK-293T cells were transfected and supernatant were utilised to transfect K562/HHDII<sup>+</sup> cells. Since PLenti-Puro/HAGE carried puromycin as a selection marker, cells were selected post-transfection by the antibiotic puromycin at 1µg/mL to maintain HAGE gene, in addition to G418 to maintain HHDII gene. The dose of puromycin was decided according to the antibiotic titration experiment described in the methodology ([Section:2.2.2.1](#)) After being selected and re-confluent, cells were then assessed for HAGE expression at the protein level using Western blot. The blot in Figure 5.11 illustrates HAGE protein expression in the transduced cell in comparison with cells that were transduced with PLenti.Puro/empty vector, PCI-13 cells at this point were used as a positive control.

**Figure 5.11: Western blot analysis to assess HAGE transduction in K562/HHDII<sup>+</sup> cells.**

K562/HHDII<sup>+</sup>/PLenti.Puro/ empty vector cells were loaded as a negative control and PCI-13 as a positive control. 30µg of protein was loaded onto 10% w/v SDS gel and then blotted onto PVDF membrane. The membrane was probed with rabbit anti-DDX43 antibody. β-actin (42KDa) was used as a loading control. Result indicates a positive band for the successfully transduced cells in comparison with cells that were transduced with the empty vector.



Although these engineered cells are strongly positive for HHDII expression (Figure 5.10) as well as HAGE protein (Figure 5.11), it is possible that they are derived from mixed HAGE expressing populations. It is technically important to generate target exhibit high level of purity to obtain an ideal response from T cells of interest. Therefore, these cells were further cloned by seeding them at a density of single cell per well in 96-well plate and then expanded. 30µg of protein from each clone was then immune probed with human anti-DDX43 antibody using Western blot to detect and select the strongest HAGE expressing clone to be a target for cytotoxicity assay. The blot in Figure 5.12A illustrates different band densities of HAGE expression from 9 clones selected randomly, the darkest, Clone5, and the faintest, Clone9. Accordingly, Clone5 was chosen for this purpose and it was further validated using

RT-qPCR analysis and IF assay as shown in Figure 5.12B and Figure 5.13, respectively.

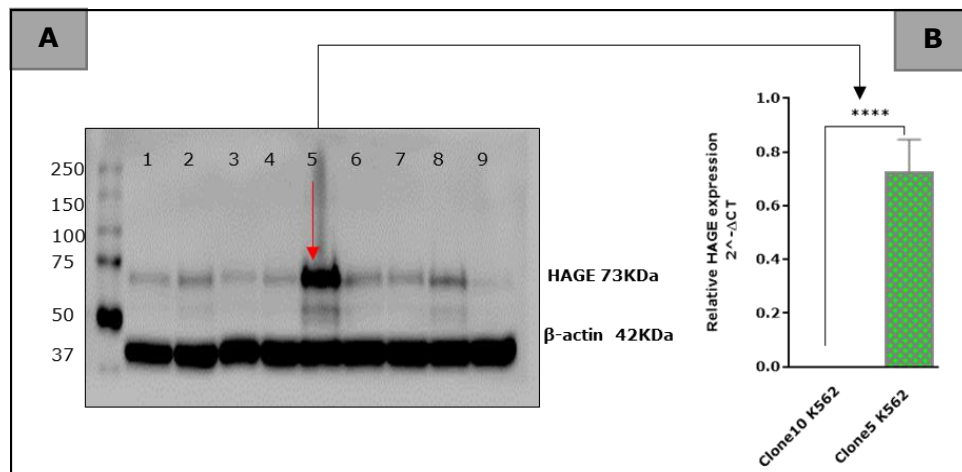


**Figure 5.12: Expressing of HAGE by different K562/HHDII<sup>+</sup>/HAGE<sup>+</sup> clones.**

**(A)** Western blot shows different band densities of HAGE expression by nine K562/HHDII<sup>+</sup>/HAGE<sup>+</sup> clones (lanes 1-9). Red arrow indicates that Clone5 exhibits the strongest HAGE expression **(B)** RT-qPCR validation of HAGE expression in Clone5 using codon optimised primers. Results indicate the highly significant difference in HAGE expression in HAGE transfected cells (Clone5) in comparison to non-transfected cells (Clone10) with *P-value*<0.0001. Clone10 refers to K562/HHDII<sup>+</sup>/HAGE<sup>-</sup> whereas Clone5 refers to K562/HHDII<sup>+</sup>/HAGE<sup>+</sup> cells.

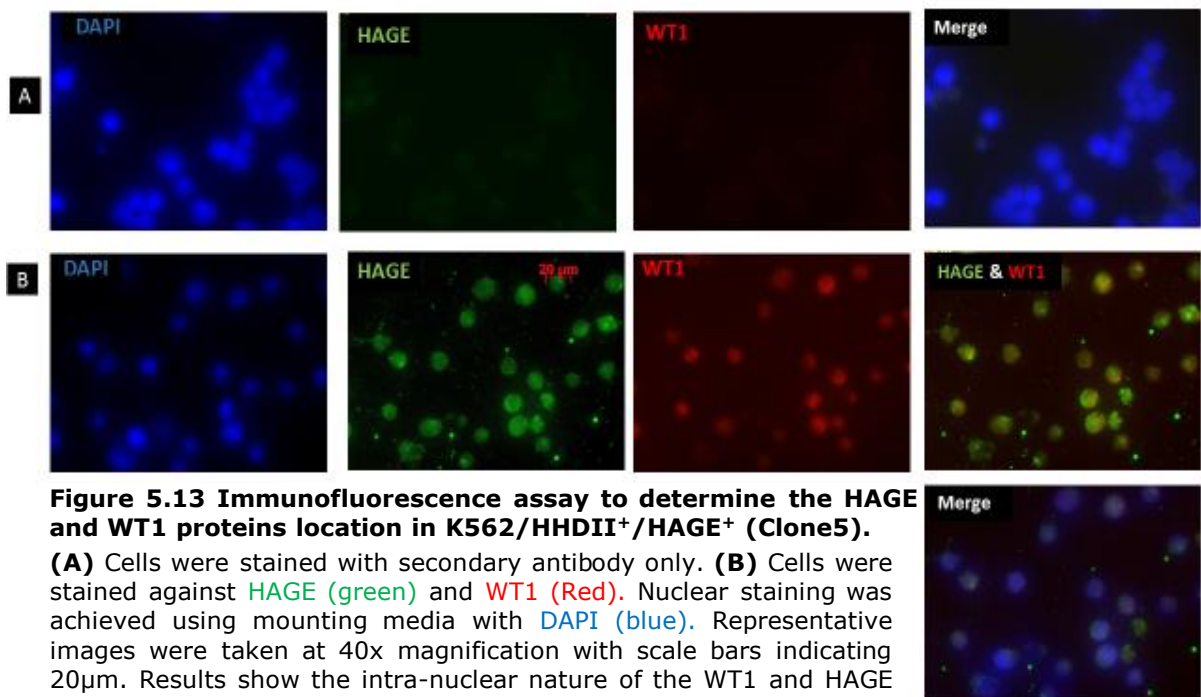


**Figure 5.13 Immunofluorescence assay to determine the HAGE and WT1 proteins location in K562/HHDII<sup>+</sup>/HAGE<sup>+</sup> (Clone5).**

**(A)** Cells were stained with secondary antibody only. **(B)** Cells were stained against HAGE (green) and WT1 (Red). Nuclear staining was achieved using mounting media with DAPI (blue). Representative images were taken at 40x magnification with scale bars indicating 20 $\mu$ m. Results show the intra-nuclear nature of the WT1 and HAGE protein expression. Images were detected under laser capture microdissection zeiss microscope.

In summary, both Clone10 (K562/HHDII<sup>+</sup>/HAGE<sup>-</sup>) and Clone5 (K562/HHDII<sup>+</sup>/HAGE<sup>+</sup>) were confirmed to express high level of HHDII at around 91%, the former being HAGE negative whereas the latter expressing high level of HAGE protein. Cells were then periodically checked for the maintenance of the transduced genes.

### 5.3.4 Generation of KCL-22/HAGE<sup>+</sup> target cells

KCL22 is another *BCR-ABL1* (Philadelphia) positive leukaemic cell line that was found to express HLA-A2 and WT1, but not HAGE protein. Hence, it was decided to transfect KCL-22 cells with HAGE to provide an additional target for the forthcoming cytotoxicity assays. KCL-22 cells were transfected by PLenti-Puro/HAGE plasmid - the same plasmid used to transduce HAGE in K562 cells. In addition to which, some other parental KCL-22 cells were transduced with PLenti-Puro/empty vector to be used as a negative control. The transduced cells were then selected using 1µg/mL puromycin, the lowest concentration of puromycin required to kill the non-transfected cells over a defined period of time. After being selected and adequately re-confluent, cells were assessed for HAGE expression at the mRNA and protein levels. Figure 5.14A illustrates the expression of HAGE in cells transfected with PLenti-Puro/HAGE construct in comparison with one that was transfected with PLenti-Puro/empty vector. Results clearly demonstrates that there is highly significance difference in the level of HAGE expression between the two cells with \*\*\*\**P-value* <0.0001. HAGE expression was also assessed at protein level using Western blot analysis, Figure 5.14B.

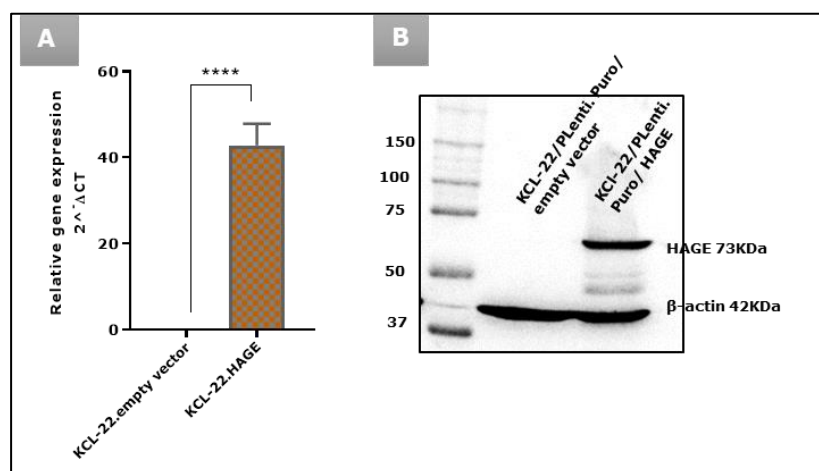


**Figure 5.14: HAGE transduction in KCL-22.**

**(A)** The transduced cells were assessed at mRNA level by RT-qPCR in comparison to the one that transduced with PLenti.Puro/empty vector using codon optimised primers. **(B)** Western blot shows the difference in the bands densities between the two cell types. Overall, results indicate successful transduction of HAGE in KCL-22.

In summary, KCL-22 cells were successfully transfected with the HAGE gene, as demonstrated by existence of transcriptional and translational products, and it is therefore ready to use for *in vitro* cytotoxicity assay.

### 5.3.5 Generation of TCC-S/WT1.shRNA target cells

As previously shown, all the leukaemic cell lines chosen for this project express WT1. The Philadelphia<sup>+</sup> leukaemic cell line, TCC-S cells, express HLA-A2, WT1 and HAGE protein. It was thought that knockdown of WT1 in these cells could establish a negative control for WT1 expressing TCC-S (Wild-type) upon assessing the effectiveness of WT1-specific CTLs in the cytotoxicity assay. In order to achieve this, two shRNA sequences targeting human WT1 were ordered from MISSION/Sigma (see the table below), and DNA derived from them were used to transfect HEK-293T cells separately using lipofectamine reagents. Supernatants (fractions-1) from the respectively transfected HEK-293T cells was collected to transduce the TCC-S cells. After being transduced, cells were selected with 1µg/mL puromycin and assessed for the WT1 expression. Data in Figure 5.15A demonstrate the outcome of WT1 knockdown in TCC-S at protein level using the two WT1.shRNA sequences in comparison with cells that were transfected with the PLentiviral carrying the empty vector (PLKO.1. Puro) as a control vector. It is clear that both sequences of shRNA were successful in the decreasing of WT1 protein expression; however, the WT1.shRNA.1 appears to be more efficient than WT1.shRNA.2, and therefore WT1.shRNA.1 clone was used in the cytotoxicity assay. Silencing of WT1 in this clone was further confirmed by RT-qPCR as shown in Figure 5.15B.

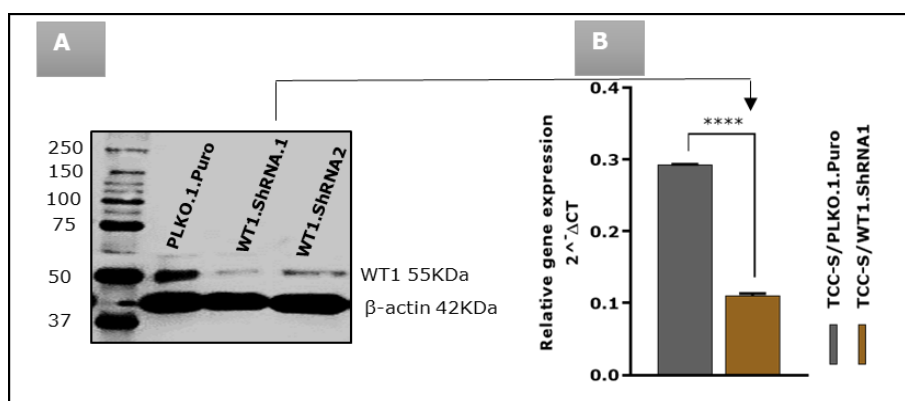


**Figure 5.15: Knockdown of WT1 in TCC-S cells.**

**(A)** Western blot demonstrates WT1 expression in TCC-S transfected by two WT1.shRNA sequences in comparison with cells that transfected with PLKO.1. Puro. Results point out that silencing in both clones was successful. However, WT1.shRNA.1 was more efficient in decrease WT1 expression. This clone was chosen for future cytotoxicity assay. **(B)** RT-qPCR analysis assessing shRNA.1/WT1 knockdown in TCC-S cells.

In summary, WT1 was successfully knocked down in TCC-S cells, and the TCC-S/WT1.shRNA.1 cells will be used to test the role of WT1 in the forthcoming cytotoxicity assay.

**Table 5.5.1: Two shRNA sequences targeting WT1 gene.**

Catalogue #	Name	ShRNA sequences
TRCN0000010466	WT1.shRNA.1	CCGGATGAACTTAGGAGCCACCTTCTCGAGAAGGTGGCTC CTAAGTTCATCTTTTTG
TRCN0000040064	WT1.shRNA.2	CCGGGCAGTGACAATTTATACCAAACCTCGAGTTTGGTATA AATTGTCACCTGCTTTTTG

### 5.3.6 Profile of $hB16/HAGE^+/Luc^+$ cells:

#### 5.3.6.1 Gene expression by the engineered B16 melanoma cells

Tumours model using B16 melanoma cells have been extensively used by many projects as a “proof-of-concept” to assess the efficacy of many immunotherapeutic strategies (Overwijk, Restifo 2000). In order to be able to grow tumours in the HHDII/DR1 transgenic mice using these cells, murine MHC was knocked-out and replaced by the HHDII/HLA-DR1 construct. These “humanised” B16 cells were kindly provided by Prof. Lindy Durrant (Scancell). Thereafter, HAGE and firefly luciferase (Luc) reporter constructs were transfected into these cells by Divya Nagarajan (Previous PhD student). The expression of HHDII/DR1 and HAGE genes was confirmed by flow cytometry and Western blotting, respectively as shown in Figure 5.16. Stable gene expression was assessed before every *in vitro* and *in vivo* study.

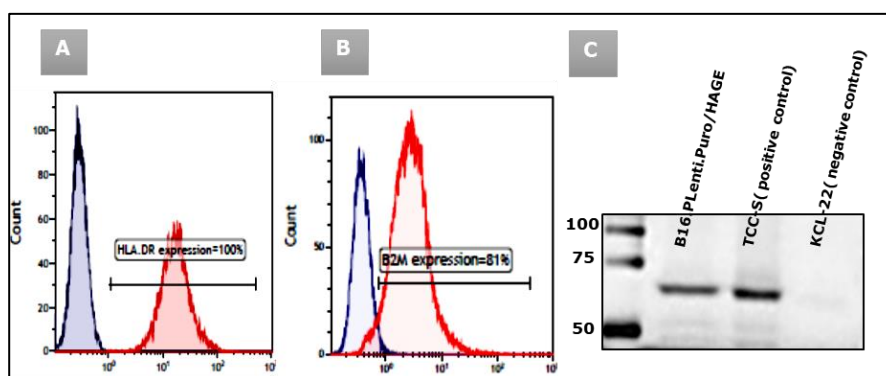


**Figure 5.16: Stable genes expression by  $hB16/HAGE^+/Luc^+$  cells.**

The expression of the HLA-DR and chimeric HLA-A2 on the surface of the  $hB16$  cells (knockout for murine MHC and knocked-in for HHDII and DR1 genes) was confirmed by flow cytometry (shown in A and B, respectively), wherein the stained candidate cells (red histograms) were compared with control non-stained samples (blue histograms). (C) HAGE protein expression after cells being further transfected, as confirmed by Western blotting. TCC-S cells were loaded as a positive control and KCL-22 as a negative control.

The modified B16 melanoma cells were also assessed for constitutive expression of WT1 using immunofluorescence (IF) and DAB immunochemical staining, as shown in Figure 5.17A and B, respectively.

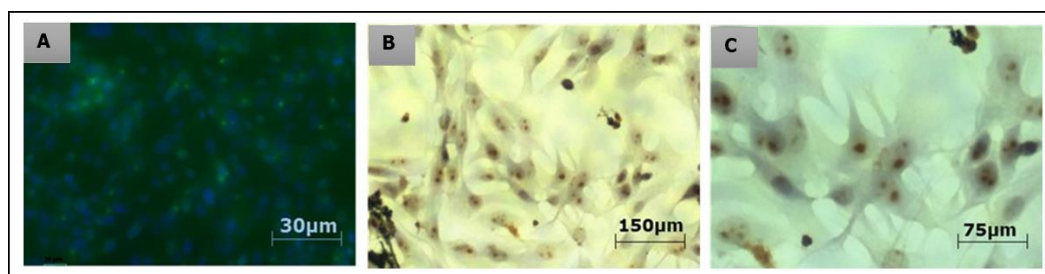


**Figure 5.17: Constitutive WT1 expression by  $hB16/HAGE^+/Luc^+$  cells using IF and DAB immunochemical staining.**

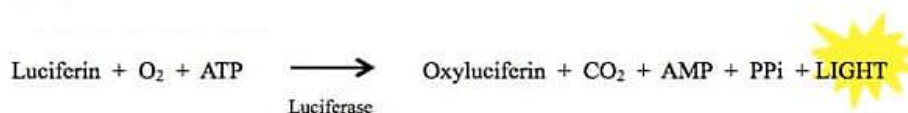
(A) WT1 detection using IF, image was taken at 20X magnification with scale bar of  $30\mu m$ , where WT1 positive areas are represented by green fluorescent staining and the nuclei of cells are shown to be stained blue. (B) and (C) are DAB immunochemical staining of WT1 in B16 cells, image shown in (B) was taken at 20X magnification and scale bar equal to  $150\mu m$  whereas image in (C) was taken at 40X magnification and scale bar equal to  $75\mu m$ . WT1 (dark stained area) appears to be localised in the nucleus as well as in the cytoplasm.

In summary, the expression of HHDII, DR1, HAGE and WT1 proteins was confirmed in the  $hB16$  cells. Luc expression was also verified, as it will be shown in the following section.

### 5.3.6.2 *In vitro* optimisation of $hB16/HAGE^+/Luc^+$ bioluminescence

After having confirmed the expression of the modified genes in the engineered B16 cells, the luciferase activity and the tumorigenicity were then evaluated. The latter will be covered in Chapter-7.

As mentioned previously, the murine melanoma B16 cell line was stably transfected with firefly luciferase reporter gene (Luc) to be detected by imaging system. Fireflies are able to emit light when luciferin is converted to oxyluciferin by the luciferase enzyme. Some of the energy released by this reaction is in the form of light.



When this reaction happens *in vivo*, the bioluminescence emitted from tumour cells can be captured and quantified by *in vivo* live imaging system. The amount of the generated luciferin should correlate to the tumour size, therefore, to monitor tumour growth, several imaging sessions are required. However, prior to tumour implantation, B16 cells were assessed for *in vitro* and *in vivo* optimisation of luciferin bioluminescence. Cells were titrated and plated in a black 96-well microplate and  $0.15\mu g$  of D-Luciferin was then added. Plate was covered with foil and immediately sent to measure the total flux of bioluminescence. Results in Figure 5.18 illustrate *in vitro* kinetics imaging signal of B16  $Luc^+$  cells bioluminescence where data show a static correlation between the total flux and cells density, indicating cells validity for

imaging system. Taking advantage of already prepared hB16 tumour cell line with dual expression of HAGE and WT1 proteins and according to data of cytotoxicity assay (in Chapter-6), these cells were chosen as tumour model in "a proof-of-concept" for our *in vivo* study (Chapter-7).

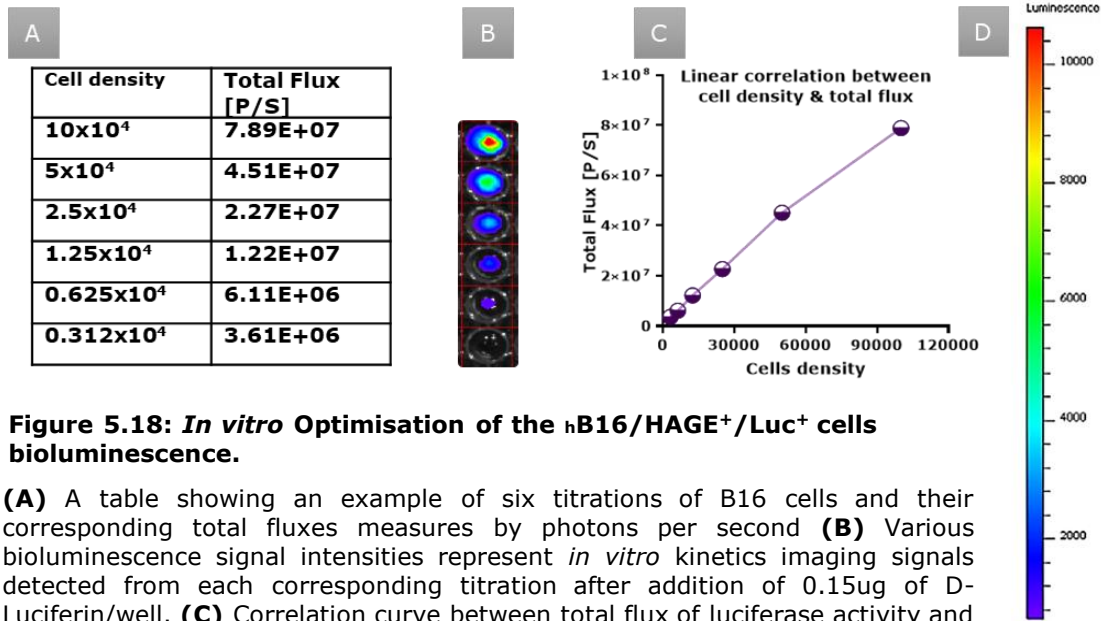


**Figure 5.18: *In vitro* Optimisation of the hB16/HAGE<sup>+</sup>/Luc<sup>+</sup> cells bioluminescence.**

(A) A table showing an example of six titrations of B16 cells and their corresponding total fluxes measures by photons per second (B) Various bioluminescence signal intensities represent *in vitro* kinetics imaging signals detected from each corresponding titration after addition of 0.15ug of D-Luciferin/well. (C) Correlation curve between total flux of luciferase activity and the cells population is plotted from data in the table shown in (A). Scale of illuminances shown in (D).

### 5.3.7 Diverse biological functions of IFN- $\gamma$ on the respective CML cells:

#### 5.3.7.1 Assessing the expression of IFN- $\gamma$ receptor (CD119)

The previous chapter demonstrated the ability of the vaccine-induced T cells to produce high levels of IFN- $\gamma$ . Positive and negative impacts of IFN- $\gamma$  on cells of interest was therefore important to be assessed. First, the existence of IFN- $\gamma$  receptors on the surface of K562, KCL-22 and TCC-S cells were confirmed. These receptors are necessary for signal transduction upon engagement of IFN- $\gamma$  molecule. Therefore, cells were firstly stained with interferon gamma receptor 1 (IFNGR1)/PE-conjugated anti-human CD119 monoclonal antibody and analysed using flow cytometer. IFNGR1 tends to be expressed by almost all cells in the body except erythrocytes. Hence, the results below confirm the abundant expression of CD119 in the selected CML cell lines. The effect of IFN- $\gamma$  could now be confidently assessed.

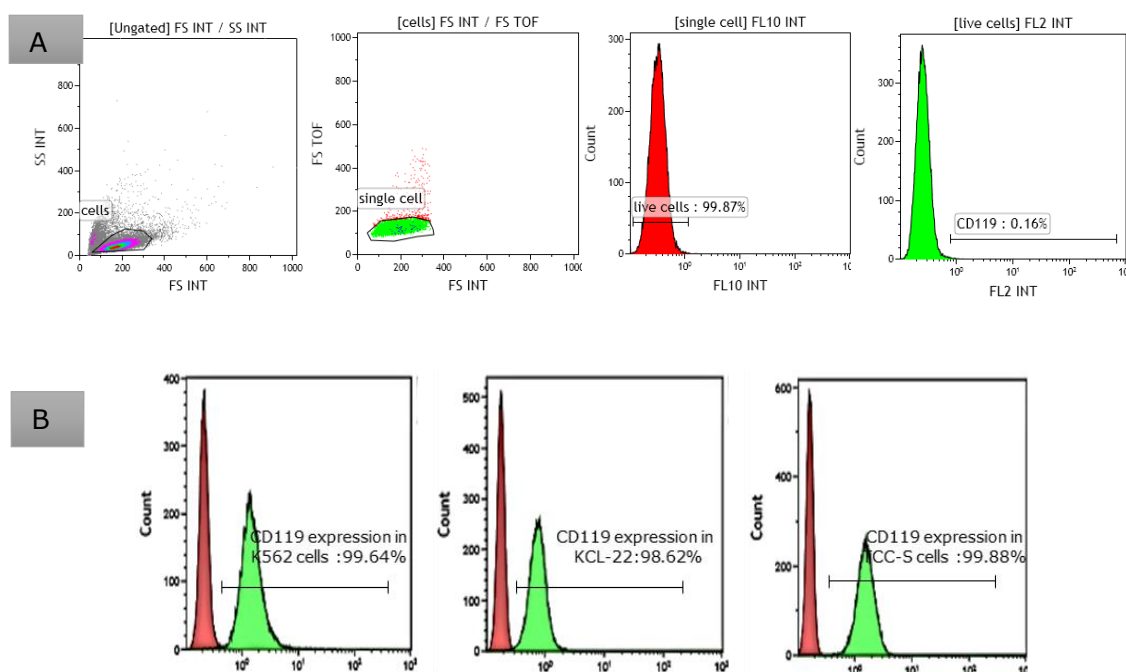


**Figure 5.19: CD119 constitutive expression on CML-derived target cells.**

Cells were stained with PE-conjugated anti-human CD119 monoclonal antibody (detected at FL2) and LIVE/DEAD™ Yellow stain (detected at FL10) and analysed using a Beckman Coulter Gallios™ flow cytometer. **(A)** Gating strategy used in this type of analysis wherein cells were first gated at single cell level and then per live cell, the level of CD119 expression was determined on basis of right shift in peaks that gated on unstained samples. **(B)** Overlay histograms illustrate CD119 expression in the respective cells in comparison to negative controls (non-stained samples). Red histograms represent non-stained controls and green histograms reflects CD119 expression. All tested cells were found to express CD119 molecules.

Having confirmed the expression of IFNGR1, cells were then treated with 100ng/mL of IFN- $\gamma$  and incubated for 24, 48 and 72 hours before staining. This dose was previously used by previous researchers to study the effect of IFN- $\gamma$  on leukaemic blast, wherein authors found that this dose is able to upregulated the expression of IDO1 in leukaemic human samples (Folgiero, Goffredo *et al.* 2014). For each time point, cells were stained for a panel of antibodies to assess the expression of the following costimulatory molecules; HLA-A, B, C, MICA/MICB, CD80, CD86 and CD40, and the inhibitory molecules; HLA-E, HLA-G, PD-L1 and FasL using flow cytometry. In order to determine their viability, cells were also stained with LIVE/DEAD™ Yellow which is an amine reactive dye. Cells that have compromised membranes, LIVE/DEAD™ Yellow interreacts with free amines expressed both intracellularly and on the surface of these cells, producing a strong fluorescent signal. Whereas in viable cells, dye interaction is limited to the cell surface amines only, resulting in fewer fluorescence. Such big difference in the intensity of fluorescence allows the discrimination between live and dead cells easily.

The level of IDO1 expression and function was also assessed upon IFN- $\gamma$  treatment by RT-qPCR and kynurenine assay, respectively.

### 5.3.7.2 Influence of IFN- $\gamma$ treatment on immuno-activating molecules expressed by the respective CML cells

The aim of this experiment was to test the possible upregulation of HLA-A, B, C molecules and other costimulatory molecules such as MICA/MICB, CD80, CD86 and CD40 upon IFN- $\gamma$  treatment. Binding of these molecules with their respective ligands will indeed determine whether T cells end up activated or rendered unresponsive (anergised).

Overall, Figure 5.20 (A&B) shows that HLA-A, B, C and CD40 expression were significantly upregulated in response to IFN- $\gamma$  treatment in comparison to the control cells, where it was decided to compare the intensity of expression (MFI) instead of the % positive because the percentage of the cells were already 100% for the majority of the markers studied prior to IFN- $\gamma$  treatments. In contrast, no statistically significant upregulation of MICA/MICB, CD80 and CD86 in comparison with control non-treated cells could be detected within the range of incubation time points used and treatment dose applied in the all three cell lines (data not shown).

Figure 5.20A demonstrates an impressive upregulation of HLA-A, B, C expression in comparison to the control non-treated samples in a time-dependent manner for almost in all incubation times and in all cell lines studied. Interestingly, although all cells responded significantly to IFN- $\gamma$  treatment, TCC-S cells were the highest responder, as it can be seen by the rise MFI values going from less than 10 in the control groups to almost 200, 300 and 400 at 24, 48 and 72 hours of treatments, respectively. MFI values in the treated KCL-22 were similar those for IFN- $\gamma$  treated TCC-S cells, whereas K562 cells were the least responsive. Nonetheless, all the results were found to be statistically significant at almost \*\*\*\* $P$ -value<0.0001.

Similarly, CD40 expression level was also found to be upregulated by IFN- $\gamma$  treatment, as shown in Figure 5.20B, in a time-dependent manner for the majority of incubations performed in all studied cells. However, TCC-S cells also showed the highest upregulation at \*\*\*\* $P$ -value<0.0001.

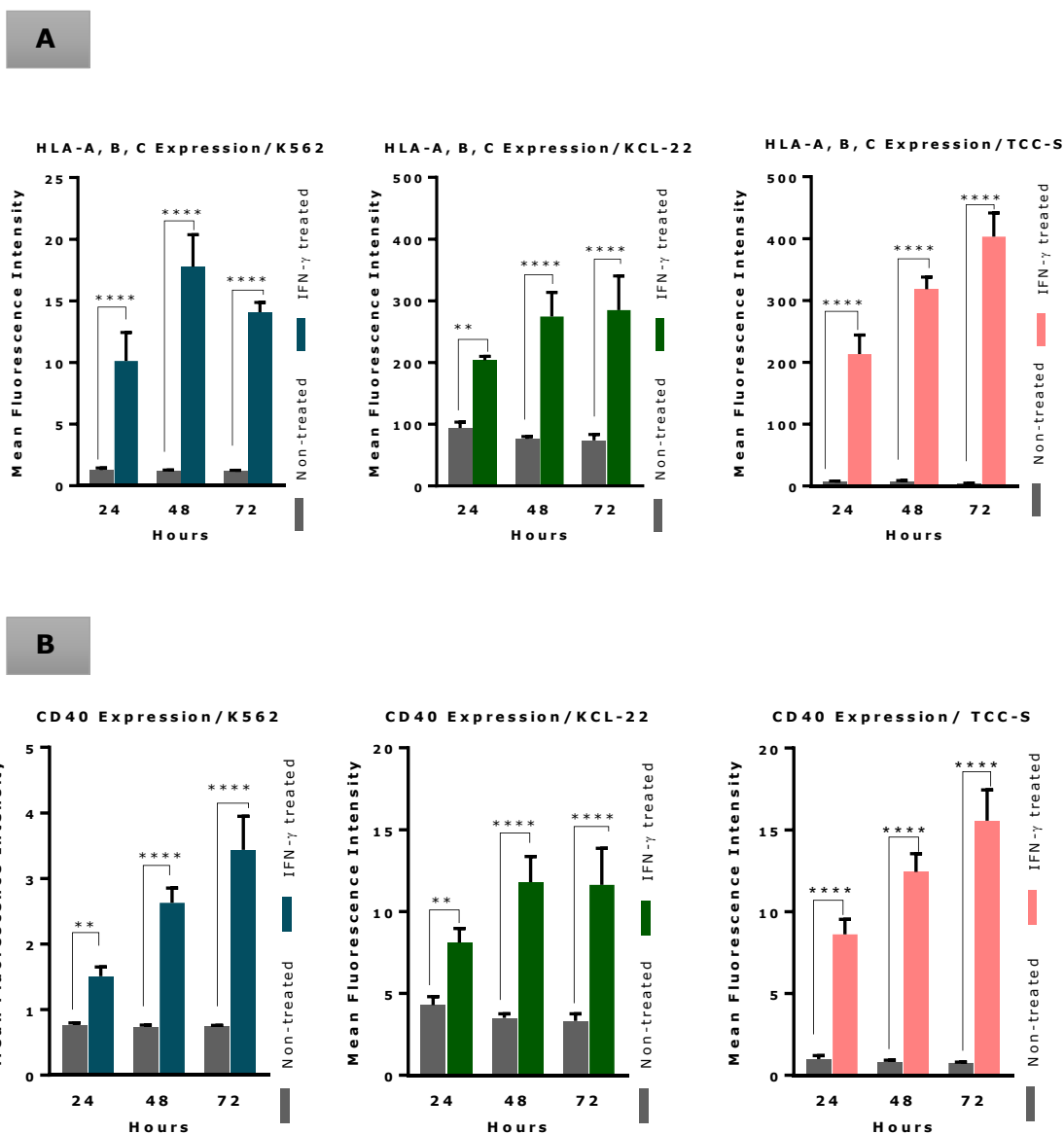


**Figure 5.20: Upregulation of HLA-A, B, C and CD40 expression on CML-derived target cells after IFN- $\gamma$  treatment.**

Expression analysis of HLA-A, B, C on three targets shown in **(A)** and CD40 shown in **(B)** in comparison to control non-treated cells.  $2 \times 10^6$  cells were challenged with 100ng/mL of IFN- $\gamma$  and incubated for three different time points; 24, 48 and 72 hours. After each incubation, cells were washed, stained with the respective antibodies and run using flow cytometer. Values are expressed as the mean  $\pm$  SD of three independent experiments and the level of significance was assessed using Two Way ANOVA. Results show that there is a significant upregulation of HLA-A, B, C and CD40 molecules in the treated samples in comparison with non-treated at \*\*\*\* $P$ -value $<0.0001$  almost in all treatments and in all cell lines studied. This upregulation was time dependent as reflected by a steady increase of MFI levels with the duration of the incubation after IFN- $\gamma$  treatment. HLA-A, B, C, CD40 and Live/Dead Yellow stain are detected at FL8, FL7 and FL10, respectively.  $n=3$ .

### 5.3.7.3 Influence of IFN- $\gamma$ treatment on the expression of immune inhibitory molecules by the respective CML cells

The expression of HLA-E, HLA-G, FasL CD178 (CD95L) and PD-L1(CD274) molecules was assessed before and following 24, 48 and 72 hours treatment with IFN- $\gamma$ . Many studies point out that the overexpression of these molecules by tumour cells favours tumour escape from immune-surveillance. Therefore, since it was shown that the vaccine-induce T cells can secrete high levels of IFN- $\gamma$ , it is worth investigating the impacts that IFN- $\gamma$  treatment may have on these known inhibitory molecules. As previously indicated, the CML cell lines were treated with 100ng/mL of IFN- $\gamma$  and incubated for three time points 24, 48 and 72 hours, thereafter, stained with the considered antibodies and analysed using flow cytometry.

Summary of the findings can be found in Figure 5.21, wherein once again TCC-S are shown to be the most sensitive cells to the treatment and upregulated HLA-E molecule the most, whereas HLA-E expression in KCL-22 cells is less upregulated in comparison to TCC-S cells.

HLA-G expression, on the other hand, was found to be high in K562 cells even before treatment and was not significantly altered after IFN- $\gamma$  treatment within the range of time-points and dose of IFN- $\gamma$  applied (Figure 5.21B). With regards to KCL-22, although cells expressing low HLA-G level, it responded to the treatment and upregulated HLA-G after 48 hours and 72 hours incubation, albeit moderate at \**P-value* and \*\**p-value*, respectively. Finally, moderate induction of HLA-G expression in TCC-S cells is noticed upon the challenges at \*\**p-value*, even though that the cells already express high percentage of the molecules before treatment.

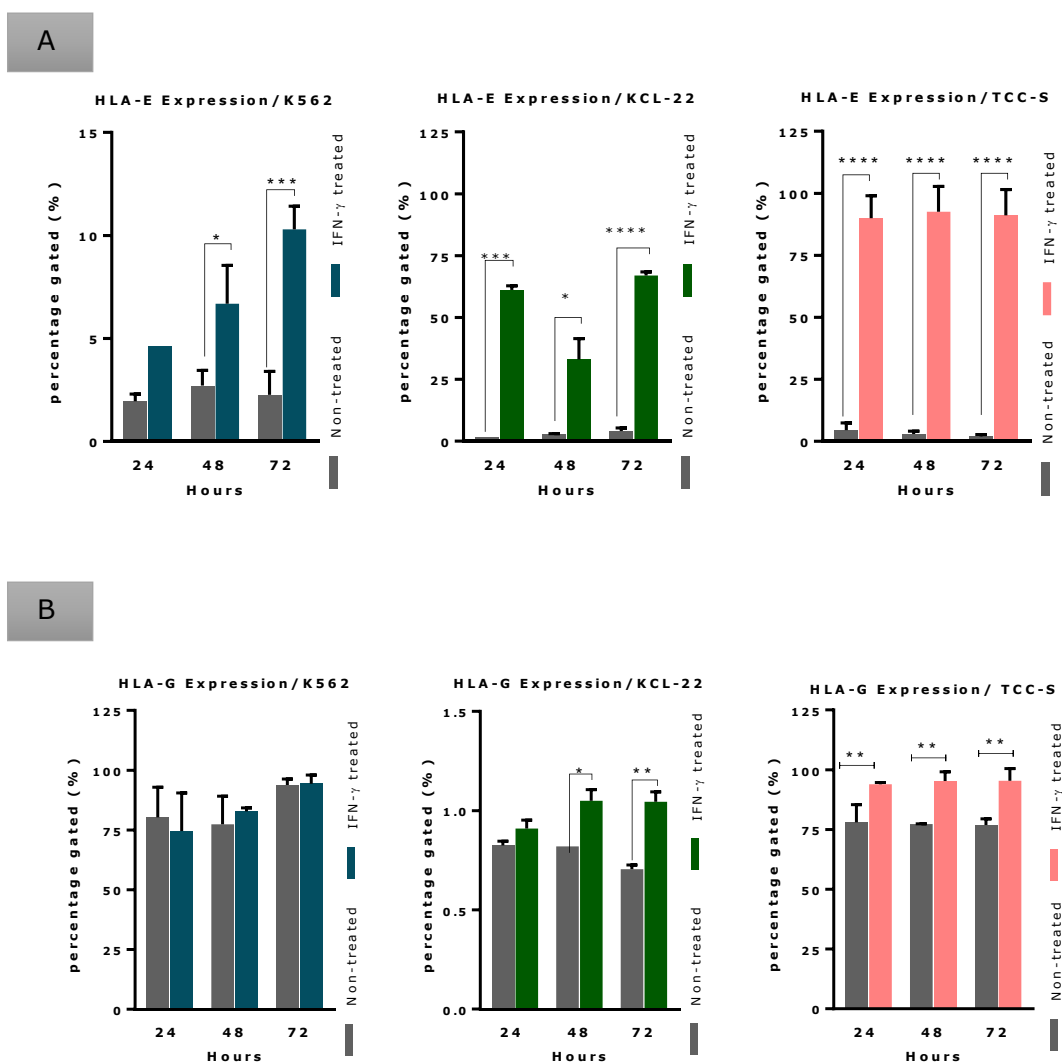


**Figure 5.21: Upregulation of HLA-E and HLA-G expression on CML-derived target cells after IFN- $\gamma$  treatment.**

Expression analysis of HLA-E on three targets shown in (A) and HLA-G shown in (B) in comparison to control non-treated cells. Cells were treated with IFN- $\gamma$  and incubated for three different time points; 24, 48 and 72 hours. After each incubation, cells were washed, stained with respective antibodies and run using flow cytometry. Values are expressed as the mean $\pm$ SD of three independent experiments. The level of significance was assessed using Two Way ANOVA. Results show that there is a significant upregulation in HLA-E and HLA-G expression in studied cells in comparison with non-treated cells. HLA-E upregulation is more than HLA-G specially with high concentrations, and most responder cells are TCC-S cells. However, no upregulation in HLA-G expression in K562 cells was detected. HLA-E, HLA-G and LIVE/DEAD<sup>TM</sup> YELLOW stain are detected at FL4, FL5 and FL10, respectively. n=3.

Similarly, PD-L1 molecule is shown to be significantly upregulated in all treated leukaemic cell lines in comparison with non-treated ones and also in time dependent manner (Figure 5.22). Although upregulation was observed for all cell lines, TCC-S cells again responded the most to these treatments with highly significant upregulation is prompted as early as the 24 hours incubation.

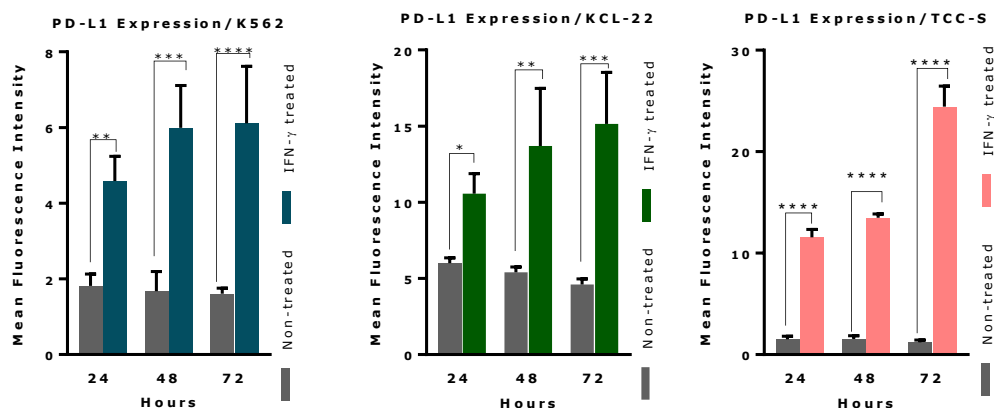


**Figure 5.22: Upregulation of PD-L1 expression on CML-derived target cells after IFN- $\gamma$  treatment.**

Cells were treated with IFN- $\gamma$  and incubated for three different time points; 24, 48 and 72 hours. After each incubation, cells were washed, stained with respective antibodies and run on flow cytometer. Values are expressed as the mean $\pm$ SD of three independent experiments. The level of significance was assessed using Two Way ANOVA. Results show that there is a significant upregulation in PD-L1 expression in all studied cells in comparison with non-treated cells. PD-L1 upregulation is noticed to be a time dependent manner and most upregulation is seen in TCC-S. n=3.

The expression of FasL, on the other hand, does not express any response upon this treatment in any of the cells or time points studied, as shown in Figure 5.23. It is therefore further optimisation might be indicated.

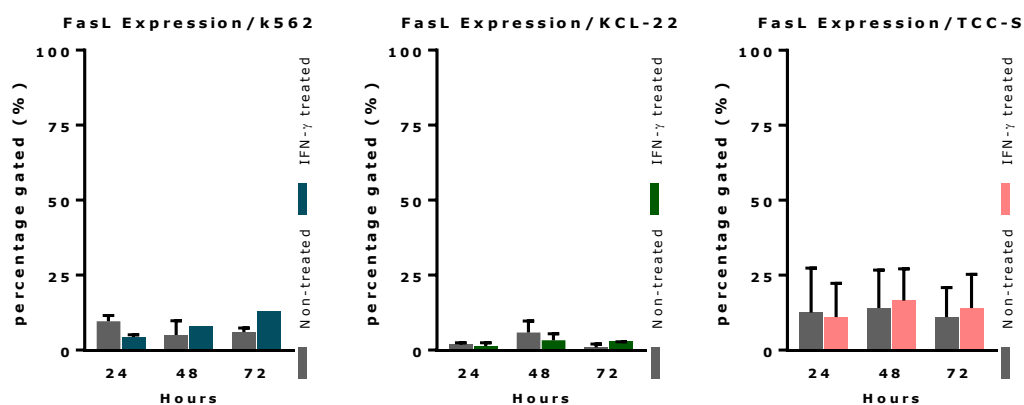


**Figure 5.23: The effect of IFN- $\gamma$  treatment on FasL expression by CML-derived target cells.**

Cells were treated with IFN- $\gamma$  and incubated for three different time points; 24, 48 and 72 hours. After each incubation, cells were washed, stained with respective antibodies and run on flow cytometer. Values are expressed as the mean $\pm$ SD of two independent experiments. The level of significance was assessed using Two Way ANOVA. Results show that there is no significant upregulation in FasL expression in all studied cells in comparison with non-treated cells. n=2.

#### 5.3.7.4 Influence of IFN- $\gamma$ treatment on Indoleamine 2,3-dioxygenase 1 (IDO1) expression by the respective CML cells

The influence of IFN- $\gamma$  on the expression of the powerful inhibitory molecule, IDO1, was also assessed at three time points of IFN- $\gamma$  treatment: 24, 48 and 72 hours at a dose of 100ng/mL. The chosen of this dose is based on previous leukaemic blast studies which found that IFN- $\gamma$  was able to upregulate IDO1 expression in leukaemic human samples at the indicated dose (Folgiro, Goffredo *et al.* 2014). After each treatment, cells were assessed for direct induction of IDO1 expression at mRNA level using RT-qPCR, and for IDO1 activity by assessing kynurenine production in supernatants collected from each time point. At the same time, HAGE and WT1 at mRNA level and protein level were assessed to detect any meaningful associated upregulation upon IFN- $\gamma$  treatment.

Overall, data in the Figure 5.24 below demonstrate the influence of IFN- $\gamma$  treatment on IDO1 expression by K562 and TCC-S cells. It is apparent from Figure 5.24 (A) that IDO1 expression was more markedly upregulated on TCC-S cells and that it had no effects on WT1 and HAGE expression in these cell lines within the range of the used dose and the incubated time.

As with TCC-S cells, K562 cells show enhancement of IDO1 upon the treatment. The highest level of upregulation occurred after 48 hours of treatment (\*\**P-value*=0.003). A small increase in the expression of IDO1 appeared after 24 hours (\**P-value*=0.0132), whereas no statistically significant upregulation of IDO1 after 72 hours of treatment. The same upregulation pattern of HAGE expression is noticed in this cell line and no upregulation of WT1 was seen.

With regards to KCL-22, no induction of IDO1 level was noticed when the cells were treated with IFN- $\gamma$ . Also, there was no change in either HAGE or WT1 expression in all time points used (data is not shown).

In addition, IDO1 activity mediated by IFN- $\gamma$  was assessed indirectly by measuring kynurenine accumulation in supernatants collected from the indicated time points using the kynurenine assay, presuming that the presence of IDO1 can cause L-tryptophan consumption and kynurenine production. Overall, the baseline amount of kynurenine was barely detectable in all cell lines. Figure 5.25B shows that IFN- $\gamma$  treated K562 cells resulted in a significant increase in the level of kynurenine (\*\*\*\**p-value*<0.0001 at 48 and 72 hours). Taken together the upregulation of IDO1 mRNA and increased kynurenine production, suggesting a functional upregulation of IDO1 in K562 cells. However, even though TCC-S cells show remarkable IDO1 upregulation at the mRNA level, the level of kynurenine did not change in comparison to the non-

treated cells, suggesting non-functional upregulation of IDO1 upon IFN- $\gamma$  treatment in TCC-S cells.

In the case of IFN- $\gamma$  treated KCL-22, there was neither upregulation of IDO expression at the mRNA level nor increase in the level of kynurenine products.

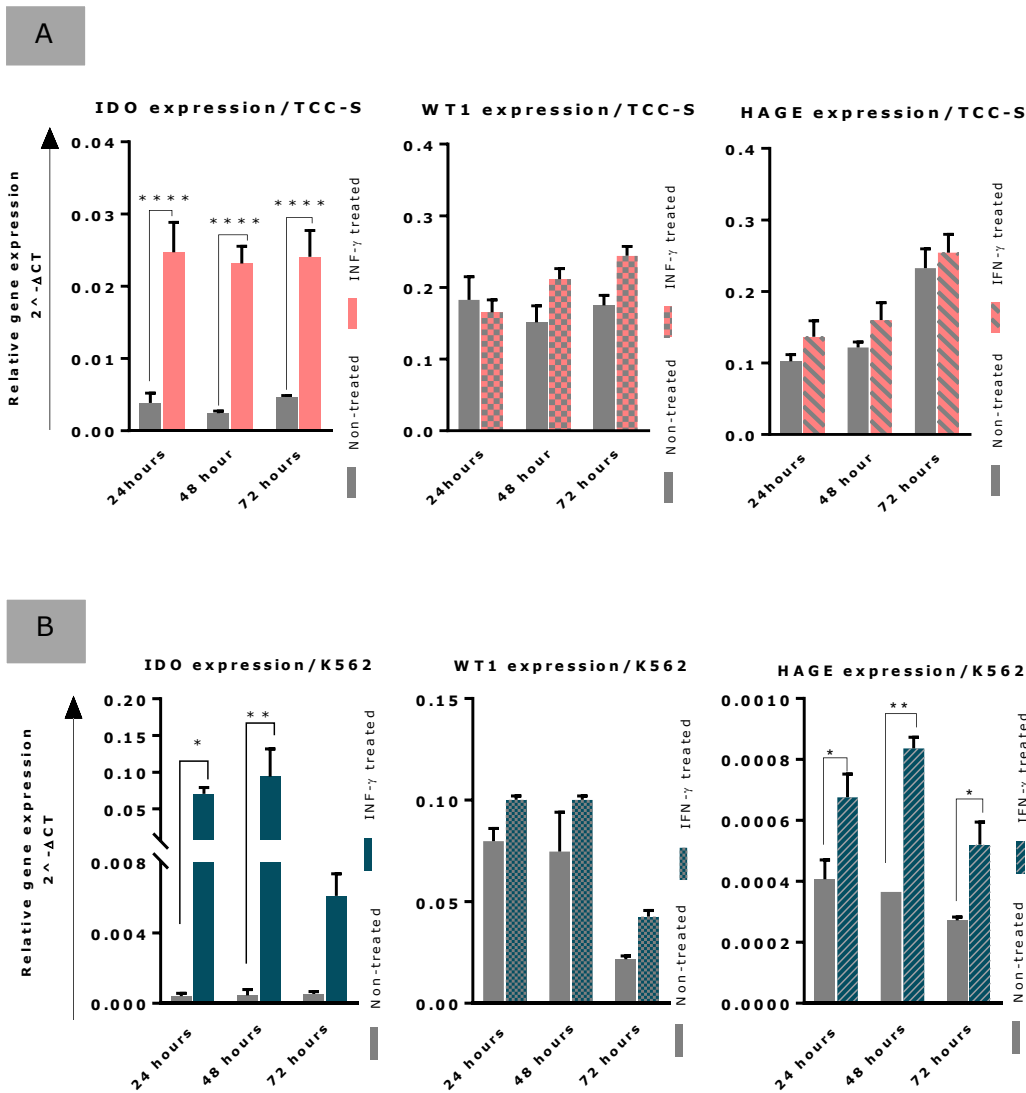
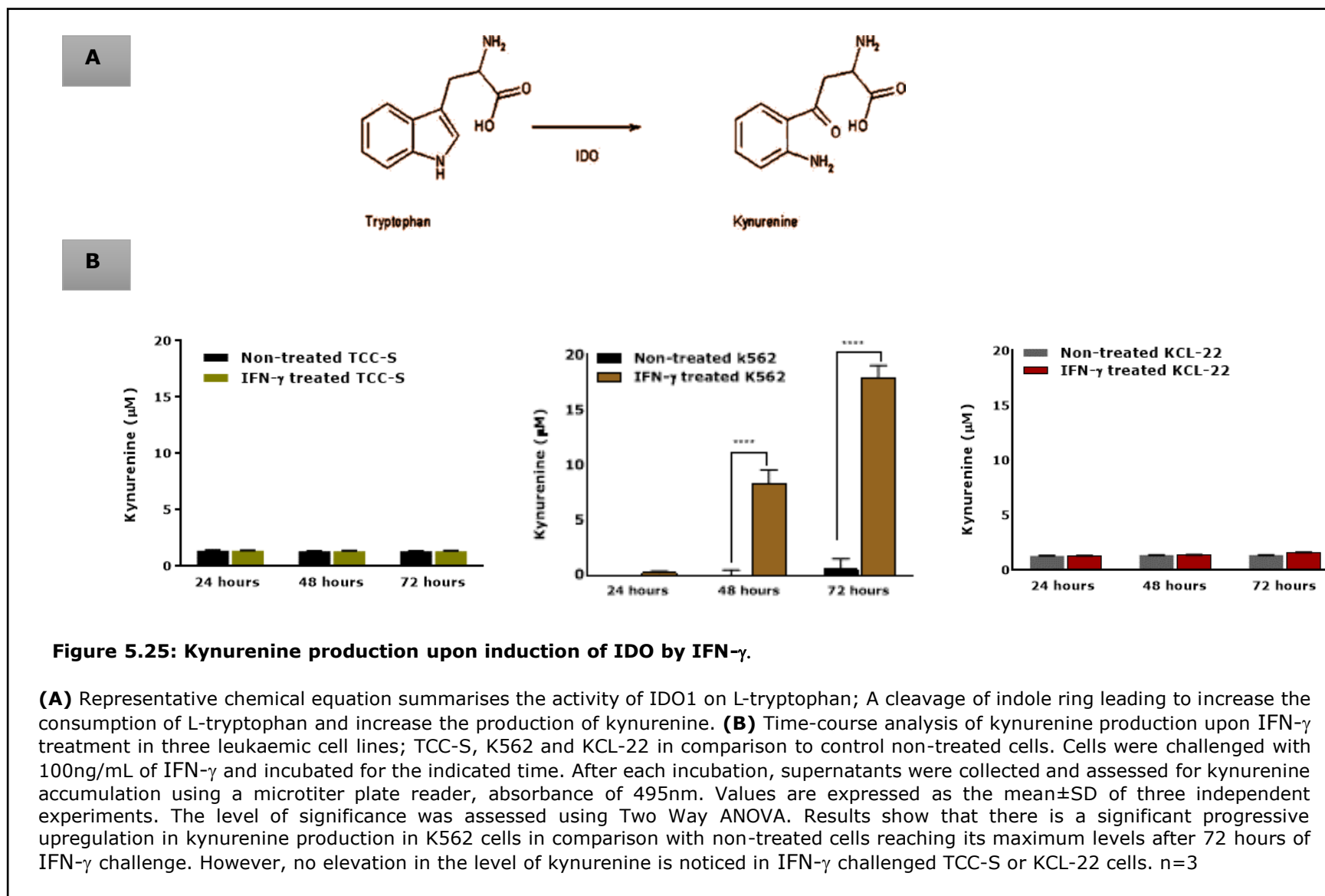


**Figure 5.24: The effect of IFN- $\gamma$  on the expression of IDO1, WT1 and HAGE gene in TCC-S and K562 cells.**

Cells were treated with IFN- $\gamma$  and harvested after three time points 24, 48, and 72 hours. mRNA was extracted followed by cDNA synthesis and PCR amplification. Gene expression level was assessed by calculating  $2^{-\Delta CT}$  value and normalised by GUSB housekeeping gene. **(A)** IDO1, WT1 and HAGE genes expression in TCC-S cells **(B)** genes expression in K562 cells. Values are expressed as the mean  $\pm$  SD of two independent experiments and the level of significance was assessed using Two Way ANOVA. Results show a significance upregulation of IDO1 expression in TCC-S and K562 cells in comparison to non-treated cells, upregulation of HAGE in K562 cells and no changes in the level of WT1 expression neither in TCC-S nor in K562 cells. n=2



## 5.4 Discussion

After having been demonstrated the immunogenicity of the prospective vaccines in HHDII/DR1 mice (Chapter-4), T cells derived from such mice needs to be evaluated for their capability to recognise and specifically kill targets harbouring the relevant antigens and HLA haplotype using *in vitro* cytotoxicity assays (the next chapter), that is why herein different CML target cells with/without the considered antigens and HLA haplotype were prepared.

In the recent years, immortalised haematopoietic cell lines have become increasingly important tools to study leukaemia-associated fusion genes analysis, such as cloning, characterisation, and functional studies (Drexler, Matsuo *et al.* 2000). These cell lines have also been instrumental in evaluating biological efficacy of newly developed drugs. Hence, herein, three Philadelphia positive leukaemic cell lines namely, K562, KCL-22 and TCC-S cells were chosen to be targets for *in vitro* cytotoxicity assays.

CML targets were assessed for HLA-A2 surface expression to validate their compatibility with the T cells derived from HHDII/DR1 mice. Both KCL22 and TCC-S were shown to exhibit high level of HLA-A2. However, surface HLA-A2 was barely detectable in K562 cells, therefore, they were transfected with HHDII gene. In the first instance, lipofectamine reagents were used to transfect K562 cells; however, only low efficiency rate was achieved, and therefore electroporation technique was tried. We have found that electroporation technique is superior to lipofectamine in HHDII gene transfection of K562 cells.

With regards to HAGE overexpression, two cell lines, K562 and KCL-22, were successfully transduced using PLenti.Puro/HAGE plasmid. TCC-S cells did not require to be knocked-in for any genes since they were found to naturally express HAGE, HLA-A2 and WT1. The latter antigen being found constitutively expressed by all three cell lines. However, TCC-S cells were chosen to have its WT1 gene expression knocked-down and thereby serve as a control for WT1-specific killing. K562/HHDII<sup>+</sup> cells (Clone10) do not constitutively express HAGE, and therefore were chosen to be used as negative control for HAGE-specific recognition upon targeting K562/HHDII<sup>+</sup>/HAGE<sup>+</sup> cells (Clone5). All genetically manipulated cells were periodically assessed for the stable expression of genes of interest prior to every cytotoxicity assay. Unfortunately, attempts to stably knock-down WT1 in Clone5, Clone10 K562 and KCL-22 were not successful.

Regarding *in vivo* studies, the genetically modified murine B16 melanoma cells were kindly donated to our group by Prof. Lindy Durrant. These had been previously knocked-out for murine MHC molecules and double transfected to express both the

chimeric HLA-A2 (HHDII) and HLA-DR1 molecules. These cells were also found to naturally express murine WT1 but not HAGE. So, these were further transfected with HAGE and firefly luciferase reporter gene (by previous PhD student; Divya Nagarajan) in order to be used as a “proof of concept” in pre-clinical tumour model. The firefly luciferase reporter gene was previously inserted in B16 cells to monitor *in vivo* tumour growth by detection of bio-luminescence signals produced in the live mice and then captured by imaging system (more details will be covered in Chapter-7).

Since the vaccines used in this project are aimed to provoke T cell stimulation which will result in the release of cytokines, including IFN- $\gamma$ , this chapter explore the effect of IFN- $\gamma$  treatment on the considered CML cells by assessing time-course analysis on selected stimulatory and inhibitory molecules after being challenged with 100ng/mL of IFN- $\gamma$ , a dose that has been shown to be associated with IFN- $\gamma$  response (IDO induction) in leukaemic studies dose (Folgiro, Goffredo *et al.* 2014). It has recently become apparent that IFN- $\gamma$  has dual contrasting effects, anti-tumour and pro-tumour effects. Under both scenarios, IFN- $\gamma$  has direct and indirect effects on tumour cells and their microenvironment. The anti-tumour function stems from the direct inhibition of cancerous cell growth, and from recognition and elimination of the malignant cells by IFN- $\gamma$  secreted immune cells. The pro-tumorigenic effects, on the other hand, include promoting proliferative and anti-apoptotic signals, and tumour escape from CTLs and NK cells. Which battle going to ultimately win the war, depends on the context of cancer specificity, signalling intensity and microenvironment reaction (Zaidi, M. R., Merlino 2011).

Loss of tumour immunogenicity due to downregulation of MHC class I molecule and subsequent malpresentation of tumour antigens is a hallmark of tumour escape process. In the context of tumour vaccine development, T cell recognition of cancerous cells essentially depends on tumour antigen presentation, and therefore lacking/diminishing of an appropriate peptide-HLA complex on the cell surface results in that peptide mediate immunotherapy will unlikely propagate an efficient anti-tumour CTL response. Adding to that scenario, the existence of the second signal transduction mediated by the costimulatory molecules is required to promote effective T cell activation and function. For instance, it has been reported that upregulation of CD40 molecule has an important immunomodulatory function, adding to its direct role in enhancement of antigen presentation by DCs and the subsequent elicitation of CTL function, CD40 engagement with its ligand promotes tumour lysis by CTLs through direct induction of apoptosis on cancerous cells (von Leoprechting, van der Bruggen *et al.* 1999). Collectively, it is apparent that there is a critical prerequisite to generate an efficient peptide-MHC system and deliver appropriate costimulatory molecule signals in order to initiate a basic step of vaccine development. Hence, in this study and a part of anti-tumour functions of IFN- $\gamma$ ,

upregulation of costimulatory molecules, such as HLA-class Ia molecules (A, B and C), MICA/MICB, CD80, CD86 and CD40 was assessed in the respective CML cells. Interestingly, in all cell lines treated, results show that there was a significant increase in the level of HLA-A, B, C molecules in comparison with non-treated samples. CD40 molecules were also significantly upregulated, whereas the expression of the other surface proteins studied (MICA/MICB, CD80 and CD86) remained essentially unaffected. The enhancement of MHC class Ia concurrent with the increase in the costimulatory CD40 signals upon IFN- $\gamma$  challenges indicates that IFN- $\gamma$  is capable of manipulating the process of immunoediting by promote priming and presentation of peptide-MHC complex to T cells, and according to Stewart, Abrams 2008, such findings are indicators of immune stimulation and cytotoxic killing of the abnormal cells (Stewart, Abrams 2008b). These trends were apparent in all cell lines studied and more prominent in TCC-S cells, however, primary leukaemic cells might differ from cell lines in the basal line level of HLA class Ia expression and the response to IFN- $\gamma$  treatment, tumour cells might display a large diversity in HLA class Ia expression and thus different efficiencies of tumour antigens might be eventually presented.

However, growing lines of evidence indicate that cancerous cells can employ IFN- $\gamma$  to diminish anti-tumour immune response and so promote their progression. It has been reported that IFN- $\gamma$  upregulate several inhibitory molecules involved in tumour immune evasion process, such as the non-classical MHC class Ib antigens, PD-L1, PD-L2, IDO1, CTLA-4, CIITA, CXCL12, etc. (Garcia-Diaz, Shin *et al.* 2017, Ayers, Lunceford *et al.* 2017, Zaidi, M. Raza, Davis *et al.* 2011). The non-classical MHC class Ib molecules, such as HLA-E and HLA-G, are known to favour tumour escape from immune-surveillance by engaging with the inhibitory receptors of CTLs and NK cells. Induction of PD-L1 and PD-L2 expression in tumour cells as well as in other stromal cells including immune infiltrating cells upon IFN- $\gamma$  also suppresses the activity of tumour-specific T cells and or NK cells by interacting with the PD-1 receptor (Abiko, Matsumura *et al.* 2015, Bellucci, Martin *et al.* 2015, Spranger, Spaapen *et al.* 2013). Moreover, Benci *et al.* demonstrated that prolonged IFN- $\gamma$  signalling in cancer cells can create epigenetic and transcriptional alterations in malignant cells which in turn induced multiple ligands for T cell inhibitory receptors that eventually promotes their PD-L1-independent resistance to immune checkpoint therapy (Benci, Xu *et al.* 2016). Herein, we therefore studied the possible potential upregulation of inhibitory surface molecules, such as HLA-E, HLA-G, FasL CD178 (CD95L) and PD-L1(CD274) in response to *in vitro* IFN- $\gamma$  treatment. Interestingly, we have shown that each cell line demonstrated a considerable increase in the expression of HLA-E and PD-L1, with a lower level of HLA-G upregulation, which was found to be constitutively high. These phenotypic modifications represent essential means by which the recognition function

of the effector cells can be misled, a situation might deliver a cancer protective milieu that favours tumour growth and spread. In addition, it has been reported that HLA-E upregulation could be induced by HLA-G, however this correlation cannot be clearly detected in our experiments, one possible reason is that the assessments of HLA-E and HLA-G molecules were herein limited on the membrane-bound type rather than assessing both surface and circulating types, a soluble molecule that known of its enhancement upon IFN- $\gamma$  treatment, so possibly there were upregulation of the soluble HLA-E and HLA-G molecules.

Regarding FasL, no consistent increase in the expression of surface FasL could be noticed within the range of our experimental design, although Xia, Li *et al* in 2017 were able to demonstrate the suppressor effects of IFN- $\gamma$  on K562 cell proliferation and induction of cell apoptosis by enhancing both Fas and FasL proteins expressions (Xia, Li *et al.* 2017).

IDO1 has gained emerging attention in both basic and clinical research essentially because of critically hostile microenvironment created upon its activation. While kynurenine derived from IDO1 activity promotes the development and activation of Tregs cells, the effector T cells are concomitantly suppressed due to tryptophan deprivation. In addition, a study conducted by Sharma *et al.* in 2017 reported that IDO activated Tregs greatly upregulated PD-L1 and PD-L2 expression on DCs (Sharma, Baban *et al.* 2007), and that the activation of such pathway (in addition to IDO direct effect) can indeed intensify the already immunosuppressed microenvironment. IDO induction has been detected in many solid malignancies and in a considerable number of AML patients indicating a substantial role of this enzyme in the disease pathophysiology and response to the therapy. Assessment of IDO transcript was therefore assessed in the respective cell lines, as well as its function by assessing the degradation product, kynurenine. RT-qPCR findings show that there was a significant upregulation of IDO in K562 and TCC-S. Kynurenine accumulation produced as a result of the activity of IDO1 on L-tryptophan in K562 cells implies that overall treatments cause translation of transcripts into functionally active IDO1 as reflected by a sharp production of kynurenine mainly in prolong incubations at 48- and 72-hours treatments. However, despite upregulation of the IDO1 transcripts in TCC-S cells detected by RT-qPCR, the enhancement seems to be non-functional one as reflected by unchanged levels of kynurenine in treated samples in relation to non-challenged control. On the other hand, IDO1 level/activity in KCL-22 after addition of IFN- $\gamma$  have shown no detectable changes within the limit of the experimental conditions.

At the same time, the expression of HAGE and WT1 were also assessed in the target cells at mRNA and protein levels under the same experimental conditions applied for

IDO induction mentioned above. In all cell lines and incubations applied, trends for mRNA upregulation were noticed, but were not of statistical significance, apart from mild upregulation of HAGE mRNA level in K562 cells from already low constitutive levels. However, it is accepted that significant effects might be induced at higher doses of IFN- $\gamma$  and/or after more prolonged incubations.

Several clinical studies of various malignancies have shown that IDO1 expression is associated with poor prognosis, thus, IDO inhibitors have emerged as promising therapeutics in the field of immunotherapy, mainly in combination with other treatment options, such as PD-1 inhibitors (Bilir, Sarisozen 2017). However, although early studies that were designed to involve the incorporation of IDO1 inhibitor with PD-1 inhibitor, indicated a quite promising antitumor activity with minimal toxicity, a phase 3 ECHO-301/KEYNOTE-252 ([accession number: NCT02752074](#)) was disappointing. The purpose of the study was to evaluate the efficacy and safety of IDO1 inhibitor with PD-1 inhibitor *versus* placebo with PD-1 inhibitor in untreated unresectable or metastatic melanoma in a total of 706 participants. Findings reveal that the addition of IDO1 enzyme inhibitor to PD-1 inhibitor did not associate with statistical significance in the clinical advantages over PD-1 inhibitor monotherapy, although the safety profile of this combination was comparable to the previous studies (Long, Dummer *et al.* 2018). As there was no improving in progression-free survival, the study will be stopped after failing to meet its primary endpoint. Collectively, it might be concluded that, although there is clear evidence of IDO1 inhibitors to modulate the immune process, it might be a matter of finding the right combination with IDO inhibition to effectively activate the immune responses.

## 5.5 Conclusion and chapter impacts

In this chapter, target cell lines were successfully prepared to be utilised to assess the efficacy of the putative vaccines in *in vitro* assays and *in vivo* model studies. In addition, the possible immunomodulatory effects of IFN- $\gamma$  treatments on the considered CML cells was assessed *in vitro*. Findings demonstrated a contradictory behaviour of IFN- $\gamma$  as it showed simultaneous induction of stimulatory and inhibitory molecules. Given the fact that HLA-E was significantly upregulated upon IFN- $\gamma$  and therefore in the future it might be an idea to combine the vaccine with an anti-HLA-E antibody, a subject which could be explored more in-depth in the future experiments in order to get better understanding about controlling the possible complex immune mechanisms.

## **6 Chapter VI: *In vitro* cytotoxic activity of CTLs derived from mice immunised with the HAGE- and WT1-ImmunoBody<sup>®</sup> vaccines**

In the previous chapter, targets were prepared in order to have cells either expressing or not the genes of the interest. In this chapter, these cells have been used as targets to evaluate the capability of T cells from immunised animals to specifically recognise and kill cancer cells in an antigen and HLA-A-restricted manner.

### **6.1 Introduction**

It is widely known that monitoring cellular immune responses during the course of clinical or pre-clinical trials is an important prerequisite for the development of cancer immunotherapies (Malyguine, Strobl *et al.* 2012). The key objective of immune monitoring is to assess the ability of the vaccine to generate vaccine-specific CTLs that specifically recognise and effectively kill cells expressing the relevant peptide(s). Cytotoxicity assays are fundamental means to study CTL functionality. The mechanism(s) involved in CTL-mediated cytotoxicity, assays for monitoring cytotoxicity and the key parameters that could affect monitoring of cell-mediated cytotoxicity in each assay will be briefly explained in the following sections.

#### **6.1.1 T Cell-mediated cytotoxicity**

Among the different components of the immune system, T cells and particularly CD8<sup>+</sup> cytotoxic T lymphocytes (CTLs) are the most effective cells in recognizing alterations occurring inside cells, such as viral infection and/or cancerous transformation. CTLs can destroy the transformed cells upon recognition of peptide-MHC-I complex expressed on the cell surface by one of at least three mechanisms (Andersen, M. H., Schrama *et al.* 2006). The first and the principal mechanism is direct cell-cell contact, granule-mediated killing. This killing encompasses powerful Ca<sup>2+</sup>-dependent events involving the release of specialised lytic granules that contain at least two distinct classes of effector proteins selectively expressed by CTLs. These granules are produced and stored in an active form inside the cytosol, but they do not perform killing until after their release. These lytic proteins are perforin which has the ability to create holes in the target cell membrane through which serine proteases called granzymes can enter target and induce apoptotic death (Smyth, Trapani 1995). The second mechanism by which CTLs induce cell contact killing is Fas/FasL interactions. Ligation of Fas (CD95) on the cell membrane of the targets with FasL on the cell

membrane of CTLs triggers a classical caspase-dependent apoptosis resulting in programmed cell death of targets in a  $\text{Ca}^{2+}$ -independent manner (Nagata, Golstein 1995). The third mechanism involves indirect target killing (contact independent) via the release of cytokines such as  $\text{IFN-}\gamma$  and  $\text{TNF-}\alpha$ . These cytokines are produced and released if TCR stimulation is maintained. Once  $\text{TNF-}\alpha$  engages its receptor on the target cell it causes an induction of caspase signalling pathway leading to the destruction of the target by apoptosis (Ratner, Clark 1993). Moreover,  $\text{IFN-}\gamma$  induces the expression of MHC class I and activates macrophages that offer both effector and APC functions, in addition to stimulating Fas-mediated target-cell lysis (Mullbacher, Lobigs *et al.* 2002). Whatever the mechanism, targeted cells undergoing apoptosis are engulfed rapidly by nearby phagocytic cells without contributing to or stimulating immune responses.

As a sequence of the features summarised above, cytotoxic T cells have been described as a rapid killer, highly selective action and have the propensity to destroy multiple targets bearing the same antigens, either simultaneously or serially. This prompt response is attributed to the fact that the effector molecules of the cytotoxic T cells are pre-synthesised and stored since the first encounter of a naïve cytotoxic precursor T cell with its specific antigen. Whenever a stable adhesion with the target cells takes place, an immediate signal is then sent to Golgi apparatus and the microtubule-organizing centre which induces the release of a concentrated dose of granules precisely at the point of contact with the target cell. That is why a lethal hit delivered by the narrowly focused action of CTLs allows such a specific killing of solitary target cells without damaging adjacent normal tissues. Therefore, cytotoxic T cells should, in theory, be able to attack and destroy any cells that undergo malignant transformation or are infected with a cytosolic pathogen (Janeway, Travers *et al.* 2005), and this is why immunotherapy is preferable over the traditional chemotherapy.

Like  $\text{CD8}^+$  CTLs, NK cells can also kill targets by granules production, FasL and TNF. However, unlike  $\text{CD8}^+$  CTLs, NK cells recognise the expression of stress signals or the absence/down-regulation of classical MHC class I molecules on the surface of the cells, whereas  $\text{CD8}^+$  CTLs require at least three signals to become activated; TCR ligation with specific peptide-MHC class I complex, co-stimulation and cytokine production signals (Zaritskaya, Shurin *et al.* 2010).

## 6.1.2 Assays for monitoring cell-mediated cytotoxicity

Many new techniques to determine *in vitro* cytotoxic activity of antigen-specific CTLs have emerged. However, one of the most convenient and oldest method used by many laboratories is the <sup>51</sup>chromium (<sup>51</sup>Cr) release assay. This assay was developed by Brunner around 50 years ago (Brunner, Mauel *et al.* 1968) and since that time, has been considered to be the 'gold-standard' approach for determining cytotoxic T cell activity. The principle of this assay relies on measuring the amount of radioactivity released from <sup>51</sup>Cr labelled target cells into the cell culture medium because of the cytolytic function of CTLs against targets. Radioactivity is measured in the supernatant collected from the co-culture medium either directly in a gamma counter or mixed with solid scintillant on a LumaPlate™ (Wallace, Hildesheim *et al.* 2004). However, although it has the advantage of being reproducible, relative low cost and easy to screen many targets in one run, this assay has several drawbacks. Firstly, radioisotope biohazard, low level of sensitivity and the needs to stimulate cytotoxic cells prior to testing which in turn might distort the activity of the original populations, poor labelling efficacy, and high spontaneous release from some targets (Kim, G., Donnenberg *et al.* 2007).

Another popular and highly sensitive technique has been to rely on the release of cytokines and granzyme B by the effector cells upon recognition of their targets which can be captured and visualised using the ELISpot assay. It was firstly introduced by Sedgwick and Holt in 1983 and relies on the ability of immobilised antibodies to capture proteins secreted by effector cells upon recognition of targets. Thereafter a biotinylated/streptavidin antibody recognising different parts of the same protein is used to amplify the signal. The complex is then visualised by the addition of a colorimetric substrate which forms an insoluble precipitate when catalysed by particular enzyme. Each spot represents the release of protein by one T cell. The larger is the spot the more of that protein has been released and the higher the number of spots the higher the frequency of cells that responded to the stimuli. Such molecules include IFN- $\gamma$ , TNF- $\alpha$ , granzymes or perforin. This assay has a number of advantages over the <sup>51</sup>Cr release assay as it provides both qualitative and quantitative information, has a higher level of sensitivity and specificity, and no concern of radioactive biohazard or problem with targets labelling efficiency (Malyguine, Strobl *et al.* 2012).

Currently, multiparametric data delivered by multi-colour flow cytometry enable the quantification of the functionally active cells at single cell levels and measurement of simultaneous expression of numerous markers (Smith, S. G., Smits, Joosten, van Meijgaarden, Satti, Fletcher, Caccamo, Dieli, Mascart, and McShane 2015). Multi-

colour flow cytometry has the specific advantage of enabling the simultaneous assessment of specific subset of responder T cells (such as CD4<sup>+</sup> or CD8<sup>+</sup> T cells), associated markers of differentiation (such as memory or activation markers), function markers (such as cytokine secretion and cytotoxicity-associated markers) and markers of proliferation (Smith, S. G., Smits, Joosten, van Meijgaarden, Satti, Fletcher, Caccamo, Dieli, Mascart, and McShane 2015b). However, the technique remains expensive and tedious when the assessment involves multiple ratios of target/effector cells, large number of target cells and many patients/mice, especially when the outcome is uncertain.

With the development of new technologies, additional killing assays have emerged. XCELLigence® Real Time Cell Analysis (RTCA), for example, allows a real-time cell monitoring and automatic data analysis. This assay is based on measuring cellular impedance; as cells grow and adhere on electronic plate (E-Plate), the flow of electric current between electrodes is gradually impeded (obstructed), therefore, the value of impedance increases, and when cells reach 100% confluence, the impedance reaches its highest value. In cytotoxicity assays, a decrease in impedance value (means cell detached from the plate surface) is the key indicator for tumour cells being attacked and killed by the effector T cells. This assay provides a highly sensitivity, label-free and real-time measurements (Erskine, Henle *et al.* 2012). The IncuCyte® S3 Live-Cell Analysis System is another highly sensitive technique that provides real-time cell death records by analysing images around the clock and translate them automatically into computing data. However, the main disadvantages of this assay are the cost and requirement for cell labelling.

Because RTCA and IncuCyte® systems are both very expensive, they were excluded from the presented study.

## 6.2 Rationale of the chapter

1. To assess the ability of CD8<sup>+</sup> CTLs derived from the spleen of animals immunised using the HAGE- or WT1-ImmunoBody® vaccines separately or in combination to recognise and kill relevant targets using <sup>51</sup>Cr release and ELISpot assays.
2. To characterise intracellular cytokine expression profiles of CD8<sup>+</sup> T cells derived from the respective ImmunoBody® vaccines upon recognition of specific antigens expressed by relevant targets in comparison with suitable control using multi-colour flow cytometry.

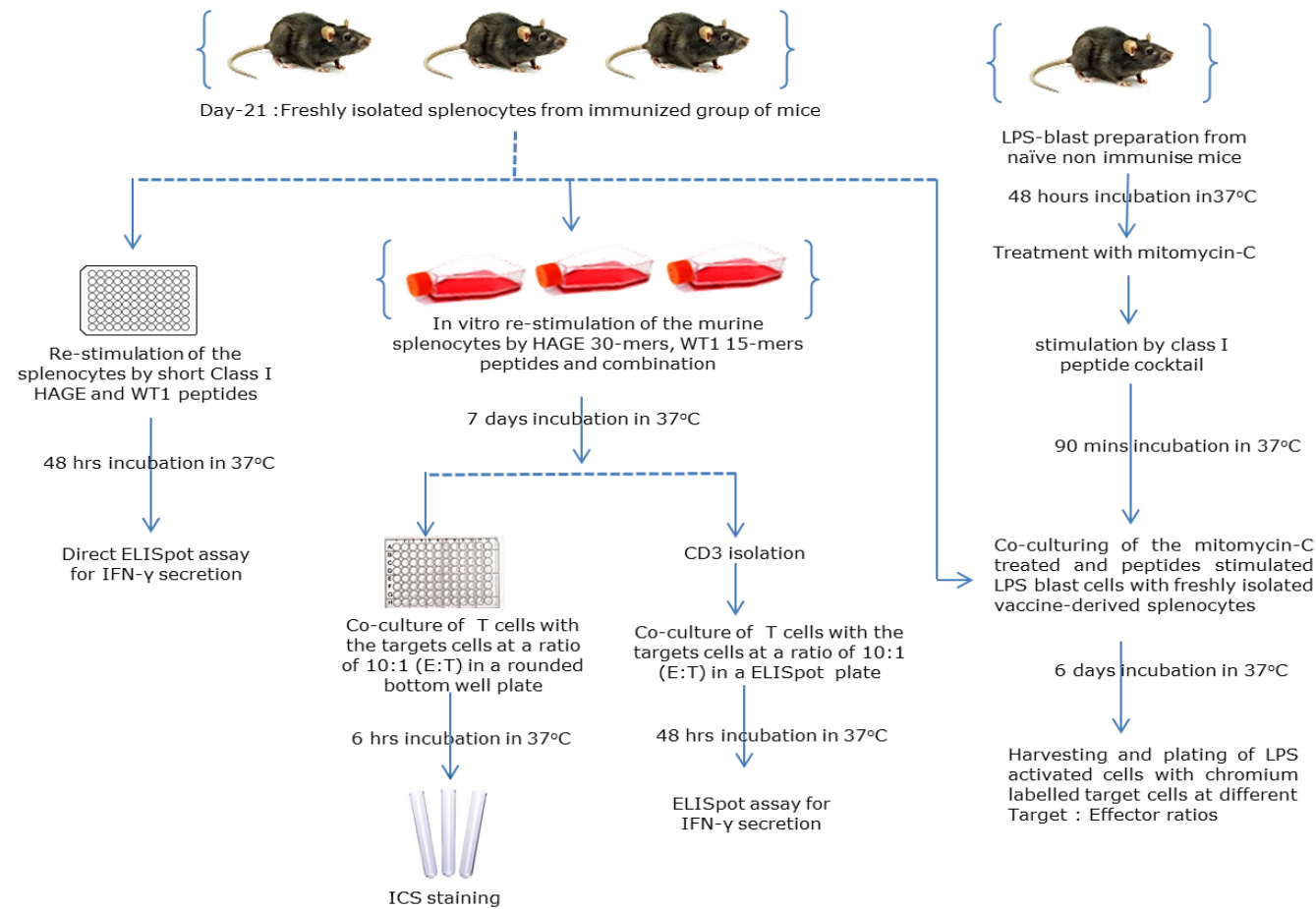


**Figure 6.1: A workflow summarises cytotoxicity assays used in the present study.**

For  $^{51}\text{Cr}$  release assay, T cells were stimulated with LPS-blast/peptide for 6 days before being incubated with labelled-targets, whereas for the ELISpot assay and intracellular staining (ICS), T cells were stimulated with either HAGE 30-mer, WT1 15-mer or both for 7 days before they were incubated with the respective targets.

## 6.3 Results:

### 6.3.1 Targets used in the cytotoxicity assay

The wild-type and modified leukaemic target cells (K562, TCC-S and KCL-22), the hB16 melanoma cells (with/without HAGE) and four groups of unpulsed T2 cells and T2 cells pulsed overnight with a cocktail of the immunogenic short class I peptides (HAGE, WT1, combined both HAGE and WT1) were used as targets *in vitro* to assess the effector function of CTLs derived from the candidate vaccines. Details related to their MHC, HAGE and WT1 expression are mentioned in Chapter-5. Table 6.1 summarises HLA-A2, HHDII, DR1, HAGE and WT1 expression, as determined at the protein level using Western blot and flow cytometry.

**Table 6.1: Summary information of targets used in the cytotoxicity assay**

#	Cell line	Targets	MHC status	HAGE expression	WT1 expression
1.	T2	Non-pulsed	HLA-A2 <sup>+</sup>	non	non
2.		HAGE pulsed	HLA-A2 <sup>+</sup>	+	-
3.		WT1 pulsed	HLA-A2 <sup>+</sup>	-	+
4.		HAGE&WT1 pulsed	HLA-A2 <sup>+</sup>	+	+
5.	K562	K562 Clon10	HHDII <sup>+</sup>	-	+
6.		K562 Clone5	HHDII <sup>+</sup>	+	+
7.	KCL-22	KCL-22 wild-type	HLA-A2 <sup>+</sup>	-	+
8.		KCL-22/HAGE <sup>+</sup>	HLA-A2 <sup>+</sup>	+	+
9.	TCC-S	TCC-S wild-type	HLA-A2 <sup>+</sup>	+	+
10.		TCC-S/ (WT1.shRNA)	HLA-A2 <sup>+</sup>	+	low
11.	B16	B16/HAGE <sup>-</sup>	HHDII <sup>+</sup> /DR1	-	+
12		B16/HAGE <sup>+</sup>	HHDII <sup>+</sup> /DR1	+	+

These targets were utilised to demonstrate *in vitro* cytotoxicity using <sup>51</sup>Cr release, IFN- $\gamma$  ELISpot and flow cytometry assays as it will be elaborated in the following sections. For the <sup>51</sup>Cr release assay, targets producing a ratio of more than 30% of spontaneous release/maximum release were excluded from analysis, as shown in Figure 9.3 (see Appendix).

## **6.3.2 Specific CTL activity against HAGE and WT1 peptide-pulsed T2 cells:**

### **6.3.2.1 HAGE- and WT1-ImmunoBody® vaccines individually or in combination provoke a specific cytotoxicity capable of lysing the cognate peptide-pulsed T2 cells using the <sup>51</sup>Cr release assay**

A well-established procedure to probe antigen recognition by CTLs in the field of vaccine development is the use of the TAP deficient T2 cells. Its principle relies on the induction of T2 cells to display an exogenously administered peptide in association with MHC class I molecules on the surface of T2 cells (Bossi, Gerry *et al.* 2013). The popularity of using these cells for monitoring the effectiveness of vaccines is attributed to their failure of correctly translocate the endogenous peptides to MHC loading site in the ER or Golgi apparatus due to the fact of the TAP deficiency (Hosken, Bevan 1990). T2 cells can therefore efficiently display exogenously administered peptide in a non-competitive environment.

In this study, splenocytes from non-immunised naïve and mice immunised with HAGE-, WT1-ImmunoBody® vaccines, individually and in combination, were co-cultured *in vitro* with mitomycin-C treated and peptide-pulsed LPS blast cells at a ratio of 1:5 (1 LPS blast cell: 5 T cell) for 6 days and then plated with <sup>51</sup>Cr labelled peptide-pulsed and non-pulsed T2 cells, typically at target: effector ratios of 1:100, 1:50, 1:25, 1:12.5 for 4 hours at 37°C. Supernatants (50µL) were then transferred onto Lumaplates and read with Top count beta scintillation counter. For this assay, T2 cells were loaded with a cocktail of the immunogenic short class I peptides the night before <sup>51</sup>Cr release assay. This involved the allocation of T2 cells into four groups of targets: HAGE-pulsed group, WT1-pulsed group, combined HAGE and WT1 pulsed group (at equal percentages) and non-pulsed group as a control for other groups. Each group of T2 targets (except the combined peptides group) were incubated overnight with their respective peptides at a final concentration of 50µg/mL together with 3µg/mL β<sub>2</sub>m in serum-free medium at 26°C, apart from the control (non-stimulating T2 group) to which no peptide was added. For the generation of the combined peptide-pulsed T2 cells group, a calculated number of cells from the overnight HAGE-pulsed and WT1-pulsed T2 cells were mixed together at equal percent just prior to <sup>51</sup>Cr labelling in order to give an equal opportunity for both peptides to be taken up by T2 cells, typically in a non-competitive state. By doing so, the problem of predominant peptides overtaken at expense of the weaker one was potentially avoided. These groups of targets were used for every cytotoxicity assay to assess the overall success of <sup>51</sup>Cr experiments.

In the first instance, lysis produced from the effect of the stimulated CTLs derived from naïve mice against each group of peptides-pulsed and non-pulsed T2 targets was compared to activity derived from immunised mice. It is obvious from data shown in Figure 6.2 that there is a trivial amount of lysis produced per each group, reflecting the low prevalence of effector cells against different groups of T2 targets in these mice.

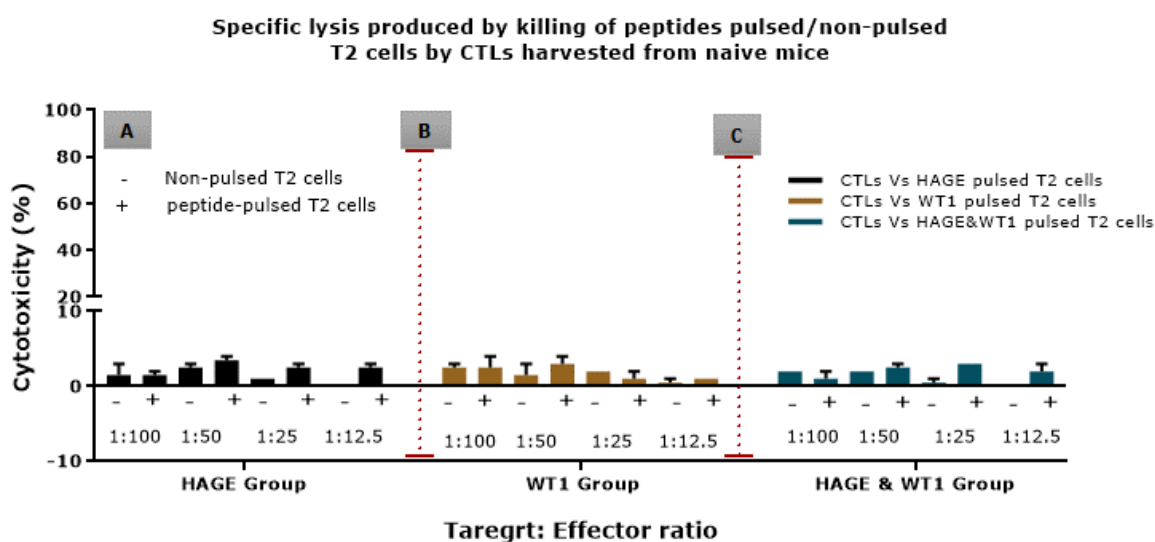


**Figure 6.2: Specific *in vitro* cytotoxicity induced by T cells derived from naïve mice against peptide pulsed/non-pulsed T2 cells, as assessed by the  $^{51}\text{Cr}$  release assay.**

Splenocytes from naïve mice were co-cultured *in vitro* with mitomycin-C treated and peptide-pulsed LPS T cells for 6 days and then plated with  $^{51}\text{Cr}$  labelled-peptide pulsed T2 cells at various ratios for 4 hours at  $37^{\circ}\text{C}$ , followed by measuring the release of  $^{51}\text{Cr}$  into the medium. Data are expressed as a percentage of lysis produced by the effect of T cells against peptide-pulsed in comparison to the non-pulsed T2 cells. Values are expressed as the mean  $\pm$  SEM of two independent experiments (1 mouse/group).

On the other hand, results in Figure 6.3 demonstrate that lysis produced by effector cells from the HAGE, WT1 and combined HAGE and WT1 immunised groups is significantly higher than their respective controls (non-peptide pulsed T2 cells) in all ratios used with  $****p\text{-value} < 0.0001$ . This indicates that these peptides either individually or in combination were taken up by T2 cells and displayed in association with MHC class I molecules on their surface, and that CTLs specifically recognised and efficiently killed these targets upon the engagement of TCR with peptide-MHC class I complex.

Additionally, comparing data in Figure 6.2 with that from immunised mice in Figure 6.3 provides evidence that our ImmunoBody<sup>®</sup> vaccines are transcribed into mRNA and then protein which are then endogenously processed and expressed on the surface of APCs in sufficient amount to enable the generation of CTLs repertoires.

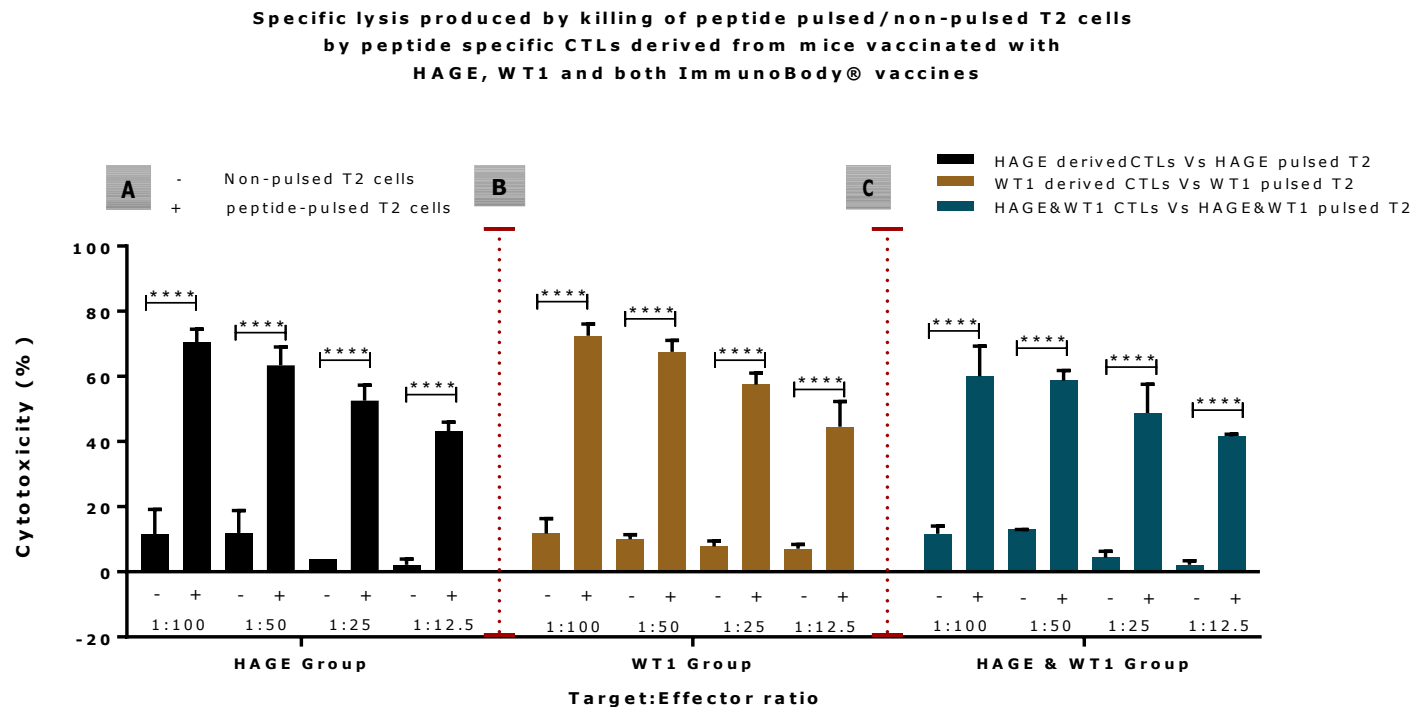


**Figure 6.3: Specific *in vitro* cytotoxicity induced by CTLs derived from ImmunoBody® immunised groups of mice against peptide pulsed/non-pulsed T2 cells, as assessed by the  $^{51}\text{Cr}$  release assay.**

Splenocytes from mice immunised with HAGE, WT1 and both were co-cultured *in vitro* with mitomycin-C treated and peptide-pulsed LPS T cells for 6 days and then plated with  $^{51}\text{Cr}$  labelled-target cells at various ratios for 4 hours at  $37^\circ\text{C}$ , followed by measuring the release of  $^{51}\text{Cr}$  into the medium. Data are expressed as a percentage of T2 lysis by the corresponding effector CTLs in comparison to non-peptide pulsed T2 cells. Values are expressed as the mean  $\pm$  SEM and the level of the significance was assessed using Two Way ANOVA followed by Tukey's multiple comparisons test. n=3 (3 mice/group),

### **6.3.2.2 HAGE and WT1 vaccines elicit peptide-specific CTLs upon recognition of specific peptide-pulsed T2 cells, as assessed using the IFN- $\gamma$ ELISpot assay.**

In the field of immunotherapy, the IFN- $\gamma$  ELISpot assay has gained increasing popularity to monitor both frequency and function of CTLs, as it was used here, to confirm the results obtained by the  $^{51}\text{Cr}$  release assay. However, IFN- $\gamma$  can also be produced by other immune cells, and thus isolation of CD3<sup>+</sup> cells was therefore required. It is also important to compare data produced from ELISpot with  $^{51}\text{Cr}$  to cross-correlate the functionality and cytotoxicity of the generated effector CTLs. In this context, splenocytes derived from groups of mice immunised with HAGE, WT1, and combined vaccines were isolated and stimulated individually with the HAGE long 30-mer peptide, WT1 long 15-mer and in combination, respectively at a dose of 1 $\mu\text{g}/\text{mL}$  peptide and 50U/mL mIL-2 per group for 7 days. Cells were then washed and CD3<sup>+</sup> cells were isolated, as indicated in the Methodology ([Section:2.2.6.4](#)) to ensure that other cells do not mask measurements of effector T cell function. The purity of populations before and after isolation (>95%) was assessed using flow cytometry, the gating strategy and data for which are provided in the Appendix (Figure 9.2). The isolated cells were counted and plated at 0.1x10<sup>6</sup> cells/well in IFN- $\gamma$  coated ELISpot plate and co-cultured with peptide-pulsed/non-pulsed T2 cells at a ratio of 1:10 (target: effector) for 48 hours at 37°C.

Figure 6.4 demonstrates the number of IFN- $\gamma$  secreting CTLs against T2 cells in their corresponding groups, where the frequency of cells responding to T2 pulsed with peptide is significantly greater than the one produces when non-pulsed T2 cells are being used in all groups with *\*\*\*p-value*<0.0001. Correlation of these data with those obtained from  $^{51}\text{Cr}$  release assay confirmed that both HAGE- and WT-ImmunoBody<sup>®</sup> vaccines either alone or in combination were able to stimulate immune responses against HAGE and WT1-vaccine-derived peptides expressed by the targets. Like the  $^{51}\text{Cr}$  release assay, the ELISpot assay does not show superiority of the combined vaccines over the individual ones when T2 cells are used, but neither do they show antigen competition.

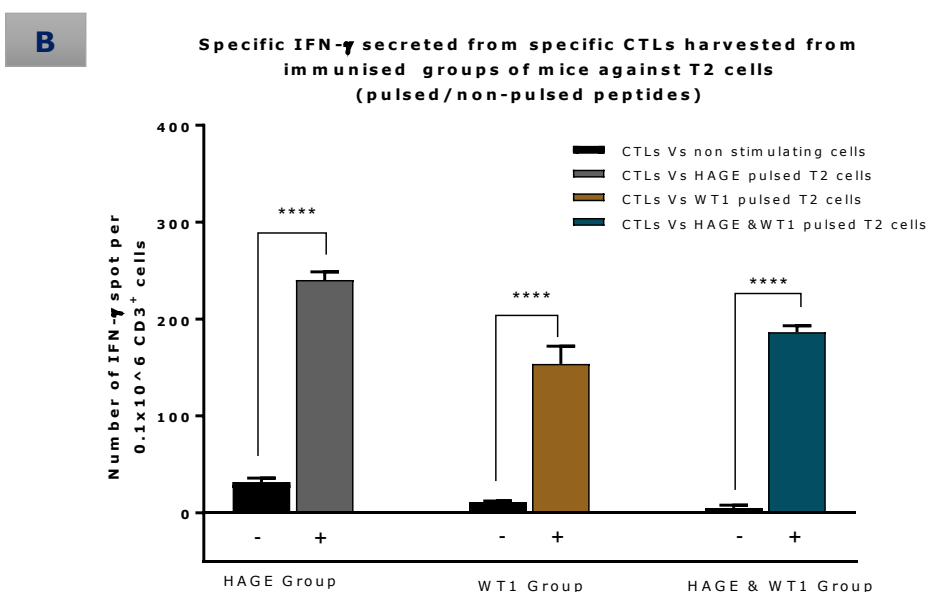
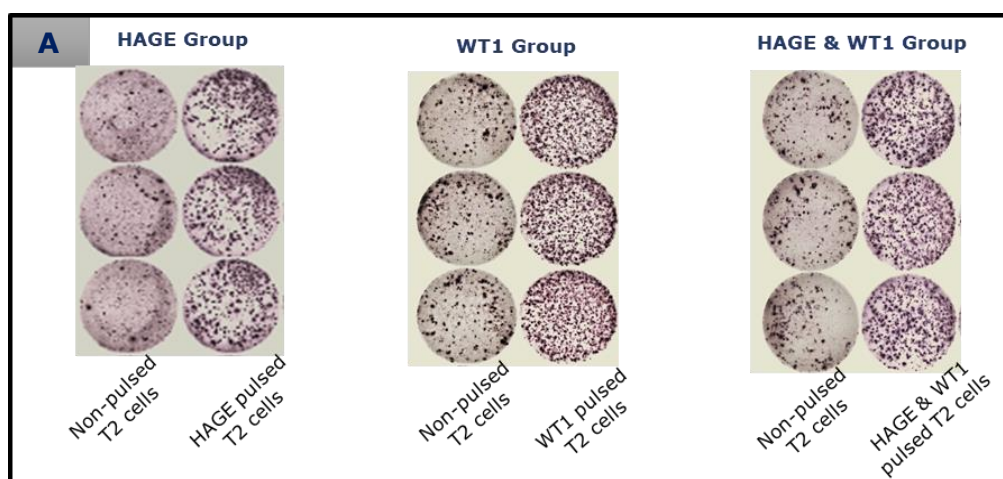


**Figure 6.4: IFN- $\gamma$  response of CTLs produced by HAGE- and WT1-specific CTLs against peptide-pulsed T2 cells, as assessed using the IFN- $\gamma$  ELISpot assay.**

Splenocytes were stimulated for 1-week, pure CD3 $^+$  cells were isolated and plated at  $0.1 \times 10^6$  cells/well and co-cultured with peptide pulsed/non-pulsed T2 cells at a ratio of 10:1, respectively. **(A)** Representative ELISpot well images demonstrate the number of spots produced per group. **(B)** Bar chart shows the number of spots produced from each group, expressed as an average number of IFN- $\gamma$  spots per well produced by CTLs derived from the immunised mice with respective vaccines in comparison with non-stimulated T2 cells, background was subtracted in each group. Values are expressed as the mean  $\pm$  SEM of three independent experiments (3 mice/group), and the level of the significance was assessed using TWO Way ANOVA followed by Tukey's multiple comparisons test.

### **6.3.3 Specific CTL activity against HHDII<sup>+</sup>/HAGE<sup>+</sup> and HHDII<sup>+</sup>/HAGE<sup>-</sup> K562 cells**

#### **6.3.3.1 HAGE- and WT1-ImmunoBody<sup>®</sup> vaccines either individually or in combination provoke a specific cytotoxicity capable of lysing K562/HHDII<sup>+</sup> (with/without HAGE), as assessed using the <sup>51</sup>Cr release assay**

In the previous chapter, K562 cells were genetically modified, and two clones were generated. K562/HHDII<sup>+</sup>/HAGE<sup>+</sup> (Clone5) and K562/HHDII<sup>+</sup>/HAGE<sup>-</sup> (control, Clone10) were used as targets to test and compare CTL responses produced using different vaccine strategies.

Splenocytes harvested from immunised animals (HAGE, WT1 and combination) and naïve mice were co-cultured *in vitro* with mitomycin-C treated and peptide-pulsed LPS blasts at ratio of 1:5 (LPS blast:T cell) for 6 days. Cells were then plated with <sup>51</sup>Cr labelled-Clone5 and -Clone10 K562 cells at various target:effector ratios (1:100, 1:50, 1:25, and 1:12.5) for 24 hours at 37°C. Supernatants were then transferred onto Lumaplates and read using a Top count beta scintillation counter.

In the previous section, it was demonstrated that LPS and peptide-stimulated T cells derived from these vaccines could recognise and kill peptide-pulsed T2 cells. In Figure 6.5, the same CTLs are now showing that they can specifically recognise the naturally endogenously processed antigen against which mice were vaccinated. Indeed, in a group which received the HAGE only, vaccine shows a significant difference between the killing of Clone5 which expresses HAGE and Clone10 which does not (shown in A), while the cells derived from mice immunised with WT1-ImmunoBody<sup>®</sup> demonstrate an equal killing between Clone5 and Clone10 because both express the WT1 antigen and originally, they derived from the same clone (shown in B). Interestingly, while cells derived from the mice immunised with both HAGE- and WT1-ImmunoBody<sup>®</sup> vaccines (C) could kill both clones, a significantly higher killing of Clone5 was achieved, a finding which is indicative of a synergistic effect of the combined vaccines, as is illustrated in Figure 6.6, at \*\*\*\**P*-value<0.0001 in almost all ratios used.

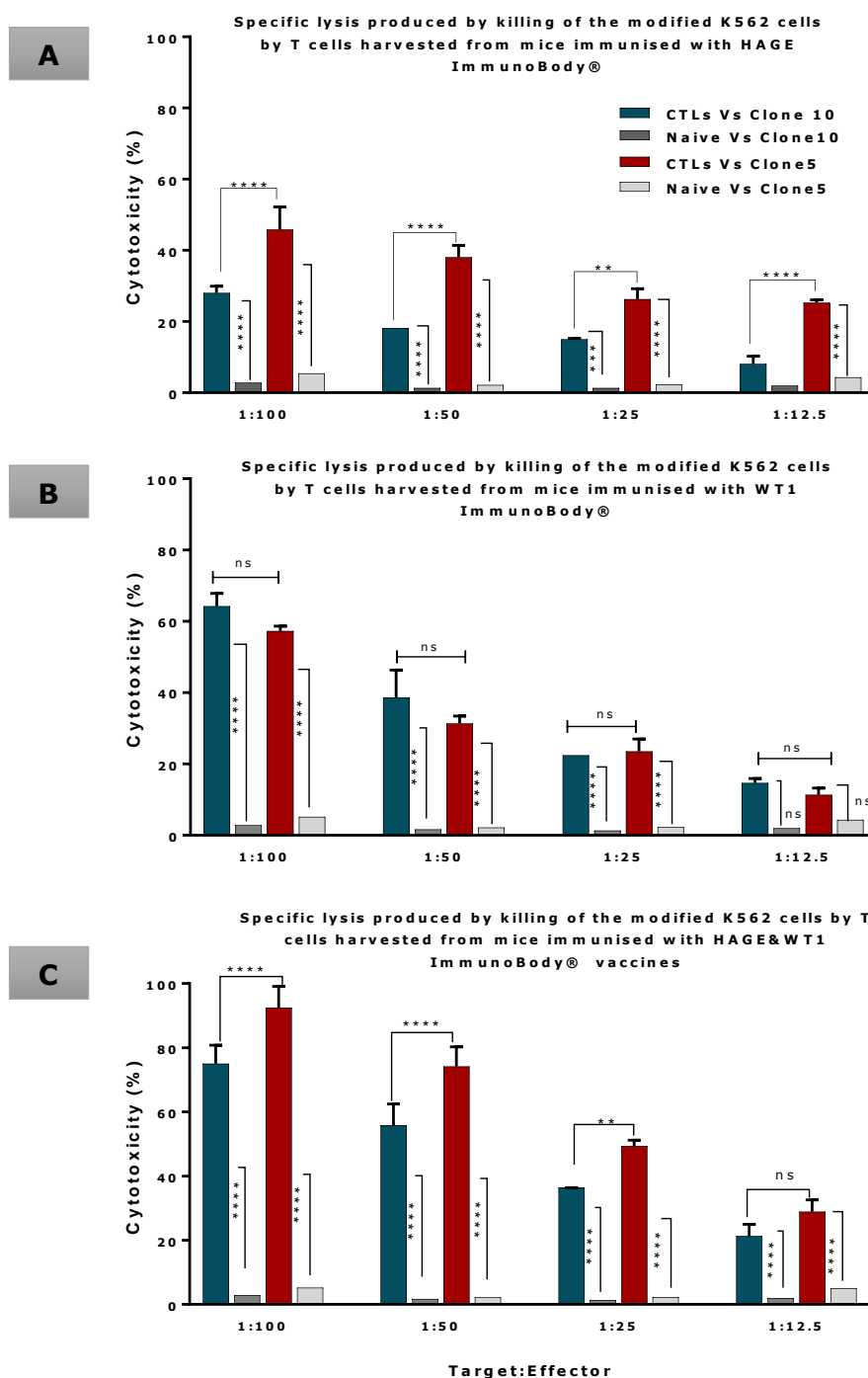


**Figure 6.5: Specific *in vitro* cytotoxicity induced by CTLs derived from ImmunoBody® vaccinated groups of mice against K562 cells, as assessed using the  $^{51}\text{Cr}$  release assay.**

Splenocytes from mice immunised with HAGE, WT1 and combined, and from naïve non-immunised mice were co-cultured *in vitro* with mitomycin-C treated and peptide-pulsed LPS T cells for 6 days and then plated with  $^{51}\text{Cr}$  labelled-K562 cells at various ratios for 24 hours at  $37^\circ\text{C}$ , followed by measuring  $^{51}\text{Cr}$  in the medium. Values are expressed as the mean $\pm$ SEM of three independent experiments (3mice/group) and the level of the significance was assessed using Two Way ANOVA followed by Tukey's multiple comparisons test. Results demonstrate that percentage of lysis generated from the combined vaccines is higher than individual vaccines.

**Percentage of the specific lysis produced by killing of Clone5 K562 by T cells harvested from mice immunised with HAGE&WT1 ImmunoBody® vaccines (individually and in combination)**

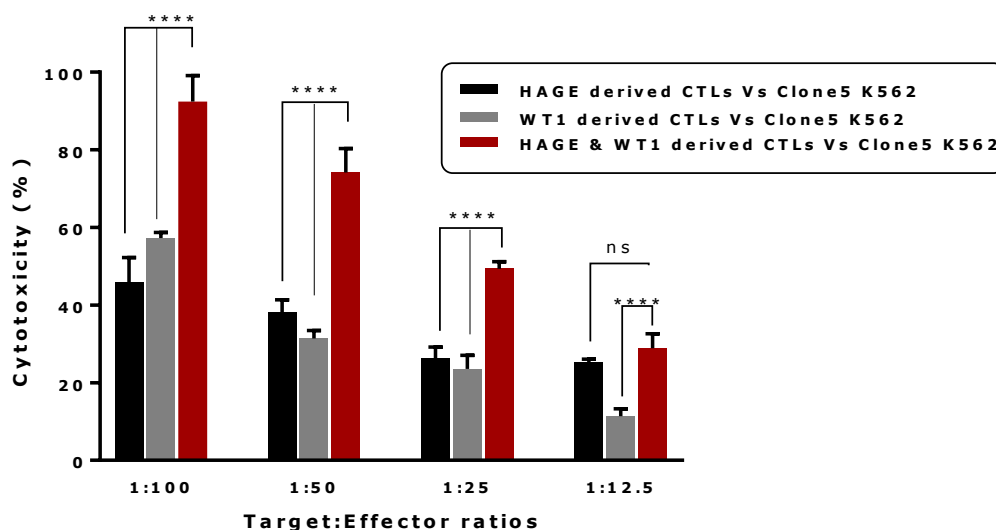


**Figure 6.6: Specific *in vitro* cytotoxicity induced by the CTLs from ImmunoBody® immunised mice against the modified K562 “Clone5” cells, as assessed using the  $^{51}\text{Cr}$  release assay.**

Splenocytes from mice immunised with HAGE, WT1 and both were co-cultured *in vitro* with mitomycin-C treated and peptide-pulsed LPS T cells for 6 days and then plated with  $^{51}\text{Cr}$  labelled-K562 cells at various ratios for 24 hours, followed by measuring the release of  $^{51}\text{Cr}$  into the medium. Values are expressed as the mean  $\pm$  SEM of three independent experiments (3 mice/group), and the level of the significance was assessed using Two Way ANOVA followed by Tukey's multiple comparisons test. Results demonstrate that lysis produced upon the administration of the combined vaccines is significantly higher than when either vaccine is administered individually at all ratios studied.

Overall, these findings indicate that both HAGE- and WT1-ImmunoBody® derived peptides either individually or in combination were endogenously processed and displayed in association with MHC class I molecules on the surface of APCs leading to the development of professional CTLs which are able to specifically recognise and kill these targets. They also indicate that the combination approach induces better CTL responses.

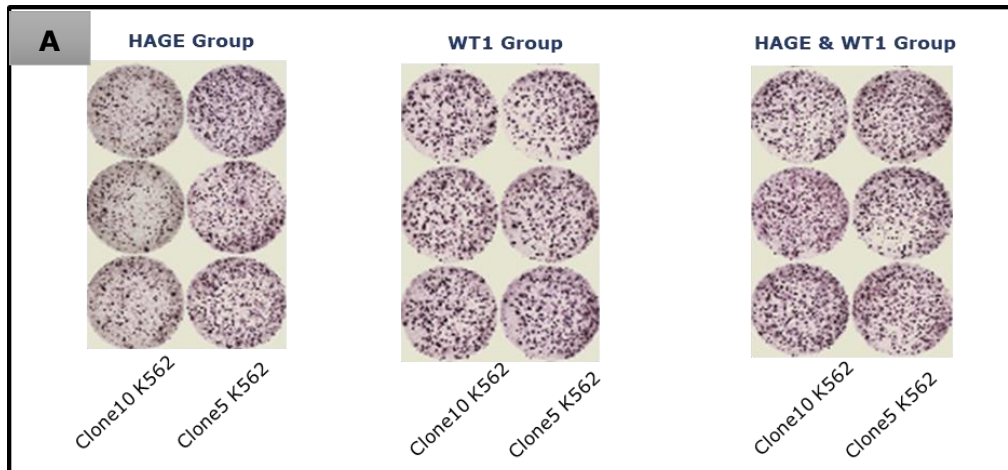
### **6.3.3.2 HAGE and WT1 vaccines elicit a peptide specific CTLs IFN- $\gamma$ secretion response upon recognition of K562/HHDII<sup>+</sup> (with/without HAGE), as assessed using the IFN- $\gamma$ ELISpot assay**

Splenocytes from each group of mice were stimulated with long 30-mer HAGE peptide, long 15-mer WT1 peptide and a combination of these, respectively at a dose of 1 $\mu$ g/mL and 50U/mL murine IL-2 per group for 7 days. After incubation, CD3<sup>+</sup> cells were isolated and then plated at 0.1 $\times$ 10<sup>6</sup> cells per well in IFN- $\gamma$  coated ELISpot plate and co-cultured with the modified K562/HHDII<sup>+</sup> cells (with/without HAGE) Clone5 and Clone10, respectively at ratio of 1:10 (target: effector) for 48 hours at 37<sup>o</sup>C.

The produced spots shown in the Figure 6.7 point out the number of IFN- $\gamma$  secreted from CD3<sup>+</sup> cells against the considered targets in their respective group. Interestingly, there is significant more killing of Clone5 than Clone10, with \*\*\*\**p*-value<0.0001. These data are consistent with the findings of the <sup>51</sup>Cr assay, and both assays are confirming that HAGE vaccine can produce CTLs with high degree of specific recognition and killing.

For the WT1 group, the IFN- $\gamma$  response of CTLs against both clones is also high, and this is not surprising given the constitutive expression of WT1 by both. This result is also in line with findings from the <sup>51</sup>Cr release assay, reflecting the ability of WT1 to induce an appropriate immune response.

With respect to the combined vaccines, IFN- $\gamma$  production induced by both clones were similar. However, unlike the <sup>51</sup>Cr release assay, the ELISpot does not demonstrate a superiority of the combined approach over the individual approaches.

**B**

Specific IFN- $\gamma$  response generated from specific CTLs harvested from different groups of vaccinated mice against the modified k562 clones (HHDII<sup>+</sup>HAGE-/+)

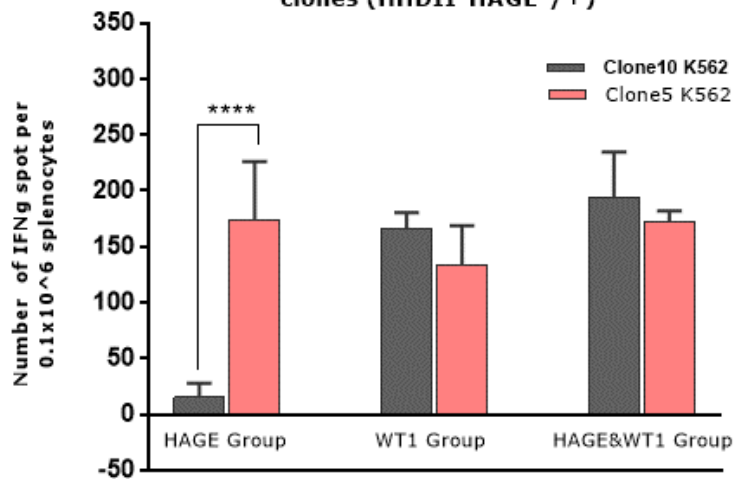


**Figure 6.7: IFN- $\gamma$  secretion by HAGE- and WT1-specific CTLs in response to K562/HHDII<sup>+</sup> cells (with/without HAGE) cells, as assessed using the IFN- $\gamma$  ELISpot assay.**

Splenocytes were stimulated for 1-week, pure CD3<sup>+</sup> cells were isolated and plated at  $0.1 \times 10^6$  cells/well and co-cultured with K562/HHDII<sup>+</sup> cells (with/without HAGE) at ratio of 10:1, respectively. (A) Representative ELISpot well images demonstrate the number of spots produced per group. (B) Bar chart shows the average number of IFN- $\gamma$  spots per well produced by CTLs from immunised mice with the respective vaccines against Clone10 and Clone5 after backgrounds being subtracted. Values are expressed as the mean  $\pm$  SEM of three independent experiments (3 mice/group), and the level of significance was assessed using One Way ANOVA followed by Tukey's multiple comparisons test.

## **6.3.4 Specific CTL activity against KCL-22 and TCC-S cells**

### **6.3.4.1 HAGE- and WT1-ImmunoBody® vaccines either individually or in combination induce specific cytotoxicity capable of lysing KCL-22 cells (with/without HAGE)**

In addition to K562 cell, specific CTL activity against KCL-22 cells (with/without HAGE) was evaluated. These cells were chosen to ensure the reproducibility of the results obtained with K562 cells. Accordingly, splenocytes from animals immunised using the three regimes and naïve mice were isolated and stimulated in a similar way to that previously described for K562 experiments and incubated with <sup>51</sup>Cr labelled KCL-22 cells with/without HAGE.

Figure 6.8 demonstrates the specific killing of the HAGE<sup>+</sup> cells when the effector cells were derived from mice immunised with HAGE vaccine only (shown in A), and the killing of both KCL-22 (HAGE<sup>+</sup>) and KCL-22 (HAGE<sup>-</sup>) for those derived from mice immunised with WT1 vaccine alone (shown in B), due to the existence of WT1 in both targets. Interestingly, when effector cells from mice immunised with both vaccines were used against those, more KCL-22 (HAGE<sup>+</sup>/WT1<sup>+</sup>) killing was achieved at around 80% than when the effector cells were derived from either WT1 (58%) or HAGE (60%) only vaccine. As shown in Figure 6.9 (at 1:100 ratio), this result confirms that the combined approach is more advantageous than the single vaccine approach.

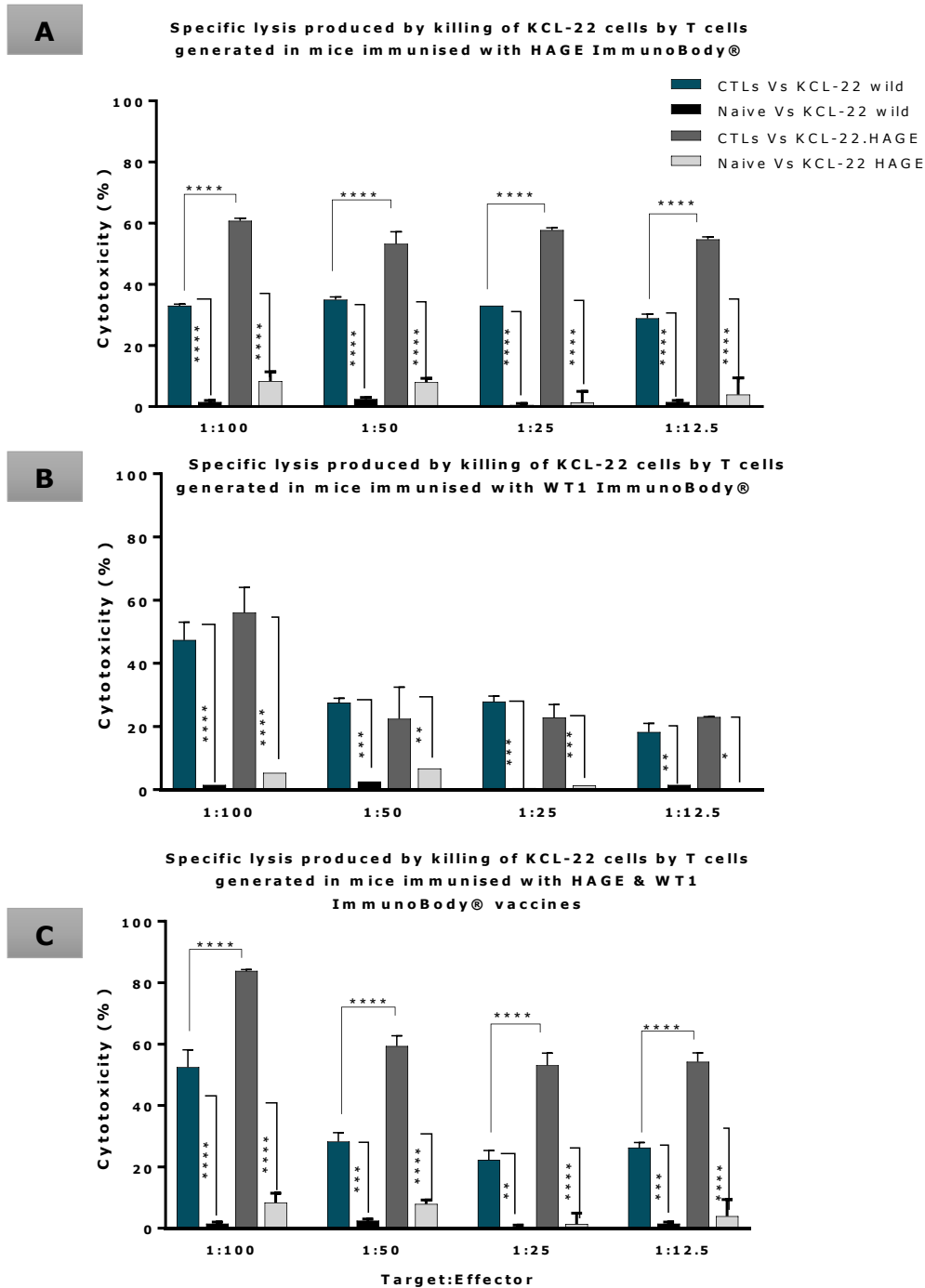


**Figure 6.8: Specific *in vitro* cytotoxicity induced by CTLs derived from ImmunoBody® immunised mice against KCL-22 cells (with/without HAGE), as assessed using the  $^{51}\text{Cr}$  release assay.**

Splenocytes from mice immunised with HAGE, WT1 and both, and also from non-immunised naïve mice were co-cultured *in vitro* with mitomycin-C treated and peptide-pulsed LPS T cells for 6 days and then plated with  $^{51}\text{Cr}$  labelled-KCL-22 cells at various ratios for 24 hours at  $37^\circ\text{C}$ , followed by measuring the release of  $^{51}\text{Cr}$  into the medium. Values are expressed as the mean $\pm$ SEM of two independent experiments (3 mice/group), and the level of the significance was assessed using Two Way ANOVA followed by Tukey's multiple comparisons test.

Specific lysis produced by killing of KCL-22.HAGE<sup>+</sup> cells by T cells generated in mice immunised with HAGE & WT1 ImmunoBody<sup>®</sup> vaccines (individually and in combination)

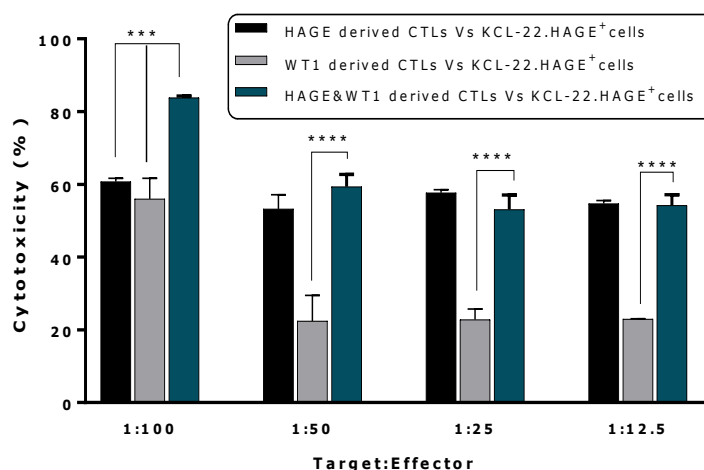


**Figure 6.9: Specific *in vitro* cytotoxicity of CTLs from ImmunoBody<sup>®</sup> immunised mice against KCL-22/HAGE<sup>+</sup> cells, as assessed using the <sup>51</sup>Cr release assay.**

Splenocytes from mice immunised with HAGE, WT1 and both were co-cultured *in vitro* with mitomycin-C treated and peptide-pulsed LPS T cells for 6 days and then plated with <sup>51</sup>Cr labelled KCL-22/HAGE<sup>+</sup> cells at various ratios for 24 hours, followed by measuring the release of <sup>51</sup>Cr into the medium. Values are expressed as the mean±SEM of two independent experiments (3 mice/group), and the level of significance was assessed using Two Way ANOVA followed by Tukey's multiple comparisons test. Results demonstrate that the lysis produced upon the administration of the combined vaccines is significantly higher than when either vaccines are administered individually.

#### 6.3.4.2 HAGE- and WT1-ImmunoBody<sup>®</sup> vaccines induce specific cytotoxicity capable of lysing TCC-S cells (with/without WT1)

As mentioned in Chapter-5, TCC-S cells were shown to naturally express both WT1 and HAGE proteins and HLA-A2 on their surface. In order to test the cytotoxic activity of ImmunoBody<sup>®</sup> derived CTLs induced by the individual and the combined vaccines, and specifically to test WT1-specific CTLs recognition, i.e. what will be happened if the WT derived CTLs do not encounter WT1 peptide expressed on the target? The wild-type TCC-S cells (HAGE<sup>+</sup>/WT1<sup>+</sup>) were knocked down of WT1 using shRNA plasmid to produce modified WT1.shRNA TCC-S cells (HAGE<sup>+</sup>/WT1<sup>Low</sup>), Both targets were then used as a separate tool to compare CTLs immune responses produced from three occasions of vaccination, together with a naïve group using <sup>51</sup>Cr release assay.

Figure 6.10 firstly highlights the level of significant difference in the percentages of lysis produce by the indicated group in comparison to the naïve non-immunised mice, which confirming overall vaccine capability to induce *in vitro* cytotoxicity.

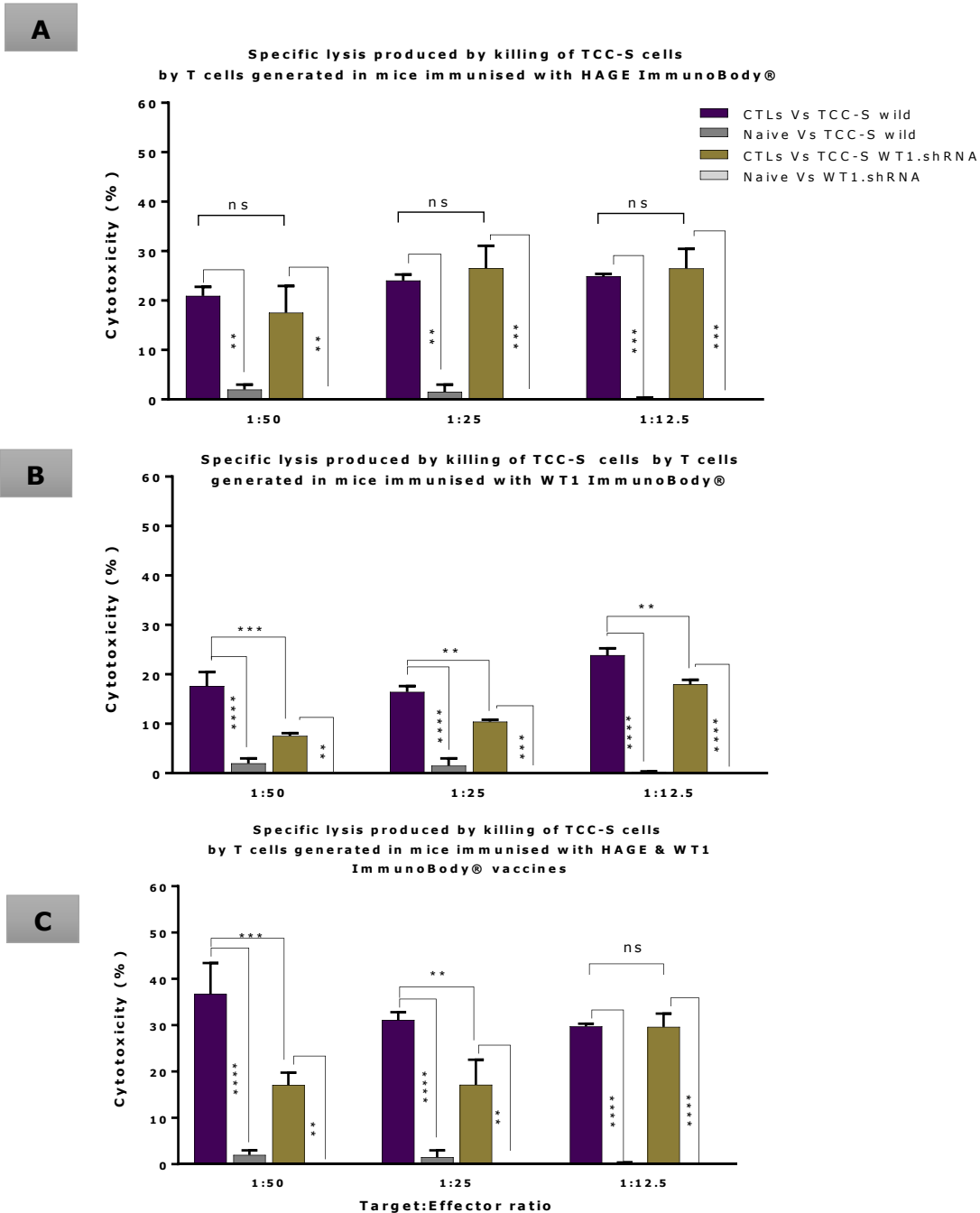


**Figure 6.10: Specific *in vitro* cytotoxicity of CTLs from ImmunoBody® immunised mice against wild type and WT1-shRNA TCC-S cells, as assessed using the  $^{51}\text{Cr}$  release assay.**

Splenocytes from mice immunised with HAGE, WT1, and both, and from non-immunised naïve mice were co-cultured *in vitro* with mitomycin- C treated and peptide-pulsed LPS T cells for 6 days and then plated with  $^{51}\text{Cr}$  labelled-TCC-S cells at various ratios for 24 hours at  $37^\circ\text{C}$ , followed by measuring the release of  $^{51}\text{Cr}$  into the medium. Values are expressed as the mean $\pm$ SD of two independent experiments (3 mice/ group) and the level of the significance was assessed using Two Way ANOVA, followed by Tukey's multiple comparisons test.

The figure also demonstrates the capacity of CTLs from different animal groups to recognise wild-type (HAGE<sup>+</sup>/WT1<sup>+</sup>) and WT1.shRNA (HAGE<sup>+</sup>/WT1<sup>low</sup>) TCC-S cells. There was no difference in the level of cytotoxicity against both cells types elicited by CTLs from HAGE-immunised mice (shown in A), which was expected since both targets are expressing HAGE. There was a significant difference in the killing of TCC-S (HAGE<sup>+</sup>/WT1<sup>+</sup>) cells and WT1.shRNA TCC-S cells by CTLs from mice immunised against WT1 (shown in B), thereby highlighting WT1-specific killing. The killing of these target cells by CTLs from animals immunised using the combined approach was also evaluated (shown in C). Data in Figure 6.11 demonstrate an increase in the percentage of cytotoxicity against TCC-S wild-type (almost doubled at 1:50 ratio) from ~20% at the individual vaccines to ~38% when both are incorporated, suggesting amplified recognition and killing by the HAGE-specific and WT1-specific CTLs against this co-expressing peptides targets.

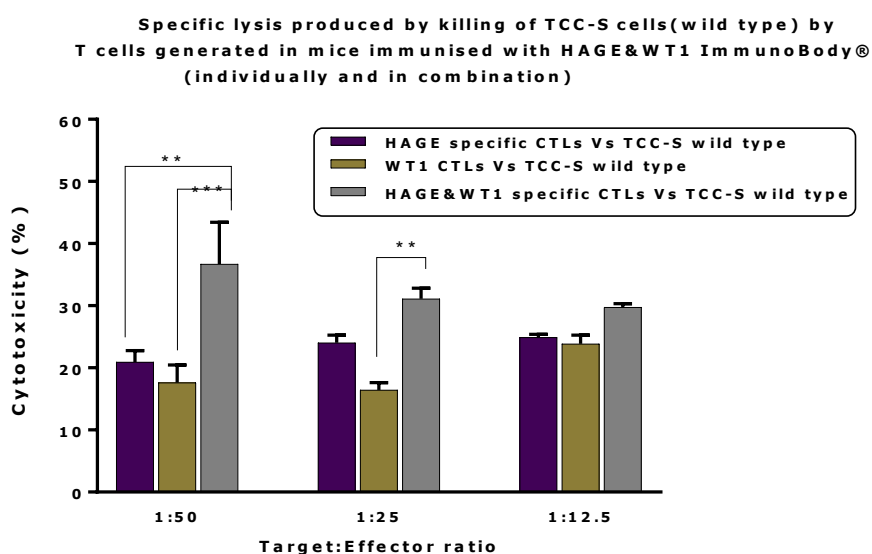


**Figure 6.11: Specific *in vitro* cytotoxicity of CTLs from ImmunoBody® immunised mice against the wild type TCC-S (HAGE<sup>+</sup>/WT1<sup>+</sup>) cells, as assessed using the <sup>51</sup>Cr release assay.**

Splenocytes from mice immunised with HAGE, WT1 and both were co-cultured *in vitro* with mitomycin-C treated and peptide-pulsed LPS T cells for 6 days and then plated with <sup>51</sup>Cr labelled-TCC-S cells at various ratios for 24 hours, followed by measuring the release of <sup>51</sup>Cr into the medium. Values are expressed as the mean±SEM of three independent experiments (3mice/group) and the level of the significance was assessed using Two Way ANOVA followed by Tukey's multiple comparisons test. Results demonstrate that lysis produced upon the administration of the combined vaccines is significantly higher than when either vaccine is administrated individually.

## 6.3.5 Specific CTL activity against humanised B16 cells

### 6.3.5.1 HAGE- and WT1-ImmunoBody<sup>®</sup> vaccines either individually or in combination provoke specific cytotoxicity capable of lysing <sup>h</sup>B16 cells (with/without HAGE)

In the previous chapter, the “humanised” B16 murine melanoma cell line (with/without HAGE) was described, wherein a constitutive WT1 protein expression was confirmed. Herein, this cell line was used to assess the capability of HAGE- and WT1-ImmunoBody<sup>®</sup> vaccines derived CTLs to provoke *in vitro* cytotoxic activity. By confirming this, cells then used to establish tumours in the HHDII/DR1 double transgenic mice. However, the WT1-ImmunoBody<sup>®</sup> construct was designed to carry the gene coding for the 15-mer human WT1 (VRDLNALLPAVPSLG) peptide which has been inserted in the heavy variable region (see vector map in Figure 4.5 A/ Chapter-4). As B16 is a murine cell line, then it should express the murine type of WT1. As a consequence, WT1 sequences from both species were aligned to assess the degree of homology using “Align Sequences Protein BLAST” tool available at: [https://blast.ncbi.nlm.nih.gov/Blast.cgi?PROGRAM=blastp&PAGE\\_TYPE=BlastSearch&BLAST\\_SPEC=blast2seq&LINK\\_LOC=blasttab](https://blast.ncbi.nlm.nih.gov/Blast.cgi?PROGRAM=blastp&PAGE_TYPE=BlastSearch&BLAST_SPEC=blast2seq&LINK_LOC=blasttab).

We have found that the homology between the sequences is 92% and there is only a single amino acid difference in the 15-mer human WT1 peptide (VRDLNALLPAV**P**SLG) and the corresponding murine WT1 sequence (VRDLNALLPAV**S**SLG) (underlined bold in both above sequences, serine (S) in murine WT1 is replaced by Proline (P) in human WT1). In the context of HLA binding affinity, it was previously demonstrated that the predicted binding scores of the long 15-mer human WT1/P1 (VRDLNALLPAVPSLG) and the short 9-mer peptides derived from it; WT1/P3 (ALLPAVPSL) and WT1/P5 (DLNALLPAV) were 31, 33, 27, respectively using the SYFPEITHI score (see Table 4.2 / Chapter-4). Hence, it was necessary to rescore peptides derived from the murine WT1 and compare with human once again to ensure that will not affect binding score predicated by the same software. After being rescored, results indicate that almost identical values were obtained, details in Figure 6.12 and Figure 6.13.

Regarding the HAGE-ImmunoBody<sup>®</sup> construct, it was also designed to encode the human HAGE protein, but it was assumed that will not create a problem since the <sup>h</sup>B16 cell line was already transfected with a construct engineered to express the human HAGE sequence.



**Figure 6.12: A comparative alignment between the murine and human WT1 protein sequences using "Align Sequences Protein BLAST" tool.**

(A) and (B) sequence of the murine and the human (isoform B) WT1 proteins where the peptide of the interest is highlighted by green. (C) Alignment of WT1 proteins derived from both species using "Align Sequences Protein BLAST" tool available in NCBI, showing a 92% homology in amino acids, and a single amino acid difference between the human 15-mer WT1 peptide (VRDLNALLPAVPSLG) and the corresponding murine WT1 sequence (VRDLNALLPAVSSLG) - serine (S) in the murine WT1 is replaced by Proline (P) in human.

Murine WT1																
Pos	1	2	3	4	5	6	7	8	9	Score						
114	A	S	A	Y	G	S	L	G	G	P	A	P	P	P	A	35
70	G	S	D	V	R	D	L	N	A	L	L	P	A	V	S	34
365	I	Q	D	V	R	R	V	S	G	V	A	P	T	L	V	32
73	V	R	D	L	N	A	L	L	P	A	V	S	S	L	G	31

Pos	1	2	3	4	5	6	7	8	9	Score
78	A	L	L	P	A	V	S	S	L	32
75	D	L	N	A	L	L	P	A	V	27

Human WT1																
Pos	1	2	3	4	5	6	7	8	9	Score						
42	G	G	I	W	A	K	L	G	A	E	A	S	A	E	37	
118	A	S	A	Y	G	S	L	G	G	P	A	P	P	P	A	35
75	G	S	D	V	R	D	L	N	A	L	L	P	A	V	P	34
370	I	Q	D	V	R	R	V	P	G	V	A	P	T	L	V	32
78	V	R	D	L	N	A	L	L	P	A	V	P	S	L	G	31

Pos	1	2	3	4	5	6	7	8	9	Score
83	A	L	L	P	A	V	P	S	L	33
80	D	L	N	A	L	L	P	A	V	27

**Figure 6.13: A comparison in the binding affinity scores between the murine and the human WT1 derived peptides toward HLA molecule, as determined using SYFPEITHI.**

These images were exported from the SYFPEITHI website after epitope prediction scoring was performed. The figure demonstrates that the human WT1/P1 (blue arrows) and WT1/P5 (green arrows) have affinity scores for HLA exactly as the murine counterpart at 31 and 27, respectively. WT1/P3 (red arrows) got a very closed score to the corresponding murine sequence at 33 and 32, respectively.

Having demonstrated such similarity between the human and the murine WT1 protein, and that a single amino acid difference in the sequence of the interest which shown does not affect the binding score, the candidate B16 (with/without HAGE) was then  $^{51}\text{Cr}$  labelled to assess CTLs derived from three ImmunoBody<sup>®</sup> vaccination regimes.

Figure 6.14 highlights the significant difference in the lysis produced by each indicated group in all ratios studied. Here again, a statistically significant difference was found between the killing of B16 cells expressing HAGE (almost 50%) and HAGE-negative B16 (20%) at 1:100 ratio (shown in A), whereas no differences in killing were found against these two targets when the effector cells used were derived from mice immunised with only WT1 (shown in B), since both express murine WT1. This indicates that the WT1 peptide used in this study was naturally endogenously processed and presented on the surface of the B16 cells and was recognised by CTLs generated against a mutated version of that peptide.

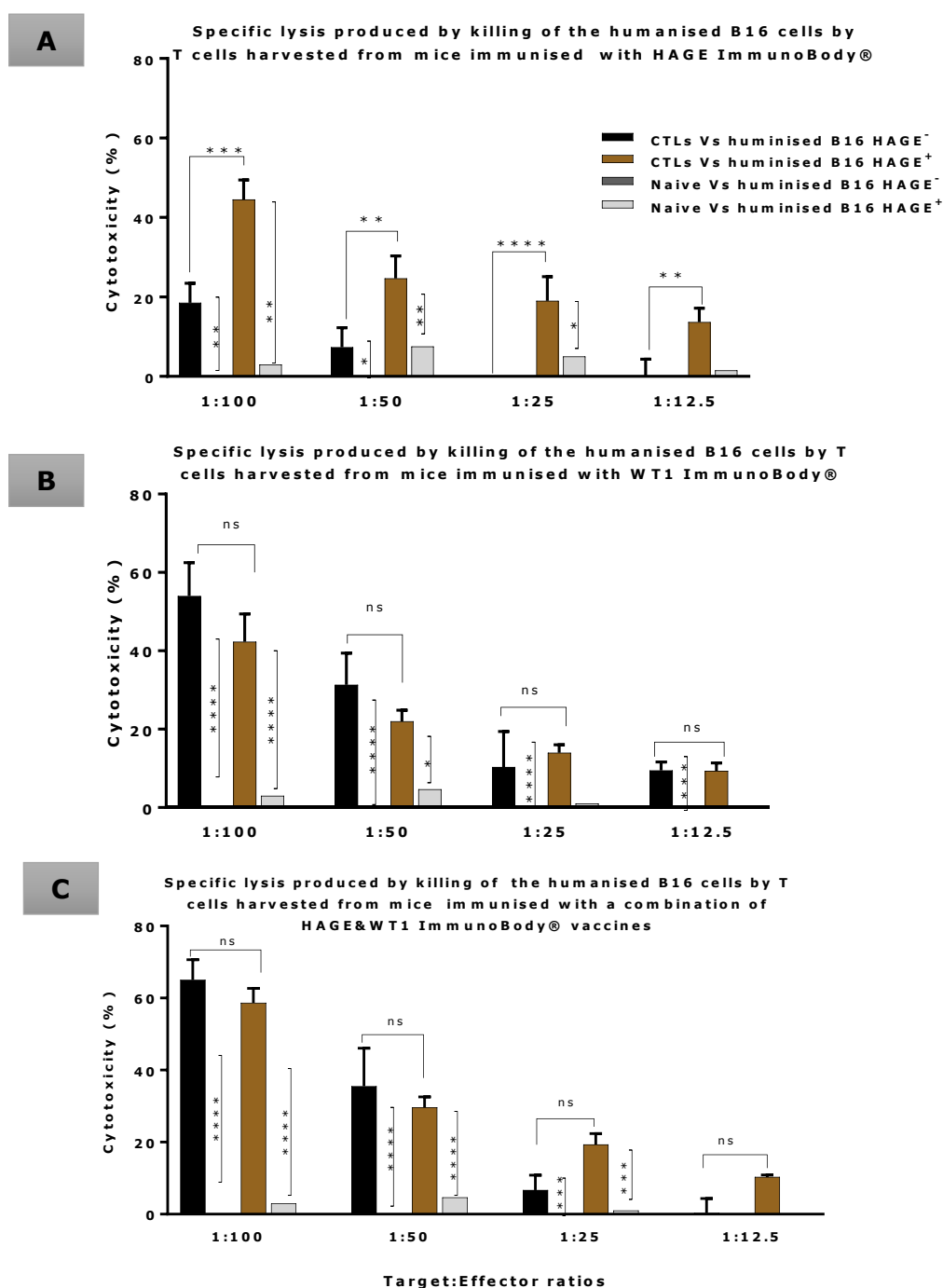


**Figure 6.14: Specific *in vitro* cytotoxicity of CTLs derived from ImmunoBody® vaccinated mice against the hB16 cells, as assessed using the  $^{51}\text{Cr}$  release assay.**

Splenocytes from mice immunised with HAGE, WT1 and both, and from naïve non-immunised mice were co-cultured *in vitro* with mitomycin-C treated and peptide-pulsed LPS T cells for 6 days, and then plated with  $^{51}\text{Cr}$  labelled-B16 cells at various ratios for 24 hours followed by measuring the release of  $^{51}\text{Cr}$  into the medium. Values are expressed as the mean  $\pm$  SEM of two independent experiments (3 mice/group), and the level of significance was assessed using Two Way ANOVA followed by Tukey's multiple comparisons test. Results demonstrate the lysis produce in each group are peptide-specific, and that the combined vaccines induces the highest level of killing.

Interestingly, B16/HAGE<sup>+</sup> cells are killed in a higher level when CTLs are derived from mice immunised with the combined approach (Figure 6.15, at almost 60%) than when they are derived from mice immunised with either HAGE or WT1 vaccine individually (50% and 45%, respectively). This difference is shown to be a statistically significance at 1:100 (target: effector ratio) with\*\**P-value*=0.0032 and \*\*\**P-value*=0.0002 in HAGE and WT1 groups, respectively.

Overall, these findings indicate that both HAGE and WT1 peptides encoded by the human ImmunoBody<sup>®</sup> were endogenously processed and displayed in the context of MHC class I on the surface of the APCs and generated CTL repertoires that recognise the identical sequence expressed by B16 cells when they are co-cultured *in vitro* and ultimately kill them. Therefore, these cells can be used to assess the efficacy of the vaccine in preventing/slowing down the growth of tumours produce by implantation of these cells in the HHDII/DR1 mice (more details will be covered in the next chapter).

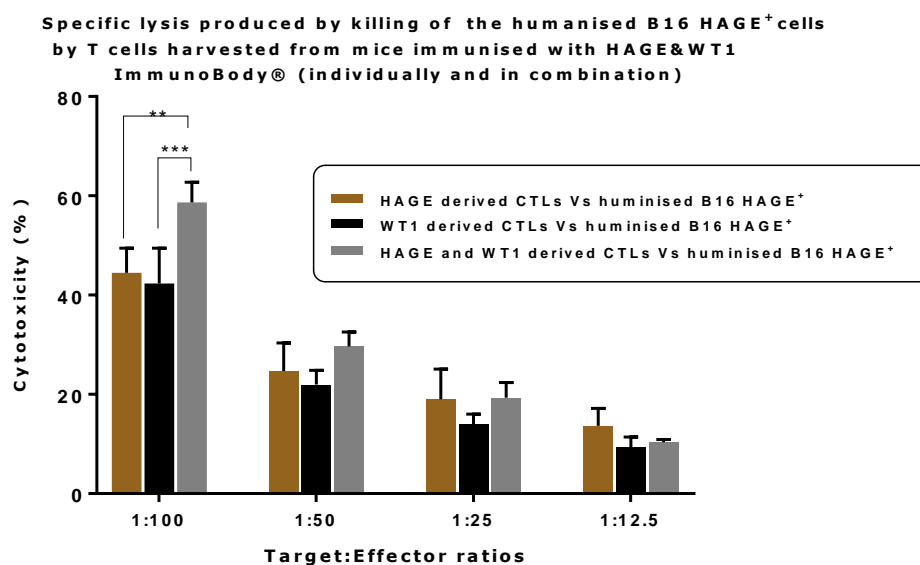


**Figure 6.15: Specific *in vitro* cytotoxicity of CTLs from ImmunoBody<sup>®</sup> immunised mice against the hB16/HAGE<sup>+</sup> cells, as assessed using the <sup>51</sup>Cr release assay.**

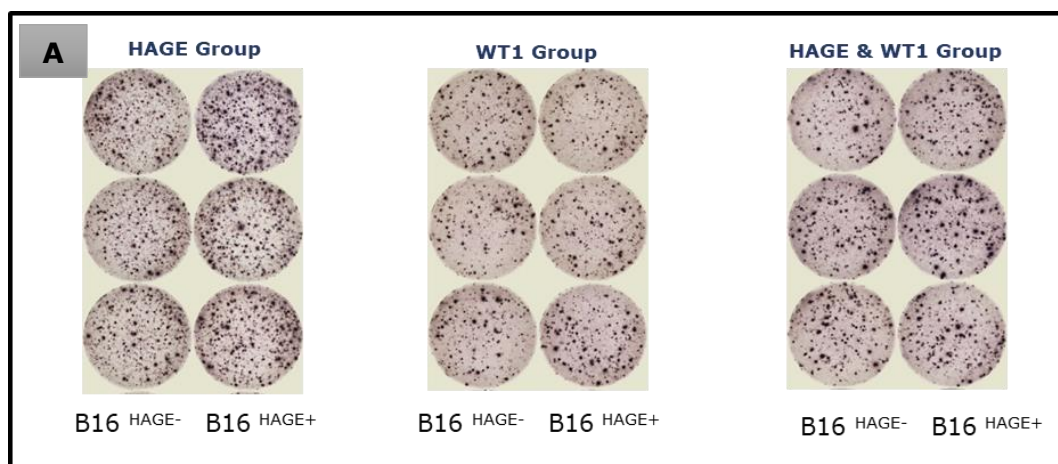
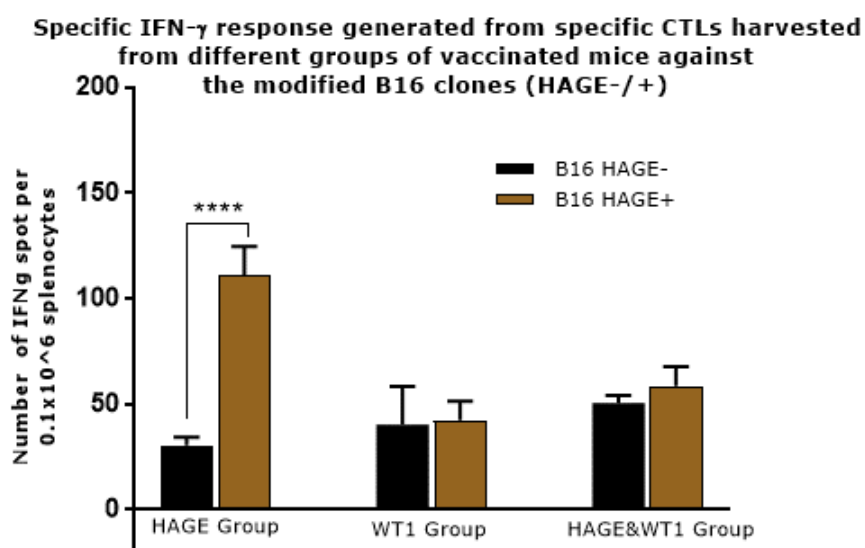
Splenocytes from mice immunised with HAGE, WT1 and both were co-cultured *in vitro* with mitomycin-C treated and peptide-pulsed LPS T cells for 6 days and then plated with <sup>51</sup>Cr labelled-B16 cells at various ratios for 24 hours, followed by measuring the release of <sup>51</sup>Cr into the medium. Values are expressed as the mean±SEM of two independent experiments (3 mice/group) and the level of significance was assessed using Two Way ANOVA followed by Tukey's multiple comparisons test. Results demonstrate that lysis produced upon the administration of the combined vaccines (at 1:100 ratio) is significantly higher than that induced when vaccines are given individually.

### **6.3.5.2 HAGE and WT1 vaccines elicit peptide specific CTLs that secrete IFN- $\gamma$ upon recognition of the $^h$ B16 cells (with/without HAGE)**

The previously described approach for the *in vitro* stimulation of splenocytes was used, after which CD3<sup>+</sup> cells were isolated and then plated at  $0.1 \times 10^6$  cells per well in IFN- $\gamma$  coated ELISpot plate and co-cultured with  $^h$ B16 cells (with/without HAGE) at a ratio of 1:10 (target: effector) for 48 hours. Figure 6.16 indicates the prevalence of responding cells based on the IFN- $\gamma$  ELISpot assay.

The response of CTLs from HAGE-immunised mice to HAGE positive cells was significantly higher than that in response to HAGE negative cells, with \*\*\*\**p*-value < 0.0001. These data are consistent with the  $^{51}\text{Cr}$  release assay and both assays confirmed that CTLs derived for HAGE immunised mice can recognise and kill target cells in a HAGE-specific manner.

For the WT1 vaccine, the number of CTLs producing IFN- $\gamma$  was similar for both targets, reflecting the fact of that both express murine WT1. This result is also in parallel with  $^{51}\text{Cr}$  finding and both reflecting the ability of WT1 to induce an appropriate immune response. The same was obtained when effector cells were derived from mice immunised with both vaccines. However, the overall number of cells producing IFN- $\gamma$  was much lower in both cases and while 3 mice per group were used these were the results of only one experiments and would have benefitted from being repeated in order to confirm this phenomenon.

**B**

**Figure 6.16: Specific *in vitro* responses of CTLs from ImmunoBody® immunised mice against hB16/HAGE<sup>+</sup> cells (with/without HAGE), as assessed using the IFN- $\gamma$  ELISpot assay.**

Splenocytes were stimulated for 1-week, pure CD3<sup>+</sup> cells were isolated and plated at  $0.1 \times 10^6$  cells per well and co-cultured with the hB16 cells (with/without HAGE) at ratio of 10:1. **(A)** Represent ELISpot wells images demonstrate the number of spots produced from each group. **(B)** Bar chart shows the number of spots generated in each group after background being subtracted. Values are expressed as the mean  $\pm$  SEM of triplicate (3 mic/group)- experiment done once. The level of significance was assessed using Two Way ANOVA followed by Tukey's multiple comparisons test.

### 6.3.6 Functional characterisation of CD8<sup>+</sup> T cells derived from the immunised animals

Intracellular staining (ICS) for assessing the expression of cytokines and other relevant proteins is commonly used to characterise immune responses upon antigenic stimuli. Herein, we wanted to profile TNF- $\alpha$ , IL-2, IFN- $\gamma$  and granzyme B production by CD8<sup>+</sup> T cells from animals immunised with the ImmunoBody<sup>®</sup> vaccines in response to incubation with target cells expressing relevant peptides using flow cytometry. The assay also examined the expression of functional markers, such as the Lysosome-Associated Membrane Protein 1 (LAMP-1 or CD107a) as a marker of CD8<sup>+</sup> T cell degranulation and Ki-67 as a marker of cell proliferation.

Hence, splenocytes were isolated and stimulated as described above. Cells were then washed and given a short-term stimulation upon co-culturing with the respective targets at a ratio of 1:10 (target: effector) for 6 hours at 37°C. Two types of target cells were selected for this study, peptide pulsed/non-pulsed T2 cells and Clone10/Clone5 K562 cells, as illustrated in Figure 6.17. Secreted cytokines/proteins were retained intracellularly using inhibitors of secretion, namely brefeldin A and monensin, and their expression in response to stimulation was then determined using an intracellular and cell surface staining. Similar analytical approach to that demonstrated in Chapter-4 was herein applied.

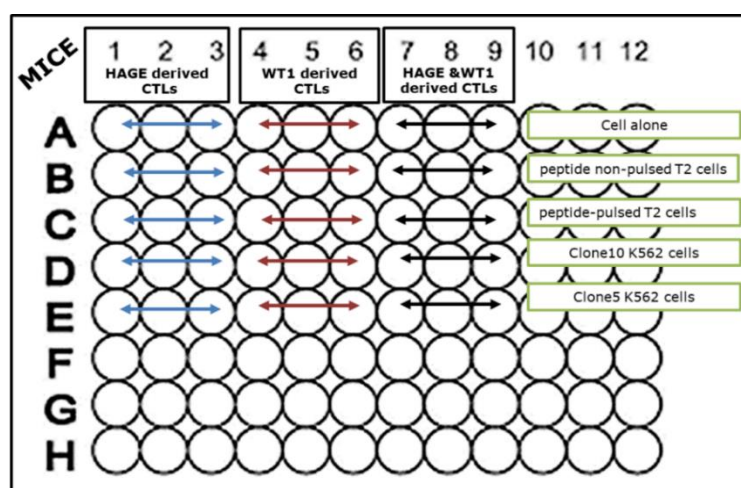


**Figure 6.17: Representative plate layout to assess responsiveness of CD8<sup>+</sup> T cells from ImmunoBody<sup>®</sup> immunised animals upon co-culture with targets.**

Targets used herein were pulsed/non-pulsed T2 cells and Clone10/Clone5 K562 cells. Splenocytes were isolated from each group (3 mice/group) and stimulated with the peptides and murine IL-2 for 1 week (IVS). Cells were then washed and seeded with respective targets at a ratio of 1:10 (target: effector) together with inhibitors of protein secretion in 96-rounded bottoms well plates and then incubated for 6 hours in a 37°C incubator. Plates were then foiled and stored overnight at 4°C for flow cytometric staining and analysis the next day.

### 6.3.6.1 Responsiveness of CD8<sup>+</sup> T cells from animals immunised with the ImmunoBody<sup>®</sup> vaccine to peptide-pulsed/non-pulsed T2 cells

Cytokines/proteins produced per single CD8<sup>+</sup> T cells derived from the candidate vaccines was determined for i) T cells alone; wherein T cells incubated with medium instead of a target, thereby the background level of the markers of the interests can be removed, ii) T cells *versus* non-pulsed T2 cells co-culture, in which the percentages of the markers gated in this group represents the control groups, and iii) T cells *versus* peptide-pulsed T2 cells co-culture, in which the percentages of the markers gated in this group represents the test groups. In the test group, T cells from animals immunised with the HAGE vaccine were co-cultured with the HAGE-pulsed T2 cells, T cells from animals immunised with the WT1 vaccine were co-cultured with the WT1-pulsed T2 cells, and T cells from animals immunised with the combined HAGE and WT1 vaccine were co-cultured with HAGE- and WT1-pulsed T2 cells. The fold change was determined as a ratio between the percentage of CTLs responding to peptide-pulsed T2 cells and the percentage of CTLs responding to non-pulsed T2 cells for each individual mouse.

Figure 6.18 shows the responses of CTLs from different animal groups to co-culture with peptide-pulsed T2 cells relative to non-pulsed T2 cells. Overall, findings demonstrate that there was at least a 1.5-fold increase, indicating that the production of these markers are triggered/induced by the recognition of peptides on the surface of the T2 cells. Although, there was no notable difference in the responses of CTLs generated from the different vaccine strategies for the majority of proteins examined, TNF- $\alpha$  responses were notable, with a 34-fold increase (compared to the response induced by non-pulsed cells) being observed for CTLs derived from animals receiving the combined vaccines, a 12-fold increase for those receiving the WT1 vaccine and a 4-fold increase for those receiving the HAGE vaccine. Although the expression of IFN- $\gamma$  and Ki-67 were also increased, the differences were not of statistical significance.

In summary, HAGE- and WT1-ImmunoBody<sup>®</sup> vaccines either individually or in combination were able to induce CTLs that could be triggered to express key proteins which are necessary for CD8<sup>+</sup> cells to carry out cytotoxic activity and proliferation on encounter with using peptide-pulsed T2 cells *in vitro*. Of the markers, TNF- $\alpha$  was found to be the most upregulated cytokine, with the combined vaccines generating the highest production, highlighting again the benefit of using both vaccines together.

**Intracellular cytokines/proteins production by CD8<sup>+</sup> CTLs generated from different ImmunoBody® vaccines against the peptides-pulsed T2 cells**

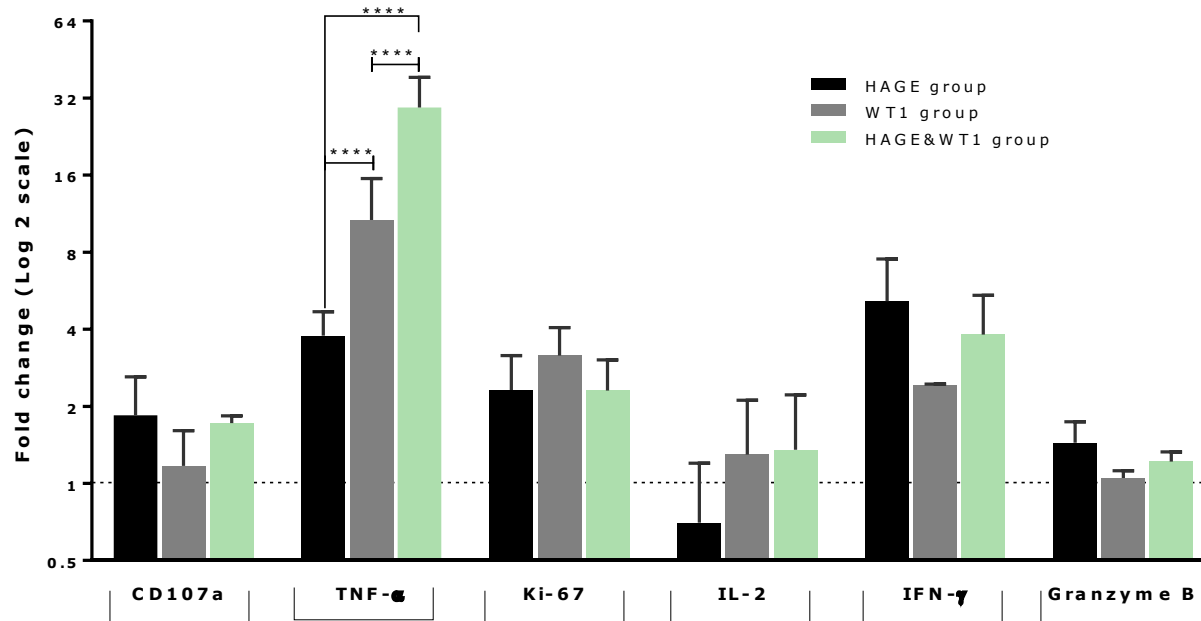


**Figure 6.18: Responsiveness of CD8<sup>+</sup> CTLs from immunised animals to peptide-pulsed/non-pulsed T2 cells.**

The percentage of positive cells was determined for each vaccine group and the fold changes were then calculated as ratios. Values are expressed as the mean  $\pm$  SEM of two independent experiments (3 mice/group). The level of significance was assessed using Two Way ANOVA followed by Tukey's multiple comparisons test. Findings, in general, demonstrate an increase in the ratios almost in all ImmunoBody® vaccination groups, and that TNF- $\alpha$  is the predominant cytokine, especially in the combined vaccines. Note: all calculations were done using percentage gated except for granzyme B, wherein MFI was applied since the percentage gated for it was already closed to the 100%.

### **6.3.6.2 Responsiveness of CD8<sup>+</sup> T cells from animals immunised with HAGE- and WT1-ImmunoBody<sup>®</sup> to K562/HHDII<sup>+</sup> cells**

Similar to previous assay, the responsiveness of CD8<sup>+</sup> T cells from animals immunised with HAGE- and WT1-ImmunoBody<sup>®</sup> to K562/HHDII<sup>+</sup> cells was determined; i) T cells alone, thus the background level can be identified, ii) T cells co-cultured with Clone10, (represents the control group), and iii) T cells co-cultured with Clone5 (representing the test group). The fold change increase in expression was calculated as a ratio between the percentage of CTLs expressing the relevant protein in response to Clone5 (HAGE<sup>+</sup>/WT1<sup>+</sup>) relative to the expression induced in response to Clone10 (HAGE<sup>-</sup>/WT1<sup>+</sup>) for each individual mouse. Figure 6.20 shows the fold changes increase in the expression by the different CD8<sup>+</sup> CTL populations.

For cells derived from animals immunised with HAGE and WT1 alone, co-culturing with the K562 cells had little effect on the expression of the measured proteins, except for TNF- $\alpha$  in the case of CTLs from animals immunised with HAGE alone (fold change reaching around 2, Figure 6.19). Although this finding would be expected for the cells derived from mice vaccinated with WT1 (WT1 being expressed by both Clone5 and Clone10), this was not expected for those derived from mice immunised with HAGE alone, since Clone10 does not express HAGE.

Responses of cells from animals that had been immunised with the combined vaccine were almost all higher than those for cells from animals immunised with the single vaccine. Interestingly, IL-2 and Ki-67 were the two most upregulated markers in cells from the combined vaccine group, indicating that such incorporation might be useful in CML in terms of the induction of CD8<sup>+</sup> cells specific IL-2 and Ki-67. Similar trend was also noticed for granzyme B which shows an increase in MFI values in comparison to the single vaccines although, it was statistically not significant.

In summary, IL-2, Ki-67 and granzyme B responses of cells from the combined HAGE and WT1 vaccine group are better than those generated by cells from the single vaccine groups.

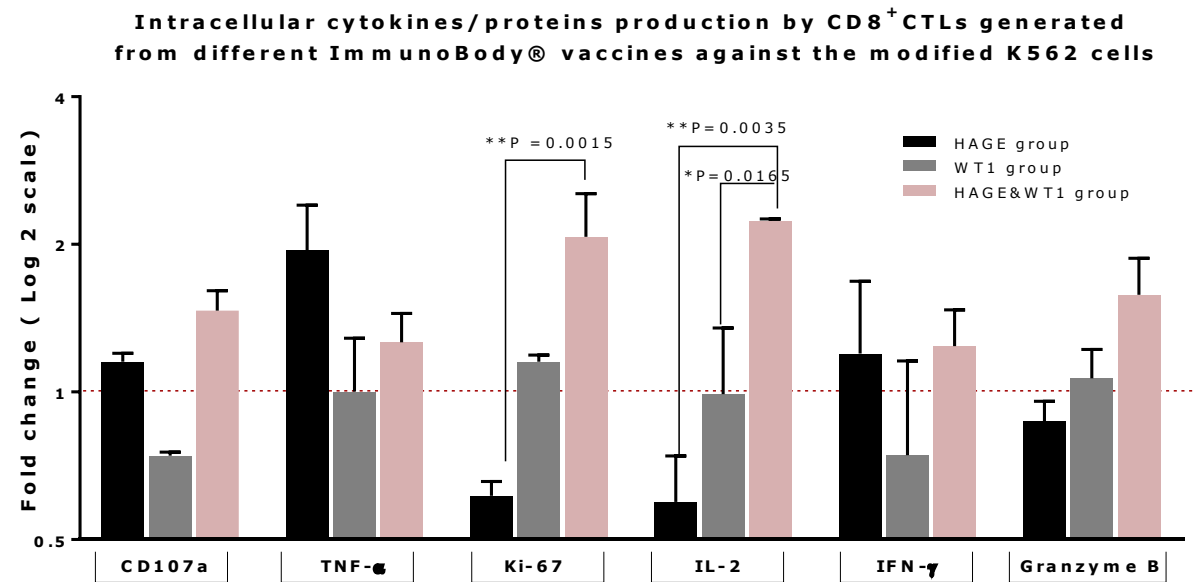


**Figure 6.19: Responsiveness of CD8<sup>+</sup> CTLs from immunised animals to HAGE<sup>+</sup>/WT1<sup>+</sup> (Clone5) and HAGE<sup>-</sup>/WT1<sup>+</sup> (Clone10) K562/HHDII<sup>+</sup> cells.**

The percentages of the positive cells for cytokines production was determined in each vaccine group against Clone10 and Clone5 K562 cells and the fold changes were calculated as ratios. Values are expressed as the mean±SEM of two independent experiments (3 mice /group). The level of significance was assessed using Two Way ANOVA followed by Tukey's multiple comparisons test. Findings in general demonstrate an increase in the ratios in some cytokines in HAGE derived CTLs, no changes in WT1 CTLs and upregulation of IL-2 and Ki-67 in the combined vaccines. Note: all calculations were done using percentage gated except for granzyme B wherein MFI was applied since the percentage gated for it was already closed to the 100%.

## 6.4 Discussion

CTLs are a fundamental subset involved in cell mediated cytotoxicity and therefore their monitoring is regarded as a key element in the evaluation of a vaccine success. In some contexts, while it is important to quantify the frequency of antigen-specific CD8<sup>+</sup> T cells using assays such as ELISpot, ELISA or flow cytometry, it is often critical to ascertain their functionality via killing assays (Knutson, dela Rosa *et al.* 2006). <sup>51</sup>Cr release has long been a gold standard assay for CD8<sup>+</sup> T cell functionality study (Andersen, Schrama *et al.* 2006). Nevertheless, due to limitations associated with <sup>51</sup>Cr release assay, other assays have been developed, such as IFN- $\gamma$  ELISpot and multicolour flow cytometry assays. However, IFN- $\gamma$  ELISpot assay individually might not be quite practical since other non-cytotoxic cells can also produce IFN- $\gamma$  and CTLs with cytotoxic activity do not constitutively produce IFN- $\gamma$  (Derby, Reddy *et al.* 2001). Hence, whenever it is appropriate, combining assays would provide more comprehensive outcomes of specific immune responses. Therefore, this chapter, in addition to <sup>51</sup>Cr release assay, has employed IFN- $\gamma$  ELISpot and multiparametric flow cytometry-based assays to confirm and validate findings.

Hence, the frequency and functionality of CTLs derived from animals immunised with the individual and combined HAGE- and WT1-ImmunoBody<sup>®</sup> vaccines have been assessed, as has their ability to respond to, and kill, relevant target cells. These targets are CML cell lines (wild-type and modified) and the TAP deficient T2 cells loaded with cognate peptides. The  $\mu$ B16 melanoma cells were also studied to get a preliminary information of *in vitro* cytotoxicity before being used as "a proof-of-concept" in tumour model studies.

T2 cells was chosen as a target to study *in vitro* cytotoxicity based on their expression of HLA-A\*0201 molecules and defective endogenous peptide presentation (Salter, Cresswell 1986). In this respect, we have clearly demonstrated the capability of peptide-specific CTLs to mediate peptide-pulsed T2 killing, and release IFN- $\gamma$  upon encountering of the candidate peptides on the surface of T2 cells using <sup>51</sup>Cr and IFN- $\gamma$  ELISpot assays, respectively. The findings generated from both assays were consistent, and both confirm that HAGE- and WT1-ImmunoBody<sup>®</sup> derived CTL repertoires are frequent and functionally efficient to specifically kill their targets. To the best of our knowledge, this is the first study to have assessed the responsiveness and functionality (cytotoxicity) of CTLs from animals immunised with the WT1-ImmunoBody<sup>®</sup> vaccine individually and in combination with HAGE-ImmunoBody<sup>®</sup>. The immunogenicity of the HAGE vaccine has been studied previously, where these studies demonstrated the capability of HAGE-specific CTLs derived from mice immunised with similar HAGE insert ImmunoBody<sup>®</sup> to kill T2 cells pulsed with a

cocktail of class I HAGE peptides using the  $^{51}\text{Cr}$  release assay (Divya Nagarajan, PhD thesis 2018). Findings of the current and previous studies are consistent. Although there was no significant difference in the killing capacity of CTLs derived from immunised animals using the single and combined vaccines observed in the current study, no peptide competition or inhibition could be identified.

Examining responsiveness to K562 and KCL-22 cells (CML cell lines) confirmed the capacity of these vaccines to generate relevant CTL populations. The results of these two cell lines seem to be quite similar, as highlighted by the capacity of HAGE-specific CTLs to specifically recognise and kill HAGE<sup>+</sup> K562 (Clone5) and the HAGE<sup>+</sup> KCL-22 in comparison to their respective HAGE<sup>-</sup> cell lines, and the production of IFN- $\gamma$  in response to the HAGE<sup>+</sup> clone. These findings suggest that target killing by such CTLs is initiated by the recognition of HAGE epitopes. Adding this to data produce by killing/IFN- $\gamma$  production against HAGE-pulsed T2 cells by the same CTL repertoires, the HAGE-ImmunoBody<sup>®</sup> vaccine seems to be capable of producing fully functional effector HAGE-specific CTLs. K562 and KCL-22 were also previously shown to constitutively express high levels of WT1 and so were used as a useful tool for testing the responsiveness of CTLs from animals immunised with the WT1 vaccine. As with WT1-pulsed T2 cells, CTLs response to WT1 have been shown to lyse CML targets upon recognition of WT1 and this was also confirmed by ELISpot assay. Collective data produce by WT1-specific CTLs against these CML targets and WT1 loaded T2 cells, has confirmed that the suitability of the WT1 vaccine for inducing effector CTL repertoires.

Interestingly, CTLs generated from mice immunised with the combined HAGE- and WT1-ImmunoBody<sup>®</sup> vaccines elicit even higher level of cytotoxicity of CML targets than mice receiving the vaccines individually, thereby suggesting the development of an abundant level of highly efficient and specific CTL repertoires and the concurrent expression of HAGE and WT1 epitopes on a target surface. This is reflected by the percentages of lysis obtained in this group which are obviously greater in targets with co-expression (HAGE<sup>+</sup> and WT<sup>+</sup>) than those with an individual expression; Clone5 K562 cells lysis percent is greater than Clone10, and KCL-22/HAGE<sup>+</sup> lysis is greater than KCL-22 wild-type. However, as with IFN- $\gamma$  production upon the administration of the combined vaccines against T2 pulsed with both HAGE and WT1 peptides mixture, the combined regime in this case does not show superiority over the individual vaccines in term of the number of spots produced in response to the K562 target. However, at the same time, it does not lead to a decline in IFN- $\gamma$  production in this group. These data are not consistent with those from the  $^{51}\text{Cr}$  release assay (shown above) which revealed superiority of the combination over single vaccine regime. This discrepancy could be partially reasoned by the fact that not all CTLs with lytic activity are constantly producing IFN- $\gamma$  (Derby, Reddy *et al.* 2001) and it was for

reasons such as these, multiple assays were herein applied to test the producibility of the results.

Adding to above finding, we provide additional evidence of *in vitro* cytotoxicity, wherein, the activity of WT1-specific CTLs against the TCC-S/WT1.shRNA (HAGE<sup>+</sup> and WT1<sup>Low</sup>) is significantly lower in comparison to wild-type TCC-S (HAGE<sup>+</sup> and WT1<sup>+</sup>), suggesting that low WT1 expression by this target would attenuate overall recognition ability of CTLs and eventual reduce the level of killing compared to the wild-type. This indicates that CTLs generated by the WT1 vaccine are indeed specific for WT1 and that the low density of antigen expressed by tumour cells would negatively impact the overall CTLs response. Also, this experiment has provided evidence of the ability of HAGE vaccine-derived CTLs to lyse both TCC-S targets (which constitutively express HAGE) in almost equal percentages which is no wonder since both are originally derived from the same cell line. Moreover, CTLs generated by the combined vaccines exert a greater cytotoxicity against the wild-type TCC-S, probably due to the synergistic effect of dual peptide recognition by HAGE-specific and WT1-specific CTLs, a result that again highlights the beneficial effect of our novel vaccine approach.

The encouraging cytotoxicity data mentioned-above has given incentive to study the hB16 cells with/without HAGE to demonstrate *in vitro* cytotoxicity before being using in an animal tumour model. It has been found that the pattern of CTLs activity generated against these targets is similar to those obtained against the CML targets in terms of the high percentages of lysis and IFN- $\gamma$  production generated by HAGE-specific CTLs against B16/HAGE<sup>+</sup> cells in comparison to the HAGE<sup>-</sup> clone. These results are in line with previous data (Divya Nagarajan, PhD Thesis 2018), wherein, HAGE-specific CTL activity against the hB16/HAGE<sup>+</sup> cells was demonstrated using the <sup>51</sup>Cr release assay, ELISpot assay and impedance-based assays (RTCA). Interestingly, although the WT1-ImmunoBody<sup>®</sup> vaccine-induced CTLs encodes human WT1 sequence antigen, B16 clones which original express the murine sequence were killed by the CTLs. This might be due to the fact that a single amino acid difference between human 15-mer WT1 peptide sequence and its mutated version does not significantly impact the ability of human WT1-specific CTLs to kill B16 cells expressing the murine WT1. Although the IFN- $\gamma$  ELISpot assay suggested a low frequency of CTLs, this needs further focused study in the future work to confirm or identify reasons behind this result. The combined regime results in a higher degree of hB16/HAGE<sup>+</sup> cell lysis than the single vaccines. The B16 was therefore used as tumour model to confirm *in vivo* vaccine efficacy in the next chapter.

Recently, multi-parametric flow cytometry-based assays measured cytotoxicity, and assess T cells degranulation, proliferation and cytokine production has been developed. Upon specific-peptide recognition expressed by targets, T cells could

promptly proliferate and differentiate to effector cells that in the context of immune responses should be associated with the secretion of effector markers of immunity. In this study, CTLs from animals immunised with different vaccines were assessed for the production of essential markers, TNF- $\alpha$ , IFN- $\gamma$ , granzyme B, IL-2, CD107a and Ki-67 upon incubation with targets expressing the relevant cognate peptides.

Initial experiments demonstrated that the frequency of specific CD8<sup>+</sup> CTLs upon the recognition of peptides on peptide-pulsed T2 cells relative to non-pulsed T2 cells was slightly higher for the combined vaccines group, and that the most notable response was TNF- $\alpha$  production specially for cells from animals immunised by the combined vaccines (34-fold increase *versus* control). Although not of statistical significance *versus* the single vaccine regimens, the combined immunisation also increases the responsiveness to stimulation, as indicated on the basis of Ki-67 and IFN- $\gamma$  expression, thereby confirming proliferation and effector function potential. Although CD107a, IL-2 and granzymes B was also increased, these were only moderate. Comparing IFN- $\gamma$  production assessed by flow cytometry with IFN- $\gamma$  ELISpot upon using T2 cells as a target, it seems that data are almost consistence; IFN- $\gamma$  is upregulated in each group of ImmunoBody<sup>®</sup> derived CTLs upon recognition of the cognate peptide loaded on T2 cells in comparison with non-pulsed ones, however vaccines combination does not upregulate IFN- $\gamma$  over the individual vaccine.

The HAGE<sup>+</sup>/WT1<sup>+</sup> and HAGE<sup>-</sup>/WT1<sup>+</sup> K562 cells were also employed as CML model targets for studying the responsiveness of T cells from immunised animals to *in vitro* stimulation. However, one limitation of this study is that it could only provide information about responses of CTLs from animals immunised with the HAGE vaccine, as both cell lines expressed WT1 - previous attempts to knockdown WT1 from these cells were unsuccessful. Incubation of cells from animals immunised with the HAGE vaccine with Clone5 (HAGE<sup>+</sup>) slightly increased their expression of CD107a, TNF- $\alpha$  (mostly) and IFN- $\gamma$  compared to control (incubation with Clone10, HAGE<sup>-</sup>), but not IL-2 or Ki-67. In contrast, both IL-2 and Ki-67 were the two most upregulated markers from CD8<sup>+</sup> cell derived from animals immunised with the HAGE and WT1 vaccines upon incubation with Clone5 compared to Clone10. This upregulation is found to be significantly higher in comparison to those induced by single vaccine group, indicating that such incorporation is beneficial in CML disease in term of induction of Ki-67 and IL-2, two markers that are known for their critical role in T cells proliferation and differentiation, respectively. Similarly, granzyme B secreted by both HAGE and WT1 derived CTLs is shown to be increase when both vaccines are administered together.

In summary, the efficacy of HAGE- and WT1-ImmunoBody<sup>®</sup> vaccines to induce *in vitro* cytotoxicity either individually or in combination are confirmed. However, while

the vaccines combination is shown to be clearly superior over the individual vaccines in all targets assessed by the  $^{51}\text{Cr}$  release assay, observations made using the IFN- $\gamma$  ELISpot-do not confirm these findings. This might be due to the fact that CTLs with lytic activity do not necessary constitutively produce IFN- $\gamma$  (Derby, Reddy *et al.* 2001) and that the ELISpot and  $^{51}\text{Cr}$  release assays - measure different aspects of cell-mediated cytotoxicity; effector cell function and target cell death, respectively, it is therefore assumed that CTLs generated upon combination of both vaccines could kill targets by additional means of cell-mediated cytotoxicity. These assumptions are supported by data generated from the multicolour flow cytometry, including i) a remarkable upregulation of TNF- $\alpha$  production in response to peptide-pulsed T2 cells -TNF- $\alpha$  is a potent inducer of cytotoxicity, ii) an increase of IL-2 in response to K562 cells used as a target - IL-2 is essential for promoting T cell differentiation into effector and memory T cells, iii) an increase of Ki-67 expression, thereby indicating that CTLs are proliferating and are likely entering the active phases of the cell division, and iv) an upregulation of granzyme B expression - granzyme B is intimately involved in target cells killing upon direct contact. Collectively, these findings support the advantageous effect of vaccines combination and highlighted the mechanisms that the combined vaccines could kill the target by, excluding IFN- $\gamma$  production.

## 6.5 Conclusion and chapter impacts

Previously, it was confirmed the immunogenicity of the HAGE- and WT1-ImmunoBody<sup>®</sup> derived peptides, and herein, their ability to provoke specific *in vitro* cytotoxicity has been confirmed. While both vaccines independently associated with substantial cell-mediate killing indicative of professional CTL repertoires, our novel approach of vaccines combination delivers a particularly superior killing over the individual vaccines. It has also been demonstrated that targets killing was variable and seems to depend on the peptide density displayed by target surface, a feature would be of clinical significance in the context of using demethylating agents prior to immunotherapy to re-express the peptides of the interest on the tumour cell surface, thereby increasing their recognition and killing by CTLs. However, this project was carried out on CTLs generated in mice and it would be important to demonstrate that PBMCs from patients with CML or other cancers can be stimulated *in vitro* using a combination of WT1 and HAGE derived peptides, co-culture with K562 (HAGE<sup>+</sup>/WT1<sup>+</sup>/HLA-A2<sup>+</sup> (not HHDII)) cells and their cytokine production determined by flow cytometry, ELISPOT assay and/or ELISA. However, the availability of such samples has been problematic, and these studies are beyond the scope of the current thesis. The hB16 cells transfected with HAGE will be used in the next chapter as "a proof-of-concept" to confirm the efficacy of the combined HAGE and WT1 vaccine in *in vivo* models.

## **7 Chapter VII: The efficacy of HAGE/ WT1 ImmunoBody<sup>®</sup> combined regime as immunotherapeutic target in tumour models**

### **7.1 Introduction**

In the previous chapters, the immunogenicity of HAGE- and WT1-ImmunoBody<sup>®</sup> vaccines in HHDII/DR1 mice either individually or in combination was confirmed. It was also confirmed that these vaccines were able to induce potent CTLs able to specifically recognise and kill targets expressing these antigens in *in vitro* assays. The administration of both vaccines on opposite flanks of the mice interestingly induced higher percentage of killing than either alone.

The anti-tumour efficacy of this combination was herein assessed using the “humanised” HHDII/DR1 mice in the prophylactic and therapeutic tumour challenges. Among targets that were employed in the previous chapter to carry out the cytotoxicity assays was the “humanised” B16 cells (<sub>h</sub>B16/HAGE<sup>+</sup>/Luc<sup>+</sup>), which also constitutively expressing WT1. It was found that these cells were killed by HAGE-specific and WT1-specific CTLs derived from the combined HAGE/WT1 ImmunoBody<sup>®</sup> vaccines more efficiently than when single regimes were implemented. This cell line is derived from a well-known aggressive type of skin cancer, melanoma tumour, and has been extensively used by many laboratories in pre-clinical studies as a “proof-of-concept” to assess vaccines efficacy before being used in clinical trials (Overwijk, Restifo 2000). This chapter employed these cells to evaluate the effectiveness of the combined HAGE- and WT1-ImmunoBody<sup>®</sup> vaccines as immunotherapeutic target in the HHDII/DR1 mice, as it will be demonstrated in the following sections. In this respect, a brief understanding of the pre-clinical mice models in general and the HHDII/DR1 in particular is initially provided.

#### **7.1.1 Mouse cancer models in pre-clinical research**

In human cancer research, using mice as a model has proven to be a quite beneficial and practical due to the potential similarity between mice and humans in many genomic and physiological characteristics of tumour biology. It has been reported that mice tumour shared certain characteristics with human tumours, such as cellular, molecular and anatomical, that are known to have essential properties and functions in malignancies (Lamprecht Tratar, Horvat *et al.* 2018). It has been also

found that the proportion of ortholog genes between mice and human is at approximately 80% (Mouse Genome Sequencing Consortium, Waterston *et al.* 2002), hence, mice models provide valuable tools to investigate various mechanistic underpinning carcinogenesis and to study different aspects of the immunotherapeutic agents, such as safety and efficacy before being translated into clinics. Recent advancement in the field of genetic engineering of mice models have offered excellent opportunities to mimic genetic and biological evolution of human malignancies. These models are of great value in the validation of targets, assessment of tumour-immune interaction, and drug toxicity studies.

The earliest generations of mouse models are the transplant models and orthotopic models, wherein, in the first case, tumour cells are engrafted subcutaneously and in the second model, tumour cells are transplanted in the correct physiological site of origin. The graft could be derived from human tumour and in this case called "xenografts" where immune-compromised mice have to be used in this instance, or from murine tissue and so-called "syngeneic tumours". Monitoring growth of a transplanted tumour is usually performed using caliper while orthotopic models require an imaging system, such as bioluminescence imaging. The transplanted tissue can be labelled with chemiluminescent marker, such as luciferase as reporter gene, prior to the implantation to permit tumour detection and growth follow-up. The syngeneic and xenografted tumours transplanted subcutaneously or orthotopically in immunocompetent and immunodeficient mice have been widely used due to their widespread availability and relative low cost (House, Hernandez *et al.* 2014).

Transgenic mice are another type of mice that are routinely used in cancer studies. This model was introduced in the early 1980s and when first emerged was a revolution for cancer research development. The concept relies on the insertion of mutations in mice genome, which activate permanently or temporarily oncogenes while silencing tumour suppressor genes. These traditional models have been very important in studies of carcinogenesis and tumour pathogenesis, as well as in studies evaluating the development of resistance to therapies; however, one criticism regarding the use of traditional mouse transgenic models lies in their limitations with respect to the low degree of heterogeneity in tumours derived from mice in comparison to the very heterogeneous tumour derived from human. Later on, more advance genomic modifications were achieved, known as; knockout and knock-in mice where in the first model, the gene is depleted/silenced to cause a "loss-of-function". In translational cancer research, this type represents potent means to assess the function of the gene silenced. It is also important to elucidate the cause-effect relationship in cancer development and assessment of many classes of genes, such as oncogenes and tumour-suppressor genes. In general, two subtypes of knockout mouse models have been often used, either constitutive/permanent inactivation of the candidate gene expression in all cells of the organism, or

conditional/inducible inactivation of the gene of interest which can involve a specific target tissue/cell. In second type (Knock-in models), the transgenic mice are produced with “gain-of-function” mutation. This type is often used to study how could oncogene drive carcinogenesis *in vivo*. Details of these transgenic mice can be found in a comprehensive review provided by (Lamprecht Tratar, Horvat *et al.* 2018).

Historically, some researchers have used the nomenclature “transgenic mice” as a distinct set from “knockout and knock-in mice” (Hanahan, Wagner *et al.* 2007); however, after the release of the Federation of European Laboratory Animal Science Associations guidelines for the production and nomenclature of transgenic rodents, mice are now often termed as transgenic mice, but it is also referred to as germline genetically engineered mouse models, including both knock-in and knockout models (Cano, Soto-Moreno *et al.* 2014).

### 7.1.2 Generation of transgenic mice

Several methods have been used to introduce DNA into a mouse genome (as shown in Figure 7.1), these includes; i) retroviral infection of mouse embryos at different stages of the developmental, this method is rarely used nowadays due to limitations associated with this procedure, such as silencing of the transgene of viral origin due to *de novo* DNA methylation after viral vector insertion (Doyle, McGarry *et al.* 2012), and random integration that can affect the expression of the adjacent genes causing faulty phenotypic expression, ii) microinjection of DNA constructs, but this method is associated with some limitations including the fact that the transgene may end up being inserted into a critical locus resulting in unexpected serious genetic alterations. Secondly, the DNA might get inserted into a locus that is subjected to gene silencing (Chicas, Macino 2001). Thirdly, DNA construct might be inserted several times which would result in many copies being produced leading to extreme overexpression and non-physiological phenotypic effects. Under this categories, a more advance technology has been developed to increase the accuracy of the insertion thereby reducing significantly the side effect mentioned, thus fairly recent technique involves the microinjection of endonuclease-based mixtures; such as Cas9–sgRNA–ssDNA mixture, wherein, reagents are directly injected into the pronucleus of fertilized oocytes, but the genetic modification occurs at a targeted site. The clustered regularly interspaced short palindromic repeat system (CRISPR)/-associated (Cas9) mediates an effective and simple engineered nuclease system to generate transgenic mice (Yang, Wang *et al.* 2014). In addition, for it being easy and efficient in creating the desirable genome editing, targeted mutations in multiple genes can be achieved. The principle is based on that single guide RNA (sgRNA) directs Cas9 nuclease enzyme to specifically cut the targeted sequence in the DNA. iii) gene-targeted transgene approach; this method is routinely used to produce conventional knockout transgenic

mice, often with a constitutive loss-of-function mutation (Kumar, Larson *et al.* 2009). It includes the manipulation of mouse embryonic stem cells at selected loci by introducing DNA with targeted transgene, the modified cells are then microinjected into the mouse blastocysts (early mouse embryo) and implanted into pseudo-pregnant recipient mouse. The embryonic stem cells and donor blastocysts originally derived from two different coat-colours mice, and thus successful incorporation is indicated by production of chimeric offspring displaying variegated coat-colour. The chimeric mice will only transmit the recombinant genotype to the offspring if the embryonic stem cells contributed to germ cells (Hanson, Sedivy 1995). The hybrid offspring are then further mated with wild-type mice and assessed for homozygosity of the mutations to select the most stable line.

The course of generating and characterising such mice takes several years to be completed, and in addition to being time and labour consuming, it is also expensive. However, several companies have since specialised in making these transgenic mice which can be purchased and used for pre-clinical experiments in many different research fields.

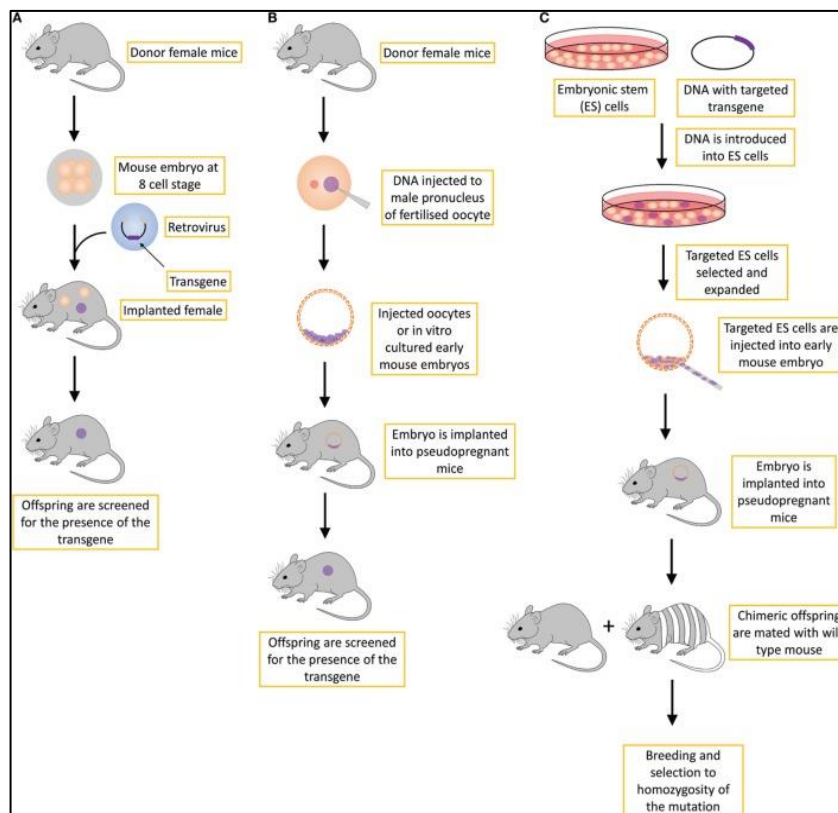


**Figure 7.1: Various approaches for manufacturing transgenic mice.** (A) Retroviral approach. (B) Standard transgene approach. (C) Gene-targeted transgene approach. Figure is reused with a reference from (Lamprecht Tratar, Horvat and Cemazar 2018).

## 7.1.3 Humanised mouse

Humanised mice are defined as mice that have been engrafted with functional cells or tissues derived from human (including their products encoded by human genes), to investigate the development and the function of human cells or tissues in the *in vivo* context of these animal (Fujiwara 2018).

### 7.1.3.1 Patient-derived xenograft (PDX)

PDX models are generated by the engraftment of patient primary tumours cells/tissues into immunodeficient mice. The logic of using PDX is that the molecular, cellular, and genetic characterisations of PDXs are similar to the original tumours in comparison to established tumour cell lines, and hence, in principal, it should offer results with higher translational potential (Tentler, Tan *et al.* 2012). Several groups of immunodeficient mice exist, including athymic nude, SCID, NOD-SCID and recombination-activating gene 2 (*Rag2*) knockout mice (Morton, Houghton 2007). The nude mutation in the first model prevents the development of functional T cells; however, due to the existence of an intact humoral and innate immunity, including NK cell activity, engraftment of solid tumour and normal/malignant haematopoietic cells were limited or even prevented (Fogh, Fogh *et al.* 1977). The next version was the C.B-17/severe combined immunodeficiency (SCID), the SCID mutation prevents the development of both mature T cells and B cells of the adaptive immune system. This model could be engrafted with a wider range of human derived solid tumours than nude mice (Phillips, Jewett *et al.* 1989), and it also allowed, for the first time, the engraftment of human normal and malignant haematopoietic cells that did not grow in nude mice albeit of low levels. To reduce the activity of NK cell and other components of innate immunity in the murine host, nonobese diabetic/severe combined immunodeficiency (NOD/SCID) was then developed. The background of NOD strain confers intrinsic defects in the innate immunity of NK cells, macrophages and DCs. Combining these defects with ablation of the adaptive immunity using targeted mutations in the recombination activating genes 1 and 2 (*Rag1<sup>null</sup>/Rag2<sup>null</sup>*) led to the development of a murine host with features of being more receptive for human solid human cancer and haematopoietic cells than previous versions (Williams, S. S., Alosco *et al.* 1993, Hudson, Li *et al.* 1998). However, due to residual innate immune function, such as remaining NK cells activity, many malignancies, solid or haematological fail to engraft efficiently and grow in NOD/SCID mice. Hence, a great leap forward in the area of engraftment was then developed, which involves the development of NOD/SCID mice with *IL2rg* mutations (NSG). These mice have the ability to support the growth of almost all types of human cancer due to their severe immunodeficiency (Shultz, Goodwin *et al.* 2014). NSG mice carrying a

targeted mutation in the IL2-receptor common gamma chain (IL2rg<sup>null</sup>), which is necessary for high-affinity ligand binding and signalling through various cytokine receptors, including IL-2, IL-4, IL-7, IL-9, IL-15, and IL-21. Inhibiting signalling through these receptors can cripple both adaptive and innate immune systems (Cao, Shores *et al.* 1995, Ohbo, Suda *et al.* 1996).

The process of PDX implantation usually involves engrafting a small fragment of tumours or cell suspensions either heterotopically or orthotopically. Implanting cells/tissue heterotopically offers certain advantages over the orthotopically implantation including simplicity of the procedure and the ease of tumour measurement. Subcutaneous and intravenous PDX models have been frequently used in cancer research for studying solid tumour and leukaemia, while, orthotopic models are better if one wants to study metastasis because tumour cells disseminate throughout the body of the animal in a similar manner that in human cancer progression (Paez-Ribes, Man *et al.* 2016).

Due to the current advancement in immunotherapy and the evidence supporting the role of immune system in tumour progression and treatment, new PDX models have been developed called humanised mouse xenograft models. This model has been developed to better mimic cancerous cells/tissues heterogeneity and cross-talk between the tumour and immune cells (Lai, Wei *et al.* 2017), providing extremely valuable models for the assessment of the investigational cancer therapy, in particularly new immunotherapies. One such model has been produced by the transplantation of human CD34<sup>+</sup> HSCs or precursor cells derived from umbilical cord blood, peripheral blood or bone marrow into NSG mice. In these mice, the stem cell expand, the entire haematopoiesis happens, and this is followed by long-term engraftment, with functional human antibody being produced and cellular immune responses taking place (Tanner, A., Taylor *et al.* 2013).

### **7.1.3.2 Chimeric MHC transgenic mice**

Modest vaccines efficacy observed in many clinical trials may be partially explained by the different effects that human and mice MHC have on the final outcomes of the immune responses, due the fact that both human and animal MHC molecules do not present the same epitopes (Röttschke, Falk *et al.* 1990). Hence, albeit some limitations, transgenic mice engineered to express human HLA provide advantageous improvement over wild type as a preclinical model for assessing vaccine candidates, the risk of autoimmunity that the vaccines could induce, and develop better therapeutic approaches based on the human restriction component. One of the initial versions of such "humanised" mice involved a manipulation in the MHC class I molecule only, such model is: HLA-A2.1transgenic/H-2 class I-knockout mice, in

which the chimeric HLA-A2.1 (HHD) gene was inserted and H-2 class I removed. This model was found to mount HLA-A2.1-restricted responses more than HLA-A2.1-transgenic mice that kept the expression of the endogenous murine H-2 class I molecules (Pascolo, S., Bervas *et al.* 1997, Pajot, Pancré *et al.* 2004). Similar observations were noticed with MHC class II HLA-DR1-transgenic mice based on whether or not they are deficient in the murine class II H-2 molecules (Pajot, Pancré *et al.* 2004). From these studies, it was noticed that the lack of competition from murine MHC molecules in both situations (the HLA-A2.1-transgenic/H-2 class I-knockout mice or HLA-DR1-transgenic/H-2 class II-knockout mice models) generated only HLA-restricted immune responses, thereby enabling the monitoring of HLA-restricted CD8<sup>+</sup> or CD4<sup>+</sup>T cell responses. However, in order to obtain a long lasting CD8<sup>+</sup> T-cell immune response, CD4<sup>+</sup> T helper also need to be activated, a concept that cannot be studied in a single HLA class I or HLA class II transgenic mice. Therefore, the same group (Pajot, Michel *et al.* 2004) incorporated the distinct advantages of the two models by creating a model that has been double transgenic for both class I and class II molecules, HLA-A2.1 (HHD) and HLA-DR1 molecules, in a context that is deficient for both murine H-2 class I and class II molecules.

Therefore, the present study is entirely based on the “humanised” double transgenic HHDII/DR1 models to study and assess the efficacy of HAGE/WT1 ImmunoBody<sup>®</sup> combined regime as immunotherapeutic target. This model is of C57BL6 origin was developed by Dr. Lemmonier’s group in France, by knocking-out both murine class I and class II H-2 genes, and knocked-in a chimeric HLA-A2 (HHD) gene and the human HLA-DR1 gene (Pajot, Michel *et al.* 2004). The chimeric part is called so, because it contained human and murine compartments, of which, the  $\alpha 1$  and  $\alpha 2$  loops of the HLA-A2 molecules are human, while the  $\alpha 3$  loop with its transmembrane domain is murine. At its NH3 terminus, the chimeric molecule linked to the human  $\beta 2m$  by a peptide linker of 15 amino acid in length (Pascolo, Steve, Bervas *et al.* 1997). This chimeric structure, as it is demonstrated in Figure 7.2B, permits HLA-A2 restricted antigens to be presented within the murine context of immunity. This is by allowing the processed peptide to be presented completely in the human portion of the HLA-A2 molecules whereas the CD8 co-receptor expressed by the murine T cells can be recognised by the  $\alpha 3$  chain for further signal transduction. The HLA-DR1 molecules expressed by the murine cells are, however, completely human. Thus, murine T cells generated in response to peptide-MHC complex can recognise both human HLA-A2 and HLA-DR1 molecules expressing on the murine target cells (Vitiello, Marchesini *et al.* 1991).

A

This image has been removed by the author for copyright reasons

B

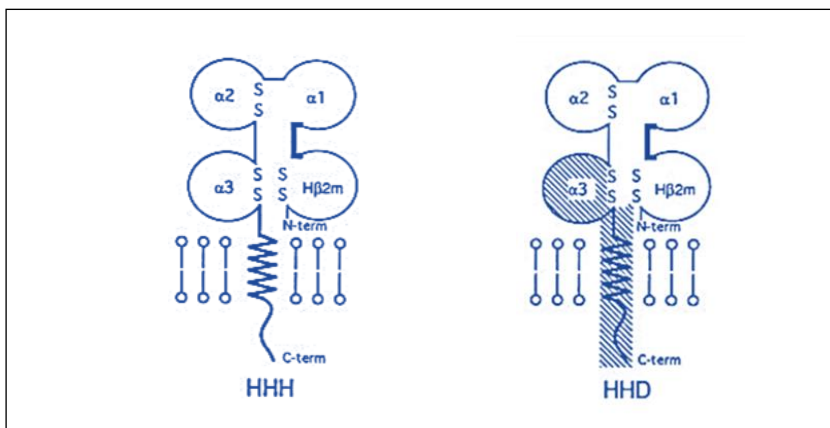


**Figure 7.2: Schematic representation of human (HLA) genes, mouse (H-2) MHC genes and the chimeric MHC (HHD) molecule.**

A comparison between mouse and human MHC gene maps is demonstrated in (A), image is reused from (Abbas, Lichtman and Pillai 2014). Schematic representation of the human MHC molecule (HHH) *versus* the chimeric MHC (HHD) molecule is shown in (B) where the open area refers to human origin and the hatched area refers to mouse origin. The 15-amino acid linker is shown as a thick line connect  $\alpha 1$  portion and human  $\beta 2m$  molecules. Permission is obtained to reuse this image with a reference from (Pascolo, Steve, *et al.* 1997).

## 7.2 Rationale of the chapter

The main aim of this chapter is to investigate the anti-tumour efficacy of the combined HAGE- and WT1-ImmunoBody<sup>®</sup> vaccines in prophylactic and therapeutic tumour challenge settings using humanised B16 cell line ( $hB16/HAGE^+/Luc^+$ ) as a “proof-of-concept” in the double transgenic HHDII/DR1 mice. A summary of experimental workflow is provided in Figure 7.3.

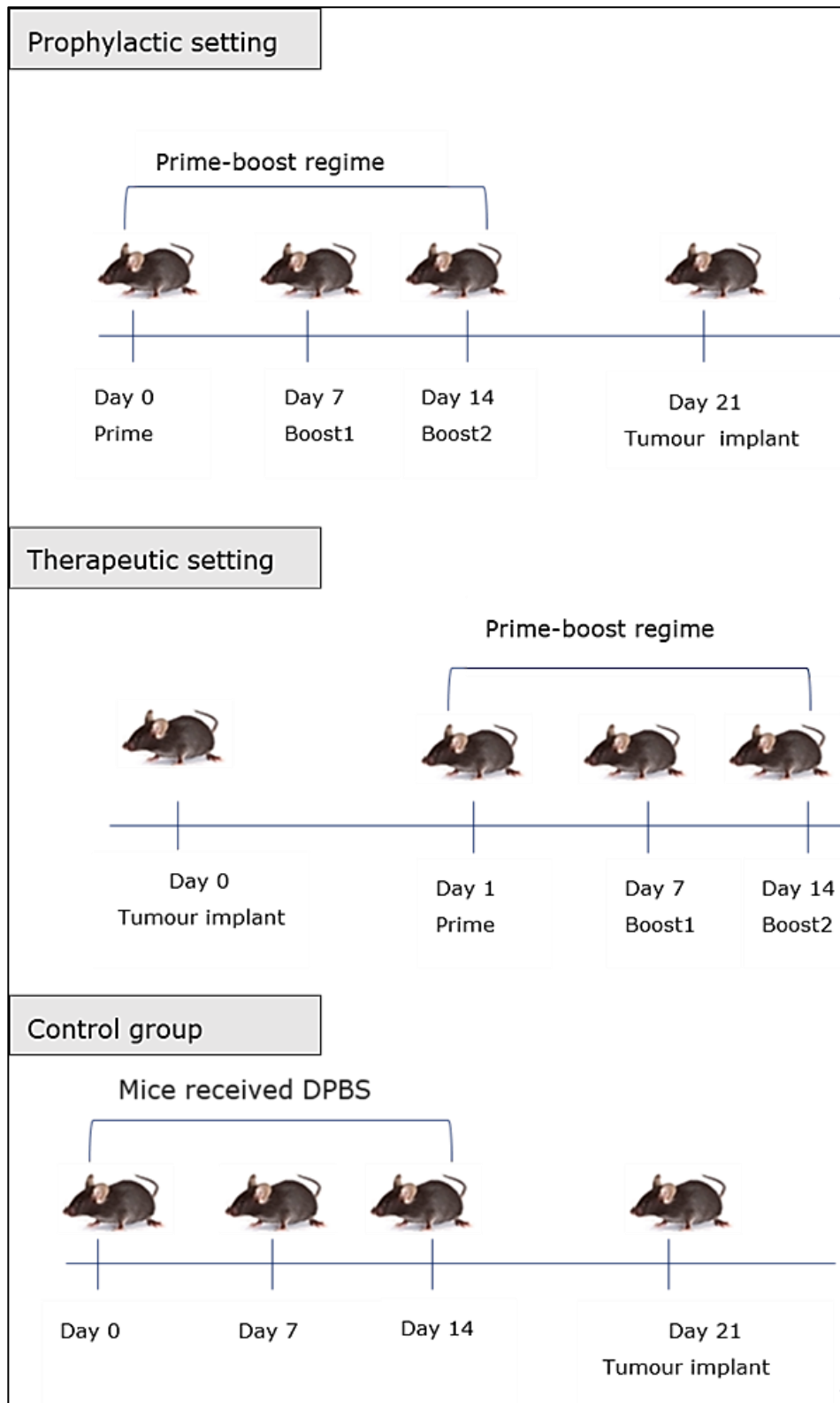


**Figure 7.3: Schematic representation of the *in vivo* experimental design.**

Three groups of mice were used in this study, 10 mice /group, prophylactic, therapeutic and control groups. In the prophylactic setting, prime-boost regime was applied, mice were then challenged with  $\text{B16}/\text{HAGE}^+/\text{Luc}^+$  cells on day 21, whereas, in the therapeutic setting, cells were implanted, followed by vaccination in the determined days. The control group of mice received DPBS instead of the vaccine.

## 7.3 Results

### 7.3.1 Profile of ${}_{\text{h}}\text{B16}/\text{HAGE}^+/\text{Luc}^+$ cells

#### 7.3.1.1 Genes expression by ${}_{\text{h}}\text{B16}/\text{HAGE}^+/\text{Luc}^+$ cells

In the target cells preparation Chapter-5 ([Section:5.3.6.1](#)), the profile of the modified B16 cells was described. Briefly, the “humanised” murine melanoma B16 cell line was kindly provided by Scancell Ltd, wherein, the murine  $\beta 2\text{m}$  was knocked-out and replaced by the chimeric HHDII/HLA-DR1 constructs to be able to grow tumours in the humanised HHDII/DR1 double transgenic mice. Furthermore, the previous PhD student transfected these cells further with the HAGE and firefly luciferase (Luc) constructs. The expression of these genes in addition to the constitutive expression of WT1 were all confirmed in Chapter-5.

#### 7.3.1.2 Tumorigenicity and kinetic optimisation of ${}_{\text{h}}\text{B16}/\text{HAGE}^+/\text{Luc}^+$ bioluminescence in naïve HHDII/DR1 mice

Luciferin bioluminescence produced by the  ${}_{\text{h}}\text{B16}/\text{HAGE}^+/\text{Luc}^+$  cells was also confirmed in Chapter-5 ([Section:5.3.6.2](#)), wherein, *in vitro* a static correlation between the total photons flux of the luciferin and cell population was demonstrated, indicating the validity of these cells for being imaged, this correlation was assessed prior to every tumour challenge experiment. Taking advantage of the already prepared  ${}_{\text{h}}\text{B16}$  tumour cells with the dual expression of HAGE and WT1 proteins and based on the *in vitro* cytotoxicity assay obtained in Chapter-6, these cells were herein chosen as tumour model in a “proof-of-concept” for our *in vivo* studies.

Before being used in tumour challenges experiments, both the tumorigenicity of B16 cells and *in vivo* luciferase activity measured over time in naïve HHDII/DR1 mice were determined. In this respect, three escalating doses of  ${}_{\text{h}}\text{B16}/\text{HAGE}^+/\text{Luc}^+$  cells were used in three independent experiments;  $0.25 \times 10^6$ ,  $0.5 \times 10^6$  and  $0.75 \times 10^6$  cells/100 $\mu\text{L}$  serum free medium/mouse were injected subcutaneously. Mice were monitored for tumour growth upon detection of bioluminescent signal of luciferin captured by Perkin Elmer IVIS Lumina III system. Results show that a dose of  $0.75 \times 10^6$  cells was the most reliable as it was able to induce a steady growth in the majority of mice used (Figure 7.4C), and therefore it was used to assess the anti-tumour efficacy of the HAGE/WT1 ImmunoBody<sup>®</sup> vaccines combination regime in the tumour challenges experiments. Whereas with a dose of  $0.25 \times 10^6$  cells, an increase in the total flux was noticed in the first two sessions but then after day-15 post implantation, tumour size started to decline. The dose of  $0.5 \times 10^6$  cells; however,

shows a constant correlation only in a half of the mice studied, therefore, both doses were exclude from further studies.

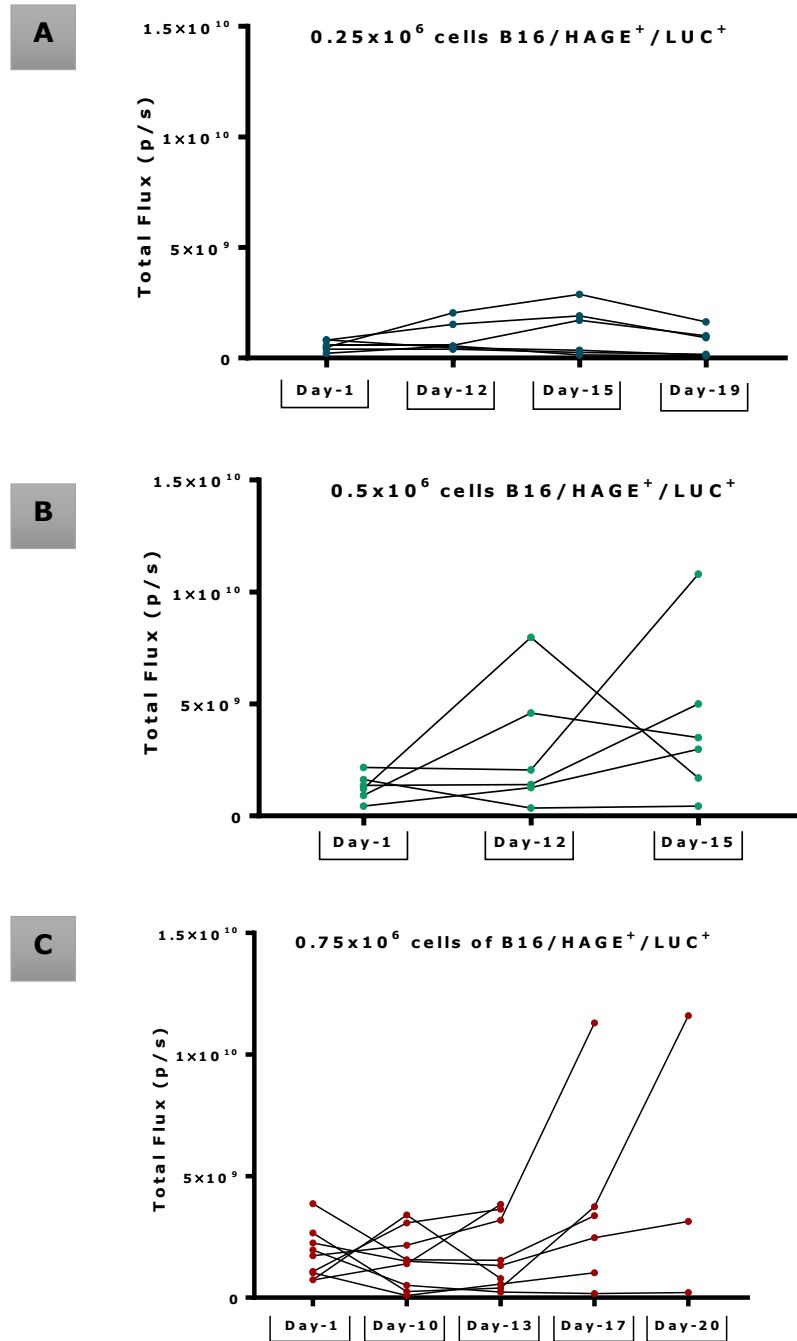


**Figure 7.4: *In vivo* kinetic optimisation of hB16/HAGE<sup>+</sup>/Luc<sup>+</sup> bioluminescence in naïve HHDII/DR1 mice.**

Total flux of luciferase activity in living animal was measured in photons per second upon the administration of three escalating doses of the hB16/HAGE<sup>+</sup>/Luc<sup>+</sup> cells;  $0.25 \times 10^6$  (shown in A),  $0.5 \times 10^6$  (shown in B) and  $0.75 \times 10^6$  (shown in C). Results show that the total flux of luciferin from  $0.75 \times 10^6$  does was proportional to growth in tumour size in the majority of mice tested, and therefore it was chosen for further studies.

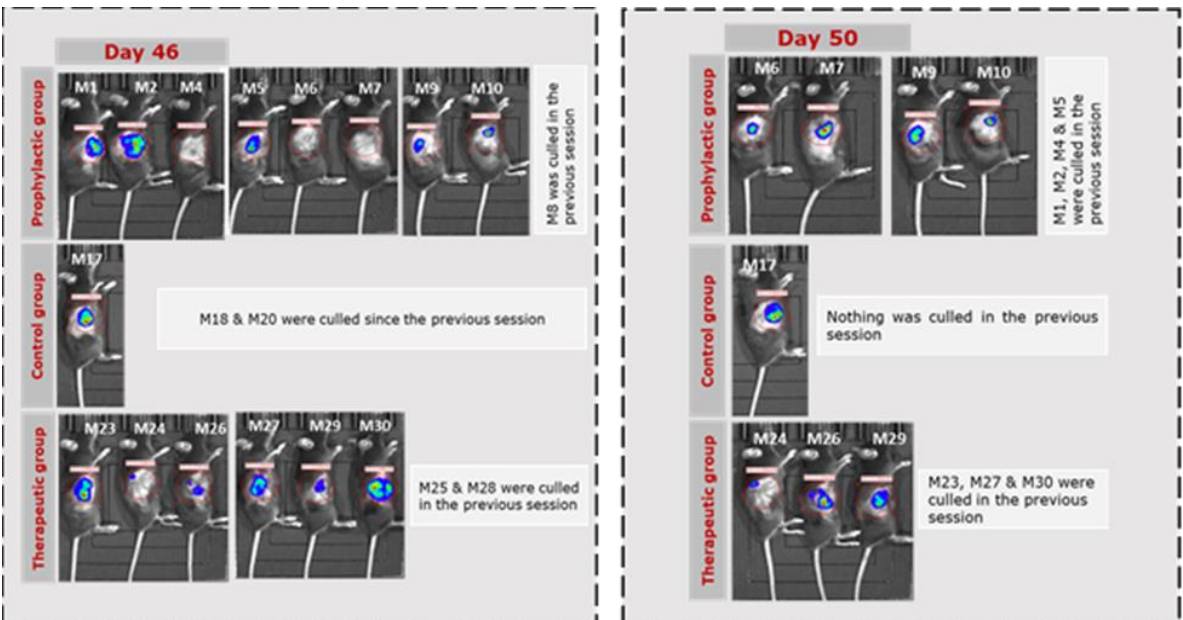
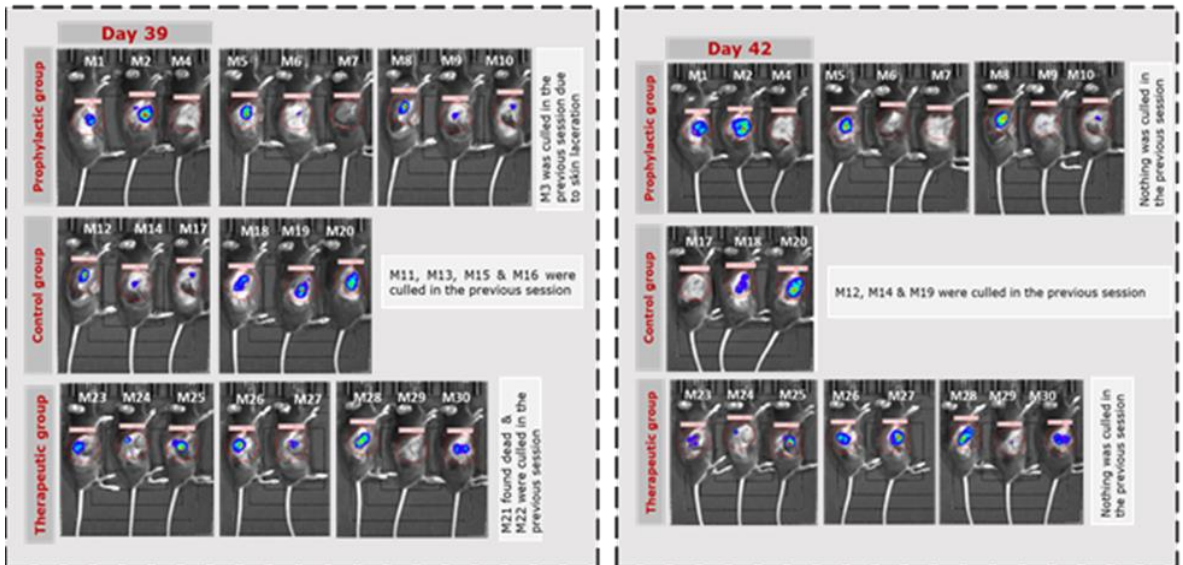
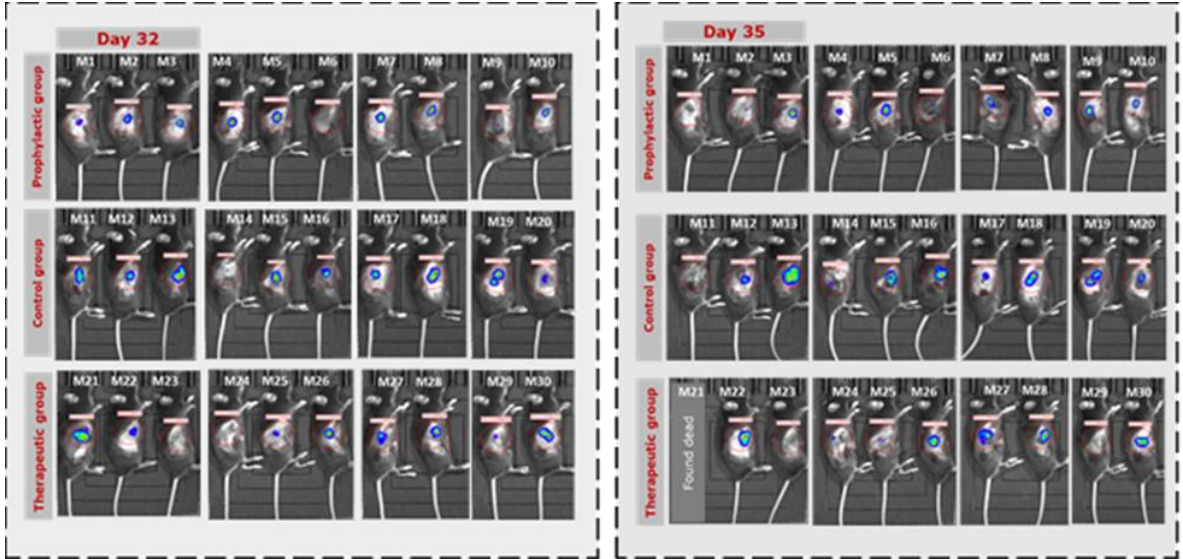
### **7.3.2 Prophylactic and therapeutic efficacy of the combined HAGE/WT1 ImmunoBody<sup>®</sup> vaccines in HHDII/DR1 mice bearing the aggressive $hB16/HAGE^+/Luc^+$ tumour**

After carrying out tumorigenicity for the  $hB16/HAGE^+/Luc^+$  cells, the efficacy of the combined HAGE/WT1 ImmunoBody<sup>®</sup> vaccines was tested in both prophylactic and therapeutic settings in HHDII/DR1 mice with a group of 10 mice/group.

As per written in the methodology Chapter-2 ([Section: 2.2.7.4](#)), each mouse in the prophylactic setting was given the HAGE- and WT1-ImmunoBody<sup>®</sup> vaccines, and then on day-21 post-transplantation, they received subcutaneous implant of the  $hB16/HAGE^+/Luc^+$  cells. Whereas in the therapeutic group, mice were given the same dose of the cells, and then on the next day, they received the combined vaccines as for the prophylactic group (summarised in Figure 7.3). The control group received no vaccine.

Details of bioluminescence images and mice culling per session are shown in Figure 7.5. Eight sessions at day-32, -35, -39, -42, -46, -50, -54 and -56 post-implantation are demonstrated in a sequential real-time analysis of tumour burden in live animals. The figure clearly demonstrates that mice that did not receive the vaccine had to be sacrificed as early as day-39 post-implantation session due to tumour size endpoint, whereas mice that received the combined vaccines continue to survive and showing a delay of tumour growth in comparison to the control. Indeed, one can see that at around day-46 post-implantation, the number of surviving mice were 8/10 (80%) for the prophylactic group and 6/10 (60%) for the therapeutic group, in comparison with only 1/10 (10%) for the control group. Tumour growth, as measured by the total flux for each group was recorded and plotted in Figure 7.6.

Eventually, 4 mice from the prophylactic group (Mouse-6, Mouse-7, Mouse-9 and Mouse-10) and one mouse from the therapeutic group (Mouse-24) were the last mice to be culled. The study was then terminated after day-56 post-implantation session, which was before tumours reached their maximum growth. This was purposely done in order to be able to perform some immune characterisation of the tumour infiltrating lymphocytes and performed some functional assay with the splenocytes extracted from these mice.



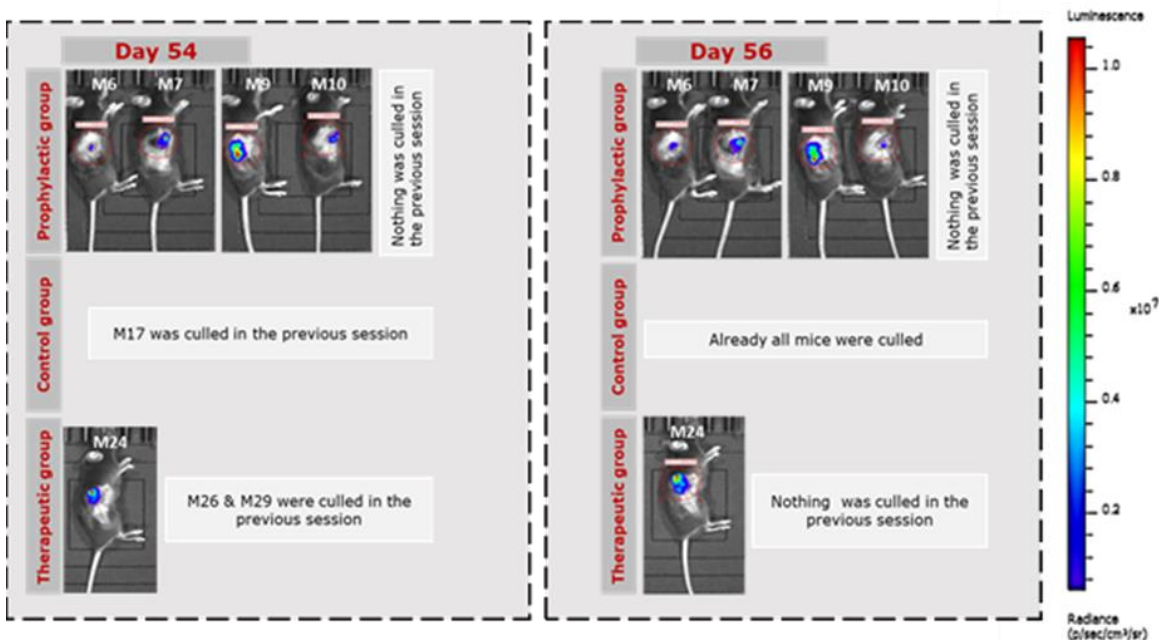


**Figure 7.5: Sequential real-time *in vivo* analysis of tumour burden in live animals, as assessed by Perkin Elmer IVIS Lumina III system.**

The figure reflects intra-tumoural luciferin bioluminescence signals in anaesthetised HHDII/DR1 mice bearing  $hB16/HAGE^+/Luc^+$  tumour. Images from different groups point out a decline in tumour size and prolonged mice survival in vaccinated group in comparison with the control. Colours overlying mice represent the rate of photons emission of the luciferin per second, wherein, red refers to the highest photons density and violet corresponding to the least detectable emission.

Intra-tumoural luciferin bioluminescent signals detected in  $hB16/HAGE^+/Luc^+$  tumour from both groups were demonstrated in Figure 7.6. Interestingly, while the total flux signals, as expected, were very similar on day-22 (one day post-transplant), 10 days later, statistical difference was detected between the size of tumours for the prophylactic group and those for the control. Thereafter, tumour size in the prophylactic group and therapeutic stayed, for the majority of the tumour, below the  $1 \times 10^9$  threshold. However, by day-39 a distinct group consisting of 4 mice separated from the rest of the prophylactic group, continuing to grow until they had to be culled on day-46. In the future, it would be interesting to re-immunise animals showing such a trend before their tumour become too big. It is also evident from these graphs that 7 out of the 10 mice that received the vaccine after tumour implantation, their tumour first regressed below the  $1 \times 10^9$  threshold while the size of the tumour from the control group was, for the majority of them above or very near this value (with the exception of one mouse) but then by day-39 these increased again. This demonstrates the ability of the combined vaccines to delay the growth of tumour but required either further vaccination on day-39 or adding additional interventions, such as checkpoint inhibitors.

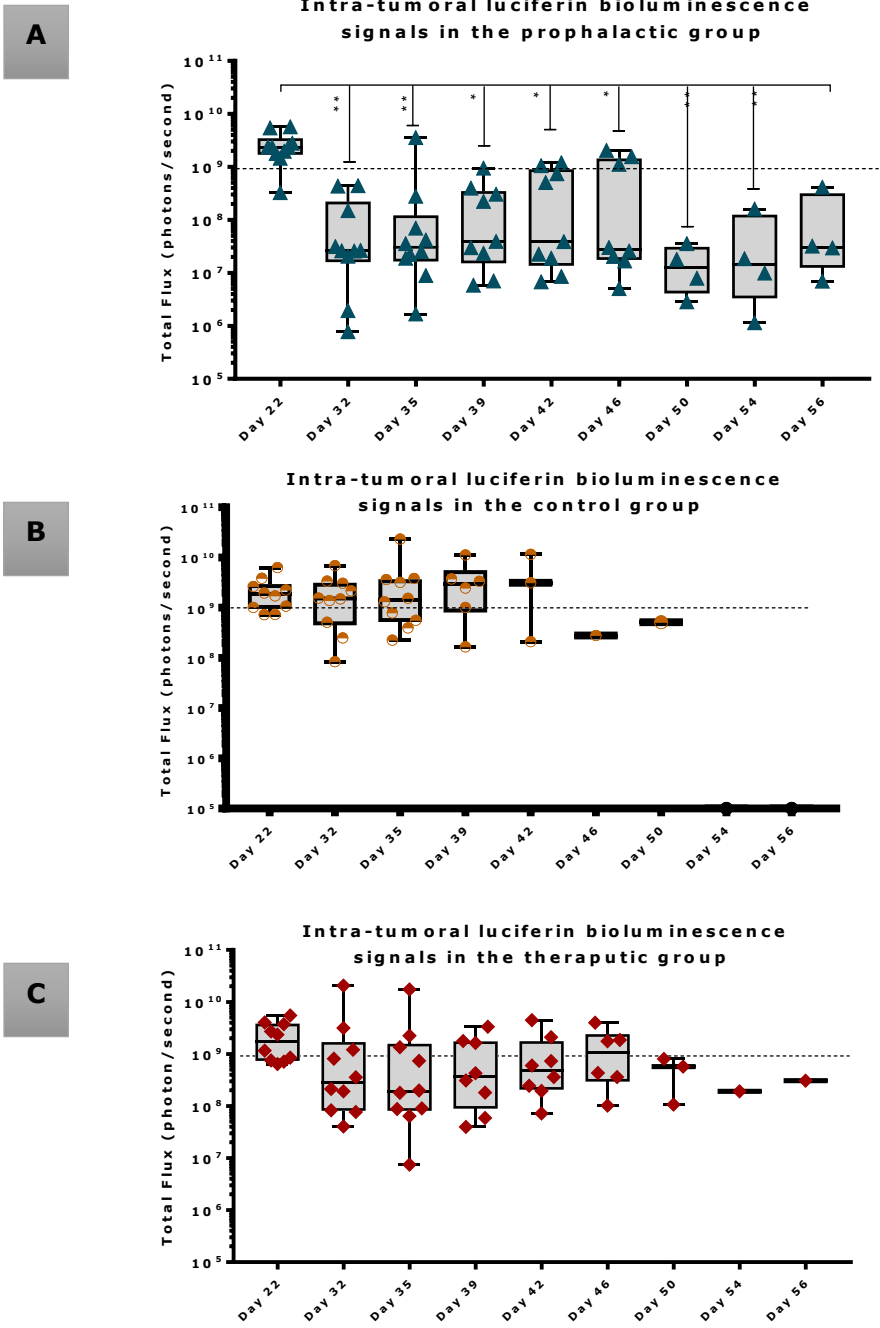


**Figure 7.6: Intra-tumoural luciferin bioluminescent signals in the vaccinated HHDII/DR1 mice bearing the aggressive  $\text{hB16/HAGE}^+/\text{Luc}^+$  tumour in comparison to the control.**

The figure demonstrates the prophylactic and therapeutic efficacy of the combined HAGE/WT1 ImmunoBody<sup>®</sup> vaccines, wherein luciferin bioluminescent signals were detected in the prophalactic (A), control (B), and therapeutic (C) groups as a total flux measured by photons/second. Data shows that the total flux in the prophalactic group and therapeutic was declined in comparison with the control, and that both treatment settings lead to prolong mice survival rate. The vast majority of mice from the control group were culled after day-39 post transplantation session whereas mice in the vaccinated groups survive while they were holding small size tumours.

Furthermore, tumour volume and weight were calculated for each tumour taken as soon as animals were culled. Data in Figure 7.7B, demonstrate that there is a significance difference in the tumour volume in the prophylactic and therapeutic group in comparison to the control at  $**P\text{-value} = 0.0030$  and  $*P\text{-value} = 0.0271$ , respectively. However, no statistical difference in tumour weights *versus* control was detected.

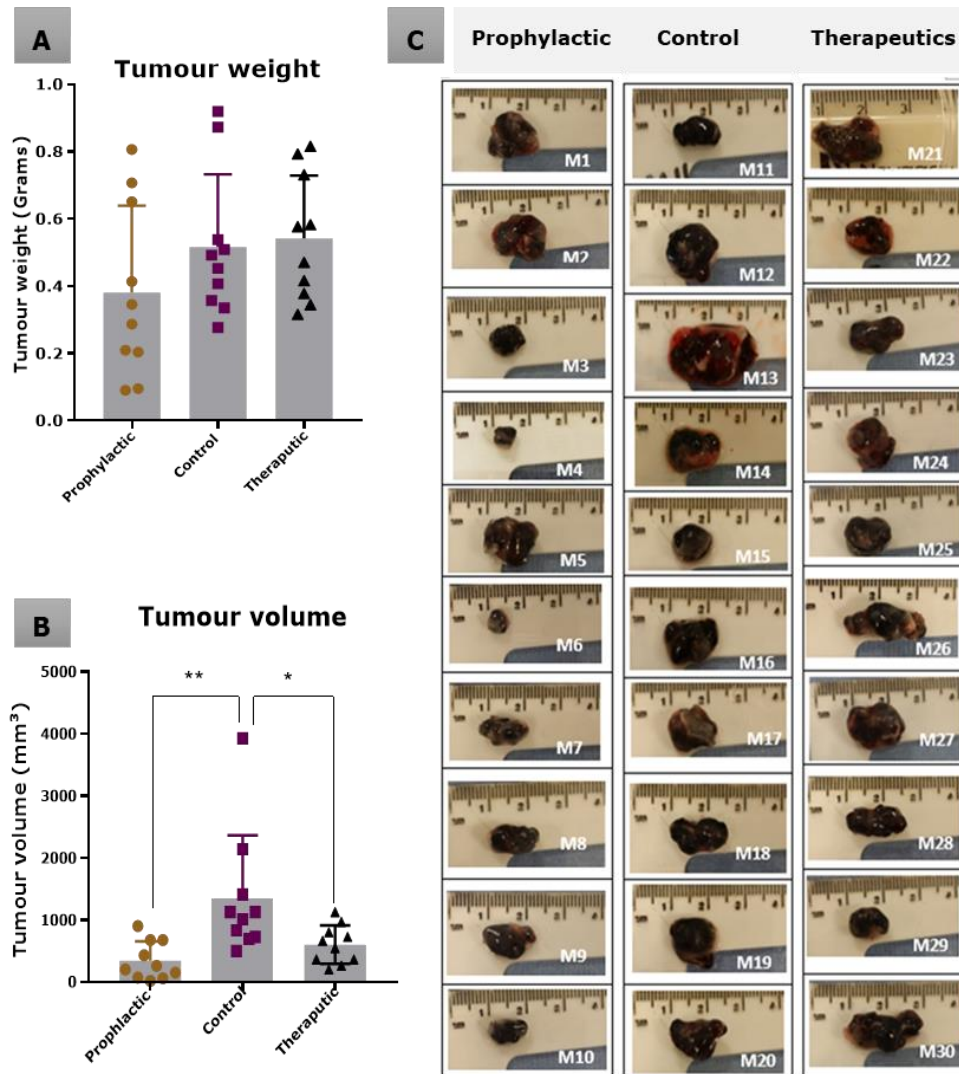


**Figure 7.7: Post-culled hB16/HAGE<sup>+</sup>/Luc<sup>+</sup> tumour weight and volume.**

The figure demonstrates the prophylactic and therapeutic efficacy of the combined HAGE/WT1 ImmunoBody<sup>®</sup> vaccines in HHDII/DR1 mice bearing the aggressive hB16/HAGE<sup>+</sup>/Luc<sup>+</sup> tumour. For each indicated group, tumour weight in grams shown in (A), tumour volume in mm<sup>3</sup> shown in (B) and post-culled tumour images highlighted the tumour size shown in (C) were determined. Mice were euthanized when tumour size reached endpoint threshold (12 mm<sup>3</sup> for the prophylactic setting and 15 mm<sup>3</sup> for the therapeutic setting). In graph A and B, data is expressed as the mean±SD, and the level of the significance was determined using one-way ANOVA analysis followed by Dunnett's multiple comparisons test.

After the experiment was completed, a survival curve was plotted (shown in Figure 7.8), wherein data clearly demonstrate that the combined HAGE/WT1 ImmunoBody® vaccines is able to significantly delays the aggressive growth of B16 melanoma cells and increases the overall survival of the prophylactic group, at  $**P\text{-value}<0.01$  in comparison to the control group. The therapeutic efficacy of the vaccines is shown to be also improved slightly the survival rate of the mice, but the rate was not statistically significant.

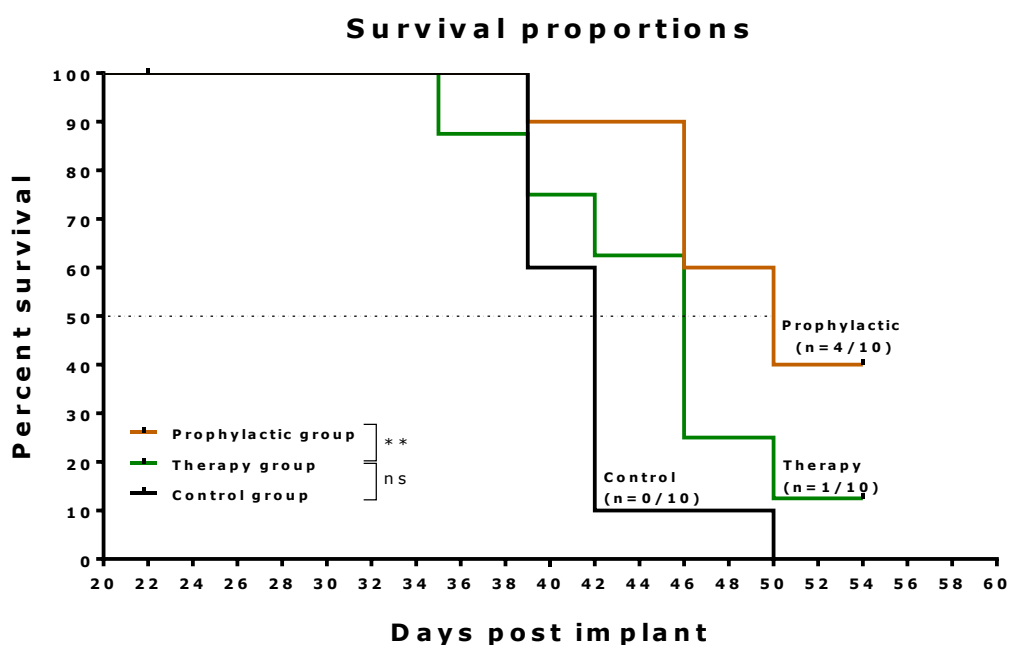


**Figure 7.8: Survival analysis demonstrates the antitumor efficacy of the combined HAGE/WT1 ImmunoBody® vaccines in vaccinated tumour bearing mice.**

Results shows that the combined HAGE/WT1 vaccines is significantly protective in the prophylactic group in comparison to the control group at  $**P\text{-value}<0.01$ , but not in the therapeutic setting. The significance of the difference was evaluated by both Gehan-Breslow-Wilcoxon test and log-rank test. The total number of mice is 30, (10/group).

### **7.3.3 Capability of the combined HAGE/WT1 ImmunoBody® vaccines to provoke *in vivo* anti-tumour effector T cell function**

As mentioned above, four mice from the prophylactic group (Mouse-6, Mouse-7, Mouse-9 and Mouse-10) and one mouse from the therapeutic group (Mouse-24) were able to survive until day-56 post-implantation. Although tumour volume had not reached the indicated endpoint thresholds, these mice were euthanised in order to assess some immunological responses at this particular stage of resistance before their tumours become bigger. Thus, some functional assay was performed, such as IFN- $\gamma$  ELISpot, in addition to TILs study.

IFN- $\gamma$  response generated in these mice was compared to a set of mice that were culled early in the study, which involves four from the control group (Mouse-11, Mouse-13, Mouse-15 and Mouse-16) and one from the therapeutic (Mouse-22), shown in Figure 7.9 (A&B). Interestingly, data show that IFN- $\gamma$  production was significantly greater in the surviving mice than those which were culled early in the study due to their tumour size reaching the maximum size allowed, indicating the ability of the combined vaccines to trigger specific anti-tumour immune protection in the form of IFN- $\gamma$  release in the responder mice which lead to prolong mice survival and tumours regression. It is also probably indicating that vaccinated mouse which had to be sacrificed early in the study due to tumour size (Mouse-22) lacked the development of specific anti-tumour immune response and therefore they maintained tumour growth in a similar pattern as the control.

IFN- $\gamma$  production from spleens of these mice was also assessed after 1week *in vitro* stimulation (IVS) using IFN- $\gamma$  ELISpot assay. As demonstrated in Figure 7.9C, IFN- $\gamma$  secretion was increased after IVS in comparison with those obtained by straight *ex-vivo*. Furthermore, the frequency of HAGE- specific and WT1-specific T cells producing IFN- $\gamma$  was demonstrated for each mouse to find out whether there was any correlation between the number IFN- $\gamma$  spots and the size of the tumour measured post-culling (Figure 7.10). There was, however, no consistent correlation between a tumour size and the level of IFN- $\gamma$  production. It is possible that the difference is to be found elsewhere such as the number of Tregs, MDSC or the level of IDO1 expressed by the tumour.

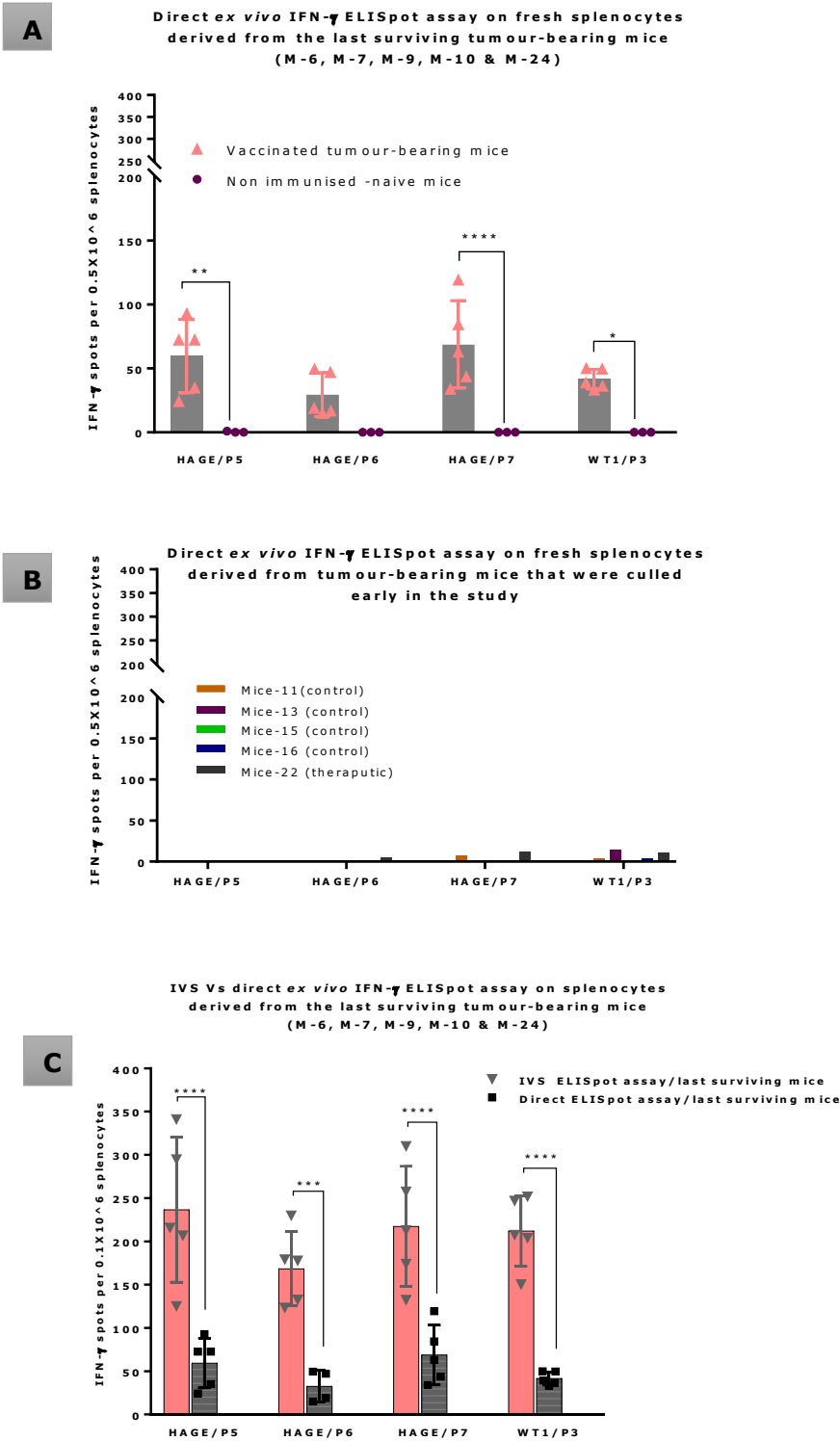
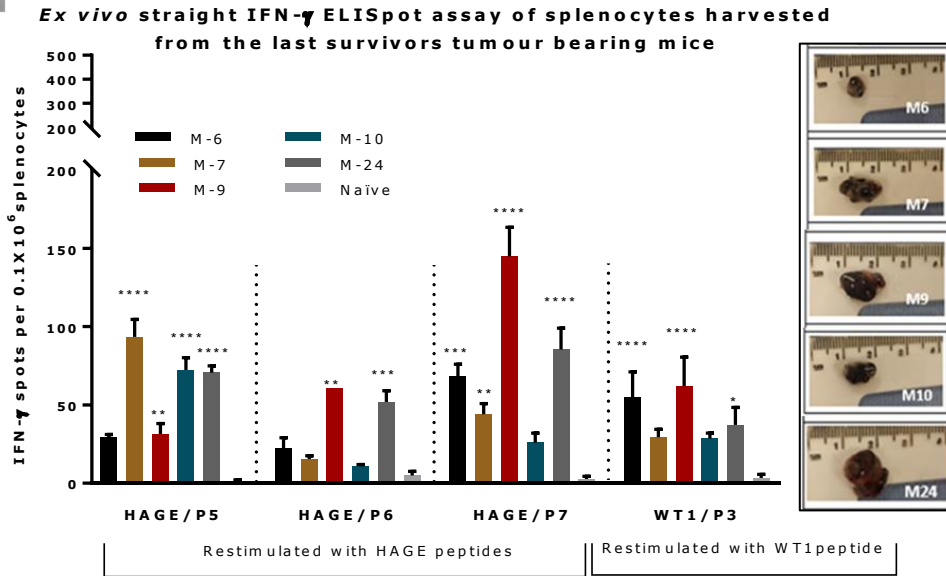


**Figure 7.9: Ex vivo IFN- $\gamma$  ELISpot results of splenocytes derived from HHDII/DR1 tumour bearing mice vaccinated by the combined HAGE/WT1 ImmunoBody<sup>®</sup> vaccines.** Result of direct ELISpot assay on fresh splenocytes derived from the last surviving tumour-bearing mice from the prophylactic group (Mouse-6 ,Mouse-7 ,Mouse-9 and Mouse-10) and one mice from therapeutic group (Mouse-24) shown in **(A)** versus samples from mice culled earlier shown in **(B)**, cells were harvested and plated at a density of  $0.5 \times 10^6$  cells/well and re-stimulated with  $1 \mu\text{g/mL}$  of short peptides for 48hours. Results demonstrate that IFN- $\gamma$  is much greater in the surviving mice than the control. These fresh splenocytes were also assessed *in vitro* after one-week stimulation using IVS assay, wherein, cells were incubated at a density of  $0.1 \times 10^6$  cells/well with  $1 \mu\text{g/mL}$  short peptides shown in **(C)**. Results reveal that there was a significance induction of IFN- $\gamma$  secretion after 1-week IVS. Data plotted as an average of spots/mouse, expressed as the mean $\pm$ SEM of all 5 mice and the level of the significance was assessed using two-way ANOVA.

A



B

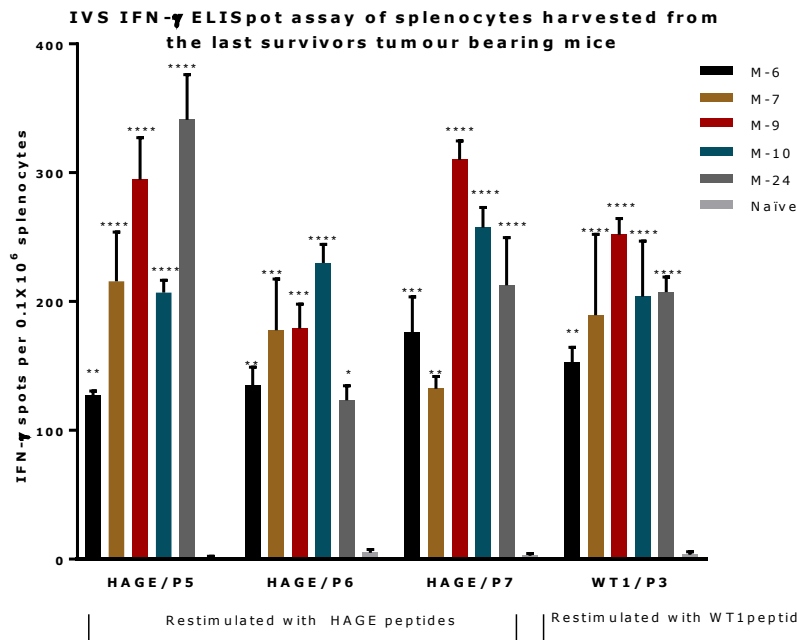


**Figure 7.10: Ex-vivo IFN- $\gamma$  ELISpot assay of splenocytes processed from the last surviving tumour bearing mice assessed individually.**

Results of IFN- $\gamma$  ELISpot of fresh splenocytes is shown in (A), wherein, splenocytes were harvested and plated at a density of  $0.5 \times 10^6$  cells/well and *in vitro* re-stimulated with  $1 \mu\text{g/mL}$  of short peptides for 48 hours. After 1-week *in vitro* stimulation (IVS) results are shown in (B). Results show that there is a significance induction of IFN- $\gamma$  secretion after 1-week IVS. Error bar of each bar in the graph is expressed as the mean  $\pm$  SEM of triplicate of single mouse and the level of significance were assessed by two-way ANOVA followed by Dunnett's multiple comparisons test.

Furthermore, splenocytes derived from these survivor mice and stimulated for one week were co-cultured with different targets to assess the responsiveness of T cells upon recognition of the relevant targets as assessed by the release of IFN- $\gamma$ . Results in Figure 7.11 show that a specific immunity was generated, although the number of mice was not enough to make a final judgement on the result, there were a trend to produce more IFN- $\gamma$  against targets that hold dual expression of HAGE and WT1 antigens than the one expressing a single antigen.

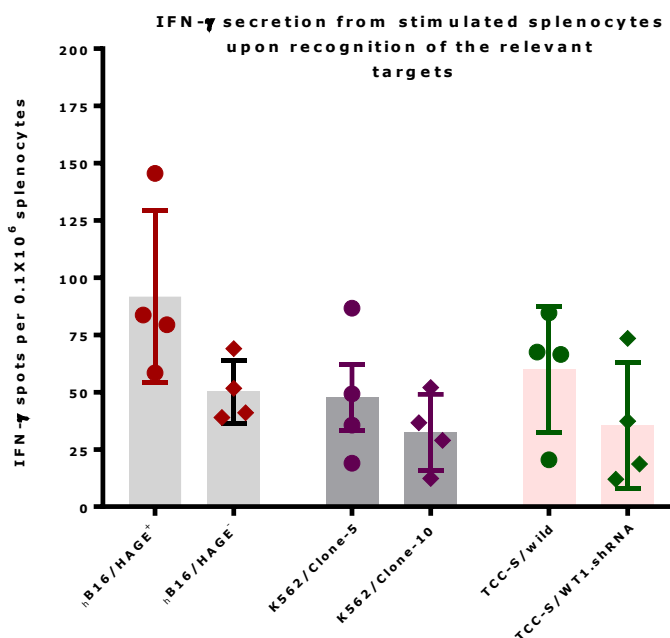


**Figure 7.11: IFN- $\gamma$  secretion from splenocytes harvested from the last survivor tumour bearing mice, upon the recognition of the relevant targets, as assessed by ELISpot IFN- $\gamma$  assay.**

Splenocytes isolated from the last survivor tumour bearing mice immunised with the combined vaccines were stimulated for one-week, plated at  $0.1 \times 10^6$  cells per well and then co-cultured with the modified targets at a ratio of 10:1, respectively. Bar chart shows the number of spots produced by CTLs from these mice against different targets after backgrounds being subtracted. Values are expressed as the mean  $\pm$  SEM of the 4 survivors, and the level of significance was assessed using Dunn's multiple comparisons test. Results show that there is an induction of IFN- $\gamma$  secretion after 1-week against different targets.

Moreover, the cytokines/proteins released upon the recognition of the specific antigens were assessed from CD8<sup>+</sup> T cells (which were stimulated by IVS) from the last survivor mice co-cultured with targets. Results in Figure 7.12A and B show fold increase in the CD8<sup>+</sup> secreting cytokines upon incubation with T2 cells and hB16 cells. Fold change calculated as a ratio of (CTLs *versus* peptides-pulsed T2 cells) to (CTLs *versus* non-pulsed T2 cells). Similarly, a ratio of (CTLs *versus* hB16/HAGE<sup>+</sup>/Luc<sup>+</sup> cells) to (CTLs *versus* hB16/HAGE<sup>-</sup>/Luc<sup>+</sup> cells) was also calculated. Results demonstrate that the average fold increase in cytokines/proteins secretion is higher in targets holding dual expression of the antigens than the target hold no or single peptide, although it

was not statistically significant. Interestingly, one mouse demonstrates a notable upregulation in IFN- $\alpha$ , Ki-67 and IL-2 release, shown in Figure 7.12B.

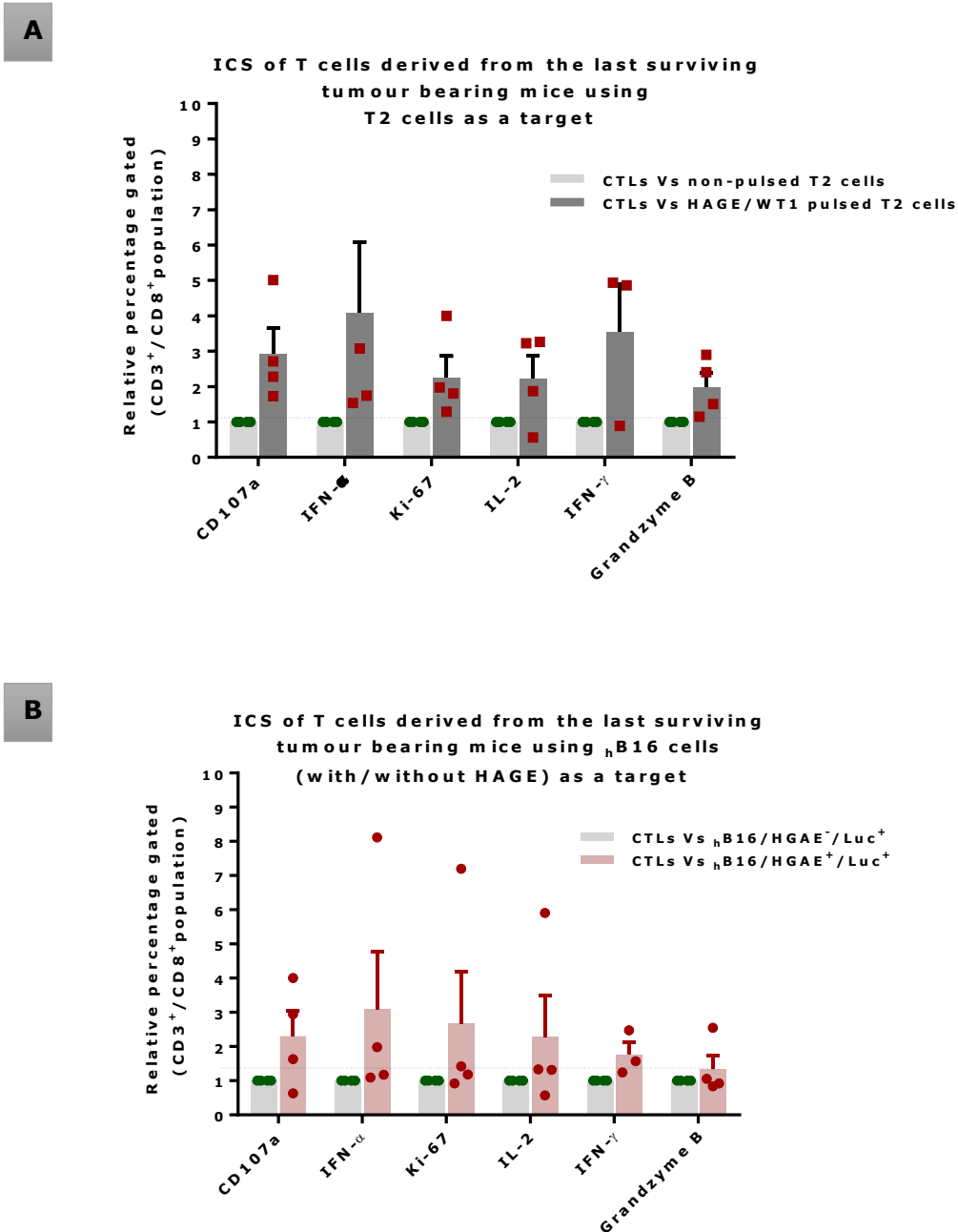


**Figure 7.12: ICS of CTLs harvested from the last survivor tumour bearing mice in the prophylactic mice, induced by the HAGE/WT1 ImmunoBody<sup>®</sup> combined vaccines upon the recognition of the cognate peptides expressed by targets.**

Splenocytes were stimulated for one-week by IVS and then plated at  $0.1 \times 10^6$  cells per well and co-cultured with targets; T2 cells shown (A) and B16 cells shown in (B) at a ratio of 10:1(E:T) for 6 hours using ICS assay, the level of the cytokines were then assessed using flow cytometry. Bar chart shows fold increase in cytokines produced by CTLs from the last survivor mice against different targets. Values are expressed as the mean  $\pm$  SEM of the 4 mice and the level of significance was assessed using two-way ANOVA.

### 7.3.4 Phenotypical characterisation of T cells and TILs from mice bearing $_{h}B16/HAGE^{+}/Luc^{+}$ tumour

The profile of tumour-infiltrating lymphocytes (TILs) was assessed and compared with T cells extracted from spleens of tumour bearing mice. Therefore, after each culling, a small piece of tissue was immediately digested and stained with Brilliant Violet 421™ anti-mouse CD3 antibody, Alexa-fluor700 anti-mouse CD4 antibody, APC/CY7 anti-mouse CD8a antibody and APC anti-mouse CD279 PD-1 antibody. Cells were also stained with ZOMBI or LIVE/DEAD™ Yellow to exclude dead cells. After that, samples were assessed by flow cytometry and analysed according to gating strategy in Figure 7.13.

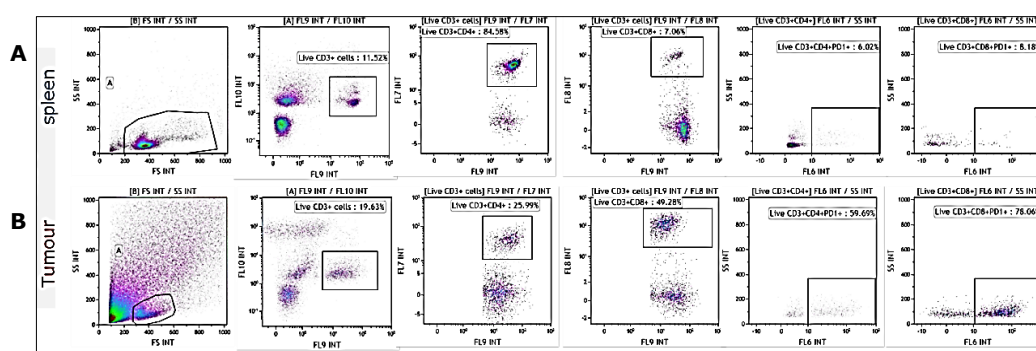


**Figure 7.13: Gating strategy of splenocytes (A) and TILs (B) from immunised tumour bearing mice treated with HAGE/WT1-derived vaccine.**

Figure 7.14 demonstrates the expression pattern of CD3<sup>+</sup>, CD4<sup>+</sup>, CD8<sup>+</sup> and PD-1 on TILs and T cells from fresh spleens isolated from tumour bearing mice in both treatment settings in comparison to the control group. From these data, the following points can be concluded, firstly; the majority of CD3<sup>+</sup> T cells that recruited in spleens was CD4<sup>+</sup> cells whereas the majority of CD3<sup>+</sup> T cells in all tumours studied was CD8<sup>+</sup> cells, as shown in (A&B), indicating a reverse CD4<sup>+</sup>/CD8<sup>+</sup> ratio of TILs in comparison with those derived from spleens. This trend is seen overall in the vaccinated and non-vaccinated groups, but the percentage of CD8<sup>+</sup> T cells within tumour of the prophylactic and therapeutic mice was significantly more than the control at *\*\*\*P-value*= 0.0003 and *\*P-value*= 0.0323, respectively, shown in (B), indicating that the combined vaccines were able to recruit more CD8<sup>+</sup> cells in the vaccinated group in both the prophylactic and therapeutic settings.

Secondly, more than 60% of CD4<sup>+</sup> and CD8<sup>+</sup> T cells infiltrated tumour tissues were expressing PD-1 compare to 5-10% in spleens, as shown in (C& D), suggesting that T cells of both types CD4<sup>+</sup> and CD8<sup>+</sup> in the tumour microenvironment have been jeopardised by immunosuppressive elements, PD-1, which might be induced by immune immunosuppressive cells in the hostile B16 microenvironment. Finally, the

percentage of CD4<sup>+</sup>PD-1<sup>+</sup> cells in tumours was higher in the prophylactic group at \*\**P*-value= 0.0046 than the control.

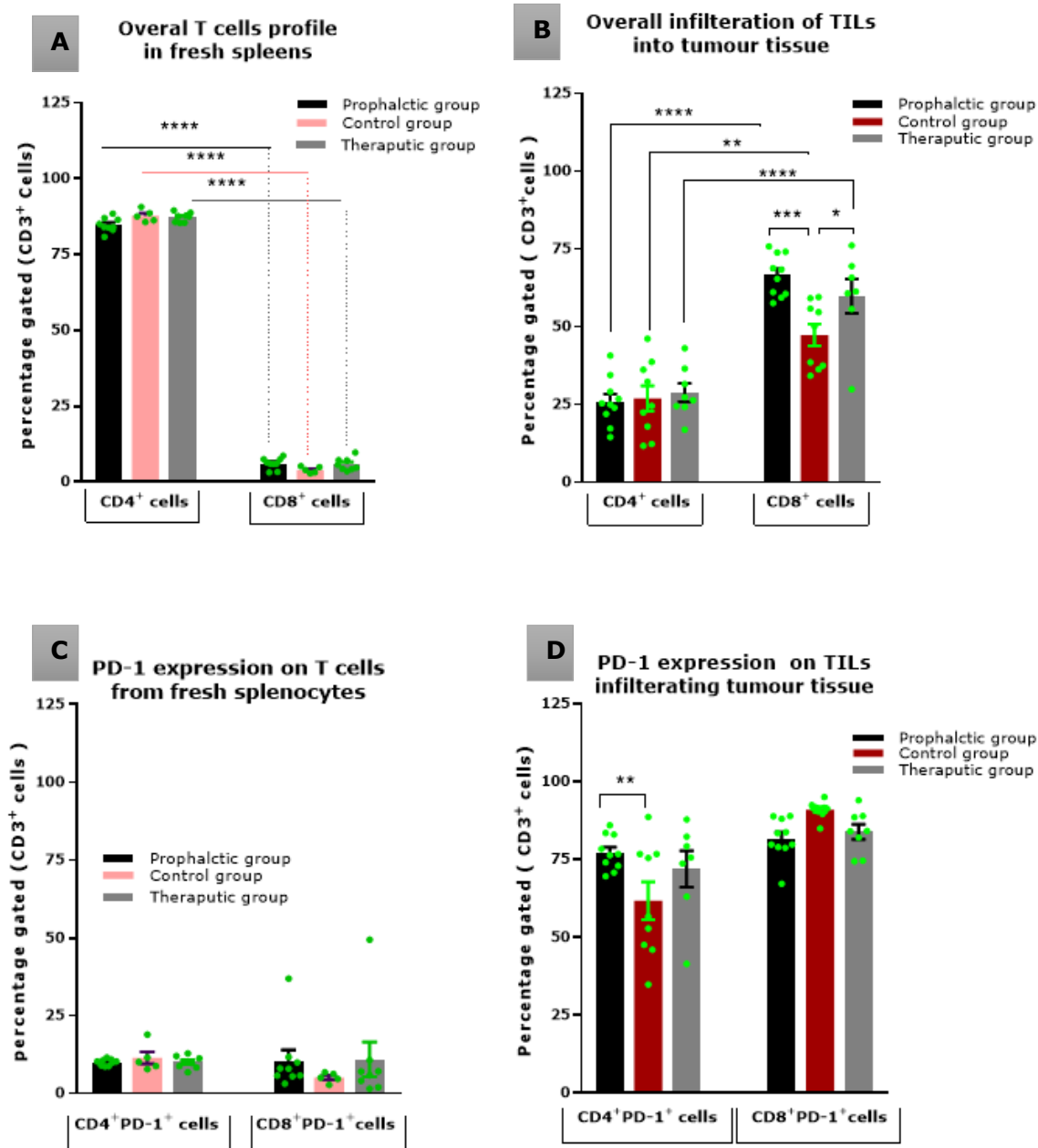


**Figure 7.14: Overall T cells profile of spleens and TILs harvested from vaccinated and non-vaccinated tumour-bearing mice, as assessed by flow cytometry.**

Cells were processed and incubated with anti-mouse FCR block at 1 $\mu$ g/test for 15 minutes at 4°C and then stained with surface antibody; anti-CD3, -CD4, -CD8, -PD-1 and Live/Dead Yellow stain for 30 minutes at 4°C, cells were then assessed by flow cytometry. Data are expressed as the means $\pm$  SEM of at around 10 mice/group and the level of significance were assessed by two-way ANOVA followed by Dunnett's multiple comparisons test. Data demonstrate an inversed CD4:CD8 ratio derived from tumour in comparison to spleens, and also demonstrates PD-1 upregulation in the T cells derived from tumour tissues.

Moreover, T cells profile from fresh spleens and TILs isolated from the last survivor tumour bearing mice from the prophylactic group were analysed and compared separately and data demonstrated in Figure 7.15 and Figure 7.16 below.

Similar to the data above obtain from the overall mice studied, CD4<sup>+</sup> cells in spleens harvested from this group of mice were found to be significantly higher than those present in the tumours at \*\*\*\**P-value*<0.0001. The tumours, in contrast, demonstrated a significant higher expression of CD8<sup>+</sup> than CD4<sup>+</sup> cells at \*\*\*\**P-value*<0.0001. Moreover, CD4<sup>+</sup> and CD8<sup>+</sup> cells derived from tumours are both predominantly expressing PD-1.

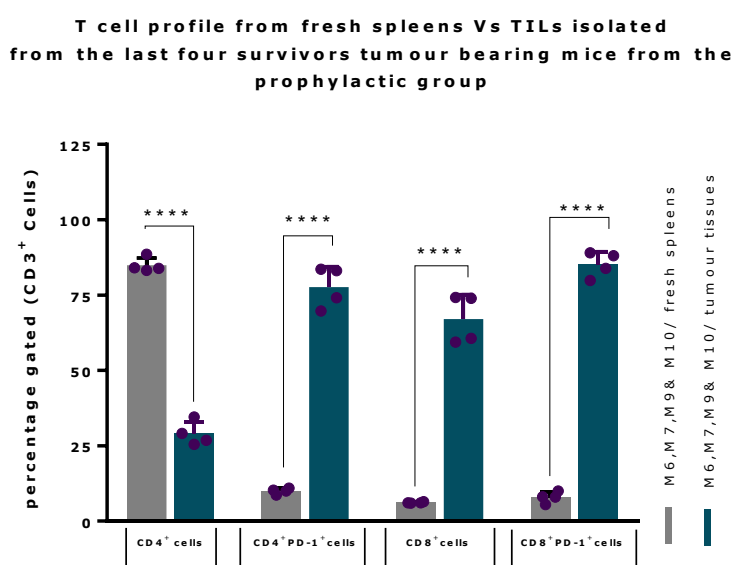


**Figure 7.15: T cell profile from fresh spleens versus TILs isolated from the last four survivor tumour bearing mice from the prophylactic group.**

Cells were processed and incubated with anti-mouse FCR block at 1µg/test for 15 minutes at 4°C and then stained with surface antibody; anti-CD3, -CD4, -CD8, -PD-1 and Live/Dead Yellow stain for 30 minutes at 4°C, cells were then assessed by flow cytometry. Data are expressed as the mean ± SEM, and the level of significance were assessed by two-way ANOVA followed by Dunnett's multiple comparisons test. Results highlight the significance difference in CD4<sup>+</sup> and CD8<sup>+</sup> expression in tumours in comparison to spleens, as well as the PD-1 expression on each subset.

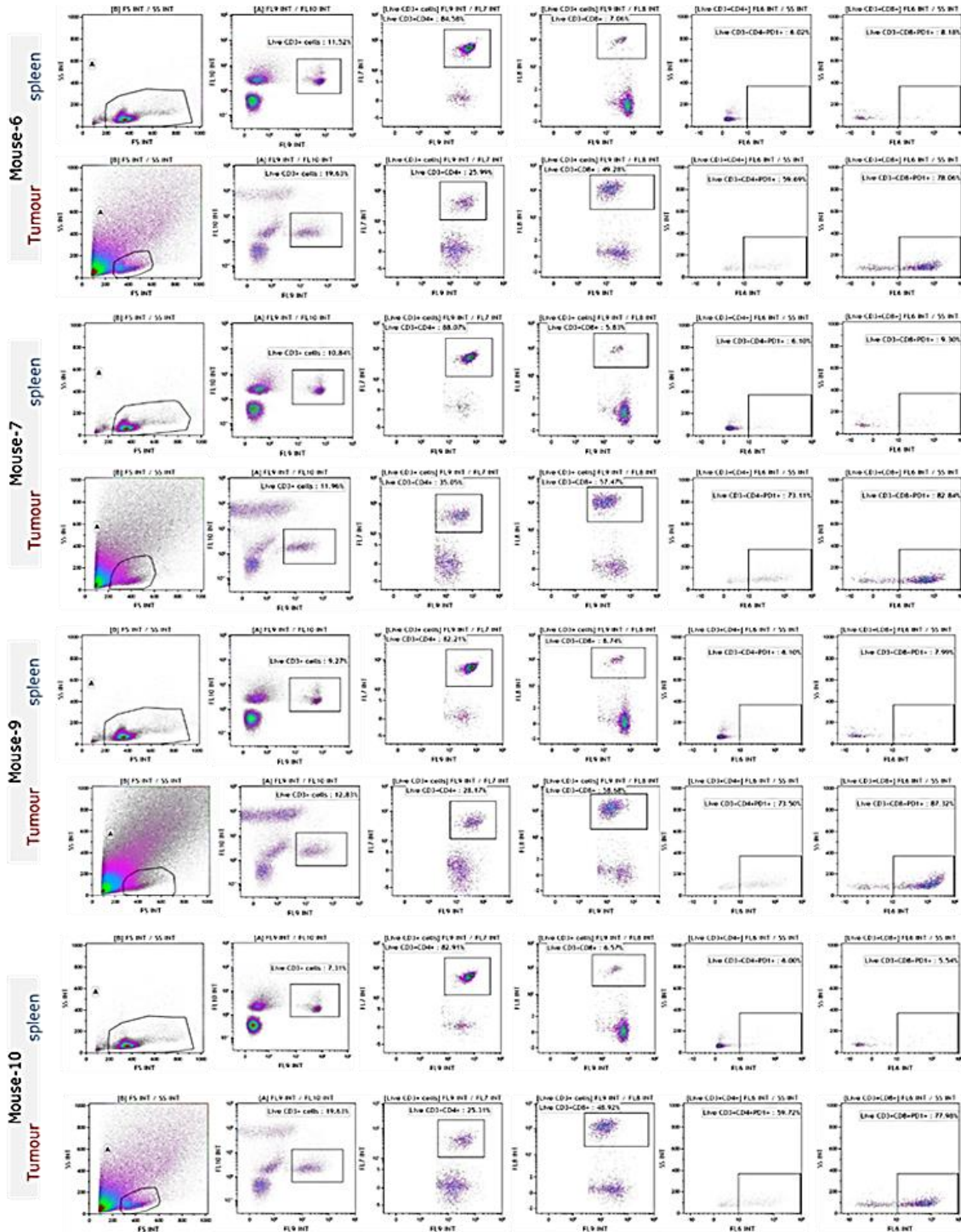


**Figure 7.16: Representative images of flow cytometry staining analysis of T cells profile derived from splenocytes and tumours from the latest surviving tumour bearing mice from prophylactic group.** Results highlight the difference in the expression of PD-1 between spleens and tumours.

## 7.4 Discussion

Murine syngeneic tumour models constitute an essential pre-clinical element in the development of novel immunotherapies, of which, the subcutaneous model has been commonly used in pre-clinical tumour challenge experiment to evaluate the efficacy of these therapies. One of the commonest subcutaneous tumour model approaches that has been extensively used to establish tumours transplants in the C57BL/6 is the murine B16 melanoma cells and its sublines B16-1 and B16-F10 (Ya, Hailemichael *et al.* 2015). Tumours from B16 cell lines have been described as more immunologically 'silent' in comparison with other tumour types, and they express low MHC class I and II pathway genes (Mosely, Prime *et al.* 2017, Nanni, Colombo *et al.* 1983). Hence, this project has employed a genetically modified version of the B16 "humanised" provided by Scancell Ltd to be implanted in "humanised" HHDII/DR1 mice. As described previously, the B16 cells were humanised by knockout  $\beta 2m$  to remove the murine MHC antigens, and then were transfected with the chimeric HHDII and HLA-DR1 genes. These cells were further modified by the previous PhD student by transfecting of HAGE and the firefly luciferase constructs. Expression of these genes in addition to the natural expression of WT1 were all confirmed in Chapter-5 (5.3.6.) before these were used in tumour challenge experiments.

Using the traditional caliper measurement for subcutaneous tumours is problematic because of its lower limits of detection. A palpable subcutaneous tumour can be detectable only when tumour cells are present first at more than million cells, and at this level of sensitivity, complete clearance of tumours, however, cannot be accurately determined. Another matter related to subcutaneous tumours monitoring is that central tumour necrosis, skin ulceration, and treatment-induced apoptosis might not be fully accounted for by gross tumour mass measurements (Puaux, Ong *et al.* 2011). For these reasons, developing a tumour monitoring system associated with higher degree of sensitivity and quantifying only live cells is an important necessity.

Hence, various technologies to study tumours in live animals have been developed, including micro-computed tomography, magnetic resonance imaging, micro-positron emission topography, and bioluminescent imaging. The first three technologies offer the advantage of high level of accuracy by delivering three-dimensional structural images; however, they are all quite expensive, and time consuming as only a single animal can be imaged at a time (Craft, Bruhn *et al.* 2005). Bioluminescent imaging has the merits of being less expensive, convenient as many animals can be imaged concurrently, and is quite sensitive. The main drawbacks of this technique; however, is that it does less resolution than other systems, and delivering only two-dimensional tumour signals. Additionally, bioluminescent image based on the expression of a reporter gene (foreign gene) inserted in the tumours cells being assessed, hence,

limiting its usage in endogenous tumours (Contag, Ross 2002, Hollingshead, Bonomi *et al.* 2004).

Studies herein have employed mainly the bioluminescent imaging system to monitor tumour growth, and thus the following optimisation steps were required; Firstly, to characterise the available imaging system with the modified B16 tumours and to validate our results. Previously, in the target preparation Chapter-5 ([Section: 5.3.6.1](#)) we demonstrated the rates of photons emitted due to luciferase activity with tumour burden *in vitro*, wherein, a static linear correlation between luciferin emission and B16 at both very low and high densities was observed, thereby, demonstrated the validity of these cells for being used as a tumour model and being monitored by the available imaging system.

Moreover, the tumorigenicity of the  $hB16/HAGE^+/Luc^+$  cells *in vivo* prior to the tumour challenge experiments was established. Three different doses of cells were implanted subcutaneously in naïve HHDII/DR1 mice, and tumours were then monitored for a steady kinetic growth, a dose of  $0.75 \times 10^6$  cells of  $hB16/HAGE^+/Luc^+$  was associated with kinetic steady tumour growth detected almost in all mice, this dose was therefore chosen for the tumour challenge experiments.

Having determined the tumorigenicity of the  $hB16/HAGE^+/Luc^+$ , tumour challenging experiment in the prophylactic and therapeutic settings were then set up. Upon analysing the bioluminescent signals, it has been clearly demonstrated mice that did not receive the vaccine had to be sacrificed earlier due to tumour size endpoint being reached, whereas mice that received the combined vaccines continue to survive and showed a delayed tumour growth in comparison to the control. Interestingly, while the total flux signal for all the groups was very similar on day-22 (one day post-transplant) which was expected, 10 days later, a statistically difference was found between the size of the tumour for the prophylactic group and those for the control. While the majority of the mice in the prophylactic group developed a slowly growing tumour, interestingly a distinct group of 4 mice exhibited quicker tumour growth and these had to be culled earlier than the remaining 6 mice, but it is also clear that such growth is still slower than those seen in the control group, and hence, mice bearing such tumour were culled at days later than the control. In the future, it would be interesting to either re-immunise the animals showing such a trend before their tumour become too big or continue the vaccination even after the tumour started to appear. Mice in the therapeutic group exhibited a reduction in tumour size while the immunisation was still happening, but as soon as the last injection of the vaccine was performed, tumours started to grow, highlighting again the importance of do not stopping the vaccine injection while tumours can still be detected.

The survival curve further demonstrated the efficacy of the combined vaccines in protecting mice from tumour challenge and in delaying tumour growth in the

prophylactic group. These results were achieved after a set number of vaccine injections and could be improved by the continuation of vaccines inoculations.

Furthermore, comparing outcomes of mono *versus* combined vaccines, results obtained herein with the combined HAGE/WT1 ImmunBody® vaccines are better than those obtained with either vaccine alone. Indeed, tumour challenge experiments were previously conducted in our group to assess the efficacy of HAGE ImmunBody® vaccine as a monotherapy (Divya Nagarajan/ manuscript in preparation submitted to immunology and cell biology), wherein a statistically significant result was achieved in the prophylactic setting in terms of delaying tumour growth and prolonging the survival rate of mice, however, the efficacy generated was less than those provided in the present study (see the survival curve in Figure 9.4/Appendix). In addition, we previously assessed the efficacy of WT1-ImmunBody® vaccine monotherapy, we found that there was no statistically significant improvement in the survival rate of mice in comparison to the control group (survival curve in Figure 9.5/Appendix). Both studies employed HAGE- and WT1-ImmunBody® as monotherapies while they were combined in the present study, strongly highlighting the important of incorporated HAGE with WT1 for future vaccine development.

At the end of the experiment, anti-tumour immune response generated in spleens of 4 mice from the prophylactic group and one from the therapeutic group were assessed in order to demonstrate the nature of immune protection that the combined vaccines provided. HAGE/P5 and HAGE/P6, class-I peptides, as well as HAGE/P7 class-II peptide and one class-I WT1/P3 peptide were associated with high IFN- $\gamma$  release. In order to confirm the hypothesis that both HAGE- and WT1-specific T cells are responsible for the tumour growth delay, splenocytes from the last survivors mice were harvested and tested *in vitro* for IFN- $\gamma$  production following *in vitro* re-stimulation with the identified naturally processed and immunogenic peptides for 48 hours using IFN- $\gamma$  ELISpot assay. High level of IFN- $\gamma$  secretion was obtained with these splenocytes in comparison with the level of IFN- $\gamma$  produced from mice that were culled from control and therapeutic groups due to tumour size endpoint occurred earlier in the study, indicating that the combined vaccines induced a strong immune response which was involved in the prolong surviving of mice.

In addition, these cells were stimulated *in vitro* using 1week IVS, we found that a greater induction of IFN- $\gamma$  secretion was produced in comparison with straight ELISpot assay. This observation is of a particularly clinical importance as one could potentially expand *in vitro* pre-existing HAGE- and WT1-specific T cells before being re-injected into patient's blood circulation.

The pre-existing immunity within the tumour microenvironment plays an important prognostic value in a wide range of malignancies (Fridman, Pages *et al.* 2012), and it perhaps serves a prognostic biomarker of response to many types of immuno-

based therapies (Tumeh, Harview *et al.* 2014, Ji, Chasalow *et al.* 2012). Based on the infiltration of T cells into tumour compartment, tumours can be roughly classified into hot and cold tumours, wherein, in the former, an abundance tumour-infiltrating lymphocytes (TILs) is detected and exert the immune response but are then dampened by immune checkpoints upregulation and/or increased activity of immunosuppressive cells. Cold tumours, by contrast, are identified by the absence of an adequate population of established TILs. Thus, immunophenotypic analysis of TILs extracted from the B16 tumour tissues and splenocytes was performed using flow cytometry. Data demonstrated a clear reverse CD4<sup>+</sup>/CD8<sup>+</sup> of TILs ratio in comparison with those derived from spleens. While the majority of CD3<sup>+</sup> T cells in the spleens were CD4<sup>+</sup> (80%), more than 75% of them were CD8<sup>+</sup> T cells in the tumours. The high recruitment percent of CD8<sup>+</sup> cells were noticed in the vaccinated and non- vaccinated group of mice; this indicates the that B16 that we have used was immunogenic, which was not surprising since these cells are modified to overexpress foreign antigens, the HAGE antigen is totally human and immunogenic, in addition to the firefly luciferase report gene. However, it is clear that CD8<sup>+</sup> cells of TILs isolated from mice that were vaccinated with combined vaccines in the prophylactic and the therapeutic settings are significantly higher than those derived from the control group, suggesting that these cells were the principal cell type involved in the process of tumour rejection.

However, we have also found that more than 80% of these CD4<sup>+</sup> and CD8<sup>+</sup> T cells which infiltrated tumour tissue expressed PD-1 compare to 5-10% in the spleen. As it well-know, PD-1 expression is promptly induced on T cells surface after TCR activation (Chikuma, Terawaki *et al.* 2009), and this expression is transient, declines when antigen is cleared. PD-1 is; however, maintained and become constitutively expressed on antigen-specific T cells in cases of cancer or chronic disease (Youngblood, Oestreich *et al.* 2011). This might support the evidence that TILs could be hindered by immune checkpoint signals in the tumour microenvironment. Hostility of such milieu can include upregulation of ligands for the immune checkpoint, B7-1 and PD-L1, on the surface of the MDSCs and tumours *per se* leading to profound inhibitory signal to T cells causing T cell anergy and apoptosis (Okazaki, Honjo 2007, Gabilovich, Nagaraj 2009b). B16 cells express high quantity of PD-L1, one could assume that PD-1/PD-L1 mediated immune suppressions might have occurred in this *in vivo* model, in particular the therapeutic one. Therefore, future experiments should assess the use of the immune checkpoint inhibitors to enhance further the efficacy of the combined HAGE/WT1-ImmunoBody<sup>®</sup> vaccines.

## 7.5 Conclusion and chapter impacts

In the previous chapters, the capability of HAGE- and WT1-ImmunoBody® vaccines to elicit *ex vivo* specific CTLs was demonstrated. This work is the first piece of work that demonstrates the value of combining HAGE- and WT1-ImmunoBody® vaccines in inducing *in vitro* specific killing of targets expressing both antigens.

In this chapter, anti-tumour capability of the combined vaccines was demonstrated for the first time to significantly delay the growth of the aggressive B16 tumours in both prophylactic setting and increases the overall mice survival in comparison to the non-immunised group of mice. This combination was also found to be effective in the induction of potentially potent *in vivo* HAGE- and WT1-specific T cell responses compared to the control non-vaccinated group. Collectively, these findings hold indeed a great promise to treat a wide-variety of cancer and might provide a supplement to standard surgical and or chemotherapeutic approaches, or in combination with other therapeutic vaccines, based on immune-mediated cytotoxicity against cancer.

However, PD-1 expression, was found to be expressed in high level on TILs cells which might be the reason behind the low effect that the vaccine provided in preventing outgrowth of the established tumour. Thus, these findings would provide a rationale for using anti-PD-1 in combination with the combined regime to enhancing the efficacy in eliminating of established tumours; however, due to the lack of time it was not possible to assess this combination strategy at this point of time.

## 8 Chapter VIII: Summary of discussion and recommendations

### 8.1 Introduction

Conventional cancer treatments, such as chemotherapy/radiotherapy, are not specific to cancer cells but rather target any rapidly-dividing cells, this is why severe cytotoxicity of normal tissue can occur, such as organs damage and suppression of bone marrow. Active immunotherapy, however, represents a cancer specific approach that works by eliciting patient's own immune system to recognise and kill only cancerous cells, thus minimising the likelihood of undesirable effects. Importantly, the greatest advantage that active immunotherapy can offer is the establishment of long-term memory thereby offering a durable therapeutic effect. In this regard, many targeted immunotherapies have been investigated in clinical and preclinical settings to treat various malignancies. Of these, CML in particular has gained a special attention in the field of the immunotherapy, due to several reasons; i) the circulating cancerous cells in the blood render them an easy target for the immunotherapy, unlike solid tumours which shield themselves from immune attack by a thick layer of stromal cells; ii) the well-known mechanistic underpinning CML carcinogenesis allowing the development of immunotherapy that could specifically target particular oncogenic element; iii) potential selective overexpression of several immunogenic TAAs which involve in the process of the development of the disease, iv) the high percentage in cure of CML patients post allo-SCT highlights the involvement of a well-established immunity to reject CML stem cells; v) the prolong chronic phase provides considerable time for monitoring the effect of the immunotherapy during the course of therapy; vi) the beneficial "off-target" effects that imatinib has on the immune system, in addition to its "on-target" effects.

However, even though Tyrosine Kinase Inhibitors (TKIs) have considerably improved the outcome of CML, these therapies fail to eradicate CML stem cells which are ultimately responsible for the disease relapse upon treatment withdrawal. It has been reported that imatinib therapy faces three major challenges; i) the development of resistance in almost 20-40% of patients due to mutations in the *BCR-ABL1* gene, ii) limited response in patients with blast crisis, which might be attributed to establishment of additional chromosomal and molecular changes; the resulting cells of which might be not solely depend on *BCR-ABL1* for their survival, iii) finally, and the hardest overall, is the insensitivity of CML stem cells to both imatinib and other generations of TKIs. It has been found that while imatinib exerts a strong toxicity against differentiated leukaemic progenitors, CML stem cells demonstrate a relative or even complete resistance to the treatment. Indeed, even though CML patients who

have reached complete remission, their primitive leukaemic progenitors continue to be readily detectable. Notably, resistance to imatinib therapy in CML patients often occurs in the advanced stages particularly due to *BCR-ABL1* gene amplification and mutations. The second-generation TKIs, dasatinib and nilotinib, which are much more specific and potent than imatinib have also been shown to be associated with clinical resistance because of a range of point mutations. Such drug-insensitivity is the reason behind selective leukaemic stem cells outgrowth and disease relapse even years after cessation of TKIs. Thus, finding of assistant agents to enhance the therapeutic efficacy of TKIs is critically needed to obtain a state of relapse-free durable remission.

Active immunotherapeutic strategy aiming to enhancement T cell responses against specific antigens in patients on imatinib therapy could increase the number of patients experiencing relapse-free survival following cessation of imatinib.

In addition to many benefits of combining T cell-based vaccine with imatinib in CML patients, one interesting advantage is that while the former has the capability to induce T cells for IFN- $\gamma$  secretion which has strong immunostimulatory effect but also immunoinhibitory function due to the IDO induction associated with the IFN- $\gamma$  production, the latter may be able to inhibit IDO production, and so prevents subsequent downstream immunosuppressive events of IDO activity.

Historically, the interest in the vaccine innovation for treatment of CML has dramatically increased since the identification of CML-specific tumour antigen, the *BCR-ABL1*. The immunogenicity of the *BCR-ABL1*, however, has been subjected to much dispute. Its role in the development of CML and its unique sequence encompassing the breakpoint junction region, make it "in theory" an ideal target for immunotherapy and these were therefore thought to be able to induce high avidity T cells. However, a limited number of immunogenic epitopes across the junctional region has been identified, which are restricted to only a few HLA types. In this aspect, Clark and colleagues provided indeed the first direct evidence that haematologic malignancy derived cells (represented by both K562/HLA-A3<sup>+</sup> cells and primary CML cells from HLA-A3<sup>+</sup> patients) were able to express a leukaemia-specific peptides derived from *BCR-ABL1* protein (KQSSKALQR) on the cell surface in association with HLA class I antigens (HLA-A3) using a sensitive technique, the tandem nanospray mass spectrometry (NSI/MS). The authors were also able to demonstrate that those patients could induce a specific CTL response against the junctional peptide (KQSSKALQR) expressed on CML cells *in vitro* which was also found capable to kill autologous CML cells. Moreover, the authors demonstrated the occurrence of circulating specific anti-KQSSKALQR T cells detected by tetramer staining assay (Clark, Dodi *et al.* 2001).

Hence, because *BCR-ABL1* is a completely novel tumour-specific antigen, it was thought less likely that tolerance or anergy could develop in comparison with normal

self-antigen. However, failure of *BCR-ABL1* to induce effective CTLs *in vivo* in CML patients has often been described, this failure could be attributed to a number of possible reasons, such as weak antigen expression, low TCR avidity or development of T cell tolerance in patients with severe leukaemic burden. For example, it has been found that b3a2 specific CD4<sup>+</sup> T cells could be detected in normal volunteers but not in CML patients, it is therefore assumed that CD4<sup>+</sup> T cells which are essential for most CD8<sup>+</sup> T cell responses may be either absent or anergic.

Several other studies have demonstrated encouraging observations to target *BCR-ABL1* in treatment of CML, however, it was assumed that the success of such strategy depends on finding the optimal peptide composition, adjuvants, route, and timing of administration. Due to these limitations/disputes against this antigen, *BCR-ABL1* was excluded from this project.

A number of additional LAAs have been considered as promising targets for immunotherapy because of their ability to elicit specific immune responses against antigen-bearing cancerous cells while sparing normal tissues. The present study has focused on DDX43 (HAGE) and WT1 proteins as promising candidates for immunotherapeutic strategy. These groups of TAAs have been described as potentially reliable targets for the development of T cell-based immunotherapy on the basis of their restricted expression to cancer, their involvement in cell proliferation and tumorigenesis, and their limited expression in normal organs. These two antigens were tested in HHDRII/DR1 mice using a novel system of DNA delivery called ImmunoBody<sup>®</sup> (Scancell).

The overall goal of the proposed project was to develop a combined HAGE and WT1 based vaccines to create a state of definitive cure in CML patients. We hypothesised that combining both HAGE and WT1 vaccines would be more effective against cancerous cells expressing both antigens than a vaccine incorporating peptides derived from either of these antigens alone. We believe that developing such combination would benefit patients who are already on imatinib therapy to achieve a "definitive cure" by eradication of residual CML cells, patients who developed resistance to imatinib during the course of the disease, and patients who are in the blast crisis and not eligible to SCT. To develop these vaccines, this thesis has therefore studied and compared the following aspects; firstly, the HAGE and WT1 overexpression in peripheral blood mononuclear cells (PBMCs) derived from human leukaemic samples, secondly, the immunogenicity of HAGE- and WT- derived peptides upon the administration of HAGE and WT1 vaccines individually and in combination in HHDRII/DR1 mice, thirdly, the capability of the vaccines given individually and in combination to induce active cytotoxic T cells that can specifically recognise and kill peptide-expressing targets *in vitro*, and finally *in vivo* capability of the vaccines to induce tumour rejection using HAGE<sup>+</sup>/WT1<sup>+</sup> expressing hB16 cells as a "proof-of-concept" in tumour challenge experiments.

## 8.2 Validation of HAGE and WT1 as potential targets for immunotherapy

Although recent strategies to harness the immune system upon targeting cancer antigens have been heavily investigated, the clinical benefits of which are often associated with disappointing outcomes, principally due to the lack of suitable targets. Therefore, it is an important first requirement to confirm that the chosen antigens are overexpressed in the cancerous cells and absent/diminished in the normal cells.

Cancer testis (C/T) antigens have emerged as valuable targets for the development of cancer vaccines due to their restrictive expression in tumour cells and low or non-existent expression in normal cells, except testis and placenta. Many studies have confirmed that, in normal tissues and certain cancers, the promoters of C/T genes are hypermethylated and the use of demethylation agents can restore the expression of these antigens.

The candidate helicase antigen (DDX43), a member of the C/T antigen family, a relatively newly discovered antigen, and the oncogenic Wilms tumour (WT1) antigen have been both described by their overexpression in several solid tumours and haematological malignancies (Oka *et al.* 2006b, Martelange, De Smet *et al.* 2000, Mathieu, Linley *et al.* 2010). Adams and colleagues detected HAGE overexpression at the mRNA level in 55% and 71% of CML patients in chronic and blast crisis phases, respectively, and in 23% of AML samples (Adams, Sahota *et al.* 2002). In addition, Chen, Lin *et al.* in 2011 detected HAGE transcript overexpression in 9 CML cases (34.6%) (Chen, Q., Lin *et al.* 2011).

Hence, HAGE expression was herein initially assessed in several CML derived cell lines, and it was found that none of these cells express HAGE at protein level and few of them express HAGE at mRNA level, except TCC-S cells which express HAGE at both the mRNA and the protein levels. Some of these cells were previously studied and found to be highly hypermethylated, and that HAGE expression could be restored after treatments with demethylating agents (Lin, Jiang, Chen *et al.* 2014). Also, a previous PhD student in our group (Morgan Mathieu, 2007) found the same observation where a significantly enhancement of HAGE transcript expression was obtained upon treating K562 and KYO-1 cells with a demethylating agent (5'-aza-2'-deoxycytidine).

Similar mechanism was described for the expression of WT1 in leukaemia. McCarty and Loeb in 2015, for example, correlated CpG island methylation status in some myeloid derived cell and primary AML samples with WT1 expression, wherein the authors demonstrated that hypomethylation of the Intron 1 CpG island increases WT1 expression. Both K562, and HL60 found to be expressing WT1 and that their DNA were unmethylated. U937 cells; however, which do not express WT1, demonstrated

a significantly upregulation of WT1 upon treatment with the demethylating agent 5-azacytidine (McCarty, Gregory, Loeb 2015), thereby a solid correlation between methylation of the Intron 1 CpG island and silencing of WT1 in leukaemia was demonstrated. We found that WT1 was constitutively expressed virtually by all leukaemia cells lines studies.

We have also assessed the expression of HAGE and WT1 transcripts in cDNA samples obtained from PBMCs from leukaemic patients at the time of the diagnosis, provided by collaborators from other universities in the UK. HAGE transcripts were expressed at around 54% of CML samples, a result comparable to those found by Adam and colleagues at 55% (Adams, Sahota *et al.* 2002), and that WT1 transcripts were expressed by all CML samples studied with 70% of them expressing it at a level higher than that found in TCC-S cells. High percentage of WT1 overexpression in CML has also been reported in other studies (Inoue, Sugiyama *et al.* 1994, Karakas, Miething *et al.* 2002). Furthermore, HAGE and WT1 expression in these samples were compared and the results showed that the majority of the samples overexpressing WT1 also overexpressed HAGE, while those expressing low level of WT1, also expressed low level of HAGE. The observation of concomitant co-expression is of a particular importance since we hypothesised a promising outcome upon HAGE and WT1 vaccines incorporation.

In addition, we have assessed HAGE and WT1 expression in four paired samples, pre-treatment and post-imatinib failure. It has been found that a significant concomitant increase in the expression of both HAGE and WT1 transcripts in 2/4 pairs post-imatinib failure in comparison with pre-treatment samples. Nonetheless, two separate studies by (Abdel-Fatah, McArdle *et al.* 2016) and (Coluzzi, Introcaso *et al.* 2016) showed that as the disease progresses in CML, an increase in HAGE and WT1 expression occurs, leading to poor prognosis. It would be therefore very interesting if one could follow HAGE and WT1 expression over time in a large cohort of patients to confirm the validity of HAGE and/or WT1 as biomarkers for poor prognosis/imatinib failure in CML.

In addition to CML, HAGE and WT1 expression was studied in PBMCs of AML patients, HAGE was found to be overexpressed in all the patients studied (although the cohort was relatively small) in comparison with healthy controls. This percentage seems to be high in comparison with Adam, *et al.* 2002 who found that 23% of AML bone marrow and peripheral blood samples expressed HAGE (Adams, Sahota *et al.* 2002). These discrepancies could be attributed to the specificity of the primers and or sensitivity of PCR applied or disease stages as well as the number of samples. Interestingly, WT1 transcripts were also found to be overexpressed in all AML patient samples studied. Previous studies have also demonstrated that WT1 is overexpressed in all the AML samples taken at diagnosis (Aydin, Riera *et al.* 2013). The interesting observation that both HAGE and WT1 are co-overexpressed in these AML samples in

a high proportion of AML patients could provide an evidence of the feasibility of using HAGE and WT1 combined vaccines for the treatment of AML.

In addition to the above-mentioned assessments, a large-scale of publicly available microarray clinical datasets for AML and CML samples (at the time of diagnosis) was used to study the expression of WT1 and HAGE as well as a comprehensive number of C/T genes. WT1 gene was found to be significantly upregulated in both AML and CML diseases in comparison to control healthy individuals, a result which is in line with what was found in the above-mentioned findings. However, there was a discrepancy regarding HAGE expression in comparison with the above-mentioned results, indeed in this analysis no significant difference in HAGE expression between CML and control samples was found, instead there was a significant downregulation of HAGE in AML. These findings are in direct contradiction with both what has been in the limited number of samples that have been studied here and what other authors have published. It is entirely plausible that the primers used in the microarray are the source of the discrepancies, where the probes in the microarrays might have been affected by the methylation status of HAGE. Indeed, in a study by Lin, Chen *et al.* (2014), the majority (85%) of HAGE DNA of AML patients were found to be methylated and the remaining samples were hypomethylated, the authors further demonstrated that HAGE expression is epigenetically controlled and a significant correlation with HAGE hypomethylation was found, using Real-Time Quantitative Methylation-Specific PCR (RQ-MSP) and bisulfite sequencing (Lin, Jiang, Chen *et al.* 2014). In any case, patients with AML could be given a demethylating agent such as Azacytidine (AZA) or Decitabine (DAC) prior to the administration of the HAGE-derived vaccine to circumvent heterogeneity and restore the process of transcription. Other C/T genes microarray analysis also demonstrated different patterns of expression, with the majority of them being overexpressed in both AML and CML, few were found not to be different in comparison to the control or even downregulated. Overall, exploring such a large number of C/T genes trying different probes could open an avenue to many researchers to develop a specific C/T derived vaccine for treating leukaemia.

In summary, HAGE and WT1 combined vaccines in CML and AML preceded by a dose of demethylating agents could help patients whose genes are particularly hypermethylated especially during the blast phase. Another advantage of using demethylating agents in CML blast phase is to restore the expression of several tumour suppressor genes that were reported to be often methylated in CML patients and cell lines during the blast crisis (Janssen, Denkers *et al.* 2010).

## 8.3 Immunogenicity of HAGE- and WT1 derived peptides

The second important prerequisite in cancer vaccine development is to determine the immunogenicity of vaccine derived peptides. The ideal vaccine should stimulate both arms of adaptive cell immunity, T helper CD4<sup>+</sup> T cells and cytotoxic CD8<sup>+</sup>T cells. While the former helps the development of CTLs, the latter destroys specifically an aberrant cell. Importantly, various factors have been found to affect the overall cancer vaccines success, such as type of the vaccine used, route of administration, system of vaccine delivery, optimal period between vaccine priming and boosting, optimising different adjuvants combination, and finally and the most advance strategy is the incorporation of a vaccine with different other modalities, such as the incorporation with the traditional therapy and/or with immunomodulatory molecules, such as anti PD-1/PD-L1 pathway blockade.

This project is based on the use of a novel delivery system, called ImmunoBody<sup>®</sup>, provided by Scancell Ltd. This DNA vaccine encodes an antibody protein engineered to express specifically chosen peptide sequences incorporated into the CDR of the antibody. DCs at the site of injection take-up these antibodies via their Fc receptors resulting in the stimulation of high frequency/high avidity T cells of both helper and cytotoxic T cell repertoire presenting the encoded peptides by both direct and cross-presentations.

A previous PhD researcher in our group, Divya's Nagarajan, identified a 30-mer length peptide [QTGTGKTLCYLMPGFIHLVLQPSLKGQRNR] in the human HAGE protein as containing several predicted class I and class II epitopes of which 3 were predicted to HLA-A2 and two to HLA-DR1 haplotypes. The efficacy of this 30-mer sequence in the form of HAGE-ImmunoBody<sup>®</sup> was compared with that of the HAGE 30-mer peptide/adjuvant simple vaccination programme. The HAGE-ImmunoBody<sup>®</sup> was found to be more potent in term of the number of high frequency/high avidity T cells produced as assessed by IFN $\gamma$  ELISpot assay. Similarly, a 15-mer length WT1 peptide [VRDLNALLPAVPSLG], and two derived smaller peptides; WT1/P3 (ALLPAVPSL) and WT1/P5 (DLNALLPAV), were assessed for their immunogenicity in peptide/adjuvant simple vaccination programme and also in the form of ImmunoBody<sup>®</sup> vaccine in HHDII/DR1 mice. Results have shown that the WT1-ImmunoBody<sup>®</sup> vaccine (as it was the case for HAGE) was significantly better than the simple vaccination at enhancing WT1 immunogenicity, and therefore, the rest of the proposed project only used this novel system of delivery in the development and comparing of the HAGE- and WT1-based vaccines.

Prior to test the immunogenicity of these ImmunoBody® vaccines, the binding affinity as well as the stability of this binding were assessed for all the HLA-A2 HAGE- and WT1-derived peptides using T2 binding and Brefeldin A decay assays. Peptides with low binding affinity and/or with low stability are not be able to generate fully activated T cells. HAGE/P4, HAGE/P5, HAGE/P6 were found to be all strong binders and demonstrated prolong stability on T2 cell surface. Similarly, WT1/P3 also demonstrated high HLA-A2 binding capability and resistance to internalisation. However, WT1/P5 was found to be weak HLA-A2 binder and was not able to stabilise the peptide/MHC complex which was rapidly dissociated and internalised.

After that, HAGE- and WT1-ImmunoBody® vaccination was implemented individually and in combination. According to the Scancell Ltd standardisation, the vaccines were injected in a prime-boost regime, wherein, priming at day-0, then two boosts at 7 days intervals through intradermal route of injection using gene gun technology (Pudney, *et al.* 2010), this route can deliver the DNA directly into Langerhans cells (DCs under the skin) at high efficient rate, followed by rapid migration of APCs into the regional lymph nodes (Porgador, Irvine *et al.* 1998).

It has been reported that one detrimental issue in the development of combination vaccines is the possible competition between vaccines in processing and presentation of peptides derived from the vaccines by the APCs. However, in the present study no decline was found in the immunogenicity of WT1 or HAGE peptides when both vaccines were given simultaneously but in different flanks, and therefore this incorporation was implemented in all our *in vitro* and *in vivo* studies. In this scenario, it was found that splenocytes derived from immunised animals responded strongly against two class I HAGE derived peptide, HAGE/P5 and HAGE/P6, one class II peptide, HAGE/P7, and class I WT1/P3 assessed by IFN- $\gamma$  ELISpot assay, whereas HAGE/P4 and HAGE/P8 and WT1/P5 did not, as the number of spots generated being close to that of the background, and therefore, they were excluded from further study.

Next, the avidity of the HAGE and WT1 HLA-A2 restricted peptides was assessed. Avidity is defined as the amount of peptide that is needed for the activation of effector T cell function (Kroger, Alexander - Miller 2007), and therefore measures the overall strength of a CTL interaction with a target cell (Sandberg, Franksson *et al.* 2000), which was herein measured by half maximal activation (EC<sub>50</sub>).

Splenocytes derived from mice immunised with either HAGE or WT1 ImmunoBody® were co-cultured with decreasing concentrations of corresponding class I short peptides and assessed for IFN- $\gamma$  secretion using ELISpot assay. These peptides were able to continue stimulating the production of IFN- $\gamma$  even at a very low concentration

at  $EC_{50} = 5.46e-008$  for HAGE/P5,  $EC_{50} = 6.203e-009$  for HAGE/P6 and  $EC_{50} = 7.538e-009$  for WT1/P3.

Upon encountering a specific antigenic stimulus, naïve T cells proliferate and differentiate into effector cells. During this process, upregulation or downregulation of various surface markers occur to produce a specific cell function (Oehen, Brduscha-Riem 1998). Therefore, the proliferation and the effector functions of CTLs derived from the candidate vaccines that were generated upon individual and combined vaccinations in comparison to T cells derived from naïve mice were studied using 10 colour panel flow cytometric intracellular staining with surface staining assays.

Interestingly, TNF- $\alpha$  and Ki-67 produced per single CD8<sup>+</sup> cell in the immunised group were found to be higher than those generated in the naïve group, at almost equal rates, with no predominant response induced upon using a particular type of vaccine is noticed. However, CD107a and IFN- $\gamma$  are shown to be higher in the incorporated type of vaccines. These data indicate that all three vaccines were able to induce effector functions of CD8<sup>+</sup> T cells; however, the combined regime is able to induce higher degree of degranulation and IFN- $\gamma$  secretion than the individual vaccines.

To further characterise the responses induced by ImmunoBody<sup>®</sup> vaccines, a particular proliferating population of CD8<sup>+</sup> cells (Ki-67<sup>+</sup>CD8<sup>+</sup> cells) was found to produce significantly high TNF- $\alpha$ , IFN- $\gamma$  and granzyme B in all three vaccine strategies, of which, the combined vaccines shown to induce more production of TNF- $\alpha$  than when HAGE and WT1 were given individually. This observation is of particular clinical importance as one could potentially expand *in vitro* such cells before being re-injected into patient's blood circulation. This is once again highlighting the benefit of combining HAGE and WT1 vaccines.

Moreover, this study investigated whether a phenotypic polarisation toward memory pool was occurring over the course of vaccination, using two surface markers CD62L and CD44. Both HAGE- and WT1-ImmunoBody<sup>®</sup> vaccines independently or together were able to induce the differentiation of naïve T cells into memory repertoires (CD62L<sup>low</sup> CD44<sup>high</sup> population), and the use of both vaccines increased further the memory pool in term of the downregulation of CD62L<sup>high</sup>/CD44<sup>low</sup> population.

Some activation and exhaustion markers expressed by CTLs derived from mice immunised with the ImmunoBody<sup>®</sup> vaccines were also assessed in comparison to the naïve T cells, although other markers of T cell exhaustion were normal, PD-1 was the only upregulated marker which perhaps indicate T cell exhaustion, although it is necessary to demonstrate concomitant upregulation of other inhibitory markers to confirm such statement.

In summary, both HAGE- and WT1-derived sequences were found to induce stronger response when delivered as ImmunoBody<sup>®</sup> vaccines more than peptides/CpG/IFA.

The percentage of CD8<sup>+</sup> T cells producing IFN- $\gamma$  in response to short *in vitro* stimulation with the HAGE and WT1 HLA-A2 restricted peptides was found to be slightly higher than when either of the vaccines were used alone. The CD8<sup>+</sup> T cells derived from these vaccines administered individually and in combination were found to proliferate (Ki-67<sup>+</sup>) and produce both IFN- $\gamma$  and TNF- $\alpha$ . It would be interesting to assess whether the response obtained with peptide 7 for HAGE was generated from the activation of CD4<sup>+</sup> T cells or whether the peptide was further cleaved during the 48 hours incubation of the ELISpot assay into peptide 5 or peptide 6 and stimulated CD8<sup>+</sup> T cells rather than the CD4<sup>+</sup> T cells.

Finally, PD-1 expression was significantly increased on the surface of T cells derived from the immunised mice after a short *in vitro* stimulation with the peptide, which could reflect a state of T cell exhaustion.

## 8.4 *in vitro* cytotoxic activity of HAGE- and WT1- specific CTLs

For any vaccine development, it is crucial to demonstrate that the generated T cells can kill target cells expressing the correct HLA-A haplotype and antigens first *in vitro* and then in *in vivo* tumour model challenges experiments. To do so, various target cells were modified to purposely express or repress HAGE and/or WT1 proteins as well as the chimeric HLA-A2 (HHDII construct). All leukaemic cell lines were found to constitutively express WT1. The K562 cells do not express class-I molecules on their surface nor did they express HAGE. These were first transfected with the HHDII constructs and then some of these were further transfected with the HAGE construct, thereafter, these were cloned to obtain K562/HHDII<sup>+</sup>/HAGE<sup>+</sup> (Clone5) and K562/HHDII<sup>+</sup>/HAGE<sup>-</sup> (Clone10). KCL-22 cells express HLA-A2 but do not express HAGE and were therefore transfected with the HAGE construct to obtain the KCL-22/HAGE<sup>+</sup> cells to be compare with KCL-22/HAGE<sup>-</sup> (wild-type). TCC-S cells were the only cells that found to express all three HAGE, WT1 and HLA-A2. These were transfected with the shRNA targeting WT1 in order to suppress WT1 expression and produce TCC-S/shRNA.WT1 cells to be compare with wild TCC-S. Finally, the humanised B16 cells already knockout for the murine  $\beta$ 2m and transfected with HHDII/DR1 and then transfected with luciferase construct, with and without HAGE were inherited from a previous PhD student (hB16/HAGE<sup>+</sup>/Luc<sup>+</sup> cells) and (hB16/HAGE<sup>-</sup>/Luc<sup>+</sup> cells). The success of these modifications was confirmed by means of RT-qPCR, flow cytometry and Western blotting.

T2 cells, a TAP deficient cell line, were also used to confirm the ability of the vaccine-induced T cells to at least kill peptide-pulsed T2 cells. While the use of the T2 cells would confirm that the peptide responsible for the production of IFN- $\gamma$  from the vaccine-induced T cells, the modified cells would demonstrate that the same T cells

could kill target cells expressing the correct antigen. Technically, CTLs activity against these targets were assessed upon co-culture of the effector and the target cells at predefined ratios using  $^{51}\text{Cr}$  release assay, IFN- $\gamma$  ELISpot assay and ICS, wherein, the following findings were obtained:

Firstly, both HAGE and WT1 vaccines derived T cells were able to kill T2 cells that were pulsed with the HAGE and WT1 HLA-A2 restricted peptides respectively, as well as release IFN- $\gamma$  upon encountering of the candidate peptides on the surface of T2 cells using  $^{51}\text{Cr}$  release assay and IFN- $\gamma$  ELISpot assay, respectively. In a similar finding with T2 cells, the modified K562, KCL-22 and TCC-S cells as leukaemic cell models in comparison with their control versions demonstrate once again the frequency and functionality of the respective peptide-specific CTLs to specifically recognise and kill the clone expressing the specific antigen. Moreover, the  $\text{hB16}$  with/without HAGE cells were also studied to generate a preliminary information of *in vitro* cytotoxicity before being used as "a proof-of-concept" in tumour model studies. Interestingly, the pattern of specific CTLs activity generated against this murine but humanised target was quite similar to the ones obtained against the CML targets in term of the high percentages of killing and IFN- $\gamma$  production in comparison to the HAGE $^-$  clone.

Secondly, in all targets used, while HAGE and WT1 vaccines independently have shown to be associated with substantial cell mediated killing indicative of professional CTLs repertoires (as mentioned-above), the use of vaccines together induced a significantly higher percentage of killing over the use of either vaccines alone, mainly seen in  $^{51}\text{Cr}$  release assay against all targets studied. However, no significant differences were found using the IFN- $\gamma$  ELISpot. This might be due to the fact that CTLs with lytic activity do not necessary constitutively produce IFN- $\gamma$  (Derby, Reddy *et al.* 2001) and that the ELISpot and  $^{51}\text{Cr}$  release assays measure different aspects of cell-mediated cytotoxicity; effector cell function and target cell death, respectively, it is therefore assumed that CTLs generated upon combination of both vaccines could kill targets by additional means of cell-mediated cytotoxicity.

Thirdly, results obtained from the ICS using a multicolour flow cytometry demonstrates that cytokines/proteins released from HAGE-specific and/or WT1-specific CTLs upon encountering targets expressing the antigen of the interest are more than those produced upon encountering targets that do not express the correct antigen. Of which, CTLs derived from the combined vaccines were able to produce more than those derived from the vaccines alone, as it was demonstrated by a notable upregulation of TNF- $\alpha$  production (at approximately 34-fold) from CD8 $^+$  cell derived from mice immunised with the combined vaccines upon incubation with T2 cell pulsed with both HAGE and WT1 peptides relative to non-pulsed T2 cells. Nevertheless, only a 12- and 4-fold increase for those receiving the WT1 vaccine and

HAGE vaccine alone, respectively were noticed. There was also upregulation of IL-2, Ki-67 and granzyme B by the same CD8<sup>+</sup> cells upon recognition of (HAGE<sup>+</sup>/WT<sup>+</sup>) Clone5 K562 cells relative to (HAGE<sup>-</sup>/WT<sup>+</sup>) Clone10 K562.

It has also been demonstrated that peptide density on the target surface affects the percentage of target cells killing as it has been demonstrated upon WT1 knock-down in TCC-S cells led to a decrease in the percentage of target lysis. This feature is of clinical importance, since HAGE expression and also WT1 are epigenetically controlled and studies proved that demethylating agents can enhance their expression, therefore, it would be ideal if this can be applied prior to the used of the vaccine to increase the chance of recognition and subsequent killing.

However, the presented cytotoxicity assay was carried out on CTLs generated in mice, and it would be more practical if PBMCs derived from patients with cancer could be obtained, where one could stimulate them *in vitro* using a combination of the immunogenic peptides (WT1/P3, HAGE/P5 and HGAE/P6), co-culture with K562/HAGE<sup>+</sup>/WT1<sup>+</sup>/HLA-A2<sup>+</sup>, and then assess the immune responses. However, the availability of such samples has been problematic, and these studies are beyond the scope of the current thesis.

## 8.5 *In vivo* tumour challenge studies

Having demonstrated the capability of the combined vaccines to induce potentially fully activated T cells in *in vitro* cytotoxicity, the efficacy of this regime was then tested in *in vivo* tumour challenge experiments, wherein a predefined dose of the modified hB16/HAGE<sup>+</sup>/Luc<sup>+</sup> cells, which also naturally express WT1, was injected subcutaneously as a "proof-of-concept" to form tumour. Data generated from the prophylactic setting showed that the combination of HAGE- and WT1-ImmunoBody<sup>®</sup> was able to delay tumour growth and prolong mice survival rate in a significant proportion of mice in comparison to the control. Indeed, tumours implanted in mice that did not receive the vaccines grew faster than those received the vaccines, and they had to be sacrificed earlier due to tumour size endpoint being reached. Interestingly, while the vast majority of the mice in the prophylactic group developed a slowly growing tumour, a distinct group of 4 mice exhibited quicker tumour growth and these had to be culled earlier than the remaining 6 mice, but it is also clear that such growth is still slower than those seen in the control group, and hence, mice bearing such tumour were culled at days later than the control. Having seen such pattern of tumour development detected by the bioluminescent, it would be interesting, in the future work, to re-immunise animals showing such a trend before their tumour size become too big. Mice in the therapeutic group exhibited a reduction in tumour size while the immunisation was still happening, but as soon as the last injection of the vaccine was performed, tumours started to grow, highlighting again

the importance of not stopping the vaccines injections if the tumours can still be detected.

Comparing the outcomes of the present study with previous studies which used either HAGE- or WT1-ImmunoBody® vaccination programme as a monotherapy, the combined HAGE/WT1 ImmunoBody® vaccines used herein was found to further improve the delayed in the tumour growth of mice pre-immunised mice (prophylactic group). These observations highlight the importance of incorporating both HAGE and WT1 for immunotherapy for future vaccine development.

Moreover, this novel combination was found to induce notable amount of IFN- $\gamma$  secretion from HAGE- and WT1-specific T cells in the last survivor's tumour bearing mice in comparison to the mice that were euthanised early in the study, as it was assessed by IFN- $\gamma$  ELISpot assay. Interestingly, *in vitro* expansion of cells carrying such response was achieved using 1-week IVS, wherein a greater induction of IFN- $\gamma$  was generated. This observation is of particular clinical importance as once could potentially expand *in vitro* pre-existing HAGE- and WT1-specific T cells before being re-injected into patient's blood circulation.

One interesting finding in this study is that immunophenotypic analysis on TILs *versus* splenocytes isolated from mice from different groups demonstrated an obvious reverse CD4<sup>+</sup>/CD8<sup>+</sup> ratio of TILs in comparison with those derived from spleens. While the majority of CD3<sup>+</sup> T cells in spleens were CD4<sup>+</sup> (80%), more than 75% of them were CD8<sup>+</sup> T cells in tumours. High percent of recruited CD8<sup>+</sup> cells was found in both vaccinated and non-vaccinated mice; this indicates that B16 tumour that we have used was immunogenic, which is not surprising since this cells were modified to express the human HAGE antigen which would therefore have been seen as completely foreign. In addition, the cells were also transfected with the firefly luciferase report gene which has been reported to induce immunogenicity in mice tumours (Contag, Ross 2002, Hollingshead, Bonomi *et al.* 2004).

However, the frequency of CD8<sup>+</sup> cells of TILs isolated from mice that were vaccinated with the combined vaccines in the prophylactic and therapeutic settings was significantly higher than those derived from the control group, implying that these cells were the principal T cell type involved in controlling tumour growth.

It has been also noticed that the <sup>h</sup>B16/HAGE<sup>+</sup>/Luc<sup>+</sup> tumour model was associated with a remarkable upregulation of PD-1 on TILs, in both CD4<sup>+</sup> and CD8<sup>+</sup> T cells, that were derived from the immunised and non-immunised mice in comparison to cells derived from splenocytes. It has been reported that PD-1 expression is promptly induced on T cells surface after TCR activation (Chikuma, Terawaki *et al.* 2009), and this expression is temporary, declines when the immunogen is cleared. PD-1 is, however, maintained and become persistently expressed on antigen-specific T cells in cases of cancer or chronic disease (Youngblood, Oestreich *et al.* 2011). This might support the evidence that TILs could be hindered by immune checkpoint signals in

the tumour microenvironment. B16 is well-known to express PD-L1 (PD-1 ligand), therefore, it is possible that there was an activation of PD-1/PD-L1 pathway which could be attributed to the low efficacy noticed in the therapeutic setting. The prophylactic setting, however, shows significant results in term of prolonged mice survival and resistance to tumour growth despite the upregulation of PD-1 on TILs, suggesting an occurrence of other mechanisms that could make the combined vaccines in the prophylactic treatment overcome activity PD-1/PD-L1 pathway. Because of the low response seen in the therapeutic setting, it is therefore recommended to incorporate anti-PD-1/anti-PD-L1 with the novel combined vaccines and study enhancement that could be obtained.

## 8.6 Conclusion, limitations and future work

In conclusion, HAGE was found to be significantly overexpressed in the CML samples that were tested in the lab in comparison to healthy blood samples, but there was no significant overexpression by samples taken from MILE's study. This discrepancy might be due to the insufficient sample size of the samples assessed in the lab compared with the number of samples utilised from the online database, and also probably due to the difference in methods used for detection of HAGE. However, HAGE can still be considered a good candidate target for immunotherapy treatment against leukaemia after patients have received demethylating agents to restore its expression. On the other hand, WT1 antigen was found to be overexpressed by both the clinical samples assessed in the lab and those taken from the online database.

Interestingly, the present study also demonstrated that HAGE- and WT1-ImmunoBody<sup>®</sup> vaccines are more immunogenic than their respective peptide/adjuvant counterpart and that the response generated was CD8<sup>+</sup> T cells driven and included effector and memory CD8<sup>+</sup> T cells. The study also revealed that the combined HAGE and WT1 vaccines was more effective than either vaccine given individually, demonstrating the superiority of using an anti-HAGE and anti-WT1 vaccines. CTLs generated upon using this combination were also shown to specifically recognise and kill relevant targets. Interestingly, the "superiority" of the combined vaccines was not observed in ELISpot assays. The CD8<sup>+</sup> T cells restriction was, however, not demonstrated since in all assays presented here, either *in-vitro* stimulated splenocytes or CD3<sup>+</sup> isolated cells were used for these studies. Thus, in the future, isolated CD8<sup>+</sup> T cells would need to be used and/or anti-CD8<sup>+</sup> antibody should be used during the assay.

It worth mentioning that the WT1 sequence used herein is completely human and differs from the murine WT1 by a single amino-acid, and while this had no

consequences when used in double transgenic mice, the same vaccine failed to generate any detectable immune responses in syngeneic C57BL/6 mice, as assessed by a PhD student, Joshua Pearson, studying the combined use of TRP2 and WT1.

The combined HAGE- and WT1-ImmunoBody® vaccines also generated cells that responded to two HLA-DR1 15-mers (one derived from WT1 and one derived from HAGE), however the CD4<sup>+</sup> T cells restriction was not proven. Again, the use of isolated CD4<sup>+</sup> T cells and/or the use of anti-CD4<sup>+</sup> antibody would allow to ascertain that CD4<sup>+</sup> T cells are responsible for the observed response.

This study used, as a “proof-of-concept”, the B16/HHDII<sup>+</sup>/DR1<sup>+</sup>/Luc<sup>+</sup>/HAGE<sup>+</sup>/WT1<sup>+</sup> cells for *in vivo* tumour challenge experiments. It has been found that for the first time, that a novel combination of HAGE- and WT1-ImmunoBody® vaccine was able to delay the tumour growth and prolong mice survival rate in the prophylactic setting; however, it remains a melanoma model and not a leukaemia model. It would have been more relevant if the combined vaccines efficacy had been assessed against a leukaemic tumour model. Such model using mice that have completely human immune system and have received patient’s derived leukaemic cells, but such model is extremely difficult to establish and very expensive due to the need of human materials. It would also have beneficial to assess whether leukaemic patients do have circulating anti-HAGE and/or anti-WT1 T cells in their blood. Nonetheless, the study clearly demonstrated that the CD3<sup>+</sup> T cells generated after vaccination were able to kill several human CML derived targets, thereby highlighting the real potential of this strategy to target leukaemic cells.

The delayed growth of the implanted tumour cells was only significantly demonstrated in the prophylactic study, however these results also showed that the mice would have benefitted from a more sustained vaccination strategy. Moreover, the fact that B16 cells are PD-L1 positive and that CD3<sup>+</sup> T cells were also positive for PD-1, means that future studies should consider these facts and not only vaccinate the mice before challenge but continue vaccination after implantation, as well as include an anti-PD-1 antibody.

Overall, data obtained herein would certainly support the development of vaccine strategies based on a combination of both HAGE- and WT1-ImmunoBody® vaccines which could be further improved with the use of immune checkpoint inhibitors.

# 9 Appendix

European LeukemiaNet Recommendations for the Management of Chronic Myeloid Leukemia (CML)			
<b>Response definitions for any TKI first line, and 2nd line in case of intolerance, all patients (CP, AP, and BC)</b>			
Time	Optimal response	Warning	Failure
Baseline		High risk Major route CCA/Ph+	
3 mos.	BCR-ABL <sup>15</sup> ≤10%* Ph+ ≤35% (PCyR)	BCR-ABL <sup>15</sup> >10%* Ph+ 36-95%	No CHR* Ph+ >95%
6 mos.	BCR-ABL <sup>15</sup> <1%* Ph+ 0% (CCyR)	BCR-ABL <sup>15</sup> 1-10%* Ph+ 1-35%	BCR-ABL <sup>15</sup> >10%* Ph+ >35%
12 mos.	BCR-ABL <sup>15</sup> ≤0.1%* (MMR)	BCR-ABL <sup>15</sup> 0.1-1%*	BCR-ABL <sup>15</sup> >1%* Ph+ >0%
Then, and at any time	MMR or better	CCA/Ph- (-7, or 7q-)	Loss of CHR Loss of CCyR Loss of MMR, confirmed** Mutations CCA/Ph+
*and/or **in 2 consecutive tests, of which one ≥1% IS: BCR-ABL on International Scale			
Treatment recommendations			
Line	Event	TKI, standard dosage <sup>1</sup>	Transplantation
Chronic phase			
		Imatinib 400 mg/qd Nilotinib 300 mg/bid Dasatinib 100 mg/qd Bosutinib 500 mg/qd Ponatinib 45 mg/qd	Search for HLA type + sibs unrelated donor consider recommended Chemotherapy
1 <sup>st</sup>	Baseline	X X X	X <sup>2</sup>
2 <sup>nd</sup>	Intolerance to 1 <sup>st</sup> TKI	Any other TKI approved 1 <sup>st</sup> line	
	Failure 1 <sup>st</sup> line of	imatinib	X <sup>3</sup> X X X X X
		dasatinib	X <sup>3</sup> X X X X X
3 <sup>rd</sup>	Intolerance to/failure of two TKI	Any remaining TKI	X
Any	T3151 mutation		X X X X X
Accelerated or blast phase			
In newly diagnosed, TKI naive patients	start with	X <sup>3</sup> X <sup>4</sup>	X X
	no optimal response, BP		X <sup>7</sup> X <sup>5</sup>
TKI pre-treated patients	Any other TKI	X <sup>6</sup>	X <sup>7</sup> X <sup>5</sup>
<sup>1</sup> choice of the TKI consider tolerability and safety, and patient characteristics (age, comorbidities). <sup>2</sup> only in case of baseline warnings (high risk, major route CCA/Ph+), <sup>3</sup> 400 mg/bid, <sup>4</sup> 70 mg/bid or 140 mg/qd, <sup>5</sup> may be required before SCT to control disease and to make patients eligible to alloSCT, <sup>6</sup> in case of T3151 mutation, <sup>7</sup> only patients who are eligible for alloSCT, not in case of uncontrolled, resistant BP. <sup>8</sup> 400 mg bid in failure setting qd: Once daily bid: Twice daily			
References: 1. Baccarani M, Deininger M, Rossi G, et al. European LeukemiaNet recommendations for the management of chronic myeloid leukemia: 2013. Blood 122:872-884, 2013. 2. Baccarani M, Cortes J, Pane F, et al. Chronic myeloid leukemia. An update of concepts and management Recommendations of the European LeukemiaNet. J Clin Oncol. 27:5041-51, 2009. 3. Baccarani M, Saglio G, Goldman J, et al. Evolving concepts in the management of chronic myeloid leukemia: recommendations from an expert panel on behalf of the European LeukemiaNet. Blood 108:1809-1820, 2006.			

Other definitions			
CCA	Clonal chromosome abnormalities		
CCA/Ph+	CCA in Ph+ cells which define failure if newly arisen		
CHR	Complete hematologic response: Platelet count < 450 x 10 <sup>9</sup> /L; WBC count <10 x 10 <sup>9</sup> /L; Differential: no immature granulocytes, basophils <5%; no palpable spleen		
High risk	Evaluated by Sokal-Score (>1.2), Euro-Score (>1.480) or EUTOS-Score (>87)		
Major route CCA/Ph+	Major route CCA/Ph+ are trisomy 8, 2 <sup>nd</sup> Ph+ [+der(22)t(9;22)(q34;q11)], isochromosome 17 [i(17)(q10)], trisomy 19, and ider(22)(q10)t(9;22)(q34;q11)		
Mutations	BCR-ABL kinase domain point mutations (not to be confused with ABL1 polymorphisms), Mutational analysis by conventional Sanger sequencing is recommended in case of progression, failure and warning.		
Timing of Cytogenetic and Molecular Monitoring			
At diagnosis	CBA, FISH in case of Ph- (for cryptic or variant translocations), qualitative PCR (transcript type)		
During treatment	RQ-PCR every 3 months until MMR has been achieved, then every 3 to 6 months and/or CBA at 3, 6, and 12 months until CCyR has been achieved, then every 12 months. Once CCyR is achieved, FISH on blood cells can be used.		
Failure, progression	RQ-PCR, mutational analysis, and CBA. Immunophenotyping in blast phase.		
Warning	Molecular and cytogenetic tests more frequently, CBA in case of myelodysplasia or CCA/Ph-		
CBA: Chromosome banding analysis of marrow cell metaphases at least 20 metaphases analysed			
Response definitions to 2 <sup>nd</sup> line therapy in case of failure of imatinib (can be used provisionally, NOT for the response to 3 <sup>rd</sup> line treatment).			
Time	Optimal response	Warnings	Failure
Baseline		No CHR Loss of CHR on imatinib Lack of CyR to 1 <sup>st</sup> line TKI High risk	
3 mos.	BCR-ABL <sup>15</sup> ≤10%* Ph+ <65%	BCR-ABL <sup>15</sup> >10%* Ph+ 65-95%	No CHR, or Ph+ >95%, or New mutations
6 mos.	BCR-ABL <sup>15</sup> ≤10%* Ph+ <35% (PCyR)	BCR-ABL <sup>15</sup> ≤10%* Ph+ 35-65%	BCR-ABL <sup>15</sup> >10%* Ph+ >65%* New mutations
12 mos.	BCR-ABL <sup>15</sup> <1%* Ph+ 0 (CCyR)	BCR-ABL <sup>15</sup> 1-10%* Ph+ 1-35%	BCR-ABL <sup>15</sup> >10%* Ph+ >35%* New mutations
Then, and at any time	MMR or better	CCA/Ph- (-7 or 7q-) or BCR-ABL <sup>15</sup> >0.1%	Loss of CHR, or Loss of CCyR or PCyR New mutations Loss of MMR** CCA/Ph+
*and/or **in 2 consecutive tests, of which one ≥1% IS: BCR-ABL on International Scale			
Definition of response			
Optimal response	Best long-term outcome No indication for a change of treatment.		
Failure	Patient should receive a different treatment to limit the risk of progression and death		
Warning	Characteristics of disease and response to treatment require more frequent monitoring to permit timely changes in therapy, in case of treatment failure.		

**Figure 9.1: European LeukemiaNet recommendations for the management of CML: 2013.**

The table (A&B) summarises the last-update for CML management in 2013 where the following aspects were covered; i) response to TKIs: three definitions termed as optimal, warning and failure to response are defined according to the expression of *BCR-ABL1* gene and the presence of Philadelphia chromosome, as it should be assessed by molecular and chromosomal analysis, ii) treatment recommendation; TKIs generations, standard dosage and transplantation option are all described *versus* three possible lines of treatment, iii) update some definitions, iv) timing of cytogenetic and molecular monitoring, and v) 2<sup>nd</sup> line treatment in case of failure to imatinib therapy. Tables are reused from European LeukemiaNet website, available at: [https://www.leukemia-net.org/content/leukemias/cml/recommendations/index\\_eng.html](https://www.leukemia-net.org/content/leukemias/cml/recommendations/index_eng.html)

**Table 9.1: Pattern of C/T and WT1 genes expression in CML samples analysed from MILE study**

<b>Upregulated expression</b>	<b>Non-upregulated expression</b>	<b>Down-regulated expression</b>
WT1/(206067_s_at)	DDX43 (220004_at)	PBK (219148_at)
SSX1/(206626_x_at)	SSX1 (206627_s_at)	TTK (204822_at)
SSX4/SSX4B/ (all probs)	SYCP1 (206740_x_at)	SPA17 (205406_s_at)
MAGEA1/(207325_x_at)		
MAGEA3/MAGEA6 (209942_x_at)	CTAG1A/CTAG1B (217339_x_at)	
MAGEA4 (214254_at)	TMEFF2/(223557_s_at)	
MAGEA12(210467_x_at)	PRAME (204086_at)	
MAGEB2 (206218_at)		
MAGEC1 (206609_at)		
MAGEC2 (220062_s_at)	TPTE (220205_at)	
MAGEC2 (215932_at)		
CTCFL (1552368_at)	BAGE (207712_at)	
CTAG1A/CTAG1B (210546_x_at)	SEMG1 (206442_at)	
CTAG1A/CTAG1B /(211674_x_at)	GAGE1/(208283_at)	
CT45A1/CT45A10/CT45A3/CT45A4/ CT45A5/ CT45A6/ CT45A7/ CT45A8 CT45A/91567912_s_at)	CT45A1/CT45A2/CT45A3/CT45A4/ CT45A5/ CT45A6// LOC1 (235700_at)	
CTCFL/1552368_at		
SYCP1 (216917_s_at)		
PRM1 (206358_at)		
PASD1 (240687_at)		
ROPN1/(233203_at)		
TMEFF2 (233910_at)		
TMEFF2/ (224321_at)		

**Table 9.2: Pattern of C/T and WT1 genes expression in AML samples analysed from MILE study**

<b>Upregulated expression</b>	<b>Non-upregulated expression</b>	<b>Down-regulated expression</b>
WT1/(206067_s_at)	GAGE1/(208283_at)	DDX43/(220004_at)
SSX4/SSX4B/ (all probes)	MAGEA4/(214254_at)	SEMG1/(206442_at)
MAGEB2/(206218_at)	MAGEA12/(210467_x_at)	PBK/(219148_at)
MAGEC2/ (both probes)	MAGEC1/(206609_at)	TTK/(204822_at)
CTCF1/(1552368_at)	SYCP1/(206740_x_at)	SPA17/(205406_s_at)
CT45A1/CT45A2/CT45A3/CT45A4/ CT45A5/CT45A6/LOC1_235700_at	CTAG1A/CTAG1B/(211674_x_at)	
CTAG1A/CTAG1B/ (210546_x_at)	PRM1/(206358_at)	
SYCP1/(216917_s_at)	PASD1/(240687_at)	
PRAME/(204086_at)	ROPN1/(233203_at)	
ROPN1/(231535_x_at)		
TMEFF2/(233910_at)	TPTE/(220205_at)	
TMEFF2/(224321_at)	BAGE/(207712_at)	
CT45A1/CT45A10/CT45A3/CT45A4/ CT45A5/ CT45A6/ CT45A7/ CT45A8 CT45A/91567912_s_at)	SSX1/(206626_x_at)	
	SSX1/(206627_s_at)	
	MAGEA3/(MAGEA6(209942_x_at)	
	MAGEA1/(207325_x_at)	
	CTAG1A/CTAG1B/(217339_x_at)	
	TMEFF2/(223557_s_at)	

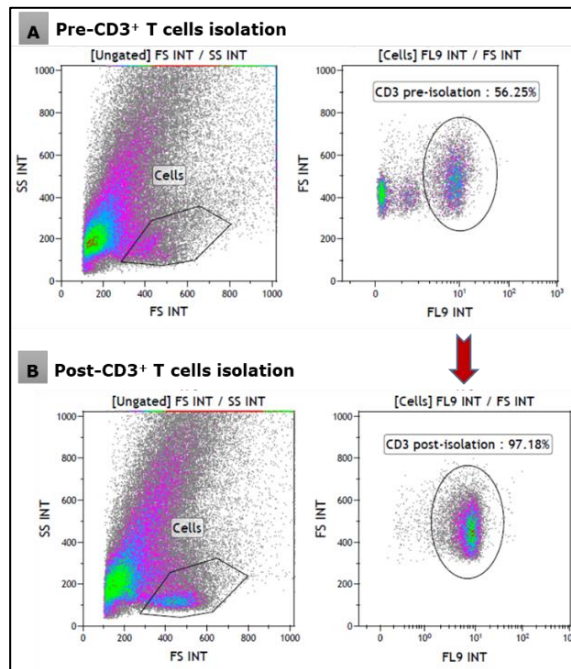


**Figure 9.2: Representative density blot analysis to assess the purity of CD3<sup>+</sup> T cells before and after isolation using flow cytometer.**

Splenocytes were stimulated by after one-week IVS, CD3<sup>+</sup> T cells were then isolated before being incubated with relevant target cells in the IFN- $\gamma$  ELISpot plate. The top graphs show that percentage of CD3<sup>+</sup> T cells at 56.25% (pre-isolation) and the bottom row demonstrate post isolation purity at around 97.18%.

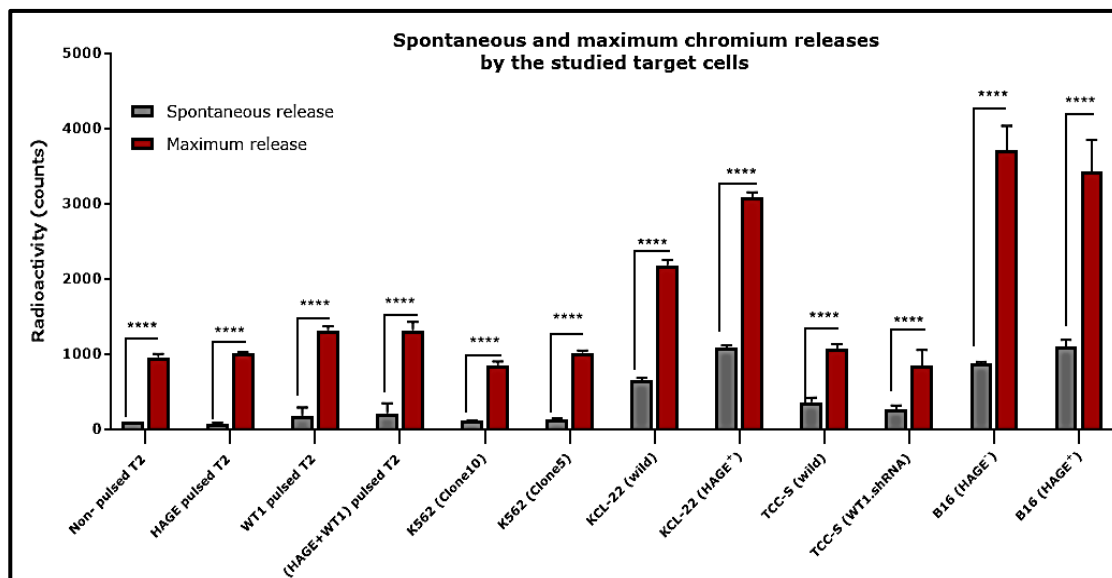


**Figure 9.3: Spontaneous and maximum release of <sup>51</sup>Cr by targets.**

All targets were labelled with <sup>51</sup>Cr. Targets were then washed and rested for 1hour at 37°C until plated in rounded bottom 96 well plates at 5x10<sup>3</sup>/well. Four wells for the spontaneous and maximum release were loaded with target cells and target cells with 1% SDS respectively for 4-24 hours at culture conditions. After incubation, 50 $\mu$ L of supernatants were transferred onto Lumaplates and read with Top count beta scintillation. Results are presented as mean  $\pm$  SEM of two independent experiments (3 mouse per group) and the level of significance was assessed using Two Way ANOVA followed by Tukey's multiple comparisons test. Data show that the maximum releases by the studied targets are considerably higher than the corresponding spontaneous releases with \*\*\*\**P*-value < 0.0001.

## Survival proportions: B16/HAGE+ tumour studies

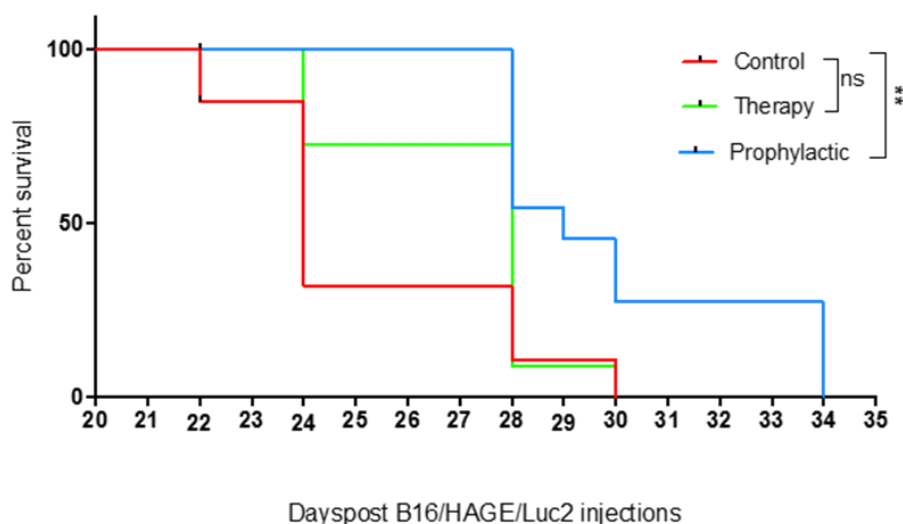


**Figure 9.4: Survival curve demonstrates prophylactic and therapeutic efficacy of the HAGE ImmunoBody® vaccines monotherapy in HHDII/DR1 mice bearing  $\mu$ B16/HAGE<sup>+</sup>/Luc<sup>+</sup> tumour.**

Results shows the significant effect of the HAGE vaccines in the prophylactic group, and lack of protection in the therapeutic group. Figure is obtained with permission from (Divya Nagarajan, 2019)/ manuscript in preparation submitted to immunology and cell biology.

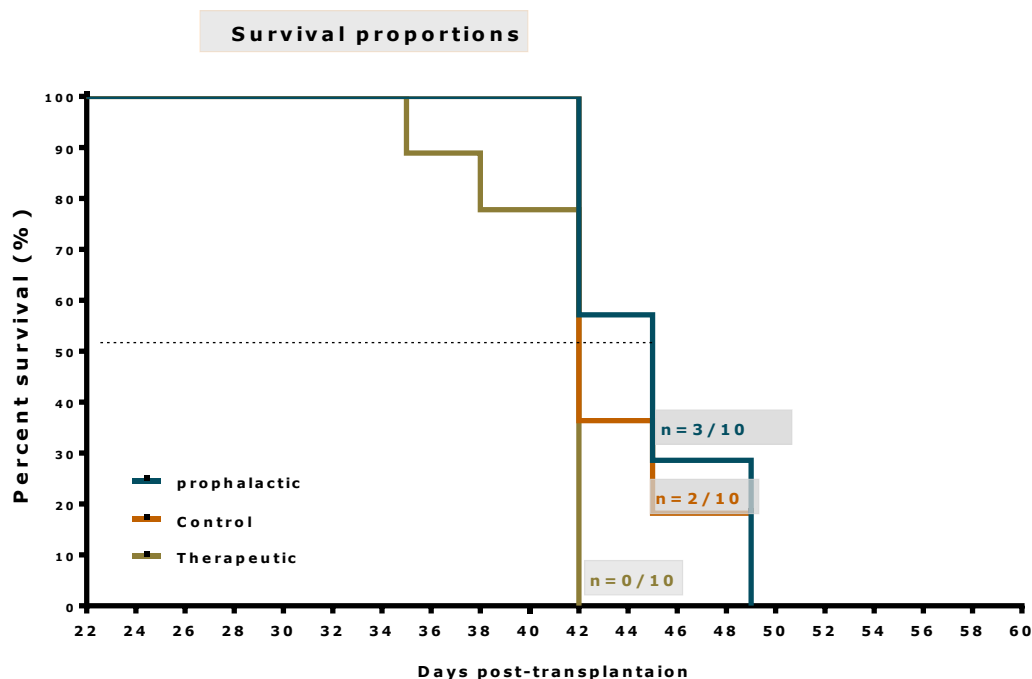


**Figure 9.5: Survival curve demonstrates the prophylactic and therapeutic efficacy of the WT1-ImmunoBody® vaccines monotherapy in HHDII/DR1 mice bearing  $\mu$ B16/HAGE<sup>+</sup>/Luc<sup>+</sup> tumour.**

Results shows modest effect of the WT1 vaccines in the prophylactic group, and lack of the protection in the therapeutic group. The level of significance in the animal survival was evaluated by log-rank test (*p-value*) between control and treatment groups, (total mice=30, 10/group).

**Table 9.3: Human WT1 protein isomers sequences**

<b>Human WT1 protein isoform A (502 amino acid protein)</b>
MDFLLLQDPASTCVPEPASQHTLRSGPGCLQQPEQQGVDRDPGGIWAKLGAAEASAERLQGRRSRGASGSEPQQM GSDVRDLNALLPAVPSLGGGGGCALPVSGAAQWAPVLDFAFPGASAYGSLGGPAPPAPPPPPPPHFSFIKQEPSW GGAEPHEEQCLSAFTVHFSGQFTGTAGACRYGPFPPPPSQASSGQARMFPNAPYLPSCLESQPAIRNQGYSTVTF DGTSPSYGHTPSHHAAQFPNHSFKHEDPMGQQGSLGEQQYSVPPVYGCHTPTDSTGSQALLLRTPYSSDNLYQM TSQLECMTWNQMNLGATLKGHSTGYESDNHTTTPILCGAQYRIHTHGVRGIQDVRRVPGVAPTLVRSASETSEKRP FMCAYPGCNKRYFKLSHLQMHSRKHTGEKPYQCDFKDCERRFSRSDQLKRHQRRHTGVKPFQCKTCQRKFSRSD HLKTHTRTHTGEKPFSCRWPSCQKFFARSDELVRHHNMHQ RNMTKLQ LAL
<b>Human WT1 protein isoform B (519 amino acid protein)</b>
MDFLLLQDPASTCVPEPASQHTLRSGPGCLQQPEQQGVDRDPGGIWAKLGAAEASAERLQGRRSRGASGSEPQQM GSDVRDLNALLPAVPSLGGGGGCALPVSGAAQWAPVLDFAFPGASAYGSLGGPAPPAPPPPPPPHFSFIKQEPS WGGAEPHEEQCLSAFTVHFSGQFTGTAGACRYGPFPPPPSQASSGQARMFPNAPYLPSCLESQPAIRNQGYSTVTF FDGTSPSYGHTPSHHAAQFPNHSFKHEDPMGQQGSLGEQQYSVPPVYGCHTPTDSTGSQALLLRTPYSSDNLYQ MTSQLECMTWNQMNLGATLKGVAAGSSSSVKWTEGQSNHSTGYESDNHTTTPILCGAQYRIHTHGVRGIQDVRR VPGVAPTLVRSASETSEKRPFMCAYPGCNKRYFKLSHLQMHSRKHTGEKPYQCDFKDCERRFSRSDQLKRHQRRH TGKPFQCKTCQRKFSRSDHLKTHTRTHTGEKPFSCRWPSCQKFFARSDELVRHHNMHQ RNMTKLQ LAL
<b>Human WT1 protein isoform D (522 amino acid protein)</b>
MDFLLLQDPASTCVPEPASQHTLRSGPGCLQQPEQQGVDRDPGGIWAKLGAAEASAERLQGRRSRGASGSEPQQM GSDVRDLNALLPAVPSLGGGGGCALPVSGAAQWAPVLDFAFPGASAYGSLGGPAPPAPPPPPPPHFSFIKQEPS WGGAEPHEEQCLSAFTVHFSGQFTGTAGACRYGPFPPPPSQASSGQARMFPNAPYLPSCLESQPAIRNQGYSTVTF FDGTSPSYGHTPSHHAAQFPNHSFKHEDPMGQQGSLGEQQYSVPPVYGCHTPTDSTGSQALLLRTPYSSDNLYQ MTSQLECMTWNQMNLGATLKGVAAGSSSSVKWTEGQSNHSTGYESDNHTTTPILCGAQYRIHTHGVRGIQDVRR VPGVAPTLVRSASETSEKRPFMCAYPGCNKRYFKLSHLQMHSRKHTGEKPYQCDFKDCERRFSRSDQLKRHQRRH TGKPFQCKTCQRKFSRSDHLKTHTRTHTGKTSEKPFSCRWPSCQKFFARSDELVRHHNMHQ RNMTKLQ LAL
<b>Human WT1 protein isoform E (302 amino acid protein): No long mer</b>
MEKGYSTVTFDGTSPSYGHTPSHHAAQFPNHSFKHEDPMGQQGSLGEQQYSVPPVYGCHTPTDSTGSQALLLRT PYSSDNLYQMTSQLECMTWNQMNLGATLKGVAAGSSSSVKWTEGQSNHSTGYESDNHTTTPILCGAQYRIHTHGVR FRGIQDVRRVPGVAPTLVRSASETSEKRPFMCAYPGCNKRYFKLSHLQMHSRKHTGEKPYQCDFKDCERRFSRSDQ LKRHQRRHTGVKPFQCKTCQRKFSRSDHLKTHTRTHTGEKPFSCRWPSCQKFFAR SDELVRHHNMHQ RNMTKLQ LAL
<b>Human WT1 protein isoform F (288 amino acid protein): No long mer</b>
MEKGYSTVTFDGTSPSYGHTPSHHAAQFPNHSFKHEDPMGQQGSLGEQQYSVPPVYGCHTPTDSTGSQALLLRT PYSSDNLYQMTSQLECMTWNQMNLGATLKGHSTGYESDNHTTTPILCGAQYRIHTHGVRGIQDVRRVPGVAPTLV RSASETSEKRPFMCAYPGCNKRYFKLSHLQMHSRKHTGEKPYQCDFKDCERRFSRSDQLKRHQRRHTGVKPFQCK TCQRKFSRSDHLKTHTRTHTGKTSEKPFSCRWPSCQKFFARSDELVRHHNMHQ RN MTKLQ LAL

Table demonstrates the location of the long 15-mer peptide (VRDLNALLPAVPSLG) within each full sequence, available at: <https://www.ncbi.nlm.nih.gov/protein/?term=human+WT1>

# 10 Bibliography

Abbas, A.K., Lichtman, A.H. and Pillai, S., 2014. *Cellular and molecular immunology E-book*. Elsevier Health Sciences.

Abdel-Fatah, T.M., *et al.*, 2016. HAGE in Triple-Negative Breast Cancer Is a Novel Prognostic, Predictive, and Actionable Biomarker: A Transcriptomic and Protein Expression Analysis. *Clinical Cancer Research: An Official Journal of the American Association for Cancer Research*, 22 (4), 905-914.

Abelson, H.T. and Rabstein, L.S., 1970. Lymphosarcoma: virus-induced thymic-independent disease in mice. *Cancer Research*, 30 (8), 2213-2222.

Abiko, K., *et al.*, 2015. IFN- $\gamma$  from lymphocytes induces PD-L1 expression and promotes progression of ovarian cancer. *British Journal of Cancer*, 112 (9), 1501.

Adam, J.K., Odhav, B. and Bhoola, K.D., 2003. Immune responses in cancer. *Pharmacology & Therapeutics*, 99 (1), 113-132.

Adams, S.P., *et al.*, 2002. Frequent expression of HAGE in presentation chronic myeloid leukaemias. *Leukemia*, 16 (11), 2238-2242.

Ahmed, R. and Gray, D., 1996. Immunological memory and protective immunity: understanding their relation. *Science (New York, N.Y.)*, 272 (5258), 54-60.

Akcakanat, A., *et al.*, 2004. NY-ESO-1 expression and its serum immunoreactivity in esophageal cancer. *Cancer Chemotherapy and Pharmacology*, 54 (1), 95-100.

Akiyama, H., *et al.*, 2003. A synergistic increase of apoptosis utilizing Fas antigen expression induced by low doses of anticancer drug. *Rinsho Byori.the Japanese Journal of Clinical Pathology*, 51 (8), 733-739.

Alimohammadi, F., *et al.*, 2018. Evaluation of Wilms' Tumor (WT1) Gene Methylation in Acute Lymphocytic Leukemia Patients. *Basic & Clinical Cancer Research*, 10 (4), 26-29.

Almeida, J.R., *et al.*, 2007. Superior control of HIV-1 replication by CD8+ T cells is reflected by their avidity, polyfunctionality, and clonal turnover. *The Journal of Experimental Medicine*, 204 (10), 2473-2485.

Almeida, J.R., *et al.*, 2009. Antigen sensitivity is a major determinant of CD8+ T-cell polyfunctionality and HIV-suppressive activity. *Blood*, 113 (25), 6351-6360.

Andersen, M.H., *et al.*, 2006. Cytotoxic T cells. *Journal of Investigative Dermatology*, 126 (1), 32-41.

Andersen, R.S., *et al.*, 2012. Dissection of T-cell antigen specificity in human melanoma. *Cancer Research*, 72 (7), 1642-1650.

Anderson, R.J. and Schneider, J., 2007. Plasmid DNA and viral vector-based vaccines for the treatment of cancer. *Vaccine*, 25 Suppl 2, B24-34.

Andersson, A., *et al.*, 2005. Gene expression profiling of leukemic cell lines reveals conserved molecular signatures among subtypes with specific genetic aberrations. *Leukemia*, 19 (6), 1042.

- Andrea Erika Held, S., et al., 2013. Advances in immunotherapy of chronic myeloid leukemia CML. *Current Cancer Drug Targets*, 13 (7), 768-774.
- Anichini, A., et al., 1999. An expanded peripheral T cell population to a cytotoxic T lymphocyte (CTL)-defined, melanocyte-specific antigen in metastatic melanoma patients impacts on generation of peptide-specific CTLs but does not overcome tumor escape from immune surveillance in metastatic lesions. *The Journal of Experimental Medicine*, 190 (5), 651-667.
- Appay, V., Douek, D.C. and Price, D.A., 2008. CD8 T cell efficacy in vaccination and disease. *Nature Medicine*, 14 (6), 623.
- Appay, V., et al., 2002. Memory CD8 T cells vary in differentiation phenotype in different persistent virus infections. *Nature Medicine*, 8 (4), 379.
- Appay, V. and Iglesias, M.C., 2011. Antigen sensitivity and T-cell receptor avidity as critical determinants of HIV control. *Current Opinion in HIV and AIDS*, 6 (3), 157-162.
- Appel, S., et al., 2004. Imatinib mesylate affects the development and function of dendritic cells generated from CD34+ peripheral blood progenitor cells. *Blood*, 103 (2), 538-544.
- Appel, S., et al., 2005. Effects of imatinib on monocyte-derived dendritic cells are mediated by inhibition of nuclear factor-kappaB and Akt signaling pathways. *Clinical Cancer Research: An Official Journal of the American Association for Cancer Research*, 11 (5), 1928-1940.
- Apperley, J.F., 2015. Chronic myeloid leukaemia. *The Lancet*, 385 (9976), 1447-1459.
- Apperley, J.F., et al., 2002. Response to imatinib mesylate in patients with chronic myeloproliferative diseases with rearrangements of the platelet-derived growth factor receptor beta. *The New England Journal of Medicine*, 347 (7), 481-487.
- Aswald, J.M., et al., 2002. Increased IFN-gamma synthesis by T cells from patients on imatinib therapy for chronic myeloid leukemia. *Cytokines, Cellular & Molecular Therapy*, 7 (4), 143-149.
- Atanackovic, D., et al., 2011. Cancer-testis antigen expression and its epigenetic modulation in acute myeloid leukemia. *American Journal of Hematology*, 86 (11), 918-922.
- Aydin, S., et al., 2013. *WT1 Expression in Acute Myeloid Leukaemia: A Useful Marker for Improving Therapy Response Evaluation*.
- Ayers, M., et al., 2017. IFN- $\gamma$ -related mRNA profile predicts clinical response to PD-1 blockade. *The Journal of Clinical Investigation*, 127 (8), 2930-2940.
- Ayyoub, M., et al., 2003a. Tumor-reactive, SSX-2-specific CD8+ T cells are selectively expanded during immune responses to antigen-expressing tumors in melanoma patients. *Cancer Research*, 63 (17), 5601-5606.
- Babiak, A., et al., 2014. Frequent T cell responses against immunogenic targets in lung cancer patients for targeted immunotherapy. *Oncology Reports*, 31 (1), 384-390.

Baccarani, M., *et al.*, 2012. Chronic myeloid leukemia: ESMO Clinical Practice Guidelines for diagnosis, treatment and follow-up. *Annals of Oncology*, 23 (suppl\_7), vii72-vii77.

Baccarani, M., *et al.*, 2009. Chronic myeloid leukemia: an update of concepts and management recommendations of European LeukemiaNet. *Journal of Clinical Oncology: Official Journal of the American Society of Clinical Oncology*, 27 (35), 6041-6051.

Baccarani, M., *et al.*, 2013. European LeukemiaNet recommendations for the management of chronic myeloid leukemia: 2013. *Blood*, 122 (6), 872-884.

Baccarani, M., *et al.*, 2006. Evolving concepts in the management of chronic myeloid leukemia: recommendations from an expert panel on behalf of the European LeukemiaNet. *Blood*, 108 (6), 1809-1820.

Bachy, E., *et al.*, 2011. Quantitative and functional analyses of CD4(+) CD25(+) FoxP3(+) regulatory T cells in chronic phase chronic myeloid leukaemia patients at diagnosis and on imatinib mesylate. *British Journal of Haematology*, 153 (1), 139-143.

Baker, B.M., *et al.*, 2000. Conversion of a T cell antagonist into an agonist by repairing a defect in the TCR/peptide/MHC interface: implications for TCR signaling. *Immunity*, 13 (4), 475-484.

Balachandran, V.P., *et al.*, 2011. Imatinib potentiates antitumor T cell responses in gastrointestinal stromal tumor through the inhibition of Ido. *Nature Medicine*, 17 (9), 1094.

Ball, H.J., *et al.*, 2007. Characterization of an indoleamine 2, 3-dioxygenase-like protein found in humans and mice. *Gene*, 396 (1), 203-213.

Banchereau, J. and Steinman, R.M., 1998. Dendritic cells and the control of immunity. *Nature*, 392 (6673), 245.

Banchereau, J. and Steinman, R.M., 1998. Dendritic cells and the control of immunity. *Nature*, 392 (6673), 245-252.

Baniyash, M., 2004. TCR zeta-chain downregulation: curtailing an excessive inflammatory immune response. *Nature Reviews. Immunology*, 4 (9), 675-687.

Barbolina, M.V., *et al.*, 2008. Wilms tumor gene protein 1 is associated with ovarian cancer metastasis and modulates cell invasion. *Cancer*, 112 (7), 1632-1641.

Baren, V., 1998. PRAME, a gene encoding an antigen recognized on a human melanoma by cytolytic T cells, is expressed in acute leukaemia cells. *British Journal of Haematology*, 102 (5), 1376-1379.

Beatty, G.L., Li, Y. and Long, K.B., 2017. Cancer immunotherapy: activating innate and adaptive immunity through CD40 agonists. *Expert Review of Anticancer Therapy*, 17 (2), 175-186.

Bell, R.B., *et al.*, 2018. 15 – Immunotherapy. Oral, Head and Neck Oncology and Reconstructive Surgery. Elsevier. 2018, pp.314-340. Available at: <https://www.sciencedirect.com/topics/biochemistry-genetics-and-molecular-biology/ctla-4>. [Accessed 27 May 2019].

- Bellantuono, I., *et al.*, 2002. Two distinct HLA-A0201-presented epitopes of the Wilms tumor antigen 1 can function as targets for leukemia-reactive CTL. *Blood*, 100 (10), 3835-3837.
- Bellucci, R., *et al.*, 2015. Interferon- $\gamma$ -induced activation of JAK1 and JAK2 suppresses tumor cell susceptibility to NK cells through upregulation of PD-L1 expression. *Oncoimmunology*, 4 (6), e1008824.
- Benci, J.L., *et al.*, 2016. Tumor interferon signaling regulates a multigenic resistance program to immune checkpoint blockade. *Cell*, 167 (6), 1540-1554. e12.
- Bennett, K., *et al.*, 1992. Antigen processing for presentation by class II major histocompatibility complex requires cleavage by cathepsin E. *European Journal of Immunology*, 22 (6), 1519-1524.
- Bennour, A., Saad, A. and Sennana, H., 2016. *Chronic myeloid leukemia: Relevance of cytogenetic and molecular assays*.
- Bergant, M., *et al.*, 2006. Preparation of native and amplified tumour RNA for dendritic cell transfection and generation of in vitro anti-tumour CTL responses. *Immunobiology*, 211 (3), 179-189.
- Bertram, J.S., 2000. The molecular biology of cancer. *Molecular Aspects of Medicine*, 21 (6), 167-223.
- Berzofsky, J.A., Ahlers, J.D. and Belyakov, I.M., 2001. Strategies for designing and optimizing new generation vaccines. *Nature Reviews. Immunology*, 1 (3), 209-219.
- Bhatia, R., *et al.*, 2003. Persistence of malignant hematopoietic progenitors in chronic myelogenous leukemia patients in complete cytogenetic remission following imatinib mesylate treatment. *Blood*, 101 (12), 4701-4707.
- Bijker, M.S., *et al.*, 2007. CD8+ CTL priming by exact peptide epitopes in incomplete Freund's adjuvant induces a vanishing CTL response, whereas long peptides induce sustained CTL reactivity. *Journal of Immunology (Baltimore, Md.: 1950)*, 179 (8), 5033-5040.
- Bikoff, E.K., *et al.*, 1993. Defective major histocompatibility complex class II assembly, transport, peptide acquisition, and CD4+ T cell selection in mice lacking invariant chain expression. *The Journal of Experimental Medicine*, 177 (6), 1699-1712.
- Bilir, C. and Sarisozen, C., 2017. Indoleamine 2, 3-dioxygenase (IDO): only an enzyme or a checkpoint controller? *Journal of Oncological Sciences*, 3 (2), 52-56.
- Binotto, G., *et al.*, 2014. *Comparative Analysis of NK Receptor and T-Cell Receptor Repertoires in Patients with Chronic Myeloid Leukemia Treated with Different Tyrosine Kinase Inhibitors*.
- Bjorkman, P.J. and Parham, P., 1990. Structure, function, and diversity of class I major histocompatibility complex molecules. *Annual Review of Biochemistry*, 59 (1), 253-288.
- Blackburn, S.D., *et al.*, 2008. Selective expansion of a subset of exhausted CD8 T cells by alphaPD-L1 blockade. *Proceedings of the National Academy of Sciences of the United States of America*, 105 (39), 15016-15021.

- Blank, C., *et al.*, 2006. Blockade of PD-L1 (B7-H1) augments human tumor-specific T cell responses in vitro. *International Journal of Cancer*, 119 (2), 317-327.
- Bocchia, M., *et al.*, 2005. Effect of a p210 multipeptide vaccine associated with imatinib or interferon in patients with chronic myeloid leukaemia and persistent residual disease: a multicentre observational trial. *The Lancet*, 365 (9460), 657-662.
- Bocchia, M., *et al.*, 1995. Specific binding of leukemia oncogene fusion protein peptides to HLA class I molecules. *Blood*, 85 (10), 2680-2684.
- Bodine, D.M., *et al.*, 1993. In vivo administration of stem cell factor to mice increases the absolute number of pluripotent hematopoietic stem cells. *Blood*, 82 (2), 445-455.
- Boissel, N., *et al.*, 2006. BCR/ABL oncogene directly controls MHC class I chain-related molecule A expression in chronic myelogenous leukemia. *Journal of Immunology (Baltimore, Md.: 1950)*, 176 (8), 5108-5116.
- Boissel, N., *et al.*, 2004. Defective blood dendritic cells in chronic myeloid leukemia correlate with high plasmatic VEGF and are not normalized by imatinib mesylate. *Leukemia*, 18 (10), 1656-1661.
- Bol, K.F., *et al.*, 2016. Dendritic Cell-Based Immunotherapy: State of the Art and Beyond. *Clinical Cancer Research: An Official Journal of the American Association for Cancer Research*, 22 (8), 1897-1906.
- Bolhassani, A., Safaiyan, S. and Rafati, S., 2011. Improvement of different vaccine delivery systems for cancer therapy. *Molecular Cancer*, 10 (1), 3.
- Borg, C., *et al.*, 2004. Novel mode of action of c-kit tyrosine kinase inhibitors leading to NK cell-dependent antitumor effects. *The Journal of Clinical Investigation*, 114 (3), 379-388.
- Boss, J.M., 1997. Regulation of transcription of MHC class II genes. *Current Opinion in Immunology*, 9 (1), 107-113.
- Bossi, G., *et al.*, 2013. Examining the presentation of tumor-associated antigens on peptide-pulsed T2 cells. *Oncoimmunology*, 2 (11), e26840.
- Braciale, T.J., 1992. Antigen processing for presentation by MHC class I molecules. *Current Opinion in Immunology*, 4 (1), 59-62.
- Braud, V.M., *et al.*, 1998. HLA-E binds to natural killer cell receptors CD94/NKG2A, B and C. *Nature*, 391 (6669), 795.
- Brentjens, R.J. and Curran, K.J., 2012. Novel cellular therapies for leukemia: CAR-modified T cells targeted to the CD19 antigen. *Hematology. American Society of Hematology. Education Program*, 2012, 143-151.
- Brentjens, R.J., *et al.*, 2013. CD19-targeted T cells rapidly induce molecular remissions in adults with chemotherapy-refractory acute lymphoblastic leukemia. *Science Translational Medicine*, 5 (177), 177ra38.
- Brett, A., Pandey, S. and Fraizer, G., 2013. The Wilms' tumor gene (WT1) regulates E-cadherin expression and migration of prostate cancer cells. *Molecular Cancer*, 12, 3-4598-12-3.

- Brown, C.E., *et al.*, 2016. Regression of Glioblastoma after Chimeric Antigen Receptor T-Cell Therapy. *The New England Journal of Medicine*, 375 (26), 2561-2569.
- Brunner, K.T., *et al.*, 1968. Quantitative assay of the lytic action of immune lymphoid cells on 51-Cr-labelled allogeneic target cells in vitro; inhibition by isoantibody and by drugs. *Immunology*, 14 (2), 181-196.
- Brusic, A., *et al.*, 2012. Detecting T-cell reactivity to whole cell vaccines: Proof of concept analysis of T-cell response to K562 cell antigens in CML patients. *Oncoimmunology*, 1 (7), 1095-1103.
- Buonaguro, L. and HEPAVAC Consortium, 2016. Developments in cancer vaccines for hepatocellular carcinoma. *Cancer Immunology, Immunotherapy: CII*, 65 (1), 93-99.
- Burnet, M., 1957. Cancer-a biological approach. 3. Viruses associated with neoplastic conditions. *British Medical Journal*, 1 (APR 13), 841-846.
- Butt, N.M., *et al.*, 2005. Circulating bcr-abl-specific CD8+ T cells in chronic myeloid leukemia patients and healthy subjects. *Haematologica*, 90 (10), 1315-1323.
- Butte, M.J., *et al.*, 2007. Programmed death-1 ligand 1 interacts specifically with the B7-1 costimulatory molecule to inhibit T cell responses. *Immunity*, 27 (1), 111-122.
- Call, K.M., *et al.*, 1990. Isolation and characterization of a zinc finger polypeptide gene at the human chromosome 11 Wilms' tumor locus. *Cell*, 60 (3), 509-520.
- Cano, D.A., Soto-Moreno, A. and Leal-Cerro, A., 2014. Genetically engineered mouse models of pituitary tumors. *Frontiers in Oncology*, 4, 203.
- Carr JH, Rodak BF., 2009. Clinical Hematology Atlas, 3<sup>rd</sup> ed. Philadelphia, Saunders. Available online at: <https://slideplayer.com/slide/13569767/release/woothee> . [Accessed 29 February 2019].
- Cao, X., *et al.*, 1995. Defective lymphoid development in mice lacking expression of the common cytokine receptor  $\gamma$  chain. *Immunity*, 2 (3), 223-238.
- Carulli, G., *et al.*, 2010. Abnormal phenotype of bone marrow plasma cells in patients with chronic myeloid leukemia undergoing therapy with Imatinib. *Leukemia Research*, 34 (10), 1336-1339.
- Catellani, S., *et al.*, 2011. Imatinib treatment induces CD5+ B lymphocytes and IgM natural antibodies with anti-leukemic reactivity in patients with chronic myelogenous leukemia. *PLoS One*, 6 (4), e18925.
- Cathcart, K., *et al.*, 2004. A multivalent bcr-abl fusion peptide vaccination trial in patients with chronic myeloid leukemia. *Blood*, 103 (3), 1037-1042.
- Cavnar, M.J., *et al.*, 2013. KIT oncogene inhibition drives intratumoral macrophage M2 polarization. *The Journal of Experimental Medicine*, 210 (13), 2873-2886.
- Cawthon, A.G., Lu, H. and Alexander-Miller, M.A., 2001. Peptide requirement for CTL activation reflects the sensitivity to CD3 engagement: correlation with CD8 $\alpha$  versus CD8 $\alpha$  $\alpha$  expression. *Journal of Immunology (Baltimore, Md.: 1950)*, 167 (5), 2577-2584.
- Cebo, C., *et al.*, 2006. The Decreased Susceptibility of Bcr/Abl Targets to NK Cell-Mediated Lysis in Response to Imatinib Mesylate Involves Modulation of NKG2D

- Ligands, GM1 Expression, and Synapse Formation. *The Journal of Immunology*, 176 (2), 864-872.
- Cella, M., Sallusto, F. and Lanzavecchia, A., 1997. Origin, maturation and antigen presenting function of dendritic cells. *Current Opinion in Immunology*, 9 (1), 10-16.
- Champagne, P., et al., 2001. Skewed maturation of memory HIV-specific CD8 T lymphocytes. *Nature*, 410 (6824), 106.
- Chang, C., et al., 2007. Expression of CD80 and CD86 costimulatory molecules are potential markers for better survival in nasopharyngeal carcinoma. *BMC Cancer*, 7 (1), 88.
- Chappell, D.B. and Restifo, N.P., 1998. T cell-tumor cell: a fatal interaction? *Cancer Immunology, Immunotherapy*, 47 (2), 65-71.
- Chapuis, A.G., et al., 2013. Transferred WT1-reactive CD8+ T cells can mediate antileukemic activity and persist in post-transplant patients. *Science Translational Medicine*, 5 (174), 174ra27.
- Cheever, M.A., et al., 2009. The prioritization of cancer antigens: a national cancer institute pilot project for the acceleration of translational research. *Clinical Cancer Research: An Official Journal of the American Association for Cancer Research*, 15 (17), 5323-5337.
- Chen, F., et al., 2012. In vitro and in vivo identification of a novel cytotoxic T lymphocyte epitope from Rv3425 of Mycobacterium tuberculosis. *Microbiology and Immunology*, 56 (8), 548-553.
- Chen, Q., et al., 2012. Aberrant hypomethylation of DDX 43 promoter in myelodysplastic syndrome. *British Journal of Haematology*, 158 (2), 293-296.
- Chen, Y., et al., 2009. Cancer/testis antigen CT45: analysis of mRNA and protein expression in human cancer. *International Journal of Cancer*, 124 (12), 2893-2898.
- Chen, Z., et al., 2018. Impact of protamine I on colon cancer proliferation, invasion, migration, diagnosis and prognosis. *Biological Chemistry*, 399 (3), 265-275.
- Chen, C.I., et al., 2012. NK cells are dysfunctional in human chronic myelogenous leukemia before and on imatinib treatment and in BCR-ABL-positive mice. *Leukemia*, 26 (3), 465-474.
- Chen, G., et al., 2002. Discordant protein and mRNA expression in lung adenocarcinomas. *Molecular & Cellular Proteomics: MCP*, 1 (4), 304-313.
- Chen, L. and Han, X., 2015. Anti-PD-1/PD-L1 therapy of human cancer: past, present, and future. *The Journal of Clinical Investigation*, 125 (9), 3384-3391.
- Chen, S., et al., 2009. TCR zeta chain expression in T cells from patients with CML. *Hematology (Amsterdam, Netherlands)*, 14 (2), 95-100.
- Chen, Q., et al., 2011. Gene expression of helicase antigen in patients with acute and chronic myeloid leukemia. *Zhongguo Shi Yan Xue Ye Xue Za Zhi*, 19 (5), 1171-1175.
- Chen, Q., et al., 2013. The methylation status of the DDX43 promoter in Chinese patients with chronic myeloid leukemia. *Genetic Testing and Molecular Biomarkers*, 17 (6), 508-511.

- Chiba, Y., *et al.*, 2014. Immunological Control of Chronic Myeloid Leukemia Leading to Treatment-Free. *In: .*
- Chicas, A. and Macino, G., 2001. Characteristics of post-transcriptional gene silencing. *EMBO Reports*, 2 (11), 992-996.
- Chikuma, S., *et al.*, 2009. PD-1-mediated suppression of IL-2 production induces CD8+ T cell anergy in vivo. *Journal of Immunology (Baltimore, Md.: 1950)*, 182 (11), 6682-6689.
- Chiusa, L., *et al.*, 2006. Prognostic value of quantitative analysis of WT1 gene transcripts in adult acute lymphoblastic leukemia. *Haematologica*, 91 (2), 270-271.
- Chlichlia, K., Schirrmacher, V. and Sandaltzopoulos, R., 2005. Cancer immunotherapy: Battling tumors with gene vaccines. *Current Medicinal Chemistry-Anti-Inflammatory & Anti-Allergy Agents*, 4 (4), 353-365.
- Cho, B., *et al.*, 2003. Promoter hypomethylation of a novel cancer/testis antigen gene CAGE is correlated with its aberrant expression and is seen in premalignant stage of gastric carcinoma. *Biochemical and Biophysical Research Communications*, 307 (1), 52-63.
- Christiansson, L., *et al.*, 2013. Increased level of myeloid-derived suppressor cells programmed death receptor ligand 1/programmed death receptor 1, and soluble CD25 in Sokal high risk chronic myeloid leukemia. *PLoS One*, 8 (1), e55818.
- Cilloni, D., *et al.*, 2004. Sensitivity to imatinib therapy may be predicted by testing Wilms tumor gene expression and colony growth after a short in vitro incubation. *Cancer*, 101 (5), 979-988.
- Ciszak, L., *et al.*, 2016. CTLA-4 affects expression of key cell cycle regulators of G0/G1 phase in neoplastic lymphocytes from patients with chronic lymphocytic leukaemia. *Clinical and Experimental Medicine*, 16 (3), 317-332.
- Clark, R.E., *et al.*, 2001. Direct evidence that leukemic cells present HLA-associated immunogenic peptides derived from the BCR-ABL b3a2 fusion protein. *Blood*, 98 (10), 2887-2893.
- Clarke, C.J. and Holyoake, T.L., 2017. Preclinical approaches in chronic myeloid leukemia: from cells to systems. *Experimental Hematology*, 47, 13-23.
- Clinical care option oncology. Providing Optimal Care for Patients with Chronic Myeloid Leukemia, LLC; Reston, Virginia, USA. Available at: <https://www.clinicaloptions.com/oncology/programs/managing-cml/interactive-virtual-presentation>. [Accessed 26 February 2020].
- Coluzzi, S., *et al.*, 2016. WT1 ANALYSIS IN CHRONIC MYELOID LEUKEMIA (CML) PATIENTS. *In: HAEMATOLOGICA*, FERRATA STORTI FOUNDATION VIA GIUSEPPE BELLI 4, 27100 PAVIA, ITALY, pp. S101-S101.
- Contag, C.H. and Ross, B.D., 2002. It's not just about anatomy: in vivo bioluminescence imaging as an eyepiece into biology. *Journal of Magnetic Resonance Imaging: An Official Journal of the International Society for Magnetic Resonance in Medicine*, 16 (4), 378-387.

- Contini, P., *et al.*, 2000. Soluble HLA class I/CD8 ligation triggers apoptosis in EBV-specific CD8 cytotoxic T lymphocytes by Fas/Fas-ligand interaction. *Human Immunology*, 61 (12), 1347-1351.
- Contini, P., *et al.*, 2003. Soluble HLA-A,-B,-C and-G molecules induce apoptosis in T and NK CD8 cells and inhibit cytotoxic T cell activity through CD8 ligation. *European Journal of Immunology*, 33 (1), 125-134.
- Corbin, A.S., *et al.*, 2011. Human chronic myeloid leukemia stem cells are insensitive to imatinib despite inhibition of BCR-ABL activity. *The Journal of Clinical Investigation*, 121 (1), 396-409.
- Cortes, J. and Kantarjian, H., 2012. How I treat newly diagnosed chronic phase CML. *Blood*, 120 (7), 1390-1397.
- Cortes, J.E., *et al.*, 2013. A phase 2 trial of ponatinib in Philadelphia chromosome-positive leukemias. *The New England Journal of Medicine*, 369 (19), 1783-1796.
- Corthay, A., 2014. Does the immune system naturally protect against cancer? *Frontiers in Immunology*, 5, 197.
- Corzo, C.A., *et al.*, 2009. Mechanism regulating reactive oxygen species in tumor-induced myeloid-derived suppressor cells. *Journal of Immunology (Baltimore, Md.: 1950)*, 182 (9), 5693-5701.
- Goss, V.L., *et al.*, 2006. A common phosphotyrosine signature for the Bcr-Abl kinase. *Blood*, 107 (12), 4888-4897.
- Coulie, P.G., *et al.*, 2014. Tumour antigens recognized by T lymphocytes: at the core of cancer immunotherapy. *Nature Reviews Cancer*, 14 (2), 135.
- Cox, J.C. and Coulter, A.R., 1997. Adjuvants—a classification and review of their modes of action. *Vaccine*, 15 (3), 248-256.
- Craft, N., *et al.*, 2005. Bioluminescent imaging of melanoma in live mice. *Journal of Investigative Dermatology*, 125 (1), 159-165.
- Cross, N., *et al.*, 2012. Standardized definitions of molecular response in chronic myeloid leukemia. *Leukemia*, 26 (10), 2172.
- Cruz, C.R., *et al.*, 2013. Infusion of donor-derived CD19-redredirected virus-specific T cells for B-cell malignancies relapsed after allogeneic stem cell transplant: a phase 1 study. *Blood*, 122 (17), 2965-2973.
- Curti, A., *et al.*, 2007. Modulation of tryptophan catabolism by human leukemic cells results in the conversion of CD25<sup>-</sup> into CD25<sup>+</sup> T regulatory cells. *Blood*, 109 (7), 2871-2877.
- Daley, G.Q., Van Etten, R.A. and Baltimore, D., 1990. Induction of chronic myelogenous leukemia in mice by the P210bcr/abl gene of the Philadelphia chromosome. *Science (New York, N.Y.)*, 247 (4944), 824-830.
- Daniel, P.T., *et al.*, 1997. Costimulatory signals through B7.1/CD28 prevent T cell apoptosis during target cell lysis. *Journal of Immunology (Baltimore, Md.: 1950)*, 159 (8), 3808-3815.

- Dao, T., et al., 2017. An immunogenic WT1-derived peptide that induces T cell response in the context of HLA-A\* 02: 01 and HLA-A\* 24: 02 molecules. *Oncoimmunology*, 6 (2), e1252895.
- Davies, M., 2014. New modalities of cancer treatment for NSCLC: focus on immunotherapy. *Cancer Management and Research*, 6, 63-75.
- de Klein, A., et al., 1982. A cellular oncogene is translocated to the Philadelphia chromosome in chronic myelocytic leukaemia. *Nature*, 300 (5894), 765.
- De Smet, C., et al., 1999. DNA methylation is the primary silencing mechanism for a set of germ line- and tumor-specific genes with a CpG-rich promoter. *Molecular and Cellular Biology*, 19 (11), 7327-7335.
- Deininger, M., et al., 2009. *International Randomized Study of Interferon Vs STI571 (IRIS) 8-Year Follow Up: Sustained Survival and Low Risk for Progression Or Events in Patients with Newly Diagnosed Chronic Myeloid Leukemia in Chronic Phase (CML-CP) Treated with Imatinib*.
- Deininger, M.W., et al., 2000. BCR-ABL tyrosine kinase activity regulates the expression of multiple genes implicated in the pathogenesis of chronic myeloid leukemia. *Cancer Research*, 60 (7), 2049-2055.
- Denhardt, D.T., 1996. Signal-transducing protein phosphorylation cascades mediated by Ras/Rho proteins in the mammalian cell: the potential for multiplex signalling. *The Biochemical Journal*, 318 (Pt 3) (Pt 3), 729-747.
- Dermime, S., et al., 2002. Cancer vaccines and immunotherapy. *British Medical Bulletin*, 62, 149-162.
- Dermime, S., et al., 2004. Vaccine and antibody-directed T cell tumour immunotherapy. *Biochimica Et Biophysica Acta*, 1704 (1), 11-35.
- Diekmann, D., et al., 1991. Bcr encodes a GTPase-activating protein for p21 rac. *Nature*, 351 (6325), 400.
- Dietz, A.B., et al., 2004. Imatinib mesylate inhibits T-cell proliferation in vitro and delayed-type hypersensitivity in vivo. *Blood*, 104 (4), 1094-1099.
- Disis, M.L., 2014. Mechanism of action of immunotherapy. *In: Seminars in oncology*, Elsevier, pp. S3-S13.
- Divya Nagarajan, 2018. Towards the development of HAGE -based vaccines for the treatment of patients with triple negative breast cancers [online]. Ph.D. thesis, Nottingham Trent University. Available at: <http://irep.ntu.ac.uk/id/eprint/34884/>. [Accessed 29 January 2019].
- Dolcetti, L., et al., 2010. Hierarchy of immunosuppressive strength among myeloid-derived suppressor cell subsets is determined by GM-CSF. *European Journal of Immunology*, 40 (1), 22-35.
- Dolstra, H., et al., 1999. A human minor histocompatibility antigen specific for B cell acute lymphoblastic leukemia. *The Journal of Experimental Medicine*, 189 (2), 301-308.
- Dong, H., et al., 2002. Tumor-associated B7-H1 promotes T-cell apoptosis: a potential mechanism of immune evasion. *Nature Medicine*, 8 (8), 793.

- Doria-Rose, N.A. and Haigwood, N.L., 2003. DNA vaccine strategies: candidates for immune modulation and immunization regimens. *Methods*, 31 (3), 207-216.
- Doyle, A., et al., 2012. The construction of transgenic and gene knockout/knockin mouse models of human disease. *Transgenic Research*, 21 (2), 327-349.
- Drexler, H.G., Matsuo, Y. and MacLeod, R.A., 2000. Continuous hematopoietic cell lines as model systems for leukemia-lymphoma research. *Leukemia Research*, 24 (11), 881-911.
- Druker, B.J., et al., 2001. Efficacy and safety of a specific inhibitor of the BCR-ABL tyrosine kinase in chronic myeloid leukemia. *The New England Journal of Medicine*, 344 (14), 1031-1037.
- Du, Y., et al., 2014. SMG1 acts as a novel potential tumor suppressor with epigenetic inactivation in acute myeloid leukemia. *International Journal of Molecular Sciences*, 15 (9), 17065-17076.
- Dulphy, N., et al., 2013. *Low Natural Killer (NK) Cell Counts and Functionality Are Associated With Molecular Relapse After Imatinib Discontinuation In Patients (pts) With Chronic Phase (CP)-Chronic Myeloid Leukemia (CML) With Undetectable BCR-ABL Transcripts For At Least 2 Years: Preliminary Results From Immunostim, On Behalf Of STIM Investigators.*
- Dutoit, V., et al., 2001. Heterogeneous T-cell response to MAGE-A10(254-262): high avidity-specific cytolytic T lymphocytes show superior antitumor activity. *Cancer Research*, 61 (15), 5850-5856.
- Dutton, R., Bradley, L. and Swain, S., 1998. T cell memory. *Annual Review of Immunology*, 16 (1), 201-223.
- Eisendle, K., et al., 2003. Phenotypic and functional deficiencies of leukaemic dendritic cells from patients with chronic myeloid leukaemia. *British Journal of Haematology*, 120 (1), 63-73.
- ELN European LeukemiaNet. European LeukemiaNet recommendations for the management of CML, 2013 Available at: [https://www.leukemia-net.org/content/leukemias/cml/recommendations/index\\_eng.html](https://www.leukemia-net.org/content/leukemias/cml/recommendations/index_eng.html). [Accessed 28 January 2019].
- Emens, L.A., 2008. Cancer vaccines: on the threshold of success. *Expert Opinion on Emerging Drugs*, 13 (2), 295-308.
- Erskine, C.L., Henle, A.M. and Knutson, K.L., 2012. Determining optimal cytotoxic activity of human Her2neu specific CD8 T cells by comparing the Cr51 release assay to the xCELLigence system. *Journal of Visualized Experiments: JoVE*, (66):e3683. doi (66), e3683.
- Faderl, S., et al., 1999. The biology of chronic myeloid leukemia. *The New England Journal of Medicine*, 341 (3), 164-172.
- Farrar, M.A. and Schreiber, R.D., 1993. The molecular cell biology of interferon-gamma and its receptor. *Annual Review of Immunology*, 11 (1), 571-611.
- Figuroa, M.E., et al., 2013. Integrated genetic and epigenetic analysis of childhood acute lymphoblastic leukemia. *The Journal of Clinical Investigation*, 123 (7), 3099-3111.

- Fijak, M. and Meinhardt, A., 2006. The testis in immune privilege. *Immunological Reviews*, 213 (1), 66-81.
- Fioretti, D., *et al.*, 2010. DNA vaccines: developing new strategies against cancer. *Journal of Biomedicine & Biotechnology*, 2010, 174378.
- Fitzpatrick, K.E., *et al.*, 2012. Incidence and risk factors for placenta accreta/increta/percreta in the UK: a national case-control study. *PLoS One*, 7 (12), e52893.
- Fogh, J., Fogh, J.M. and Orfeo, T., 1977. One hundred and twenty-seven cultured human tumor cell lines producing tumors in nude mice. *Journal of the National Cancer Institute*, 59 (1), 221-226.
- Folgiero, V., *et al.*, 2014. Indoleamine 2,3-dioxygenase 1 (IDO1) activity in leukemia blasts correlates with poor outcome in childhood acute myeloid leukemia. *Oncotarget*, 5 (8), 2052-2064.
- Fourcade, J., *et al.*, 2009. PD-1 is a regulator of NY-ESO-1-specific CD8+ T cell expansion in melanoma patients. *Journal of Immunology (Baltimore, Md.: 1950)*, 182 (9), 5240-5249.
- Fourcade, J., *et al.*, 2010. Upregulation of Tim-3 and PD-1 expression is associated with tumor antigen-specific CD8+ T cell dysfunction in melanoma patients. *The Journal of Experimental Medicine*, 207 (10), 2175-2186.
- Fraser, C.K., *et al.*, 2007. Improving vaccines by incorporating immunological adjuvants. *Expert Review of Vaccines*, 6 (4), 559-578.
- Freeman, G.J., *et al.*, 1993. Cloning of B7-2: a CTLA-4 counter-receptor that costimulates human T cell proliferation. *Science (New York, N.Y.)*, 262 (5135), 909-911.
- Fridman, W.H., *et al.*, 2012. The immune contexture in human tumours: impact on clinical outcome. *Nature Reviews Cancer*, 12 (4), 298.
- Fujiwara, S., 2018. Humanized mice: A brief overview on their diverse applications in biomedical research. *Journal of Cellular Physiology*, 233 (4), 2889-2901.
- Funakoshi, S., *et al.*, 1994. Inhibition of human B-cell lymphoma growth by CD40 stimulation. *Blood*, 83 (10), 2787-2794.
- Gabrilovich, D.I. and Nagaraj, S., 2009a. Myeloid-derived suppressor cells as regulators of the immune system. *Nature Reviews Immunology*, 9 (3), 162.
- Gannage, M., *et al.*, 2005. Ex vivo characterization of multiepitopic tumor-specific CD8 T cells in patients with chronic myeloid leukemia: implications for vaccine development and adoptive cellular immunotherapy. *Journal of Immunology (Baltimore, Md.: 1950)*, 174 (12), 8210-8218.
- Gantt, S., *et al.*, 2014. The role of myeloid-derived suppressor cells in immune ontogeny. *Frontiers in Immunology*, 5, 387.
- Gao, H., *et al.*, 2005. Imatinib mesylate suppresses cytokine synthesis by activated CD4 T cells of patients with chronic myelogenous leukemia. *Leukemia*, 19 (11), 1905-1911.

- Garcia-Diaz, A., *et al.*, 2017. Interferon receptor signaling pathways regulating PD-L1 and PD-L2 expression. *Cell Reports*, 19 (6), 1189-1201.
- Gattinoni, L., *et al.*, 2005. Acquisition of full effector function in vitro paradoxically impairs the in vivo antitumor efficacy of adoptively transferred CD8+ T cells. *The Journal of Clinical Investigation*, 115 (6), 1616-1626.
- Gehring, A.J., *et al.*, 2009. Profile of tumor antigen-specific CD8 T cells in patients with hepatitis B virus-related hepatocellular carcinoma. *Gastroenterology*, 137 (2), 682-690.
- Genard, G., Lucas, S. and Michiels, C., 2017. Reprogramming of Tumor-Associated Macrophages with Anticancer Therapies: Radiotherapy versus Chemo- and Immunotherapies. *Frontiers in Immunology*, 8, 828.
- Gerber, J.M., *et al.*, 2011. Characterization of chronic myeloid leukemia stem cells. *American Journal of Hematology*, 86 (1), 31-37.
- Gerdemann, U., *et al.*, 2011. Cytotoxic T lymphocytes simultaneously targeting multiple tumor-associated antigens to treat EBV negative lymphoma. *Molecular Therapy: The Journal of the American Society of Gene Therapy*, 19 (12), 2258-2268.
- Germain, R.N., 1995. The biochemistry and cell biology of antigen presentation by MHC class I and class II molecules. Implications for development of combination vaccines. *Annals of the New York Academy of Sciences*, 754, 114-125.
- Gessler, M., *et al.*, 1990. Homozygous deletion in Wilms tumours of a zinc-finger gene identified by chromosome jumping. *Nature*, 343 (6260), 774.
- Ghanem, A., Healey, R. and Adly, F.G., 2013. Current trends in separation of plasmid DNA vaccines: a review. *Analytica Chimica Acta*, 760, 1-15.
- Ginhoux, F., Guilliams, M. and Naik, S.H., 2016. Editorial: Dendritic Cell and Macrophage Nomenclature and Classification. *Frontiers in Immunology*, 7, 168.
- Gismondi, A., *et al.*, 2015. Effector Functions of Natural Killer Cell Subsets in the Control of Hematological Malignancies. *Frontiers in Immunology*, 6, 10.3389/fimmu.2015.00567.
- Gjerstorff, M., *et al.*, 2006. Restriction of GAGE protein expression to subpopulations of cancer cells is independent of genotype and may limit the use of GAGE proteins as targets for cancer immunotherapy. *British Journal of Cancer*, 94 (12), 1864.
- Gjerstorff, M.F., Burns, J. and Ditzel, H.J., 2010. Cancer-germline antigen vaccines and epigenetic enhancers: future strategies for cancer treatment. *Expert Opinion on Biological Therapy*, 10 (7), 1061-1075.
- Gjerstorff, M.F., Andersen, M.H. and Ditzel, H.J., 2015. Oncogenic cancer/testis antigens: prime candidates for immunotherapy. *Oncotarget*, 6 (18), 15772-15787.
- Glover, D.J., Lipps, H.J. and Jans, D.A., 2005. Towards safe, non-viral therapeutic gene expression in humans. *Nature Reviews Genetics*, 6 (4), 299.
- Gnjatic, S., *et al.*, 2003. Survey of naturally occurring CD4+ T cell responses against NY-ESO-1 in cancer patients: correlation with antibody responses. *Proceedings of the National Academy of Sciences of the United States of America*, 100 (15), 8862-8867.

- Goldman, J.M., 2009. Initial treatment for patients with CML. *Hematology.American Society of Hematology.Education Program*, 453-460.
- Gourley, T.S., et al., 2004. Generation and maintenance of immunological memory. *In: Seminars in immunology*, Elsevier, pp. 323-333.
- Graham, S.M., et al., 2002. Primitive, quiescent, Philadelphia-positive stem cells from patients with chronic myeloid leukemia are insensitive to STI571 in vitro. *Blood*, 99 (1), 319-325.
- Greiner, J., Dohner, H. and Schmitt, M., 2006. Cancer vaccines for patients with acute myeloid leukemia--definition of leukemia-associated antigens and current clinical protocols targeting these antigens. *Haematologica*, 91 (12), 1653-1661.
- Greiner, J. and Schmitt, M., 2008. Leukemia-associated antigens as target structures for a specific immunotherapy in chronic myeloid leukemia. *European Journal of Haematology*, 80 (6), 461-468.
- Greve, K., et al., 2014. SSX2-4 expression in early-stage non-small cell lung cancer. *Tissue Antigens*, 83 (5), 344-349.
- Grewal, I.S. and Flavell, R.A., 1998. CD40 and CD154 in cell-mediated immunity. *Annual Review of Immunology*, 16 (1), 111-135.
- Gridelli, C., et al., 2009. Vaccines for the treatment of non-small cell lung cancer: a renewed anticancer strategy. *The Oncologist*, 14 (9), 909-920.
- Grivennikov, S.I., Greten, F.R. and Karin, M., 2010. *Immunity, Inflammation, and Cancer*.
- Grunau, C., et al., 2005. Frequent DNA hypomethylation of human juxtacentromeric BAGE loci in cancer. *Genes, Chromosomes and Cancer*, 43 (1), 11-24.
- Grunebach, F., et al., 2006. BCR-ABL is not an immunodominant antigen in chronic myelogenous leukemia. *Cancer Research*, 66 (11), 5892-5900.
- Grupp, S.A., et al., 2013. Chimeric antigen receptor-modified T cells for acute lymphoid leukemia. *The New England Journal of Medicine*, 368 (16), 1509-1518.
- Guinn, B., et al., 2005. Humoral detection of leukaemia-associated antigens in presentation acute myeloid leukaemia. *Biochemical and Biophysical Research Communications*, 335 (4), 1293-1304.
- Guy, B., 2007. The perfect mix: recent progress in adjuvant research. *Nature Reviews Microbiology*, 5 (7), 505.
- Haferlach, T., et al., 2010. Clinical utility of microarray-based gene expression profiling in the diagnosis and subclassification of leukemia: report from the International Microarray Innovations in Leukemia Study Group. *Journal of Clinical Oncology: Official Journal of the American Society of Clinical Oncology*, 28 (15), 2529-2537.
- Han, J.F., et al., 2006. Identification of a new HLA-A\*0201-restricted cytotoxic T lymphocyte epitope from CML28. *Cancer Immunology, Immunotherapy: CII*, 55 (12), 1575-1583.

- Hanahan, D., Wagner, E.F. and Palmiter, R.D., 2007. The origins of oncomice: a history of the first transgenic mice genetically engineered to develop cancer. *Genes & Development*, 21 (18), 2258-2270.
- Hanson, K.D. and Sedivy, J.M., 1995. Analysis of biological selections for high-efficiency gene targeting. *Molecular and Cellular Biology*, 15 (1), 45-51.
- Haass, W., et al., 2015. Clonal Evolution and Blast Crisis Correlate with Enhanced Proteolytic Activity of Separase in BCR-ABL b3a2 Fusion Type CML under Imatinib Therapy. *PloS One*, 10 (6), e0129648.
- Hastie, N.D., 2017. Wilms' tumour 1 (WT1) in development, homeostasis and disease. *Development (Cambridge, England)*, 144 (16), 2862-2872.
- Hehlmann, R., Hochhaus, A. and Baccarani, M., 2007. Chronic myeloid leukaemia. *The Lancet*, 370 (9584), 342-350.
- Hehlmann, R., 2012. How I treat CML blast crisis. *Blood*, 120 (4), 737-747.
- Heisterkamp, N., et al., 1982. Chromosomal localization of human cellular homologues of two viral oncogenes. *Nature*, 299 (5885), 747.
- Herberman, R.B., et al., 1975. Natural cytotoxic reactivity of mouse lymphoid cells against syngeneic and allogeneic tumors. II. Characterization of effector cells. *International Journal of Cancer*, 16 (2), 230-239.
- Herman, H., et al., 2003. Trans allele methylation and paramutation-like effects in mice. *Nature Genetics*, 34 (2), 199.
- Hernandez-Boluda, J.C., et al., 2005. Survivin expression in the progression of chronic myeloid leukemia: a sequential study in 16 patients. *Leukemia & Lymphoma*, 46 (5), 717-722.
- Herrada, A.A., et al., 2012. Harnessing DNA-induced immune responses for improving cancer vaccines. *Human Vaccines & Immunotherapeutics*, 8 (11), 1682-1693.
- Hodge, J.W., et al., 2005. Multiple costimulatory modalities enhance CTL avidity. *Journal of Immunology (Baltimore, Md.: 1950)*, 174 (10), 5994-6004.
- Hoebe, K., Janssen, E. and Beutler, B., 2004. The interface between innate and adaptive immunity. *Nature Immunology*, 5 (10), 971.
- Hofmann, O., et al., 2008. Genome-wide analysis of cancer/testis gene expression. *Proceedings of the National Academy of Sciences of the United States of America*, 105 (51), 20422-20427.
- Holler, P.D. and Kranz, D.M., 2003. Quantitative analysis of the contribution of TCR/pepMHC affinity and CD8 to T cell activation. *Immunity*, 18 (2), 255-264.
- Hollingshead, M., et al., 2004. A potential role for imaging technology in anticancer efficacy evaluations. *European Journal of Cancer*, 40 (6), 890-898.
- Holmen, S.L., et al., 1995. Efficient lipid-mediated transfection of DNA into primary rat hepatocytes. *In Vitro Cellular & Developmental Biology-Animal*, 31 (5), 347-351.

- Holyoake, T.L. and Vetrie, D., 2017. The chronic myeloid leukemia stem cell: stemming the tide of persistence. *Blood*, 129 (12), 1595-1606.
- Horowitz, M.M., *et al.*, 1990. Graft-versus-leukemia reactions after bone marrow transplantation. *Blood*, 75 (3), 555-562.
- Hosken, N.A. and Bevan, M.J., 1990. Defective presentation of endogenous antigen by a cell line expressing class I molecules. *Science (New York, N.Y.)*, 248 (4953), 367-370.
- House, C.D., Hernandez, L. and Annunziata, C.M., 2014. Recent technological advances in using mouse models to study ovarian cancer. *Frontiers in Oncology*, 4, 26.
- Huang, X., Cortes, J. and Kantarjian, H., 2012. Estimations of the increasing prevalence and plateau prevalence of chronic myeloid leukemia in the era of tyrosine kinase inhibitor therapy. *Cancer*, 118 (12), 3123-3127.
- Huang, B., *et al.*, 2006. Gr-1+CD115+ immature myeloid suppressor cells mediate the development of tumor-induced T regulatory cells and T-cell anergy in tumor-bearing host. *Cancer Research*, 66 (2), 1123-1131.
- Hudson, W., *et al.*, 1998. Xenotransplantation of human lymphoid malignancies is optimized in mice with multiple immunologic defects. *Leukemia*, 12 (12), 2029.
- Hughes, A., *et al.*, 2017. CML patients with deep molecular responses to TKI have restored immune effectors and decreased PD-1 and immune suppressors. *Blood*, 129 (9), 1166-1176.
- Iachininoto, M.G., *et al.*, 2013. Cyclooxygenase-2 (COX-2) inhibition constrains indoleamine 2, 3-dioxygenase 1 (IDO1) activity in acute myeloid leukaemia cells. *Molecules*, 18 (9), 10132-10145.
- Ichinohasama, R., *et al.*, 2010. Sensitive immunohistochemical detection of WT1 protein in tumors with anti-WT1 antibody against WT1 235 peptide. *Cancer Science*, 101 (5), 1089-1092.
- Ilander, M.M., *et al.*, 2014. *Early Disease Relapse after Tyrosine Kinase Inhibitor Treatment Discontinuation in CML Is Related Both to Low Number and Impaired Function of NK-Cells.*
- Inoue, K., *et al.*, 1994. WT1 as a new prognostic factor and a new marker for the detection of minimal residual disease in acute leukemia. *Blood*, 84 (9), 3071-3079.
- Jabbour, E. and Kantarjian, H., 2018. Chronic myeloid leukemia: 2018 update on diagnosis, therapy and monitoring. *American Journal of Hematology*, 93 (3), 442-459.
- Jabbour, E. and Kantarjian, H., 2014. Chronic myeloid leukemia: 2014 update on diagnosis, monitoring, and management. *American Journal of Hematology*, 89 (5), 547-556.
- Jain, K.K., 2004. Applications of biochips: from diagnostics to personalized medicine. *Current Opinion in Drug Discovery & Development*, 7 (3), 285-289.
- Janeway, C.A., *et al.*, 2005. Immunobiology: the immune system in health and disease.

- Janitz, M., *et al.*, 1994. Analysis of mRNA for class I HLA on human gametogenic cells. *Molecular Reproduction and Development*, 38 (2), 231-237.
- Janssen, J.J., *et al.*, 2010. Methylation patterns in CD34 positive chronic myeloid leukemia blast crisis cells. *Haematologica*, 95 (6), 1036-1037.
- Jarmoskaite, I. and Russell, R., 2014. RNA helicase proteins as chaperones and remodelers. *Annual Review of Biochemistry*, 83, 697-725.
- Jayakumar Vadakekolathu, 2013. Characterisation of high and low avidity peptide specific CD8<sup>+</sup> T cells using immunologic, transcriptomic and proteomic tools. [online]. Ph.D. thesis, Nottingham Trent University. Available at: <http://irep.ntu.ac.uk/id/eprint/228/>. [Accessed 30 March 2017].
- Jensen, M.C., *et al.*, 2010. Antitransgene rejection responses contribute to attenuated persistence of adoptively transferred CD20/CD19-specific chimeric antigen receptor redirected T cells in humans. *Biology of Blood and Marrow Transplantation: Journal of the American Society for Blood and Marrow Transplantation*, 16 (9), 1245-1256.
- Ji, R., *et al.*, 2012. An immune-active tumor microenvironment favors clinical response to ipilimumab. *Cancer Immunology, Immunotherapy*, 61 (7), 1019-1031.
- Jin, H.T., *et al.*, 2010. Cooperation of Tim-3 and PD-1 in CD8 T-cell exhaustion during chronic viral infection. *Proceedings of the National Academy of Sciences of the United States of America*, 107 (33), 14733-14738.
- Jones, P.A. and Baylin, S.B., 2002. The fundamental role of epigenetic events in cancer. *Nature Reviews Genetics*, 3 (6), 415.
- Jonuleit, H., *et al.*, 2001. A comparison of two types of dendritic cell as adjuvants for the induction of melanoma-specific T-cell responses in humans following intranodal injection. *International Journal of Cancer*, 93 (2), 243-251.
- Jorgensen, H.G., *et al.*, 2007. Nilotinib exerts equipotent antiproliferative effects to imatinib and does not induce apoptosis in CD34+ CML cells. *Blood*, 109 (9), 4016-4019.
- Jungbluth, A.A., *et al.*, 2005. The cancer-testis antigens CT7 (MAGE-C1) and MAGE-A3/6 are commonly expressed in multiple myeloma and correlate with plasma-cell proliferation. *Blood*, 106 (1), 167-174.
- Kaech, S.M., Wherry, E.J. and Ahmed, R., 2002. Vaccines: effector and memory T-cell differentiation: implications for vaccine development. *Nature Reviews Immunology*, 2 (4), 251.
- Kalos, M., *et al.*, 2011. T cells with chimeric antigen receptors have potent antitumor effects and can establish memory in patients with advanced leukemia. *Science Translational Medicine*, 3 (95), 95ra73.
- Kansas, G.S., *et al.*, 1993. Regulation of leukocyte rolling and adhesion to high endothelial venules through the cytoplasmic domain of L-selectin. *The Journal of Experimental Medicine*, 177 (3), 833-838.
- Karakas, T., *et al.*, 2002. The coexpression of the apoptosis-related genes bcl-2 and wt1 in predicting survival in adult acute myeloid leukemia. *Leukemia*, 16 (5), 846.

- Karre, K., *et al.*, 1986. Selective rejection of H-2-deficient lymphoma variants suggests alternative immune defence strategy. *Nature*, 319 (6055), 675-678.
- Kaur, G. and Dufour, J.M., 2012. *Cell Lines: Valuable Tools Or Useless Artifacts*, .
- Kelly, R.J., Gulley, J.L. and Giaccone, G., 2010. Targeting the immune system in non-small-cell lung cancer: bridging the gap between promising concept and therapeutic reality. *Clinical Lung Cancer*, 11 (4), 228-237.
- Kerst, G., *et al.*, 2008. WT1 protein expression in childhood acute leukemia. *American Journal of Hematology*, 83 (5), 382-386.
- Kessler, J., *et al.*, 2006. BCR-ABL fusion regions as a source of multiple leukemia-specific CD8 T-cell epitopes. *Leukemia*, 20 (10), 1738.
- Kessler, J.H., *et al.*, 2001. Efficient identification of novel HLA-A(\*)0201-presented cytotoxic T lymphocyte epitopes in the widely expressed tumor antigen PRAME by proteasome-mediated digestion analysis. *The Journal of Experimental Medicine*, 193 (1), 73-88.
- Kim, G., *et al.*, 2007. A novel multiparametric flow cytometry-based cytotoxicity assay simultaneously immunophenotypes effector cells: comparisons to a 4 h 51Cr-release assay. *Journal of Immunological Methods*, 325 (1-2), 51-66.
- Kim, R., Emi, M. and Tanabe, K., 2007. Cancer immunoediting from immune surveillance to immune escape. *Immunology*, 121 (1), 1-14.
- Kim, T.K. and Eberwine, J.H., 2010. Mammalian cell transfection: the present and the future. *Analytical and Bioanalytical Chemistry*, 397 (8), 3173-3178.
- Kim, H.P., Imbert, J. and Leonard, W.J., 2006. Both integrated and differential regulation of components of the IL-2/IL-2 receptor system. *Cytokine & Growth Factor Reviews*, 17 (5), 349-366.
- Kipreos, E.T. and Wang, J.Y., 1992. Cell cycle-regulated binding of c-Abl tyrosine kinase to DNA. *Science (New York, N.Y.)*, 256 (5055), 382-385.
- Klattig, J., *et al.*, 2007. WT1-mediated gene regulation in early urogenital ridge development. *Sexual Development: Genetics, Molecular Biology, Evolution, Endocrinology, Embryology, and Pathology of Sex Determination and Differentiation*, 1 (4), 238-254.
- Kloetzel, P. and Ossendorp, F., 2004. Proteasome and peptidase function in MHC-class-I-mediated antigen presentation. *Current Opinion in Immunology*, 16 (1), 76-81.
- Knights, A.J., *et al.*, 2006. A novel MHC-associated proteinase 3 peptide isolated from primary chronic myeloid leukaemia cells further supports the significance of this antigen for the immunotherapy of myeloid leukaemias. *Leukemia*, 20 (6), 1067-1072.
- Kochan, G., *et al.*, 2013. Role of non-classical MHC class I molecules in cancer immunosuppression. *Oncoimmunology*, 2 (11), e26491.
- Kochenderfer, J.N., *et al.*, 2012a. B-cell depletion and remissions of malignancy along with cytokine-associated toxicity in a clinical trial of anti-CD19 chimeric-antigen-receptor-transduced T cells. *Blood*, 119 (12), 2709-2720.

- Kochenderfer, J.N., *et al.*, 2010. Eradication of B-lineage cells and regression of lymphoma in a patient treated with autologous T cells genetically engineered to recognize CD19. *Blood*, 116 (20), 4099-4102.
- Kondo, M., *et al.*, 2003. Biology of hematopoietic stem cells and progenitors: implications for clinical application. *Annual Review of Immunology*, 21 (1), 759-806.
- Kowolik, C.M., *et al.*, 2006. CD28 costimulation provided through a CD19-specific chimeric antigen receptor enhances in vivo persistence and antitumor efficacy of adoptively transferred T cells. *Cancer Research*, 66 (22), 10995-11004.
- Kreuzer, K.A., *et al.*, 2001. Fluorescent 5'-exonuclease assay for the absolute quantification of Wilms' tumour gene (WT1) mRNA: implications for monitoring human leukaemias. *British Journal of Haematology*, 114 (2), 313.
- Kroger, C.J. and Alexander-Miller, M.A., 2007. Dose-dependent modulation of CD8 and functional avidity as a result of peptide encounter. *Immunology*, 122 (2), 167-178.
- Krummel, M.F. and Allison, J.P., 1995. CD28 and CTLA-4 have opposing effects on the response of T cells to stimulation. *The Journal of Experimental Medicine*, 182 (2), 459-465.
- Kumar, T.R., *et al.*, 2009. Transgenic mouse technology: principles and methods. *In: Transgenic mouse technology: principles and methods. Molecular Endocrinology*. Springer, 2009, pp. 335-362.
- Lai, Y., *et al.*, 2017. Current status and perspectives of patient-derived xenograft models in cancer research. *Journal of Hematology & Oncology*, 10 (1), 106.
- Lamprecht Tratar, U., Horvat, S. and Cemazar, M., 2018. Transgenic Mouse Models in Cancer Research. *Frontiers in Oncology*, 8, 268.
- Lane, P., 1995. A molecular basis for T-dependent B cell activation. *Behring Institute Mitteilungen*, (96) (96), 7-12.
- Laneville, P., 1995. Abl tyrosine protein kinase. *In: Seminars in immunology*, Elsevier, pp. 255-266.
- Lanier, L.L., *et al.*, 1986. The relationship of CD16 (Leu-11) and Leu-19 (NKH-1) antigen expression on human peripheral blood NK cells and cytotoxic T lymphocytes. *Journal of Immunology (Baltimore, Md.: 1950)*, 136 (12), 4480-4486.
- Le Bouteiller, P. and Lenfant, F., 1996. Antigen-presenting function (s) of the non-classical HLA-E, -F and -G class I molecules: the beginning of a story. *Research in Immunology*, 147 (5), 301-313.
- Lee, K.H., *et al.*, 1999. Increased vaccine-specific T cell frequency after peptide-based vaccination correlates with increased susceptibility to in vitro stimulation but does not lead to tumor regression. *Journal of Immunology (Baltimore, Md.: 1950)*, 163 (11), 6292-6300.
- Legros, L., *et al.*, 2004. Imatinib mesylate (STI571) decreases the vascular endothelial growth factor plasma concentration in patients with chronic myeloid leukemia. *Blood*, 104 (2), 495-501.

- Lemoli, R.M., *et al.*, 2009. Molecular and functional analysis of the stem cell compartment of chronic myelogenous leukemia reveals the presence of a CD34<sup>-</sup> cell population with intrinsic resistance to imatinib. *Blood*, 114 (25), 5191-5200.
- Lenschow, D.J., Walunas, T.L. and Bluestone, J.A., 1996. CD28/B7 system of T cell costimulation. *Annual Review of Immunology*, 14 (1), 233-258.
- Lesokhin, A.M., *et al.*, 2015. On being less tolerant: enhanced cancer immunosurveillance enabled by targeting checkpoints and agonists of T cell activation. *Science Translational Medicine*, 7 (280), 280sr1.
- Lesterhuis, W.J., *et al.*, 2011. Route of administration modulates the induction of dendritic cell vaccine-induced antigen-specific T cells in advanced melanoma patients. *Clinical Cancer Research: An Official Journal of the American Association for Cancer Research*, 17 (17), 5725-5735.
- Li, H., *et al.*, 2009. Cancer-expanded myeloid-derived suppressor cells induce anergy of NK cells through membrane-bound TGF-beta 1. *Journal of Immunology (Baltimore, Md.: 1950)*, 182 (1), 240-249.
- Li, L. and Petrovsky, N., 2017. Molecular Adjuvants for DNA Vaccines. *Current Issues in Molecular Biology*, 22, 17-40.
- Li, Y., *et al.*, 2011. Restricted TRBV repertoire in CD4<sup>+</sup> and CD8<sup>+</sup> T-cell subsets from CML patients. *Hematology (Amsterdam, Netherlands)*, 16 (1), 43-49.
- Li, Y., Lin, C. and Schmidt, C.A., 2012. New insights into antigen specific immunotherapy for chronic myeloid leukemia. *Cancer Cell International*, 12 (1), 52-2867-12-52.
- Lim, J.H., *et al.*, 2005. Activation of human cancer/testis antigen gene, XAGE-1, in tumor cells is correlated with CpG island hypomethylation. *International Journal of Cancer*, 116 (2), 200-206.
- Lim, S., *et al.*, 1999. Expression of testicular genes in haematological malignancies. *British Journal of Cancer*, 81 (7), 1162.
- Lim, S.H., *et al.*, 2001. Sperm protein 17 is a novel cancer-testis antigen in multiple myeloma. *Blood*, 97 (5), 1508-1510.
- Lin, J., *et al.*, 2014. DDX43 promoter is frequently hypomethylated and may predict a favorable outcome in acute myeloid leukemia. *Leukemia Research*, 38 (5), 601-607.
- Lin, J., *et al.*, 2018. Arresting of miR-186 and releasing of H19 by DDX43 facilitate tumorigenesis and CML progression. *Oncogene*, 37 (18), 2432-2443.
- Linder, P. and Jankowsky, E., 2011. From unwinding to clamping - the DEAD box RNA helicase family. *Nature Reviews.Molecular Cell Biology*, 12 (8), 505-516.
- Ljunggren, H.G. and Karre, K., 1990. In search of the 'missing self': MHC molecules and NK cell recognition. *Immunology Today*, 11 (7), 237-244.
- Lob, S., *et al.*, 2008. Levo- but not dextro-1-methyl tryptophan abrogates the IDO activity of human dendritic cells. *Blood*, 111 (4), 2152-2154.

- Lohman, T.M. and Bjornson, K.P., 1996. Mechanisms of helicase-catalyzed DNA unwinding. *Annual Review of Biochemistry*, 65, 169-214.
- Long, G.V., et al., 2018. *Epacadostat (E) Plus Pembrolizumab (P) Versus Pembrolizumab Alone in Patients (Pts) with Unresectable Or Metastatic Melanoma: Results of the Phase 3 ECHO-301/KEYNOTE-252 Study*.
- Lu, C., et al., 2017. A novel multi-epitope vaccine from MMSA-1 and DKK1 for multiple myeloma immunotherapy. *British Journal of Haematology*, 178 (3), 413-426.
- Mach, B., et al., 1996. Regulation of MHC class II genes: lessons from a disease. *Annual Review of Immunology*, 14 (1), 301-331.
- Maher, J., et al., 2002. Human T-lymphocyte cytotoxicity and proliferation directed by a single chimeric TCRzeta /CD28 receptor. *Nature Biotechnology*, 20 (1), 70-75.
- Mahmoud, A.M., 2018. Cancer testis antigens as immunogenic and oncogenic targets in breast cancer. *Immunotherapy*, 10 (9), 769-778.
- Mahon, F., et al., 2010. Discontinuation of imatinib in patients with chronic myeloid leukaemia who have maintained complete molecular remission for at least 2 years: the prospective, multicentre Stop Imatinib (STIM) trial. *The Lancet Oncology*, 11 (11), 1029-1035.
- Maker, A.V., Attia, P. and Rosenberg, S.A., 2005. Analysis of the cellular mechanism of antitumor responses and autoimmunity in patients treated with CTLA-4 blockade. *Journal of Immunology (Baltimore, Md.: 1950)*, 175 (11), 7746-7754.
- Malyguine, A.M., et al., 2012. ELISPOT assay for monitoring cytotoxic T lymphocytes (CTL) activity in cancer vaccine clinical trials. *Cells*, 1 (2), 111-126.
- Mamsen, L.S., et al., 2012. The migration and loss of human primordial germ stem cells from the hind gut epithelium towards the gonadal ridge. *The International Journal of Developmental Biology*, 56 (10-12), 771-778.
- Manz, M.G., et al., 2001. Dendritic cell potentials of early lymphoid and myeloid progenitors. *Blood*, 97 (11), 3333-3341.
- Marmont, A.M., et al., 1991. T-cell depletion of HLA-identical transplants in leukemia. *Blood*, 78 (8), 2120-2130.
- Martelange, V., et al., 2000. Identification on a human sarcoma of two new genes with tumor-specific expression. *Cancer Research*, 60 (14), 3848-3855.
- Mathieu, M.G., et al., 2010. HAGE, a cancer/testis antigen expressed at the protein level in a variety of cancers. *Cancer Immunity*, 10, 2.
- Maude, S.L., et al., 2014. Chimeric antigen receptor T cells for sustained remissions in leukemia. *The New England Journal of Medicine*, 371 (16), 1507-1517.
- Maupetit-Mehouas, S., et al., 2018. DNA methylation profiling reveals a pathological signature that contributes to transcriptional defects of CD 34 CD 15– cells in early chronic-phase chronic myeloid leukemia. *Molecular Oncology*, 12 (6), 814-829.
- Maus, M.V., et al., 2014. Antibody-modified T cells: CARs take the front seat for hematologic malignancies. *Blood*, 123 (17), 2625-2635.

- Mbongue, J.C., *et al.*, 2015. Induction of indoleamine 2, 3-dioxygenase in human dendritic cells by a cholera toxin B subunit—Proinsulin vaccine. *PLoS One*, 10 (2), e0118562.
- McCarty, G. and Loeb, D.M., 2015. Hypoxia-sensitive epigenetic regulation of an antisense-oriented lncRNA controls WT1 expression in myeloid leukemia cells. *PLoS One*, 10 (3), e0119837.
- McCarty, G., Awad, O. and Loeb, D.M., 2011. WT1 protein directly regulates expression of vascular endothelial growth factor and is a mediator of tumor response to hypoxia. *The Journal of Biological Chemistry*, 286 (51), 43634-43643.
- McKee, M.D., Roszkowski, J.J. and Nishimura, M.I., 2005. T cell avidity and tumor recognition: implications and therapeutic strategies. *Journal of Translational Medicine*, 3 (1), 35.
- McWhirter, J.R. and Wang, J., 1993. An actin-binding function contributes to transformation by the Bcr-Abl oncoprotein of Philadelphia chromosome-positive human leukemias. *The EMBO Journal*, 12 (4), 1533-1546.
- McWhirter, J.R., Galasso, D.L. and Wang, J.Y., 1993. A coiled-coil oligomerization domain of Bcr is essential for the transforming function of Bcr-Abl oncoproteins. *Molecular and Cellular Biology*, 13 (12), 7587-7595.
- Mehier-Humbert, S. and Guy, R.H., 2005. Physical methods for gene transfer: improving the kinetics of gene delivery into cells. *Advanced Drug Delivery Reviews*, 57 (5), 733-753.
- Meklat, F., *et al.*, 2007. Cancer-testis antigens in haematological malignancies. *British Journal of Haematology*, 136 (6), 769-776.
- Meklat, F., *et al.*, 2009. Identification of protamine 1 as a novel cancer-testis antigen in early chronic lymphocytic leukaemia. *British Journal of Haematology*, 144 (5), 660-666.
- Melief, C.J. and Van Der Burg, Sjoerd H, 2008. Immunotherapy of established (pre) malignant disease by synthetic long peptide vaccines. *Nature Reviews Cancer*, 8 (5), 351.
- Mellqvist, U.H., *et al.*, 2000. Natural killer cell dysfunction and apoptosis induced by chronic myelogenous leukemia cells: role of reactive oxygen species and regulation by histamine. *Blood*, 96 (5), 1961-1968.
- Menard, C., *et al.*, 2009. Natural killer cell IFN-gamma levels predict long-term survival with imatinib mesylate therapy in gastrointestinal stromal tumor-bearing patients. *Cancer Research*, 69 (8), 3563-3569.
- Mendoza-Salas, I., *et al.*, 2016. Frequency of cancer testis antigens in chronic myeloid leukemia. *Revista Médica Del Hospital General De México*, 79 (2), 46-54.
- Menssen, H.D., *et al.*, 1995. Presence of Wilms' tumor gene (wt1) transcripts and the WT1 nuclear protein in the majority of human acute leukemias. *Leukemia*, 9 (6), 1060-1067.
- Metz, R., *et al.*, 2007. Novel tryptophan catabolic enzyme IDO2 is the preferred biochemical target of the antitumor indoleamine 2,3-dioxygenase inhibitory compound D-1-methyl-tryptophan. *Cancer Research*, 67 (15), 7082-7087.

- Miao, R., *et al.*, 2016. Utility of the dual-specificity protein kinase TTK as a therapeutic target for intrahepatic spread of liver cancer. *Scientific Reports*, 6, 33121.
- Milne, K., *et al.*, 2008. Tumor-infiltrating T cells correlate with NY-ESO-1-specific autoantibodies in ovarian cancer. *PLoS One*, 3 (10), e3409.
- Mocellin, S., *et al.*, 2004. Part II: Vaccines for haematological malignant disorders. *The Lancet.Oncology*, 5 (12), 727-737.
- Mohty, M., *et al.*, 2002. Low blood dendritic cells in chronic myeloid leukaemia patients correlates with loss of CD34+/CD38- primitive haematopoietic progenitors. *British Journal of Haematology*, 119 (1), 115-118.
- Mohty, M., *et al.*, 2001. Circulating blood dendritic cells from myeloid leukemia patients display quantitative and cytogenetic abnormalities as well as functional impairment. *Blood*, 98 (13), 3750-3756.
- Mojic, M., Takeda, K. and Hayakawa, Y., 2017. The dark side of IFN- $\gamma$ : its role in promoting cancer immunoevasion. *International Journal of Molecular Sciences*, 19 (1), 89.
- Molldrem, J.J., *et al.*, 1997. Cytotoxic T lymphocytes specific for a nonpolymorphic proteinase 3 peptide preferentially inhibit chronic myeloid leukemia colony-forming units. *Blood*, 90 (7), 2529-2534.
- Molldrem, J.J., *et al.*, 2000. Evidence that specific T lymphocytes may participate in the elimination of chronic myelogenous leukemia. *Nature Medicine*, 6 (9), 1018-1023.
- Mollenhauer, H.H., Morr , D.J. and Rowe, L.D., 1990. Alteration of intracellular traffic by monensin; mechanism, specificity and relationship to toxicity. *Biochimica Et Biophysica Acta (BBA)-Reviews on Biomembranes*, 1031 (2), 225-246.
- Moretta, A., *et al.*, 2001. Activating receptors and coreceptors involved in human natural killer cell-mediated cytotoxicity. *Annual Review of Immunology*, 19 (1), 197-223.
- Morgan G. Mathieu, 2007. HAGE, a novel cancer/testis antigen with strong potential as a target for immunotherapy against cancers [online]. Ph.D. thesis, Nottingham Trent University. Available at: <http://irep.ntu.ac.uk/id/eprint/33>, [Accessed 26 July 2015].
- Morton, C.L. and Houghton, P.J., 2007. Establishment of human tumor xenografts in immunodeficient mice. *Nature Protocols*, 2 (2), 247.
- Mosely, S.I., *et al.*, 2017. Rational Selection of Syngeneic Preclinical Tumor Models for Immunotherapeutic Drug Discovery. *Cancer Immunology Research*, 5 (1), 29-41.
- Mosmann, T.R., *et al.*, 2009. T helper cytokine patterns: defined subsets, random expression, and external modulation. *Immunologic Research*, 45 (2-3), 173.
- Mothe, B., *et al.*, 2012. CTL responses of high functional avidity and broad variant cross-reactivity are associated with HIV control. *PLoS One*, 7 (1), e29717.
- Motz, G.T., *et al.*, 2014. Tumor endothelium FasL establishes a selective immune barrier promoting tolerance in tumors. *Nature Medicine*, 20 (6), 607.

- Mouse Genome Sequencing Consortium, *et al.*, 2002. Initial sequencing and comparative analysis of the mouse genome. *Nature*, 420 (6915), 520-562.
- Mullbacher, A., *et al.*, 2002. Antigen-dependent release of IFN-gamma by cytotoxic T cells up-regulates Fas on target cells and facilitates exocytosis-independent specific target cell lysis. *Journal of Immunology (Baltimore, Md.: 1950)*, 169 (1), 145-150.
- Muller, A.J., *et al.*, 1991. BCR first exon sequences specifically activate the BCR/ABL tyrosine kinase oncogene of Philadelphia chromosome-positive human leukemias. *Molecular and Cellular Biology*, 11 (4), 1785-1792.
- Mumprecht, S., *et al.*, 2009a. Programmed death 1 signaling on chronic myeloid leukemia-specific T cells results in T-cell exhaustion and disease progression. *Blood*, 114 (8), 1528-1536.
- Mumprecht, S., *et al.*, 2009b. Programmed death 1 signaling on chronic myeloid leukemia-specific T cells results in T-cell exhaustion and disease progression. *Blood*, 114 (8), 1528-1536.
- Munn, D.H. and Mellor, A.L., 2016. IDO in the tumor microenvironment: inflammation, counter-regulation, and tolerance. *Trends in Immunology*, 37 (3), 193-207.
- Munn, D.H., *et al.*, 2005a. GCN2 kinase in T cells mediates proliferative arrest and anergy induction in response to indoleamine 2, 3-dioxygenase. *Immunity*, 22 (5), 633-642.
- Nagata, S. and Golstein, P., 1995. The Fas death factor. *Science (New York, N.Y.)*, 267 (5203), 1449-1456.
- Nandi, A., *et al.*, 2004. Protein expression of PDZ-binding kinase is up-regulated in hematologic malignancies and strongly down-regulated during terminal differentiation of HL-60 leukemic cells. *Blood Cells, Molecules, and Diseases*, 32 (1), 240-245.
- Nanni, P., *et al.*, 1983. IMPAIRED H-2 EXPRESSION IN B 16 MELANOMA VARIANTS. *International Journal of Immunogenetics*, 10 (5), 361-370.
- Napier, R.J., *et al.*, 2015. Low doses of imatinib induce myelopoiesis and enhance host anti-microbial immunity. *PLoS Pathogens*, 11 (3), e1004770.
- Narita, M., *et al.*, 2010. WT1 peptide vaccination in combination with imatinib therapy for a patient with CML in the chronic phase. *International Journal of Medical Sciences*, 7 (2), 72-81.
- Neefjes, J.J. and Momburg, F., 1993. Cell biology of antigen presentation. *Current Opinion in Immunology*, 5 (1), 27-34.
- Niemeyer, P., *et al.*, 2003. Expression of serologically identified tumor antigens in acute leukemias. *Leukemia Research*, 27 (7), 655-660.
- Nierkens, S., *et al.*, 2013. Antigen cross-presentation by dendritic cell subsets: one general or all sergeants? *Trends in Immunology*, 34 (8), 361-370.
- Nievergall, E., *et al.*, 2014. Monoclonal antibody targeting of IL-3 receptor alpha with CSL362 effectively depletes CML progenitor and stem cells. *Blood*, 123 (8), 1218-1228.

NIH. U.S. National library of medicine. The National Center for Biotechnology Information (NCBI). Align Sequences Protein BLAST, available at: [https://blast.ncbi.nlm.nih.gov/Blast.cgi?PROGRAM=blastp&PAGE\\_TYPE=BlastSearch&BLAST\\_SPEC=blast2seq&LINK\\_LOC=blasttab](https://blast.ncbi.nlm.nih.gov/Blast.cgi?PROGRAM=blastp&PAGE_TYPE=BlastSearch&BLAST_SPEC=blast2seq&LINK_LOC=blasttab). [Accessed 6 May 2019].

Nolz, J.C., Starbeck-Miller, G.R. and Harty, J.T., 2011. Naive, effector and memory CD8 T-cell trafficking: parallels and distinctions. *Immunotherapy*, 3 (10), 1223-1233.

Nomenclature, 2019. HLA Alleles Numbers. Available at: <http://hla.alleles.org/nomenclature/stats.html>, [Accessed 2 January 2019].

Nowell, P.C. and Hungerford, D.A., 1960. Chromosome studies on normal and leukemic human leukocytes. *Journal of the National Cancer Institute*, 25 (1), 85-109.

Oberlies, J., *et al.*, 2009. Regulation of NK cell function by human granulocyte arginase. *Journal of Immunology (Baltimore, Md.: 1950)*, 182 (9), 5259-5267.

Oehen, S. and Brduscha-Riem, K., 1998. Differentiation of naive CTL to effector and memory CTL: correlation of effector function with phenotype and cell division. *Journal of Immunology (Baltimore, Md.: 1950)*, 161 (10), 5338-5346.

Oh, S., *et al.*, 2003. Selective induction of high avidity CTL by altering the balance of signals from APC. *Journal of Immunology (Baltimore, Md.: 1950)*, 170 (5), 2523-2530.

O'hare, T., *et al.*, 2012. Pushing the limits of targeted therapy in chronic myeloid leukaemia. *Nature Reviews Cancer*, 12 (8), 513.

Ohbo, K., *et al.*, 1996. Modulation of hematopoiesis in mice with a truncated mutant of the interleukin-2 receptor gamma chain. *Blood*, 87 (3), 956-967.

Oji, Y., *et al.*, 2010. WT1 peptide vaccine induces reduction in minimal residual disease in an Imatinib-treated CML patient. *European Journal of Haematology*, 85 (4), 358-360.

Oji, Y., *et al.*, 2009. WT1 IgG antibody for early detection of nonsmall cell lung cancer and as its prognostic factor. *International Journal of Cancer*, 125 (2), 381-387.

Oka, Y., *et al.*, 2006a. Development of WT1 peptide cancer vaccine against hematopoietic malignancies and solid cancers. *Current Medicinal Chemistry*, 13 (20), 2345-2352.

Oka, Y., *et al.*, 2008. WT1 peptide vaccine for the treatment of cancer. *Current Opinion in Immunology*, 20 (2), 211-220.

Oka, Y., *et al.*, 2004. Induction of WT1 (Wilms' tumor gene)-specific cytotoxic T lymphocytes by WT1 peptide vaccine and the resultant cancer regression. *Proceedings of the National Academy of Sciences of the United States of America*, 101 (38), 13885-13890.

Okazaki, T. and Honjo, T., 2007. PD-1 and PD-1 ligands: from discovery to clinical application. *International Immunology*, 19 (7), 813-824.

Oriss, T.B., *et al.*, 2014. Dendritic cell c-kit signaling and adaptive immunity: implications for the upper airways. *Current Opinion in Allergy and Clinical Immunology*, 14 (1), 7-12.

- Orsini, E., *et al.*, 2006. Circulating myeloid dendritic cell directly isolated from patients with chronic myelogenous leukemia are functional and carry the bcr-abl translocation. *Leukemia Research*, 30 (7), 785-794.
- Ostrand-Rosenberg, S. and Sinha, P., 2009. Myeloid-derived suppressor cells: linking inflammation and cancer. *Journal of Immunology (Baltimore, Md.: 1950)*, 182 (8), 4499-4506.
- Otahalova, E., *et al.*, 2009. WT1 expression in peripheral leukocytes of patients with chronic myeloid leukemia serves for the prediction of Imatinib resistance. *Neoplasma*, 56 (5), 393-397.
- Ottmann, O.G., *et al.*, 2002. A phase 2 study of imatinib in patients with relapsed or refractory Philadelphia chromosome-positive acute lymphoid leukemias. *Blood*, 100 (6), 1965-1971.
- Overwijk, W.W. and Restifo, N.P., 2000. B16 as a mouse model for human melanoma. *Current Protocols in Immunology*, 39 (1), 20.1. 1-20.1. 29.
- Özlü, F., *et al.*, 2017. New biomarkers for antenatal infection: MICA and MICB gene expression in preterm babies. *The Journal of Maternal-Fetal & Neonatal Medicine*, , 1-5.
- Padua, R.A., *et al.*, 2003. PML-RARA-targeted DNA vaccine induces protective immunity in a mouse model of leukemia. *Nature Medicine*, 9 (11), 1413-1417.
- Paez-Ribes, M., *et al.*, 2016. Development of patient derived xenograft models of overt spontaneous breast cancer metastasis: a cautionary note. *PloS One*, 11 (6), e0158034.
- Pajot, A., *et al.*, 2004. A mouse model of human adaptive immune functions: HLA-A2.1/HLA-DR1-transgenic H-2 class I/class II-knockout mice. *European Journal of Immunology*, 34 (11), 3060-3069.
- Pajot, A., *et al.*, 2004. Comparison of HLA-DR1-restricted T cell response induced in HLA-DR1 transgenic mice deficient for murine MHC class II and HLA-DR1 transgenic mice expressing endogenous murine MHC class II molecules. *International Immunology*, 16 (9), 1275-1282.
- Pane, F., *et al.*, 2002. BCR/ABL genes and leukemic phenotype: from molecular mechanisms to clinical correlations. *Oncogene*, 21 (56), 8652-8667.
- Parmiani, G., *et al.*, 2007. Unique human tumor antigens: immunobiology and use in clinical trials. *Journal of Immunology (Baltimore, Md.: 1950)*, 178 (4), 1975-1979.
- Patel, H., *et al.*, 2008. Subcellular distribution of p210 BCR-ABL in CML cell lines and primary CD34 CML cells. *Leukemia*, 22 (3), 559-571.
- Pascolo, S., *et al.*, 1997. HLA-A2.1-restricted education and cytolytic activity of CD8(+) T lymphocytes from beta2 microglobulin (beta2m) HLA-A2.1 monochain transgenic H-2Db beta2m double knockout mice. *The Journal of Experimental Medicine*, 185 (12), 2043-2051.
- Pascolo, S., *et al.*, 1997. HLA-A2.1-restricted Education and Cytolytic Activity of CD8+ T Lymphocytes from  $\beta$ 2 Microglobulin ( $\beta$ 2m) HLA-A2.1 Monochain Transgenic H-2D<sup>b</sup>  $\beta$ 2m Double Knockout Mice.

- Patel, P.M., *et al.*, 2018. Targeting gp100 and TRP-2 with a DNA vaccine: Incorporating T cell epitopes with a human IgG1 antibody induces potent T cell responses that are associated with favourable clinical outcome in a phase I/II trial. *Oncoimmunology*, 7 (6), e1433516.
- Pauken, K.E. and Wherry, E.J., 2015. Overcoming T cell exhaustion in infection and cancer. *Trends in Immunology*, 36 (4), 265-276.
- Perez-Garcia, A., *et al.*, 2009. CTLA-4 genotype and relapse incidence in patients with acute myeloid leukemia in first complete remission after induction chemotherapy. *Leukemia*, 23 (3), 486-491.
- Perrotti, D., *et al.*, 2017. Cellular and Molecular Networks in Chronic Myeloid Leukemia: The Leukemic Stem, Progenitor and Stromal Cell Interplay. *Current Drug Targets*, 18 (4), 377-388.
- Petrovas, C., *et al.*, 2006. PD-1 is a regulator of virus-specific CD8+ T cell survival in HIV infection. *The Journal of Experimental Medicine*, 203 (10), 2281-2292.
- Phillips, R., Jewett, M. and Gallie, B., 1989. Growth of human tumors in immune-deficient scid mice and nude mice. *In: Growth of human tumors in immune-deficient scid mice and nude mice. The Scid Mouse*. Springer, 1989, pp. 259-263.
- Pianko, M.J., *et al.*, 2017. Immune checkpoint blockade for hematologic malignancies: a review. *Stem Cell Investigation*, 4, 32.
- Pierson, B.A. and Miller, J.S., 1996. CD56+bright and CD56+dim natural killer cells in patients with chronic myelogenous leukemia progressively decrease in number, respond less to stimuli that recruit clonogenic natural killer cells, and exhibit decreased proliferation on a per cell basis. *Blood*, 88 (6), 2279-2287.
- Pinilla-Ibarz, J., *et al.*, 2006a. Improved human T-cell responses against synthetic HLA-0201 analog peptides derived from the WT1 oncoprotein. *Leukemia*, 20 (11), 2025.
- Pinilla-Lbarz, J., Shah, B. and Dubovsky, J.A., 2009. The biological basis for immunotherapy in patients with chronic myelogenous leukemia. *Cancer Control: Journal of the Moffitt Cancer Center*, 16 (2), 141.
- Pistoia, V., *et al.*, 2007. Soluble HLA-G: Are they clinically relevant? *In: Seminars in cancer biology*, Elsevier, pp. 469-479.
- Platten, M., *et al.*, 2015. Cancer immunotherapy by targeting IDO1/TDO and their downstream effectors. *Frontiers in Immunology*, 5, 673.
- Pogribny, I.P. and Beland, F.A., 2009. DNA hypomethylation in the origin and pathogenesis of human diseases. *Cellular and Molecular Life Sciences*, 66 (14), 2249-2261.
- Poltorak, M.P. and Schraml, B.U., 2015. Fate mapping of dendritic cells. *Frontiers in Immunology*, 6, 199.
- Ponta, H., Sherman, L. and Herrlich, P.A., 2003. CD44: from adhesion molecules to signalling regulators. *Nature Reviews Molecular Cell Biology*, 4 (1), 33.

- Porgador, A., *et al.*, 1998. Predominant role for directly transfected dendritic cells in antigen presentation to CD8+ T cells after gene gun immunization. *The Journal of Experimental Medicine*, 188 (6), 1075-1082.
- Porter, D.L., *et al.*, 2011. Chimeric antigen receptor-modified T cells in chronic lymphoid leukemia. *The New England Journal of Medicine*, 365 (8), 725-733.
- Porter, D. and Levine, J.E., 2006. *Graft-Versus-Host Disease and Graft-Versus-Leukemia After Donor Leukocyte Infusion*.
- Posthuma, E.F., *et al.*, 2004. Proteosomal degradation of BCR/ABL protein can generate an HLA-A\*0301-restricted peptide, but high-avidity T cells recognizing this leukemia-specific antigen were not demonstrated. *Haematologica*, 89 (9), 1062-1071.
- Powell, D.J., Jr and Rosenberg, S.A., 2004. Phenotypic and functional maturation of tumor antigen-reactive CD8+ T lymphocytes in patients undergoing multiple course peptide vaccination. *Journal of Immunotherapy (Hagerstown, Md.: 1997)*, 27 (1), 36-47.
- Prendergast, G.C., *et al.*, 2014. IDO2 in immunomodulation and autoimmune disease. *Frontiers in Immunology*, 5, 585.
- Prosper, F. and Verfaillie, C.M., 2001. Regulation of hematopoiesis through adhesion receptors. *Journal of Leukocyte Biology*, 69 (3), 307-316.
- Puaux, A.L., *et al.*, 2011. A comparison of imaging techniques to monitor tumor growth and cancer progression in living animals. *International Journal of Molecular Imaging*, 2011, 321538.
- Pudney, V.A., *et al.*, 2010. DNA vaccination with T-cell epitopes encoded within Ab molecules induces high-avidity anti-tumor CD8 T cells. *European Journal of Immunology*, 40 (3), 899-910.
- Punt, J., 2013. *Cancer Immunotherapy: Chapter 4. Adaptive Immunity: T Cells and Cytokines*. Elsevier Inc. Chapters.
- Puré, E. and Cuff, C.A., 2001. A crucial role for CD44 in inflammation. *Trends in Molecular Medicine*, 7 (5), 213-221.
- Pyle, A.M., 2008. Translocation and unwinding mechanisms of RNA and DNA helicases. *Annual Review of Biophysics*, 37, 317-336.
- Qi, X.W., *et al.*, 2015. Wilms' tumor 1 (WT1) expression and prognosis in solid cancer patients: a systematic review and meta-analysis. *Scientific Reports*, 5, 8924.
- Qian, F., *et al.*, 2004. Th1/Th2 CD4+ T cell responses against NY-ESO-1 in HLA-DPB1\*0401/0402 patients with epithelial ovarian cancer. *Cancer Immunity*, 4, 12.
- Quatromoni, J.G. and Eruslanov, E., 2012. Tumor-associated macrophages: function, phenotype, and link to prognosis in human lung cancer. *American Journal of Translational Research*, 4 (4), 376-389.
- Quintarelli, C., *et al.*, 2011. High-avidity cytotoxic T lymphocytes specific for a new PRAME-derived peptide can target leukemic and leukemic-precursor cells. *Blood*, 117 (12), 3353-3362.

- Raska, M. and Turanek, J., 2015. DNA vaccines for the induction of immune responses in mucosal tissues. *In: DNA vaccines for the induction of immune responses in mucosal tissues. Mucosal Immunology*. Elsevier, 2015, pp. 1307-1335.
- Ratner, A. and Clark, W.R., 1993. Role of TNF-alpha in CD8+ cytotoxic T lymphocyte-mediated lysis. *Journal of Immunology (Baltimore, Md.: 1950)*, 150 (10), 4303-4314.
- Recillas-Targa, F., 2006. Multiple strategies for gene transfer, expression, knockdown, and chromatin influence in mammalian cell lines and transgenic animals. *Molecular Biotechnology*, 34 (3), 337-354.
- Reith, W. and Mach, B., 2001. The bare lymphocyte syndrome and the regulation of MHC expression. *Annual Review of Immunology*, 19 (1), 331-373.
- Reits, E.A., *et al.*, 2000. The major substrates for TAP *in vivo* are derived from newly synthesized proteins. *Nature*, 404 (6779), 774.
- Rezvani, K., *et al.*, 2007. Graft-versus-leukemia effects associated with detectable Wilms tumor-1 specific T lymphocytes after allogeneic stem-cell transplantation for acute lymphoblastic leukemia. *Blood*, 110 (6), 1924-1932.
- Ribas, A., *et al.*, 2003. Current developments in cancer vaccines and cellular immunotherapy. *Journal of Clinical Oncology*, 21 (12), 2415-2432.
- Rice, J., Ottensmeier, C.H. and Stevenson, F.K., 2008. DNA vaccines: precision tools for activating effective immunity against cancer. *Nature Reviews.Cancer*, 8 (2), 108-120.
- Riether, C., Schürch, C. and Ochsenbein, A., 2015. Regulation of hematopoietic and leukemic stem cells by the immune system. *Cell Death and Differentiation*, 22 (2), 187.
- Riva, G., *et al.*, 2010. Emergence of BCR-ABL-specific cytotoxic T cells in the bone marrow of patients with Ph+ acute lymphoblastic leukemia during long-term imatinib mesylate treatment. *Blood*, 115 (8), 1512-1518.
- Riva, G., *et al.*, 2014. Long-term molecular remission with persistence of BCR-ABL1-specific cytotoxic T cells following imatinib withdrawal in an elderly patient with Philadelphia-positive ALL. *British Journal of Haematology*, 164 (2), 299-302.
- Rodgers, J.R. and Cook, R.G., 2005. MHC class Ib molecules bridge innate and acquired immunity. *Nature Reviews Immunology*, 5 (6), 459.
- Rodriguez, P.C., *et al.*, 2004. Arginase I production in the tumor microenvironment by mature myeloid cells inhibits T-cell receptor expression and antigen-specific T-cell responses. *Cancer Research*, 64 (16), 5839-5849.
- Roemer, M.G., *et al.*, 2016. PD-L1 and PD-L2 Genetic Alterations Define Classical Hodgkin Lymphoma and Predict Outcome. *Journal of Clinical Oncology : Official Journal of the American Society of Clinical Oncology*, 34 (23), 2690-2697.
- Rogel, A., *et al.*, 1985. p53 cellular tumor antigen: analysis of mRNA levels in normal adult tissues, embryos, and tumors. *Molecular and Cellular Biology*, 5 (10), 2851-2855.
- Romani, N., *et al.*, 1994. Proliferating dendritic cell progenitors in human blood. *The Journal of Experimental Medicine*, 180 (1), 83-93.

- Rooney, M.S., *et al.*, 2015. Molecular and genetic properties of tumors associated with local immune cytolytic activity. *Cell*, 160 (1-2), 48-61.
- Rosalia, R.A., *et al.*, 2013. Dendritic cells process synthetic long peptides better than whole protein, improving antigen presentation and T-cell activation. *European Journal of Immunology*, 43 (10), 2554-2565.
- Rosenberg, S.A., 2004. Development of effective immunotherapy for the treatment of patients with cancer. *Journal of the American College of Surgeons*, 198 (5), 685-696.
- Rosenfeld, C., Cheever, M. and Gaiger, A., 2003. WT1 in acute leukemia, chronic myelogenous leukemia and myelodysplastic syndrome: therapeutic potential of WT1 targeted therapies. *Leukemia*, 17 (7), 1301-1312.
- Ross, D.M., *et al.*, 2010. Patients with chronic myeloid leukemia who maintain a complete molecular response after stopping imatinib treatment have evidence of persistent leukemia by DNA PCR. *Leukemia*, 24 (10), 1719-1724.
- Ross, D.M., *et al.*, 2013. Safety and efficacy of imatinib cessation for CML patients with stable undetectable minimal residual disease: results from the TWISTER study. *Blood*, 122 (4), 515-522.
- Ross, D.M. and Hughes, T.P., 2014. How I determine if and when to recommend stopping tyrosine kinase inhibitor treatment for chronic myeloid leukaemia. *British Journal of Haematology*, 166 (1), 3-11.
- Rötzschke, O., *et al.*, 1990. Isolation and analysis of naturally processed viral peptides as recognized by cytotoxic T cells. *Nature*, 348 (6298), 252.
- Rouas-Freiss, N., *et al.*, 2005. HLA-G proteins in cancer: do they provide tumor cells with an escape mechanism? *Cancer Research*, 65 (22), 10139-10144.
- Rudolph, M.G., *et al.*, 2001. The crystal structures of Kbm1 and Kbm8 reveal that subtle changes in the peptide environment impact thermostability and alloreactivity. *Immunity*, 14 (3), 231-242.
- Saadi, M., Karkhah, A. and Nouri, H.R., 2017. Development of a multi-epitope peptide vaccine inducing robust T cell responses against brucellosis using immunoinformatics based approaches. *Infection, Genetics and Evolution : Journal of Molecular Epidemiology and Evolutionary Genetics in Infectious Diseases*, 51, 227-234.
- Saitoh, A., *et al.*, 2011. WT1 peptide vaccination in a CML patient: induction of effective cytotoxic T lymphocytes and significance of peptide administration interval. *Medical Oncology*, 28 (1), 219-230.
- Sakuishi, K., *et al.*, 2010. Targeting Tim-3 and PD-1 pathways to reverse T cell exhaustion and restore anti-tumor immunity. *The Journal of Experimental Medicine*, 207 (10), 2187-2194.
- Sallusto, F., *et al.*, 1999. Two subsets of memory T lymphocytes with distinct homing potentials and effector functions. *Nature*, 401 (6754), 708.
- Sallusto, F. and Lanzavecchia, A., 1994. Efficient presentation of soluble antigen by cultured human dendritic cells is maintained by granulocyte/macrophage colony-stimulating factor plus interleukin 4 and downregulated by tumor necrosis factor alpha. *The Journal of Experimental Medicine*, 179 (4), 1109-1118.

- Sandberg, J.K., *et al.*, 2000. T cell tolerance based on avidity thresholds rather than complete deletion allows maintenance of maximal repertoire diversity. *Journal of Immunology (Baltimore, Md.: 1950)*, 165 (1), 25-33.
- Sang, M., *et al.*, 2011. Melanoma-associated antigen genes—an update. *Cancer Letters*, 302 (2), 85-90.
- Santoni, A., *et al.*, 2007. Natural killer (NK) cells from killers to regulators: distinct features between peripheral blood and decidual NK cells. *American Journal of Reproductive Immunology*, 58 (3), 280-288.
- Sato, T., *et al.*, 2009. Interferon regulatory factor-2 protects quiescent hematopoietic stem cells from type I interferon-dependent exhaustion. *Nature Medicine*, 15 (6), 696-700.
- Saussele, S., *et al.*, 2016. The concept of treatment-free remission in chronic myeloid leukemia. *Leukemia*, 30 (8), 1638-1647.
- Savoldo, B., *et al.*, 2011. CD28 costimulation improves expansion and persistence of chimeric antigen receptor-modified T cells in lymphoma patients. *The Journal of Clinical Investigation*, 121 (5), 1822-1826.
- Scheich, F., *et al.*, 2007. The immunogenicity of Bcr-Abl expressing dendritic cells is dependent on the Bcr-Abl kinase activity and dominated by Bcr-Abl regulated antigens. *Blood*, 110 (7), 2556-2560.
- Schenborn, E.T. and Goiffon, V., 2000. DEAE-dextran transfection of mammalian cultured cells. *In: DEAE-dextran transfection of mammalian cultured cells. Transcription Factor Protocols*. Springer, 2000, pp. 147-153.
- Schmied, S., *et al.*, 2015. Analysis of the functional WT 1-specific T-cell repertoire in healthy donors reveals a discrepancy between CD 4 and CD 8 memory formation. *Immunology*, 145 (4), 558-569.
- Schmitt, M., *et al.*, 2006. Chronic myeloid leukemia cells express tumor-associated antigens eliciting specific CD8+ T-cell responses and are lacking costimulatory molecules. *Experimental Hematology*, 34 (12), 1709-1719.
- Sedlik, C., *et al.*, 2000. In vivo induction of a high-avidity, high-frequency cytotoxic T-lymphocyte response is associated with antiviral protective immunity. *Journal of Virology*, 74 (13), 5769-5775.
- Seggewiss, R., *et al.*, 2005. Imatinib inhibits T-cell receptor-mediated T-cell proliferation and activation in a dose-dependent manner. *Blood*, 105 (6), 2473-2479.
- Shahrabi, S., *et al.*, 2017. Wilms' tumor gene 1 in leukemia: Prognostic or predictive biomarker. *Clinical Cancer Investigation Journal*, 6 (6), 233.
- Shapiro-Shelef, M. and Calame, K., 2005. Regulation of plasma-cell development. *Nature Reviews.Immunology*, 5 (3), 230-242.
- Sharma, M.D., *et al.*, 2007. Plasmacytoid dendritic cells from mouse tumor-draining lymph nodes directly activate mature Tregs via indoleamine 2,3-dioxygenase. *The Journal of Clinical Investigation*, 117 (9), 2570-2582.

- Shi, L., *et al.*, 2013. The role of PD-1 and PD-L1 in T-cell immune suppression in patients with hematological malignancies. *Journal of Hematology & Oncology*, 6 (1), 74.
- Shin, J.Y., *et al.*, 2014. High c-Kit expression identifies hematopoietic stem cells with impaired self-renewal and megakaryocytic bias. *The Journal of Experimental Medicine*, 211 (2), 217-231.
- Shinohara, Y., *et al.*, 2013. A multicenter clinical study evaluating the confirmed complete molecular response rate in imatinib-treated patients with chronic phase chronic myeloid leukemia by using the international scale of real-time quantitative polymerase chain reaction. *Haematologica*, 98 (9), 1407-1413.
- Shultz, L.D., *et al.*, 2014. Human cancer growth and therapy in immunodeficient mouse models. *Cold Spring Harbor Protocols*, 2014 (7), 694-708.
- Sigalotti, L., *et al.*, 2004. Intratumor heterogeneity of cancer/testis antigens expression in human cutaneous melanoma is methylation-regulated and functionally reverted by 5-aza-2'-deoxycytidine. *Cancer Research*, 64 (24), 9167-9171.
- Simpson, A.J., *et al.*, 2005. Cancer/testis antigens, gametogenesis and cancer. *Nature Reviews Cancer*, 5 (8), 615.
- Singleton, M.R., Dillingham, M.S. and Wigley, D.B., 2007. Structure and mechanism of helicases and nucleic acid translocases. *Annual Review of Biochemistry*, 76, 23-50.
- Sivori, S., *et al.*, 1999. Nkp46 is the major triggering receptor involved in the natural cytotoxicity of fresh or cultured human NK cells. Correlation between surface density of Nkp46 and natural cytotoxicity against autologous, allogeneic or xenogeneic target cells. *European Journal of Immunology*, 29 (5), 1656-1666.
- Slingluff Jr, C.L., *et al.*, 2000. Melanomas with concordant loss of multiple melanocytic differentiation proteins: immune escape that may be overcome by targeting unique or undefined antigens. *Cancer Immunology, Immunotherapy*, 48 (12), 661-672.
- Slingluff, C.L., Jr, 2011. The present and future of peptide vaccines for cancer: single or multiple, long or short, alone or in combination? *Cancer Journal (Sudbury, Mass.)*, 17 (5), 343-350.
- Sloma, I., *et al.*, 2010. Insights into the stem cells of chronic myeloid leukemia. *Leukemia*, 24 (11), 1823.
- Smith, S.G., *et al.*, 2015a. Intracellular cytokine staining and flow cytometry: considerations for application in clinical trials of novel tuberculosis vaccines. *PLoS One*, 10 (9), e0138042.
- Smith, H.A. and McNeel, D.G., 2010. The SSX family of cancer-testis antigens as target proteins for tumor therapy. *Clinical & Developmental Immunology*, 2010, 150591.
- Smyth, M.J. and Trapani, J.A., 1995. Granzymes: exogenous proteases that induce target cell apoptosis. *Immunology Today*, 16 (4), 202-206.
- Sopper, S., *et al.*, 2017. Reduced CD62L Expression on T Cells and Increased Soluble CD62L Levels Predict Molecular Response to Tyrosine Kinase Inhibitor Therapy in

- Early Chronic-Phase Chronic Myelogenous Leukemia. *Journal of Clinical Oncology : Official Journal of the American Society of Clinical Oncology*, 35 (2), 175-184.
- Spranger, S., et al., 2013. Up-regulation of PD-L1, IDO, and T(regs) in the melanoma tumor microenvironment is driven by CD8(+) T cells. *Science Translational Medicine*, 5 (200), 200ra116.
- Sprent, J. and Tough, D.F., 2001. T cell death and memory. *Science (New York, N.Y.)*, 293 (5528), 245-248.
- Srivastava, M.K., et al., 2010. Myeloid-derived suppressor cells inhibit T-cell activation by depleting cystine and cysteine. *Cancer Research*, 70 (1), 68-77.
- Srivastava, P., et al., 2016. Induction of cancer testis antigen expression in circulating acute myeloid leukemia blasts following hypomethylating agent monotherapy. *Oncotarget*, 7 (11), 12840-12856.
- Stegmann, J.L., et al., 2003. Chronic myeloid leukemia patients resistant to or intolerant of interferon alpha and subsequently treated with imatinib show reduced immunoglobulin levels and hypogammaglobulinemia. *Haematologica*, 88 (7), 762-768.
- Stevens, W.B., et al., 2016. 'Trained immunity': consequences for lymphoid malignancies. *Haematologica*, 101 (12), 1460-1468.
- Stevenson, B.J., et al., 2007. Rapid evolution of cancer/testis genes on the X chromosome. *Bmc Genomics*, 8 (1), 129.
- Stewart, T. and Abrams, S., 2008a. How tumours escape mass destruction. *Oncogene*, 27 (45), 5894.
- Suemori, K., et al., 2008. Identification of an epitope derived from CML66, a novel tumor-associated antigen expressed broadly in human leukemia, recognized by human leukocyte antigen-A\*2402-restricted cytotoxic T lymphocytes. *Cancer Science*, 99 (7), 1414-1419.
- Sugiyama, H., 2001. Wilms' tumor gene WT1: its oncogenic function and clinical application. *International Journal of Hematology*, 73 (2), 177-187.
- Sultan, H., et al., 2017. Designing therapeutic cancer vaccines by mimicking viral infections. *Cancer Immunology, Immunotherapy*, 66 (2), 203-213.
- Taieb, J., et al., 2004. Imatinib mesylate impairs Flt3L-mediated dendritic cell expansion and antitumor effects in vivo. *Blood*, 103 (5), 1966-7; author reply 1967.
- Takahashi, N., et al., 2012. Discontinuation of imatinib in Japanese patients with chronic myeloid leukemia. *Haematologica*, 97 (6), 903-906.
- Takahashi, T., et al., 2003. Dendritic cell vaccination for patients with chronic myelogenous leukemia. *Leukemia Research*, 27 (9), 795-802.
- Takikawa, O., et al., 1988. Mechanism of interferon-gamma action. Characterization of indoleamine 2,3-dioxygenase in cultured human cells induced by interferon-gamma and evaluation of the enzyme-mediated tryptophan degradation in its anticellular activity. *The Journal of Biological Chemistry*, 263 (4), 2041-2048.

- Takikawa, O., *et al.*, 1986. Tryptophan degradation in mice initiated by indoleamine 2,3-dioxygenase. *The Journal of Biological Chemistry*, 261 (8), 3648-3653.
- Talwar, T., *et al.*, 2017. The DEAD-box protein DDX43 (HAGE) is a dual RNA-DNA helicase and has a K-homology domain required for full nucleic acid unwinding activity. *The Journal of Biological Chemistry*, 292 (25), 10429-10443.
- Tanner, A., *et al.*, 2013. Humanized mice as a model to study human hematopoietic stem cell transplantation. *Stem Cells and Development*, 23 (1), 76-82.
- Tanner, N.K., *et al.*, 2003. The Q motif: a newly identified motif in DEAD box helicases may regulate ATP binding and hydrolysis. *Molecular Cell*, 11 (1), 127-138.
- Tentler, J.J., *et al.*, 2012. Patient-derived tumour xenografts as models for oncology drug development. *Nature Reviews Clinical Oncology*, 9 (6), 338.
- Terme, M., Tartour, E. and Taieb, J., 2013. VEGFA/VEGFR2-targeted therapies prevent the VEGFA-induced proliferation of regulatory T cells in cancer. *Oncoimmunology*, 2 (8), e25156.
- Thaker, A.I., *et al.*, 2013. IDO1 metabolites activate  $\beta$ -catenin signaling to promote cancer cell proliferation and colon tumorigenesis in mice. *Gastroenterology*, 145 (2), 416-425. e4.
- The National Center for Biotechnology Information (NCBI). Protein, WT1-WT1 transcription factor. Homo sapiens (human). Available at: <https://www.ncbi.nlm.nih.gov/protein/?term=human+WT1>. [Accessed 4 May 2019].
- Thielen, N., *et al.*, 2013. Imatinib discontinuation in chronic phase myeloid leukaemia patients in sustained complete molecular response: A randomised trial of the Dutch-Belgian Cooperative Trial for Haemato-Oncology (HOVON). *European Journal of Cancer*, 49 (15), 3242-3246.
- Thoren, L.A., *et al.*, 2008. Kit regulates maintenance of quiescent hematopoietic stem cells. *Journal of Immunology (Baltimore, Md.: 1950)*, 180 (4), 2045-2053.
- Ting, J.P. and Trowsdale, J., 2002. Genetic control of MHC class II expression. *Cell*, 109 (2), S21-S33.
- Tiptiri-Kourpeti, A., *et al.*, 2016. DNA vaccines to attack cancer: Strategies for improving immunogenicity and efficacy. *Pharmacology & Therapeutics*, 165, 32-49.
- Topalian, S.L., Drake, C.G. and Pardoll, D.M., 2015. Immune checkpoint blockade: a common denominator approach to cancer therapy. *Cancer Cell*, 27 (4), 450-461.
- Toska, E. and Roberts, S.G., 2014. Mechanisms of transcriptional regulation by WT1 (Wilms' tumour 1). *The Biochemical Journal*, 461 (1), 15-32.
- Traver, D., *et al.*, 2000. Development of CD8 $\alpha$ -positive dendritic cells from a common myeloid progenitor. *Science (New York, N.Y.)*, 290 (5499), 2152-2154.
- Trimble, C., *et al.*, 2003. Comparison of the CD8 T cell responses and antitumor effects generated by DNA vaccine administered through gene gun, biojector, and syringe. *Vaccine*, 21 (25-26), 4036-4042.
- Trinchieri, G., 1989. Biology of natural killer cells. *Advances in Immunology*, 47, 187-376.

- Tsang, K.Y., *et al.*, 1995. Generation of human cytotoxic T cells specific for human carcinoembryonic antigen epitopes from patients immunized with recombinant vaccinia-CEA vaccine. *Journal of the National Cancer Institute*, 87 (13), 982-990.
- Tsuboi, A., *et al.*, 2000. Cytotoxic T-lymphocyte responses elicited to Wilms' tumor gene WT1 product by DNA vaccination. *Journal of Clinical Immunology*, 20 (3), 195-202.
- Tsuji, T., *et al.*, 2009. Characterization of preexisting MAGE-A3-specific CD4+ T cells in cancer patients and healthy individuals and their activation by protein vaccination. *Journal of Immunology (Baltimore, Md.: 1950)*, 183 (7), 4800-4808.
- Tumeh, P.C., *et al.*, 2014. PD-1 blockade induces responses by inhibiting adaptive immune resistance. *Nature*, 515 (7528), 568.
- Türeci, Ö., *et al.*, 1998. Expression of SSX genes in human tumors. *International Journal of Cancer*, 77 (1), 19-23.
- Turnis, M.E. and Rooney, C.M., 2010. Enhancement of dendritic cells as vaccines for cancer. *Immunotherapy*, 2 (6), 847-862.
- Tyler, E.M., *et al.*, 2013. WT1-specific T-cell responses in high-risk multiple myeloma patients undergoing allogeneic T cell-depleted hematopoietic stem cell transplantation and donor lymphocyte infusions. *Blood*, 121 (2), 308-317.
- Usherwood, E.J., *et al.*, 1999. Functionally heterogeneous CD8(+) T-cell memory is induced by Sendai virus infection of mice. *Journal of Virology*, 73 (9), 7278-7286.
- Uyttenhove, C., *et al.*, 2003. Evidence for a tumoral immune resistance mechanism based on tryptophan degradation by indoleamine 2, 3-dioxygenase. *Nature Medicine*, 9 (10), 1269.
- Vacchelli, E., *et al.*, 2014. Trial Watch: Chemotherapy with immunogenic cell death inducers. *Oncoimmunology*, 3 (3), e27878.
- Valverde, R., Edwards, L. and Regan, L., 2008. Structure and function of KH domains. *The FEBS Journal*, 275 (11), 2712-2726.
- van Baren, N., *et al.*, 1999. Genes encoding tumor-specific antigens are expressed in human myeloma cells. *Blood*, 94 (4), 1156-1164.
- van den Elsen, Peter J, *et al.*, 1998. Regulation of MHC class I and II gene transcription: differences and similarities. *Immunogenetics*, 48 (3), 208-221.
- van der Burg, S.H., *et al.*, 1996. Immunogenicity of peptides bound to MHC class I molecules depends on the MHC-peptide complex stability. *Journal of Immunology (Baltimore, Md.: 1950)*, 156 (9), 3308-3314.
- van Dongen, M., *et al.*, 2010. Anti-inflammatory M2 type macrophages characterize metastasized and tyrosine kinase inhibitor-treated gastrointestinal stromal tumors. *International Journal of Cancer*, 127 (4), 899-909.
- Van Driessche, A., Berneman, Z.N. and Van Tendeloo, V.F., 2012a. Active specific immunotherapy targeting the Wilms' tumor protein 1 (WT1) for patients with hematological malignancies and solid tumors: lessons from early clinical trials. *The Oncologist*, 17 (2), 250-259.

- Van Etten, R.A., Jackson, P. and Baltimore, D., 1989. The mouse type IV c-abl gene product is a nuclear protein, and activation of transforming ability is associated with cytoplasmic localization. *Cell*, 58 (4), 669-678.
- van Mierlo, G.J., *et al.*, 2002. CD40 stimulation leads to effective therapy of CD40(-) tumors through induction of strong systemic cytotoxic T lymphocyte immunity. *Proceedings of the National Academy of Sciences of the United States of America*, 99 (8), 5561-5566.
- van Rhee, F., *et al.*, 2005. NY-ESO-1 is highly expressed in poor-prognosis multiple myeloma and induces spontaneous humoral and cellular immune responses. *Blood*, 105 (10), 3939-3944.
- Van Thanh, P.N., *et al.*, 2005. Establishment and characterization of A novel Philadelphia-chromosome positive chronic myeloid leukemia cell line, TCC-S, expressing P210 and P190 BCR/ABL transcripts but missing normal ABL gene. *Human Cell*, 18 (1), 25-33.
- Vanneman, M. and Dranoff, G., 2012. Combining immunotherapy and targeted therapies in cancer treatment. *Nature Reviews Cancer*, 12 (4), 237.
- Vatakis, D.N., Koh, Y.T. and McMillan, M., 2005. CD4+ T cell epitope affinity to MHC II influences the magnitude of CTL responses elicited by DNA epitope vaccines. *Vaccine*, 23 (20), 2639-2646.
- Vitiello, A., *et al.*, 1991. Analysis of the HLA-restricted influenza-specific cytotoxic T lymphocyte response in transgenic mice carrying a chimeric human-mouse class I major histocompatibility complex. *The Journal of Experimental Medicine*, 173 (4), 1007-1015.
- Vivier, E., *et al.*, 2012. Targeting natural killer cells and natural killer T cells in cancer. *Nature Reviews Immunology*, 12 (4), 239-252.
- von Leoprechting, A., *et al.*, 1999. Stimulation of CD40 on immunogenic human malignant melanomas augments their cytotoxic T lymphocyte-mediated lysis and induces apoptosis. *Cancer Research*, 59 (6), 1287-1294.
- Volpe, G., *et al.*, 2007. Alternative BCR/ABL splice variants in Philadelphia chromosome-positive leukemias result in novel tumor-specific fusion proteins that may represent potential targets for immunotherapy approaches. *Cancer Research*, 67 (11), 5300-5307.
- Vonka, V. and Petrackova, M., 2015. Immunology of chronic myeloid leukemia: current concepts and future goals. *Expert Review of Clinical Immunology*, 11 (4), 511-522.
- Voron, T., *et al.*, 2015. VEGF-A modulates expression of inhibitory checkpoints on CD8+ T cells in tumors. *The Journal of Experimental Medicine*, 212 (2), 139-148.
- Wallace, D., Hildesheim, A. and Pinto, L.A., 2004. Comparison of benchtop microplate beta counters with the traditional gamma counting method for measurement of chromium-51 release in cytotoxic assays. *Clinical and Diagnostic Laboratory Immunology*, 11 (2), 255-260.
- Walunas, T.L., *et al.*, 1994. CTLA-4 can function as a negative regulator of T cell activation. *Immunity*, 1 (5), 405-413.

- Wang, Y., *et al.*, 2004. Cancer/testis antigen expression and autologous humoral immunity to NY-ESO-1 in gastric cancer. *Cancer Immunity Archive*, 4 (1), 11.
- Wang, Z., *et al.*, 2006. SPAN-Xb expression in myeloma cells is dependent on promoter hypomethylation and can be upregulated pharmacologically. *International Journal of Cancer*, 118 (6), 1436-1444.
- Wang, Z., *et al.*, 2003. Gene expression and immunologic consequence of SPAN-Xb in myeloma and other hematologic malignancies. *Blood*, 101 (3), 955-960.
- Wang, Z., *et al.*, 2004. The spermatozoa protein, SLLP1, is a novel cancer-testis antigen in hematologic malignancies. *Clinical Cancer Research : An Official Journal of the American Association for Cancer Research*, 10 (19), 6544-6550.
- Warda, W., *et al.*, 2019. *CML Hematopoietic Stem Cells Expressing IL1RAP Can Be Targeted by Chimeric Antigen Receptor-Engineered T Cells.*
- Washbourne, P. and McAllister, A.K., 2002. Techniques for gene transfer into neurons. *Current Opinion in Neurobiology*, 12 (5), 566-573.
- Wei, G., Rafiyath, S. and Liu, D., 2010. First-line treatment for chronic myeloid leukemia: dasatinib, nilotinib, or imatinib. *Journal of Hematology & Oncology*, 3, 47-8722-3-47.
- Weissman, I.L., 2000. Translating stem and progenitor cell biology to the clinic: barriers and opportunities. *Science (New York, N.Y.)*, 287 (5457), 1442-1446.
- Weiss-Steider, B., *et al.*, 2011. Expression of MICA, MICB and NKG2D in human leukemic myelomonocytic and cervical cancer cells. *Journal of Experimental & Clinical Cancer Research*, 30 (1), 37.
- Weng, N., Araki, Y. and Subedi, K., 2012. The molecular basis of the memory T cell response: differential gene expression and its epigenetic regulation. *Nature Reviews Immunology*, 12 (4), 306.
- Weon, J.L. and Potts, P.R., 2015. The MAGE protein family and cancer. *Current Opinion in Cell Biology*, 37, 1-8.
- Wherry, E.J., 2011. T cell exhaustion. *Nature Immunology*, 12 (6), 492.
- Williams, D.B. and Watts, T.H., 1995. Molecular chaperones in antigen presentation. *Current Opinion in Immunology*, 7 (1), 77-84.
- Williams, S.S., *et al.*, 1993. The study of human neoplastic disease in severe combined immunodeficient mice. *Laboratory Animal Science*, 43 (2), 139-146.
- Wilmotte, R., *et al.*, 2005. B7-homolog 1 expression by human glioma: a new mechanism of immune evasion. *Neuroreport*, 16 (10), 1081-1085.
- Wolchok, J.D., *et al.*, 2010. Ipilimumab monotherapy in patients with pretreated advanced melanoma: a randomised, double-blind, multicentre, phase 2, dose-ranging study. *The Lancet. Oncology*, 11 (2), 155-164.
- Wolchok, J.D., *et al.*, 2013. Four-year survival rates for patients with metastatic melanoma who received ipilimumab in phase II clinical trials. *Annals of Oncology : Official Journal of the European Society for Medical Oncology*, 24 (8), 2174-2180.

- Wong, P. and Pamer, E.G., 2003. CD8 T cell responses to infectious pathogens. *Annual Review of Immunology*, 21 (1), 29-70.
- Wurm, F.M., 2004. Production of recombinant protein therapeutics in cultivated mammalian cells. *Nature Biotechnology*, 22 (11), 1393.
- Xia, H., et al., 2017. Interferon-gamma affects leukemia cell apoptosis through regulating Fas/FasL signaling pathway. *Eur Rev Med Pharmacol Sci*, 21 (9), 2244-2248.
- Xu, S., et al., 2003. Rapid high efficiency sensitization of CD8+ T cells to tumor antigens by dendritic cells leads to enhanced functional avidity and direct tumor recognition through an IL-12-dependent mechanism. *Journal of Immunology (Baltimore, Md.: 1950)*, 171 (5), 2251-2261.
- Ya, Z., et al., 2015. Mouse model for Pre-Clinical study of human cancer immunotherapy. *Current Protocols in Immunology*, 108 (1), 20.1. 1-20.1. 43.
- Yamamoto, R., et al., 2008. PD-1-PD-1 ligand interaction contributes to immunosuppressive microenvironment of Hodgkin lymphoma. *Blood*, 111 (6), 3220-3224.
- Yamane, H. and Paul, W.E., 2013. Early signaling events that underlie fate decisions of naive CD 4 T cells toward distinct T-helper cell subsets. *Immunological Reviews*, 252 (1), 12-23.
- Yan, Q., et al., 2007. A DNA vaccine constructed with human papillomavirus type 16 (HPV16) E7 and E6 genes induced specific immune responses. *Gynecologic Oncology*, 104 (1), 199-206.
- Yang, H., Wang, H. and Jaenisch, R., 2014. Generating genetically modified mice using CRISPR/Cas-mediated genome engineering. *Nature Protocols*, 9 (8), 1956.
- Yin, D., et al., 1999. Ligation of CD28 in vivo induces CD40 ligand expression and promotes B cell survival. *Journal of Immunology (Baltimore, Md.: 1950)*, 163 (8), 4328-4334.
- Youngblood, B., et al., 2011. Chronic virus infection enforces demethylation of the locus that encodes PD-1 in antigen-specific CD8 T cells. *Immunity*, 35 (3), 400-412.
- Yu, L., et al., 2016. Chronic Myelocytic Leukemia (CML) Patient-Derived Dendritic Cells Transfected with Autologous Total RNA Induces CML-Specific Cytotoxicity. *Indian Journal of Hematology & Blood Transfusion : An Official Journal of Indian Society of Hematology and Blood Transfusion*, 32 (4), 397-404.
- Yu, Z. and Restifo, N.P., 2002. Cancer vaccines: progress reveals new complexities. *The Journal of Clinical Investigation*, 110 (3), 289-294.
- Zahran, A.M., Badrawy, H. and Ibrahim, A., 2014. Prognostic value of regulatory T cells in newly diagnosed chronic myeloid leukemia patients. *International Journal of Clinical Oncology*, 19 (4), 753-760.
- Zaidi, M.R., et al., 2011. Interferon- $\gamma$  links ultraviolet radiation to melanomagenesis in mice. *Nature*, 469 (7331), 548.

Zaidi, M.R. and Merlino, G., 2011. The two faces of interferon-gamma in cancer. *Clinical Cancer Research : An Official Journal of the American Association for Cancer Research*, 17 (19), 6118-6124.

Zanetti, M., Castiglioni, P. and Ingulli, E., 2010. Principles of memory CD8 T-cells generation in relation to protective immunity. *In: Principles of memory CD8 T-cells generation in relation to protective immunity. Memory T cells*. Springer, 2010, pp. 108-125.

Zaritskaya, L., *et al.*, 2010. New flow cytometric assays for monitoring cell-mediated cytotoxicity. *Expert Review of Vaccines*, 9 (6), 601-616.

Zarour, H.M., 2016. Reversing T-cell Dysfunction and Exhaustion in Cancer. *Clinical Cancer Research : An Official Journal of the American Association for Cancer Research*, 22 (8), 1856-1864.

Zeh, H.J., 3rd, *et al.*, 1999. High avidity CTLs for two self-antigens demonstrate superior in vitro and in vivo antitumor efficacy. *Journal of Immunology (Baltimore, Md.: 1950)*, 162 (2), 989-994.

Zendman, A.J., *et al.*, 2001. Expression profile of genes coding for melanoma differentiation antigens and cancer/testis antigens in metastatic lesions of human cutaneous melanoma. *Melanoma Research*, 11 (5), 451-459.

Zha, X., *et al.*, 2012. Alternative expression of TCRzeta related genes in patients with chronic myeloid leukemia. *Journal of Hematology & Oncology*, 5, 74-8722-5-74.

Zhang, W., *et al.*, 2019. Phase I/II clinical trial of a Wilms' tumor 1-targeted dendritic cell vaccination-based immunotherapy in patients with advanced cancer. *Cancer Immunology, Immunotherapy*, 68 (1), 121-130.

Zhang, Y., *et al.*, 2003. Pattern of gene expression and immune responses to Semenogelin 1 in chronic hematologic malignancies. *Journal of Immunotherapy*, 26 (6), 461-467.

Zhang, L., 2018. Multi-epitope vaccines: a promising strategy against tumors and viral infections. *Cellular & Molecular Immunology*, 15 (2), 182-184.

Zhang, L., Gajewski, T.F. and Kline, J., 2009. PD-1/PD-L1 interactions inhibit antitumor immune responses in a murine acute myeloid leukemia model. *Blood*, 114 (8), 1545-1552.

Zitvogel, L., *et al.*, 2013. Mechanism of action of conventional and targeted anticancer therapies: reinstating immunosurveillance. *Immunity*, 39 (1), 74-88.

Zitvogel, L., *et al.*, 2016. Immunological off-target effects of imatinib. *Nature Reviews. Clinical Oncology*, 13 (7), 431-446.

National Care Institution. Principle of CAR therapy [online]: Available at: <https://www.cancer.gov/images/cdr/live/CDR774647-750.jpg> [Accessed 20 April 2019].

Smart Servicer Medical Art [online]: Available at: <https://smart.servier.com/>.

NIH. U.S National library of medicine, 2015. Administration of Donor Multi TAA-Specific T cells for AML or MDS(ADSPAM). Available at: <https://www.clinicaltrials.gov/ct2/show/NCT02494167> ,[Accessed 21 January 2019].